ID Design Press, Skopje, Republic of Macedonia
Open Access Macedonian Journal of Medical Sciences. 2019 Dec 30; 7(24):4189-4193.
https://doi.org/10.3889/oamjms.2019.343
eISSN: 1857-9655
Basic and Clinical Medical Researches in Vietnam

Correction of Upper Incisor Proclination by Applying Lingual Crown Torque with Pre adjusted Lingual Brackets in a Skeletal-Class III Patient – Case Report

Viet Anh Nguyen[1*], Nguyen Vu Thai Lien[2], Vu Thi Nga[3]

[1]Viet Anh Orthodontic Clinic, Nam Tu Liem, Hanoi, Vietnam; [2]Department of Pediatric Dentistry, Faculty of Dentistry, Hanoi University of Business and Technology, Hanoi, Vietnam; [3]Institute for Research and Development, Duy Tan University, 03 Quang Trung, Danang, Vietnam

Citation: Nguyen VA, Lien NVT, Nga VT. Correction of Upper Incisor Proclination by Applying Lingual Crown Torque with Pre adjusted Lingual Brackets in a Skeletal-Class III Patient – Case Report. Open Access Maced J Med Sci. 2019 Dec 30; 7(24):4189-4193. https://doi.org/10.3889/oamjms.2019.343

Keywords: Lingual bracket; Lingual Crown Torque; Skeletal class III relationship

***Correspondence:** Viet Anh Nguyen. Viet Anh Orthodontic Clinic, Nam Tu Liem, Hanoi, Vietnam. E-mail: nvatk16@gmail.com

Received: 09-Sep-2019; **Revised:** 20-Nov-2019; **Accepted:** 21-Nov-2019; **Online first:** 15-Oct-2019

Funding: This research did not receive any financial support

Competing Interests: The authors have declared that no competing interests exist

Abstract

BACKGROUND: After levelling and alignment in skeletal Class III patients with upper anterior crowding, the upper incisors usually have excessive proclination. In these cases, the upper incisors' axial proclination need to be reduced to improve esthetics.

CASE REPORT: This case report presents an invisible orthodontic treatment of a 24-year-old adult female patient with skeletal Class III relationship, anterior crossbite, proclined upper incisors, and reduced incisor showing. Patients denied extraction and interproximal reduction. With multi-slotted lingual brackets and straight archwires, we applied lingual crown torque to upper anterior teeth to reduce axial proclination. The resulting uprighted position of upper incisors led to increased incisor showing. A good smile and stable occlusion were obtained after 15 months of active treatment.

CONCLUSION: The use of lingual brackets to apply lingual crown torque helps to reduce axial proclination and increasing upper incisor showing without interproximal reduction nor extraction in skeletal Class III patients with upper anterior crowding.

Introduction

Since the first introduction of multilingual bracket system by K. Fujita in 1979 [1], lingual orthodontic treatment has become popular. Recent advances in lingual orthodontics include the transition from mushroom archwire to straight wire concept [2], [3], the use of multi-slot lingual bracket [4], [5], the application of self-ligating lingual brackets [6], [7], the customised lingual bracket, and individual robot-bending archwire [8]. The fifth generation of Dr Fujita's lingual brackets was the first lingual bracket with the multi-slot concept. Based on this concept, CLB lingual brackets was developed to have the additional advantages of the straight lingual archwire.

Skeletal Class III patients have proclined upper incisors due to the dentoalveolar compensation to the skeletal discrepancies. In compensation Class III cases with crowding, after levelling the upper arch with nonextraction approach, upper incisors usually have increased proclination. Also, the vertical maxillary deficiency accompanying with skeletal Class III may express as decreased upper incisor showing. By uprighting the upper incisors, orthodontists can increase the incisor display to create a better smile arc. In this case report, the authors applied lingual crown torque to upright the upper incisors, using preadjusted lingual appliances with straight tandem archwire mechanics.

Case Report

Diagnosis and Treatment Plan

A 24-year-old female patient presented to the author's clinic with the request to correct anterior crossbite using an invisible appliance. She also wanted to reduce upper incisor proclination and have more incisor showing on a smile without neither tooth extraction nor orthognathic surgery.

On clinical examination, she showed a straight profile with normal nasolabial angle and labiomental sulcus without facial asymmetry (Figure 1). On smile, she has reduced incisor showing with a flat smile arc. Intraoral examination revealed a crossbite involving the upper right central and lateral incisors, overerupted lower incisors and dental midline deviation. She had a Class I molar and canine relationship on the left, a mild Class II canine and Class I molar on the right.

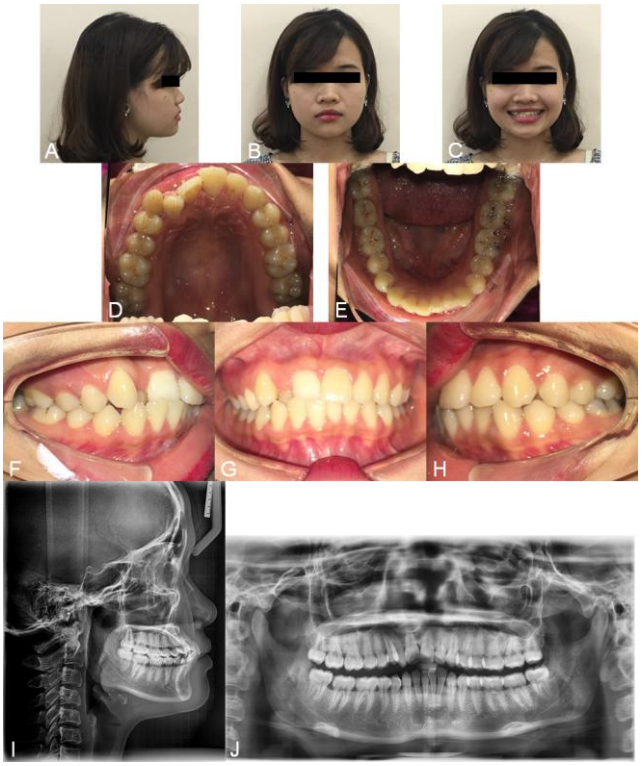

Figure 1: 24-year-old female patient with anterior crossbite and mild skeletal Class III relationship before treatment. A) Extraoral profile view; B) Extraoral straight view; C) Smile straight view; D) Maxillary occlusal view; E) Mandibular occlusal view; F) Intraoral right lateral view; G) Intraoral straight view; H) Intraoral left lateral view; I) Cephalometric radiograph; J) Panoramic radiograph

The panoramic radiograph revealed the presence of all teeth, including the third molars. She also had an impacted supernumerary tooth in the right central incisor region. Cephalometric analysis (Table 1) showed a mild skeletal Class III relationship (ANB = –1.8°) with prognathic mandible (SNB = 85.5°) and horizontal growth pattern (FMA = 16°). Both upper and lower incisors were proclined labial (U1-SN = 124.1°and IMPA = 106.2°).

Table 1: Cephalometric Analysis

	Pretreatment	Post-treatment
SNA	83.7°	84.4°
SNB	85.5°	85.4°
ANB	-1.8°	-0.9°
FMA	16°	16.2°
U1-SN	124.1°	112.2°
Wit appraisal	-0.9 mm	-1.9 mm
IMPA	106.2°	104°
Interincisal Angle	107.9°	122.2°
L1-NB	5.6 mm	5.9 mm
U1 protrusion (U1-APo)	9.3 mm	8.7 mm
L1 protrusion (L1-APo)	6.4 mm	6.0 mm
Upper lip to E-line	-2.2 mm	-1.4 mm
Lower lip to E-line	0.3 mm	0.7 mm

The treatment objectives were to eliminate the anterior crossbite, level the curve of Spee, obtain normal overjet and overbite, correct the dental midlines, establish Class I molar and canine relationship, upright and extrude the upper incisors to reduce incisor proclination and increase incisor show. The patient was explained about the need for surgical removal of the supernumerary tooth but she denied this invasive surgery and accepting the risk of root resorption of adjacent teeth during orthodontic treatment.

After correcting the anterior crossbite and aligning the upper teeth without extraction of premolars, upper incisors flaring would be inevitable. There were three possible treatment options to reduce upper incisor proclination. The first option would be the interproximal reduction and anterior teeth retraction. The second option would involve third molars extraction and the entire arch distalization. The third option would be uprighting the upper incisors by applying lingual crown torque. Because the patient wanted neither tooth extraction nor tooth stripping, she chose the third option.

Treatment progress

CLB lingual brackets were bond indirectly in both arches using a thermoplastic splint. A large.012" Ni-Ti continuous straight archwire was inserted in the upper arch, and a medium wire of the same type was inserted in the lower arch. Bite turbos were placed on lower molars for allowing the upper right incisors to move forward. In the next months, archwire size was increased to .014" and .016" Ni-Ti. Bite turbos were gradually grinded at each appointment. After four months of levelling, the anterior crossbite was eliminated but the inclination of upper right lateral incisors had not been corrected, it's root was still in the palatal side (Figure 2). Two months later, .018" x .018" stainless steel archwires were inserted to both gingival and occlusal slots in both arches. Labial brackets were bonded to upper and lower molars to control the molars. After another two months, .018" x .025" stainless steel archwire was inserted to the occlusal slots of upper incisor and canine brackets for torque control.

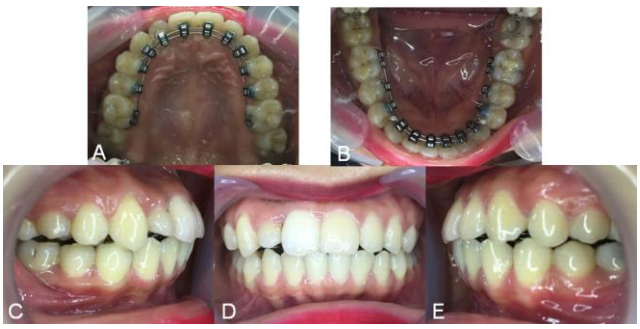

Figure 2: After four months of levelling with lingual appliances and nickel-titanium archwires, the anterior crossbite was eliminated but the upper right lateral incisors had excessive proclination; A) Maxillary occlusal view; B) Mandibular occlusal view; C) Intraoral right lateral view; D) Intraoral straight view; E) Intraoral left lateral view

Two months later, the upper right lateral incisor's torque was improved (Figure 3). At this time, the upper incisors still had excessive proclination.

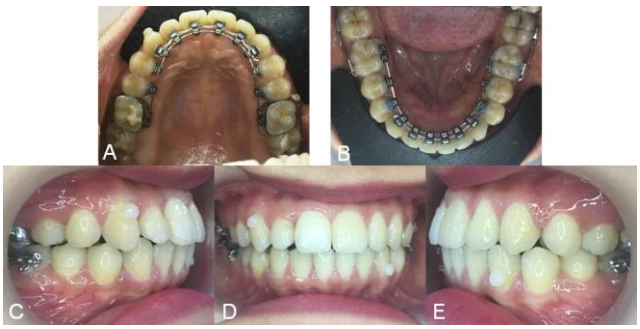

Figure 3: Progress after 10 months of treatments. The upper right lateral incisor's torque was improved. Composite buttons were bonded for using intermaxillary elastics; A) Maxillary occlusal view; B. Mandibular occlusal view; C) Intraoral right lateral view; D) Intraoral straight view; E) Intraoral left the lateral view

Both upper main archwire and anterior segmental wire were applied 15° lingual crown torque in the anterior teeth to further upright them. The main archwire had detorque bends distal to the canine to maintain the torque of buccal segments (Figure 4).

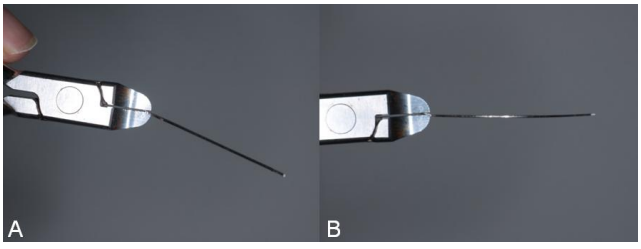

Figure 4: A) The main archwire has 15° lingual crown torque in the anterior teeth; B) Zero torque of the main archwire in the buccal segments

Steel ligature was used for full engagement of the archwires to the bracket slot. Composite buttons were bonded to lower canines and upper right canine for Class III elastic on the right side and anterior diagonal elastic. After three months of applying lingual crown torque, the upper incisors' proclination was improved (Figure 5). Intermaxillary elastics continued to be used for midline correcting and settling the occlusion.

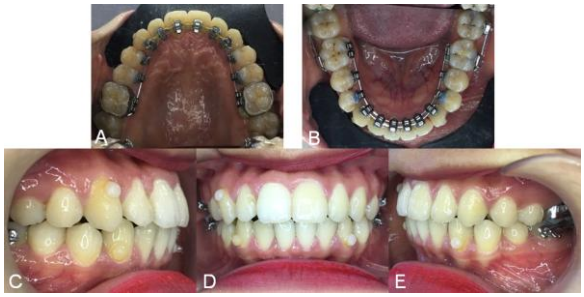

Figure 5: After three months of inserting main archwire and anterior segmental wire with – 15° torque toupper anterior brackets, the upper incisors were uprighted; A) Maxillary occlusal view; B) Mandibular occlusal view; C) Intraoral right lateral view; D) Intraoral straight view; E. Intraoral left the lateral view

Treatment result

Class I canine and molar relationships were established with normal overjet and overbite (Figure 6). The anterior crossbite was eliminated, dental midlines of both arches were straightened, the curve of Spee was levelled. The smile arc became more curved, and the upper incisor show upon smile was increased. The patient satisfied with the treatment results.

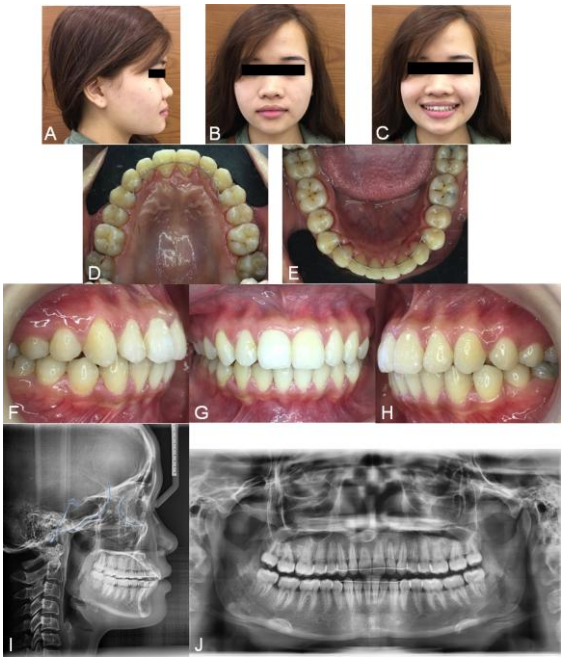

Figure 6: Patient after 14 months of treatment; A) Extraoral profile view; B) Extraoral straight view; C) Smile straight view; D) Maxillary occlusal view; E) Mandibular occlusal view; F) Intraoral right lateral view; G) Intraoral straight view; H) Intraoral left lateral view; I) Cephalometric radiograph; J) Panoramic radiograph

The panoramic radiograph showed proper root parallelism with moderate root resorption on the right central incisor. This resorption may be due to root contact with the impacted supernumerary tooth during orthodontic tooth movement, as explained with

the patient before treatment. The cephalometric analysis demonstrated the reduction in upper incisors' proclination (Table 1). Cephalometric superimposed revealed the upright and extrusion of upper incisors and the intrusion and slightly lingual tipping of lower incisors (Figure 7).

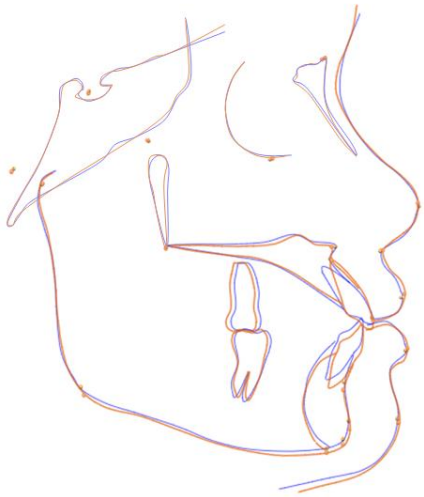

Figure 7: Superimposition of pre- and post-treatment cephalometric tracings

The total active treatment period was 15 months. Following bracket removal, fixed retainers were bonded on the lingual surface of teeth from right first premolars to the left first premolars to keep the alignment in both arches. Besides, removable thermoforming retainers were made for both maxillary and mandibular arch. The patient was instructed to wear the removable retainers only at night. The treatment result remained stable 1 year follow up (Fig 8).

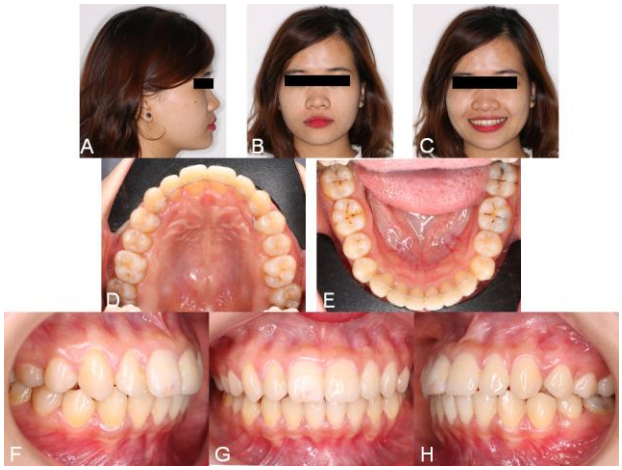

Figure 8: Patients after 1 year of retention; A) Extraoral profile view; B) Extraoral straight view; C) Smile straight view; D) Maxillary occlusal view; E) Mandibular occlusal view; F) Intraoral right lateral view; G) Intraoral straight view; H) Intraoral left the lateral view

The use of lingual brackets to apply lingual crown torque helps to reduce axial proclination and increasing upper incisor showing without neither interproximal reduction nor extraction. The result is a better esthetic improvement for skeletal Class III patients with upper anterior crowding.

Discussion

Since the first introduction of multilingual bracket system by K. Fujita in 1979, there have been many improvements to overcome the disadvantages of lingual orthodontic treatment [2]. Two of them are the transition from mushroom archwire to straight wire concept [2], [3], and the use of multi-slot lingual bracket [4], [5]. The application of straight lingual archwire leads to the elimination of offset bends between canines and premolars, and between premolars and molars so that the technique becomes simpler and the chair time may be reduced. Because of the small inter bracket distance and bracket size, it is hard to engage the archwire into bracket slots fully, so controlling three-dimensional tooth movement in lingual orthodontics become difficult. There is two main slot design in lingual orthodontics: vertical and horizontal slot. The vertical slot is efficient for in-and-out and rotational control and the horizontal slot is efficient for angulation (tip) control [5] (Figure 9). By combining the advantages of two-slot design into one bracket system, the multi-slot lingual brackets allow inserting simultaneously to the archwire so that the traditional complex double overtie method may be eliminated. However, the tooth movement is still well controlled.

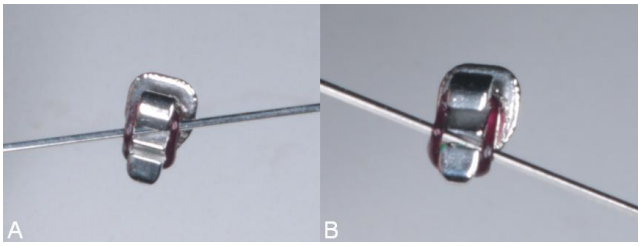

Figure 9: Because it is difficult to engage the archwire into bracket slots fully, the horizontal slots can't control in-out and rotation well A), and the vertical slots find difficultly in controlling tip B)

In this case, report, applying lingual crown torque to upper incisors helped to limit incisor proclination after decrowding, as many Asians prefer uprighted incisors to proclined incisors [9]. In labial orthodontics, some authors advocate using the low-torque bracket for upper anteriors to upright maxillary incisors in non-extraction cases, such as Dr Pitts, he inverted upper incisor brackets to have negative torque value [10]. Another advantage of uprighting upper incisors, in this case, was more upper incisor extrusion to increase incisor show and create a more harmonious smile arc. This effect increases in lingual orthodontic treatment because vertical tooth movement is greater with a lingual bracket than with a

labial bracket when applying torque to bracket slot [11].

Informed Consent

Informed consent was obtained from the patient included in the study

References

1. Fujita K. New orthodontic treatment with lingual bracket mushroom archwire appliance. American Journal of Orthodontics. 1979; 76(6):657-75. https://doi.org/10.1016/0002-9416(79)90211-2

2. Takemoto K, Scuzzo, G. The straight-wire concept in lingual orthodontics. Journal of Clinical Orthodontics. 2001; 35:46-52.

3. Kyung HM, Park HS, Bae SM, Sung JH, Kim IB. The lingual plain-wire system with Micro-Implant Anchorage. Journal of Clinical Orthodontics. 2004; 38:388-95.

4. Hong RK, Lim SM. The Tandem Archwire Technique in Lingual Orthodontics. Journal of Clinical Orthodontics. 2013; 47(4):232-40.

5. Choi YB, Choi SH.Tandem mechanism with multi-slot bracket.Journal of the Japan Lingual Orthodontic Association. 2012; 23:65-73.

6. Geron S. Self-Ligating Brackets in Lingual Orthodontics. Seminars in Orthodontics. 2008; 14(1):64-72. https://doi.org/10.1053/j.sodo.2007.12.007

7. Fillion D. The Lingual Liberty system: Advantages of a digital lingual straight wire system. Seminars in Orthodontics. 2018; 24(3):286-96. https://doi.org/10.1053/j.sodo.2018.08.005

8. Wiechmann D, Rummel V, Thalheim A, Simon J-S, Wiechmann L. Customized brackets and archwires for lingual orthodontic treatment. American Journal of Orthodontics and Dentofacial Orthopedics. 2013; 124(5):593-99. https://doi.org/10.1016/j.ajodo.2003.08.008 PMid:14614428

9. Cao L, Zhang K, Bai D, Jing Y, Tian Y, Guo Y. Effect of maxillary incisor labiolingual inclination and anteroposterior position on smiling profile esthetics. Angle Orthodontist. 2011; 81(1):121-29. https://doi.org/10.2319/033110-181.1 PMid:20936964

10. Pitts TR. Bracket positioning for smile arc protection. Journal of Clinical Orthodontics. 2017; 51(3):142-56.

11. Hong RK. The mushroom archwire technique in Lingual Orthodontic Treatment. ed RK Hong and HM Kyung, Dentos, Daegu, Korea, 2009:95-103.

ID Design Press, Skopje, Republic of Macedonia
Open Access Macedonian Journal of Medical Sciences. 2019 Dec 30; 7(24):4194-4198.
https://doi.org/10.3889/oamjms.2019.355
eISSN: 1857-9655
Basic and Clinical Medical Researches in Vietnam

Closed Reduction and Percutaneous Pinning for Supracondylar Fractures of Humerus in Vietnamese Children

Dung Tran Trung[1, 2], Nam Le Van[2], Vien Nguyen Huu[2], Chinh Dao Nguyen[2], Ha Nguyen Ngoc[1], Vu Thi Nga[3], Toi Chu Dinh[4*]

[1]Hanoi Medical University, Hanoi, Vietnam; [2]Saint Paul hospital, Hanoi, Vietnam; [3]Institute for Research and Development, Duy Tan University, 03 Quang Trung, Danang, Vietnam; [4]Department of Human and Animal Physiology, Faculty of Biology, Hanoi National University of Education, Hanoi, Vietnam

Citation: Tran Trung D, Le Van N, Nguyen Huu V, Dao Nguyen C, Nguyen Ngoc H, Nga VT, Chu Dinh T. Closed Reduction and Percutaneous Pinning for Supracondylar Fractures of Humerus in Vietnamese Children. Open Access Maced J Med Sci. 2019 Dec 30; 7(24):4194-4198. https://doi.org/10.3889/oamjms.2019.355

Keywords: Supracondylar of the humerus fracture; CRPP; Garland classification; Flynn 's criteria

***Correspondence:** Toi Chu Dinh. Department of Human and Animal Physiology, Faculty of Biology, Hanoi National University of Education, Hanoi, Vietnam. E-mail: chudinhtoi@hnue.edu.vn

Received: 10-Sep-2019; **Revised:** 20-Nov-2019; **Accepted:** 21-Nov-2019; **Online first:** 15-Oct-2019

Funding: This research did not receive any financial support

Competing Interests: The authors have declared that no competing interests exist

Abstract

BACKGROUND: Pediatric supracondylar humerus fracture (SHF) is a complicated injury which can result in severe sequela. Nowadays, closed reduction and percutaneous pinning (CRPP) is the most popular treatment.

AIM: This study had two aims (1) checking the result of treating pediatric SHF patients without neurovascular injury by CRPP under image intensifier, and (2) analysing neurovascular complications of CRPP in treating these patients.

METHODS: We conducted a research on 42 patients from February 2018 to March 2019. The age of patients ranged from 3 to 11 years old, with a mean of 5. There was a male predominance with a male / female ratio of 3/1. The average duration of the procedure was 46 minutes, and there was no failed case.

RESULTS: Result evaluation based on Flynn criteria (1974): 85.74 % excellent, 9.5% good, 2.38% fair, and 2.38% poor. There was 1 patient how got ulnar nerve injury complication after medial-lateral crossed pinning, making up 2.38% of all cases. This case was a late admission – 3 days after being injured – and the elbow was badly swollen, so locating the medial condyle for pin placement was very problematic, this the ulnar nerve could be damaged during K-wire pinning. The K-wires are removed after 4 weeks.

CONCLUSION: CRPP under image intensifier in treating pediatric supracondylar humerus fracture is an effective treatment and with good treatment result.

Introduction

SHF account for 60 percent of all elbow fractures in kids with a maximum incidence between 4 and 7 years of age [1]. The fracture typically happens to owe to a falling out of an elbow joint hyperextension of an extended side. These fractures were previously handled with casting or traction in the closed decrease [2]. The method, however, has usually been abandoned due to problems in keeping appropriate alignment and circulation with the limb at the same time, especially with displaced bones (type II and III Gartland). The present technique for treating displaces fractures is closed decrease with percutaneous pin stabilisation, allowing casting in larger elbow extension [3], [4], [5], [6], [7].

Two significant complications connected with this fracture's percutaneous pinning are iatrogenic ulnar nerve injury and decrease loss, cubitus varus / valgus growth or deformity of hyperextension.

There continues a discussion about the ideal pin setup that gives sufficient stability of the fracture to preserve reductions in bondage and to minimise the risk of neurovascular damage. One popular technique of fixation is the cross-pin configuration, where on the pin is placed at the lateral epicondyle and the other at the medial epicondyle. Although this setup has been linked with adequate reproducible stabilisation of the fracture, there is a danger of complications such as ulnar nerve and brachial artery injury when the medial pin is inserted, or periprosthetic infection which will result in the severe sequel. Therefore, the research aimed to assess the outcome of the treatment of patients with pediatric

supracondylar humerus fracture without neurovascular complications of this method on them.

Methods

From February 2018 to March 2019, 42 cases of SHF were performed in our department. Twenty-seven cases were found to be Gartland type III fracture [8] (with a completely displaced extension fracture type). Demographic, examination, radiological data were recorded from medical documents. Also, the patients were called back for history and physical examination in a special follow-up assessment clinic. All final assessments were performed by one of the authors.

During this review, we also noted the delayed time to admission and whether the patient and been treated elsewhere before being admitted to our centre. The timing of the operative procedure, the preoperative neurovascular status of the forearm and the hand, the anaesthetic time, other associated injuries, and the postoperative morbidity were all documented [9].

The instances have been handled by CRPP used image intensifier at the earliest possible time (Figure 1).

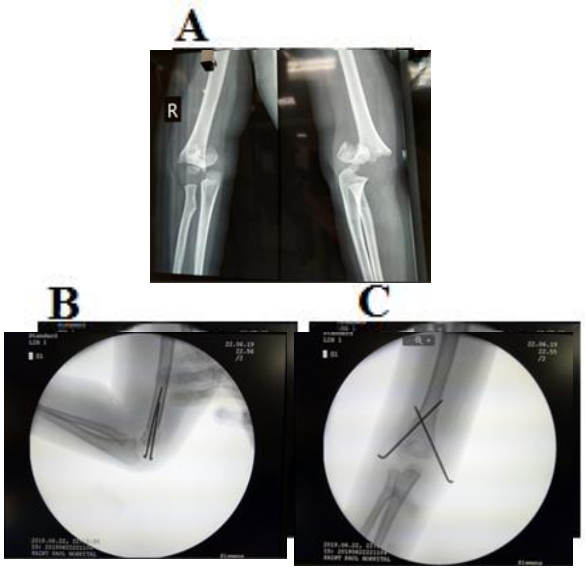

Figure 1: Xray of a 7-year-old boy with supracondylar of the right humerus fracture grade IV (Garland classification); A) Pre-op; B) and C) Post-op Xray of the same patient under image intensifier

Open reduction and pinning were to be performed if the closed reduction and pining failed. For closed pining, a modified technique was performed. A particularly contracted small arm table was used rather than the Bracket inverted in the U form of Flynn, which we found difficult to use with the image intensifier. Using the special armboard, the arm was the table is solved using bandaging, and the patient lay in the seated position with the abducted arm 90°. The arm could be imaged easily in both the AP and lateral views.

During the reduction, the bandage was intended to immobilise the top armed forces, ameliorate them and to allergic, he reduced fracture when the pins were inserted. Our study applied the cross pining technique with one Kirschner wire inserted medially and another laterally the primary benefit of the crossed pin is greater stability, which prevents secondary displacement and malunion [10].

All pins were twisted beyond the skin at the correct angles and protected by a lengthy cast arm. In the outpatient clinic at the end of the 4th week, the cast and the pins were removed without anaesthesia depending on the radiological assessment. Mobilisation exercise was performed under the supervision of a physiotherapist for children > 4 years old until the elbow regained ≈ 85% of the normal range of motion.

Results

Age and Sex Distribution

Among the 42 cases with SHF, the proportion between male and female was 3: 1 (Figure 2). The peak incidence of the fracture in this study was at the age of 6, with a gradual and significant decrease to the age of 10 and after.

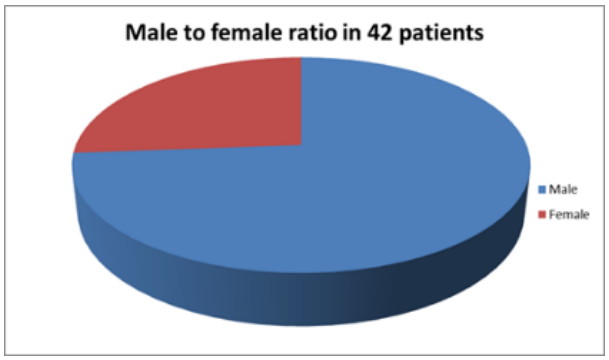

Figure 2: Gender ratio

The peak incidence of the fracture in this study was at the age of 6, with a gradual and significant decrease to the age of 10 and after (Figure 3).

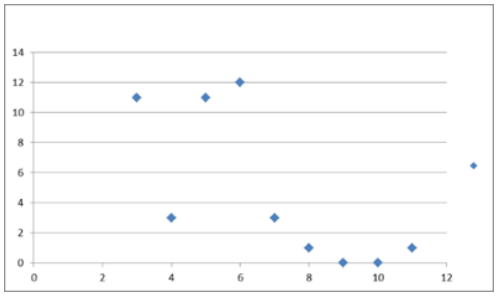

Figure 3: Age distribution of 42 patients

Side of fracture

Twenty-five patients had a fracture of the dominant right side, and 17 involved the nondominant left side (ratio 1: 0,68) (Figure 4).

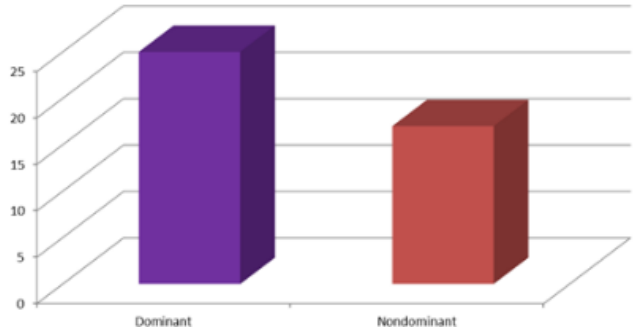

Figure 4: Side of fracture

Time of presentation

Most of the patients submitted on the injury day. However, 16.7% sought hospital treatment after a delay of > 24 h. For those cases that presented late, many had initially sought various forms of traditional medicine treatment (Table 1).

Table 1: Time of presentation

Time of presentation	Patient
< 24h	35 (83.3%)
> 24h	7 (16.7%)

Associated Injuries

Two patients (4.7%) had ipsilateral fractures. They were fractures of the distal radius. At the moment of presentation, there was no case of related neurological injury. 2 people had radial pulse absent at presentation. Still, the clinical assessments were normal so there was no exploration of the radial artery performed, and the pulse fully recovered 12 hours after the operation (Table 2).

Table 2: Associated injuries

Associated injuries	Patient
Distal radius Fx	2
Pulseless radial artery	2
Total	4

Treatment

All the 42 types II or III patients received primary CRPP. Thirty-nine patients were available for a complete detailed assessment with a follow-up period ranging from 2 to 12 months (average 7.3 months) (Table 3).

Table 3: Periods of follow-up

Time follow-up	Patient
2 to 12 months	39
Non-information	3
Total	42

Cross pinning was used in all cases. Smooth Kirschner wire of 1.6 mm diameter was used. There was 1 case got prosthetic osteomyelitis and one iatrogenic ulnar nerve palsy with cross pinning. The one with ulnar nerve palsy fully recovered after 8 months while the one with osteomyelitis had to be re-operated once more and then got elbow stiffness. 5% of patients were operated within 24 hours of receipt and 93% were operated within the first 48 hours. The mean anaesthesia time required for the closed reduction and pinning procedure was 46 min. The length of stay in hospital ranged between 1 and 5 days (mean 2 days).

Final Assessment

Of the 39 cases with CRPP and complete subsection assessment, 3 cases (7.7%) had > 10 degrees of deficit in the elbow movement spectrum.

None had a loss of motion of more than 20°. Two (5.1%) had varus deformity > 10° compared to the normal side. None had varus deformity > 20°. The Flynn criteria were used to assess the results of treatment [11]. Excellent to good results (loss in carrying angle and elbow motion of < 10 degrees) were achieved in 82% (Table 4).

Table 4: Flynn's criteria for the outcome of supracondylar fracture of the humerus in children

Evaluation	The factor of cosmetics: angle of transport (°)	Functional factor loss of movement (°)
Excellent	38	40
0° – 5°	90.5%	95.2%
Good	3	1
6° – 10°	7.1%	2.4%
Fair	0	1
11° – 15°		2.4%
Poor	1	0
> 15°	2.4%	
Total	42	42
	100%	100%

According to parental evaluation, 90% considered their children to have good elbow movement; all of them regarded the function as good, and no patient had any pain at the elbow joint.

We subjected various parameters to statistical analysis for correlation. The only positive correlation was the deviation of carrying angle between the injured and normal side and the difference in Baumann's angles measured on radiographs taken during surgery and on the day of the final assessment, which well correlated (Pearson's reference coefficient of 0.4920 and $p < 0.001$).

Discussion

Displaced SHF in children is difficult to treat. As a result, various modes of treatment had been advocated in the past. Simple plaster immobilisation no longer seems acceptable. The problem that the orthopaedic surgeon has to face in choosing this mode of treatment is obvious. To firmly immobilise the reduced fracture, the elbow must be hyper-flexed, which in turn might predispose to vascular compromise as ischemical contracture of

Volkmann. Skin traction or skeletal traction is generally unaccepted because of the long hospital stay and the difficulties in monitoring the fracture alignment [12].

ORIF requires surgical dissection in an already swollen elbow, which might be hazardous. Also, the open reduction has been associated with a greater residual rigidity in the elbow joint and a substantial varus deformity proportion [13].

Fowles and Kassab [14] and Flynn et al., [11], were known for their pioneering work on CRPP. Our research further supports the fact that a good outcome can be obtained with this method of treatment. It was shown in this study that 95.24% of cases had Excellent to good result using Flynn's original criteria of assessment [11] with 7.3 months of average tracking [15]. None had varus deformity > 20°. Particularly notable was the achievement of the elbow joint movement. Only 7.7% of cases had stiffness > 10%. In comparison with several published series of CRPP, the overall excellent to good results in this series is equal to the average of 90-95% [2], [11], [13], [16].

The overall open reduction rate in our study was 2.38% (1 case). That case was an 11-year-old male patient with a bodyweight of 55 kg and Gartland type III fracture. The muscle tone of the arm was high even under general anaesthesia, therefore, closed reduction failed and we had to shift to open procedure. The cross-pinning method was applied in every case. In 4 cases, one more lateral smooth Kirschner wires were used with satisfactory results. The operating time was also decreased significantly in our study.

We found that the adoption of the modified supine positioning of the patient greatly improved many intraoperative population, reduction, and imaging. The primary goals were achieving good initial reduction and good Kirschner wire placement.

In correlating the results of treatment with various parameters, we found no correlation with age, sex, time of presentation, or side of the fracture. The only important correlation was Baumann angle difference before and instantly after decrease was considerably associated with follow-up angles and axial defect ($p < 0.001$). Thus, it would be reasonable to recommend taking a proper radiograph immediately after reduction, measuring Baumann's angle accurately and comparing the results with the normal side. By fixing the reduced fracture in < 5° of deviation from the normal Baumann's angle, the results could be further improved. This was the advance of procedure performed under the intensified image.

The lack of the pulse was no sign that the artery had been investigated. The clinical assessment of the distal circulation was more important. After effective, fast fracture decrease and fixation, the two instances with no radial pulse had constant healthy distal circulation without residual complications. This is in agreement with the findings of Shaw's series [17].

There was 1 (2.38%) nerve palsies detected post operation which had a complete recovery after 8 months. Like many other investigators, we recommend adopting a more conservative approach to associated nerve palsies. We referred this patient to the rehabilitation department with neurological agents prescribed. Ipsilateral fractures were not uncommon [18], [19].

About 4.7% of our cases had such fractures, mostly of the distal radius. They should be reduced and internally fixed appropriately.

From this series we can conclude that cross percutaneous pinning after meticulously closed reduction under good radiographic imaging and anaesthesia is a reliable and secure method for the treatment of type II, III completely displaces SHF in children.

Ethical approval

This study is approved by Saint Paul hospital. The date is a meticulous, sufficient collection, accurate analysis, scientific, confidence.

Informed consent

The consent and commitment were signed by the patients in the Study.

Reference

1. Farnsworth CL, Silva PD, Mubarak SJ. Etiology of supracondylar humerus fractures. J Pediatr Orthop. 1998; 18(1):38-42. https://doi.org/10.1097/01241398-199801000-00008 PMid:9449099

2. Pirone AM, Graham HK, Krajbich JI. Management of displaced extension-type supracondylar fractures of the humerus in children. The Journal of bone and joint surgery. American volume. 1988; 70(5):641-50. https://doi.org/10.2106/00004623-198870050-00002

3. Vaquero-Picado A, González-Morán G, Moraleda L. Management of supracondylar fractures of the humerus in children. EFORT open rev. 2018; 3(10):526-40. https://doi.org/10.1302/2058-5241.3.170049 PMid:30662761 PMCid:PMC6335593

4. Wingfield JJ, et al. Open reduction techniques for supracondylar humerus fractures in children. JAAOS-Journal of the American Academy of Orthopaedic Surgeons. 2015; 23(12):e72-e80. https://doi.org/10.5435/JAAOS-D-15-00295 PMid:26507292

5. Barton KL, et al. Reliability of a modified Gartland classification of supracondylar humerus fractures. Journal of Pediatric Orthopaedics. 2001; 21(1):27-30. https://doi.org/10.1097/01241398-200101000-00007 PMid:11176349

6. Skaggs DL, et al. How safe is the operative treatment of Gartland type 2 supracondylar humerus fractures in children? Journal of Pediatric Orthopaedics. 2008; 28(2):139-141.

https://doi.org/10.1097/BPO.0b013e3181653ac8 PMid:18388704

7. Skaggs DL, et al. Lateral-entry pin fixation in the management of supracondylar fractures in children. JBJS. 2004; 86(4):702-707. https://doi.org/10.2106/00004623-200404000-00006 PMid:15069133

8. Gartland JJ. Management of supracondylar fractures of the humerus in children. Surg Gynecol Obstet. 1959; 109(2):145-54.

9. Williamson DM, et al. Normal characteristics of the Baumann (humerocapitellar) angle: an aid in assessment of supracondylar fractures. J Pediatr Orthop. 1992; 12(5):636-9. https://doi.org/10.1097/01241398-199209000-00014 PMid:1517426

10. Lee KM, et al. Medial and lateral crossed pinning versus lateral pinning for supracondylar fractures of the humerus in children: decision analysis. J Pediatr Orthop. 2012; 32(2):131-8. https://doi.org/10.1097/BPO.0b013e3182471931 PMid:22327446

11. Flynn JC, Matthews JG, Benoit RL. Blind pinning of displaced supracondylar fractures of the humerus in children. Sixteen years' experience with long-term follow-up. J Bone Joint Surg Am. 1974; 56(2):263-72. https://doi.org/10.2106/00004623-197456020-00004 PMid:4375679

12. Sutton WR, et al. Displaced supracondylar humeral fractures in children. A comparison of results and costs in patients treated by skeletal traction versus percutaneous pinning. Clin Orthop Relat Res. 1992; (278):81-7. https://doi.org/10.1097/00003086-199205000-00013

13. France J, Strong M. Deformity and function in supracondylar fractures of the humerus in children variously treated by closed reduction and splinting, traction, and percutaneous pinning. J Pediatr Orthop. 1992; 12(4):494-8. https://doi.org/10.1097/01241398-199207000-00015 PMid:1613094

14. Fowles JV, Kassab MT. Displaced supracondylar fractures of the elbow in children. A report on the fixation of extension and flexion fractures by two lateral percutaneous pins. J Bone Joint Surg Br. 1974; 56B(3):490-500. https://doi.org/10.1302/0301-620X.56B3.490

15. Pretorius J, Rollinson P, Rasool M. Outcome of displaced supracondylar fractures in children after manipulation and backslab. SA Orthopaedic Journal. 2015; 14(4):35-41. https://doi.org/10.17159/2309-8309/2015/v14n1a4

16. Boyd DW, Aronson DD. Supracondylar fractures of the humerus: a prospective study of percutaneous pinning. Journal of pediatric orthopedics. 1992; 12(6):789-794. https://doi.org/10.1097/01241398-199211000-00017 PMid:1452752

17. Shaw BA, et al., Management of vascular injuries in displaced supracondylar humerus fractures without arteriography. Journal of orthopaedic trauma. 1990; 4(1):25-29. https://doi.org/10.1097/00005131-199003000-00004 PMid:2313426

18. Biyani A, Gupta S, Sharma J. Ipsilateral supracondylar fracture of humerus and forearm bones in children. Injury. 1989; 20(4):203-207. https://doi.org/10.1016/0020-1383(89)90112-5

19. Williamson D, Cole W. Treatment of ipsilateral supracondylar and forearm fractures in children. Injury. 1992; 23(3):159-161. https://doi.org/10.1016/S0020-1383(05)80034-8

ID Design Press, Skopje, Republic of Macedonia
Open Access Macedonian Journal of Medical Sciences. 2019 Dec 30; 7(24):4199-4203.
https://doi.org/10.3889/oamjms.2019.358
eISSN: 1857-9655
Basic and Clinical Medical Researches in Vietnam

Evaluate the Results at Minimum 2-Years of Treating Rotator Cuff Tear by Arthroscopic Surgery

Dung Tran Trung[1, 2, 3*], Duc Nguyen Anh[4], Tuan Tran Duc[5], Van Nguyen Trung[6], Thien Chu Dinh[7]

[1]Saint Paul General Hospital, Hanoi, Vietnam; [2]Hanoi Medical University Hospital, Hanoi, Vietnam; [3]Hanoi Medical University, Hanoi, Vietnam; [4]198 Hospital, Hanoi, Vietnam; [5]Ha Tinh General Hospital, Ha Tinh, Vietnam; [6]Nam Dinh General Hospital, Nam Dinh, Vietnam; [7]Institute for Research and Development, Duy Tan University, 03 Quang Trung, Danang, Vietnam

Citation: Trung DT, Anh DN, Duc TT, Trung VN, Chu Dinh T. Evaluate the Results at Minimum 2-Years of Treating Rotator Cuff Tear by Arthroscopic Surgery. Open Access Maced J Med Sci. 2019 Dec 30; 7(24):4199-4203. https://doi.org/10.3889/oamjms.2019.358

Keywords: Rotator cuff tear; Shoulder arthroscopy; UCLA; Quality of life

***Correspondence:** Tran Trung Dung. Hanoi Medical University, Hanoi, Vietnam; E-mail: dungbacsy@dungbacsy.com

Received: 10-Sep-2019; **Revised:** 20-Nov-2019; **Accepted:** 21-Nov-2019; **Online first:** 15-Oct-2019

Funding: This research did not receive any financial support

Competing Interests: The authors have declared that no competing interests exist

Abstract

BACKGROUND: Rotator cuff tear (RCT) is a common injury of the shoulder, especially middle-aged people. Nonoperative treatment, cortisone injections are only effective at an early stage. Open surgery causes postoperative atrophy of the deltoid muscle, so results are limited. Arthroscopic rotator cuff repair surgery has been performed in Vietnam for about ten years, with many advantages such as the ability to accurately assess the lesions and less invasive procedure. In order to have a clearer view, we performed a mid-term assessment of the effectiveness of this surgery.

AIM: Evaluate results over 2 years of patients with rotator cuff tears treated with arthroscopic surgery and their quality of life.

METHOD: A group of 30 patients were diagnosed with RCT and surgery by arthroscopy to treat at Hanoi Medical University Hospital and Saint Paul Hospital between Jun 2015 and April 2017. The results of the surgeries were assessed by the degree of pain, muscle power, motion of the shoulder joint according to UCLA shoulder score. Evaluate the quality of life through the Rotator Cuff-Quality of Life (RC-QoL) index.

RESULTS: The average age was 60.7 years. Female / male ratio was 1.3. Thirty-six months ± 6.41 was the average follow-up time (min 27 – max 50 months). The shoulder function is recorded according to UCLA has an average score of 30.9, therein good and excellent result were 90 %. The mean RC-QoL index was 91.5%.

CONCLUSION: Treatment of RCT by arthroscopic surgery that has been evaluated for a minimum of 2 years follow-up showed good results and high quality of patient's life.

Introduction

Rotator cuff (RC) is a muscle-tendon group that attaches to the head of the humerus, includes 4 muscles (in order from anterior to posterior) which are the supraspinatus, subscapularis, infraspinatus and teres minor. Rotator cuff tear (RCT) is a common injury of the shoulder [1], especially middle-aged people. The characteristic of a rotator cuff tear injury is that once it is torn, it cannot heal by itself, so if the suture is not performed, the progression of the torn tendon will be more and more widespread so that it cannot be stitched recover again [2]. The final consequence is that the head of the humerus will be migrated superiorly lead to limit shoulder movement and degeneration [3].

Arthroscopic rotator cuff repair surgery has been performed in Vietnam for a decade; it has many advantages such as the ability to accurately assess the lesions and minimally invasive procedure, so it facilitates patients to recover after surgery earlier [4], [5]. Previously, the authors had performed open surgery to treat rotator cuff tear, but it caused postoperative atrophy of the deltoid muscle, so the results were still limited [6]. Nonoperative measures such as rest, physical therapy, NSAIDs [7] or cortisone injections are only effective at an early stage [8]. Thus, with the current surgery trend, the gold standard for RCT treatment is arthroscopic surgery [9].

In Vietnam, there has not been any

assessment focusing on the mid-term outcomes of arthroscopic surgery for the treatment of RCT. Therefore, for a clearer view of the effectiveness of this surgery in Vietnam, we chose the time to assess the outcomes is at least 2 years after surgery, especially considering the quality of patient's life.

Materials and Method

Research method

A retrospective descriptive study.

Inclusion criteria

Thirty patients were diagnosed with RCT from partial-thickness tear grade 3 (Ellman's classification) to large tear (De Orio and Cofiled classification) and surgery by arthroscopy to treat at Hanoi Medical University Hospital and Saint Paul Hospital between Jun 2015 and April 2017.

Patients with complete records of research content and re-examination after at minimum 2-years of surgery.

Exclusion criteria

Massive and irreparable RCTs. **RCTs** *but no tendon suture indication, just* debridement of the lesion, acromioplasty. Patients lost follow-up and did not re-examination after at minimum 2-years of surgery.

Operative technique

We placed the patient in the "Beach Chair" position. Probing the shoulder joint through a posterior portal, the corresponding point between the infraspinatus and teres minor. Then we opened the lateral portal to view into subacromial space and anterior-lateral portal for working. Performed debride of the lesion, acromioplasty (especially at one – third anterior-lateral position of acromion), identify rotator cuff tear.

Refreshing the tendons tear, release and mobilise the tendons, prepare footprint. RCTs were repaired by single-row suture anchor technique.

Place a hemovac drain into the shoulder joint, after that patient was worn the sling with a small pillow to abductor 20 degrees of their shoulder and keep it up to 4 weeks. All patients after surgery are rehabilitated at the same facility with a team of experts agreed on the viewpoint and practice method.

Evaluation

Patients were invited to re-examination, then they *were assessed according to the UCLA score and* RC-QoL index [10].

Statistic

Data were processed by SPSS 20.0 software. Comparing the average values of the groups, we used the Student's t-test. *A significant difference was defined as* $p < 0.05$.

Result

The mean age of 30 patients in the study group was 60.7 years old (36-79). In which, the age group over 65 accounts for the highest rate, 46.66%. Female: male ratio is 1.3:1. The average follow-up time is 36 months ± 6.41 months (min 27 – max 50 months). Tearing partial-thickness RC tendon is 4 cases, accounted for 13.33%. Tearing full-thickness RC tendon is 26 cases (86.66%), among all sizes of total tear, medium-sized tears prevail 11 / 26 or 42%.

All of the patients had subacromial impingement syndrome, and they all proceed an acromioplasty***,*** the tendon tears were repaired by single-row suture anchor technique (Figure 1). No patients with trauma to the shoulder had surgery lead to re-tear.

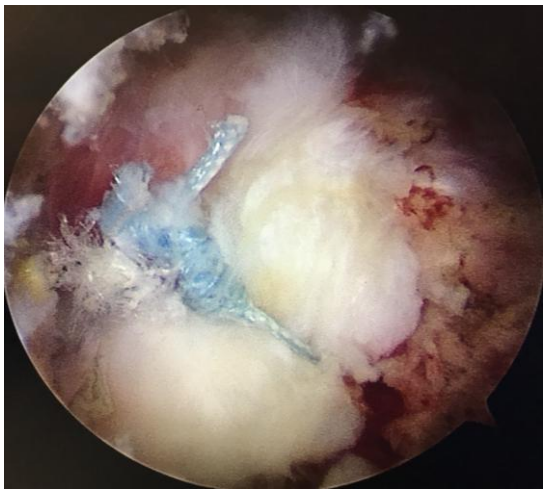

Figure 1: Single-row technique

The mean UCLA score is 30.9 (range 23-35), therein good and excellent result is 90 %. Particularly for pain assessment, the rate of painless patients was 86.66%; the remaining 13.33% were occasional and slight pain. The rate of patients satisfied with the current situation is 29 / 30 patients (96.66%).

The mean RC-QoL index at the final of the study was 91.5% ± 5.6 (78.33 – 99.1%). The rate of

patients returning to previous work is 100%.

Comparing the correlation of UCLA and RC-QoL average score with the characteristics of study subjects such as gender, age, trauma factor or between sizes of complete tear were the surgical results did not depend on the above factors. The p-value in these tests was all > 0.05. Details are recorded according to Table 1.

Table 1: Correlation of UCLA and RC-QoL average score with the characteristics of study subjects

Characteristics	Patients (n)	UCLA score	P (UCLA)	RC – QoL index	P (RC – QoL)
Gender					
Male	13	30.69 ± 3.83		91.62 ± 5.46	
Female	17	31.06 ± 2.83	0.76	91.45 ± 5.87	0.93
Age					
< 55	8	31.88 ± 3.64		92.07 ± 7.23	
55 – 65	8	31.13 ± 3.37	0.518	92.41 ± 4.80	0.762
≥ 65	14	30.21 ± 3.04		90.70 ± 5.30	
Trauma factor					
Yes	12	30.42 ± 3.96		91.33 ± 5.30	
No	18	31.22 ± 2.75	0.51	91.65 ± 5.94	0.879
Sizes of total tear					
Small	6	31.0 ± 4.33		92.29 ± 6.04	
Medium	11	31.36 ± 2.58	0.17	92.23 ± 4.2	0.86
Large	9	28.78 ± 3.17		87.37 ± 5.46	

However, the correlation of both UCLA and RC-QoL mean between the partial-tear group and the total-tear group found a statistically significant difference. The p-value of the two tests was all > 0.05 (table2). In other words, the type of tear is the impact factor on the outcome of shoulder function after surgery. This means that the quality of a patient's life with partial-thickness tear has significantly better postoperative results than the group with a full-thickness tear.

Table 2: Correlation of UCLA and RC-QoL average score with the type of tear

Characteristics	Patients (n)	UCLA score	P (UCLA)	RC – QoL index	P (RC – QoL)
Type of tear					
Partial-thickness	4	34.25 ± 0.95		97.75 ± 0.83	
Full-thickness	26	30.38 ± 3.17	0.024	90.56 ± 5.40	0.00

At the last re-examination, none of the patients had delta muscle atrophy, no patients had numbness of the shoulder injury, no cases of shoulder stiffness, but there was a common point in patients with large tear is limited hand movements behind the back.

Discussion

The mean age in this study was 60.7 years, with most of the participants were in the over 65 groups. This observation was in line with the etiologies in which the intrinsic causes are the tendon degeneration due to reduced vascularisation, thinning of the collagen fibres while the extrinsic causes are subacromial impingement syndrome and microtrauma [3]. Besides, 17 patients had rotator cuff tear without the history of trauma; they suffered from progressive shoulder pain in many years. Only 13 patients had a traumatic factor, but some of them are even minor trauma. As a result, trauma is a positive factor which helps deteriorate the existing rotator cuff degeneration or tear. Therefore, age is a bad prognosis factor to heal of RC tendon. This idea is also supported by several authors [11], [12]. However, this is not the only factor involves the outcome of shoulder joint function because, when comparing the scores of UCLA and RC-QoL between the under 55 group, 55 to 65 group and over 65 groups, there was no statistical significance. The mean satisfaction reached 96.66% because the elderly subjects only need the shoulder joint to perform basic daily activities. Additionally, the traumatic factor does not influence the final result of the surgery.

The average UCLA score for the whole group is 30.9, which belongs to the group with good results; this result is similar to some domestic studies [13]. When compared with the results of other international authors such as Marrero [14] who showed the average UCLA score of 31.8 (33 patients, regardless of tear size) or Castagna [15] with the score of 30.8 (29 patients, with minimum 24 months follow-up), one thing must be pointed out that the above results were the scores of the affected shoulder joint. However, when examining the unaffected shoulder joint with both scales, the maximum score could not be reached. The reason is the rotator cuff of the unaffected shoulder is also degenerative and starts to hurt. Many patients even complained that the unaffected shoulder is more painful than the operated shoulder. The pain reduction or pain elimination is the main factor determining the quality of life of the patient (this assertion is also postulated by many authors, typically Arrigoni [16]), which is consistent with the average RC-QoL score in this study of 91.5%. Some patients have forgotten which side has been operated until being called for follow-up.

The mean score of both UCLA and RC-QoL between the partial-thickness tear group and the full-thickness tear group found a statistically significant difference. Thus, the type of tear is the prognostic factor affecting the outcome of shoulder joint function. Some studies by Park [17] or Marrero [14] do not support this view, saying that the results of these two groups were equal. Perhaps, there is no randomisation in term of quantity, age and gender in these 2 groups in our study. More studies with larger sample sizes are needed to assess this judgment accurately. However, in the total tear type, all authors agreed that the grade 2 rotator cuff is the most common. Haviv [18] conducted a study on 607 patients and found that small and medium tear accounted for 69%; this proportion in our study was 65.38% (17/26). This study has the limitation that does not evaluate the time before surgery, the early results after surgery but focusing on assessing at least the minimum 2 years, so it is not possible to compare the level of improvement before and after the

surgery, or whether good results are maintained up to mid-term.

We used the Beach-chair position to surgery for all patients in our research. This position has the advantage of not needing to use a commercially available arm supporter like a lateral decubitus position, and importantly it objectively assesses the extent of *subacromial impingement* and easily identifies whether *the* subacromial space after acromioplasty has been suitable. We selected a single-row suturing method for all groups of patients in this study with the reason that although there have been a lot of investigations arguing about different suturing techniques, in the long-term study of Spennacchio [19], no difference in clinical results between single-row suture anchor technique and double-row. Also, a systematic review [20] concluded that there was no statistically significant difference in the shoulder joint function different suturing techniques. Moreover, this option is suitable for the financial conditions of many patients in Vietnam and still delivers acceptable outcomes.

Following the analysis results of this research, we recommend that if the patient has been diagnosed with rotator cuff tear (even if they are older patient) and nonoperative measures do not improve; it does not need to wait for sufficient time, number of treatment sessions that should proactively conduct surgery early (when still in the partial-tear grade) to solve the current symptoms, causes, reduce and overcome the consequences of rotator cuff tear injury.

In conclusion, through research 30 patients who have undergone arthroscopic repair of RCTs, can be determined that in addition to the advantages such as small incision the advantages of small incision, minimally invasive, accurately assess the lesions, after over 2 years (the average evaluation time was 36 months) arthroscopic surgery to repair RC tendon give good results of shoulder function and high quality of patient life. Patients satisfaction reached 96.66%.

Ethical Approval

The medical ethics committee of Hanoi Medical University agreed to approve this study in Decision No. 4235.

Informed consent

The consent and commitment were signed by the patients in this research.

References

1. White J, et al. An epidemiological study of rotator cuff pathology using The Health Improvement Network database. The bone & joint journal. 2014; 96(3):350-353. https://doi.org/10.1302/0301-620X.96B3.32336 PMid:24589790

2. Nho SJ, et al. Rotator cuff degeneration: etiology and pathogenesis. The American journal of sports medicine. 2008; 36(5):987-993. https://doi.org/10.1177/0363546508317344 PMid:18413681

3. Angelo RL, Esch J, Ryu RK. AANA Advanced Arthroscopy: The Shoulder E-Book: Expert Consult: Online, Print and DVD. Elsevier Health Sciences; 2010.

4. Gartsman GM, Khan M, Hammerman SM. Arthroscopic repair of full-thickness tears of the rotator cuff. JBJS. 1998; 80(6):832-40. https://doi.org/10.2106/00004623-199806000-00007 PMid:9655101

5. Miyazaki AN, et al. Avaliação dos resultados das reoperações de pacientes com lesões do manguito rotador. Rev Bras Ortop. 2011; 46(1):45-50. https://doi.org/10.1590/S0102-36162011000100009 PMid:27026985

6. Hata Y, et al. Atrophy of the deltoid muscle following rotator cuff surgery. JBJS. 2004; 86(7):1414-1419. https://doi.org/10.2106/00004623-200407000-00008 PMid:15252087

7. Mantone JK, Burkhead Jr WZ, Noonan Jr J. Nonoperative treatment of rotator cuff tears. Orthopedic Clinics of North America. 2000; 31(2):295-311. https://doi.org/10.1016/S0030-5898(05)70149-8

8. CHARLES S NEER II. Anterior acromioplasty for the chronic impingement syndrome in the shoulder: a preliminary report. JBJS. 1972; 54(1):41-50. https://doi.org/10.2106/00004623-197254010-00003

9. Duquin TR, Buyea C, Bisson LJ. Which method of rotator cuff repair leads to the highest rate of structural healing? A systematic review. Am J Sports Med. 2010; 38(4):835-41. https://doi.org/10.1177/0363546509359679 PMid:20357403

10. Hollinshead RM, et al. Two 6-year follow-up studies of large and massive rotator cuff tears: comparison of outcome measures. J Shoulder Elbow Surg. 2000; 9(5):373-81. https://doi.org/10.1067/mse.2000.108389 PMid:11075319

11. Dung TT. Corticoid injection for subacromial impingement syndrome treatment. J Practical Medicine. 2014; 1:32-34.

12. Chung SW, et al. Quality of life after arthroscopic rotator cuff repair: evaluation using SF-36 and an analysis of affecting clinical factors. The American journal of sports medicine. 2012; 40(3):631-639. https://doi.org/10.1177/0363546511430309 PMid:22190415

13. Anh THN. Result of arthroscopic rotator cuff repair. Ho Chi Minh City Medicine and Pharmacy University: Ho Chi Minh City, 2014.

14. Marrero LG, Nelman KR, Nottage WM. Long-term follow-up of arthroscopic rotator cuff repair. Arthroscopy. 2011; 27(7):885-8. https://doi.org/10.1016/j.arthro.2011.02.019 PMid:21620635

15. Castagna A, et al. Arthroscopic repair of rotator cuff tear with a modified Mason-Allen stitch: mid-term clinical and ultrasound outcomes. Knee Surg Sports Traumatol Arthrosc. 2008; 16(5):497-503. https://doi.org/10.1007/s00167-007-0461-2 PMid:18273602

16. Arrigoni P, et al. Functional repair in massive immobile rotator cuff tears leads to satisfactory quality of living: results at 3-year follow-up. Musculoskelet Surg. 2013; 97(1):73-7. https://doi.org/10.1007/s12306-013-0252-5 PMid:23588825

17. Park JY, Chung KT, Yoo MJ. A serial comparison of arthroscopic repairs for partial-and full-thickness rotator cuff tears. Arthroscopy: The Journal of Arthroscopic & Related Surgery. 2004; 20(7):705-711. https://doi.org/10.1016/S0749-8063(04)00598-5

18. Haviv B, et al. Arthroscopic rotator cuff repair: clinical outcome

of 607 patients. Knee Surg Sports Traumatol Arthrosc. 2010; 18(12):1707-11. https://doi.org/10.1007/s00167-010-1091-7 PMid:20217391

19. Spennacchio P, et al. Long-term outcome after arthroscopic rotator cuff treatment. Knee Surg Sports Traumatol Arthrosc. 2015; 23(2):523-9. https://doi.org/10.1007/s00167-014-3234-8 PMid:25145945

20. Saridakis P, Jones G. Outcomes of single-row and double-row arthroscopic rotator cuff repair: a systematic review. J Bone Joint Surg Am. 2010; 92(3):732-42. https://doi.org/10.2106/JBJS.I.01295 PMid:20194334

ID Design Press, Skopje, Republic of Macedonia
Open Access Macedonian Journal of Medical Sciences. 2019 Dec 30; 7(24):4204-4208.
https://doi.org/10.3889/oamjms.2019.361
eISSN: 1857-9655
Basic and Clinical Medical Researches in Vietnam

Anatomical Characteristics and Variants of Prostatic Artery in Patients of Benign Hyperplasia Prostate by Digital Subtraction Angiography

Hien Nguyen Xuan[1], Hoang Do Huy[1], Ngoc Nguyen Thi Bich[1*], Giang Phan Hoang[1], Khanh Le Van[1], Trinh Nguyen Duy[1], Tuan Anh Tran[1], Vu Thi Nga[2], Le Bui Minh[3]

[1]Bach Mai Radiology Center, Bach Mai Hospital, Hanoi Vietnam; [2]Institute for Research and Development, Duy Tan University, Danang, Vietnam; [3]NTT Hi-tech Institute, Nguyen Tat Thanh University, 300A Nguyen Tat Thanh St., Ward 13, District 4, Ho Chi Minh City, Vietnam

Citation: Nguyen Xuan H, Do Huy H, Nguyen Thi Bich N, Phan Hoang G, Le Van K, Nguyen Duy T, Anh Tran T, Thi Nga V, Bui Minh L. Anatomical Characteristics and Variants of Prostatic Artery in Patients of Benign Hyperplasia Prostate by Digital Subtraction Angiography. Open Access Maced J Med Sci. 2019 Dec 30; 7(24):4204-4208.
https://doi.org/10.3889/oamjms.2019.361

Keywords: Prostatic artery; DSA; F. Carnevalle classification

***Correspondence:** Hien Nguyen Xuan Bach. Mai Radiology Center, Bach Mai Hospital, Hanoi Vietnam, email: ngochienduylocbm@gmail.com

Received: 12-Apr-2019; **Revised:** 13-Jul-2019; **Accepted:** 14-Jul-2019; **Online first:** 13-Jul-2019

Funding: This research did not receive any financial support

Competing Interests: The authors have declared that no competing interests exist

List of abbreviations: BPH: benign prostatic hyperplasia, CBCT: cone-beam computed tomography software, DSA: digital subtraction angiography, IIA: internal iliac artery, LUTS: lower urinary tract symptoms, PAE: prostatic artery embolisation, PA: prostatic artery, SVA: superior vesical artery

Abstract

AIM: This work is aimed to describe anatomical features and variants of the prostatic artery (PA) using digital subtraction angiography (DSA).

METHODS: This is a descriptive statistic study. We reviewed the DSA of 348 patients, who had a PA embolisation to reduce the benign prostatic hyperplasia (BPH) symptoms at Radiology Department of Bach Mai Hospital from Oct – 2014 to Oct – 2018.

RESULTS: PA was found at 660 pelvic halves, of which 30 pelvic halves (4.5%) had two PAs, 630 pelvic halves had one PA. In terms of the origin of PA, in total 690 PAs, the percentage of type 1, 2, 3, 4 and 5 was successively 33.9%, 13.9%, 18.3%, 23.9% and 10.4%, respectively. Atherosclerosis of PA observed in 20.9%. The 'corkscrew' pattern was found in 30.4%. The average diameter of PA was 1.5 ± 0.34mm. The anastomosis of PA with surrounding arteries was common. PA may supply rectum (6.1%), seminal vesical (9.6%), bladder (5.2%), contralateral prostatic parenchyma (13.0%), surrounding soft-tissues (3.5%).

CONCLUSION: The common trunk with SVA superior vesical artery was the most common origin of PA. Anastomoses of PA with surrounding tissues were complex.

Introduction

Benign prostatic hyperplasia (BPH) is a common disease in older men; it can cause lower urinary tract symptoms (LUTS). Prostatic artery embolisation (PAE) for BPH is a new mini-invasive treatment in Vietnam as well as in the world. It has demonstrated the therapeutic effect and safety in improving the symptoms of LUTS, reducing the prostatic volume [1], [2], [3], [4]. The key to the success of this method is to understand the anatomy of the prostatic artery. However, the anatomy of PA is very variable in number and the position of origin. In male cadaveric studies, many researchers agreed that the origin of PA is very diverse and inconstant. Some authors also revealed cases of 2 or even 3 PAs in the same pelvic side [5-7]. Recent studies on the anatomy of PA on DSA had similar results. A single PA in each pelvic side was found in the majority of cases, a double vascularisation was rare [8], [9], [10]. The most common origin of PA is the branches of the anterior division of internal iliac artery (IIA) like an internal pudendal artery, common trunk with the superior vesical artery (SVA), obturator artery. The proportion of PA originating from the middle rectal artery, the accessory obturator artery, the gluteal artery, the accessory pudendal artery is rare. Carnevale was the first author to classify prostatic arteries by origin of

PA, which is relatively easy to apply [8]. According to this classification, the prostatic arteries divide into 5 different groups (Table 1).

Table 1: Classification of PA by FC Carnevale et al., [8]

Type	1	2	3	4	5
Origin of PA	Common trunk with SVA	The anterior division of IIA, inferior to SVA	Obturator artery	Internal pudendal artery	Less common origins

Also, PA has complex anastomosis with surrounding organs such as penis, rectum, seminal vesicle, and bladder [11]. Therefore, the risk of necrosis of surrounding organs during PAE is not negligible. Several researchers revealed the role of CBCT software in the PAE procedure [9], [12]. Currently, in Vietnam, Bach Mai hospital is the first place to apply this technique to treat BPH. However, to our knowledge, no study in Vietnam has been conducted to evaluate the anatomy of PA on the DSA. Therefore, the *purpose* of the present *study* is to (1) classify the prostatic arteries in Vietnamese by origin according to the classification of FC. Carnevale et al., and (2) describe other anatomical features of the prostatic artery, including anastomoses to adjacent arteries, number, shape, and diameter.

Material and Methods

Patient selection

This retrospective study was approved by the Department of Radiology, Bach Mai Hospital between 10/2014 and 10/2018.

Inclusion criteria

1. Moderate to severe symptoms: IPSS index > 19 and the quality of life (QoL) > 3.

2. PSA index ≤ 4 ng/ml or PSA ≤ 10 ng/ml (the ratio free PSA/total PSA ≥ 0.20, PSA density < 0.15).

3. No response to 6-month medical treatment.

4. The patient does not want surgery, accepting complications that may occur during the intervention.

5. Complete medical records

6. Successfully unilateral or bilateral PA catheterisation.

Exclusion criteria

1. Prostatic cancer.

2. Urethral stenosis, narrowing of the bladder neck, large diverticula, and large stones.

3. General contraindications of angiography: serious infection, and liver failure, severe renal failure etc.

4. Active urinary infection.

5. Do not have enough medical records.

Imaging modalities

We used Philips single-plane fluoroscopy (AluraHD) with Road-mapping and Cone-beam computed tomography software (CBCT). In this study, we only applied CBCT software in the following cases: suspect anastomosis of PA with surrounding organs, suspect whether or not the investigated artery supplies the prostate.

Technical process

1. Put a bladder catheter with contrast product into a Foley balloon before performing the vascular procedure.

2. Angiogram of the internal iliac artery was performed with the ipsilateral oblique projection of 35-45 degrees and caudal-cranial angulation of 10 degrees.

3. Selective DSA of PA was used to measure the diameter of PA.

4. Injection of 1ml nitroglycerin 10% into PA was employed to evaluate better the anastomosis of PA.

5. Angiogram of PA was repeated to evaluate the anastomosis of PA.

6. In cases of suspected anastomosis of PA with surrounding organs, uncertain whether or not the investigated artery supplies the prostate, a CBCT was performed.

Statistical analysis

All data are statistically processed and computerised under the SPSS program (version 16.0). Descriptive statistics with variables on anatomical characteristics of the prostate artery.

Results

In the study period, 348 PAE procedures performed at Department of Radiology, Bach Mai hospital were included, the mean age of patients was 69.6 years, mean Qmax was 6.8 ml/s, and mean prostatic volume was 61.6 gram. In 348 these patients, 21 patients had an only unilateral selection of

prostatic artery due to occlusive atherosclerosis. Other 327 patients were treated with bilateral PAE. A total of 675 pelvic sides were studied.

In 675 pelvic sides, double vascularisation was found in 15 cases, a single PA in 660 pelvic sides. So, the number of PA in our study was 690, with the average diameter of PA was 1.5 ± 0.35 mm (from 0.7 to 2.6 mm).

The most common origin of PA was the trunk with the SVA (33.9%), followed by internal pudendal artery (23.5%), and obturator artery (18.3%). The proportion of PA originating from the anterior division of IIA and other positions was 10.4% and 13.9%, respectively (Table 2).

Table 2: Classification of PA

Type	1	2	3	4	5	Total
N	234	72	126	162	96	690
Incidence (%)	33.9	10.4	18.3	23.5	13.9	100

An identifying feature of PA on DSA is the corkscrew pattern. However, in this study, the typical feature of PA was found in only 30.4% (Table 3).

Table 3: Incidence of "corkscrew pattern" of PA

Shape	Presence of the corkscrew pattern	Absence of the corkscrew pattern	Total
N	210	480	690
%	30.4	69.6	100

Atherosclerosis of PA can also be observed by DSA. Atherosclerosis is defined as a defect of contrast in the artery. In our study, atherosclerosis was seen in 20.9% of cases (Table 4).

Table 4: Incidence of the atherosclerosis of PA

Atherosclerosis	Presence	Absence	Total
N	144	546	690
%	20.9	79.1	100

The most common anastomosis was seen with the opposite PA (13%). The remaining types of anastomosis had lower rates like with seminal vesicle (9.6%), penis (8.7%), rectum (6.1%), bladder (4.3%), and soft tissue (3.5%) (Table 5).

Table 5: Anastomosis between PA and surrounding arteries

Anastomosis	Bladder	Seminal vesicle	Penis	Rectum	Soft tissue	Contralateral prostate tissue I.
N	30	66	60	42	24	90
%	4.3	9.6	8.7	6.1	3.5	13

Discussion

Regarding the origin of prostatic arteries, based on the classification of FC. Carnevale, in this study, the most popular origin of the PA was the common trunk with SVA (33.9%), followed by internal pudendal artery (23.5%). This result is similar to the study of FC. Carnevale and T. Bilhimet al., [8], [10]. According to a study by Wang et al., the most common origin of PA was also common trunk with SVA (37.1%) but followed by the anterior pelvic artery branch (31.1%), then the internal pudendal artery (24.2%) [9].

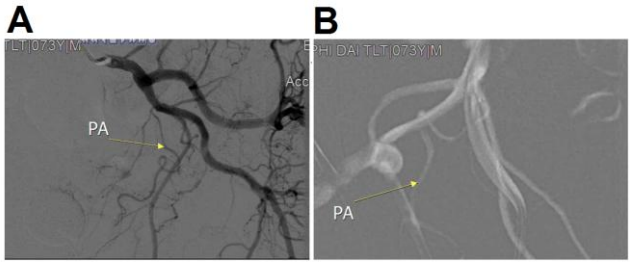

Figure 1: Prostatic arterial type 1 (A) and type 2 (B)

The less common origins of the PA were the middle rectal artery, the accessory obturator artery, the gluteal artery, and the accessory pudendal artery. However, in this study, the incidence of these PA types was relatively high (13.9%). There were 2 cases in which PA was originated from the accessory obturator artery-a branch of the external iliac artery (1.7%). According to T. Bilhim et al., the ratio of PA originated from the external iliac artery was 1.8% [13]. Thus, in the case of absence of PA on internal iliac artery angiogram, catheterisation of the external iliac artery is necessary to find PA from the accessory obturator artery.

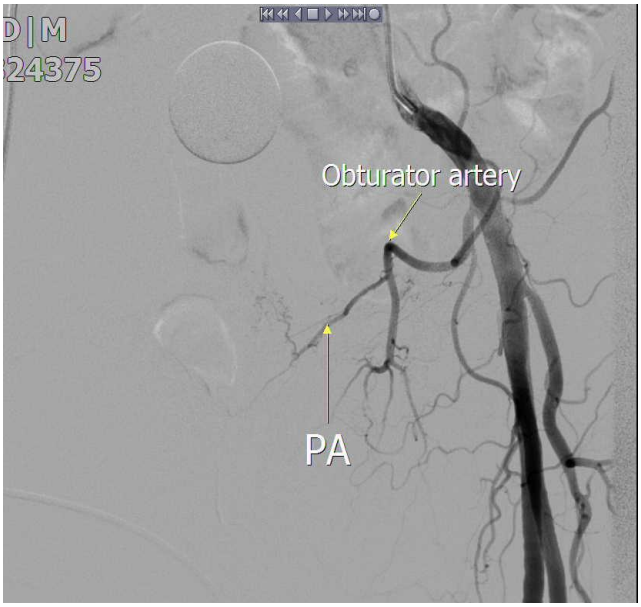

Figure 2: PA type 5, originating from the accessory obturator artery

Regarding the number of independent PA, there was one PA in 95.5% of pelvic sides and two independent PAs in the other 4.5%, for a total of 115 PA. This result was similar to the study done by Wang and FC Carnevale et al., [8], [9]. However, according to T. Bilhim, the incidence of two independent ipsilateral PA was very high (43%) [10]. Mean

diameter of PA was 1.5 mm. Therefore, the types of micro-catheters used must also be small in size. We always used microcatheter types with diameter ≤ 2F (equivalent to 0.67 mm).

The presence of the corkscrew pattern was found in 30.4%. It is unlike the uterine artery, which always has the corkscrew pattern on DSA imaging. This result was similar to the study of T. Bilhim [10]. Although less common, however, the presence of the corkscrew pattern can be considered as a suggestion of PA on DSA. Another difficulty in the embolisation of PA is atherosclerosis. Atherosclerosis was found in 20.9% of PA, most commonly in the proximal course of PA.

About anastomoses of PA, we saw them in 21% of cases. This result was similar to the study of Wang (22.6%). However, that rate was lower than those in studies done by T. Bilhim and JM. Pisco et al., (60%) [9], [10], [11].

In our study, the most common anastomosis was with contralateral PA (13%), followed by the penis (8.7%), bladder (4.3%), rectum (6.1%), seminal vesicle (9.6%), and soft tissue (3.5%). However, the presence of anastomosis of PA is not a contraindication to the embolisation. In the presence of small-sized anastomosis, a slow infusion under the control of fluoroscopy and usage of big embolisation particles (> 200 um) may avoid the complication of non-target ischemia to the surrounding tissues (bladder, rectum, anus, or corpus cavernosum).

In cases with significant of PA anastomosis, before injecting particles for embolisation, maybe we need to cut off anastomosis by coils or other materials.

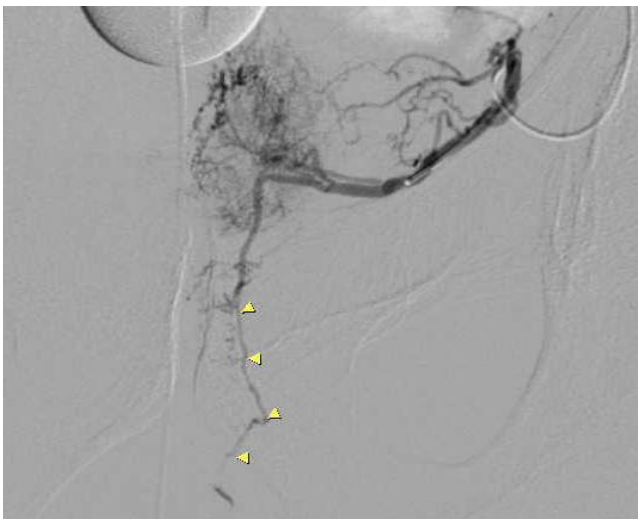

Figure 3: Anastomosis of PA with penis in AP views (arrowhead)

This study still has limitations. First, we acknowledge the retrospective nature of our patient group from a single centre. Second, we do not systematically use CBCT software to evaluate the anastomosis of PA, due to the risk of increasing the irradiation dose and increasing the procedure times. This may affect the assessment of anastomosis of PA.

In conclusion, we found that the most popular origin of PA was the common trunk with SVA, followed by the interne pudendal artery and obturator artery. The anastomosis of PA was very diverse; it is possible to supply blood to bladder, rectum, seminal vesicles, and contralateral prostatic tissue. Therefore, perfect knowledge of PA is fundamental to assure the success of the procedure, avoid complications, and reduce procedure times and radiation exposure.

Ethical Statement

This research was approved by the scientific ethics committee of Bach Mai hospital and allowed to be implemented at the Department of Radiology of Bach Mai hospital.

Informed Consent

The patients were consulted and agreed to participate in the study. Informed consent was obtained from the patient included in the study.

Acknowledgement

We would like to thank Ms Bui Nhat Le (Faculty of Clinical Pharmacy, University of Pharmacy, Hanoi, Vietnam) for checking and improving the English in the manuscript.

References

1. Christidis DCE, Ly V, et al. Prostatic artery embolization for benign prostatic obstruction: assessment of safety and efficacy. World J Urol. 2018; 36: 575-584. https://doi.org/10.1007/s00345-018-2220-z PMid:29445846

2. DeMeritt JS, Elmasri FF, Esposito MP, Rosenberg GS. Relief of benign prostatic hyperplasia-related bladder outlet obstruction after transarterial polyvinyl alcohol prostate embolization. Journal of Vascular and Interventional Radiology. 2000; 11(6):767-70. https://doi.org/10.1016/S1051-0443(07)61638-8

3. Ray AF, Powell J, Speakman MJ, Longford NT, DasGupta R, Bryant T, Modi S, Dyer J, Harris M, Carolan-Rees G, Hacking N. Efficacy and safety of prostate artery embolization for benign prostatic hyperplasia: an observational study and propensity-matched comparison with transurethral resection of the

prostate (the UK-ROPE study). BJU international. 2018; 122(2):270-82. https://doi.org/10.1111/bju.14249 PMid:29645352

4. Bagla S, Smirniotopoulos J, Orlando J, van Breda A. Safety and Efficacy of Prostate Artery Embolization in Small-Volume Benign Prostatic Hyperplasia. Journal of Vascular and Interventional Radiology. 2015; 26(1):148-9. https://doi.org/10.1016/j.jvir.2014.10.032

5. Ambrósio JD, De Almeida JS, De Souza A. Origin of prostatic arteries in man. Rev Paul Med. 1980; 96(3-4):52.

6. Bouissou H, Talazac A. Arterial vascularization of the normal and the pathological prostate. InAnnales d'anatomie pathologique. 1959; 4(1):63-79.

7. Garcia-Monaco R, Garategui L, Kizilevsky N, Peralta O, Rodriguez P, Palacios-Jaraquemada J. Human cadaveric specimen study of the prostatic arterial anatomy: implications for arterial embolization. Journal of Vascular and Interventional Radiology. 2014; 25(2):315-22. https://doi.org/10.1016/j.jvir.2013.10.026 PMid:24325930

8. de Assis AM, Moreira AM, de Paula Rodrigues VC, Harward SH, Antunes AA, Srougi M, Carnevale FC. Pelvic arterial anatomy relevant to prostatic artery embolisation and proposal for angiographic classification. Cardiovascular and interventional radiology. 2015; 38(4):855-61. https://doi.org/10.1007/s00270-015-1114-3 PMid:25962991

9. Wang MQ, Duan F, Yuan K, Zhang GD, Yan J, Wang Y. Benign prostatic hyperplasia: cone-beam CT in conjunction with DSA for identifying prostatic arterial anatomy. Radiology. 2017:282. https://doi.org/10.1148/radiol.2016152415 PMid:27467466

10. Bilhim T, Pisco JM, Tinto HR, Fernandes L, Pinheiro LC, Furtado A, Casal D, Duarte M, Pereira J, Oliveira AG, O'Neill JE. Prostatic arterial supply: anatomic and imaging findings relevant for selective arterial embolization. Journal of Vascular and Interventional Radiology. 2012; 23(11):1403-15. https://doi.org/10.1016/j.jvir.2012.07.028 PMid:23101913

11. Bilhim T, Tinto HR, Fernandes L, Pisco JM. Radiological anatomy of prostatic arteries. Techniques in vascular and interventional radiology. 2012; 15(4):276-85. https://doi.org/10.1053/j.tvir.2012.09.006 PMid:23244724

12. Bagla S, Rholl KS, Sterling KM, van Breda A, Papadouris D, Cooper JM, van Breda A. Utility of cone-beam CT imaging in prostatic artery embolization. Journal of Vascular and Interventional Radiology. 2013; 24(11):1603-7. https://doi.org/10.1016/j.jvir.2013.06.024 PMid:23978461

13. Bilhim T, Pisco J, Pinheiro LC, Tinto HR, Fernandes L, Pereira JA. The role of accessory obturator arteries in prostatic arterial embolization. Journal of Vascular and Interventional Radiology. 2014; 25(6):875-9. https://doi.org/10.1016/j.jvir.2014.03.005 PMid:24857944

ID Design Press, Skopje, Republic of Macedonia
Open Access Macedonian Journal of Medical Sciences. 2019 Dec 30; 7(24):4209-4213.
https://doi.org/10.3889/oamjms.2019.362
eISSN: 1857-9655
Basic and Clinical Medical Researches in Vietnam

Perforator Mapping of the Superficial and Deep Inferior Epigastric Artery in the Abdominal Region of the Vietnamese

Tran Dang Khoa[1], Nguyen Duy Bac[2*], Cao Ngoc Bich[3], Hoang-Long Vo[4], Nguyen Vu Thai Lien[5], Thien Chu Dinh[6]

[1]Pham Ngoc Thach University of Medicine (PNTU), Ho Chi Minh City, Vietnam; [2]Vietnam Military Medical University (VMMU), Hanoi, Vietnam; [3]Thanh Van Cosmetic Surgery Hospital, Ho Chi Minh City, Vietnam; [4]Institute for Preventive Medicine and Public Health, Hanoi Medical University, Hanoi, Vietnam; [5]School of Odonto Stomatology, Hanoi Medical University, Hanoi, Vietnam; [6]Institute for Research and Development, Duy Tan University, 03 Quang Trung, Danang, Vietnam

Citation: Khoa TD, Bac ND, Bich CN, Vo H-L, Lien NVT, Dinh TC. Perforator Mapping of the Superficial and Deep Inferior Epigastric Artery in the Abdominal Region of the Vietnamese. Open Access Maced J Med Sci. 2019 Dec 30; 7(24):4209-4213. https://doi.org/10.3889/oamjms.2019.362

Keywords: Deep inferior epigastric artery; Superficial epigastric artery; Fourth space; Eight regions; Perforators

***Correspondence:** Nguyen Duy Bac. Vietnam Military Medical University (VMMU), Hanoi, Vietnam. E-mail: nguyenduybac@vmmu.edu.vn

Received: 26-May-2019; **Revised:** 20-Aug-2019; **Accepted:** 19-Jun-2019; **Online first:** 15-Oct-2019

Funding: This research did not receive any financial support

Competing Interests: The authors have declared that no competing interests exist

Abstract

BACKGROUND: Previous studies worldwide have investigated the anatomy of the perforators of the deep inferior epigastric arteries to figure out the navigation patterns of the perforators on the abdominal wall. This has been inconsistent amongst the researchers about how to select the perforator to increase the blood supply area for the flap.

AIM: To explore the blood supply area of the perforators of the superficial and deep inferior epigastric artery in the abdominal region of the Vietnamese by dissection and 64-slice multislice computed tomography (64-slice MSCT).

METHODS: A descriptive cross-sectional study Center from September 2014 to September 2016 on two groups including 30 cadavers fixed by formalin 10% in Anatomy Department of UPNT, and 37 patients getting the 64-slice MSCT abdominal arteries angiogram.

RESULTS: The superficial epigastric arteries at the level of the inguinal ligament were located in the middle region, with 96% (right) and 88.5% (left). The anterior superior iliac spine level was in the middle, and lateral regions of 68% and 32% respectively. The level of the umbilical cord was in the lateral region with 66.7% and 85.7%, respectively. There were about 6 perforators of the deep inferior epigastric arteries located in the navel area. These perforators were 70% in the medial region and 30% in the middle region.

CONCLUSION: Mapping the blood supply based on the fourth space in the abdominal region in which the superfical inferior epigastric arteries supplied the lateral area. The middle and the internal ones were the perforators of the deep inferior epigastric arteries.

Introduction

Abdominoplasty is one of the aesthetic procedures performed increasingly commonly. Despite this made procedure for a long time, the outcome has not satisfied both physicians and cosmetic surgery clients due to its esthetic effects and safety. Particularly, the most important complication is the necrosis of the residual abdominal skin with various levels, which results from lacking of blood supply after the operation. Thus, the adequate knowledge about the characteristics of blood supply of the superficial and deep inferior epigastric artery as well as their perforators plays an important role that helps the surgeons calculate the dimensions of the removable flap in the operation procedure so that this procedure is ensured safely [1]. Up to now, previous studies worldwide have investigated the anatomy of the perforators of the deep inferior epigastric arteries to figure out the navigation patterns of the perforators on the abdominal wall. From that, they can identify four standard blood supply spaces as Hartrampf [2], [3], [4]. However, this has been inconsistent amongst the researchers forward how to select the perforator to increase the blood supply area for the flap. A Quynh et al.' study reported this issue in Vietnam, which has been not yet systematic for both the arteries [3]. The present study, therefore, aimed to explore blood supply area of the perforators of the superficial and deep inferior epigastric artery in the abdominal region of Vietnamese by dissection and 64-slice multislice computed tomography (64-slice MSCT).

Material and methods

Study design and participants

A descriptive cross-sectional study was conducted between September 2014 and September 2018. The participants in the study were divided into two groups. A group included 30 cadavers fixed with formalin 10% in Anatomy Department of UPNT. Other group included 37 adult patients getting the 64-slice MSCT angiography of the abdominal artery in Hoa Hao Medical Center. The participants were selected in this study with the convenience sampling method. We included the Vietnamese patients (i) over 18 years and (ii) not undergoing any surgery in the groin and thigh areas. We excluded the patients (i) with the distortions in the groin and thigh areas (congenital, pathological abnormalities, and previous surgery), and (ii) vascular malformation in these areas (transplantation, binding vessels, etc.).

Procedures

In the cadaver group, we performed an incision in the abdominal area along to inguinal ligament in the supine position of the cadavers. Then we determined the origins of the superficial and deep inferior epigastric artery. We continued to dissect along the deep inferior epigastric artery until we could not determine the vessel in the abdominal wall. Moreover, we dissected along the superficial epigastric artery to find perforators. We examined them about position, direction and their relationship with the medial or lateral of the anterior abdominal wall as well as their coordination.

In the patient group, the patients getting 64-slice MSCT contrast injection undergo function tests of liver and kidney, abdominal sonography, blood pressure, height and weight measurement. The contrast dose was 2 ml/kg. The patient was conducted with 64-slice MSCT in the supine position (the depth of slice: 1mm (0.8) overlap 0.2). The outcomes were evaluated by the same diagnostic imaging doctor and the same researcher. We identified the number of perforators of the deep inferior epigastric artery, their position and relationship with the medial or lateral of the anterior abdominal wall.

Data analysis

Data were collected and analysed with IBM SPSS 21 software package. Descriptive statistics (percentages, frequencies, means and standard deviations) for the various groups distinguished, were computed. Independent t-tests were applied to test the significance of differences between groups. The significance level was considered at $p < 0.05$.

Results

The blood supply area of the superficial epigastric artery in the abdominal wall: Characteristics of the direction of the superficial epigastric artery

In the cadaver group, the direction of the superficial epigastric artery which toward the anterior superior iliac spine was 64% in the right and 69.2% in the left. In the patient group with 64-slice MSCT, the patient percentage of the direction of the arteries, which straight down the hypochondriac region was more than 50% than.

Table 1: Direction of the superficial epigastric artery in the abdominal wall of cadavers and patients with 64-slice MSCT

Sample	Direction	To the right	To the left	p
Cadavers (nR = 25, nL = 26)	Toward to anterior superior iliac spine	17 (68%)	20 (76.9%)	0.26
	Toward to middle line	4 (16%)	3 (11.5%)	
	Straight down hypochondriac region	4 (16%)	3 (11.5%)	
	Superficial epigastric artery-inguinal ligament angle	50 ± 15.94	46 ± 12.6	0.35
64-slice MSCT (nR = 5, nL = 4)	Toward to anterior superior iliac spine	1 (20%)	1 (25%)	0.09
	Toward to middle line	1 (20%)	1 (25%)	
	Straight down hypochondriac region	3 (60%)	2 (50%)	
	Superficial epigastric artery-inguinal ligament angle	42.0 ± 22.3	53.5 ± 16.8	0.29

The proportion of the angle of the superficial epigastric artery and inguinal ligament was smaller in the patient group than in the cadaver group. There were no significant differences in directions from two sides (Table 1and Figure 1).

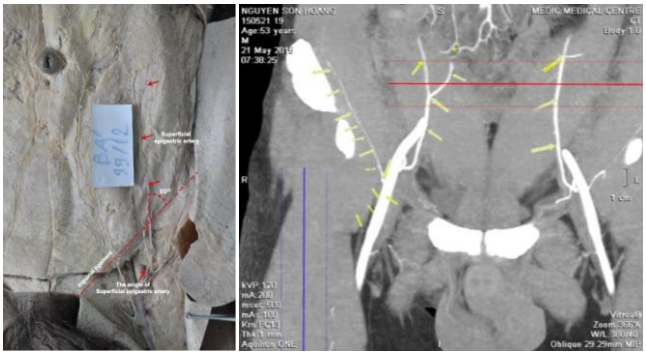

Figure 1: The angle of the superficial epigastric artery and the left hypochondriac region (Right); the right superficial epigastric artery goes toward to anterior superior iliac spine, then goes into lateral line toward to the hypochondriac region in 64-slice MSCT (Left)

Mapping the blood supply area of the superficial epigastric artery based on three lines in the abdominal wall

In the cadaver group, the relative position of the superficial epigastric artery which is at the level of an inguinal ligament in the middle line accounted for the highest percentage with both right and left sides (96.0% and 88.5%, respectively), followed by in the lateral line. No observation in the medial line. At level of anterior superior iliac spine, the artery running into the lateral line started to increase to 32% in the right side and to 50% in the left side (the lower the

percentage of artery in the middle line became, the upper the percentage of artery in the lateral line became), and once at level of navel, the position of the artery in the lateral line was up to 66.7% in the right side and up to 85.7% in the left side. This supported that, in the cadaver group, the direction of the superficial epigastric artery ran from the medial to the lateral line, and the cases of the superficial epigastric artery at that level decreased to ½ in the right side and about ¼ in the left side. Moreover, there was a significant difference in the relative position of the superficial epigastric artery based on three lines amongst the sides ($p < 0.05$).

Table 2: Localizing the superficial epigastric artery based on three lines in the abdominal wall of cadaver and patient groups

Location		Cadaver group		64-slice MSCT group	
Standard landmark	Line	Right	Left	Right	Left
Level of inguinal ligament	Medial	0	0	1 (20%)	1 (25%)
	Middle	24 (96%)	23 (88.5%)	4 (80%)	3 (75%)
	Lateral	1 (4%)	3 (11.5%)	0	0
	Total	25	26	4	3
	p-values	0.143		0.25	
Level of anterior superior iliac spine	Medial	0 (0,0%)	1 (3,8%)	1 (25,0%)	1 (33,3%)
	Middle	17 (68,0%)	12 (46,2%)	3 (75,0%)	1 (33,3%)
	Lateral	8 (32,0%)	13 (50%)	0	1 (33,3%)
	Total	25	26	4	3
	p-values	0.008*		1	
Level of navel	Medial	0	0	1 (33.3%)	1 (50%)
	Middle	4 (33.3%)	1 (14.3%)	1 (33.3%)	1 (50%)
	Lateral	8 (66.7%)	6 (85.7%)	1 (33.3%)	0
	Total	12	7	3	2
	p-values	0.248		1	

*: significant at 0.05.

There is no significant difference at the level of the navel, perhaps because the numbers of the arteries at that level were very few.

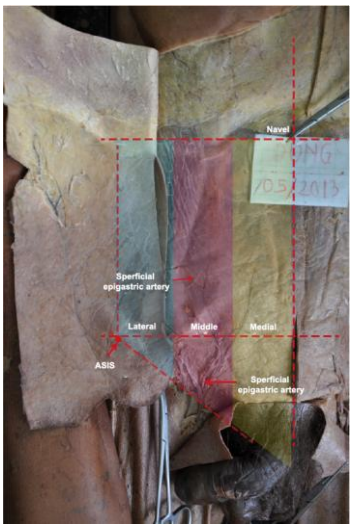

Figure 2: Mapping the right superficial epigastric artery based on three lines: at the level of the inguinal ligament, the right superficial epigastric artery is in the middle line; at level of anterior superior iliac spine, it is still in the middle line; and at level of navel, it is at the lateral line

In, the relative position of the superficial epigastric artery which is at the level of the anterior superior iliac spine is the highest in both right and left sides (80.0% and 75.0%, respectively), this is still at the middle line when the artery runs into the level of the anterior superior iliac spine.

However, in the patient group with 64-slice MSCT, it is difficult to identify the branches of the superficial epigastric artery which were more than 0.5 mm in diameter, so there was an extremely significant difference in the frequency of the appearance of the superficial epigastric artery amongst cadaver and patient groups (Table 2 and Figure 2).

The blood supply area of the perforators of the deep inferior epigastric artery in the abdominal wall

We documented the position of perforators of the deep inferior epigastric artery based on 3 lines and the vertical axis going through the navel. We could not observe any perforators in the lateral line, but the number of the perforators in the medial line was the highest (approximately 70%), followed by in the middle line (30%). By dividing based on three lines (medial, middle and lateral lines) which were different in the distance from the anterior superior iliac spine and the axis going through navel, the number of perforators in the medial line decreased to 30%, and in the middle line, there was an increase reported (Table 3).

Table 3: The proportion of perforators based on these landmarks

Artery	Side	Medial line	Middle line	At level about ¼ under the navel	Right	Left	At the level at the navel and about ¼ upper	Right	Left
1	Right	25 (83.3%)	5 (16.7%)	Space 1	27 (96.4%)	21 (77.8%)	Space 1	2 (100%)	3 (100%)
	Left	27 (90%)	3 (10%)	Space 2	1 (3.6%)	6 (22.2%)	Space 2,3,4	-	-
2	Right	19 (67.9%)	9 (32.1%)	Space 1	21 (100%)	23 (100%)	Space 1	7 (100%)	6 (100%)
	Left	24 (82.8%)	5 (17.2%)	Space 2	-	-	Space 2,3,4	8 (80%)	7 (58.3%)
3	Right	20 (76.9%)	6 (23.1%)	Space 1	16 (100%)	16 (100%)	Space 1	2 (20%)	5 (41.7%)
	Left	20 (71.4%)	8 (28.6%)	Space 2	-	-	Space 2 Space 3,4	- 10 (71.4%)	- 5 (62.5%)
4	Right	15 (71.4%)	6 (28.6%)	Space 1	7 (100%)	13 (100%)	Space 1	4 (28.6%)	3 (37.5%)
	Left	14 (66.7%)	7 (33.3%)	Space 2	-	-	Space 2 Space 3,4	- 12 (70.6%)	- 8 (72.7%)
5	Right	13 (72.2%)	5 (27.8%)	Space 1	1 (100%)	5 (100%)	Space 1	5 (29.4%)	2 (18.2%)
	Left	12 (75%)	4 (25%)	Space 2	-	-	Space 2 Space 3 Space 4	- - 8 (61.5%)	1 (9.1%) - 11 (73.3%)
6	Right	10 (71.4%)	4 (28.6%)	Space 1	1 (100%)	-	Space 1	3 (23.1%)	2 (13.3%)
	Left	9 (60%)	6 (40%)	Space 2	-	-	Space 2 Space 3 Space 4	2 (15.4%) - 2 (100.0%)	1 (6,.7%) 1 (6.7%) 3 (100.0%)

As was shown in Table 3, the percentage of perforator 1 under the navel was 90%. While the percentage of the perforators number 2, 3, 4 under the navel decreased to 50%, the figures for the perforators number 2, 3, 4 upper the navel increased. Most of the perforator number 6 to number 11 were upper the navel. As the results from 64-slice MSCT, most perforators number 1 were under the navel (90%). The percentage of the perforators number 2, 3, 4 under the navel decreased to 50%, while the figures for the perforators number 2, 3, 4 upper the navel increased, but the slope in the patient group was recorded to be smaller than in the cadaver group.

With the perforators number 6 to number 11, most of them were upper the navel. In summary, the presence of each perforator was absolutely under the navel about 40 mm (unless the left perforator number 1 lies up to space 2, the percentage of these cases is about 22.2%). The percentage of perforators number 1 and 2 staying in space 1 was 100%, while the percentage of perforators number 3, 4, 5 which stayed in space 1 decreased from 80% to 60%. However, there had the perforators number 3, 4, 5 in the space 2 and 3, and the percentage of these cases were about 20%.

Discussion

The division pattern which divided the abdominal wall into 8 spaces along the axis going through the navel of N.T.Quynh was consistent with us, however, Quynh's pattern was considered as easier than ours. In the upper navel space, Quynh used the line going through the middle point of navel and xiphisternum to divide that space into space 3-4 (space 3 is medial and space 4 is lateral) and space 1-2 (space 1 is medial and space 2 is lateral), which were space 1-2 and space 3-4 respectively in our study (2 spaces in our study was consistent with 1 space in N.T.Quynh' study). The similar statistics was also applied in our study; we found that our results were strongly consistent with others. The distribution of the perforators originated from ½ under the navel, and the highest concentration around the navel and the distribution decreased from there to xiphisternum. Therefore, the artery supplying blood for upper navel space is the deep inferior epigastric artery, not the superior epigastric artery. This was an important note in designing the flap. No similarity in the distribution of the perforators based on the horizontal axis going through the navel between N.T.Quynh' study and our ones. This could be because of N.T.Quynh divided the medial and lateral space based on the rectus abdominis muscle [3].

When research investigated the sample study, he often gives a series of different dimensions such as 4 cm, 5 cm, 8 cm, 10 cm or a few centimetres. This is a general disadvantage because the dimension has no rule. In this study, we found that our data was followed the rule of 4 (a distance equals 4cm long) and the distance was followed the fifty-fifty rule, which is the easy way for the practice because it did not depend on height, size and weight of the patient. If we multiplied the 4 cm-distance twice or ½, our result might be consistent with previous studies (8 cm equals two 4cm-distances, 10 cm is 2.5 times of 4 cm-distance) [2], [3], [4].

We offered a division pattern with 4cm-distance in the abdominal wall to map the branches of the superficial epigastric artery and the deep inferior epigastric artery. Firstly, a line from the pubis to navel need drawing, then divide that line into two equal segments and continue to divide each segment into two equal segments. So, we will have 4 segments (each segment which is called 4 cm-distance is 4 cm long). With this segment, we can identify that (i) the place where the inferior epigastric artery runs into muscle is at the point which divides navel-pubis distance into two segments; (ii) the place which has the first perforator is at the point which ¾ long from navel to pubis; (iii) perforators round up 100% at the 4cm-distance under navel. Secondly, with the medial point in the inguinal ligament, we draw a circle whose radius equals a 4 cm-distance from the pubis to navel, the probability to find the origin of the superficial epigastric artery is 90.2%. Thirdly, we draw 2 parallel lines which divide the distance from anterior superior iliac spine to the medial line of the abdomen into 3 rows (medial, middle and lateral rows) whose width equals a 4 cm-distance from the pubis to the navel. With 3 rows, we can identify the blood supply area of the arteries, such as the lateral row is the area which is supplied by the superficial epigastric artery, the middle row is the area we can find 30% perforators, and the medial row has 70% perforators of the deep inferior epigastric artery.

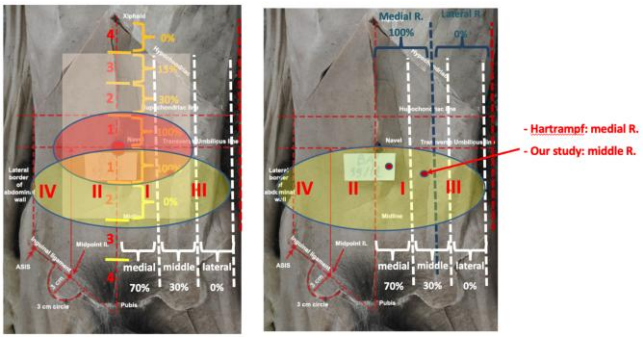

Figure 3: Mapping the perforators based on the vertical and horizontal axes which run through navel in our study (right), compared with the division pattern of Hartrampf (left)

The division pattern dividing the abdominal wall into 3 rows exists several advantages. The dimension of each segment is equivalent so that we can use it to estimate a distance. Secondly, segment ¼ upper navel, ¼ under the navel, ⅓ anterior superior iliac spine - navel have a similar measurement regardless of anyone. Thus, we offered using this segment as a unit measurement to estimate the distance in the abdominal wall or to map the arteries as using proportion in traditional medicine. If we divided 2 rows: medial and lateral as a four-space pattern of Hartrampf or Scheflan and Dinner, most perforators are in the medial row, the result of our study is 100%. This would be an illogical appointment if we used the division pattern. This point was supported by Wong C.'s study [5], the blood supply area of perforators in the medial row near the middle row is different from the blood supply area of perforators in the medial row near the lateral row. The flat which is supplied blood by perforators in the

medial row near middle line more concentrated in the center and has an area bigger than the flat which is supplied blood by perforators in the medial row near lateral row [5]. In consequence, they are both perforators in the medial row, but near the middle line or not; their blood supply areas are different. Thus, based on the division pattern which divides abdominal wall into 3 rows in our study, perforators in the medial row near middle line belong to medial row, and perforators in the medial row far from middle line belong to medial row and the lateral row belong to the blood supply area of the superficial epigastric artery. In our point of view, 6 divided areas are logical and content with the explanation about blood supply area.

In a previous study of Eric M, et al., [6], the authors divided Hartrampf's spaces into smaller pieces followed 3 patterns: (a) 9 subspaces numbered from 1 to 9; (b) 3 subspaces near, middle, far; and (c) 3 subspaces medial, middle and lateral. The percentage of the presence of the perforators in space I was 79.43%, in space II was 6.38%, in space III was 13.48%, and in space, IV was 0.71%. The probability of finding out a perforator in space I was the highest (100%), while the probability to find out a perforator in space II, III and IV were 65%, 25% and 5%, respectively [6]. This division pattern divided each space of Hartrampf into 3 smaller pieces into horizontal and vertical axes to localise the mapping of perforators, not as the division pattern in our study. In Vietnam, N.T.Quynh divided into 2 rows including medial and lateral. However, this pattern was based on the horizontal axis of rectus abdominis muscle, not the horizontal of abdominal wall, thus, in fact, these two rows belonging the medial row in Hartrampf's pattern or the medial and lateral in our study's pattern. Wong C et al. found that the peripheral branches were larger in diameter and tent to run straight, which helped the surgeon dissect faster and easier [5]. The perforators in the lateral row were used for semi-abdominal flap having more than one centre and the risk of necrosis of a part of flap's apex or border. Thus, the semi-abdominal flaps tended to be safe when they are taken based on a simple perforator in the lateral row. Holm et al. did several studies of the blood supply area and they proved that Hartrampf's space II and III needed to be converted. The authors emphasised that the division pattern of Hartrampf was wrong and "the blood supply area which goes through middle line was always delayed and less ingrained than the other area in the same side" [7]. Hamdi M et al. found that the perforators in the lateral row were larger and dissected more easily. The perforators in the medial row supplied blood better for space III and IV, however, if the surgeons want to dissect these vessels, they have to dissect a segment of a vessel running in the muscle longer, and this procedure is much along the vertical axis. The perforator ran through the rectus muscle which has transverse tendious. The distance from this area to skin was shorter, it might be difficult to dissect these vessels.

In conclusion, the direction of the superficial epigastric artery running toward inguinal ligament was almost in the middle row. When this artery reached the anterior superior iliac spine, it belonged to the lateral row. Once mapping the perforators in the abdominal wall, most perforators were in the medial row (93-100%), and there were very few perforators in the lateral row. Mapping the perforators in the abdominal wall based on 3 rows (medial, middle and lateral) in the line between the anterior superior iliac spine and the vertical axis running through the navel, the proportion rates of the perforators in the medial and middle row were 70% and 30%, respectively. The percentage of the superficial epigastric artery running toward the anterior superior iliac spine was observed at 65%. Once mapping blood area, this artery supplied for the 4cm-distance lateral row, while the deep inferior epigastric artery supplied for the middle and medial rows.

References

1. Tran NV, Buchel EW, Convery PA. Microvascular complications of DIEP flaps. Plastic and reconstructive surgery. 2007; 119(5):1397-405. https://doi.org/10.1097/01.prs.0000256045.71765.96 PMid:17415232

2. Masia J, Kosutic D, Clavero JA, Larranaga J, Vives L, Pons G. Preoperative computed tomographic angiogram for deep inferior epigastric artery perforator flap breast reconstruction. Journal of reconstructive microsurgery. 2010; 26(01):021-8. https://doi.org/10.1055/s-0029-1223854 PMid:19742426

3. Quynh N.T. Study on anatomy of the abdomen muscle flap on Vietnamese people: Hanoi Medical University; 2006.

4. Saber AA, Meslemani AM, Davis R, Pimentel R. Safety zones for anterior abdominal wall entry during laparoscopy: a CT scan mapping of epigastric vessels. Annals of surgery. 2004; 239(2):182. https://doi.org/10.1097/01.sla.0000109151.53296.07 PMid:14745325 PMCid:PMC1356210

5. Wong C, Saint-Cyr M, Mojallal A, Schaub T, Bailey SH, Myers S, et al. Perforasomes of the DIEP flap: vascular anatomy of the lateral versus medial row perforators and clinical implications. Plastic and reconstructive surgery. 2010; 125(3):772-82. https://doi.org/10.1097/PRS.0b013e3181cb63e0 PMid:20195105

6. Erić M, Ravnik D, Žic R, Dragnić N, Krivokuća D, Lekšan I, et al. Deep inferior epigastric perforator flap: An anatomical study of the perforators and local vascular differences. Microsurgery. 2012; 32(1):43-9. https://doi.org/10.1002/micr.20944 PMid:22113874

7. Hamdi M, Rebecca A. The deep inferior epigastric artery perforator flap (DIEAP) in breast reconstruction. InSeminars in plastic surgery 2006; 20(02):095-102. https://doi.org/10.1055/s-2006-941716 PMCid:PMC2884777

ID Design Press, Skopje, Republic of Macedonia
Open Access Macedonian Journal of Medical Sciences. 2019 Dec 30; 7(24):4214-4219.
https://doi.org/10.3889/oamjms.2019.363
eISSN: 1857-9655
Basic and Clinical Medical Researches in Vietnam

The Correlation between the Structures of the Nasal Tip on the Ultrasound and the Anthropometry of the Nose in Vietnamese

Tran Dang Khoa[1*], Nguyen Thanh Van[2], Ho Nguyen Anh Tuan[1], Nguyen Duy Bac[3], Pham Dang Dieu[1], Nguyen Thi Phuong[4], Vu Thi Nga[5]

[1]Department of Anatomy, Pham Ngoc Thach University of Medicine (PNTU), Ho Chi Minh City, Vietnam; [2]Thanh Van Cosmetic Surgery Hospital, Ho Chi Minh City, Vietnam; [3]Department of Anatomy, Vietnam Military Medical University (VMMU), Hanoi, Vietnam; [4]NTT Hi-tech Institute, Nguyen Tat Thanh University, Ho Chi Minh City, Vietnam; [5]Institute for Research and Development, Duy Tan University, Danang, Vietnam

Citation: Khoa TD, Van NT, Tuan HNA, Bac ND, Dieu PD, Phuong NT, Nga VT. The Correlation between the Structures of the Nasal Tip on the Ultrasound and the Anthropometry of the Nose in Vietnamese. Open Access Maced J Med Sci. 2019 Dec 30; 7(24):4214-4219. https://doi.org/10.3889/oamjms.2019.363

Keywords: The protrusion of the nasal tip; The nasal tip; The interdomal fat pad; Tip point

***Correspondence:** Tran Dang Khoa. Department of Anatomy, Pham Ngoc Thach University of Medicine (PNTU), Ho Chi Minh City, Vietnam. E-mail: khoatrandr@gmail.com

Received: 26-May-2019; **Revised:** 20-Nov-2019; **Accepted:** 21-Nov-2019; **Online first:** 15-Oct-2019

Funding: This research did not receive any financial support

Competing Interests: The authors have declared that no competing interests exist

Abstract

BACKGROUND: Nowadays, there are few types of research held in Vietnam to investigate the anthropometric index of the nose as well as analysis the structure of nasal tip on ultrasound to identify the relationship between these parameters.

AIM: To determine the relationship between the height and the width of the nasal tip and the structures constructed these areas by anthropometric and ultrasound measurement.

METHODS: A descriptive study in Thanh Van Hospital from December 2017 to April 2019.

RESULTS: There were 94 women (62.7%), and 56 men (37.3%) and the average age were 33.6 years old. The height and width of the nasal tip are 10.1 mm and 21.7 mm, respectively. Through the ultrasound, the thickness of the adipose tissues is 3 mm. The width of the interdomal fat pad is 6.5 mm and the distance between two tip point is 5.6 mm. There are the relationships between the distance of two tip points and the width of the tip (r = 0.341), and the width of the interdomal fat pad (r = 0.72). There is also the correlation between the width of the nasal tip with the distance of two tip points (r = 0.46) and the height of the tip with the thickness of the interdomal fat pad (r = 1.23).

CONCLUSION: The thickness of the interdomal fat affects the height of the tip, and the distance of two tip points influences the width of the tip.

Introduction

The structures such as lower lateral cartilages, tip points, interdomal area, interdomal fat pad, interdomal ligament are described widely and in detail by the ENT clinicians and the cosmetic doctors. In contrast, the anatomists describe the structure of the nose at the level of morphology and simplicity [1]. Most surgeons noticed that rhinoplasty on nasal tip was extremely difficult because the nasal tip after the operation should look natural if not, people know that nose had undergone a rhinoplasty, and the complexity of nose anatomies such as tip points, interdomal fat pad, interdomal ligament and the harmony of noise on face [2]. Moreover, the characteristics of structures which build nasal tip change depending on the anthropometric index of a race, it made nose harmonise with the other structures on a face. Thus, the operation may be complex because of the mobility, variety and anthropometric index [3].

Nowadays, there are many extensive studies about the anthropometric index of nose and face. However, there are few types of research held in Vietnam to investigate these dimensions as well as analysis the structure of nasal tip on ultrasound to identify the relationship between these parameters.

Thus, we started a study "The correlation between the structures of the nasal tip on the ultrasound and the anthropometry of the nose in Vietnamese" with two objects: 1) Identify the relationship between the anthropometry of the height of nasal tip and the thickness of the soft tissues on the nasal tip by ultrasound and 2) Identify the relationship between the anthropometry of the width of nasal tip and the distance between two tip points and the interdomal fat pad by ultrasound.

Material and Methods

Study design

Descriptive cross-sectional study.

Participants

We chose 150 adults Vietnamese by convenient sampling method.

Inclusive criteria: 1. Adult Vietnamese, 18 years old and above; 2. The nasal tip is intact; the participant has never undergone any surgery on the nose; and 3. The participant has no congenital malformation, trauma, cosmetic surgery, tumour or anatomic abnormality in structures of the face.

Exclusive criteria: We excluded people who use filler in the nose area or have dyslipidemia or Cushing syndrome. - Study period: from December 2017 to April 2019 and - Study area: Thanh Van Hospital in HCMC.

Study materials: - A calliper, compass, anthropometric ruler; - Camera NIKON D90, lens Nikon AF-S Micro NIKKOR 60 mm 1: 2.8G ED; and - Ultrasound machine Accuvix with probe 12MHz.

Measuring the anthropometric index of face

We used a calliper to measure the index such as distance from nasion (n), (g) to the subnasal point (sn) directly. We recorded and measured the dimensions of nasal tip such as the protrusion of nasal tip, width and height of nasal tip.

Using ultrasound

We used ultrasound machine with probe 12 MHz to measure the thickness of the skin at the nasal tip, the thickness of the subcutaneous fat pad, the width, height and thickness of the interdomal fat pad, the thickness of the cartilage at the tipping point and the distance between two tip points.

Processing and Analysing data

Statistics, description, processing, and analysing data with the statistical test in SPSS 19. We compared the average values by the t-test and the ratios by X^2 test, CI 95%. We used multivariable linear regression to find the relationship.

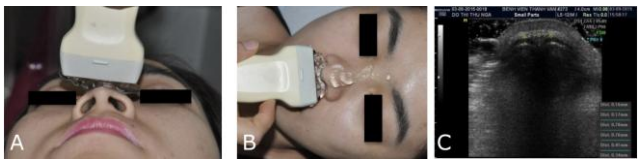

Figure 1: The patient's position when we did an ultrasound

Results

We investigated 150 patients including 94 females (62.7%), 56 male (37.3%) and the average age is 33.6 ± 13.4 years old (Table 1) (ranged from 18 to 65 years old) (E.g. 1 case in Figure 1).

The relationship between the anthropometry of the height of the nasal tip and the thickness of the soft tissues on the nasal tip by ultrasound

The average protrusion of the nasal tip is 16.9 mm; the average height of the nasal crus is 6.8 mm; the average height of the nasal tip is 10.1 mm. These dimensions are significantly different between the two sex ($p < 0.05$) and these dimensions of the male are more than ones of female (Table 1).

Table 1: The dimensions of nasal tip

The dimensions of nasal tip	Male (n = 56)	Female (n = 94)	Total (n = 150)	P-values
The protrusion of nasal tip (sn-prn)	17.8 ± 3.3	16.4 ± 3.8	16.9 ± 3.7	0.023[e]
The height of nasal crus (sn-c')	7.3 ± 1.3	6.6 ± 1.2	6.8 ± 1.3	0.001[e]
The height of nasal tip (c-prn)	10.5 ± 3.0	9.9 ± 4.0	10.1 ± 3.6	< 0.001

c. T-student test; e. Mann-Whitney test.

The thickness of the skin at interdomal area is 3 mm, the thickness of subcutaneous fat tissue at interdomal area is 3 mm.

Table 2: The thickness of soft tissue on nasal tip on ultrasound

Dimension (mm)	Male (n = 56)	Female (n = 94)	Total (n = 150)	P-values
Skin at interdomal area	3.0 ± 0.5	2.8 ± 0.5	2.9 ± 0.5	0.167[c]
Subcutaneous fat tissue at interdomal area	3.1 ± 0.7	2.9 ± 0.7	3.0 ± 0.7	0.160[c]
Interdomal fat pad	3.1 ± 0.7	2.9 ± 0.7	3.0 ± 0.5	0.09[c]

c. T-student test.

There is no significant difference in the thickness of subcutaneous fat tissue between male and female ($p > 0.05$) (Table 2) (Figure 2).

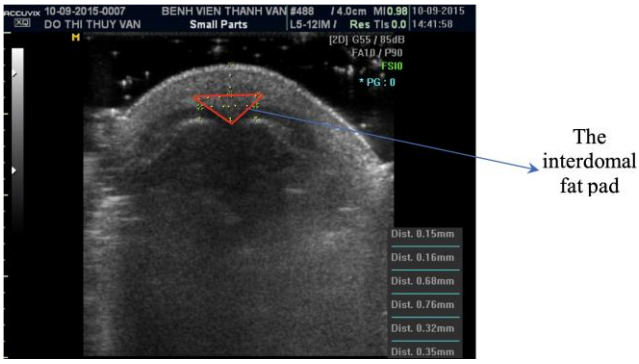

Figure: 2 The interdomal fat pad on ultrasound

The result showed that the male's cartilage at tip point is thicker than females.

Table 3: The thickness of cartilage of nasal tip on ultrasound

Thickness of cartilage	Male (n = 56)	Female (n = 94)	Total (n = 150)	p-values
The right tip point	2.2 ± 0.5 mm	1.7 ± 0.4 mm	1.9 ± 0.5 mm	0.0001[e]
The left tip point	2.2 ± 0.5 mm	1.7 ± 0.4 mm	1.9 ± 0.5 mm	0.0001[e]

e. Mann – Whitney test.

With Table 2, the patients' cartilage of tip point in both sides is thicker than on ultrasound (p = 0.0001) (Table 3) (Figure 3).

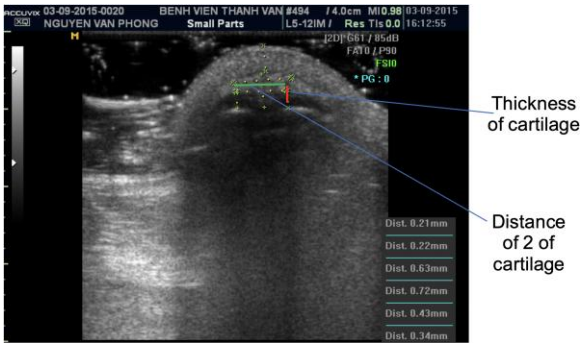

Figure: 3 The thickness of cartilage and distance between two tip points on ultrasound

Investigating the relationship between the height of the nasal tip on external and internal structures

In single variable correlation, the height of tip point is closely correlated with the thickness of interdomal fat pad, the thickness of interdomal subcutaneous fat tissue and the thickness of skin and interdomal fat pad, and it is not correlated with the thickness of interdomal skin and the thickness of cartilage on tip point (Table 4).

Table 4: The correlation between the height of the nasal tip and the other structures (in single - variable correlation)

The correlation of the height of the nasal tip and	Coefficient	p
The thickness of interdomal skin	0.18	0.764
The thickness of interdomal fat pad	1.19	0.003
The thickness of subcutaneous fat tissue	0.99	< 0.001
The thickness of cartilage on the right nasal tip point	0.11	0.862
The thickness of cartilage on the left nasal tip point	0.39	0.512
The thickness of skin and interdomal subcutaneous fat tissue	1.01	< 0.001

There is a close relationship between the height of the nasal tip and the thickness of interdomal fat pad. The equation to estimate the height of nasal tip: The height of the nasal tip (c'-prn) = 6.7 + 1.23 x the thickness of interdomal fat pad (Table 5).

Table 5: The correlation between the height of the nasal tip and the other structures (in multivariable correlation)

The correlation between the height of the nasal tip (c'-prn) and	Coefficient	p
The thickness of interdomal skin	0.003	0.996
The thickness of interdomal fat pad	1.23	0.004
The thickness of cartilage on the right nasal tip point	- 0.89	0.364
The thickness of cartilage on the left nasal tip point	0.78	0.394
Constant	6.70	0.005

The anthropometric index of the width of the nasal tip

The index of the width of the nasal tip is different between male and female (p < 0.05); these male's index is larger than female's (Table 6).

Table 6: The index of the width of nasal tip

The index of the width of nasal tip	Male (n = 56)	Female (n = 94)	Total (n = 150)	p
The width of nasal tip	23.1 ± 2.3	20.9 ± 2.0	21.7 ± 2.4	0.0001[e]
The width of crus at the bottom of nose (sn'-sn')	6.1 ± 1.0	5.5 ± 1.0	5.7 ± 1.0	0.001[e]
The width of crus at the top of nose (c'-c')	11.1 ± 1.8	9.9 ± 1.5	10.3 ± 1.7	0.0001[e]

c. T-student test; e. Mann-Whitney test.

The distance between two tip points and the width of interdomal fat pad

The male's distance between two tip points is 5.8 ± 1.7 mm, the female's one is 5.6 ± 1.2 mm, and the average distance is 5.6 ± 1.4 mm, there is no significant difference about these indexes between male and female (p = 0.319) (Table 7).

Table 7: Classification of the distance between two tip points on ultrasound

Classification of the distance between two tip points	Male (n = 56)		Female (n = 94)		Total (n = 150)	
	n	%	n	%	n	%
2 – 4 mm	8	14.3	9	9.6	17	11.3
4 – 6 mm	24	42.9	51	54.3	75	50.0
6 – 8 mm	17	30.4	30	31.9	47	31,3
8 – 10 mm	6	10.7	3	3.2	9	6.0
> 10 mm	1	1.8	1	1.1	2	1.3

The distance between two tip points on ultrasound is more than 6 mm, which would decrease 38.6%, and there is no significant difference in this distance between male and female.

Table 8: The dimension of interdomal fat pad on ultrasound

Dimensions	Male (n = 56)	Female (n = 94)	Total (n = 150)	p-values
The width of interdomal fat pad	6.5 ± 1.9	6.4±1.8	6.5 ± 1.4	0.89[e]
The thickness of interdomal fat pad	3.1 ± 0.7	2.9±0.7	3.0 ± 0.5	0.09[c]

c. T – student test; e. Mann – Whitney test.

The thickness of cartilage on tip point in male is 2.2 mm, which thicker than in female (1.7 mm); and

the thickness of cartilage on tip point in patient is thicker than in cadaver on both sides.

The thickness of interdomal fat pad equals ½ the width (6.5 mm in average), and there is a significant difference between male and female, the male's one is thicker than female's ($p < 0.05$) (Table 8) (Figure 4).

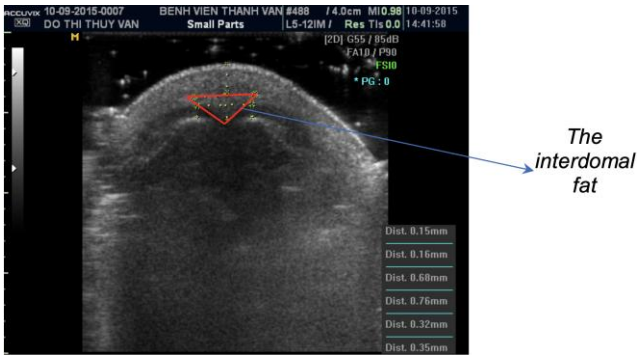

Figure: 4 The interdomal fat pad on ultrasound

Investigating the relationship between the width of the nasal tip on external anatomy and internal structures

By investigating the relationship between two nasal tip points with the width of the nasal tip on ultrasound, we found that the relative coefficient (r) = 0.341 with $p = 0.001$.

We also considered the correlation between the distance of two tip points and the width of interdomal fat pad in population study and we found that the relative coefficient $r = 0.72$ ($p = 0.001$).

The linear correlation equation: the distance between two tip points = 2.356 + 0.612 x the width of interdomal fat pad.

In single variable correlation, we found that there is a correlation between the width of nasal tip and the distance between two tip points, the width of interdomal fat pad and two factors above (Table 9).

Table 9: The relationship between the width of the nasal tip and the other structure (in single variable correlation)

The correlation between the width of the nasal tip and	Coefficient	p
The distance between two tip points	0.6	< 0.001
The width of interdomal fat pad	0.39	< 0.001
The distance between two tip points and the thickness of interdomal fat pad	0.28	< 0.001

When analysing with multivariable correlation, we noted that the width of the nasal tip correlates with the distance between two tip points.

Table 10: The correlation between the width of the nasal tip and the other structure (in multivariable correlation)

The correlation between the width of the nasal tip and	Coefficient	p
The distance between two tip points	0.46	0.012
The width of interdomal fat pad	0.16	0.250
Constant	18.12	< 0.001

The equation to estimate the width of the nasal tip: The width of the nasal tip = 18.12 + 0.46 x the distance between two tip points (Table 10).

Discussion

The relationship between the anthropometry of the height of the nasal tip and the thickness of the soft tissues on the nasal tip by ultrasound

In our study, the protrusion of the nasal tip is shorter, compared with the other foreign studies. It demonstrated that Vietnamese nose is shorter, the length of the alar nostril is shorter than the foreigners; the difference is mostly based on the race of the population study (Table 11).

Table 11: The protrusion of nasal tip in some other studies

Dimension	Ngeow W.C. [4]	Anderson K.J. [5]	Duskova M. [6]	Khandekar B. [7]	Choe K.S. [8]	Farkas L.G. [9]	Our research
The protrusion of nasal tip (mm)	17.8	Male: 24.9 Female: 23.0	21.4	Male: 20.4 Female: 16.9	19.6	19.3	Male: 17.8 Female: 16.4

The ratio of the width of nasal tip and the width of nasal soft tissues (al-al) is 0.6, smaller the result of Porter J.P. [10] with white population study (0.75), the difference may be due to the population study. The ratio of the width of nasal tip and the width of the nose in anatomy is 80%, which much higher than the result of Prendergast P.M. [11] (35-45%), it demonstrated that the Vietnamese nasal tip is bigger than the others. The big nasal tip is one of the characteristics of Asian and African people, the factors contributing the big nasal tip are the distance between two tip points, the divergent angle of the nasal tip, the interdomal fat pad and the thickness of nasal SMAS. Thus, how to choose an appropriate method to diminish the width of the nasal tip is too difficult for the surgeon. These methods include interdomal suture, transdermal suture, SMAS resection.

The ratio of the height of nasal tip and the height of nasal base in our study is 0,6 or ⅗, which larger than the result of Prendergast P.M. [11] (⅓ in White people), Porter J.P. [11] (2:1), and Farkas L.G. [9] (58,2). It demonstrated that the height of the Vietnamese nasal tip is more than ½ the protrusion of nasal tip. In other word, the Vietnamese nasal tip is thick, big and nasal crus is short.

All the values and ratios made a general point of view about Vietnamese naval base, whose characteristics are short, wide, nasal nostril is puff, nasal crus is short and nasal tip is big and thick. These are reasons which make rhinoplasty become one of the most popular cosmetic surgery to

restructure nasal tip and base by diminishing nasal tip and alar base reduction, lengthening nasal crus.

We investigated the relationship between the height of nasal tip and the other structures such as the thickness of cartilage at nasal tip point, the thickness of interdomal fat pad, the skin of interdomal area, interdomal subcutaneous fat tissue. In single variable correlation, the height of tip point is closely correlated with the thickness of interdomal fat pad, the thickness of interdomal subcutaneous fat tissue and the thickness of skin and interdomal fat pad, and it is not correlated with the thickness of interdomal skin and the thickness of cartilage on tip point. When investigating the multivariable correlation between the factors affecting the height of the nasal tip, we found that there is a close relationship between the height of the nasal tip and the thickness of the interdomal fat pad.

By investigating the single and multi-variable correlations, we found that the height of the nasal tip is affected most by the thickness of interdomal fat pad. This object should be noted in the rhinoplasty on a nasal tip because it can change the dimensions of this area when interceding the interdomal fat pad.

The relationship between the anthropometric index of the width of the nasal tip and ultrasound

We found that the thickness of cartilage on tip point in male is 2.2 mm, which thicker than in female (1.7 mm). Our results are consistent with the other foreign studies which showed that the nasal tip point has the thickest cartilage, the tip points of two domain area in both sides would build up the nasal tip. Thus, the distance between the two tip points would affect the nasal tip.

In our study, the distance between two tip points on ultrasound is more than 6 mm, which would decrease by 38.6%, and there is no significant difference in this distance between male and female. So, the prevalence of big Vietnamese nose is about 40%. The Asian nasal tip is often bigger and less prominent than the White people because [1] the fat fibre tissue of interdomal area is thicker and the distance between the tip points is larger, [2] the medial crus of LLC does not adhere to the nasal septum cartilage, [3] the Asian LLC develop less than the White's one. However, it is not smaller [1] and [4] the last important reason which affects the nasal tip is the thickness of nasal SMAS.

The results showed that this fat pad is subcutaneous, thickest at the nasal tip area, it covered all the interdomal area, about 50% patients having a medium-thick skin or above also have an interdomal fat pad and even when they have a thin skin, they also have this fat pad [12]. In our study, the interdomal fat pad is 1.8 – 3.2 mm, it lied in the interdomal area about 2.9 mm. Our results are consistent with the results of Copcu E. which found that the dimension 1.8 x 3.2 mm [12], but our results are larger than the results of Anderson K.J. [5], which found that the thickness of fat pad on nasal tip in male and female is 0.38 mm and 0.19 mm, respectively.

By investigating the relationship between two nasal tip points with the width of the nasal tip on ultrasound, we found that the relative coefficient ($r = 0.341$; $p = 0.001$) showed that the effect was at the medium level (perhaps the further the distance is, the bigger the nasal tip is).

We also considered about the correlation between the distance of two tip points and the width of interdomal fat pad in population study and us found that the relative coefficient $r = 0.72$ ($p = 0.001$), this means it is a close correlation, the width of interdomal fat pad would mostly affect the distance of two tip points, the thicker and wider this fat pad is, the bigger the nasal tip is. Based on this result, we designed a linear correlation equation: the distance between two tip points = 2.356 + 0.612 x the width of interdomal fat pad. We showed the interdomal fat pad has an important role more than the distance of two tip points and the domal divergent angle this fat pat attached to nasal SMAS. Thus, we could confirm that the nasal tip is big because of the interdomal fat pad and the thickness of nasal SMAS, which can be investigated before the operation procedure by ultrasound.

By investigating the single variable correlation between the width of nasal tip using anthropometric index on ultrasound such as the distance between two tip points and the width of interdomal fat pad, we found that there is a correlation between the width of nasal tip and the distance between two tip points, the width of interdomal fat pad and two factors above. When analysing with multivariable correlation, we noted that the width of the nasal tip has a close correlation with the distance between two tip points.

In conclusion, the height and width of the nasal tip, the protrusion of nasal tip is significantly different between male and female; the dimensions of the male are larger than of female. There is a relationship between the distance between two tip points and the width of interdomal fat pad. By investigating the nasal tip, we found that the thickness of interdomal fat pad would affect the height of the nasal tip, the distance of two tip points would affect the width of the nasal tip. During operation procedure of rhinoplasty, we should notice about the interdomal fat pad and the nasal tip.

Ethical approval

All procedures performed in studies involving human participants were in accordance with the

ethical standards of institutional and/or national research committee and with the 1964 Helsinki declaration and its later amendments or comparable ethical standards. This study was approved by The Pham Ngoc Thach university research committee with No 005.

Informed Consent

Informed consents were obtained from the patients included in the study.

Acknowledgement

We would like to thank Ms. Hoang Thi Anh (Faculty of Biology, Hanoi National University of Education, Hanoi, Vietnam) checking and improving the English in the manuscript.

References

1. Dieu PD. Anatomy of the Head, Face and Neck. Ho Chi Minh City: Medical Publshing House; 2010.

2. Soliemanzadeh P, Kridel RWH. Tip Grafts in Revision Rhinoplasty. Facial Plastic Surgery Clinics of North America. 2006; 14:331-41. https://doi.org/10.1016/j.fsc.2006.06.014 PMid:17088181

3. Burres S. Tip Points: Defining the Tip. Aesthetic Plastic Surgery. 1999; 23:113-8. https://doi.org/10.1007/s002669900252 PMid:10227911

4. Ngeow WC, Aljunid ST. Craniofacial anthropometric norms of Malays. Singapore Medical Journal. 2009; 50(5):525-8.

5. Anderson KJ, Henneberg M, Norris RM. Anatomy of the nasal profile. American Journal of Anatomy. 2008; 213:210-6. https://doi.org/10.1111/j.1469-7580.2008.00924.x PMid:19172735 PMCid:PMC2526105

6. Duskova M, Kristen M, Smahel Z. The Anthropometric Verification of Corrective Surgery Outcome in Cleft Secondary Deformities. The Journal Of Craniofacial Surgery. 2006; 17(3):447-53. https://doi.org/10.1097/00001665-200605000-00011 PMid:16770180

7. Khandekar B, Srinivasan S, Mokal N. Anthropometric analysis of lip-nose complex in Indian population. Indian Journal of Plastic Surgery. 2005; 38(2):128-31. https://doi.org/10.4103/0970-0358.19781

8. Choe KS, Yalamanchili HR, Litner JA. The Korean american woman's nose. Archives of Facial Plastic Surgery. 2007; 8:319-23. https://doi.org/10.1001/archfaci.8.5.319 PMid:16982988

9. Farkas LG, Kolar JC, Munro IR. Geography of the Nose: A Morphometric Study. Aesthetic Plastic Surgery. 1986; 10:191-223. https://doi.org/10.1007/BF01575292 PMid:3812136

10. Porter JP, Lee JI. Facial analysis: maintaining ethnic balance. Facial Plastic Surgery Clinics of North America. 2002; 10:343-9. https://doi.org/10.1016/S1064-7406(02)00030-5

11. Prendergast PM. Facial Proportions: Advanced surgical facial rejuvenation Art and Clinical practice, Springer; 2012. https://doi.org/10.1007/978-3-642-17838-2_2

12. Copcu E, Metin K, Ozsunar Y, et al. The interdomal fat pad of the nose: a new anatomical structure. Surgical and Radiologic Anatomy. 2004; 26:14-8. https://doi.org/10.1007/s00276-003-0172-4 PMid:14574464

ID Design Press, Skopje, Republic of Macedonia
Open Access Macedonian Journal of Medical Sciences. 2019 Dec 30; 7(24):4220-4223.
https://doi.org/10.3889/oamjms.2019.364
eISSN: 1857-9655
Basic and Clinical Medical Researches in Vietnam

Anatomical Characteristics of Thalamus-Cortical Sensory Tract in the Human Brain Using Diffusion Tensor Tractography at 3.0 Tesla Scanner

Lam Khanh[1], Nguyen Duy Bac[2*], Pham Thanh Nguyen[3], Tran Viet Tien[4], Vo Truong Nhu Ngoc[5], Thien Chu-Dinh[6], Nguyen Thi Phuong[7]

[1]108 Military Central Hospital, 1 Tran Hung Dao, Hai Ba Trung, Ha Noi, Vietnam; [2]Vietnam Military Medical University, Hanoi, Vietnam; [3]Hai Phong University of Medicine and Pharmacy, 72A Nguyen Binh Khiem, Ngo Quyen, Hai Phong, Vietnam; [4]103 Militæra Hospital, 26 Phung Hung, Phuc La, Ha Dong, Ha Noi, Vietnam; [5]Ha Noi Medical University, Ha Noi, Vietnam; [6]Institute for Research and Development, Duy Tan University, Danang, Vietnam; [7]NTT Hi-tech Institute, Nguyen Tat Thanh University, Ho Chi Minh City, Vietnam

Citation: Khanh L, Bac ND, Nguyen PT, Tien TV, Ngoc VTN, Chu-Dinh T, Phuong NT. Anatomical Characteristics of Thalamus - Cortical Sensory Tract in the Human Brain Using Diffusion Tensor Tractography at 3.0 Tesla Scanner. Open Access Maced J Med Sci. 2019 Dec 30; 7(24):4220-4223. https://doi.org/10.3889/oamjms.2019.364

Keywords: Somatosensory thalamocortical tract; Diffusion tensor tractography; 3.0 tesla scanner; Human brain

***Correspondence:** Nguyen Duy Bac. Vietnam Military Medical University, Hanoi, Vietnam. E-mail: nguyenduybac@vmmu.edu.vn

Received: 21-May-2019; **Revised:** 20-Sep-2019; **Accepted:** 21-Sep-2019; **Online first:** 15-Oct-2019

Funding: This research did not receive any financial support

Competing Interests: The authors have declared that no competing interests exist

Abstract

BACKGROUND: Our knowledge about characteristics of the thalamocortical tract (THT) according to the cerebral origin is still few of studies about this structure on Vietnamese.

AIM: Here, we aim to characterise the morphology of the thalamocortical tract in the human brain using diffusion tensor tractography (DTT) at 3.0 tesla scanner.

METHODS: Fifty healthy subjects have enrolled in this study. Reconstructed images of the thalamocortical tract in the human brain were built using DTT at 3.0 tesla scanner.

RESULTS: The median length of the right thalamocortical tract was 130.64 mm, and the left THT was 123.14 mm, and an average of two sides was 126.34 mm. The difference between the two sides was statically significance ($p < 0.001$). The median fibre number of the right THT was 401.50, and the left THT was 315.00, and an average of two sides was 365.50. There was a diverse branch of THT: two branches (5%); three branches (25%); four branches (42%); five branches (16%); six branches (12%); in which branched contralateral for the right was 50%, and for the left was 50%.

CONCLUSION: Using the DTI and 3D image reconstruction techniques allow to build the image of sensory THT intuitively and accurately, which helps to identify the morphological characteristic of the thalamocortical tract of healthy people without invasive effects.

Introduction

Understanding the connection in a region and among regions within the brain help to know the function and coordinating activities of those regions [1]. The nervous tract within the human brain can be determined using injecting fluorescent pigments after the autopsy; however, the distance for observing only about 10 millimetres [2]. The further distance can be identified by dissection of the large conduction bundle, or determined by degradation after a local injury [3]. However, they are invasive methods and impossible for applying in the living human brain. Studies on the conduction bundle by non-invasive methods were almost handled on animals [4], [5], and researches in the human brain using these methods are not much.

The diffusion tensor imaging (DTI) builds images based on the diffusion anisotropy of the water molecules in the axons [6], [7]. DTI is a new technique, which helps to determine the neural tracts, mostly in the living human brain. The anatomical images of sensory tract connected from the thalamus to other regions throughout the brain are important for clinical practice. However, it has not been studied well, especially in developing countries as Vietnam.

In this work, by using DTI and tractography, we studied the characteristics of somatosensory thalamocortical tract according to the cerebral origin in living subjects' brains.

Patients and Methods

Patients

This study included fifty healthy subjects, aged 18 and older. The selected subjects had no previous history of neurological, psychiatric disorders as well as physical illness.

This study was approved by the institutional review board of the 108 Military Central Hospital in Vietnam. Informed consents were obtained from the subjects included in the study. All procedures performed in studies involving human participants were in accordance with the ethical standards of the 1964 Helsinki Declaration and its later amendments or comparable ethical standards.

Diffusion Tensor Image

We have employed Phillips Achieva 3.0 T using SENSE NV 16 coil channels to obtain DTI data. The sections were made from the background to the top of the skull with the basic pulse chain T1W, T2W, and FLAIR. Imaging parameters as follows: acquisition matrix 128 x 128, FOV 230 x 230 mm^2, TR: 10172 ms, 93 ms, EPI factor b0 and b 1000 s/mm2, and 2 mm section thickness (acquired isotropic voxel size, 1.8 x 1.8 x 2 mm^3).

Fibre Tracking

Diffusion-weighted image (DWI) and DTI data were analysed using software Philips Extended MR Workspace 2.6.3.1. Construction 2D colour map of fractional anisotropy (FA) was used to seed regions of interests (ROI) according to known anatomy [8]. The first ROI was placed in the commissura cerebelli, dark blue region on the FA 2D map (Figure 1A); the second ROI was located in the thalamus (Figure 1B); the third ROI was placed in the posterior limb of capsula interna, dark blue area on the FA 2D map (Figure 1C). The software was employed to reconstruct a 3D image of the sensory thalamocortical tract (THT), that was used to analyse the length, number of the tract, and the morphologies.

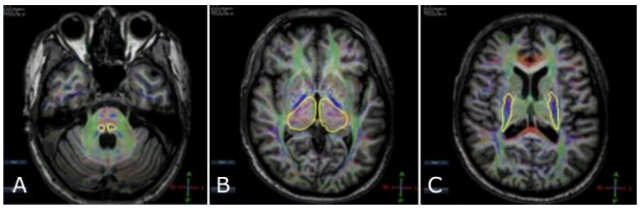

Figure 1: The seed regions of interests (ROI); The first ROI was placed in the commissura cerebelli A); The second ROI was placed in the thalamus B); The third ROI was placed in posterior of capsula interna C)

Statistical analysis

The data were statistically analysed using the SPSS software (Version 15.0; SPSS, Chicago, Illinois). The independent t-test was employed to determine the difference in length and volume of sensory THT between sexes and the two hemispheres, significant difference as $p < 0.05$. The distribution of age, sex of subjects and morphology of sensory THT was presented as the percentages.

Results

Characteristics of the subjects

In this study, subjects distributed mostly in young and middle-age with 18-39 age group accounted for 42%, the 40 – 49 age group accounted for 46%, and fewer in elder subjects with ≥ 60 age group accounted for 15%. The percentage of two genders were similar to male (52%) and female (48%) (Table 1).

Table 1: Age and genders of the subjects

	Age groups: numbers (%)			Sum
	18 – 39	40 – 59	≥ 60	
Male	9 (18%)	14 (28%)	3 (6%)	26 (52%)
Female	12 (24%)	9 (18%)	3 (6%)	24 (48%)
Both genders	21 (42%)	23 (46%)	6 (12%)	50 (100%)

Characteristics of somatosensory thalamocortical tract

The 3D reconstructed images of the somatosensory thalamocortical tract were built successfully based on diffusion tensor image and fibre tracking using the dedicated software. Then, we measured the length and counted the number of branches in each hemisphere separately (Figure 2).

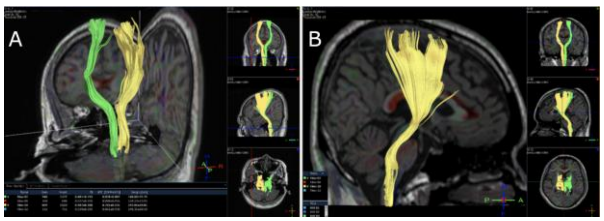

Figure 2: The 3D reconstructed images of the sensory thalamocortical tract; Green showed the tract on the right hemisphere A) and the yellow illustrated for the tract of the left hemisphere B)

The results showed that the mean length of the somatosensory thalamocortical tract on the right hemisphere (130.17 ± 11.44 mm) was statistical significance longer than the left one (121 ± 13.49 mm) ($P < 0.005$). This suggests that there were differences in the anatomical characteristics of sensory thalamocortical tract length between the right and the

left (Table 2).

Table 2: The length of the sensory of the thalamocortical tract in study subjects

The length of the sensory of the thalamocortical tract (mm)						P
Left hemisphere			Right hemisphere			
Mean (mm)	SD (mm)	N	Mean (mm)	SD (mm)	n	
121.21 mm	13.49 mm	50	130.17 mm	11.44 mm	50	< 0.05

We also investigated the influence of gender on the length of sensory of the thalamocortical tract by comparing between the sexes. Data showed that the length bunch of males tended to be longer than that of females; however, there were no significant differences between the sexes (P > 0.05) (Table 3).

Table 3: Length comparison of right and left of the sensory of the thalamocortical tract between the sexes

The length of the sensory of the thalamocortical tract (mm)							p
	Males			Females			
	Mean (mm)	SD (mm)	n	Mean (mm)	SD (mm)	n	
Left hemisphere	123.32 mm	13.22 mm	26	118.94 mm	13.70 mm	24	> 0.05
Right hemisphere	132.32 mm	12.88 mm	26	127.85 mm	9.37 mm	24	> 0.05

We counted the number of lines of the somatosensory thalamocortical tract on both sides of the hemisphere. The statistical analysis showed that the median number of the right side (401.5) tend to be higher than that of the left side (315). However, the difference was not statistically significant (P > 0.05) (Figure 3D).

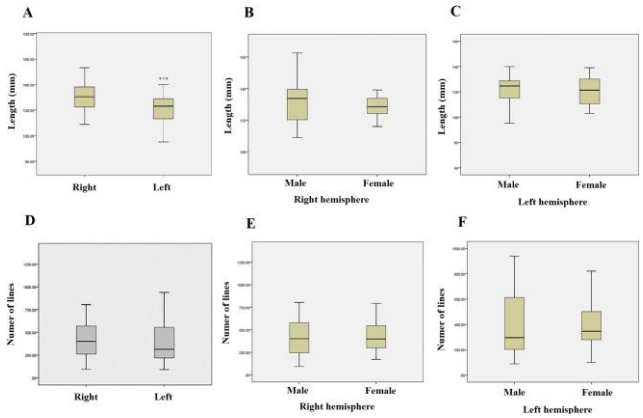

*Figure 3: The length and the number of lines of the sensory of thalamocortical tract in study subjects; Comparison of sensory thalamocortical tract length between right and left hemisphere, mean ± SD; n = 50 for each side; *** P < 0.001 left side versus right side A); Length comparison of right B) and left C) of the sensory of thalamocortical tract between the sexes, mean ± SD, males (n = 2), females (n = 24); Comparison the number of sensory thalamocortical tract lines between right and left hemisphere, mean ± SD, n = 50 for each side D); Comparison on the number of lines of right E) and left F) of the sensory of thalamocortical tract between two genders, mean ± SD, males (n = 26), females (n = 24)*

Comparison of the number of somatosensory thalamocortical tract lines between two genders showed that the lines of the right side were equivalent in the two sexes, in the left side the lines of males tend to lower than females, but no statistically significant difference (P > 0.05) (Figure 3E and 3F).

Based on the 3D reconstructed images of the somatosensory thalamocortical tract and the number of branches, we classified the branching morphology as following: 2, 3, 4, 5, 6 or contralateral branches (Figure 4 and Table 4).

Table 4: The branch morphology distribution of the sensory thalamocortical tract

	Branch morphology (%)		Sum
	Right hemisphere	Left hemisphere	
2 branches	3 (3%)	2 (2%)	5 (5%)
3 branches	14 (14%)	11 (11%)	25 (25%)
4 branches	22 (22%)	20 (20%)	42 (42%)
5 branches	6 (6%)	10 (10%)	16 (16%)
6 branches	5 (5%)	7 (7%)	12 (12%)
Contralateral branches	6 (50%)	6 (50%)	12 (100%)

The data showed that somatosensory thalamocortical tract was the polymorphic branch. Most abundance was four-branches-morphology (42%); other morphologies were found including three branches (25%), five branches (16%), six branches (12%), and the two branches (5%). Obtained images showed that the appearance of the branch was into the contralateral hemispheres, with the left and right ratio equal on each side.

Discussion

Our data showed that the length of the somatosensory thalamocortical tract on the right hemisphere (130.17 ± 11.44 mm) was statistically significantly longer than that on the left hemisphere (121 ± 13.49 mm). But, the study done by Kamali et al., on the sensations in the brain stem showed that there was similar in length between the right and the left sides [9]. The differences between our and Kamali's results can be explained by the fact that the different anatomical locations can lead to differences over the structure. Moreover, there are always differences in general function and sensory conduction, in particular, between two sides of the brain [10], which may lead to changes along the length of the somatosensory thalamocortical tract between the two sides. The length of the somatosensory thalamocortical tract in males tend to be longer than in females in this study, and this may be due to the brain of male larger than female [11]. However, the difference was not statistically significant, and this may be due to not large enough in the size of the subjects in our study.

The number of the somatosensory thalamocortical tract lines was higher in the right hemisphere (401.5) than that in the left hemisphere (315.0), but the difference was not statistically significant. This result may be due to the majority of subjects in this study were right-handed persons, which can make the sensory transduction differences between the right and left side of the body [12], [13]. In order to clarify this, extensive research with a larger

number of subjects are needed. In the relationship between gender and number of the somatosensory thalamocortical tract t lines, notably the number on the left side in males (295.5) was much lower than that in females (347.0), while the number on the right side was almost equivalent between males (401.5) and females (398.5). These differences are quite interesting, but larger studies are required to clarify these phenomena.

Our data showed that the somatosensory thalamocortical tract was the polymorphic branch. The diversity of morphology may be related to the function, distribution of nerve conduction bundles, and the diversity of subjects (gender, age, etc.).

Using the diffusion tensor imaging for studying the anatomical characteristics of the somatosensory thalamocortical tract is a new advanced technique not only in Vietnam but also in the world. So far, this is the ideal method which allows studying the white matter, designated the nerves and neurotransmitters on the non-invasive living body [14], [15].

In conclusion, the data in this study can be used as anatomical reference parameters for the understanding function of the brain in sensory transduction from the thalamus to the cortex. Our finding is also the basis for the assessment and detection of function area in the brain, and for understanding the mechanics of some diseases related to brain injury and nerve conduction clinically such as stroke, degenerative myelin, diffuse axonal injury, and Wallerian degeneration. The results of the study also open up the new directions for DTI application to study neurotransmitter activity under physiological conditions and diseases for understanding the function of neural activity in clinical applications.

References

1. Passingham RE, Stephan KE, Kötter R. The anatomical basis of functional localization in the cortex. The anatomical basis of functional localization in the cortex. Nat Rev Neurosci. 2002; 3(8):606-16. https://doi.org/10.1038/nrn893 PMid:12154362

2. Mufson EJ, Brady DR, Kordower JH. Tracing neuronal connections in postmortem human hippocampal complex with the carbocyanine dye DiI. Neurobiol Aging. 1990; 11(6):649-53. https://doi.org/10.1016/0197-4580(90)90031-T

3. Van Buren JM, Borke RC. Variations and Connections of the Human Thalamus 2. New York.: Springer-Verlag, 1972. https://doi.org/10.1007/978-3-642-88594-5 PMCid:PMC1355386

4. Scannell JW, et al. The connectional organization of the cortico-thalamic system of the cat. Cereb Cortex. 1999; 9(3):277-99. https://doi.org/10.1093/cercor/9.3.277 PMid:10355908

5. Barbas H, Pandya DN. Architecture and frontal cortical connections of the premotor cortex (area 6) in the rhesus monkey. J Comp Neurol. 1987; 256(2):211-28. https://doi.org/10.1002/cne.902560203 PMid:3558879

6. Basser PJ, Mattiello J, LeBihan D. Estimation of the effective self-diffusion tensor from the NMR spin echo. J Magn Reson B. 1994; 103(3):247-54. https://doi.org/10.1006/jmrb.1994.1037 PMid:8019776

7. Basser PJ, Mattiello J, LeBihan D. MR diffusion tensor spectroscopy and imaging. Biophys J. 1994; 66(1):259-67. https://doi.org/10.1016/S0006-3495(94)80775-1

8. Akter M, Hirai T, Sasao A, Nishimura S, Uetani H, Iwashita K, Yamashita Y. Multi-tensor tractography of the motor pathway at 3T: a volunteer study. Magn Reson Med Sci. 2011; 10(1):59-63. https://doi.org/10.2463/mrms.10.59 PMid:21441730

9. Kamali A, Kramer LA, Butler IJ, Hasan KM. Diffusion tensor tractography of the somatosensory system in the human brainstem: initial findings using high isotropic spatial resolution at 3.0 T. Eur Radiol. 2009; 19(6):1480-8. https://doi.org/10.1007/s00330-009-1305-x PMid:19189108

10. Kobayashi M, Takeda K, Kaminaga T, Shimizu T, Iwata M. Neural consequences of somatosensory extinction: an fMRI study. J Neurol, 2005; 252(11):1353-8. https://doi.org/10.1007/s00415-005-0865-1 PMid:16314997

11. Luders E, Gaser C, Narr KL, Toga AW. Why sex matters: brain size independent differences in gray matter distributions between men and women. J Neurosci. 2009; 29(45):14265-70. https://doi.org/10.1523/JNEUROSCI.2261-09.2009 PMid:19906974 PMCid:PMC3110817

12. Patel A, Mehta A. A Comparative Study Of Nerve Conduction Velocity Between Left And Right Handed Subjects. Int J Basic Appl Physiol. 2012; 1(1):19-21.

13. Tan U. Sensory nerve conduction velocities are higher on the left than the right hand and motor conduction is faster on the right hand than left in right-handed normal subjects. Int J Neurosci. 1993; 73(1-2):85-91. https://doi.org/10.3109/00207459308987214 PMid:8132422

14. Han BS, Ahn SH, Jang SH. Cortical reorganization demonstrated by diffusion tensor tractography analyzed using functional MRI activation. NeuroRehabilitation. 2008; 23(2):171-4. https://doi.org/10.3233/NRE-2008-23206 PMid:18525138

15. Hong JH, Son SM, Jang SH. Identification of spinothalamic tract and its related thalamocortical fibers in human brain. Neurosci Lett. 2010; 468(2):102-5. https://doi.org/10.1016/j.neulet.2009.10.075 PMid:19879333

ID Design Press, Skopje, Republic of Macedonia
Open Access Macedonian Journal of Medical Sciences. 2019 Dec 30; 7(24):4224-4229.
https://doi.org/10.3889/oamjms.2019.365
eISSN: 1857-9655
Basic and Clinical Medical Researches in Vietnam

Research on Macroanatomic and Histologic Characteristics of the Lower Lateral Nasal Cartilages in Vietnamese

Tran Dang Khoa[1], Ho Nguyen Anh Tuan[1], Nguyen Duy Bac[2], Nguyen Thanh Van[3], Pham Dang Dieu[1], Nguyen Thi Phuong[4], Vu Thi Nga[5], Toi Chu Dinh[6*]

[1]Department of Anatomy, Pham Ngoc Thach University of Medicine (PNTU), Ho Chi Minh City, Vietnam; [2]Department of Anatomy, Vietnam Military Medical University (VMMU), Hanoi, Vietnam; [3]Thanh Van Cosmetic Surgery Hospital, Ho Chi Minh City, Vietnam; [4]NTT Hi-tech Institute, Nguyen Tat Thanh University, Ho Chi Minh City, Vietnam; [5]Institute for Research and Development, Duy Tan University, Danang, Vietnam; [6]Department of Human and Animal Physiology, Faculty of Biology, Hanoi National University of Education, Hanoi, Vietnam

Citation: Khoa TD, Tuan HNA, Bac ND, Van NT, Dieu PD, Phuong NT, Nga VT, Chu Dinh T. Research on Macroanatomic and Histologic Characteristics of the Lower Lateral Nasal Cartilages in Vietnamese. Open Access Maced J Med Sci. 2019 Dec 30; 7(24):4224-4229. https://doi.org/10.3889/oamjms.2019.365

Keywords: Lower lateral cartilages; interdomal ligament; interdomal fat pad

***Correspondence:** Toi Chu Dinh. Department of Human and Animal Physiology, Faculty of Biology, Hanoi National University of Education, Hanoi, Vietnam. E-mail: chudinhtoi@hnue.edu.vn

Received: 28-May-2019; **Revised:** 20-Sep-2019; **Accepted:** 21-Sep-2019; **Online first:** 15-Oct-2019

Funding: This research did not receive any financial support

Competing Interests: The authors have declared that no competing interests exist

Abstract

BACKGROUND: There are recently many studies about the anatomy of lower lateral cartilage (LLC). However, the microanatomic studies to identify the segments of most LLC at the nasal tip in Vietnamese are very rare.

AIM: Investigate the macroanatomic and microanatomic characteristics of the LLC and the structures of the nasal tip.

METHODS: Descriptive study, 30 cadaver noses fixed by 10% formalin, 2 cadaver noses fixed by HE in 69 Institutes in Vietnam from December 2017 to April 2019.

RESULTS: The average length of the medial crus is 12.3 mm on the right and 13.2 mm on the left. The maximum intercrural distance is 10.7 mm. The average length of the dome is 3.7 mm and 3.9 mm on the right and left side separately, with 2 subunits are the domal and lobular segment. The average thickness of the tip points is 1.0 mm. The width of the interdomal and intercrural ligaments are 0.5-fold the height and 2-fold the thickness. The thickness of the interdomal fat pad is 3mm and about 0.5-fold the wide.

CONCLUSION: The LLC has 3 parts: intermediate, medial and lateral crus. The microanatomic structures of tip consist of the interdomal ligaments, intercrural ligaments, SMAS and interdomal fat pad.

Introduction

External nasal is one of the human organs which are operated most in cosmetic surgery, especially in Asian countries due to high demands of rhinoplasty. The characteristics of the Asian nose structure are large tips and low nose bridges [1]. The rhinoplasty is not only putting an implant to lift nose bridge, but also refining tip of the nose as well as alar base reduction, and it includes nasal osteotomies, etc. The lower lateral cartilage (LLC) plays an important role in reconstructing the tip of nose; particularly the structures form pyramidal nose such as medial and lateral crus, dome of LLC including tip point, the tripod concept as well as the definition about M-arc, the nasal tip support including interdomal ligaments, intercrural ligaments, skin cartilage make a ratio between compression and tension forces, which affect the outcome of rhinoplasty [2]. If surgeons understand clearly about these anatomies, they can choose the appropriate surgery methods for rhinoplasty of the nasal tip [3]. There are recently many studies about the anatomy of lower lateral cartilage. However, the microanatomic studies to identify the segments of most LLC at the nasal tip in Vietnamese are very rare [4], [5], [6]. Based on the upper demands, we carried out the study "Research on macroanatomic and histologic characteristics of the lower lateral nasal cartilages in Vietnamese" with two objects: *1. Investigating the macroanatomic and histologic*

characteristics of segments of LLC: lateral, medial and intermediate crus and 2. Investigating the macroanatomic and histologic characteristics of the structures related to nasal tip in Vietnamese.

Materials and Methods

Study design

Descriptive cross-sectional study

Study population

Group 1: Investigating the macroanatomic features of 30 Vietnamese adult cadavers fixed by formalin 10% at Anatomy Department of Pham Ngoc Thach University of Medicine.

Group 2: Investigating the microanatomic features of 2 noses of Vietnamese adult cadavers fixed by hematoxylin-eosin at 69 Institute (Ha Noi).

We chose the convenience sampling method:

- Inclusive criteria: 1. Vietnamese adult cadavers who were 18 years old or more; 2. The cadavers whose pyramidal noses were integrated and they had never undergone rhinoplasty before; and 3. There were no malformation, tumour or abnormalities in facial structure.

- Exclusive criteria: we excluded the cadavers who had a malformation of the pyramidal nose, had undergone in nasal cavities or had destroyed structures due to storage method or inappropriate fixing.

Study period

From December 2017 to April 2019.

Investigating anatomic features

We revealed the tip of the nose based on open nasal surgery method, then identified LLC and the related structure around the LLC near the nasal tip. We measured the length of crus and footplate, the distance between crural, the length and width of two subunits: domal and lobular segment, the thickness of cartilage at the nasal tip, the width and height of triangular soft tissue. We investigated interdomal ligaments, intercrural ligaments and interdomal fat pad.

Investigating micro anatomic features

With two cadavers, we cut all the nasal root area with the upper border is a line crossing through two internal ends of supraorbital ridge, the outer borders runs along the outer border of nasal bone, alar nostril and the lower border is a line running along the lower border of alar nostril and footplate of the nose, we fixed them with formol 10% for histopathology. Then the nasal-frontal bone samples were demineralised by acid citric 5% to become soft tissues. After blocking paraffin, we cut slices by microtome machine and collected 4 µm-width slices, then we stained the samples based on HE method (Hematoxylin – Eosin), and observed those with an optical microscope in 4, 10, 20, 40 objectives to identify the major alar nostril and the related structures.

Statistics

The histopathologic images were read by Image Pro Software at 69 Academy, Tomb Security Command. They were recorded by Olympus camera inside the microscope.

Analysing and processing the statistical tests by SPSS 19. We used the statistical tests such as t-test and χ^2 and p-value < 0.05 was considered statistically significant.

Results

Characteristics of samples: We investigated the anatomic features of 30 Vietnamese cadavers, the sample included 20 males (62.5%) and 12 females (37.5%), the average age of our sample is 67.3 ± 16.7 years old (ranging from 21 to 93 years old).

Characteristics of the lower lateral cartilage

The length of collumelar crus was more than the length of footplate crus about 2 mm, and the internal legs (tripod) in both sides were about 15 mm long, the dimensions are different between left and right side.

Table 1: The dimensions of medial crus in Vietnamese cadavers

Dimension (mm)	Right	Left	p-values
Length of medial crus	12.3 ± 2.9	13.2 ± 2.2	0.076[e]
Width of medial crus	3.5 ± 1.2	3.2 ± 1.2	0.007[e]
Thickness of cartilage	0.8 ± 0.2	1.0 ± 1.0	0.346[e]
Intercrural distance	3.2 ± 1.4		
Length of footplate crus	0.5 ± 0.8		
The maximum distance between two footplate crus	10.7 ± 2.5		

c. T - student test; e. Mann - Whitney test.

The length of the medial crus in our sample was 12 – 13 mm (Table 1). We found that the prevalence of the separation of upper crus was 60%

in both sides and there was a significant difference between left and right side, the maximum distance between two crus, which is called the intercrural space, was 3.2 mm.

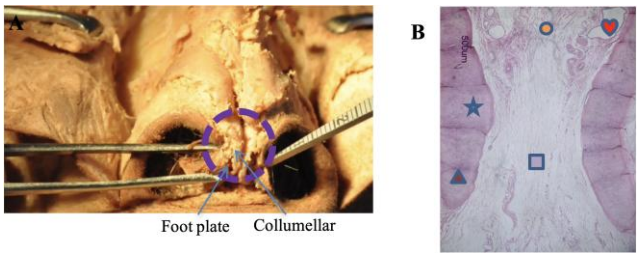

Figure 1: Medial crus in macroanatomic feature A) and in microanatomic feature, B) corresponding to the circle area in A); (*) Notes: the footplate are separated (□), the crus are converted (✱), the collagen fibres run in the intercrural space (□), the collagen fibres of interdomal ligaments ( ) and the vessels of interdomal area (♥)

Meanwhile, the part in which footplate crus (Figure 1) did not separate was very small (0.5 mm) and most of these were separated far from each other to fin nasal base, and the maximum distance between two footplates was 11 mm (about 4 times more than the intercrural space).

Table 2: The dimensions of intermediate crus in Vietnamese cadavers

Dimension (mm)	Right	Left	p-values
The length of lobular subunit	3.0 ± 1.1 mm	3.0 ± 1.1 mm	0.884[e]
The length of domal subunit	4.9 ± 2.0 mm	5.0 ± 2.3 mm	0.655[e]
The width of lobular subunit	3.7 ± 1.1 mm	3.9 ± 2.1 mm	0.434[e]
The width of domal subunit	4. ± 1.4 mm	4.5 ± 1.6 mm	0.254[e]

e. Mann-Whitney test.

The domal subunit was longer than the lobular one about 2 mm (Table 2 and Figure 2), and there was no significant difference between the dimension in both sides.

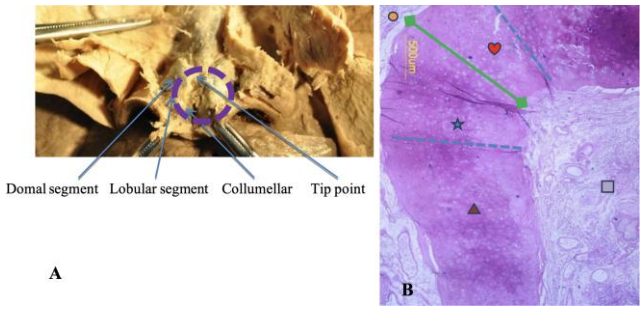

Figure 2: The boundary of lobular and domal segments in intermediate crus and tip A); the specimen of the continual zone of domal area and the medial crus B); corresponding to the circle area in A); (*) Notes: the medial crus (□), the lobular segment (✱), the collagen fibres of interdomal ligaments ( ), the domal segment (♥), the triangular soft tissue is connective tissue (□), the green arrow is the tipping point

The height of the triangular soft tissue was about 5 mm, which equals ½ the width and the dimensions in both sides were significantly different (Table 3).

Table 3: The triangular soft tissue in the cadavers

Dimension (mm)	Right	Left	p-values
Width	10.2 ± 2.4 mm	10.5 ± 3.5 mm	0.0001[e]
Height	4.7 ± 1.5 mm	4.6 ± 1.2 mm	0.020[e]

e. Mann-Whitney test.

The thickness of intermediate crus was more than 1 mm; there was no significant difference between the two sides in the cadavers. The distance between tip points was 6.8 mm.

Table 4: The thickness of cartilage of intermediate crus in Vietnamese cadavers

Dimension (mm)	Right	Left	p-values
Lobular segment	1.2 ± 0.3 mm	1.2 ± 0.3 mm	0.650[e]
Domal segment	1.2 ± 0.3 mm	1.3 ± 0.3 mm	0.065[e]
Tip points	1.0 ± 0.5 mm	0.9 ± 0.2 mm	0.386[e]
Distance between tip points	6.8 ± 2.7mm		

e. Mann-Whitney test.

The total length of right and left lateral crus were 18.5 and 17.5 mm, respectively; the width at the middle point of lateral crus was 8.5 mm; the dimensions of the tail of lateral crus were about ½ the dimensions of lateral crus; the thickness of cartilage was about 0.8 mm. The parallel direction of lateral crus was 40.0% (12 out of 30 cadavers), and the oblique direction was 60.6% (18 out of 30 cadavers) (Table 5).

Table 5: The dimensions of lateral crus in Vietnamese cadavers

Dimensions		Right	Left	p-values
Length	From lateral genu to the boundary of tail	12.3 ± 2.4 mm	12.1 ± 2.3 mm	0.626[e]
	Tail	6.1 ± 2.7 mm	5.5 ± 2.1 mm	0.150[e]
	All lateral crus	18.5 ± 3.9 mm	17.5 ± 2.9 mm	0.305[e]
Width	At lateral genu	8.0 ± 1.8 mm	8.1 ± 1.8 mm	0.750[e]
	At the middle of lateral crus	8.5 ± 1.4 mm	8.5 ± 1.2 mm	0.969[e]
	At tail	5.0 ± 1.8 mm	4.6 ± 0.9 mm	0.245[e]
Thickness of the cartilage	At lateral genu	0.9 ± 0.2 mm	0.8 ± 0.2 mm	0.524[e]
	At the middle of lateral crus	0.8 ± 0.2 mm	1.1 ± 1.7 mm	0.387[e]
	At tail	0.7 ± 0.2 mm	0.7 ± 0.2 mm	0.176[e]

e. Mann – Whitney test.

The nasal tip supports

The width of the interdomal ligaments was about 4 mm (Table 6 and Figure 3 and Figure 4), which equals ½ the height and two times the thickness.

Table 6: The dimensions of interdomal ligament in Vietnamese cadavers

Dimension	Average value
Height	8.0 ± 4.8 mm
Width	4.2 ± 2.4 mm
Thickness	1.8 ± 1.0 mm

The intercrural ligament in cadavers was average 3.1 ± 1.3 mm wide, which equals ½ the length (5.8 ± 1.6 mm) and two times the average thickness of the intercrural ligament (1.6 ± 0.8 mm).

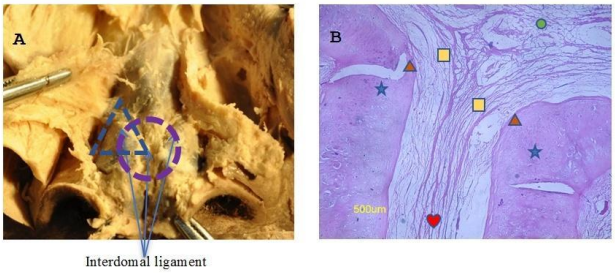

Figure 3: The interdomal ligament runs from interdomal area to the upper border of LLC and the lateral nasal valve (based on the new point of view) in anatomic feature A) and in microanatomic feature B); corresponding to the circle area in A); (*) Notes: the tip point of domal area (intermediate crus) (✶), the fat cells of the interdomal fat pad ( ), the collagen fibres in the intercrural ligament (♥), which continue with the interdomal ligament (□)

The interdomal fat pad in cadavers was average 7.9 ± 3.8 mm wide, and 11.5 ± 3.8 mm long, however, the average thickness of it was just 1.5 ± 1.1 mm.

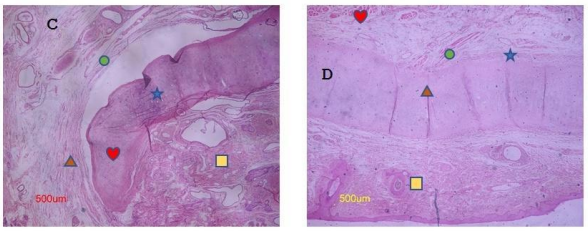

Figure 4: The microanatomic feature of the lateral crus at the tail C) and the lateral nasal valve D); corresponding to the triangle area in A); (*) Notes for C): the interdomal ligament ( ), which includes many collagen fibres running in the upper face of LLC (✶), lasts long and covers the lateral crus, lateral nasal valve and the tail of lateral crus (♥), the subcutaneous tissues in the inner face of nasal vestibule (□); (*) Notes for D): the specimen of lateral crus and lateral nasal valve; B): the lateral nasal valve area (△), which has a place for attachments of the collagen fibre bundles of nasal SMAS and the interdomal ligament, that ligament supports to the lateral nasal valve ( ), nasal muscles (♥), the collagen fibres of interdomal ligament running toward the lateral crus (✶), skin and subcutaneous tissues of the mucosa in the inner nose have a hair follicle structure (□)

The thickness of the interdomal fat pad was 3 mm, which equals ½ the width (6.5 mm), and this fat pad runs along from the interdomal area up to the nose bridge about 15 mm and the thickness was 3.3 mm (Figure 5 and Figure 6).

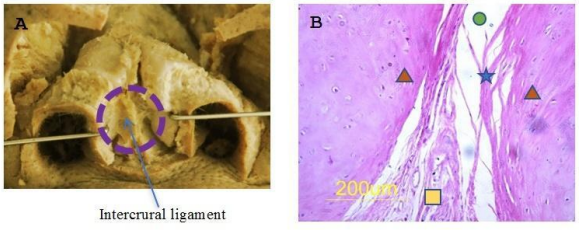

Figure 5: The intercrural ligament in anatomic feature (A) and in microanatomic feature B), corresponding to the circle area in A); (*) Notes: the medial crus of the LLC (△), the collagen fibers of the intercrural ligament (✶), the fibers run across the intercrural area ( ), the connective tissues, fat cells, vessels and the footplate (□)

Discussion

The length of medial crus in our sample was 12-13 mm, which was shorter than Polselli R. [7]; his result was 16 – 24 mm. The difference is easily explained due to the difference in races so that the crus is longer and affects to the protruding of the nose.

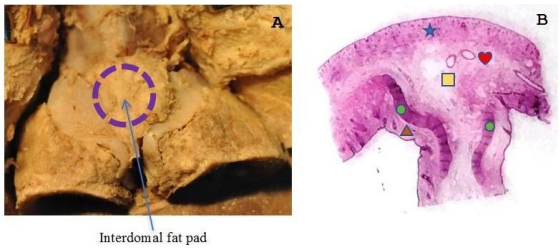

Figure 6: The interdomal fat pad in anatomic feature A) and in microanatomic feature B); corresponding to the circle area in A); (*) Notes: the thickened skin on the nasal tip (✶) and the thickened subcutaneous area (♥) mixed with the interdomal fat tissues (□), which lied on the dome of LLC (□)

The length of footplate crus, which is rarely described in standard books, in our study was about 5 – 5.7 mm and the distance between two crus was 10.7 mm. This was consistent with the results of Byrd H.S. [3], the result was 4 – 7.5 mm (average 11.4 mm). Moreover, we noticed that the prevalence of the separation of upper crus was 60% in both sides and there was a significant difference between left and right side, the maximum distance between two crus, which is called the intercrural space, was 3.2 mm. Meanwhile, the part in which footplate crus did not separate was very small (0.5 mm) and most of these were separated far from each other to fin nasal base, and the maximum distance between two footplates was 11 mm (about 4 times more than the intercrural space).

Tailing W [8] found that the distance between two tip points was the most important factor. However, it is noticed that the effect of this factor is not strong, this effect is from many other factors such as the angle of subunits, the interdomal fat pad, the thickness of skin on nasal tip and the thickness of nasal SMAS so based on one or more coherent factors, we chose the different processes. Burres S [9] concluded that the interdomal distance of the tip points was variously based on sex and race, there was no significant difference in that distance, however, there was statistically different in the distance between the interdomal subunit with tip point of nose, that meant the smaller the distance was, the higher the tipping point was. Moreover, two tip points of the pair of LLC were made of a triangular soft tissue without cartilage in the superior-inferior LLC.

The height of this triangle in our study was about 5 mm, which equals ½ the width and the area was about 25 mm^2, the dimensions of this triangle

were significantly different on both sides. This is the place which a surgeon does not notice much, and it can affect to nasal gap when we sew the wound after surgery procedure with a strict suture tightening force.

Moreover, Tai-ling W. [8] noted that the distance between two average tip points was about 5 or 6 mm if the distance was more than 6 mm, that meant the patient nasal tip was big. In our study, this distance in the cadavers was 6.8 mm, which was more than the distance measured in human by sonography (5.6 mm). Thus, if we based on this result, we could assume that the Vietnamese nasal tip had not been big. However, when being measured by anthropometry, most Vietnamese has a big nasal tip. So which factors can affect the size of the Vietnamese nasal tip although the distance between two tip points is not more than 6mm? This can be explained partly based on the reason that two domal subunits and the medial line made an angle about 80^0, which affected the distance between two tip points. The thickness of the skin in the tip is one of the negative factors for the procedure to refine the nasal tip; this thickness was investigated by observation, touch or using sonography to measure.

The lateral crus ran parallel to the border of the nostril, the outer part ran toward and made an angle 15° with the border of nostril [5]. However, Constantian M.B. [2] found that after moving out of lateral genu, the lateral crus ran parallel to ⅓ border of nostril and then toward with an angle 30-45° or more; Sheen noticed that this change would make the tip of nose bigger, the result was consistent with our study's result that 60% lateral crus run obliquely. Thus, investigating the dimensions of lateral or medial crus will help to build data for rhinoplasty in Vietnamese, the length is ranged 16 – 24 mm, the width is ranged 4 – 10 mm, the distance from the lower border of LLC to the border of nostril varies based on the measured point and the measurer, about 6mm when we chose the middle point of domal cartilage, 5 mm when we measured from the middle point of lateral crus, 13 mm when we measured from the farthest point of the end of lateral crus [5], these results are consistent with our results (the length was 18 mm, the width at the middle point was 8.5 mm and the thickness was 1 mm).

To sum up, Vietnamese noses have the medial and lateral crus, which are shorter than the white ones. Thus, most of the rhinoplasty is grafting cartilage to lengthen the legs of the tripod. It should notice that the shape of lateral crus, as well as the flexure of medial crus, will affect the dimensions. We also investigated the relationship between the lateral crus and outer leg with the shape of lateral crus to examine if the deformation of lateral crus affected these dimensions in both sides and we discovered that the deformation did not affect the length of lateral crus as well as an outer leg of the tripod.

The width of the interdomal ligaments is about 4 mm, which equals ½ the height and two times the thickness. Based on the dissection procedure in cadavers and the results of Saban Y. [6], we noticed that the definition of Anderson was not correct when we widen the origin of domal ligament.

The reason is that most of the investigated milestones were cut off during rhinoplasty along the outer incision. With the inner incision in nasal augmentation, when dissecting to put the implant, the implant may be upper or lower the domal ligament. In our study, the best position was lower the domal ligament so that the implant did not appear in the nasal tip when nasal augmentation. In other words, the interdomal ligament was just in the interdomal area, Saban Y. [6] confirmed that there was no widen interdomal area, it is just the nasal SMAS, so within the limit of our study, we cannot demonstrate that in histopathology. So, we offer more studies about the role of this area in histopathology and Vietnamese patients.

The intercrural ligament in cadavers is average 3.1 ± 1.3 mm wide, which equals ½ the length (5.8 ± 1.6 mm) and two times the average thickness of the intercrural ligament (1.6 ± 0.8 mm). During the dissection procedure, we found that this ligament was under the interdomal ligament and linked these ligaments together, there often had a fat pad being between two medial crus, that fat pad was less or more. This result was consistent with other studies [10], [11].

In our result, the thickness of the interdomal fat pad was 3mm, which equals ½ the width (6.5 mm), and in fact, this fat pad runs along from the interdomal area up to the nose bridge about 15 mm and the thickness is 3.3 mm (Pic 4). This fat pad is in most of the cadavers we investigated; it is different from the result of El-Shaarawy E.A.A [5], the researcher found that about 6.5% sample had no interdonal fat pad. However, most of the other studies found that the fat pad often exits in spite of the size of the nasal tip. In some foreign studies, this fat pad is subcutaneous, which is the thickest on the nasal tip, it covers all the interdomal area, about 50% patients with skin thickness from medium level and above always have this fat pad and even patients with thin skin still have [10], [11]. In our study, both cadaver and patient groups had the interdomal fat pad whose size ranged 1.8 – 3.2 mm, and this pad lied in the interdomal area about 2.9 mm, this result was consistent with Copcu E., in which the size of fat pad was 1.8 x 3.2 mm [4], the thickness of this in the nasal tip of male and female are 0.38 mm and 0.19 mm, respectively.

In conclusion, the lower lateral cartilages include 3 subunits: the lateral, the intermediate – domal and the medial crus. The direction of the lateral crus was running obliquely upward, that was 60% of the sample. Thus, the distance between lateral genu equals ½ the distance from the tail of LLC to the anterior border of the nostril. The intermediate crus was 8 mm long; the domal area was 4.5 mm wide, the

characteristic of Vietnamese domal area was that the angle of subunits was wide and obtuse, while two domal areas concentrate on the medial line, so the angle of two subunits is less than 90°, it is highest at the dome called the tipping point, the interdomal ligament covers that area. Between two parts of the medial crus, there are connective ligament fibres.

With the nasal tip supporting: the width of the interdomal and intercrural ligaments equals ½ the height and two times more than the thickness. The thickness of the interdomal fat pad is 3 mm, which equals ½ the width. In histopathology, we could observe these structures which the nasal tip supports.

Ethical Approval

All procedures performed in studies involving human participants were in accordance with the ethical standards of institutional and/or national research committee and with the 1964 Helsinki declaration and its later amendments or comparable ethical standards. This study was approved by the Pham Ngoc Thach University research committee with No 003.

Acknowledgements

We want to thank Ms Bui Nhat Le (Faculty of Clinical Pharmacy, University of Pharmacy, Hanoi, Vietnam) for checking and improving the English in the manuscript.

References

1. Quyen NQ. Human species. Ho Chi Minh City: Science and Technics Publishing House.1978;

2. Constantian MB. Four Common Anatomic Variants that Predispose to Unfavorable Rhinoplasty Results: A Study Based on 150 Consecutive Secondary Rhinoplasties. Plastic And Reconstructive Surgery. 2000; 105(1):316-31. https://doi.org/10.1097/00006534-200001000-00051

3. Byrd HS. Rhinoplasty. Selected readings in plastic surgery. 2001; 9(18):1-51.

4. Copcu E, Metin K, Ozsunar Y, et al. The interdomal fat pad of the nose: a new anatomical structure. Surgical and Radiologic Anatomy. 2004; 26:14-8. https://doi.org/10.1007/s00276-003-0172-4 PMid:14574464

5. El-Shaarawy EAA. Morphological and morphometrical study of the cartilaginous framwork of the dorsum and tip of the nose among populations: cadaveric study. Folia Morphol. 2016; 75(3):316-25. https://doi.org/10.5603/FM.a2016.0008 PMid:26916202

6. Saban Y, Amodeo CA, Hammou JC, et al. An Anatomical Study of the Nasal Superficial Musculoaponeurotic System. Archives of Facial Plastic Surgery. 2008; 10(2):109-15. https://doi.org/10.1001/archfaci.10.2.109 PMid:18347238

7. Polselli R, Saban Y, Braccini F. Anatomie artistique du nez. Rhinoplastie Editions: Les minographies du CCA Groupe N0 32. Livraison France, 2002.

8. Tai-ling W, Zhi-qiang X, Da-shan Y, et al. Rhinoplasty in Chinese: management of lower dorsum and bulbous nasal tip. Chinese Medical Journal. 2009; 122(3):296-300.

9. Burres S. Tip Points: Defining the Tip. Aesthetic Plastic Surgery. 1999; 23:113-8. https://doi.org/10.1007/s002669900252 PMid:10227911

10. Ishii CH. Current update in Asian rhinoplasty. Plastic and Reconstructive Surgery Global Open. 2014; 2(4):1-8. https://doi.org/10.1097/GOX.0000000000000081 PMid:25289326 PMCid:PMC4174207

11. Siemionow MZ. Plastic and Reconstructive Surgery. 313 Springer Specialist Surgery Series: Springer-Verlag London Limited, 2010.

ID Design Press, Skopje, Republic of Macedonia
Open Access Macedonian Journal of Medical Sciences. 2019 Dec 30; 7(24):4230-4238.
https://doi.org/10.3889/oamjms.2019.366
eISSN: 1857-9655
Basic and Clinical Medical Researches in Vietnam

Anatomical Characteristics of Facial Nerve Trunk in Vietnamese Adult Cadavers

Tran Dang Khoa[1], Nguyen Duy Bac[2], Hoang Van Luong[2], Tran Ngoc Anh[2], Nguyen Thi Phuong[3], Vu Thi Nga[4], Toi Chu Dinh[5*]

[1]Department of Anatomy, Pham Ngoc Thach University of Medicine (PNTU), Ho Chi Minh City, Vietnam; [2]Department of Anatomy, Vietnam Military Medical University (VMMU), Hanoi, Vietnam; [3]NTT Hi-tech Institute, Nguyen Tat Thanh University, Ho Chi Minh City, Vietnam; [4]Institute for Research and Development, Duy Tan University, Danang, Vietnam; [5]Department of Human and Animal Physiology, Faculty of Biology, Hanoi National University of Education, Hanoi, Vietnam

Citation: Khoa TD, Bac ND, Luong HV, Anh TN, Phuong NT, Nga VT, Chu Dinh T. Anatomical Characteristics of Facial Nerve Trunk in Vietnamese Adult Cadavers. Open Access Maced J Med Sci. 2019 Dec 30; 7(24):4230-4238. https://doi.org/10.3889/oamjms.2019.366

Keywords: Facial nerve; Superior ramus; Inferior ramus; Mandibular angle; Retromandibular vein

***Correspondence:** Toi Chu Dinh. Department of Human and Animal Physiology, Faculty of Biology, Hanoi National University of Education, Hanoi, Vietnam. E-mail: chudinhtoi@hnue.edu.vn

Received: 28-May-2019; **Revised:** 20-Sep-2019; **Accepted:** 21-Sep-2019; **Online first:** 15-Oct-2019

Funding: This research did not receive any financial support

Competing Interests: The authors have declared that no competing interests exist

Abstract

BACKGROUND: In medical literature, there are few studies provided a precise and detailed description of the facial nerve rami and its branches.

AIM: Identify several practical anatomic landmarks related to the facial nerve main trunk and its rami.

METHODS: A descriptive study, 30 cadavers in the anatomy department of UPNT from October 2012 to April 2015.

RESULTS: The average distance from the mandibular angle to the division of the facial nerve is 40.8 mm, and is 86.6% from range 36 – 50 mm. There is 86.7% case in which the facial nerve is in the lateral of the retromandibular vein, and there is a significant difference about both sides. Eighty percent of the case has the superior and inferior ramus in the lateral to the retromandibular vein. There are 2 cases in which the superior ramus makes the circle of the vein. Eighty percent of the facial nerve is in the lateral to the external carotid artery.

CONCLUSION: The distance from the mandibular to the division of the facial nerve is longer. The relationship between the superior/inferior ramus and the retromandibular vein maybe not the same in both sides. In some cases, it makes the circle of the vein to cause some complication in the parotid gland surgery.

Introduction

In medical literature, even though many authors already have done many studies about the facial nerve anatomy on Caucasian and non-Caucasian race, specifically about its course through the parotid gland, its rami and its branching pattern to innervate its end-organ, none of them provided precise and detailed description about its rami and its branches [1], [2]. Also, they notice that the variability of the facial nerve origin and ramification proximal to the intraparotid course have an intimate anatomic relationship with other structures such as the digastricus, the mastoid process, the mandibular angle, the retromandibular vein, the external carotid artery, etc. [1], [3]. Therefore, achieving a basic understanding of the exact course of the facial nerve in the parotid gland and its rami is critical for every surgeon to prevent facial nerve injury in parotid gland-related surgeries. There are anatomic landmarks that help pinpoint the facial nerve trunk, e.g. mastoid process, posterior belly of the digastricus, tragal "pointer", retromandibular vein, etc. [4]. The key to successfully locate the facial nerve trunk lies in those landmarks that act as reference points for the surgeons to predict the safety of nearby structures. Additionally, given that these reference points are fixed during surgery, they should be easily palpable and should permit surgeons to quickly, safely identify

and preserve anatomic structures.

Based on our assumptions as mentioned above, we've decided to conduct a study on "The anatomic characteristics of the facial nerve trunk in Vietnamese cadavers". This study aims to *(1) describe the facial nerve trunk anatomy as well as its rami in Vietnamese adult cadavers, (2) to identify several practical anatomic landmarks related to the main trunk and its rami.*

Materials and methods

Design

Descriptive cross-sectional study, on 30 hemifaces that belong to formalin-treated male and female Vietnamese cadavers, at the Department of Anatomy of Pham Ngoc Thach University of Medicine, from October 2012 to April 2015. We used a convenient sample from the available population of cadavers at the university. The average age of the cadavers is 70, in which female accounts for 33.3% and male 66.7% (10 females: 20 males).

The inclusion criteria were: 1. Vietnamese adult cadaver, older than 18 years of age; 2. The head, face, and neck must be intact with no previous surgical history in these regions; and 3 — the normal anatomy of the head, face, and neck. No deformities or tumours allowed.

Exclusion criteria: All cadavers that have deformities in the head, face and neck region, as well as damaged cadavers due to dissection errors or previous facial, parotid gland-related surgeries.

Dissection techniques and data collection

First, an incision was made along the external auditory canal – lateral canthus, and then continued the incision along the orbital rim, 30 mm above the supraorbital margin. The incision will go from the superolateral orbital rim to the aperture of the external auditory canal and run along the superior temporal line. Then make an incision from the earlobe and continue parallel with the mandibular ramus and then go along the orbicularis oris. The skin is then separated, the second layer is then exposed, continue dissecting the second layer into the third layer; the incision is perpendicular with external auditory canal – lateral canthus line and is 40mm lateral to the external ear canal, and the inferior incision still goes along the mandibular ramus. These incisions will be dissected into the third layer. Dissecting the third layer (SMAS) based on the available incisions, reflecting the SMAS the zygoma superiorly, until the flap reaches the zygomatic and orbital ligaments, masseteric ligaments anteriorly, and mandibular ligaments inferiorly. Continue dissecting the SMAS towards the orbicularis oculi muscle, the temporal, the nose, mouth, chin, and neck.

Figure 1: Exposed third layer (SMAS)

The fourth layer is exposed, namely sub-SMAS (Figure 1), the parotid fascia is dissected carefully so that facial nerve branches are not damaged. Identify anatomic landmarks such as the mastoid process, the suprasternal notch, and the clavicles to mark the anterior margin of the sternocleidomastoid muscle. Expose the following landmarks: the cartilaginous portion of the ear canal and the posterior belly of the digastricus. The facial nerve trunk usually lies deep, 10 – 15 mm below the anteroinferior margin of the cartilaginous portion of the ear canal (so-called tragal "pointer"), and 10 mm below and deep to the midpoint of the posterior belly of the digastricus. After identifying the facial nerve trunk, proceed to dissect along the main trunk to expose the two following rami: zygomaticotemporal ramus and the cervicofacial branch, sometimes a third ramus can exist. Dissect and expose the retromandibular vein and the external carotid artery.

List of parameters to be collected

- Relationship between the retromandibular vein and the facial nerve rami: whether the vein is lateral or medial to the nerve.

- Relationship between the superior, inferior division and the retromandibular vein.

- Relationship between the external carotid artery and the main trunk as well as its ramification: whether the artery is lateral or medial to the nerve.

- The number of branches of the temporofacial ramus and the cervicofacial ramus.

- Branching pattern of the facial nerve main

trunk based on Tsai's studies and branching pattern of its division based on Davis et al. classification.

- Mean distance of the facial nerve trunk from the skin surface after it emerges from the stylomastoid foramen.

- Mean angle formed by the facial nerve rami: superior, middle, inferior and other division (if available).

- Diameter and length of the facial nerve trunk, superior and inferior division.

All parameters are collected into a data sheet (see attached files). Measurement values are rounded to the nearest tenth.

Materials

Measurements and data were collected using: - A Nikon D90 digital single-lens reflex camera, Macro lens equipped; - A dissection kit: scalpel, dissection knife, Kelly clamp, Allis clamp, toothed and non-toothed forceps, single-prong hook, double-prong hook; and - Measurement devices include: analogue calliper, a compass, a depth gauge, a protractor.

Statistical procedures

- Raw data were collected from measurement records and encoded in corresponding variables. These statistics are analysed by calculating Pearson's Chi-squared exact test as well as Student's t-test using SPSS 19.0. Measurements are rounded to the nearest tenth, and $p < 0.05$ is considered statistically significant.

Results

In this study, we've done dissections on 30 hemifaces with an average of 70, in which female accounts for 33.3% and male 66.7%.

We identify the facial nerve trunk quickly and safely using the centre of the triangle formed by the temporomandibular joint, mastoid process and the angle of the mandible, as these reference points are easily palpable during the dissection. Besides, we also employ the commonly accepted classical approach to localise the facial nerve trunk for its safety as it exits the stylomastoid foramen, which is to find landmarks such as the posterior belly of the digastricus to measure its depth, the mandibular angle, the retromandibular vein, and the tragal "pointer". In this approach, the relationship between the nerve trunk and the retromandibular vein along with the bifurcation location of the former about the mandibular angle and the posterior belly of the digastricus are easily identified concerning the tragal "pointer" (Figure 2), because its reference point is difficult to localise.

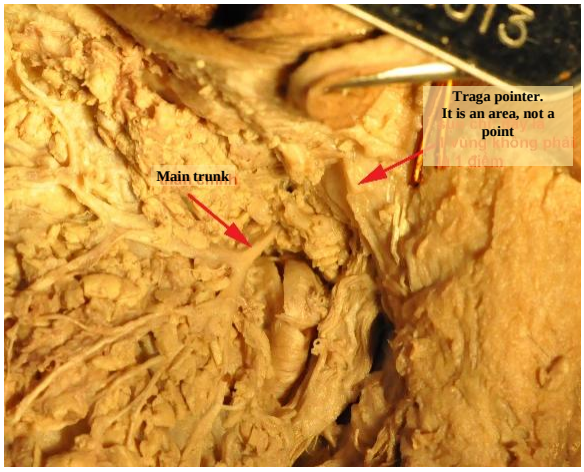

Figure 2: Tragal pointer pointing at the main trunk of the facial nerve

Anatomical characteristics of facial nerve main trunk

There is only a single facial nerve trunk (Figure 3) emerging from the stylomastoid foramen, and no specimen has been found to have a double trunk.

Mean distance of the right facial nerve trunk from the skin surface after it emerges from the stylomastoid foramen is 28.9 mm, which is deeper than that of the left side, 25.1 mm, and this difference is statistically significant.

The average length of the facial nerve trunk is 14.1 mm. The facial nerve trunk diameter is 2.5 mm.

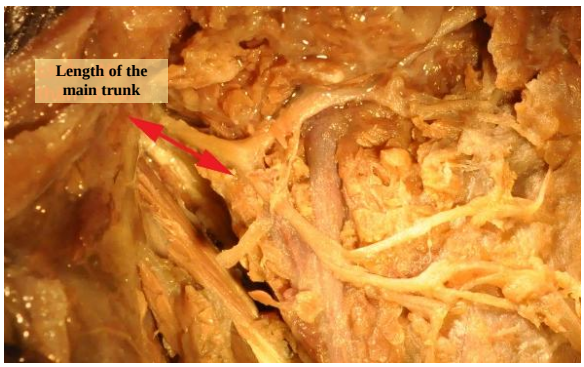

Figure 3: Length of the facial nerve trunk

The average number of divisions is 2.1 on both sides, in which bifurcation of the trunk mostly accounts for 93.3% and trifurcation only accounts for 6.7%.

The angle formed by the superior and inferior division of the main trunk appears to be almost

perpendicular to each other, an angle of 91.2°, in which 66.7% of our specimens are acute, and 33.3% are obtuse.

Mean superior division length is 15.2 mm, which is much shorter than that of inferior division, 23.6 mm.

There are three branching patterns (Figure 4) of the facial nerve trunk, according to Tsai:

- Pattern 1: the main trunk divides into superior and inferior division, closely followed by the bifurcation of the marginal and cervical branches. 20.0% of our specimens displayed this pattern.

Figure 4: Branching pattern 1 of the facial nerve trunk

- Pattern 2 (Figure 5), is the largest group (60% right-sided and 66.7% left-sided), the upper and lower trunks divide, then branch into their 5 respective classical divisions.

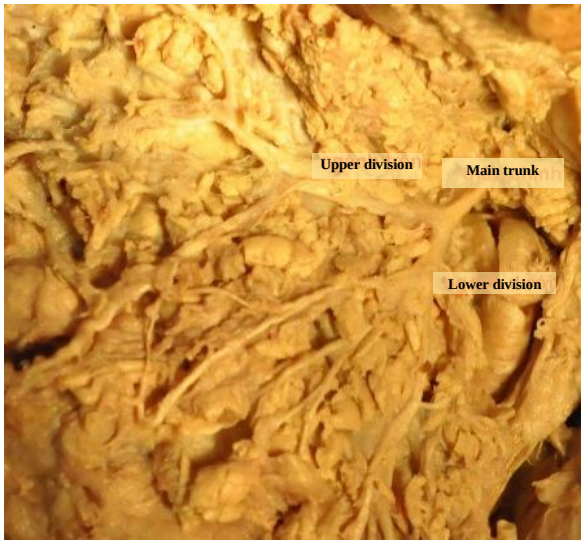

Figure 5: Branching pattern 2 of the facial nerve trunk

+ Pattern 3 (Figure 6): 20% right-sided and 13.3% left-sided, the upper-division branches immediately after the bifurcation of the upper and lower divisions.

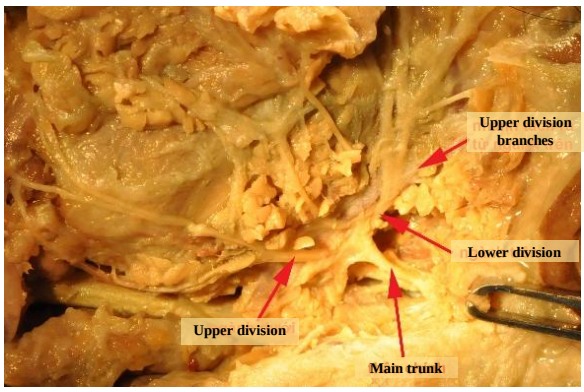

Figure 6: Branching pattern 3 of the facial nerve trunk

Facial nerve main trunk localisation method and its application

The distance (Figure 7) from the mandibular angle to the bifurcation location of the facial nerve is 40.8 mm.

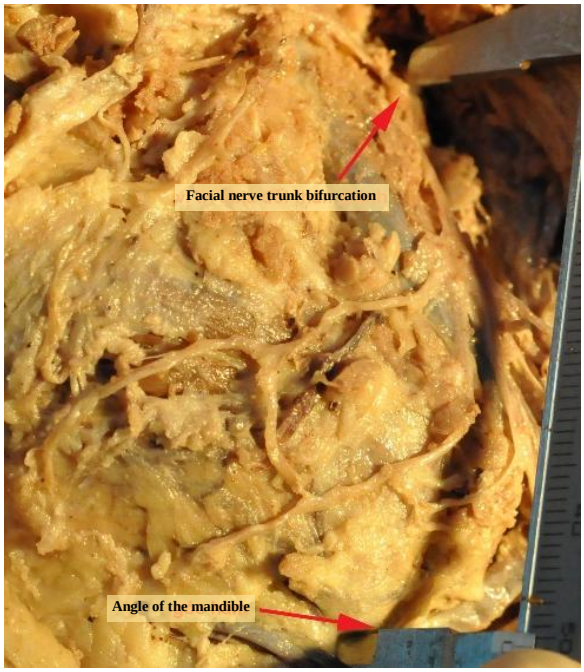

Figure 7: The distance from the angle of the mandible to the facial nerve trunk bifurcation

The distance from the mandibular angle to the bifurcation ranges from 36 – 50 mm and accounts for 86.6% on both sides.

We found that 86.7% of our specimens have facial nerves running laterally to the retromandibular vein on both sides and this difference is statistically significant about the location of the facial nerve to the retromandibular vein on both sides with p = 0.03, which means the location of the nerve about the vein is not identical on both sides.

In our study, 80% of specimens on both sides, the superior division runs laterally to the retromandibular vein, and we found this difference in the location of the superior division with the vein to be statistically significant on both sides. As for the inferior division, it runs laterally to the vein in 80% of cases on both sides, and we found no statistically significant difference about the location of the facial nerve with the vein on both sides (Figure 8).

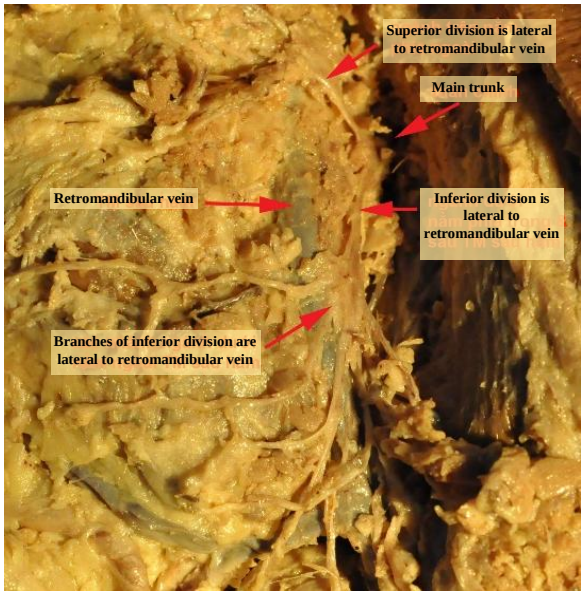

Figure 8: The inferior division's relation to the retromandibular vein, but its branches and the superior division are lateral to the vein

Discussion

Based on our findings, we conclude that there is only a single facial nerve trunk emerging from the stylomastoid foramen and no specimen has been found to have a double trunk, including one domestic study by Thanh N.V. (1997) [4]. However, a foreign study by Kilic C. has noted the existence of the double facial nerve trunk exiting the stylomastoid foramen [5]. Besides, a study by Katz and Catalano shows that 3% of their specimens have double facial nerve trunk [6], and 4.4% and 13.3% in another study by Park and Lee [7]. Does this inconsistency require a larger sample of cadavers, as well as the need for radiographic characteristics in Vietnamese adults to see whether a double facial nerve trunk exists or not?

Mean distance of the right facial nerve trunk from the skin surface after it emerges from the stylomastoid foramen is 28.9 mm, which is deeper than that of the left side, 25.1 mm. This difference is statistically significant in a way that surgeons have to take precautions when carrying out the surgery on the left hemiface and children because the facial nerve is more superficial in the latter. Therefore in our study, the location of the facial nerve regarding the skin surface appears to be deeper than that of Myint K [8] (from 10 – 20 mm deeper than the skin), but more superficial than that of Rodrigues (50 mm) [9]. This variation is influenced by many factors which can be different among individuals and races, e.g. skin thickness, subcutaneous tissue, SMAS layer, sub-SMAS layer, and the parotid parenchyma (Table 1).

Table 1: Comparison of length of the facial nerve trunk in literature

Author	Length (mm)
Thanh N.V [4]	22.4
Salame [10]	16.4
Kandari [11]	10 – 15
Dias F.L [12]	13
Rodrigues [9]	10
Ekinci [13]	9
Kwak [14]	9.38
Our study	14.1

The average length of the facial nerve trunk is 14.1 mm, which is shorter when compared to studies of Thanh N.V (22.4 mm) [4] and Salame (16.44 mm) [10], but is equivalent to results from Kandari (from 10 – 15 mm) [11] and Dias F.L (13 mm) [12]. Furthermore, our measurements are longer than those of Rodrigues (about 10 mm) [9], Ekinci (9 mm) [13] and Kwak (9.38 mm) [14]; this difference might vary due to an individual's race and ramification of the main trunk. Salame emphasised the importance of its length in facial nerve anastomosis because the trunk needs to be long enough to allow anastomosis with other branches without being too overstretched or too slack [10].

The average number of divisions is 2.1 on both sides, in which bifurcation of the trunk mostly accounts for 93.3% and trifurcation only accounts for 6.7%; this is in agreement with findings of Myint K [8]. However, as Park and Lee's recommendation stated, surgeons should be suspicious for the presence of the third division as they can accidentally damage it [7]. Based on our findings, trifurcation takes up 6.7% which is in agreement with Park and Lee's findings, 4.4% [7]; but our findings are lower than that of Thanh N.V (24%) [4], Kalaycioğlu A (18.8%) [15], Ekinci (18.6%) [13] and Kopuz (18%) [16], and higher than that of Salame (2.2%) [10]. This disparity might be due to racial factors or inherent inaccuracy in our insufficient sample. Nevertheless, the probability of having the third division is non-negligible (albeit small) has an important meaning to all surgeons: pay attention to its probable existence and avoid injuring it.

Besides, we found that the angle formed by the superior and inferior division of the main trunk appears to be almost perpendicular to each other, an angle of 91.2°, in which 66.7% of our specimens are acute, and 33.3% are obtuse. This is in agreement with Myint K's findings in a way that when the nerve reaches the posterior border of the mandibular ramus, its divisions almost form a perpendicular angle [8]. Meanwhile, Thanh N.V's findings show that 56% are obtuse, and 44% are acute [4]. Mathematically, any angle greater than 90° is obtuse, and if it's less than

90°, it will be an acute angle. However, in our study, the values of the angle formed by the superior and inferior division vary around 90, or in other words, they form a perpendicular angle.

Mean superior division length is 15.2 mm, which is much shorter than that of inferior division, 23.6 mm. This finding is statistically significant and in agreement with Thanh N.V's findings, in which the former is 15.1 mm but the latter is notably shorter that of ours, 12.4 mm [4] (Table 2). This inconsistency in the inferior division is due to individual variability as in our study it travels a considerably long course after its branching from the main trunk before dividing into the mandibular branch, the cervical branch or the anastomotic branch. As for the diameter, the superior is 2 mm and inferior division is 1.4 mm, but when we use paired t-test to compare between the two, the finding isn't statistically significant ($p > 0.05$). Therefore, the diameter of the two is identical. Compared to another domestic study by Thanh N.V, the superior division diameter is 1.94 mm, which agrees with our findings, but the interior diameter is smaller, 1.07 mm [4]. In contrast with international findings by Myint K, the superior temporofacial division has a diameter nearly twice that of the inferior ramus [8]. As for Pia F's findings, the superior division runs in a superomedial fashion and has a greater diameter [17].

Table 2: Comparison of pattern ratio in literature

Author	Pattern 1 (%)	Pattern 2 (%)	Pattern 3 (%)
Tsai [18]	24.7	42.0	33.3
Thanh N.V [4]	10.0	82.0	6.0
Our study	20.0	60.0	20.0

Specifically, 60% of our specimens display pattern 2 on both sides and the ratio between patterns is not statistically significant. Pattern 1 and 3 take up 20% evenly. Compared to Tsai's findings, 24.7% of their specimens display pattern 1 (the main trunk divides into superior and inferior division, closely followed by the bifurcation of the marginal and cervical branches), which agrees with our findings; as for pattern 2 (the upper and lower trunks divide, then branch into their 5 respective classical divisions), their findings are lower than those of us (42%); regarding pattern 3, their findings are higher than those of us [18]. Compared to Thanh N.V's findings, type 1 (equivalent to Tsai pattern 2) accounts for 82%; type 2 (Tsai pattern 3) accounts only 6% and type 3 (Tsai pattern 1) accounts 10% [4].

The distance from the mandibular angle to the bifurcation location of the facial nerve is 40.8 mm, which agrees with Thanh N.V's findings of 38.6 mm [4]. This can be explained by the fact that both authors have conducted their corresponding studies on Vietnamese, so the mandibular ramus length is approximately identical. Besides, according to other authors' explanation, this distance in Caucasian is remarkably longer due to their greater body size as well as larger, stronger mandible. However, in our study, the distance from the angle to the bifurcation is longer than that of international counterparts, such as Myint K (28.06 mm, range from 11 – 40 mm) [8], McCormack (34 mm on Caucasian, range from 14 – 46.9 mm) [19], Davis et al. (32mm, range from 25 – 45 mm) [20], Park and Lee (28.8 mm on Korean, ranging from 12.1 – 39.8 mm) [7]. Is the facial nerve trunk in Vietnamese truly located at a higher position than other races? To achieve this finding, we need to conduct a study with large enough samples together with location comparison between the main trunk and the mandibular angle about the zygomatic arch.

Besides, the distance from the mandibular angle to the bifurcation ranges from 36 – 50 mm and accounts for 86.6% on both sides, which is drastically higher than Myint K's findings, in which most of their specimens (81.0%) has the bifurcation 21 – 35 mm above the mandibular angle [8] (Table 3).

Table 3: Comparison of distance from the angle of the mandible to the bifurcation of the facial nerve with Myint K's findings

Distance in mm	Myint K.		Our study	
	Number	Proportion (%)	Number	Proportion (%)
11 – 15 mm	3	3.8%	0	0%
16 – 20 mm	6	7.6%	0	0%
21 – 25 mm	12	15.2%	0	0%
26 – 30 mm	30	38.0%	0	0%
31 – 35 mm	22	27.8%	3	10.0%
36 – 40 mm	6	7.6%	14	46.7%
41 – 45 mm	0	0%	8	26.7%
46 – 50 mm	0	0%	4	13.3%
51 – 55 mm	0	0%	1	3.3%
	79	100.0%	30	100.0%

We also noticed that the distance from the mandibular angle to the bifurcation of the facial nerve ranges from 31 – 55 mm, compared to Myint K's findings of 11 – 40 mm [8], which means if we divide the distance into 5mm portion, we can miss the in-between values. This could mean that in our upcoming study, maybe we should calculate the ratio between the distances from the bifurcation to the whole mandibular ramus length so that it may be more significant. Identifying the distance from the angle of the mandible to the bifurcation is critical to clinical otolaryngology as it prevents facial nerve injury during parotid gland-related surgeries.

We found that 86.7% of our specimens have facial nerves running laterally to the retromandibular vein on both sides and this difference is statistically significant about the location of the facial nerve to the retromandibular vein on both sides with $p = 0.03$, which means the location of the nerve concerning the vein isn't identical on both sides. This finding agrees with Alzahrani, in which 83% of their specimens have facial nerve running laterally to the retromandibular vein, and 17% lies medially to the vein, and this relationship isn't identical on both sides [21]. As for Astik R.B, their findings show that 90% of retromandibular vein lies medially to the temporofacial and cervicofacial division, 10% of their specimens have divisions running laterally to the vein, as the main trunk and its divisions form a "fork" that runs between the mandibular and the superficial temporal vein [22].

In our study, 80% of specimens on both sides, the superior division runs laterally to the retromandibular vein, and we found this difference in the location of the superior division with the vein to be statistically significant on both sides. As for the inferior division, it runs laterally to the vein in 80% of cases on both sides, and we found no statistically significant difference about the location of the facial nerve with the vein on both sides. This is in agreement with Kim et al. findings, larger inferior division mostly runs laterally to the retromandibular vein (83%), and few of them (17%) goes medially to the vein [23]. As for Wang et al., 100% of cases have mandibular branch running at a more superficial layer to the retromandibular vein [3]; Dingman found that 98% of retromandibular veins run medially to the marginal branch and only 2% runs laterally [24]; Savary et al., found that the all cervicofacial division run laterally to the retromandibular vein [25]. Therefore, despite disparities in each of the division's proportion, most of the authors concluded that over 80% of the main trunk, a superior and inferior division run laterally to the retromandibular vein and the location of the facial nerve concerning the nerve might be different between the two sides. Also, we found no difference about the location of the superior and inferior division concerning the right retromandibular vein, but we found a statistically significant difference about the superior division with the left vein ($p = 0.024$). This shows that, on the same individual, the location of the superior and inferior division about the vein can be different ipsilaterally or bilaterally, and the nerve-vein relationship doesn't appear to obey any law as shown by Laing and McKerrow's findings in which the superior division runs laterally and medially to the vein while the inferior division runs laterally [1].

Unexpectedly, Toure G. et al., study shows that there are 4 cases in which the retromandibular vein forms a ring through which the facial nerve trunk travel (2 cases) and the remaining 2 cases have the inferior division goes inferiorly to this venous ring [2]. Also, Alzahrani noted that the retromandibular vein forms two rings and both superior and inferior division go through these rings [21]. This is in contrast with our study in a way that our finding shows the superior division forms a ring around the retromandibular vein (Figure 9), and as a consequence, encountering this variation may increase facial nerve injury risk or cause bleeding during parotid gland tumour removal. In normal anatomical settings, the facial nerve runs laterally to the vein, so bleeding risk due to nerve injury is negligible. However, in special cases, the retromandibular vein runs laterally to the main trunk or its division, so bleeding and facial nerve injury risk will be substantially higher in parotid gland tumour removal surgery.

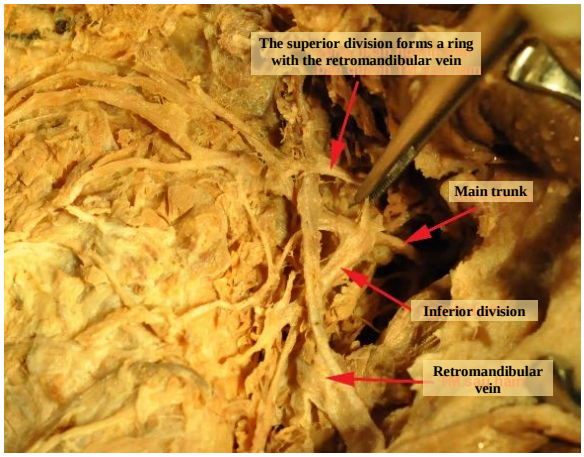

Figure 9: The superior division forms a ring with the retromandibular vein

As for otolaryngology application, Alzahrani F. R. used the retromandibular vein to identify the facial nerve by first successfully identifying the former at the cervical region and then dissect in an upwards fashion to the inferior division of the facial nerve as the latter usually lies superficial to the retromandibular vein. After successfully pinpointing the inferior division, the facial nerve will be identified and exposed [21]. This is the method commonly employed by various authors in the world. As for Ariyoshi and Shimahara [26], they provide standards based on the retromandibular vein. If the vein is pushed medially or the vein is not displaced, and the location of the tumour lies laterally to this vein, the tumour is considered to be lying in the superficial portion of the parotid gland. The method of using the retromandibular vein as an anatomic landmark in preoperative radiography has an accuracy of up to 86.4%. Therefore, a basic understanding of the existence of the changing relationship between the facial nerve and the retromandibular vein is not only important in evaluating preoperative safety but also has great value in locating the location of the parotid gland tumour, but this prediction doesn't guarantee 100% accuracy.

Application perspective of the study

The dissection technique described in the study can assist surgeons in recognising the facial nerve trunk and its rami before surgical dissection, which will avoid damage to this nerve. In particular, we defined the relationship between the retromandibular vein and the facial nerve rami; the superior, inferior division and the retromandibular vein; diameter and length of the facial nerve trunk as compared to other literature studies. This allows scientists to acknowledge the variations of facial nerve distribution in response to racial factors, individual background, personal landmarks. According to our knowledge, this study was the first research about this subject to be conducted in Southeast Asia. In general,

our results can be indicated as a useful surgical guide. Future studies are justified to determine further research on the variability in ramification patterns of the facial nerve among distinct racial and ethnic groups. Other studies using alternative research methods such as external palpation landmarks, facial nerve electrical stimulation should also be performed to optimise the accurate results, lesser time consumption and improve cost-efficiency.

Our findings about the anatomical characteristics of the facial nerve main trunk and its division include: all cadavers have a unique trunk exiting from the stylomastoid foramen, none of the specimens has been found to have double trunk, the distance of the facial nerve to the skin surface on the right side is deeper than the left side which must be respected during surgery. Mean trunk length is 14.1 mm, the diameter of 2.5 mm, an average number of divisions is 2.1 in which bifurcation proportion accounts for 93.3%, and the third division may exist and might be damaged intraoperatively. The angle formed by the superior and inferior division appears to be almost perpendicular (91.2^0), and mean superior division length is 15.2 mm, which is notably shorter than inferior division, 23.6 mm. We found that most of our specimens displayed Tsai pattern 2 (60%).

To identify the main trunk and its division, we found that the distance from the angle of the mandible to its bifurcation location is 40.8 mm, which is considerably longer than other authors due to the bifurcation lies at a higher level and the distance to the bifurcation ranges from 36 – 50 mm, which accounts for 86.6%. Based on our findings, to avoid facial nerve injury during parotid gland-related surgery, surgeons need to correctly identify the facial nerve bifurcation along the posterior border of the mandibular ramus to the mandibular angle. Approximately 86.7% of cases have facial nerve running laterally to the retromandibular vein on both sides, and over 80% of the superior and inferior division run laterally to the retromandibular vein. Based on this finding, we conclude that the location of the superior and inferior division about the retromandibular vein may not be identical ipsilaterally and bilaterally, and this nerve-vein relationship doesn't seem to obey any law. Also, we found that the superior division forms a ring around the retromandibular vein, and bleeding and facial nerve injury risk might be increased during parotid gland tumour removal procedures.

Acknowledgements

We want to thank Mr Ninh Tung Duong (Faculty of Biology, Hanoi National University of Education, Hanoi, Vietnam) and Ms Tran Uyen Ngoc (Faculty of Veterinary Medicine, Nong Lam University, Ho Chi Minh, Vietnam) checking and improving the English in the manuscript.

References

1. Laing MR, McKerrow WS. Intraparotid anatomy of the facial nerve and retromandibular vein. Br J Surg. 1988; 75(4):310-312. https://doi.org/10.1002/bjs.1800750405 PMid:3359141

2. Touré G, Vacher C. Relations of the facial nerve with the retromandibular vein: anatomic study of 132 parotid glands. Surg Radiol Anat. 2010; 32(10):957-961. https://doi.org/10.1007/s00276-010-0674-9 PMid:20473672

3. Wang TM, Lin CL, et al, Surgical anatomy of the mandibular ramus of the facial nerve in Chinese adults. Acta Anat (Basel). 1991; 142(2):126-131. https://doi.org/10.1159/000147176 PMid:1781251

4. Thanh NV. Study the types of branching of the parotid facial nerve applied in parotid gland surgery. University of Medicine and Pharmacy at Ho Chi Minh City: Master's thesis in Medicine, 1997.

5. Kirici Y, Kilic C, Kazkayasi M. Topographic anatomy of the peripheral branches of the facial nerve. Journal of Experimental and Integrative Medicine. 2011; 1(3):201-204. https://doi.org/10.5455/jeim.040711.br.005

6. Katz AD, Catalano P. The clinical significance of the various anastomotic branches of the facial nerve. Report of 100 patients. Arch Otolaryngol Head Neck Surg. 1987; 113:959-962. https://doi.org/10.1001/archotol.1987.01860090057019 PMid:3606847

7. Park IY, Lee ME. A morphological study of the parotid gland and the peripheral branches of the facial nerve in Koreans. Yonsei Med J. 1977; 18:45-51. https://doi.org/10.3349/ymj.1977.18.1.45 PMid:617028

8. Myint K, Azian AL, Khairul A. The clinical significance of the branching pattern of the facial nerve in Malaysian subjects. Med. J. Malaysia. 1992; 47(2):114-120.

9. Rodrigues AC, et al. Anatomy of the Facial Nerve and its Implication in the Surgical Procedures. Int. J. Morphol. 2009; 27(1):183-186. https://doi.org/10.4067/S0717-95022009000100031

10. Salame K, Ouaknine GER, et al. Microsurgical anatomy of the facial nerve trunk. Clin Anat. 2002; 15:93-99. https://doi.org/10.1002/ca.1102 PMid:11877786

11. Kandari QAA. Facial Paralysis: Reconstructive Surgery: State of Art Egypt. J Plast Reconstr Surg. 2011; 35(2):317-324.

12. Dias FL, Roberto AL, Jorge P. Practical Tips to Identify the Main Trunk of the Facial Nerve. Pearls and Pitfalls in Head and Neck Surgery: Basel Karger, 2008.

13. Ekinci N. A study on the branching pattern of the facial nerve of children. Kaibogaku Zasshi. 1999; 74:447-450.

14. Kwak HH, et al. Branching patterns of the facial nerve and its communication with the auriculotemporal nerve. Surg Radiol Anat. 2005; 26:494-500. https://doi.org/10.1007/s00276-004-0259-6 PMid:15368081

15. Kalaycioğlu A, Yeginoğlu G, et al. An anatomical study on the facial nerve trunk in fetus cadavers. Turkish Journal of Medical Science. 2014; 44:484-489. https://doi.org/10.3906/sag-1302-145 PMid:25558653

16. Kopuz C, Turgut S, et al. Distribution of facial nerve in parotid gland: analysis of 50 cases. Okajimas Folia Anat Jpn. 1994; 70:295-300. https://doi.org/10.2535/ofaj1936.70.6_295 PMid:8041565

17. Pia F, et al. Centripetal approach to the facial nerve in parotid surgery: personal experience. Acta Otorhinolaryngol Ital. 2003; 23:111-115.

18. Tsai SC, Hsu HT. Parotid neoplasms: diagnosis, treatment, and intraparotid facial nerve anatomy. The Journal of Laryngology & Otology. 2002; 116(5):359-62. https://doi.org/10.1258/0022215021911013 PMid:12080993

19. McCormack D, Cauldwell EW, Anson BI. The surgical anatomy of the facial nerve with special reference to the parotid gland. Surg Gynecol and Obstet. 1945; 80:620-630.

20. Davis RA, Anson BJ, et al. Surgical anatomy of the facial nerve and parotid gland based upon a study of 350 cervicofacial halves. Surg Gynecol Obstet. 1956; 102:385-412.

21. Alzahrani FR, Alqahtani KH. The facial nerve versus the retromandibular vein: a new anatomical relationship. Head Neck Oncol. 2012; 4(4):82.

22. Astik RB, Dave UH, Gajendra KS. Variant position of the facial nerve in parotid gland. International Journal of Anatomical Variations. 2011; 4:3-4.

23. Kim DI, et al. The marginal mandibular branch of the facial nerve in Koreans. Clin Anat. 2009; 22(2):207-214. https://doi.org/10.1002/ca.20739 PMid:19089998

24. Dingman RO, Grabb WC. Surgical anatomy of the mandibular ramus of the facial nerve based on the dissection of 100 facial halves. Plast Reconstr Surg Transplant Bull. 1962; 29:266-272. https://doi.org/10.1097/00006534-196203000-00005 PMid:13886490

25. Savary V, Robert R, et al. The mandibular marginal ramus of the facial nerve: An anatomic and clinical study. Surg Radiol Anat. 1997; 19:69-72. https://doi.org/10.1007/BF01628127 PMid:9210238

26. Ariyoshi Y, Shimahara M. Determining whether a parotid tumour is in the superficial or deep lobe using magnetic resonance imaging. J Oral Maxillofac Surg. 1998; 56(1):23-26. https://doi.org/10.1016/S0278-2391(98)90909-0

ID Design Press, Skopje, Republic of Macedonia
Open Access Macedonian Journal of Medical Sciences. 2019 Dec 30; 7(24):4239-4243.
https://doi.org/10.3889/oamjms.2019.367
eISSN: 1857-9655
Basic and Clinical Medical Researches in Vietnam

Quality of Life and Suitability with Vietnamese Harmonious Face Index in Class III Malocclusion Patients

Nguyen Hoang Minh[1], Truong Manh Dung[1], Vo Truong Nhu Ngoc[1], Pham Hoang Tuan[2], Nguyen Hong Ha[3], Le Van Son[1], Nguyen Thi Thu Phuong[1], Hoang Thi Doi[4], Vo Van Thanh[5], Thien Chu Dinh[6], Nguyen Thi Phuong[7], Toi Chu Dinh[1, 8*]

[1]School of Odonto Stomatology, Hanoi Medical University, Hanoi, Vietnam; [2]Hanoi National Hospital of Odontostomatology, Hanoi, Vietnam; [3]Viet Duc Hospital, Hanoi, Vietnam; [4]Hanoi Medical College, Hanoi, Vietnam; [5]Hanoi Medical University, Hanoi, Vietnam; [6]Institute for Research and Development, Duy Tan University, Danang, Vietnam; [7]NTT Hi-tech Institute, Nguyen Tat Thanh University, Ho Chi Minh City, Vietnam; [8]Department of Human and Animal Physiology, Faculty of Biology, Hanoi National University of Education, Hanoi, Vietnam

Citation: Minh NH, Dung TM, Ngoc VTN, Tuan PH, Ha NH, Son LV, Phuong NTT, Doi HT, Thanh VV, Dinh TC, Phuong NT, Chu Dinh T. Quality of Life and Suitability with Vietnamese Harmonious Face Index in Class III Malocclusion Patients. Open Access Maced J Med Sci. 2019 Dec 30; 7(24):4239-4243. https://doi.org/10.3889/oamjms.2019.367

Keywords: Oral health care; Class III malocclusion; Orthognathic surgery; Harmonious faces

***Correspondence:** Toi Chu Dinh. School of Odonto Stomatology, Hanoi Medical University, Hanoi, Vietnam; Department of Human and Animal Physiology, Faculty of Biology, Hanoi National University of Education, Hanoi, Vietnam. E-mail: chudinhtoi@hnue.edu.vn

Received: 19-Jun-2019; **Revised:** 20-Sep-2019; **Accepted:** 21-Sep-2019; **Online first:** 15-Oct-2019

Funding: This research did not receive any financial support

Competing Interests: The authors have declared that no competing interests exist

Abstract

BACKGROUND: Maxillary Lefort I osteotomy, mandibular bilateral sagittal split ramus was frequently used in correcting skeletal class III malocclusion. There was a lack of research on class III malocclusion patients' quality of life (QoL) after bimaxillary osteotomy.

AIM: Class I Intermaxillary relationship was achieved, aesthetic was significantly improved. Significant improvement in Class III skeletal patients' quality of life was acquired. The achievement of harmonious face would be beneficial to the facial aesthetics of patients, thus improving the quality of life.

METHODS: Harmonious face index is an effective criterion in assessing the surgery's outcome. In this study was conducted on 30 patients at Hanoi National Hospital of Odontostomatology, Viet Duc Hospital, and Hong Ngoc Hospital from April 2017 to April 2018, and it was a quasi-experimental study with self-comparison, 12 months follow up.

RESULTS: Orthognathic surgery effectively corrected malocclusion crossbite, dental compensation, and helped to improve facial aesthetics. 100% of patients had the quality of life improved, good quality of life consisted of 86.7%. In comparison with a harmonious facial index of Kinh ethnic in Vietnam, 70% of patients achieved skeletal harmony, 63.3% of patients achieved dental harmony, 80% achieved soft tissue harmony.

CONCLUSIONS: Vietnamese harmonious facial index should be used in planning and pre-surgical simulation.

Introduction

Malocclusion is the incorrect dental phenomena between the teeth of two arches. In America and Asian countries, this incidence of malocclusion can reach 70% of the population [1]. Class III malocclusion comprises high percentages in the population, up to 35% [2]. Class III malocclusion is the aetiology of occlusal trauma, functional decrease, and an increased risk of dental diseases, facial aesthetic and psychological problems [3]. Treatment for skeletal class III malocclusion is quite necessary to improve quality of life [4]. Most adult patients with skeletal class III malocclusion, need a combination of orthodontic and surgical treatment to achieve good outcomes in function and aesthetic. Maxillary Lefort I osteotomy and bilateral sagittal split osteotomy ramus (BSSO) are commonly applied worldwide, providing good outcome in aesthetic and function in three dimensions, as well as post-operative stability[5],[6]. Therefore, patients' physical, psychological aspects, as well as the quality of life, can make significant progress. In recent years, patients' quality of life (QoL) has been a matter of concern which has been considered to be a criterion in assessing the patients' recovery after surgery. Orthognathic Quality of Life Questionnaire (OQLQ) was created to measure patients' quality of life. OQLQ was

considered to be an effective instrument for the assessment of patients' quality of life after orthognathic surgery [7], [8]. The Vietnamese harmonious facial index is an aesthetic criterion of surgery. Thus, we conducted this study to evaluate the quality of life and the suitability with the harmonious Vietnamese facial in skeletal class III malocclusion patients after orthognathic surgery.

Subjects and Methods

Subjects: 30 skeletal class III malocclusion patients were treated with preoperative orthodontic and had orthognathic surgery in Hanoi (Hanoi National Hospital of Odontostomatology, Viet Duc University Hospital and Hong Ngoc Hospital) from April 2017 to April 2018. Patients with severe congenital facial defects were excluded.

Study method: Quasi-experimental study with self - comparison before operation (T0) and after operation 12 months (T12). All patients were operated with maxillary Lefort I osteotomy and bilateral sagittal split ramus osteotomy. The cephalometric X-ray was used to assess the patients' skeletal, dental, soft tissue before the operation and after operation 12 months. Orthognathic Quality of Life Questionnaire (OQLQ) was used to evaluate patients' quality of life before the operation and after operation 12 months (appendix A). The questionnaire contains 22 questions which were divided into four parts, including facial aesthetics, oral function, awareness of dentofacial aesthetics and social aspects of dentofacial deformity. Each question is scored on a 4-point scale, which 1 refers to "bothers you a little", 4 = "bothers you a lot", 2 and 3 = "between these statements", 0 score refers to "does not apply or does not bother". The high score presents a negative influence on the patient's QoL. The low score indicates a positive influence on the QoL. Average score: ≤ 2: good quality of life; 2-3: moderate quality of life; ≥ 3: poor quality of life.

Evaluating the effectiveness of surgery is evaluation the changes in the facial index before and after surgery by comparing skeletal, dental and soft tissue index in pre-operation (T0) and 12 months post-operation (T12).

Assess the suitability with Vietnamese harmonious facial index is assess the suitability between the post-operation facial index and Vietnamese harmonious facial index by comparing patients' cephalometric indexes after 12 months post-operation with Vietnamese Kinh Ethnic, harmonious facial index in National Research in School of Odonto& Stomatology – Hanoi Medical University.

Statistics

Data analysis: Continuous variables were skeletal, dental and soft tissue index (SNA, SNB, ANB angle, A-V, B-V, Pg-V, Wits, overjet, overbite, U1-SN, Is-V, L1-MP, Ii-V, Li-E, Ls-E, Cm-Sn – Ls angle, Li-B'-Pg' angle, Ns - Sn-Pg' angle) measured in Cephalometric X – rays and OQLQ score were analysed with SPSS 16.0 software. Pair T-tests was used to compare the normal distribution variables before and after the operation. Wilcoxon signed-rank test was used to compare OQLQ score and the non-normal distribution variables.

Results

Patch test results

There were 30 patients including14 male patients (46.7%); 16 female patients (53.3%) in the study. All the patients were Kinh ethnic. The subjects' age was in a range of 18 to 25 years old.

Table 1: Skeletal, dental and soft tissue index in 12month postoperation (T12) in comparision with preoperation (T0)

Index	T0 (N = 30)		T12 (N = 30)		P
	$\bar{X}$	SD	$\bar{X}$	SD	(T0vs T12)
SNA (degree)	80.87	3.81	82.72	3.34	< 0.001*
A-V (mm)	60.37	5.44	63.67	4.85	< 0.001*
SNB (degree)	84.98	4.22	81.67	3.78	< 0.001*
B-V (mm)	65.66	7.73	63.45	6.51	< 0.001*
Pg-V (mm)	66.59	9.36	63.89	8.62	< 0.001*
ANB (degree)	-4.11	2.65	1.05	1.01	< 0.001**
Overjet (mm)	-4.08	2.15	2.10	0.31	< 0.001**
Overbite (mm)	1.47	0.67	1.61	0.51	> 0.05**
U1-SN (degree)	110.53	9.15	107.34	8.61	< 0.001*
Is-V (mm)	67.17	7.24	69.90	6.67	< 0.001*
L1-MP (degree)	86.87	8.71	94.78	3.70	< 0.001*
Ii-V (mm)	71.44	8.01	67.24	6I46	< 0.001*
Li-E (mm)	3.68	1,12	1.45	2.20	< 0.001**
Ls-E (mm)	-3.04	1,65	-0.17	1.75	< 0.001**
Cm-Sn-Ls (degree)	81.92	4.49	94.26	4.04	< 0.001*
Li-B'-Pg' (degree)	146.29	8,94	133.75	7.81	< 0.001*
Ns-Sn-Pg' (degree)	185.54	3.41	167.41	3.56	< 0.001*

*Note: *P values were determined by Pair T-test; **P values were determined by Wilcoxon signed-rank test.*

According to Table 1, there was a forward movement of the maxilla (SNA, A-V increased), the backward movement of the mandible, prognathic chin reduced (SNB, B-V, Pg-V reduced). Class I intermaxillary relationship was achieved, crossbite was corrected. Upper incisors (Is-V increased) moved forward, lower incisors (Ii-V decreased) moved backwards. The angle between the lower incisors and mandibular plane (L1-MP) increased, the angle between the upper incisors and cranial plane (U1-SN) decreased. Forward movement of the upper lip (Ls-E increased), the backward movement of the lower lip (Li-E decreased) were seen, facial angle decreased (Ns-Sn-Pg'). Nasolabial angle was larger (Cm-Sn-Ls increased), and the labiomental angle was smaller (Li – B' – Pg' decreased) in comparison with the pre-surgery index. Above changings were statistically significant ($p < 0.05$). Overbite changing is not statistically significant ($p > 0.05$).

Table 2: The improvement of quality of life

OQLQ	Facial Aesthetics		Oral Function		Awareness of Dentofacial Aesthetics		Social Aspects of Dentofacial Deformities		SUM	
	Pre-op	Post-op	Pre-op	Post-op	Pre-op	Post-op	Pre-op	Post-op	Pre-op	Post-op
N	30	30	30	30	30	30	30	30	30	30
MEDIAN	16.5	5	17	6	14	5	26	8	72	23
MIN	12	0	12.	0	10	0	17	0	52	0
MAX	20	14	20	14	16	11	31	23	87	61
P	< 0,001		< 0,001		< 0,001		< 0,001		< 0,001	

Note: P values were determined by Wilcoxon signed-rank test.

As can be seen from Table 2, before surgery, the minimum score for OQLQ in sum was 52, and the maximum score was 87, the median score was 23. One year after surgery, all the minimum, maximum and median score decreased significantly to 0, 61 and 23, respectively ($p < 0.001$, Wilcoxon Signed Rank Test). The same trends were seen in the score for OQLQ in Facial Aesthetics, Oral Function, Awareness of Dentofacial Aesthetics, Social Aspects of Dentofacial Deformities.

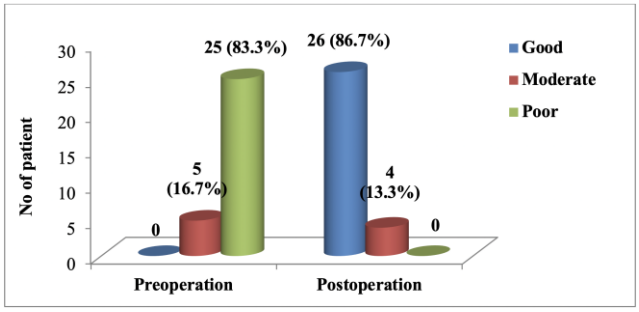

Figure 1: Quality of life-changing after surgery

From the above chart, before surgery, there was no good quality of life case, the poor quality of life consisted of 83.3%.In contrast, after surgery, 26 cases were having a good quality of life (86.7%), 4 cases having the moderate quality of life (13.3%) and there was no case having poor quality of life (Fig. 1).

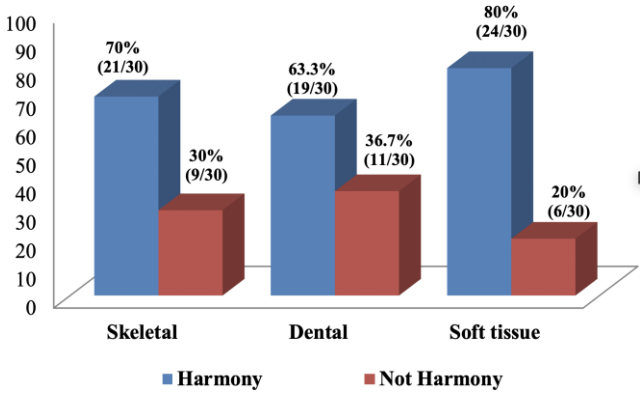

Figure 2: Suitable rate with Vietnamese harmonious facial index

Among 30 patients got 12 months postoperative following up, 21 cases were having harmonious skeletal index (70%), 19 cases having harmonious dental index (63.3%) and 24 cases having harmonious soft tissue index (80%) (Figure 2).

Discussion

Twelve months postoperative, our study observed forward movement of the maxilla, the backward movement of the mandible and the intermaxillary relationship was changed from class III (pre-operation) to class I. Overjet was increased to the positive average value, crossbite was corrected. The angle between lower incisors and the mandibular plane was increased, the angle between maxillary incisors and the basal plane was decreased, dental decompensation was achieved (palatal inclination of upper incisors and labial inclination of lower incisors), dental esthetic was improved. Soft tissue was also changed: forward movement of the upper lip, the backward movement of the lower lip, decreasing facial angle, increasing nasolabial angle as well as decreasing labiomental angle in comparison with pre-operation. These changes significantly improved facial aesthetics, the relationship between upper lip and nose, lower lip and chin. Our result was appropriate with studies conducted by Ghassemi [6], Aydemir [9].

There were a variety of articles that have mentioned the merits of orthognathic surgery in skeletal class III malocclusion patients. In recent year, other studies have directly cared about the patients' quality of life which is a wide concept related to physical health, aesthetic aspect, psychological state, social relationships.

In our study, OQLQ was chosen because OQLQ is a questionnaire designed for orthognathic. We evaluate patients' quality of life at the one-year postoperative period because we tended to asses the long-term complications, including skeletal relapse and neurosensory disturbances. Thus, it was possible to evaluate the influence of long-term complications on QoL.

In our study, the results described a highly significant degree of overall improvement in patients' quality of life after orthognathic surgery. The subjects' quality of life achieved a statistically significant improvement in all four OQLQ domains. In agreement with our outcome, other authors, including Wee, 2014 [10], Abdullad, 2015 [11], also found the improvement of patients' quality of life after orthognathic. Applying OQLQ for 41 patients, Wee found that patients' quality of life was significantly improved after two years bimaxillary osteotomies [10]. Similarly, Abdullad also used OQLQ to assess the quality of life for 17 patients, and the outcomes showed that the highly significant improvement in patients' quality of life was evident [11].

All subjects in our study underwent the combination of Lefort I maxillary advancement and BSSO mandibular setback operation with rigid fixation. The complications and surgical outcomes remarkably affected the quality of life. Long-term complications were the main factor that contributed to the changes in patients' quality of life. In BSSO, the inferior alveolar nerve was damaged, thus causing numbness of the lower lip and chin. In the study of Alolayan, in 238 patients, the percentage of nerve injury was 36.6% after mandibular procedures [12]. In our study, we found that the neurosensory disturbances reduced after one-year follow, that refer to the recovery of the nerve. After a one-year post-operation, only 5 patients were complaining about a little numbness of chin. The other long-term common complication is skeletal and dental relapse.

In our study, the percentage of patients who achieved the harmonious Vietnamese face after 12 months post-operation was high. Dental decompensation, less acute

nasolabial angle, less obtuse labiomental angle, decreasing facial angle helps improving facial esthetic significantly. Patients' facial aesthetic made remarkable progress, thus improving the patients' confidence as well as the quality of life. Therefore, Vietnamese harmonious facial index should be applied in planning and preoperative simulation to increase the surgery's outcome and the patient's quality of life.

In conclusion, maxillary Lefort I osteotomy and mandibular bilateral sagittal split ramus osteotomy were effective in correcting skeletal class III malocclusion. After surgery, class I intermaxillary relationship was acquired, esthetic was significantly improved. The study showed a highly significant improvement in Class III skeletal patients' quality of life after 12 months bimaxillary osteotomies. All four OQLQ domains improved remarkably after 12 months of surgery. The achievement of harmonious face would be beneficial to the facial aesthetics of patients, thus improving the quality of life. Vietnamese harmonious facial index should be used in planning and preoperative simulation to increase the surgery's outcome and the patient's quality of life.

Acknowledgement

We would like to express our sincere gratitude to volunteers for their participation in our study, as well as Hanoi National Hospital of Odontostomatology, Viet Duc Hospital, Hong Ngoc Hospital, School of Odonto & Stomatology – Hanoi Medical University

Ethical Approval

All procedures performed in studies involving human participants were in accordance with the ethical standards of the institutional and/or national research committee and with the 1964 Helsinki declaration and its later amendments or comparable ethical standards. This study belongs to National research of School of Odonto & Stomatology – Hanoi Medical University, which had been approved this study according to Decision No. 202/HĐĐĐĐHYHN, signed on October 20th 2016.

Acknowledgements

We want to thank Ms Nguyen Thi Yen Vy (Faculty of Biology, University of Hanoi National University of Education, Hanoi, Vietnam) checking and improving the English in the manuscript.

Informed Consent

Informed consent was obtained from the patients included in the study.

References

1. Carvalho F.S.d., et al., Epidemiology of malocclusion in children and adolescents: a critic review. RGO - Revista Gaúcha de Odontologia. 2014; 62:253-260. https://doi.org/10.1590/1981-86372014000300000041190

2. Hardy DK, Cubas YP, Orellana MF. Prevalence of angle class III malocclusion: A systematic review and meta-analysis. Open Journal of Epidemiology. 2012; 2(04):75. https://doi.org/10.4236/ojepi.2012.24012

3. Nicodemo D, Pereira MD, Ferreira LM. Self-esteem and depression in patients presenting angle class III malocclusion submitted for orthognathic surgery. Med Oral Patol Oral Cir Bucal. 2008; 13(1):48-51.

4. Huang S, et al. The changes of oral health-related quality of life and satisfaction after surgery-first orthognathic approach: a longitudinal prospective study. Head & Face Medicine. 2016; 12:2. https://doi.org/10.1186/s13005-015-0098-1 PMid:26729274 PMCid:PMC4700618

5. Aydemir H, Toygar-Memikoglu U. Facial Soft Tissue Changes in Class III Patients Treated With Bimaxillary, Maxillary Advancement or Mandibular Set Back Orthognathic Surgery. OHDM. 2015; 14:75-80.

6. Ghassemi M, et al. Evaluation of soft and hard tissue changes after bimaxillary surgery in class III orthognathic surgery and aesthetic consideration. National Journal of Maxillofacial Surgery. 2014; 5(2):157-160. https://doi.org/10.4103/0975-5950.154819 PMid:25937726 PMCid:PMC4405957

7. Momeni Danaei S, et al. Assessment of the Reliability and Validity of the Farsi Translation of the "Orthognathic Quality of Life Questionnaire" in 10-14 Year-Olds in Shiraz. The Journal of Islamic Dental Association of IRAN (JIDA). 2013; 25(4):322-328.

8. Bortoluzzi MC, Manfro R, Soares IC, Presta AA. Cross-cultural adaptation of the orthognathic quality of life questionnaire (OQLQ) in a Brazilian sample of patients with dentofacial deformities. Med Oral Patol Oral Cir Bucal. 2011; 16(5):e694-9. https://doi.org/10.4317/medoral.16938 PMid:20711138

9. Aydemir H, et al. Evaluation of long-term soft tissue changes after bimaxillary orthognathic surgery in Class III patients. The Angle Orthodontist. 2015; 85(4):631-637. https://doi.org/10.2319/062214-449.1 PMid:25271955

10. Haur Wee T, Yoke Poon C. Quality of Life Treatment Outcomes of Class III Skeletal Patients after Bimaxillary Osteotomies. Proceedings of Singapore Healthcare. 2014; 23(3):183-190. https://doi.org/10.1177/201010581402300302

11. Abdullah WA. Changes in quality of life after orthognathic surgery in Saudi patients. The Saudi Dental Journal. 2015; 27(3):161-164. https://doi.org/10.1016/j.sdentj.2014.12.001 PMid:26236131 PMCid:PMC4501467

12. Alolayan AB, Leung YY. Risk Factors of Neurosensory Disturbance following Orthognathic Surgery. PLoS ONE. 2014; 9(3):e91055. https://doi.org/10.1371/journal.pone.0091055 PMid:24599321 PMCid:PMC3945003

Appendix A

OQLQ

Please read the following statements carefully. In order to find out how important **each of the statements** is to you, please circle **1**, **2**, **3**, **4** or **N/A** where:

1 means it ***bothers you a little***
4 means it ***bothers you a lot***
2+3 lie ***between these statements***
N/A means the statement does not apply to you or does not bother you at all

1	2	3	4
Bothers you a little			Bothers you a lot

1. I am self-conscious about the appearance of my teeth **1 2 3 4 N/A**
2. I have problems biting **1 2 3 4 N/A**
3. I have problems chewing **1 2 3 4 N/A**
4. There are some foods I avoid eating because the way my teeth meet makes it difficult **1 2 3 4 N/A**
5. I don't like eating in public places **1 2 3 4 N/A**
6. I get pains in my face or jaw **1 2 3 4 N/A**
7. I don't like seeing a side view of my face (profile) **1 2 3 4 N/A**
8. I spend a lot of time studying my face in the mirror **1 2 3 4 N/A**
9. I spend a lot of time studying my teeth in the mirror **1 2 3 4 N/A**
10. I dislike having my photograph taken **1 2 3 4 N/A**
11. I dislike being seen on video **1 2 3 4 N/A**
12. I often stare at other people's teeth **1 2 3 4 N/A**
13. I often stare at other people's faces **1 2 3 4 N/A**
14. I am self-conscious about my facial appearance **1 2 3 4 N/A**
15. I try to cover my mouth when I meet people for the first time **1 2 3 4 N/A**
16. I worry about meeting people for the first time **1 2 3 4 N/A**
17. I worry that people will make hurtful comments about my appearance **1 2 3 4 N/A**
18. I lack confidence when I am out socially **1 2 3 4 N/A**
19. I do not like smiling when I meet people **1 2 3 4 N/A**
20. I sometimes get depressed about my appearance **1 2 3 4 N/A**
21. I sometimes think that people are staring at me **1 2 3 4 N/A**
22. Comments about my appearance really upset me, even when I know people are only joking **1 2 3 4 N/A**

ID Design Press, Skopje, Republic of Macedonia
Open Access Macedonian Journal of Medical Sciences. 2019 Dec 30; 7(24):4244-4249.
https://doi.org/10.3889/oamjms.2019.368
eISSN: 1857-9655
Basic and Clinical Medical Researches in Vietnam

Efficacy and Toxicity of Folfoxiri for Patients with Metastatic Colorectal Cancer

Trinh Le Huy[1], My Hanh Bui[2,3*], Toi Chu Dinh[4], Hoang Thi Hong Xuyen[5]

[1]Department of Oncology, Hanoi Medical University Hospital, Hanoi, Vietnam; [2]Tuberculosis and Lung Disease Department, Hanoi Medical University, Hanoi, Vietnam; [3]Scientific Research & International Cooperation Department, Hanoi Medical University Hospital, Hanoi, Vietnam; [4]Department of Human and Animal Physiology, Faculty of Biology, Hanoi National University of Education, Hanoi, Vietnam; [5]Center for Development of Curriculum and Human Resource in Health, Hanoi Medical University, Hanoi. Vietnam

Citation: Huy TL, Bui MH, Chu Dinh T, Xuyen HTH. Efficacy and Toxicity of Folfoxiri for Patients with Metastatic Colorectal Cancer. Open Access Maced J Med Sci. 2019 Dec 30; 7(24):4244-4249. https://doi.org/10.3889/oamjms.2019.368

Keywords: Efficacy; Toxicity; Folfoxiri; Metastatic colorectal cancer

***Correspondence:** My Hanh Bui. Tuberculosis and Lung Disease Department, Hanoi Medical University, Hanoi, Vietnam; Scientific Research & International Cooperation Department, Hanoi Medical University Hospital, Hanoi, Vietnam. E-mail: buimyhanh@hmu.edu.vn

Received: 26-Jun-2019; **Revised:** 20-Nov-2019; **Accepted:** 21-Nov-2019; **Online first:** 10-Dec-2019

Funding: This research did not receive any financial support

Competing Interests: The authors have declared that no competing interests exist

Abstract

BACKGROUND: In recent times, scientists have found new treatments for colorectal cancer patients.

AIM: The study is to evaluate the efficacy and toxicity of triplet combination chemotherapy of 5-fluorouracil/leucovorin, oxaliplatin, and irinotecan (FOLFOXIRI) for patients with metastatic colorectal cancer in stage IV.

METHODS: Uncontrolled clinical trial carried on 39 stage IV colorectal cancer patients.

RESULTS: The overall response rate of the treatment was 79.4%. The average progression-free survival was 13.4 ± 9 months. The overall survival rate at 12th month and 24th month were 90% and 76%, respectively. The proportion of granulocytopenia was 48.9%, no grade 3 or 4. Side effect beyond hematology was most seen in hepatic toxicity with 52.5%, mainly at grade 1. Vomiting was 18.3%, all at grade 1. Other adverse event was very low at percentage.

CONCLUSIONS: The triplet combination FOLFOXIRI chemotherapy improves the outcome of patients with metastatic colorectal cancer regarding rate of response, overall survival rate and progression-free survival, and the level of toxicity was acceptable.

Introduction

Colorectal cancer is a common type of gastrointestinal cancer. The disease tends to increase in recent times. Treatment of metastatic colorectal cancer is still difficult, with overall survival (OS) and 5-year survival rate reported of 16-25 months and 11%, respectively [1], [2]. At present, 5-fluorouracilimines, oxaliplatin and irinotecan are still three "backbone" drugs to the treatment for metastatic colorectal cancer.

A meta-analysis presented that the increase of overall survival rate significantly associate with the use of all 5-fluorouracil, oxaliplatin and irinotecan over the total duration of treatment [3]. Currently, in accordance with recommendation by many cancer organizations around the world, these three drugs are used step by step through two-drug regimen (FOLFOX/XELOX, FOLFIRI/XELIRI). However, not all 100% of patients are treated with all 3 these drugs because some patients abandon the following treatment lines, or their condition does not allow second-line treatment.

Thus, the idea of using all three drugs from the first-line treatment was sprouted more than 10 years ago. In 2002, the first two Phase II studies reported the efficacy and safety of the combination of Oxaliplatin/Irinotecan/5-FULV (FOLFOXIRI) at the first stage [4]. Subsequently, many phase III studies were performed with satisfactory results of this regimen. Since 2010, FOLFOXIRI were recommended in NCCN (National Comprehensive Cancer Network) Clinical Practice Guidelines in Oncology [5].

In Vietnam, the rateof colorectal cancer ranks 4th in men and 6th in women [6]. FOLFOXIRI regimen is gradually being introduced at some oncology facilities due to its efficacy and feasibility. However, since then there was no clinical trial established to evaluate the effectiveness as well as toxicity of FOLFOXIRI in Vietnamese patients with metastatic colorectal cancer.

Therefore, we carried out this work with the aim of performing an initial review in relation to the efficacy and toxicity of FOLFOXIRI in treatment for patients with metastatic colorectal cancer in stage IV.

Materials and Methods

Study design

This study was a single-arm, uncontrolled prospective clinical trial. All eligible patients were selected from October 2013 to September 2014 in the Oncology and Palliative Care Department, Hanoi Medical University Hospital.

Patient selection and study process

Main eligibility criteria were as followed: patients were diagnosed with metastatic unresectable colorectal adenocarcinoma; age from 20 to 75 years; Eastern Cooperative Oncology Group (ECOG) performance status (PS) score of 0 or 1; the patients were treated by at least 3 cycles of FOLFOXIRI in the first-line treatment (Table 1); liver, kidney and hematological functions before treatment were in normal limits; did not suffer from diseases with near-death risk and other chronic diseases. General information was collected by questioning patients and their family member to record age, gender, medical history, reasons of hospitalization, signs and symptoms of disease. Pre-treatment assessment included physical examination, performance status evaluation, complete blood profile, CEA level measurement, colonoscopy, X-ray imaging or CT (computed tomography) scan, abdominal CT scan and/or ultrasound, electrocardiogram and any other applicable method to examine metastatic sites. In the period of treatment, a physical examination was conducted once in two weeks. Metastatic sites were re-examined once within 8 weeks. Abdominal CT scan or MRI was demanded in order to evaluate liver and abdominal metastases.

Table 1: Treatment of FOLFOXIRI chemotherapy at first-line with specific dosage

Dosage	Day of receiving
Irinotecan: 165 mg/m2, intravenous infusion for 1 hour.	Day 1, 15
Oxaliplatin: 85 mg/m2, intravenous infusion for 2 hours	Day 1, 15
Calcium folinat 200 mg/m2, intravenous infusion for 2 hours	Day 1, 15
5FU 3200 mg/m2, continuous intravenous infusion during 48 hours	Day 1, 2, 3, 15, 16, 17

Note: The regimen was repeated once per 2 weeks.

Evaluation of treatment response was made in accordance with RECIST (Response Evaluation Criteria in Solid Tumors) criteria version 1.1 [7]. Overall response = Complete response + partly response [7]. The adverse event of FOLFOXIRI chemotherapy were observed weekly and categorized in accordance with standard National Cancer Institute Common Terminology Criteria for Adverse Events version 4.0. Patients with disease stability or continuous response after 6 cycles were shifted to maintenance phase with oral Capecitabine (Xeloda). During maintenance treatment, patients were re-examined before Capecitabine administration. Progression Free Survival is estimated in the period of time between the time the study starts and the time of disease progression. Overall survival was calculated at 12-month and 24-month.

Statistics

All collected data were analyzed and measured by SPSS 22.0 software. Progression-free survival (PFS) and overall survival (OS) were estimated by the Kaplan-Meier method from the day of treatment started. Dichotomous variables were analyzed by using Chi-square test and median values compa. The p values < 0.05 were recognized statistically significant.

Ethical

This study is completely voluntary and is aimed at improving the quality of treatment, not for any other purpose. Patients who have met the selection criteria will be explained in detail about the study, patients who agree to participate in the study will be signed on a volunteer to participate in the study. All details about the patient's condition are encrypted and confidential. The patient has the right to withdraw from the study.

Results

A total of 39 unresectable metastatic colorectal cancer patients were recruited to the study. There were 26 males and 13 females, with a median age of 52.9 years (range 25-70). Half of the participants had taken chemotherapy for their disease previously. The most common reason for hospitalization was abdominal pain with 74.4%. Majority of patients were with PS-1 (82.1%), while performance status (PS) score of 0 accounted for percentage of 17.9%. Bowel obstruction was the most common symptom (43.6%), followed by papable abdominal mass of 20.5% at the time of diagnosis (Table 2).

Moderately differentiated adecarcinoma was responsible for two third of the study population, followed by participants having type of histopathology as mucinous adenocarcinoma. The peritoneum was more commonly found in patients with mucinous colorectal cancer (20.5%, compared with 5.1% of patients with moderately differentiated adenocarcinoma) (Table 2).

Regarding primary tumor distribution, left-sided colorectal cancer had the highest percentage of 61.5%. Of which, primary tumors were more frequently distributed at sigmoid colon (41%) and liver (17.9%), other locations accounted for proportion of 41.1%. Liver was the most prevalent distant metastatic site (64.1%), whereas patients with peritoneal metastasis and pulmonary metastasis were 25.6% and 17.9%, respectively. Retroperitoneal lymph node occurred in 30.8% of metastatic colorectal patients. 26 patients (66.7%) had CEA levels of 20ng/ml or below before treatment (Table 2).

Table 2: Clinic-pathology features of metastatic colorectal cancer patients whose disease was not radically resectable

Characteristics		Percentage
Gender	Male	26 (66.7%)
	Female	13 (33.3%)
Age	Under 40	8 (20.5%)
	45-60	26 (66.7%)
	Over 65	5 (13.8%)
Signs	Abdominal pain	29 (74.4%)
	Hematochezia	10 (25.6%)
	Diarrhea	9 (23.1%)
Performance status	PS1	32 (82.1%)
	PS0	7 (17.9%)
Symptoms	Bowel obstruction	17 (43.6%)
	Fluid in the abdomen	1 (2,6%)
	Palpable abdominal mass	8 (20.5%)
	No symptom	13 (33.3%)
Tumor location	Sigmoid colon	16 (41%)
	Hepatic flexure	7 (18%)
	Other location	16 (41%)
Distant metastatic site	Liver metastasis	25 (64.1%)
	Pulmonary metastasis	7 (17.9%)
	Peritoneal metastasis	10 (25.6%)
	Retroperitoneal lymph node	12 (30.8%)
No. of involved organs	> 1	32 (82.1%)
	= 1	7 (17.9%)
CEA concentration	CEA > 20 ng/ml	13 (33.3%)
	CEA ≤ 20 ng/ml	26 (66.7%)
Histopathology	Moderately differentiated adenocarcinoma	26 (66.7%)
	Mucinous adenocarcinoma	13 (33.3%)

Efficacy

All participating patients had measurable disease and were evaluated for response (Table 3).

Table 3: Response rate of the treatment

Response	Percentage (%)
Completely	2 (5.9%)
Partially	25 (73.5%)
Disease stability	4 (11.8%)
Disease progression	3 (8.8%)

After 3 cycles, we recorded 5.1% of patients who responded fully after 3 cycles and the majority of patients had partial response (76.9%); 5.1% of patients with progressed disease. After 6 cycles, five patients discontinued the chemotherapy prematurely because of disease progression after 3 cycles and geographical distance. According to Table 3, 25 patients (73.5%) achieved partial remission and 2 cases (5.9%) obtained a complete response, therefore, the rate of overall response and disease control were 79.4% and 91.2%, respectively. The median dosage intensity of irinotecan, oxaliplatin and 5-FU used in the treatment for 39 colorectal cancer patients were 83.7%, 83.08% and 84.33%, respectively.

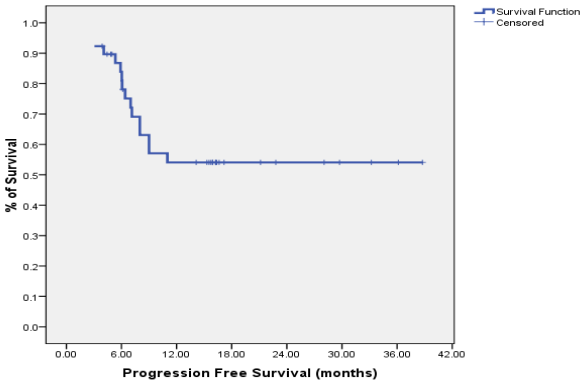

Figure 1: Progression-free survival

After 36 months of follow-up, the progression-free survival in our study was calculated as 13.4 ± 9 months (Figure 1). The overall survival rate at 12th month was 90% and 24th month was 76% (Figure 2).

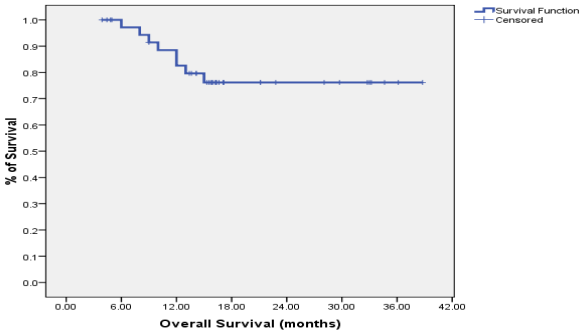

Figure 2: Overall survival rate

All patients in the study were assessable for the safety of treatment. The most prevalent adverse events included neutropenia, thrombocytopenia, anemia, vomiting, diarrhea, stomatitis, hepatic toxicity, peripheral neurotoxicity. Nevertheless, most toxicity complications were at grade 1 or 2, and grade 3 or 4 was commonly seen in neutropenia. Of which, granulocytopenia of grade 1/2 occurred in 25.5% of patients, while grade 3 and 4 occupied a lower rate of 14.1% and 9.3%, respectively. Thrombocytopenia and anemia accounted for very low percentage of 3.2% and 8.3%, mainly at grade 1. Liver toxicity was the most prevalent non-hematological adverse event and accounted for the highest proportion of 52.5%, followed by vomiting and diarrhea with the figure of 18.3% and 6.9%, respectively. All of them were scored at grade 1/2 (Table 4).

Table 4: Adverse Event of FOLFOXIRI regimen

Adverse Event	Grade 0 (%)	Grade 1-2 (%)	Grade 3-4 (%)
Granulopenia	51.1	25.5	23,4
Thrombocytopenia	96.8	3.2	0
Anemia	91.7	8.3	0
Vomiting	74.23	23	2.67
Diarrhea	93.1	6.9	0
Oral toxicity	96.57	3.63	0
Liver toxicity	47.5	52.5	0

Discussion

In recent times, the development of chemotherapy in treatment for patients with colorectal cancer has led to considerable benefit regarding antitumor activity and efficacy [5]. Documents showed that the best outcomes are obtained from patients who received all three main active substances (5-FU, irinotecan and oxaliplatin), but that in a sequential strategy only 60% to 80% of patients are able to continue the second-line treatments and thus, to be able to expose to all these three agents. These considerations assist the procedure to improve potentially more active first-line regimens which put 5-FU with both irinotecan and oxaliplatin. Thus, we conducted the study to evaluate effectiveness combo of irinotecan, oxaliplatin and 5-FU/LV (FOLFOXIRI), orderly.

In our research, the overall response rate was 79.4%. Of which, there were 5.1% of patients with full response, 73.5% with partial response, 11.8% with stable disease and 5.9% with progressive disease. Consequently, the rate of disease control was calculated as 91.2%. The overall response rate is among the highest findings which were presented in previous study on any chemotherapy regimens for treatment of metastatic colorectal cancer [4], [8], [9], [10]. The median dose intensities were 83.7% with Irinotecan, 83.08% with Oxaliplatinand 84.33% with 5-FU. This is the lowest dose intensity of chemotherapy compared with those four reference studies, except for Souglakos et al.'s study [8]. Regarding to patients' characteristics, based on three main factors: median age, prevalence of patients treated with chemotherapy before, severity of disease, our patients group presented a younger median age (54 years), the second lowest number of patients with metastases > 1 (16.7%, just behind the figure of Azmy et al.'s study with 9%), and approximately 50% of patients had been taken with chemotherapy previously (middle-ranking among 4 cited studies). Thus, the characteristics of our studied population were relatively more favorable than those of other groups in mentioned studies.

During a follow-up period of 36 months, our study showed that the median progression-free survival was recorded as 13.37 ± 9 months. This result was comparable to foreign studies using the same regimen. Particularly, Falcone et al.'s study, (2002) revealed a median progression-free survival of 10.4 months while Souglakos et al.'s study reported the progression-free survival of 13 months on average [4], [8]. Furthermore, in comparison with other regimens, FOLFOXIRI increased PFS by about 3 months, and decreased the risk of early disease progression by halfThe 12th month and 24th month overall survival rate was 90% and 76%, respectively.

A notable disadvantage of FOLFOXIRI is tohave many side-effects, but in an acceptable level. Neutropenia was the most common hematological toxic effect with proportion of 48.9%. In particular, the incidence of grade 1/2 granulocytopenia was 25.5% while grade 3/4 was found in 23.4% of patients. There was no case of fever caused by neutropenia. Interestingly, neutropenia was one of the adverse event with the highest rate in studies conducted by Falcone et al., (2002)'s which suggested that 14% of patients had at least one episode of neutropenia fever [4], and Souglakos et al., (2002) which found that grade 3 and grade 4 neutropenia happended in 14 patients (45%), two patients had neutropenia fever (6%) [8]. Compared with mentioned authors, our result of neutropenia was somewhat lower. In our study, patients were screened for blood count routinely on day 8 after chemotherapy. Cases with grade 2 or above were injected with leukocyte stimulants and closely observed, daily white blood cell counts were measured to administer leukocyte-stimulating drugs if necessary, until blood cound reached over 2000 white blood cells/ml. In addition, dosage adjustment for each patient was based on level of granulocytopenia in the period of treatment. Cases with grade 3 granulocytopenia were isolated in sterile rooms and broad-spectrum antibiotic prophylaxis was used until white blood cells increased to above 2000/ml.

Regarding anemia, the rates of anemia and thrombocytopenia in our study were 8.3% and 3.2%, respectively. Most of side effects of anemia (6.5%) and thrombocytopenia were at grade 1. The rate of grade 2 anemia was very low with 2.3% and these side effects at grade 3 and 4 did not appear in the study. Also, the percentages of anemia and thrombocytopenia of foreign studies were very low (< 10%) [11], [12]. The three drugs Oxaliplatin, 5-FU and Irinotecan have unclear effect on thrombocytopenia occurrence. Regarding anemia, only oxaliplatin can cause a small erythropoietic anemia because a small fraction (~ 7%) of oxaliplatin penetrate into red blood cells and break down the red blood cells after 48 days. Nevertheless, because only a small proportion of oxaliplatin can get into red blood cells, the levels of anemia of regimens containing oxaliplatin in general and of FOLFOXIRI in particular are not high.

Vomiting during chemotherapy occurred in 42 cases. However, no incidence of vomiting at grade 4, grade 3 occurred in 2.67% of the patients. The remaining was mainly infusions causing vomiting at grade 1 (74.23%) and grade 2 (23%). The toxicity rate

was lower than Falcone et al.'s study, in which the incidence of vomiting was 60% for grade 1, 53% for grade 2 and 13% for grade 3 [4]. The causes of this type of vomiting are usually related to psychological factors which stimulate pneumogastric nerve to cause vomiting. To solve this problem, we usually use supplements of pills (Diazepam) for patients with a history of severe vomiting in the previous infusion. In addition to using the 5-HT3 class of anti-vomiting medication, we also combined two other classes in a routine way: Corticosteroids (dexamethasone) have anti-vomiting mechanism on the central nervous system; Primperan has anti-vomiting mechanism by D4 receptor blockade. Several severe vomiting cases (grade 3) were also given Haloperidol, a chemotherapy-induced P-receptor blocker in the CTZ (chemo-trigger zone).

The incidence of diarrhea in our study group was 6.9%. Most patients developed diarrhea at later time (after 24 hours of chemical infusion). There was no case of diarrhea in grade 3 or 4. By contrast, Souglakos et al., treated on 31 stage IV colorectal cancer patients with the similar regimen and found that grade 3 and 4 diarrhea was presented in 10 cases (32%) [8]. Besides, the rate of grade 3, 4 diarrhea in Falcone et al.'s research (2007) was 20%, with no significant difference from FOLFIRI group [10]. Irinotecan, in addition to be Topoisomerase II enzyme inhibitor, inhibit Acetylcholinesterase, an enzyme that decomposes neurotransmitter of Acetylcholin receptor. Therefore, using Irinotecan will stimulate parasympathetic nervous system which intensifies bowel movement and results in diarrhea. All of our patients are taking Atropin to prevent this side effect. Depending on the severity of patient's diarrhea, Atropin is added during infusion.

Three-point six three percent of patients with oral toxicity had been detected in this study and all were at grade 1. FOLFOXIRI regimen not using bolus 5-FU as a feature causes low rate of stomatitis. Studies of Peeters M et al., (2010) [13] and Douillard JY et al., (2000) [14] also had a low incidence of this toxicity (below 5%) [13], [14]. Cases with oral toxicity was detected and treated early, which limited significantly the severity of this unwanted effects.

The most prevail non-hematological adverse event was liver toxicity, accounting for 52.5% of patients treated by FOLFOXIRI, by most of them were at grade 1 (50%), followed by grade 2 with only 2.5%. Similarly, liver toxicity in majority of foreign studies amounted to the highest percentage at grade 1 while the figure of grade 2 toxicity was very small [15], [16]. Of three drugs used in this study, Oxaliplatin is metabolized and excreted mainly in kidney so there is no effect on the liver. 5-FU and irinotecan are metabolised and excreted primarily in the liver, which can cause hepatitis due to the drug. However, the severity of hepatitis is usually mild and self-healing after chemotherapy discontinuation. In the period of treatment, we focussed on the use of infusion after chemotherapy to improve liver function, which helps reduce liver enzymes.

In conclusion, the FOLFOXIRI chemotherapy is a highly effective regimen demonstrated by an increase in response rate, progression-free survival and has side-effects at manageable and well tolerated levels during first-line treatment of metastatic colorectal cancer. The regimen needs to be conducted more in study with a larger sample size and a broader scope to prove its effectiveness and safety before being widely applied in hospitals across the country.

Ethical Approval

Ethical approval to report this case series was obtained from Hanoi Medical University Review Board (Approval Number: IRB00003117).

Informed Consent

Written or verbal informed consent was achieved from the patient(s) for their anonymized information to be published in this article.

Acknowledgment

We would like to thank Ms. Bui Nhat Le (Faculty of Clinical Pharmacy, University of Pharmacy, Hanoi, Vietnam) for checking and improving the English in the manuscript.

References

1. Ferlay J, Soerjomataram I, Dikshit R, et al. Cancer incidence and mortality worldwide: sources, methods and major patterns in GLOBOCAN 2012. Int J Cancer. 2015; 136(5):E359-86. https://doi.org/10.1002/ijc.29210 PMid:25220842

2. Jemal A, Bray F, Center MM, et al. Global cancer statistics. CA Cancer J Clin. 2011; 61(2):69-90. https://doi.org/10.3322/caac.20107 PMid:21296855

3. Grothey A, Sargent D, Goldberg RM, et al. Survival of patients with advanced colorectal cancer improves with the availability of fluorouracil-leucovorin, irinotecan, and oxaliplatin in the course of treatment. J Clin Oncol. 2004; 22(7):1209-14. https://doi.org/10.1200/JCO.2004.11.037 PMid:15051767

4. Falcone A, Masi G, Allegrini G, et al. Biweekly chemotherapy

with oxaliplatin, irinotecan, infusional Fluorouracil, and leucovorin: a pilot study in patients with metastatic colorectal cancer. J Clin Oncol. 2002; 20(19):4006-14. https://doi.org/10.1200/JCO.2002.12.075 PMid:12351598

5. Edwards MS, Chadda SD, Zhao Z, et al. 2012; A systematic review of treatment guidelines for metastatic colorectal cancer. Colorectal Dis. 2002; 14(2):e31-e47. https://doi.org/10.1111/j.1463-1318.2011.02765.x PMid:21848897 PMCid:PMC3562494

6. Duc NB, Dieu B. The situation of cancer in Vietnam in 2010 through data of 6 regions recorded in the period 2004-2008. Vietnam Journal of Oncology. 2010; 1:73-80.

7. Schwartz LH, Litière S, de Vries E, Ford R, Gwyther S, Mandrekar S, Shankar L, Bogaerts J, Chen A, Dancey J, Hayes W. RECIST 1.1-Update and clarification: From the RECIST committee. Eur J Cancer. 2016; 62:132-7. https://doi.org/10.1016/j.ejca.2016.03.081 PMid:27189322 PMCid:PMC5737828

8. Souglakos J, Mavroudis D, Kakolyris S, et al. Triplet combination with irinotecan plus oxaliplatin plus continuous-infusion fluorouracil and leucovorin as first-line treatment in metastatic colorectal cancer: a multicenter phase II trial. J Clin Oncol. 2002; 20(11):2651-7. https://doi.org/10.1200/JCO.2002.08.015 PMid:12039926

9. Azmy AM, Nasr KE, Gobran NS, et al. Infusional Fluorouracil, Leucovorin, Oxaliplatin, and Irinotecan (FOLFOXIRI) Compared with Infusional Fluorouracil, Levcovorin, and Irinotecan (FOLFIRI) as First-Line Treatment for Metastatic Colorectal Cancer. Journal of Cell Science & Therapy. 2012; 3:125. https://doi.org/10.4172/2157-7013.1000125

10. Falcone A, Ricci S, Brunetti I, et al. FOLFOXIRI plus bevacizumab versus FOLFIRI plus bevacizumab as first-line treatment of patients with metastatic colorectal cancer: updated overall survival and molecular subgroup analyses of the open-label, phase 3 TRIBE study. J Clin Oncol. 2007; 25(13):1670-6. https://doi.org/10.1200/JCO.2006.09.0928 PMid:17470860

11. Cremolini C, Loupakis F, Masi G, et al. FOLFOXIRI or FOLFOXIRI plus bevacizumab as first-line treatment of metastatic colorectal cancer: a propensity score-adjusted analysis from two randomized clinical trials. Ann Oncol. 2016; 27(5):843-9. https://doi.org/10.1093/annonc/mdw052 PMid:26861604

12. Loupakis F, Cremolini C, Salvatore L, et al. FOLFOXIRI plus bevacizumab as first-line treatment in BRAF mutant metastatic colorectal cancer. Eur J Cancer. 2014; 50(1):57-63. https://doi.org/10.1016/j.ejca.2013.08.024 PMid:24138831

13. Peeters M, Price TJ, Cervantes A, et al. Randomized phase III study of panitumumab with fluorouracil, leucovorin, and irinotecan (FOLFIRI) compared with FOLFIRI alone as second-line treatment in patients with metastatic colorectal cancer. J Clin Oncol. 2010; 28:4706-4713. https://doi.org/10.1200/JCO.2009.27.6055 PMid:20921462

14. Douillard JY, Cunningham D, Roth AD, et al. Irinotecan combined with fluorouracil compared with fluorouracil alone as first-line treatment for metastatic colorectal cancer: a multicentre randomised trial. Lancet. 2000; 355:1041-1047. https://doi.org/10.1016/S0140-6736(00)02034-1

15. Cremolini C, Loupakis F, Antoniotti C, et al. FOLFOXIRI plus bevacizumab versus FOLFIRI plus bevacizumab as first-line treatment of patients with metastatic colorectal cancer: updated overall survival and molecular subgroup analyses of the open-label, phase 3 TRIBE study. Lancet Oncol. 2015; 16(13):1306-15. https://doi.org/10.1016/S1470-2045(15)00122-9

16. Hurwitz H, Fehrenbacher L, Novotny W, et al. Bevacizumab plus irinotecan, fluorouracil, and leucovorin for metastatic colorectal cancer. N Engl J Med. 2004; 350(23):2335-42. https://doi.org/10.1056/NEJMoa032691 PMid:15175435

ID Design Press, Skopje, Republic of Macedonia
Open Access Macedonian Journal of Medical Sciences. 2019 Dec 30; 7(24):4250-4254.
https://doi.org/10.3889/oamjms.2019.369
eISSN: 1857-9655
Basic and Clinical Medical Researches in Vietnam

Frequency and Risk Factor of Lower-limb Deep Vein Thrombosis after Major Orthopedic Surgery in Vietnamese Patients

My Hanh Bui[1], Duong Duc Hung[2], Pham Quang Vinh[3], Nguyen Hoang Hiep[4], Le Lan Anh[3], Toi Chu Dinh[5*]

[1]Tuberculosis and Lung Disease Faculty, Hanoi Medical University, Hanoi, Vietnam; [2]Department of General Administration, Bach Mai Hospital, Hanoi, Vietnam; [3]Department of Hematology, Bach Mai Hospital, Hanoi, Vietnam; [4]Center for Development of Curriculum and Human Resource in Health, Hanoi Medical University, Hanoi, Vietnam; [5]Department of Hematology, Bach Mai Hospital, Hanoi, Vietnam

Citation: Bui MH, Hung DD, Vinh PQ, Hiep NH, Anh LL, Chu Dinh T. Frequency and Risk Factor of Lower-limb Deep Vein Thrombosis after Major Orthopedic Surgery in Vietnamese Patients. Open Access Maced J Med Sci. 2019 Dec 30; 7(24):4250-4254. https://doi.org/10.3889/oamjms.2019.369

Keywords: Deep Venous Thrombosis; Orthopedic; Frequency; Risk factor

***Correspondence:** My Hanh Bui. Department of Hematology, Bach Mai Hospital, Hanoi, Vietnam. E-mail: buimyhanh@hmu.edu.vn

Received: 26-Jun-2019; **Revised:** 20-Nov-2019; **Accepted:** 21-Nov-2019; **Online first:** 20-Dec-2019

Funding: This research did not receive any financial support

Competing Interests: The authors have declared that no competing interests exist

Abbreviations: DVT: Deep vein thrombosis; PE: Pulmonary embolism; THA: Total hip arthroplasty; TKA: Total knee arthroplasty

Abstract

BACKGROUND: Deep venous thrombosis (DVT) is a prevalent complication of orthopedic surgery. According in many studies. The incidence of DVT may be up to 50% if thromboprophylaxis is not available.

AIM: The objective of this study was to check the degree of disease, clinical characteristics and analyzed factors in vulnerabilities with lower-limp DVT after orthopedic surgery in a Vietnam teaching hospital.

METHODS: Orthopedic patients who met criteria were recruited at our hospital between August 2017 and June 2018. Ultrasound was used to discovering lower-limp DVT in pre-surgery and 7 days after surgery in all patients.

RESULTS: The incidence of DVT after orthopedic surgery was 7.2%. Patients with older age (> 60) have a risk of 2 times higher of DVT after surgery than normal people ($p < 0.05$). The incidence of postoperative DVT was higher in immobile individuals > 72 hours ($p < 0.05$). Patients with prolonged surgical time (>120 minutes) had a higher risk of postoperative DVT than non-surgical patients' surgery ($p < 0.05$).

CONCLUSIONS: DVT remains a common complication following orthopedic surgery. Older age, immobility status, and surgical time have been found to be risky factors for the development of postoperative lower-limp DVT in orthopedic patients.

Introduction

Deep vein thrombosis (DVT) occurs when blood clots are formed and cause partial or complete blockage of the veins, most commonly the lower-limb veins Complications can include pulmonary embolism (PE), as a result of a blood clot moving to the lungs, and syndrome after thrombosis. In the United States, DVT and PE caused up to 600,000 hospitalizations a year, approximately 50,000 deaths from PE [1].

Orthopedic surgeries, such as total hip arthroplasty (THA) and full knee joint surgery, are favorable conditions for the formation and development of the DVT. According to current reports, in the absence of thromboprophylaxis, the vein method used to detect DVT occurs in up to 50% of orthopedic patients, and PE is cause of death of about 1.7% of patients experience THA and about 2% of patients experience TKA. Even with prophylaxis, the likelihood of DVT in orthopedic surgery is 27% [2].

However, according to the literature, the clinical symptoms of DVT is mostly atypical, only suggestive [3]. Nguyen Van Dung conducted a study of clinical characteristics of DVT and found that leg pain occurs in 45.9% of patient with thrombosis and 48.4% of patients without thrombosis, while other symptoms such as swelling, leg numbness, warmth or redness are detected in these two groups. These signs and symptoms are easily confusing with those appearing postoperatively [4]. Similarly, Ker-Kan Tan et al., implemented hospital-based case-control study

and indicated that presenting signs/symptoms relating to DVT such as leg pain, warmth, erythema and fever were not significantly different between groups [5].

We conducted this research to evaluate the incidence rate, clinical characteristics and risk factors for lower-limb DVT in patients undergoing major lower limb orthopedic surgery in our teaching Bach Mai hospital in Vietnam.

Materials and Methods

Study subjects

Patient Selection

To be included in the study, patients had to be adult (≥ 18 year of age) and had undergone one of surgical procedures including total hip arthroplasty, knee arthroplasty or repair of femur fracture, were received preoperative anticoagulant therapy with low-molecular-weight-heparin or oral rivaroxaban, and have ≥ 3 days of hospital stay after surgery. Patients who have been previously diagnosed and treated for lower extremity DVT were excluded from the study, as were patients with neurological diseases who did not have ability to co-operate and provide accurate information. All the patients were notified of the investigational nature of the research, provide oral acceptance before registration on to the study.

Time and Location

The research was proced from August 2017 to June 2018 in Bach Mai Hospital, Hanoi, Vietnam.

Methodology

Study Design: Cross-sectional descriptive examination.

Sample size and sampling method

Sample size

Method:

$$n = Z^2_{1-\alpha/2} \times \frac{p(1-p)}{d^2}$$

n: sample size for the study;

α: 95% confidence coefficient;

$Z_{1-\alpha/2} = Z_{\alpha/2} = 1{,}96$;

p: incidence of DVT after orthopedic surgery, p = 0.4;

d: absolute error, d = 0.1;

The result of calculating the sample size is that n ≈ 92.2.

Therefore, the minimum sample size required for the study is 93 patients.

Sampling method: Intentional sampling method by selecting patient according to the selection criteria in the study until the sample size is sufficient

Study Process

All patients who satisfy the criteria of study and agreed to attend in the examination were interviewed and collected data (demographic information, clinical and subclinical characteristics, surgical methods, thrombo-prophylaxis regimen), taken a blood sample to perform D-dimer levels before and after 3 days of surgery. Simultaneously, a Duplex ultrasonography of the lower limb veins was also excecuted to confirm the presentation of thrombi prior to surgery, since patients diagnosed with pre-existent DVT would be excluded from the study. After 7 days or in case of clinically suspected VTE post-operatively, patients were clinically checked-up and experienced Duplex ultrasonography of lower limb veins and were assessed using Caprini score in order to determine the diagnosis of DVT. After hospital discharge, patients were conducted to account to the reseach center promptly if any symptoms and evidences of DVT occurred at home, and were asked to visit for re-examination after 1 month or immediately when symptoms occurred.

Statistical Analysis

Consecutive variables were precented as mean ± standard deviation or median [range: min-max]. Besides, we conducted Student t test or the Wilcoxon Rank Sum test to appreciate distinction in mean or medians, respectively. Categorical data were compared using the chi-square or Fisher exact tests. Multivariate logistic regression was performed to identify risk factors independently interconnected with occurrence of post-operative DVT. Odds ratio (OR) and 95% confidence interval (CI) were computed using logistic regression. The α level for statistical significance for all test was set at 0.05. All analyses were performed using SPSS 23.0 and STATA 12.0.

Results

From August 2017 to June 2018, we enrolled 97 orthopedic surgical patients who meet criteria to be included in the study at Bach Mai Hospital. Mean age of study population was 61.1 ± 16.3 years old, with the lowest age of 25 and the highest of 95 years old. The proportion of men and women was 47.4% and 52.6%,

respectively. All patients in the study did receive thromboprophylaxis, mainly with Rivaroxaban 10 mg/day (82.5%) or Enoxaparin 40 mg/day (13.4%), for average of 10-14 days, and possibly up to 35 days after surgery [26]. During follow-up, four patients presented major bleeding complications during Enoxaparin therapy, and Rivaroxaban was used alternatively in the following days.

Table 1: Essential characteristics of orthopedic inmates

Characteristics	DVT group (n = 7)	Non-DVT group (n = 90)	p value
Age			
18-40	0	13 (14.4%)	
41-60	2 (28.6%)	27 (30.0%)	
61-74	5 (71.4%)	31 (34.4%)	P > 0,05
≥75	0	19 (21.2%)	
Mean age X ± SD (Min-Max)	65.3 ± 7.3 (55-74)	60.8 ± 16.8 (25-95)	
Gender			
Male	3 (42.9%)	43 (47.8%)	P > 0.05
Female	4 (56.1%)	47 (52.2%)	
Surgical procedures			
Total hip replacement	3 (4.8%)	59 (95.2%)	
Repair of femur fracture	0	3 (100%)	
Total knee replacement	4 (12.9%)	27 (87.1%)	P > 0.05
Acetabular labral tear surgery	0	1 (100%)	
Symptoms			
Pain in one leg	7 (100%)	67 (74.4%)	> 0.05
Erythema	5 (83.6%)	35 (38.9%)	> 0,05
Swelling	4 (57.1%)	46 (51.1%)	> 0.05
Limb numbness	2 (28.6%)	11 (12.2%)	> 0.05
D-dimer test (mg/l FEU)			
Before surgery	2.39 ± 2.52	1.15 ± 1.38	< 0.05
After surgery	6.13 ± 7.38	2.64 ± 2.31	< 0.05

Seven patients developed lower-limb DVT after surgery, and were compared versus those who did not (non-DVT group: n = 90). Patients with DVT were older than those without DVT (65.3 ± 7.3 vs. 60.8 ± 16.8 years, respectively). DVT was detected in 71.4% of patients aged 60-74 years. The distinction was not statistically considerably (p > 0.05). There were no gender differences between two subgroups. The prevalence of lower-limb DVT was mainly in the two types of surgery: 12.9% for knee arthroplasty and 4.8% for hip arthroplasty. Regarding to the clinical presentation of DVT in orthopedic patients, the rate of leg pain, erythema, swelling and limb numbness were respectively 100%, 83.6%, 57.1% and 28.6% in DVT patients, higher than those of non-DVT group (Table 1).

Table 2: Risk factors of lower-limb DVT

Risk factors	No. of patient with lower-limb DVT	Odd ratio	p value
Age > 60	5 (9.1%)	2.0 (0.38-10.86)	< 0.05
Female sex	4 (7.8%)	1.22 (0.26-5.8)	> 0.05
Current smoker	2 (12.5%)	2.17 (0.4-12.0)	> 0.05
Diabetes	1 (9.1%)	1.33 (0.1-12.3)	> 0.05
Previous major surgery (1 month or more)	2 (20.0%)	4.1 (0.8-22.1)	> 0.05
Blood transfusion	4 (13.8%)	3.5 (0.8-15.5)	> 0.05
Immobilization > 72 hour	5 (20.0%)	8.8 (1.6-48.5)	< 0.05
Operative time	4 (50.0%)	28.67 (4.7-173.7)	< 0.05

Table 2 summarizes the result of logistic regression used to analyze the association between post-operative lower-limb DVT and causative factors including age over 60, gender, smoking status, history of diabetes, previous major surgery, blood transfusion, immobilization > 72 hours and operative duration. Our analysis revealed that older age (> 60), immobilization (> 72 hours), and prolonged surgery (operation time > 120 min) were significantly associated to the high risk of DVT (p < 0.05). Particularly, the rate of post-operative lower-limb DVT was significantly higher in patients who were immobilized for ≥ 72 hours (20%), compared to those who weren't (2.8%). Immobilization increased the risk of DVT by 8.8 times in orthopedic surgical patients (95% CI, 1.6-48.5). Patients with prolonged surgical time (≥ 120 min) had elevated overall rate for lower-limb DVT and greater risk of post-operative deep venous thromboembolism (OR = 28.67; 95% CI, 4.7-173.7) compared with patients having less than 120 minutes of surgical time.

Discussion

Deep vein thrombosis is known to occur prevalently after surgery, particularly orthopedic surgery, and to be able result in PE, which can be fatal. Our study of 97 patients undergoing major orthopedic surgery reveals that the rate of DVT after orthopedic surgery was 7.2%. This finding is lower than the 40% found in the Vo Van Tam and Nguyen Vinh Thong's study conducted in Cho Ray Hospital [6]. Moreover, Kim K et al reported 18%-24% incidence of deep vein thrombosis following total hip arthroplasty (THA) and an incidence of 20%-49% following total knee arthroplasty (TKA) [7]. Although these studies were similar in time and patient's characteristics compared to our study, the patients of these studies did not receive pre-operative thromboprophylaxis while in our study it was provided to 100% of patients before surgery. Thus, the rates of DVT are higher than ours.

Regarding to the clinical characteristics of lower-limb DVT, no statistically considerably distinction was found between groups. The most found symptoms/signs were leg pain and erythema in DVT group. This suggests that these two symptoms may be indications that the patient may have had or be having lower-limb DVT. However, with the specificity of orthopedic surgery as the intervention in the limbs of the patient, so these symptoms can be confusing, difficult to identify. Author Nguyen Van Dung (2011) claimed that the clinical symptoms of lower-limb DVT are atypical, nonspecific and easy to confuse with other diseases [4]. Others such as swelling, numbness and paresthesia are somewhat related to the feeling of each patient, so there is a similarity between DVT and non-DVT patients.

Our study shows that preoperative and postoperative D-dimer test values were significantly higher in the DVT group than in the non-DVT group (p < 0.05). These values were also found similar after surgery. Si-dong Yang, et al., conducted study on D-dimer test and found the D-dimer in DVT group to be relatively greater than non-DVT group [8]. Hamidi S, et al., reported a difference in D-dimer levels after

surgery between patients with and without DVT, with D-dimer cut-off point on day 3 post-operatively of 2.1 μg/mL for 100% sensitivity, 80.7% specificity and 100% negative diagnostic result [9]. Furthermore, Sudo A, et al., indicated the increase of D-dimer level statistically significant on day 4, 7, 10 and 14 after surgery, a value of 7.0 mg/L on day 4 is significant for the diagnosis of lower extremity DVT [10]. In case Duplex ultrasound images are negative, the addition of D-dimer test eliminates the risk of DVT and patient does not need to do second ultrasound test [11], [12]. Therefore, our findings are consistent with those of foreign authors.

Ascertaining the risk factor for progessive of DVT and PE is significant as this may help clinicians determine high risk patients and give them appropriate prophylaxis. In this study, we evaluate 8 factors for their role in causation or association with development of DVT after orthopedic surgery and found age over 60, immobility > hours and prolonged operative time (> 2 hours) to be significant risk factors.

Older age is commonly related to weak venous valve dinamic, vascular sclerosis and high blood viscousness. This factor associated with limited exercise after surgery, may result in lower limb DVT. In present research, age have been found to be significantly interconnected with an increase of venous thrombosis among orthopedic patients. Our result is consistent with that of Motohashi M which showed that age over 60 years significantly increased the risk of DVT by 3.91 times ($p < 0.001$) [13]. After surgery, patients often do not exercise in bed and spend a lot of time travelling on ambulant, thus they are at high baseline risk of venous thrombosis in the lower extremity. Our study confirms that postoperative immobilization over 72 hours was considerably interconnected with high risk of lower-limb DVT (OR = 8.8, $p < 0.05$). Our finding also accords with that of Bagiaria et al. [14]. In Virchow's Triad describing the pathogenesis of venous thrombosis, one of the three factors are stasis of blood flow. Prolonged immobility can be conducive to this condition, leading to the genesis of blood clot in the lower-limb.

Table 2 shows that patients who had surgery time greater than 120 minutes increased the risk of DVT by 28.67-fold, which was statistically significant at $p < 0.001$. Bagiaria et al., suggested that a surgery performed for more than 2 hours will increase the risk of DVT by 4.318 times [14]. Besides, Kang J, et al., reported a 1.69 times higher risk in patient with prolonged operative time [15]. The finding of our study was surpassingly higher than those of the authors, perhaps because our sample size was 97 patients, which is much lower than that of Bagaria's (147 patients) and Kang J's (1025 patients). In an analysis of 611 patients who had undergone orthopedic surgery of lower extremities, Motohashi M et al. demonstrated that prolonged operation time (> 120 minute, OR = 4.52) was detected as factor that markedly impacted the occurrence of DVT in all patients. But in general, the more time the surgery take, the greater the risk for developing lower-limb DVT become [13].

In conclusion, DVT remains a common complication following orthopedic surgery. Our study conducted on 97 orthopedic surgical patients showed that the incidence of postoperative DVT was 7.2%. Common clinical symptoms are pain in one leg, swelling, paresthesia and skin color change. Old age, immobility status (> 72 hours) and prolonged operative time were associated with a higher risk of developing postoperative DVT after orthopedic surgery. Thus, plastic surgeons should carefully examine the risk factors of DVT before implementing major orthopedic surgeries and should remain aware of the likelihood of developing postoperative DVT in high-risk patients.

Acknowledgement

We would like to thank Bach Mai Hospital for providing favorable conditions to us to carry out this research. We are committed not to cause conflict of interests from research results. We would like to thank Ms. Hoang Thi Anh (Faculty of Biology, Hanoi National University of Education, Hanoi, Vietnam) checking and improving the English in the manuscript.

Ethical Approval

This research was accepted by Ethical Review Board of Hanoi Medical University (Approval No. IRB 003121).

Informed Consent

Informed consents were collected from participating patient(s) for their anonymized information to be reported in the study.

References

1. Prevention of venous thrombosis and pulmonary embolism. NIH Consensus Development. JAMA. 1986; 256(6):744-9. https://doi.org/10.1001/jama.256.6.744 PMid:3723773

2. Kim YH, Oh SH, Kim JS. Incidence and natural history of deep-

vein thrombosis after total hip arthroplasty. A prospective and randomised clinical study. J Bone Joint Surg Br. 2003; 85(5):661-5. https://doi.org/10.1302/0301-620X.85B5.14012 PMid:12892186

3. CB M, et al. Risk factors for clinically relevant pulmonary embolism and deep venous thrombosis in patients undergoing primary hip or knee arthroplasty. Anesthesiology. 2003; 99:552-60. https://doi.org/10.1097/00000542-200309000-00009 PMid:12960538

4. Dung NV. Evaluation of Wells scales and serum D-dimer levels in the diagnosis of deep vein thrombosis. Hanoi Medical University Hospital, Hanoi, 2011.

5. Tan KK, Koh WP, Chao AK. Risk factors and presentation of deep venous thrombosis among Asian patients: a hospital-based case-control study in Singapore. Ann Vasc Surg. 2007; 21(4):490-5. https://doi.org/10.1016/j.avsg.2006.06.008 PMid:17628265

6. Tam VV, Thong NV. Investigation of the frequency of deep vein thrombosis in the lower extremities in patients undergoing knee or hip replacement surgery. Ho Chi Minh Medical Journal. 2014; 18(2):250-256.

7. Kim KI, et al. Thromboprophylaxis for Deep Vein Thrombosis and Pulmonary Embolism after Total Joint Arthroplasty in a Low Incidence Population. Knee Surg Relat Res. 2013; 25(2):43-53. https://doi.org/10.5792/ksrr.2013.25.2.43 PMid:23741698 PMCid:PMC3671115

8. Yang SD, Liu H, Sun YP, Yang DL, Shen Y, Feng SQ, Zhao FD, Ding WY. Prevalence and risk factors of deep vein thrombosis in patients after spine surgery: a retrospective case-cohort study. Scientific reports. 2015; 5:11834. https://doi.org/10.1038/srep11834 PMid:26135271 PMCid:PMC4488742

9. Hamidi S, Riazi M. Cutoff Values of Plasma D-Dimer Level in Patients with Diagnosis of the Venous Thromboembolism after Elective Spinal Surgery. Asian Spine J. 2015; 9(2):232-238. https://doi.org/10.4184/asj.2015.9.2.232 PMid:25901235 PMCid:PMC4404538

10. Sudo A, Wada H, Nobori T, Yamada N, Ito M, Niimi R, Hasegawa M, Suzuki K, Uchida A. Cut-off values of D-dimer and soluble fibrin for prediction of deep vein thrombosis after orthopaedic surgery. Int J Hematol. 2009; 89(5):572-576. https://doi.org/10.1007/s12185-009-0323-4 PMid:19430861

11. SA, L., et al., Approach to the diagnosis and therapy of lower extremity deep vein thrombosis, 2014. www.Uptodate.com, 2014.

12. Working GJJ. Guidelines for the diagnosis, treatment and prevention of pulmonary thromboembolism and deep vein thrombosis. Circ J. 2011; 75(5):1258-1281. https://doi.org/10.1253/circj.CJ-88-0010 PMid:21441695

13. Motohashi M, et al. Deep vein thrombosis in orthopedic surgery of the lower extremities. Ann Vasc Dis. 2012; 5(3):328-333. https://doi.org/10.3400/avd.oa.12.00049 PMid:23555532 PMCid:PMC3595850

14. Bagaria V, Incidence and risk factors for development of venous thromboembolism in Indian patients undergoing major orthopaedic surgery: results of a prospective study. Postgrad Med J. 2006; 82(964):136-139. https://doi.org/10.1136/pgmj.2005.034512 PMid:16461477 PMCid:PMC2596707

15. Kang J, Jiang X, Wu B. Analysis of Risk Factors for Lower-limb Deep Venous Thrombosis in Old Patients after Knee Arthroplasty. Chin Med J. 2015. 128(10):1358-62. https://doi.org/10.4103/0366-6999.156782 PMid:25963358 PMCid:PMC4830317

ID Design Press, Skopje, Republic of Macedonia
Open Access Macedonian Journal of Medical Sciences. 2019 Dec 30; 7(24):4255-4259.
https://doi.org/10.3889/oamjms.2019.370
eISSN: 1857-9655
Basic and Clinical Medical Researches in Vietnam

Oral Rivaroxaban Versus Standard Therapy in Acute Venous Thromboembolism Treatment for Vietnamese Patients

My Hanh Bui[1,2*], Nguyen Truong Son[3], Pham Thanh Viet[4], Nguyen Hoang Hiep[5], Toi Chu Dinh[6]

[1]Tuberculosis and Lung Disease Department, Hanoi Medical University, Hanoi, Vietnam; [2]Scientific Research & International Cooperation Department, Hanoi Medical University Hospital, Hanoi, Vietnam; [3]Director Board, Cho Ray Hospital, Ho Chi Minh City, Vietnam; [4]Department of General Administration, Bach Mai Hospital, Hanoi, Cho Ray Hospital, Ho Chi Minh, Vietnam; [5]Center for Development of Curriculum and Human Resource in Health, Hanoi Medical University, Hanoi, Vietnam; [6]Faculty of Biology, Hanoi National University of Education, Hanoi, Vietnam

Citation: Bui MH, Son NT, Viet PT, Hiep NH, Chu Dinh T. Oral Rivaroxaban Versus Standard Therapy in Acute Venous Thromboembolism Treatment for Vietnamese Patients. Open Access Maced J Med Sci. 2019 Dec 30; 7(24):4255-4259.
https://doi.org/10.3889/oamjms.2019.370

Keywords: Oral rivaroxaban; Standard therapy; Acute venous thromboembolism; Vietnamese patients

***Correspondence:** My Hanh Bui. Tuberculosis and Lung Disease Department, Hanoi Medical University, Hanoi, Vietnam; Scientific Research & International Cooperation Department, Hanoi Medical University Hospital, Hanoi, Vietnam. E-mail: buimyhanh@hmu.edu.vn

Received: 26-Jun-2019; **Revised:** 20-Nov-2019; **Accepted:** 21-Nov-2019; **Online first:** 20-Dec-2019

Funding: This research did not receive any financial support

Competing Interests: The authors have declared that no competing interests exist

Abstract

BACKGROUND: Direct oral anticoagulant-rivaroxaban may provide a simple, fixed-dose therapy for the management of hospital-acquired, acute venous thromboembolism (VTE) and for extended treatment, its use could skip lab observation and/or parenteral treatment.

AIM: Compare the efficacy and safety (EAS) of RIV vs. standard therapy (SDTD) in a cohort of Vietnamese patients diagnosed with symptomatic, acute VTE.

METHODS: An open-label, case-control, prospective study was conducted to check the efficacy and safety (EAS) of oral rivaroxaban (RIV) alone (15 mg 2 times/day for 3 weeks, then 20 mg 1 time/day) in a comparison to the standard therapy (STDT) (enoxaparin 1.0 mg/kg 2 times/day combining with vitamin K antagonist). Patients were treated for 6 months and followed-up for suspect reoccurring VTE and bleeding.

RESULTS: A total 187 patients were enrolled into study. 83 were provided rivaroxaban and 104 received enoxaparin overlapping with vitamin K antagonist (VKAs). Recurrent VTE occurred in 3 (3.6%) rivaroxaban-received patients compared with 5 (4.8%) standard-treatment received patients (OR: 0.74, 95% CI, 0.17 to 3.20, p > 0.05). Major bleeding events were found in 1 (1,8%) and 4 (3.9%) cases in the RIV treated and STDT cohort, respectively (OR: 0.30, 95% CI, 0.03 to 2.76, p > 0.05).

CONCLUSION: The finding of this study in Vietnamese patients with acute VTE presented comparable EAS profile with RIV versus STDT, consistent with those found in global population.

Introduction

Venous thromboembolism (VTE), (for example deep venous thromboembolism (DVT) or pulmonary embolism (PE)) is a major issue which cause annual prevalence of about 100 – 200 cases per 100,000 individual in the Western countries [1], [2]. In Asia, the prevalence of VTE has increased over recent years, however, it is often knownto be lower than that in Caucasian population [3], [4]. Anticoagulant therapy effectively minimize the rate of recurrent VTE from 25% to 3% approximately within the period from 6 to 12 months, but the risk of VTE reoccurrence was stable at around 5-10% after one year of treatment [5].

Standard guidelines on antithrombotic therapy for VTE commonly suggest the application of enoxaparin (low molecular weight heparins) plus vitamin K antagonists (VKAs). However, it still has some limitations. Enoxaparin requires uncomfortable subcutaneous injection on a daily or twice daily basis while treatment with VKAs demands lab observation and cautious dosage modification and may be complicated by interacting with food and concomitant drug. After one year, the likelihood of occuring major bleeding event with regard to the use of VKAs is approximately 1 to 2% annually [6]. As a result, the debate on balancing the advantages and the disadvantages of continuous therapy were still controversial, regardless of the high likelihood of VTE reoccurrence in a long term. An absolute method to solve several of these concerns might be introduction of new oral anticoagulant that skip the requirement for parenteral medication and routine lab observation but shows effectiveness as a single factor for acute and

continued treatment of symptomatic VTE.

Rivaroxaban (RIV), a new oral anticoagulant, acts through activedirect inhibition of activated Factor Xa and shows a quick onset of peak anticoagulant effect (within 2-4 hours after dosing) and has calculable pharmacodynamic and pharmacokinetic properties, which restrain the requirement for daily observation of anticoagulation, has a low propensity for interacting with other drugs and does not need dietary restrictation [7]. The evaluation of RIV was implemented in global clinical trial in acute symptomatic VTE patients, and showed a comparable efficacy as enoxaparin plus VKA with reduced incidence of major bleeding [8], [9].

Although there are a number of published studies on using RIV for the intervention of thrombolysis conditions in the literature, this therapy is not well documented among Asian population. Therefore, we aimed to compare the efficacy and safety (EAS) of RIV vs. standard therapy (SDTD) in a cohort of Vietnamese patients diagnosed with symptomatic, acute VTE.

Methods

Study design

This was a case-control, prospective study designed to evaluate the EAS of RIV in comparison with SDTD (enoxaparin overlapping with VKAs) in treating acute hospital-acquired VTE. The research was conducted at a teaching hospital (Cho Ray Hospital, Ho Chi Minh, Vietnam).

Subject and sampling method

Convenience sampling method is applied. All eligible patients are recommended to participate into study.

Patients were enrolled in the study if they were ≥ 18-year olds and had been diagnosed as having acute, symptomatic DVT and/or PE. Patients were not included if therapeutic dosage of parenteral anticoagulant was given to patients for over 48 hours before randomization; or if thrombectomy had been performed, a vena cava filter required for the present occasion of thrombosis; or if patients were contraindicated for using anticoagulant. Other criteria for exclusion were: having significant hepatic disease; another designation for VKAs; cerebral haemorrhage; occurrence of bleeding or an increased likelihood of occurring bleeding,; renal failure with creatinine clearance levels < 30 mL/min; a systolic blood pressure (BP) of ≥ 180 mm Hg or diastolic BP of ≥ 110 mm Hg; pregnancy or breast-feeding; or a life expectancy of ≤ 3 months.

Treatment regimens

Patients using rivaroxaban for VTE treatment were received 15 mg 2 times per day for the first 3 weeks, then 20 mg were given 1 time per day continuously. Patients distributed to STDT received injection of enoxaparin with a dosage of 1.0 mg/kg of body weight two times per day, and vitamin K antagonists (warfarin or acenocoumarol), begun during 48 hours after selection. Anticoagulation with SDTD was stopped when the INR (international normalized ratio) was recorded as 2.0 or higher for two continuous days and after the patients had been given at a minimum of 5 day. The VKAs dosing was changed to sustain an INR of 2.0-3.0. Initially, the INRs were examined frequently, and when stabile, at least one time per month.

Patients follow-up

Follow-up for discharged patients was performed for intended treatment period (6 months) and evaluated at fixed intervals that were alike for both subgroups. Any signs and symptoms of VTE recurrence, bleeding and complications were elicited using a checklist among each outpatient visit. If any of signs and symptoms of these events happened, patients were guided to inform to physician. In case of clinically suspected VTE reoccurrence, objective testing was demanded.

Outcomes

The main outcome for this study was the prevalence of reoccurring VTE consisting of symptomatic DVT or PE. The criteria for detection of recurrent PE were as follow: a new intraluminal filling deficiency on pulmonary angiography or computed tomography scan, a new cutoff of a vessel of 2.5 mm or higher in caliber on pulmonary angiography, a new non-high probability perfusion defect related to DVT as determined by ultrasonography or venography. The criteria for identification of recurrent DVT were as follow: a new non-compressible venous segment or a significant enlargement (more than 4 mm) in the caliber of the blood clots during full compression in earlier uncommon sector on venous detected by ultrasound scan or on the appearance of a filling deficiency on venography.

The outcome of safety was clinically relevant bleeding. Bleeding complications were classified as critical if it was clinically overt and required a transfusion of more than two units of packed red blood cells; was intracranial or retroperitoneal, appeared in another critical site and/or conduced to mortality. Non-critical clinical bleeding was determined as observable bleeding that did not satisfy the criteria for major bleeding complication but was related to medical intervention, infrequent use of drug or abandonment of medication, unscheduled contact with doctor, or

impairment of daily activities.

Mortality was identified as being because of PE, bleeding events or other causes happening during the time of continuous treatment. Pulmonary embolism was seen as the reason of decease if objective documentation of the disease were demonstrated, or if the reason of death was not discovered and PE could not be removed.

Statistical analysis

Desciptive statistics were conducted to analyze distribution of baseline characteristics in the two treatment arms. Qualitative variables were calculated as percentages and quantitative variables were calculated as average (± SD). Proportions and absolute differences and corresponding 95% confidence intervals (CI) were reported. Exact method was applied to calculate 95% CI. The results were recognized statistically significant if $p < 0.05$.

Results

From January 2017 to August 2018, a total of 187 VTE patients were selected into the study. Of these, 83 were given RIV and 104 received enoxaparin overlapping with VKAs. Overall, 71 patients receiving rivaroxaban (85%) had isolated DVT vs. 91 (87%) from standard treatment group; Moreover, 3.6% vs. 4.8% of patients had DVT and PE, and; 10.8% vs. 6.7% of patients had PE without DVT symptoms (Table 1). Limb swelling and leg pain were found as the most frequent signs in DVT patients while dyspnea and chest pain were mostly seen in PE patients. Their baseline and clinical characteristics appear in Table 1.

Table 1: Baseline characteristics

Characteristic	RIV (n = 83)	STDT (n = 104)	p value
Average age, (± SD)	57.08 ± 19.5	60.2 ± 16.4	0.24
Male sex, n (%)	30 (36.1)	27 (25.2)	0.13
Mean weight	55.8 ± 10.1	55.4 ± 9.0	0.84
Concomitant disease, n (%)	33 (47.1%)	58 (59.8%)	0.12
Concomitant therapy, n (%)	42 (50.6%)	49 (47.1%)	0.65
Major bleeding occurring in previous month, n (%)	1 (1.2%)	0	0.27
Creatinine clearance, n (%)			0.63
30 - < 50 mL/min	7 (8.4%)	13 (12.5%)	
50 - < 80 mL/min	28 (33.7%)	34 (32.7%)	
≥ 80 mL/min	44 (53.01%)	55 (52.9%)	
Cancer	5 (6%)	9 (8.4%)	0.74
Recent surgery	2 (2.4%)	3 (2.8%)	0.99
Immobilization (≥ 4 days)	8 (9.6%)	11 (10.6%)	0.41
Estrogen therapy	1 (1.2%)	0	0.25
Previous DVT or PE	3 (3.6%)	3 (2.9%)	0.60
Any travel > 6 hours in the past 3 weeks	0	1 (0.096%)	0.37
Puerperium	1 (1.2%)	2 (1.9%)	0.54
Known thrombophilic condition	3 (3.6%)	4 (3.8%)	0.96
Unprovoked VTE	62	71	
only DVT, n (%)	71	91	
DVT/PE	3 (3.6%)	5 (4.8%)	
Only PE	9 (10.8%)	7 (6.7%)	

Among 83 patients treated with rivaroxaban, 8.3% had been immobilized for the first 3 days of treatment. Meanwhile, there were 15 enoxaparin users who had been immobilized.

Table 2: Characteristics related to anticoagulant treatment in both subgroups

Characteristic	RIV (n = 83)	STDT (n = 104)	p value
Immobilization during the first 3 days			0.45
Complete, n (%)	1 (1.2%)	1 (0.96%)	
Relative, n (%)	7 (8.3%)	15 (14.4%)	
Mean time in INR range			
< 2.0	NA	15.3%	
2.0-3.0	NA	54.8%	
> 3.0	NA	27.9%	
Mean study treatment duration, days	167.6 ± 15.8	169.2 ± 16.4	0.61
Intended duration of treatment			
3 months	12	16	
6 months	70	88	

Note: P values were determined using Chi-square test.

Besides, in both treatment arms, only one patient was immobilized at a complete degree. In the traditional treatment group, the INR being in therapeutic range (2.0-3.0) accounted for 54.8% of the time, INR values above 3.0 and below 2.0 occupied the corresponding percentage of time of 27.9% and 15.3%, respectively (Table 2). None of participants was missing during follow-up

Table 3: Clinical outcomes

Treatment Outcomes	RIV (n = 83)	STDT (n = 104)	Risk Ratio (95% CI)	p
Recurrent VTE, n (%)	3 (3.6%)	5 (4.8%)	0.74 (0.17-3.20)	0.69
Type of VTE reoccurrence				
Fatal PE	0	0		
Nonfatal PE	1	1		
Reoccurring DVT plus PE	0	0		
Reoccurring DVT	2	3		
Death from any cause – n (%)	2 (2.4%)	4 (3.9%)	0.61 (0.11-3.43)	0.57
PE	0	0		
Bleeding	0	0		
Cardiovascular	0	0		
Other	2	4		
Bleeding event, n (%)				
Major bleeding	1 (1.8%)	4 (3.8%)	0.30 (0.03-2.76)	0.26
Clinically relevant non-major bleeding, n (%)	9 (10.8%)	11 (10.6%)	1.02 (0.40-2.59)	0.97

Note: P values were determined using Cox Proportional-Hazard Regression.

The main efficacy outcome, recurrent VTE, was confirmed in 3 cases in the novel anticoagulant subgroup and in 4 cases in the STDT subgroup. There were 6 cases of death reported in the study, 2 from treatment arm using rivaroxaban and 4 from group received enoxaparin plus VKA. However, the cause of death was not associated with VTE or bleeding complications, but other diseases such as stroke, respiratory insufficiency, and diabetes. Clinically relevant non-major bleeding events were observed in 9 cases in RIV subgroup and in 11 patients in SDTD group. Major bleeding was detected in one rivaroxaban-received patient (1.8%) and in 4 (3.8%) patients who were give enoxaparin overlapping with VKA (Table 3).

Discussion

Our analysis confirms that RIV shows comparable effectiveness to STDT in Vietnamese

patients also, with parallel safety for the intervention of symptomatic, acute VTE, and for the continuous treatment. The use of rivaroxaban presented a slight decrease in the frequency of reoccurring VTE in comparison with enoxaparin/VKA and presents acceptable likelihood of occurring bleeding event.

Our study shows that the mean age of patients receiving rivaroxaban group was 56.5 ± 20.1 years, slightly younger than those on standard therapy (61.2 ± 18.8 years). Mean age of in our study population was similar to that of EISTEIN study on Chinese patients: 58.6 ± 15.8 and vs. 59.0 ± 15.0 years, respectively [10]. Male patients accounted for 36.1% in RIV group and 25.2% in STDT group. The male proportions are lower compared to those in contemporary clinical studies [11], [12]. The risk factors that were most commonly observed in our patients were immobilization, cancer, history of thrombosis, and undergoing previous major surgery, which are consistent with population-based researches from Western countries [13], [14]. Overall, 2.4% of patients given RIV and 2.8% of those receiving STDT, underwent major surgery before, which suggested that post-operative thromboprophylaxis failed in these surgical patients. The situation of low execution of thromboprophylaxis in surgical patients has been reported in previous studies [15], [16]. On the basis of these data, the enhancement of quality should highlight the importance of conducting more appropriate prophylaxis for patients at high risk. In addition, the VTE treatment in standard therapy group was done well suggesting that the proportion of time in which the INR was in the therapeutic range (2.0-3.0) was 54.8% and for INR above 3.0 was 27.9%. Our findings were consistent with the results which was showed in other contemporary studies on VTE treatment [17], [18].

We found that rivaroxaban is non-inferior to enoxaparin in relation with efficacy and safety. The prevalence of complications occurring during 6 months of follow-up is comparable to the rate demonstrated by Wang and colleagues [10]. The frequency of reoccurring VTE in that analysis was 3.2% in both STDT and RIV groups. In our study, reoccurring VTE was identified in 3.6% of patients who received RIV versus 4.8% of patients in the STDT group. Bleeding was the most prevalent complication in this study, occurring in both treatment arms during initial therapy. Interestingly, while the rate of non-critical bleeding complications in two groups was comparable to each other groups (10.8% and 10.6%, respectively), the frequency of major bleeding was less common in rivaroxaban-given patients, 1.8% vs. 3.8% (OR: 0.26; 95% CI: 0.03-2.76). Our results seem to be slightly worse than those in the randomized clinical trials. For instance, the EINSTEIN study which compares the EAS of RIV vs. STDT (enoxaparin plus VKA) found the prevalence of major bleeding event to be 0.8% and 1.2% (OR: 0.65; 95% CI: 0.33-1.30; p = 0.21) in the RIV and STDT groups, respectively. The most likely explanation for this discrepancy could be differences in the exclusion criteria to recruit patients in both studies. Moreover, the frequency of non-critical bleeding events was identical between two arms (8.1% vs. 8.1%) [17].

Prins MH et al., implemented a comparison between oral rivaroxaban and enoxaparin combined with VKA on 8282 VTE treatment and suggested that the rate of mortality was 2.3% and 2.4% in the two subgroups. Of these, PE related mortality accounted for 0.4% of patients using rivaroxaban and 0.3% of those receiving enoxaparin combined with VKA while bleeding related to death appeared in corresponding proportion of 0.1% and 0.2% of number of patients [9]. In comparison, there were 6 patients who died during follow-up in our study, but the cause of death was non-related to VTE or bleeding.

Several restrictions of our study had been noted. Firstly, since our study was designed as open-label, there could be bias in outcomes assessment. However, endeavors were performed in order to restrict bias in investigation, consisting of the demand to apply diagnostic tests in detecting suspected reoccurring VTE, identical follow-up of all patients, and central adjudication of all outcome circumstances. Second, imbalance in patients' characteristics may lead to more hospitalization or emergency department visit recorded in one treatment arm and more "recycled" VTE codes that will be carried forward instead of being associated with a "true" recurring VTE. In order to solve this, we restrained our endpoint of "recurrent VTE" only to hospital admissions, where "VTE" was the primary code. Third, the risk of bleeding is also probably modified by characteristics that alter during the course of therapy, such as the concurrent use of other drugs, or the existence of intercurrent disease. Finally, our study was conducted in only one hospital with small sample sizes, so it was not possible to assess the true efficacy of rivaroxaban on Vietnamese subjects, therefore, it was necessary to implement more clinical trials with larger sample sizes in many different centers.

To conclude, the findings of this study confirm that the EAS of RIV are compared with those monitored in the larger clinical trials with parallel EAS and better bleeding profile compared to STDT (enoxaparin combined with VKA). The results suggest that rivaroxaban offers clinician with a new, better option in treatment of VTE for Vietnamese patients.

Ethical Approval

Research only aims to protect and improve the health of patients, not for any other purpose. This research was accepted by Ethical Review Board of Hanoi Medical University (Approval No. IRB 003121).

Informed Consent

Informed consents were collected from participating patient(s) for their anonymized information to be reported in the study.

References

1. Næss IA, et al. Incidence and mortality of venous thrombosis: a population-based study. J Thromb Haemost. 2007; 5(4):692-9. https://doi.org/10.1111/j.1538-7836.2007.02450.x PMid:17367492

2. Spencer FA, et al. Incidence rates, clinical profile, and outcomes of patients with venous thromboembolism. The Worcester VTE study. J Thromb Thrombolysis. 2009; 28(4):401-9. https://doi.org/10.1007/s11239-009-0378-3 PMid:19629642 PMCid:PMC3248815

3. Jang MJ, Bang SM, Oh D. Incidence of venous thromboembolism in Korea: from the Health Insurance Review and Assessment Service database. J Thromb Haemost. 2011; 9(1):85-91. https://doi.org/10.1111/j.1538-7836.2010.04108.x PMid:20942850

4. Group JJW. Guidelines for the diagnosis, treatment and prevention of pulmonary thromboembolism and deep vein thrombosis (JCS 2009). Circ J. 2011; 75(5):1258-81. https://doi.org/10.1253/circj.CJ-88-0010 PMid:21441695

5. Edwards MS, et al. A systematic review of treatment guidelines for metastatic colorectal cancer. Colorectal Dis. 2012; 14(2):e31-e47. https://doi.org/10.1111/j.1463-1318.2011.02765.x PMid:21848897 PMCid:PMC3562494

6. Sarich TC, et al. Rivaroxaban: a novel oral anticoagulant for the prevention and treatment of several thrombosis-mediated conditions. Ann N Y Acad Sci. 2013; 1291(1):42-55. https://doi.org/10.1111/nyas.12136 PMid:23701516

7. Investigators E, et al. Oral rivaroxaban for symptomatic venous thromboembolism. N Engl J Med. 2010; 363(26):2499-510. https://doi.org/10.1056/NEJMoa1007903 PMid:21128814

8. Prins MH, Lensing AW. Derivation of the non-inferiority margin for the evaluation of direct oral anticoagulants in the treatment of venous thromboembolism. Thrombosis journal. 2013; 11(1):13. https://doi.org/10.1186/1477-9560-11-13 PMid:23829521 PMCid:PMC3710481

9. Authors/Task Force Members, Konstantinides SV, Torbicki A, Agnelli G, Danchin N, Fitzmaurice D, Galiè N, Gibbs JS, Huisman MV, Humbert M, Kucher N. 2014 ESC guidelines on the diagnosis and management of acute pulmonary embolism. Eur Heart J, 2014. 35(43):3033-69.

10. Wang Y, et al. Rivaroxaban for the treatment of symptomatic deep-vein thrombosis and pulmonary embolism in Chinese patients: a subgroup analysis of the EINSTEIN DVT and PE studies. Thrombosis Journal. 2013; 11(25). https://doi.org/10.1186/1477-9560-11-25 PMid:24341332 PMCid:PMC3896794

11. Prins MH, et al. Oral rivaroxaban versus enoxaparin with vitamin K antagonist for the treatment of symptomatic venous thromboembolism in patients with cancer (EINSTEIN-DVT and EINSTEIN-PE): a pooled subgroup analysis of two randomised controlled trials. Lancet Haematol. 2014; 1(1):e37-46. https://doi.org/10.1016/S2352-3026(14)70018-3

12. Coleman CI, et al. Effectiveness and safety of rivaroxaban versus warfarin in patients with provoked venous thromboembolism. J Thromb Thrombolysis. 2018; 46(3):339-345. https://doi.org/10.1007/s11239-018-1695-1 PMid:29881958

13. Jr, A.F., et al., A population-based perspective of the hospital incidence and case-fatality rates of deep vein thrombosis and pulmonary embolism. The Worcester DVT Study. Arch Intern Med. 1991; 151(5):933-8. https://doi.org/10.1001/archinte.1991.00400050081016

14. Heit JA, et al. Risk factors for deep vein thrombosis and pulmonary embolism: a population-based case-control study. Arch Intern Med. 2000; 160(6):809-15. https://doi.org/10.1001/archinte.160.6.809 PMid:10737280

15. Caiafa JS, et al. Managing venous thromboembolism in Latin American patients: emerging results from the Brazilian Registry. Semin Thromb Hemost. 2002; 28(Suppl 3):47-50. https://doi.org/10.1055/s-2002-34076 PMid:12232824

16. Goldhaber SZ, Dunn K, Mac Dougall RC. New onset of venous thromboembolism among hospitalized patients at Brigham and Women's Hospital is caused more often by prophylaxis failure than by withholding treatment. Chest. 2000; 118(6):1680-4. https://doi.org/10.1378/chest.118.6.1680 PMid:11115458

17. Prins MH, et al. Oral rivaroxaban versus standard therapy for the treatment of symptomatic venous thromboembolism: a pooled analysis of the EINSTEIN-DVT and PE randomized studies. Thromb J. 2013; 11(1):21. https://doi.org/10.1186/1477-9560-11-21 PMid:24053656 PMCid:PMC3850944

18. Büller HR, et al. Enoxaparin followed by once-weekly idrabiotaparinux versus enoxaparin plus warfarin for patients with acute symptomatic pulmonary embolism: a randomised, double-blind, double-dummy, non-inferiority trial. Lancet. 2012; 379(9811):123-9. https://doi.org/10.1016/S0140-6736(11)61505-5

ID Design Press, Skopje, Republic of Macedonia
Open Access Macedonian Journal of Medical Sciences. 2019 Dec 30; 7(24):4260-4265.
https://doi.org/10.3889/oamjms.2019.371
eISSN: 1857-9655
Basic and Clinical Medical Researches in Vietnam

Correcting Corneal Astigmatism with Corneal Arcuate Incisions during Femtosecond Laser Assisted Cataract Surgery

Nguyen Xuan Hiep[1], Pham Thi Minh Khanh[1], Do Quyet[2], Than Van Thai[3], Vu Thi Nga[4], Toi Chu Dinh[5], Nguyen Duy Bac[2*]

[1]Vietnam National Institute of Ophthalmology, Hanoi, Vietnam; [2]Vietnam Military Medical University (VMMU), Hanoi, Vietnam; [3]NTT Hi-tech Institute, Nguyen Tat Thanh University, Ho Chi Minh City, Vietnam; [4]Institute for Research and Development, Duy Tan University, 03 Quang Trung, Danang, Vietnam; [5]Department of Human and Animal Physiology, Faculty of Biology, Hanoi National University of Education, Hanoi, Vietnam

Citation: Hiep NX, Khanh PTM, Quyet D, Thai TV, Nga VT, Dinh TC, Bac ND. Correcting Corneal Astigmatism with Corneal Arcuate Incisions during Femtosecond Laser Assisted Cataract Surgery. Open Access Maced J Med Sci. 2019 Dec 30; 7(24):4260-4265. https://doi.org/10.3889/oamjms.2019.371

Keywords: Femtosecond laser; Corneal astigmatism; Arcuate incision

***Correspondence:** Nguyen Duy Bac. Vietnam Military Medical University (VMMU), Hanoi, Vietnam. E-mail: nguyenduybac@vmmu.edu.vn

Received: 01-Jul-2019; **Revised:** 20-Nov-2019; **Accepted:** 21-Nov-2019; **Online first:** 20-Dec-2019

Funding: This research did not receive any financial support

Competing Interests: The authors have declared that no competing interests exist

Abstract

BACKGROUND: Astigmatic management is an important step to achieve the best visual quality after refractive cataract surgery. Nowadays, along with progress in cataract surgery, the femtosecond laser can produce the arcuate incisions high precisely that help the astigmatic correction. In Vietnam, it has not yet any study about this issue, so we perform this study.

AIM: To assess the efficacy and safety of arcuate corneal incisions in treatment corneal astigmatism during femtosecond laser-assisted cataract surgery.

METHODS: In this clinical interventional study, forty-five cases with cataract and corneal astigmatism (> 0.50D) were treated with corneal arcuate incisions and femtosecond-laser assisted cataract surgery in Vietnam National Institute of Ophthalmology, from January 2017 to May 2018. The uncorrected and corrected distance visual acuity, refraction spherical equivalent, corneal astigmatism were measured (using an OPD-Scan III topographer) before, 1 week and 3 months after surgery. Some features of arcuate corneal incisions (quantity, depth, length and morphology), spectacle independence at a distance and complications were recorded.

RESULTS: The rate of postoperative spherical refraction equivalent was within ± 0.50D and ± 1.0D at 3 months (in 95.6% and 100% of the eyes respectively). Mean length of arcuate corneal incisions was 53.78o ± 17.683o (range: 20o to 85o). The average of preoperative corneal astigmatism was 1.65 ± 0.83D, decreased to 0.59 ± 0.549D in the third month after surgery. Surgical induced astigmatism was 1.05 ± 0.449D and lower than preoperative corneal astigmatism (1.65 ± 0.83D), thereby this indicated undercorrection. However, the rate of spectacle independence was 82.3%, and no complications were recorded.

CONCLUSION: Correcting of corneal astigmatism in femtosecond laser-assisted cataract surgery combined with the formation of the arcuate incisions is a new and modern method for high safety and efficacy.

Introduction

Astigmatic management is an important step to achieve the best visual quality after refractive cataract surgery. Astigmatism postoperative from 0.50D or less could result due to glare, halos, ghosting, symptomatic blur, and so on[1]. A report in Spain from 4540 cases showed that the corneal astigmatism was prevalent in patients after cataract surgery with at least 1.50D in 22.2% of cases[2]. About 38% of cataract eyes had corneal astigmatism at least 1.00D before surgery, and 72% of cases had 0.50D or more [3]. In an investigation, in 2017 to evaluating the ocular biometric index on Vietnamese patients undergoing cataract surgery that indicated around 40.4% of study eyes which have corneal astigmatism preoperative with at least 1.0D.

There are two main procedures for the treatment of corneal astigmatism in cataract surgery: using the corneal incisions, and toric intraocular lens implantation. In which toric intraocular lens is often used for high astigmatic cases, and the mild to moderate astigmatic cases may be corrected by corneal incisions (up to 2.50D to 3.0D or more) [4]. They could create a single or a paired arcuate incision at limbus or clear cornea. Their position is located at the steeper corneal meridian. They are non-penetrating arcuate incisions with 80% to 90% of

corneal pachymetry which the length depends on the amount of power corneal astigmatism. In the world, many studies showed the role of corneal incisions that may occur due to flat the steeper meridian, and at the same time, it inflates the flatter meridian of the cornea. The phenomenon has called the coupling effect. The achieved outcomes were pretty good [5], [6]. However, in the past, the creation of manual arcuate incisions with a diamond knife had a lot of potential risks such as a dislocated incision, the ability to penetrate the cornea, uncorrected depth that may cause to reduce the efficacy of arcuate corneal incisions and unpredictable results [7]. Nowadays, the appearance of femtosecond laser helps to create precisely the position, size, length and depth of the arcuate incisions [8]. Thereby, the correction of astigmatism is more effective that due to increase the visual acuity and decrease the dependence on patient's spectacles.

Materials and Methods

The design of the study

This prospective, cumulative, interventional, nonrandomized, case series included forty-five eyes undergoing Femtosecond Laser Assisted Cataract Surgery (FLACS) and IOL implantation from January 2017 to May 2018 at Vietnam National Institute of Ophthalmology (VNIO), Vietnam. Selection criteria were patients who had indicated cataract surgery and had cornea astigmatism more 0.5D. Exclusion criteria were patients with a history of trauma, previous glaucoma or intraocular surgery, small palpebral fissure, nystagmus or visible eyelid spasm, inflammatory or infectious pathology of the eye, scar or opacity of the cornea, and poorly dilated pupil (< 6 mm). The clinical study was accepted by the institutional ethics committee of VNIO. All patients understood and voluntarily participated in this study.

Preoperative and postoperative index measurements

All cases were examined carefully before surgery including slit-lamp biomicroscopy, tonometry, uncorrected and corrected distance visual acuity (UDVA and CDVA), fundus evaluation, measurement axial length, keratometry, non-contact specular microscopy, and corneal topography. At the first week, first month and third month postoperative, the UDVA and CDVA, tonometry, slit-lamp biomicroscopy, and measurement of corneal topography were repeated. The manifest refraction spherical equivalent (MRSE), corneal astigmatism, the average number and length of arcuate incisions were also measured. The rate of patient's satisfaction, spectacle independence, and complications were recorded.

Plan of arcuate incisions

Length and number of arcuate incisions were determined on a web site (http://www.lricalculator.com, last accessed May 25, 2018) to achieve lowest residual astigmatism. It was essential to reduce the length of incision because the LRIs calculator was the limbus relaxing incisions. At this moment, using the Donnenfeld Nomogram, we employed the arcuate incisions that were 2 / 3 LRI-incision size, at 8 mm optical zone, and with 85% of corneal depth in the area of incision.

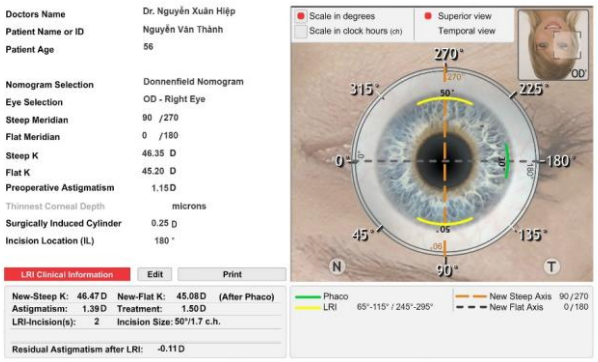

Figure 1: The Donnenfeld Nomogram is available at http://www.lricalculator.com

Surgical technique

All procedures were realized with system LenSx (Alcon, USA) for femtosecond laser and Infiniti machine (Alcon) for phacoemulsification. Before surgery, all patients have cleaned the eyelashes, eyebrow, flushing of the lacrimal drainage system, and conjunctival sac. They were also received the solution topical antibiotic, inflammation non-steroid, dilated pupil, and topical anesthesia eye drops on day surgery. We have used a speculum to fixation the palpebral, then put the patient interface (PI) (Soffit, Alcon) to docking and suction ocular. By observation the screen containing the OCT imaging of patient's eye, we could check all steps (limbus, primary incision, second incision, arcuate incisions, lens and capsulotomy), then perform the laser. After the opening the primary and second incisions by a hook, the viscoelastic solution was injected to the anterior chamber. Then, we used the capsulorhexis forceps to take off the anterior capsule, which was cut by laser before. Next, the phacoemulsification system had been responsible for performing its functions that were phacoemulsification of the nucleus and aspiration the cortex. The final steps of the procedure were implantation foldable intraocular lens in the capsular bag, and hydration the primary and second incisions.

Data analysis

Data were analyzed by using SPSS 16.0. The number of data was presented as X ± SD, and the percentage of data were shown in %. A P-value less

0.05 was considered statistically significant. Student's t-test was used to compare corneal astigmatism, UDVA, CDVA, MRSE preoperative, one week, one month, and three months postoperative. We used Chi-square test to analyze the rate of patient's satisfaction, spectacle independence, and complications. Fisher's exact test was used when the number of data was smaller than 5 to do Chi-square test.

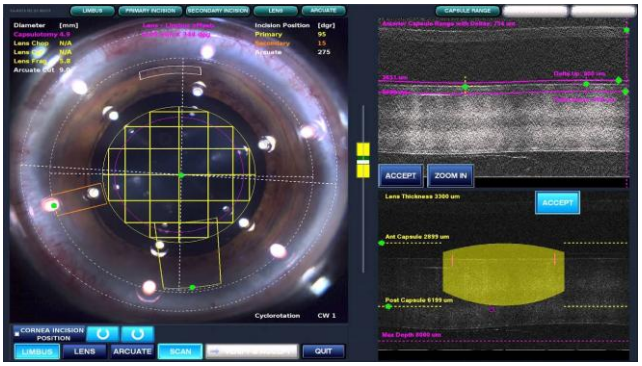

Figure 2: Screen of LenSx system shows the image OCT scan the patient's eye

Results

This study included 45 eyes of 33 patients (22 male and 11 female). The average of the age of the patients was 50.15 ± 16.672 years at the time of surgery. Among them, the most common are patients aged 40 to 60 years old.

Preoperative corneal astigmatism

		Frequency	Percent	Valid Percent	Cumulative Percent
Valid	0.53	1	2.2	2.2	2.2
	0.6	1	2.2	2.2	4.4
	0.76	1	2.2	2.2	6.7
	0.8	1	2.2	2.2	8.9
	0.84	1	2.2	2.2	11.1
	0.89	1	2.2	2.2	13.3
	0.98	1	2.2	2.2	15.6
	1	1	2.2	2.2	17.8
	1.01	1	2.2	2.2	20.0
	1.02	2	4.4	4.4	24.4
	1.07	1	2.2	2.2	26.7
	1.12	1	2.2	2.2	28.9
	1.13	1	2.2	2.2	31.1
	1.23	1	2.2	2.2	33.3
	1.26	1	2.2	2.2	35.6
	1.31	2	4.4	4.4	40.0
	1.32	1	2.2	2.2	42.2
	1.36	1	2.2	2.2	44.4
	1.38	1	2.2	2.2	46.7
	1.44	1	2.2	2.2	48.9
	1.49	1	2.2	2.2	51.1
	1.51	1	2.2	2.2	53.3
	1.64	1	2.2	2.2	55.6
	1.66	1	2.2	2.2	57.8
	1.7	1	2.2	2.2	60.0
	1.71	1	2.2	2.2	62.2
	1.75	1	2.2	2.2	64.4
	1.76	1	2.2	2.2	66.7
	1.89	2	4.4	4.4	71.1
	1.94	1	2.2	2.2	73.3
	1.97	1	2.2	2.2	75.6
	2.03	1	2.2	2.2	77.8
	2.26	1	2.2	2.2	80.0
	2.28	2	4.4	4.4	84.4
	2.33	1	2.2	2.2	86.7
	2.34	1	2.2	2.2	88.9
	2.35	1	2.2	2.2	91.1
	2.53	1	2.2	2.2	93.3
	2.86	1	2.2	2.2	95.6
	3.86	1	2.2	2.2	97.8
	4.97	1	2.2	2.2	100.0
	Total	45	100.0	100.0	

Figure 3: Preoperative corneal astigmatism

Subjects of the study were patients with cataract who had corneal astigmatism before surgery more 0.50D. Among them, mostly astigmatic eyes were from 1.0D to 2.0D with 27 / 45 eyes accounting for 60% (Table 1).

Table 1: Preoperative corneal astigmatism

Preoperative corneal astigmatism	n	%
0.50 → 1.00 (D)	8	17.8
1.00 → 2.00 (D)	27	60.0
> 2.00 (D)	10	22.2

There were 10 / 45 eyes (22.2%) with corneal astigmatism more 2.0D. In particular, there were 2 eyes of one patient with high astigmatism (3.86D and 4.97D). This patient underwent FLACS with IOL Toric T6 (Alcon) implantation, combining two arcuate corneal incisions 85 degrees by femtosecond laser, resulting in postoperative astigmatism reduced to 1.0D and 1.50D. The patient was satisfied with the visual acuity of 20 / 40 and spectacle independent.

Table 2: Preoperative and postoperative corneal astigmatism, refraction and visual acuity outcomes

	Corneal Astigmatism (D)	MRSE (D)	UDVA (logMAR)	CDVA (logMAR)
Preoperative	1.65 ± 0.828	- 1.95 ± 4.987	1.44 ± 0.714	0.72 ± 0.456
1 week postoperative	1.18 ± 0.761	- 0.27 ± 0.398	0.23 ± 0.141	0.12 ± 0.132
1 month postoperative	0.80 ± 0.599	- 0.11 ± 0.299	0.14 ± 0.122	0.08 ± 0.124
3 months postoperative	0.59 ± 0.549	- 0.08 ± 0.255	0.10 ± 0.103	0.07 ± 0.104
p (pre-op and 3 months post-op)	< 0.001	< 0.001	< 0.001	< 0.001

Note: MRSE: Manifest refraction spherical equivalent; UDVA: Uncorrected distance visual acuity; CDVA: Corrected distance visual acuit; P values were determined by comparison value data preoperative with 3 months postoperative.

The Table 2 showed that the mean preoperative corneal astigmatism was 1.65 ± 0.828D, which was significantly reduced to 0.59 ± 0.549D at 3 months postoperatively ($p < 0.001$). Thus, surgical induced astigmatism averaged 1.05 ± 0.449D, was lower than corneal astigmatism before surgery was 1.65 ± 0.828D, the correction index of surgery was 0.64 (ratio between surgical induced astigmatism and preoperative corneal astigmatism). This result indicated the undercorrection in this study that was presented in Figure 4 below.

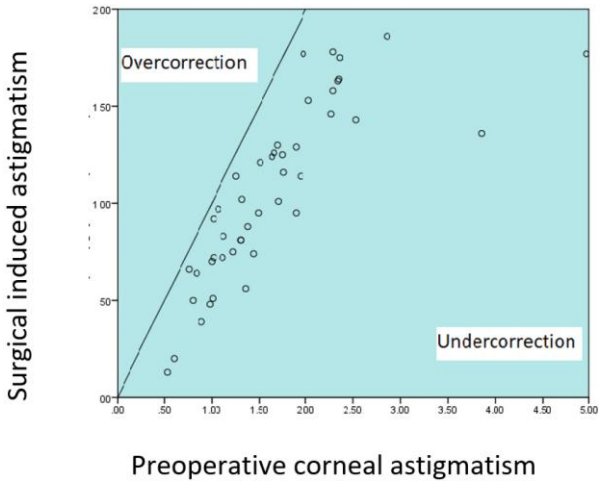

Figure 4: The scatter plot of Preoperative corneal astigmatism and

surgical induced astigmatism.

The MRSE have defined the significant increase ($p < 0.001$) between preoperative and postoperative values. Statistically significant improvements in UDVA and CDVA were determined at the third month postoperative ($p < 0.001$). Table 1 indicated the change of MRSE and visual acuity outcomes in detail.

Table 3: Manifest refraction spherical equivalent postoperative within ± 0.50D and ± 1.0D

Manifest refraction spherical equivalent (MRSE)	± 0.50D (%)	± 1.0D (%)
1 week postoperative	75.6	100
1 month postoperative	93.4	100
3 months postoperative	95.6	100

One hundred percent of study eyes that MRSE after surgery were within ± 1.0D and 95.6% was the rate of MRSE within ± 0.50D at 3 months follow up.

Table 4: The average length and number of arcuate incisions

Number of arcuate incisions	N	Length of arcuate incisions (^{0})
1 arcuate incision (opposite of primary incision)	16	62.81 ± 13.901
2 arcuate incisions (symmetry through the central cornea)	29	48.79 ± 17.761
Total	45	53.78 ± 17.683
Range		20 to 85

In the study, there were 16 eyes with astigmatic axis according to the main incision axis, so only using a single arcuate corneal incision had a mean length of 62.81 ± 13.901 degrees. Twenty-nine eyes needed to create a pair of arcuate corneal incisions symmetrically across the central cornea, at 9 mm optical zone, and the mean length of each incision was 48.79 ± 17.761 degrees. Thus, the mean length of an arcuate corneal incision to correct astigmatism in the FLACS in this study was 53.78 ± 17,638 degrees.

Discussion

Cataract surgery has been one of the most commonly performed refractive procedure worldwide. The recent progress in cataract surgery has brought excellent results as the recovery of visual acuity quickly and stably. That has met the high requirements of patients for both visual qualities as well as the independence of the patient's spectacle. Previous studies indicated the pre-existing corneal astigmatism is fairly popular in the patient undergoing cataract surgery. Residual astigmatism postoperative of 0.50D may occur due to halos, glare, monocular diplopia, asthenopia, and other visual distortions [1]. As a result, the treatment of corneal astigmatism in cataract surgery is indispensable.

To obtain at least postoperative astigmatism, the surgeons may choose the different methods such as using the limbus relaxing incisions (LRIs), toric IOL implantation, and implementation excimer laser for residual astigmatic treatment after cataract surgery. Each method has its benefits and drawbacks. The cost of Toric IOLs is reasonably high. Furthermore, some studies have shown that there was the relative rotation of the IOL after surgery cause to increase astigmatism [9], [10]. Implementation excimer laser for residual astigmatic treatment after cataract surgery also requires a high cost. Moreover, it may have the complications concerned with corneal flap and not apply for cases with thin cornea [11].

LRIs may be used in cataract surgery to treat corneal astigmatism. Its advantage is low cost and ability to perform in the operation room or at a slit lamp microscopy in the examination room. However, in the past, the creation of LRIs with a diamond knife had a lot of potential risks such as a dislocated incision, the ability to penetrate the cornea, uncorrected depth that may cause to reduce the efficacy and stability of LRIs as well as unpredictable results [12]. Moreover, LRIs also can make irregular troubles at the limbus. Anyway, they have less glare and discomfort than the clear corneal incisions [13].

At this moment, we assessed the efficacy and safety of arcuate clear corneal incisions, which were implemented by femtosecond laser in FLACS. Many previous articles presented about the role of femtosecond laser in creation the arcuate incisions with more precision and safety by creating reproducible incisions for the position, size, length and depth of the arcuate incisions [8].

Depending on the amount of preoperative corneal astigmatism and its axis, we used a single arcuate incision (opposite of the main incision) or a pair of arcuate incisions symmetrically across the central cornea to correct astigmatism. The mean length of an arcuate corneal incision to correct astigmatism in the FLACS in this study was 53.78 ± 17,638 degree (Table 4). Corneal astigmatism reduced from 1.65 ± 0.828D (preoperative) to 0.59 ± 0.549D (at 3 months postoperatively). Surgical induced astigmatism averaged 1.05 ± 0.449D, was lower than preoperative corneal astigmatism (1.65 ± 0.828D), the correction index of surgery was 0.64 (ratio between surgical induced astigmatism and preoperative corneal astigmatism). This result indicated the undercorrection in this study that was presented in Figure 4.

The study by Harry W. Roberts et al., (2018) also had similar results with this study when it showed that cataract surgery combined astigmatic correction by the arcuate corneal incision made by femtosecond laser had under correction postoperative [14]. Several other studies also have outcomes with under correction. It could be seen that researches have been still very prudent in using femtosecond laser to create the arcuate corneal incisions because of the

worry about their great effects that may lead due to unpredictable outcomes, overcorrection and increase of astigmatism with axial inversion. Therefore, most studies have remained slight residual astigmatism. In our study, residual astigmatism after surgery 3 months was 0.59 ± 0.549D, approximately to physiological astigmatism.

Moreover, by James S Wolffsohn et al., (2013), astigmatism plays a role in increasing the depth of focus of patients with healthy corneas or following laser refractive surgery [15]. Another research suggested that residual against-the-rule cylinder after cataract surgery with IOL implantation benefits the uncorrected near vision [16]. Thereby, undercorrection with astigmatism in cataract surgery may be a beneficial factor for visual quality postoperative. However, in the scope of this study, we have not yet any conditions to evaluate this issue.

Manifest refraction spherical equivalent of 100% of study eyes after surgery were within ± 1.0D, and 95.6% was the rate of MRSE within ± 0.50D at 3 months follow up. This rate was very high, contributing to explain the result of very good visual acuity. This result, according to a survey by questionnaires to evaluate the patient's satisfaction and the glasses dependence showed that the rate of spectacle independence was 83.2%. 100% of patients was the rate of patient's satisfaction with the surgical results, of which 81.8% of patients was high satisfaction. Most of the patients felt comfortable because the good vision was regardless of glasses.

The study also found that there was not any complication related to creating arcuate incisions by femtosecond laser such as corneal perforation, dislocated incision, tear of incision, inadequate depth of incision, folded edge of incision, and penetrate the epithelium into the incision.

In conclusion, correcting of corneal astigmatism in femtosecond laser-assisted cataract surgery combined with the formation of the arcuate incisions is a new and modern method for high safety and efficacy. Corneal astigmatism was reduced about 64.0% compared to before surgery (correction index was 0.64). We have not yet any complications related to creating the arcuate incisions by femtosecond laser. Uncorrected distance visual acuity after surgery 3 months was 0.10 ± 0.103, and 83.2% of patients did not depend on glasses. These results reinforced the evidence of the safety and efficacy of the surgery. However, the limitation of this study was that the sample size was small, and the follow-up time was short (3 months). The next task of the study is to collect more data to achieve a larger sample size and longer follow-up time. From that point, we could have a comprehensive view of the role, progress and stability of arcuate incisions in femtosecond laser-assisted cataract surgery. The authors also would like to find a nomogram of the arcuate corneal incision using femtosecond laser that is intended for Vietnamese patients with specific ethnic and genetic characteristics. Therefore, the research direction that is reserved for femtosecond laser remains very much and requires more time and resources in the future.

Ethical approval

Our study was accepted by the institutional ethics committee of Vietnam National Institute of Ophthalmology. All patients understood and voluntarily participated in this study.

References

1. Nichamin LD. Nomogram for limbal relaxing incisions. J Cataract Refract Surg. 2006; 32(9):1408. https://doi.org/10.1016/j.jcrs.2006.03.046 PMid:16931238

2. Ferrer-Blasco T, et al. Prevalence of corneal astigmatism before cataract surgery. J Cataract Refract Surg. 2009; 35(1):70-5. https://doi.org/10.1016/j.jcrs.2008.09.027 PMid:19101427

3. Hill, W., Expected effects of surgically induced astigmatism on AcrySof toric intraocular lens results. J Cataract Refract Surg. 2008; 34(3):364-7. https://doi.org/10.1016/j.jcrs.2007.10.024 PMid:18299058

4. Nanavaty MA, et al. Toric Intraocular Lenses Versus Peripheral Corneal Relaxing Incisions for Astigmatism Between 0.75 and 2.5 Diopters During Cataract Surgery. Am J Ophthalmol. 2017; 180:165-177. https://doi.org/10.1016/j.ajo.2017.06.007 PMid:28647461

5. Fares U, et al. Management of postkeratoplasty astigmatism by paired arcuate incisions with compression sutures. Br J Ophthalmol. 2013; 97(4):438-43. https://doi.org/10.1136/bjophthalmol-2012-302128 PMid:23390168

6. Lindstrom RL. The surgical correction of astigmatism: a clinician's perspective. Refract Corneal Surg. 1990; 6(6):441-54.

7. Cleary C, et al. Beveled femtosecond laser astigmatic keratotomy for the treatment of high astigmatism post-penetrating keratoplasty. Cornea. 2013; 32(1):54-62. https://doi.org/10.1097/ICO.0b013e31825ea2e6 PMid:22968362 PMCid:PMC3754433

8. Abbey A, et al. Femtosecond laser-assisted astigmatic keratotomy in naturally occurring high astigmatism. Br J Ophthalmol. 2009; 93(12):1566-9. https://doi.org/10.1136/bjo.2008.149971 PMid:19939795

9. Ahmed II, et al. Visual function and patient experience after bilateral implantation of toric intraocular lenses. J Cataract Refract Surg. 2010; 36(4):609-16. https://doi.org/10.1016/j.jcrs.2009.10.044 PMid:20362853

10. Khan MI, Ch'ng SW, Muhtaseb M. The use of toric intraocular lens to correct astigmatism at the time of cataract surgery. Oman J Ophthalmol. 2015; 8(1):38-43. https://doi.org/10.4103/0974-620X.149865 PMid:25709273 PMCid:PMC4333542

11. Bayramlar H, Daglioglu MC, Borazan M. Limbal relaxing incisions for primary mixed astigmatism and mixed astigmatism after cataract surgery. J Cataract Refract Surg. 2003; 29(4):723-8. https://doi.org/10.1016/S0886-3350(02)01821-7

12. Budak, K., Friedman NJ, Koch DD. Limbal relaxing incisions with cataract surgery. J Cataract Refract Surg. 1998. 24(4):503-8.

https://doi.org/10.1016/S0886-3350(98)80292-7

13. Muller-Jensen K, Fischer P, Siepe U. Limbal relaxing incisions to correct astigmatism in clear corneal cataract surgery. J Refract Surg; 1999; 15(5):586-9.

14. Roberts HW, et al. Refractive outcomes after limbal relaxing incisions or femtosecond laser arcuate keratotomy to manage corneal astigmatism at the time of cataract surgery. J Cataract Refract Surg. 2018; 44(8):955-963. https://doi.org/10.1016/j.jcrs.2018.05.027 PMid:30033111

15. Wolffsohn JS, Bhogal G, Shah S. Astigmatism and vision: should all astigmatism always be corrected? Br J Ophthalmol. 2014; 98(1):2-3. https://doi.org/10.1136/bjophthalmol-2013-303599 PMid:24338839

16. Trindade F, Oliveira A, Frasson M. Benefit of against-the-rule astigmatism to uncorrected near acuity. J Cataract Refract Surg. 1997; 23(1):82-5. https://doi.org/10.1016/S0886-3350(97)80155-1

ID Design Press, Skopje, Republic of Macedonia
Open Access Macedonian Journal of Medical Sciences. 2019 Dec 30; 7(24):4266-4271.
https://doi.org/10.3889/oamjms.2019.372
eISSN: 1857-9655
Basic and Clinical Medical Researches in Vietnam

Tissue-Cultured Human Cord Lining Epithelial Cells in Treatment of Persistent Corneal Epithelial Defect

Nguyen Dinh Ngan[1, 2], Hoang Minh Chau[3, 4], Pham Ngoc Dong[3], Le Xuan Cung[3], Nguyen Thu Thuy[3], Phan Toan Thang[5], Than Van Thai[6], Vu Thi Nga[7], Nguyen Duy Bac[8*]

[1]Department of Ophthalmology, 103 Military Hospital, Hanoi, Vietnam; [2]Department of Ophthalmology, Vietnam Military Medical University, Hanoi, Vietnam; [3]Department of Cornea and External diseases, Vietnam National Institute of Ophthalmology, Hanoi, Vietnam; [4]Department of Ophthalmology, Hanoi Medical University, Department of Ophthalmology; [5]Department of Surgery, Yong Loo Lin School of Medicine, National University of Singapore, Singapore; [6]NTT Hi-tech Institute, Nguyen Tat Thanh University, Ho Chi Minh City, Vietnam; [7]Institute for Research and Development, Duy Tan University, 03 Quang Trung, Danang, Vietnam; [8]Vietnam Military Medical University (VMMU), Hanoi, Vietnam

Citation: Ngan ND, Chau HM, Dong PN, Cung LX, Thuy NT, Thang PT, Thai TV, Nga VT, Bac ND. Tissue-Cultured Human Cord Lining Epithelial Cells in Treatment of Persistent Corneal Epithelial Defect. Open Access Maced J Med Sci. 2019 Dec 30; 7(24):4266-4271. https://doi.org/10.3889/oamjms.2019.372

Keywords: Persistent corneal epithelial defect; Cord lining epithelial cells; Tissue-cultured epithelial cells

***Correspondence:** Nguyen Duy Bac. Vietnam Military Medical University (VMMU), Hanoi, Vietnam. E-mail: nguyenduybac@vmmu.edu.vn

Received: 01-Jul-2019; **Revised:** 20-Nov-2019; **Accepted:** 21-Nov-2019; **Online first:** 20-Dec-2019

Funding: This research did not receive any financial support

Competing Interests: The authors have declared that no competing interests exist

Abstract

BACKGROUND: Persistent corneal epithelial defect (PED) is a consequence of many ocular surface disorders. Although many therapies have been suggested, the treatment of this disease have faced a lot of difficulties up to now. The transplatation of cultivated amniotic epithelial cells sheets is the new promised method for PED. Cord lining epithelial cells (CLECs) are epithelial cells of amniotic membrane of umbilical cord, so these cultivated cells sheet may be good for treating PED

AIM: To evaluate the efficacy of the transplantation of cultivated CLECs sheets in treatment of PED and analyze some influential factors of this therapy.

METHODS: A prospective interventional case series with transplantation of tissue-cultured human CLECs in 37 PED eyes in Vietnam National Institute of Ophthalmology.

RESULTS: Thirty four of 37 eyes were healed with the cells transplantation and 22 eyes of them healed within a week postoperatively. There were normal corneal scars and normal corneal epithelial cell (by impression cytology detection) on transplantation site in all 31 successful cases. The other successful eyes were done lamellar keratoplasty (respectively in 1 month, 3 months, 6 months and 27 months postoperatively) to investigate the histopathology of the CLECs transplant site. The histopathological images showed normal corneal scar and there was no appearance of CLECs in transplant site.

CONCLUSION: tissue-cultured human CLECs transplantation is a quite safe and effective treatment for persistent corneal epithelial defect. The CLECs may help the epithelial healing at early stage but do not exist at transplant site for a long time.

Introduction

Persistent epithelial defect (PED) of cornea occurs when the corneal epithelium fails to regenerate steadily over a corneal wound within due course (usually less than 2 weeks in normal corneas), although the wound has been intensively treated [1]. The potential causes of PED are myriad and its mechanisms remain unclear, related to multiple factors and hard to determine specifically. Therefore, no specific therapy for this disease has been available up to now [1]

Many therapies for PED have been suggested, such as: anti-iflammation, artificial tear, nutritious solution for ocular surface, soft contact lens, tarsorrhaphy, keratoplasty [1]. However, some PEDs were even failed to heal and the visual functions were threatened in spite of extensive treatments [2], [3], [4], [5]. Amniotic membrane transplantation has been recently employed in PED with promised result, nonetheless the success rate were varied in many studies (from 31.4% to 90%) [2], [6], [7]. Moverover, using amniotic graft may reduce the corneal transparent and visual acuity. Stem cell technologies have been applied to treat PEDs in some special situations, and supposed a new promised therapy for

this disease. Cultivated epithelial autografts (limbal stem cells, oral mucosal cells) or cultivated epithelial allografts (amniotic epithelial cells) have been tried in some rough cases with promised results [7], [8], [9], [10]. Parmar DN, et al., (2006) firstly successfully performed the trial of using tissue-cultured amniotic epithelial cells for 3 refractory PED cases [7].

Cord lining epithelial cells (CLECs) are epithelial cells of amniotic membrane of umbilical cord. These cells have been isolated and proved to be progenitor/stem cells. CLECs were differentiated to be some type of epithelium by some invitro study [11], [12], [13]. Zhou Y, MacAry PA, et al., have shown many markers of corneal and limbal epithelial cells in CLECs and the safety of CLECs human transplantation [12], [14]. Reza HM, (2011) has differentiated CLECs to corneal epithelial cells and transplanted them to rabbit eyes. The results showed that rabbits' cornea after CLECs transplatation had no limbal stem cells deficiency signs and remained transparent with normal histology structures up to 10 weeks postoperatively. These studies have suggested the CLECs application in treatment of ocular surface diseases, especially PEDs – one of the difficult treated corneal diseases [11]. From this hypothesis we carried out the prospective study to evaluate the efficacy of the transplantation of tissue-cultured CLECs in treatment of refractory PEDs.

Materials and Methods

Subjects

In this study, 37 patients with PED in Vietnam National Institute of Ophthalmology were enrolled from December 2010 to May 2014. All patients were followed up at least 36 months. All our cases had been failed to healed with other treatment therapies. The descemetocele or perforated ulcer, corneal ulcer with inflammatory infitrative site or abscess in deep stroma, the PEDs with total limbal stem cells deficiency or the eyes with eyelid malformation were excluded from the study.

This study was approved by the institutional review board of Vietnam National Institute of Ophthalmology, and informed consent was obtained from all patients.

The tissue-cultured CLECs preparation

The cells sheets were cultured in the laboratory of Department of surgery, National University of Singapore. The isolated CLECs were evaluated for the quality and expression of surface markers, and stored in single-cell suspension on culture dish with the density of 3-4 x 10^4 cells/cm^2 at -196°C. Then, they were taken out of storage tanks and thawed at 37°C in water bath. And the cells were supplemented with PTTe-1 medium to the falcon tissue culture inserts (12-well plates) at density around 10000 cells/cm^2. The next step, the culture plates were put straight into 37°C/5% CO_2 incubator. The fresh culture media was replaced every 2 days until the cells grew into a continuous surface on the scaffold (from 5 to 7 days), consists of 1-2 cell layers. Finally, the cultured CLECs were determined the markers of cornea-like epithelial cells (CK3, CK12). For transportation, the Falcon tube (50ml) with cultured fluid contained 2 wells storage in -80°C.

The tissue-cultured CLECs transplantation

The PEDs was cleaned by cresent knife to prepare transplantation site. The cells sheet with scaffold was cut to the shape and size of the ulcer. Then, the sheet was placed with the epithelium side down, and covered with soft contact lens. Two crossed Vicryl 8/0 sutures were placed over the contact lens to sclera for pressing and fixing the cells sheet. In necessary case, the combined surgeries such as hypopion lavage, pterygium excision and conjunctival autograft were done. Second cells transplantation was performed when the PEDs were ameliorated but not completely healed 4 weeks after the first surgery. The fixation sutures were removed to check the healing of the defect 7 days after surgery.

Postoperative medications included topical moxifloxacin 0.5% (Vigamox; Alcon Laboratories, Inc. Fort Worth, USA) four times daily and sodium hyaluronate 0.1% (Sanlein, Santen Pharmaceutical Company) six times daily.

The result of cells sheet transplantation was evaluated by two criteria; the time of healing and the quality of the corneal transplantation site. The treatment success meant the PED was completely healed after one or more transplatation, the failure meant the PED was not healed after transplatation or the corneal epithelial defect was recurrently appeared in 4 weeks after surgery and was not able to regraft.

The quality of the transplantation site on cornea was clinical evaluated and catergorized into 3 grades: *good* - the epithelial surface was smooth, the cornea was transparent and the anterior segment could be seen clearly. There is no neovessel at transplantation site; *moderate*-the epithelial surface was not smooth, but there is no epithelial defect. The cornea was mild opaque, but the pupil was able to see. There were neovessels in anterior stroma at transplantation site; *bad*-the epithelial surface was rough and there is epithelial defect or corneal recurrent erosion. The cornea was very opaque and the anterior segment could not be seen. There were many neovessles at at transplantation site, some of them were in posterior stroma.

To detect any abnormal cells on transplatation site, the impression cytology was done 1 month, 3

months and 6 months postoperatively in success cases. To know whether CLECs were stayed at transplantation sites, as well as partially understand the epithelial healing mechanisms of defect, some male CLECs graft were used in female cornea. Then we performed keratoplasty for those cases to take the cornea for searching for CLECs. The SRY (the specific marker of Y chromosome) were tested in the cell-received cornea by PCR to determine the existence of CLECs on transplanation site by Genetics and Molecular biology laboratory of Vietnam Military Medical Universisty.

Results

The characteristics of studied patients and PEDs before surgery

There were 37 patients (26 male, 11 female) with the age from 21 to 86 years old (average 59.6 ± 19.8 years old). All patients have unilateral corneal ulcer.

The original causes of the corneal ulcers were described in Table 1. Most of the causes were infection (26/37 eyes) with 14 herpertic eyes (37.8%).

Table 1: Original causes of the corneal ulcers

Causes		Quantity	Percentage
Infection	Herpes	14	37.8
	Bacteria	11	29.7
	Fungi	1	2.7
After surgery		3	8.1
After radiation		1	27
Eye trauma		2	5.4
Sjogren syndrome		1	2.7
Unidentified causes		4	10.9
Total		37	100

The period time of the corneal defects were from 4 weeks to 28 weeks (9.9 ± 5.2 weeks) and the period time of the PEDs were from 2 weeks to 13 weeks (5.0 ± 2.9 weeks). All patients in our study were refractory with medical treatment (stopping corneal toxic eye drop, using artificial tear, using contact lens...). There were 2 recurent PEDs after AMT (Figure 1).

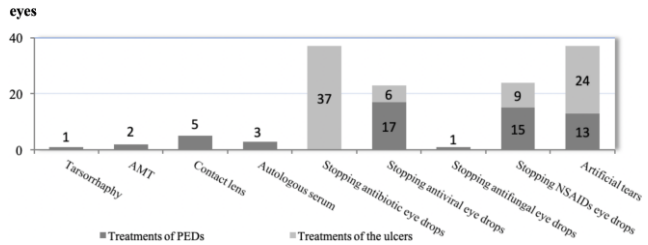

Figure 1: The previous treatments of PEDs; (AMT: amniotic membrane transplantation; NSAIDs: non steroid anti-inflammation drugs).

The size of the PEDs were from 11% to 65% corneal area (average 33.9 ± 14.9 % corneal area). The depth of PEDs were mostly less than two thirth of corneal thickness (33/37 eyes). The combined ocular lesions were shown in Figure 2.

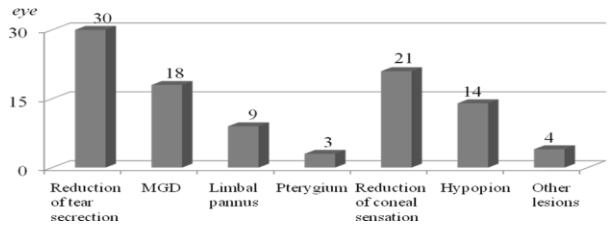

Figure 2: Combined ocular lesions; (MGD: meibomian gland dysfuntion).

The results of tissue-cultured CLECs transplantation

The success rate of our study was 91.9% (34/37 eyes). There were 31 cases completely epithelialized in 2 weeks, 2 cases in 4 weeks, only one case with healing time more than 4 weeks and need second surgery. In 3 cases that failed to heal with transplantation, there was only one case recurred epithelial defect a week after healing.

We found no association betweent healing time and some PEDs characteritics (original causes, the period time of the defects and the PED, the size of defect). Hoewever, the correlation between the time of epithelial healing and the tear secrection was 0,36 ($p < 0,05$). The healing time of eyes with the reduction of cornea sensation was longer than the healing time of the others ($p < 0.05$). The healing time of eyes that were both reduction of tear secrection and MGD (10.1 ± 5.5 days) were significant longer than the others (7.8 ± 4.1 days) ($p < 0.05$).

Table 2: The quality of the transplantation sites

Transplantation site *Follow-up time*	Good	Moderate	Bad	Total
1 month (34 eyes)	12	19	3	34
3 months (33 eyes)	20	11	2	33
6 months (32 eyes)	25	7	0	32
12 months (30 eyes)	25	5	0	30
36 months (30 eyes)	24	5	1	30
The last checked time (30 eyes)	26	4	1	30

(At the end of the study, 30 eyes were followed up from 36 to 64 months, average 45 ± 7.7 months, the others were done corneal transplant as the schedule).

One eye recurred herpes keratitis at corneal transplantation site 17 months postoperatively. After successful treated, the corneal scar was hazy with stroma neovascularization, so the transplanation site was clasified as bad quality.

The number of successful cases were done impression cytology at 1 month postoperatively was 27 cases, at 3 months was 24 cases and 6 months was 31 cases (exception 3 keratoplasty eyes). The pictures of cytologies showed normal epithelial cells: cuboidal shape, quite uniform size, and round nucleus, the same as cells on normal cornea (Figure 3B, and Figure 1D). There were no abnormal nucleus in these cells. Some cells at the bad transplantation

site were in grade of mild metaplasia (Figure 3F and 3G).

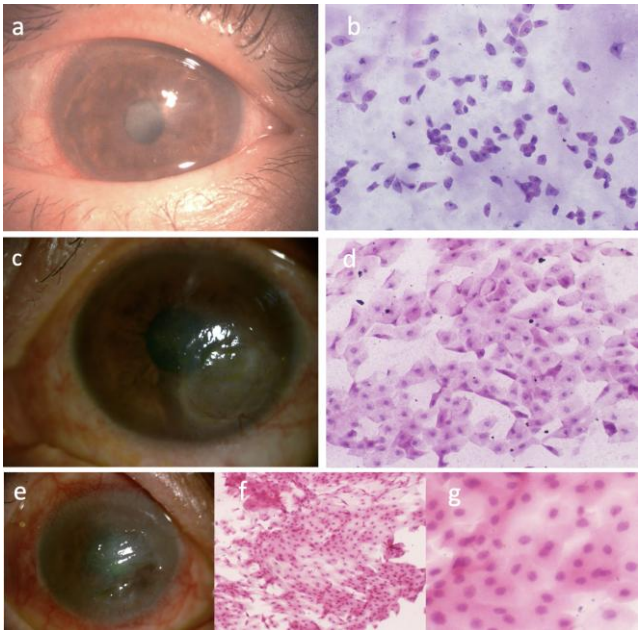

Figure 3: The corneal transplantation site and results of impression cytology; A) good transplantation site 3 months postoperatively; B) impression cytology of same patient (HE, x 100); C) moderate transplantation site 3 months postoperatively; D) impression cytology of same patient (HE, x 200); E) bad transplantation site 1 month postoperatively; F) and G) impression cytology of same patient (HE, x 100 and x 400)

In 4 corneal transplanted eyes, there were 3 females, that were done keratoplasty in 1.5 months, 3 months and 27 months postoperatively, and one male (6 months after surgery). The histology of corneal specimens showed normal epithelium at transplanation sites, but the number of layers increased (about 12-15 layers) (Figure 4). There were no inflammation cells infiltrated beneath the transplanation sites. The PCR test looking for SRY were negative in all 3 female cornea, but the test results of cells sheet and male conea were positive.

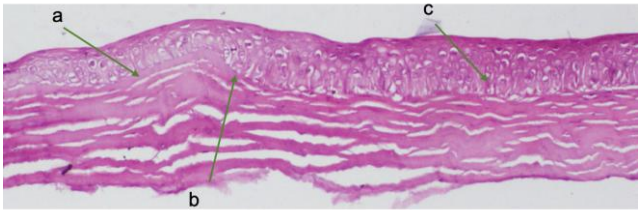

Figure 4: The histology of cell-received cornea (Trichrome-Masson, x 100); A) healthy corneal epithelium with Bowman layer; B) the connection between the healthy cornea and transplantation site; C) the transplantation site without Bowman layer

There were some mild complications in surgical procedure. Thirty eyes were subconjunctival haemorrhage without any interruption of surgical procedure. One eye was severe haemorrhage and the conjunctiva was inflated, so the contact lens had to been trephined to 10 mm in diameter to be easier to fixed.

The postoperative complications were not severe. One contact lens was lost fixation 4 days postoperatively, then the cells sheet was removed and the contact lens was replaced until the cornea was completely healed (12 days after surgery). There were 2 eyes that the cells sheets were slightly moved inspite of good fixation contact lens. After removing the fixation sutures, all these eye were completely epithelial healed.

Discussion

The mechanism of PEDs were partially specified by original causes of the corneal ulcer, the combined ocular lesions and the previous treatments. In our study, the original causes of two thirth eyes were infection (26/37 eyes, Table 1) , the remarkable combined ocular lesions were the reduction of cornea sensation, dry eye, hypopyon (Fig. 2), so that the two main mechanisms of PED in our patients might be ocular inflammation and neurotropic keratopathy. The addition mechanism was epithelial toxic from eye drops (Fig. 1). The other mechanisms may not be important role in our study group.

Amniotics membrane was proven to inhibit inflammatoty reaction, scar creation, and neovascular growth, as well as promote epithelial migration, adhesion when overlay transplantation in PED [6], [15]. These bilogical efficacies were suggested from many mediator factors (such as EGF, KGF, and HGF, macrophage inhibitory factor, Fas ligand...) inside amniotic epithelial cells and somewhat in membrane stroma [16], [17]. For amniotic membrane graft, these factor may just existed on transplantation site for short time after surgery because of nonviable amniotic epithelial cells and dissovled stroma [15], [18]. So that viable amniotic cells may be supposed more effective in treating PED than amniotic membrane transplantation. Parma (2006) showed succesful corneal epithelial healing in 3 complicated PEDs that had been failed with other therapies. Although the healing mechanism of amniotic epithelial cells transplantation in his study remains unclear, the author presumed the trans-planted cells firstly may provide an initial cellular means to repair the PED and then promote epithelialization by in situ release of anti-inflammatory and healing factors in these cells [7]. Other mentioned mechanism was tissue-cultured cells may also provide a mechanical scaffold promoting subsequent epithelial healing of the cornea. In earlier experiments, He YG had transplanted human amniotic epithelial cells onto denuded rabbit corneal surfaces, these cells had been re-polarized and tightly adhered to the recipient corneal stroma 24h after transplantation. However, the transplantation site was repopulated by host corneal epithelium after

10 days [19].

CLECs were amniotic epithelial cells around umbilical cord, so their microstructure was the same as amniotic cells. They were one kind of stem cell and were able to differentiated to corneal-liked epithelial cells [12], [13], [20]. Moreover, CLECs also were transplanted in rabbits' cornea with total limbal stem cell deficiency with good results. There were 50% cases had no limbal stem cells deficiency signs and the corneas remained transparent with normal histology structures up to 10 weeks postoperatively [11]. Therefore, transplantation tissue-cultured CLECs on PEDs may promote healing in the similar mechanisms of amniotic epithelial cells. In our study, we also found that CLECs were not able to exist long time on transplantation site after surgery. The PCR test for Y chromosome in female corneal specimens showed negative result as soon as 1.5 months postoperatively. Thus, it suggested that the donor CLECs improved the ocular surface through the secretion of factors promoting wound healing, stimulating repopulation of the remaining host corneal epithelial cells. It explained the high success rate in our studied group with most PEDs caused by inflammation and neurotrophic keratopathy.

The most important influential factors of the CLECs transplantation is tear film. The correlations between the tear secrection, situation of MGD and the quality transplantation sites as well as healing time were statitistically significant ($p < 0.05$). The healing time were statitistically significant longer in the group of reduction of cornea sensation. These factors (tear film, cornea sensation) also contributed to PEDs mechanism, so the medical treatments to ameliorate them before and after CLECs transplantation were also played important role in the result of CLECs surgery.

In our study, the cells sheet with scaffold was placed on the defect with the epithelium side down with the fixation of two Vicryl 8/0 sutures. This method showed the good result: 22/37 eyes complete healing after removing fixation sutures (a week postoperatively), 10 eyes more in 2 weeks postoperatively and 2 eyes healed in 3 weeks. Using directly scaffold of cells sheets instead of collagen shield with concave shape (in Parmar method [7]) made the cultivated procedure simplier and cheaper. However the cultured-well scaffold was flat so it was to difficult to force adherently 100% cells sheets on corneal surface, especilally when the defect was larger than 50% corneal area. Our method to fix the tissue sheet with 2 cross sutures press on soft contact lens is quite easy and simple with good effect. Although these sutures on sclera easily created subconjunctival haemorrhage that made difficult to fix contact lens. We usually used vasoconstriction eye drops to prevent this complication (adrenaline 0.1%).

In conclusion, tissued-cultured human cord lining epithelial cells transplantation is a safe and effective treatment of persistent corneal epithelial defect. This transplantation open a new method in treatment of this complicated diseased. However, more studies with long follow up time were need to re-evaluate the efficacy as well as the mechanism of corneal healing of this cells tranplantation.

Acknowledgement

We would like to acknowledge the support of many colleagues from the Departments of Ophthalmology-103 Military hospital, Department of Corneal and external diseases, Vietnam National Insitute of Ophthalmology, Scientific Research and International Co-operation at Hanoi Medical University, Hanoi, Vietnam. We gratefully acknowledge the help of the Genetics and Molecular biology laboratory of Vietnam Military Medical Universisty.

Conflict of Interests

Assoc. Prof. Phan Toan Thang is the principal investigator of human cord linning epithelial cells. He is a founding director and CSO of CellResearch Corporation Group of Companies in Singapore. Other authors have declared that no competing interests exist.

Ethical Approval

Subjects voluntarily participate in the research; patient information is confidentiality. Research subjects have the right to end the study at any time. The research was approved by the institutional ethical review board of Vietnam National Institute of Ophthalmology

Informed Consent

All patients agreed and signed an informed consent form before surgeries

References

1. MA, D, DA, HAJ. Persistent epithelial decfect, in Jakobiec's Principles and Practice of Ophthalmology, D. Albert, et al., Editors. Philadelphia: Saunders Elsevier Press, 2008:749 -759. https://doi.org/10.1016/B978-1-4160-0016-7.50058-8

2. Tsubota K, Goto E, Shimmura S, Shimazaki J. Treatment of persistent corneal epithelial defect by autologous serum application. Ophthalmology. 1999. 106(10):1984-9. https://doi.org/10.1016/S0161-6420(99)90412-8

3. de Souza Ferreira R, Kruse F, B. Seitz, Autologous serum for otherwise therapy resistant corneal epithelial defects-Prospective report on the first 70 eyes. Klinische Monatsblatter fur Augenheilkunde. 2001; 218(11):720-726. https://doi.org/10.1055/s-2001-18663 PMid:11731899

4. Jeng BH, Dupps Jr WJ. Autologous serum 50% eyedrops in the treatment of persistent corneal epithelial defects. Cornea. 2009; 28(10):1104-1108. https://doi.org/10.1097/ICO.0b013e3181a2a7f6 PMid:19730088

5. Rumelt S, et al. Persistent epithelial defects and ulcers in repeated corneal transplantation: incidence, causative agents, predisposing factors and treatment outcomes. Graefe's Archive for Clinical and Experimental Ophthalmology. 2008; 246(8):1139. https://doi.org/10.1007/s00417-008-0797-4 PMid:18500532

6. Lee SH, Tseng SC. Amniotic membrane transplantation for persistent epithelial defects with ulceration. American journal of ophthalmology. 1997; 123(3):303-12. https://doi.org/10.1016/S0002-9394(14)70125-4

7. Parmar DN, Alizadeh H, Awwad ST, Li H, Neelam S, Bowman RW, Cavanagh HD, McCulley JP. Ocular surface restoration using non-surgical transplantation of tissue-cultured human amniotic epithelial cells. American journal of ophthalmology. 2006; 141(2):299-307. https://doi.org/10.1016/j.ajo.2005.09.008 PMid:16458684

8. Cauchi P, et al. A Systematic Literature Review of Surgical Interventions for Limbal Stem Cell Deficiency in Humans. 2008; 146:251-259. https://doi.org/10.1016/j.ajo.2008.03.018 PMid:18486098

9. Kim JT, et al. The Effect of In Vivo Grown Corneal Epithelium Transplantation on Persistent Epithelial Defects with Limbal Stem Cell Deficiency. 2008; 23:502-8. https://doi.org/10.3346/jkms.2008.23.3.502 PMid:18583889 PMCid:PMC2526526

10. Ma, D., et al. Transplantation of cultivated oral mucosal epithelial cells for severe corneal burn. 2009; 23:1442-50. https://doi.org/10.1038/eye.2009.60 PMid:19373264

11. Reza HM, et al. Umbilical cord lining stem cells as a novel and promising source for ocular surface regeneration. Stem Cell Reviews and Reports. 2011; 7(4):935-947. https://doi.org/10.1007/s12015-011-9245-7 PMid:21431286

12. Zhou Y, et al. Characterization of Human Umbilical Cord Lining-Derived Epithelial Cells and Transplantation Potential. 2011; 20:1827-1841. https://doi.org/10.3727/096368910X564085 PMid:21439131

13. Huang L, et al. Stem cell-like properties of human umbilical cord lining epithelial cells and the potential for epidermal reconstitution. Cytotherapy. 2011; 13(2):145-155. https://doi.org/10.3109/14653249.2010.509578 PMid:20735166

14. Sivalingam J, et al. Biosafety assessment of site-directed transgene integration in human umbilical cord-lining cells. Molecular Therapy. 2010; 18(7):1346-1356. https://doi.org/10.1038/mt.2010.61 PMid:20424600 PMCid:PMC2911251

15. Letko E, et al. Amniotic membrane inlay and overlay grafting for corneal epithelial defects and stromal ulcers. Archives of Ophthalmology. 2001; 119(5):659-663. https://doi.org/10.1001/archopht.119.5.659 PMid:11346392

16. Li H, Niederkorn JY, Neelam S, Mayhew E, Word RA, McCulley JP, Alizadeh H. Immunosuppressive factors secreted by human amniotic epithelial cells. Investigative ophthalmology & visual science. 2005; 46(3):900-7. https://doi.org/10.1167/iovs.04-0495 PMid:15728546

17. Koizumi N, Inatomi T, Sotozono C, Fullwood NJ, Quantock AJ, Kinoshita S. Growth factor mRNA and protein in preserved human amniotic membrane. Current eye research. 2000; 20(3):173-7. https://doi.org/10.1076/0271-3683(200003)2031-9FT173

18. Tosi GM, Massaro-Giordano M, Caporossi A, Toti P. Amniotic membrane transplantation in ocular surface disorders. Journal of cellular physiology. 2005; 202(3):849-51. https://doi.org/10.1002/jcp.20181 PMid:15481064

19. He YG, et al. Experimental transplantation of cultured human limbal and amniotic epithelial cells onto the corneal surface. Cornea. 1999; 18(5):570-579. https://doi.org/10.1097/00003226-199909000-00010

20. Saleh R, Reza HM. Short review on human umbilical cord lining epithelial cells and their potential clinical applications. Stem cell research & therapy. 2017; 8(1):222. https://doi.org/10.1186/s13287-017-0679-y PMid:29017529 PMCid:PMC5634865

ID Design Press, Skopje, Republic of Macedonia
Open Access Macedonian Journal of Medical Sciences. 2019 Dec 30; 7(24):4272-4277.
https://doi.org/10.3889/oamjms.2019.373
eISSN: 1857-9655
Basic and Clinical Medical Researches in Vietnam

Outcomes of Small Incision Lenticule Extraction for Myopic Astigmatic Treatment

Nguyen Xuan Hiep[1], Pham Thi Minh Khanh[1], Do Quyet[2], Than Van Thai[3], Vu Thi Nga[4], Toi Chu Dinh[5], Nguyen Duy Bac[2*]

[1]Vietnam National Institute of Ophthalmology, Hanoi, Vietnam; [2]Vietnam Military Medical University (VMMU), Hanoi, Vietnam; [3]NTT Hi-tech Institute, Nguyen Tat Thanh University, Ho Chi Minh City, Vietnam; [4]Institute for Research and Development, Duy Tan University, 03 Quang Trung, Danang, Vietnam; [5]Department of Human and Animal Physiology, Faculty of Biology, Hanoi

Citation: Hiep NX, Khanh PTM, Quyet D, Thai TV, Nga VT, Chu Dinh T, Bac ND. Outcomes of Small Incision Lenticule Extraction for Myopic Astigmatic Treatment. Open Access Maced J Med Sci. 2019 Dec 30; 7(24):4272-4277.
https://doi.org/10.3889/oamjms.2019.373

Keywords: ReLEx SMILE; Astigmatism; Myopia

***Correspondence:** Nguyen Duy Bac. Vietnam Military Medical University (VMMU), Hanoi, Vietnam. E-mail: nguyenduybac@vmmu.edu.vn

Received: 01-Jul-2019; **Revised:** 20-Nov-2019; **Accepted:** 21-Nov-2019; **Online first:** 20-Dec-2019

Funding: This research did not receive any financial support

Competing Interests: The authors have declared that no competing interests exist

Abstract

BACKGROUND: Some studies have shown that there is a certain rotation of the eye in the sitting and lying position of the patient. The Visumax system used for the Refractive Lenticule Extraction-Small Incision Lenticule Extraction (ReLEx SMILE) surgery lacks the rotation of eye control function. So, is the ReLEx SMILE surgery for patients with astigmatism safe and effective?

AIM: To evaluate the outcomes of the ReLEx SMILE surgery in cases with myopic astigmatism.

METHODS: The case series included 120 eyes with myopic astigmatism undergoing ReLEx SMILE surgery from January 2018 to November 2018. The distribution of patients for two subgroups based on the power of astigmatism, low astigmatic group (≤ 1.50D) and high astigmatic group (> 1.50D). All patients were measured UDVA, CDVA, refractive sphere, astigmatism and sphere equivalent before and after surgery one week, one month and three months carefully. The astigmatic correction was evaluated by the vectorial analysis Alpins.

RESULTS: The mean efficacy index of the low and high astigmatic group was 1.035 and 1.082 (respectively); the mean safety index was 1.113 and 1.215 (respectively). 93% of eyes in the low astigmatic group had an angle of error (AE) within ± 15 degrees and 100% in high astigmatic group. There was an undercorrection in astigmatic treatment. No complications during and after surgery were recorded.

CONCLUSION: ReLEx SMILE surgery for the myopic astigmatic treatment was safe and effective.

Introduction

The development history of refractive surgery has gone through three generations. The first generation is photorefractive keratectomy (PRK) surgery. The second generation is LaserAssisted In Situ Keratomileusis (LASIK) surgery that creates a corneal flap. And now with the introduction of the femtosecond laser, in 2011, the third generation of refractive surgery occurred and have been called Refractive Lenticule Extraction-Small Incision Lenticule Extraction (ReLEx SMILE) with a no-flap technique [1]. Many researches have been indicated that the ReLEx SMILE had excellent results. This technique was extremely safe and effect because of avoiding the complications concerning to corneal flap. Moreover, the studies indicated that it had excellent predictability and stability for the correction of myopia. Together, the rate of dry eye syndrome and the amount of corneal aberration were also decreased [2], [3], [4], [5]. However, the Visumax system (Carl Zeiss Meditec, Germany) that has been used for this surgery lacks the rotation of eye control function. That has made the surgeons had to control the rotational eyes completely by hand and personal experience. Some surgeons have worried about the capability of this technique for the treatment of moderate or high astigmatism compared to LASIK surgery while at present, many excimer laser modern machines have cyclotorsion control function. Anyway, few papers report the results of the astigmatic correction by vector analysis, and very little researches have been still concerned with those patient's relative high astigmatism (especially > 3.0D). On the other hand, we have not found any reports about this issue in Vietnam. This study would like to assess the results of the ReLEx SMILE surgery in cases with myopic astigmatism.

Materials and Methods

The design of the study

The study method is case series. Selection criteria were patients with myopic astigmatism undergoing the ReLEx SMILE surgery from January 2018 to November 2018 at Vietnam National Institute of Ophthalmology (VNIO), Vietnam. Exclusion criteria were patients with combined systemic diseases or other problems of the eye. Distribution of patients for two subgroups was based on the power of astigmatism: low astigmatic group (astigmatism preoperative ≤ 1.50D) and high astigmatic group (astigmatism preoperative > 1.50D). The study was accepted by the institutional ethics committee of VNIO. All patients understood and voluntarily participated in this study.

Preoperative and postoperative examinations

If the patients wear contact lens, they need to discontinue at least two weeks with the soft contact lens or at least four weeks with the rigid contact lens before the initial examination.

All patients were examined carefully before surgery, including slit-lamp biomicroscopy, tonometry, uncorrected and corrected distance visual acuity (UDVA and CDVA), fundus evaluation, keratometry, non-contact specular microscopy, and corneal topography. Automated refraction was implemented before and after instilling cycloplegic solution (Cyclogyl 1%). Refractive indices were carefully measured several separated times before surgery to indicate the final refractive result for the treatment program.

After surgery one week, one month and three months, the UDVA and CDVA, tonometry, slit-lamp biomicroscopy and measurement of corneal topography were repeated. The refractive sphere, refractive astigmatism, the axis of astigmatism, manifest refraction spherical equivalent (MRSE) were also measured. The complications were recorded.

Astigmatic correction

The astigmatic correction was based on the method of Alpins, which allowed to analyze astigmatic vectors. Through the amount of astigmatic treatment, they could evaluate the efficacy of astigmatic correction. The first vector had been determined was the target induced astigmatism vector (TIA), which was manifest initial astigmatism, and needed to treat. The second vector had been known was the surgically induced astigmatism vector (SIA), which was the amount of astigmatic correction caused by surgery. The third vector was the difference between the TIA and the SIA, called the difference vector (DV) [6], [7]. Based on these above three vectors, many other indices have been identified to evaluate the characteristics of astigmatic correction further. The index of success (IOS) [8] would like to indicate the proportion of residual astigmatism, and was the value obtained by the DV division for the TIA; the ideal value was zero. The correction index (CI) was the ratio achieved by the SIA division for the TIA. If the CI was higher than 1.0, the treatment had shown overcorrection, while CI was lower than 1.0, the procedure had been under correction. The magnitude of error (ME) was the arithmetic difference between the magnitude of the SIA and the TIA. If the ME was positive the treatment had been an overcorrection, and if the ME was negative, the treatment had occurred under correction. The angle of error (AE) was the arithmetic difference between the angle of the SIA and the TIA. If the TIA was positive, the correction had shown counter clockwise with the initial astigmatic axis, and if the TIA was negative, the treatment had defined clockwise with the initial astigmatic axis.

Surgical technique

The procedure was performed by using the VisuMax system (Carl Zeiss Meditec, Germany) which emits femtosecond laser beam with near-infrared wavelengths in an extremely short time (10^{-15} seconds). The diameter of lenticule was set between 6.3 and 7.0 mm; the thickness of cap that was established 110 μm or 120 μm depends on the power of spherical refraction equivalent. The length of the incision was set 2 mm. In all cases, the patient was lying on the operation bed and align the head and the body. It was necessary to avoid head tilt. Topical anesthesia was achieved with one drop proparacaine hydrochloride (Alcaine, Alcon) every three minutes for three times before surgery. The time of treatment laser was 23 seconds. Then, a hook was used to separate two planes of the lenticule. The first, the surgeon delineated the upper interface and then was the lower interface. When both interfaces had been completely separated, the lenticule was extracted through the small incision. Finally, one drop antibiotic solution (Ofloxacin 0.3%, Santen) was instilled.

Statistical analysis

Data were analyzed using SPSS 16.0. The number of data was presented as X ± SD, and the percentage of data were shown in %. A p-value less 0.05 was considered statistically significant. Student's t-test was used to compare refractive indices, UDVA, CDVA, MRSE, corneal thickness, average keratometry, TIA, SIA, DV, ME, AE, CI, IOS…between two groups (low and high astigmatism). To compare proportions, using Fisher's exact test if the number of data was too small to do the Chi-square test.

Results

The Table 1 showed the characteristics of patients were presented, and no significant differences about the patient's age as well as the MRSE, refractive sphere, corneal thickness and average keratometry were found in both groups (low and high astigmatism) with p > 0.05.

Table 1: Preoperative patient characteristics

Characteristics	Total (74 patients)	Low Astigmatism (≤ -1.50D)	High Astigmatism (> -1.50D)	P
Female/male sex (n)	50/24	40/20	10 /4	
Patients (n)	74	60	14	
Eyes (n)	120	97	23	
Age (X ± SD)	21.21 ± 3.84	21.30 ± 3.66	20.83 ± 4.56	0.648
CDVA (X ± SD)	0.02 ± 0.06	0.004 ± 0.019	0.08 ± 0.12	< 0.001
MRSE (D)	-4.31 ± 1.74	-4.20 ± 1.59	-4.77 ± 2.25	0.262
Refractive Sphere (D) [9]	-3.75 ± 1.68 (-0.50 to -8.00)	-3.77 ± 1.59 (-0.50 to -6.50)	-3.66 ± 2.07 (-0.50 to -8.00)	0.826
Refractive Astigmatism (D) [9]	-1.14 ± 0.67 (-0.50 to -4.50)	-0.88 ± 0.33 (-0.50 to -1.50)	-2.22 ± 0.64 (-1.75 to -4.50)	< 0.001
Corneal Thickness (µm)	544.10 ± 24.47	544.45 ± 23.73	542.61 ± 27.89	0.771
Average Keratometry (D)	43.74 ± 1.15	43.73 ± 1.15	43.75 ± 1.18	0.957

Note: CDVA = corrected distance visual acuity; MRSE = manifest refraction spherical equivalent.

The corrected distance visual acuity (CDVA) in the group of patients with low astigmatic myopia was worse than that in the group of patients with high astigmatic myopia (p < 0.001). The average refractive astigmatism preoperative was -0.88 ± 0.33D in the low astigmatic group and -2.22 ± 0.64D in the high astigmatic group. The significant difference was less than 0.001. The minimum astigmatic value was -0.05D and maximum was -4.50D.

Table 2: Parameters during surgery

Parameter	Value
Thickness of cap (%)	
120 µm	97
110 µm	3
Central thickness of lenticule (µm)	70 ± 36
Minimum lenticule thickness (µm)	13 ± 3
Optical zone (mm)	6.4 ± 0.3
[9]	(6.3 to 7.0)

Some technical parameters during surgery were showed in table 2. The popular cap thickness was 120 µm in 97% of cases. The mean of the lenticule central thickness was 70 ± 36 µm. The average of the optical zone was 6.4 ± 0.3 mm with ranged from 6.3 mm to 7.0 mm.

The refractive outcomes of both groups were presented in Table 3. A significant difference was found in the UDVA logMar postoperative between the low astigmatic group and high astigmatic group (0.004 ± 0.105; 0.057 ± 0.099, respectively, p = 0.031). However, the CDVA logMar postoperative in both groups had no significant difference with p = 0.136. Most of the refractive outcomes had not statistic significant between 2 groups (p > 0.05), such as the sphere, cylinder, MRSE, efficacy index, safety index, DV [10], MA, and AE. The TIA and the SIA in the low astigmatic group were less than those in the high astigmatic group (p < 0.001). The CI and IOS [9] were also significantly lower in the low astigmatic group than in the high astigmatic group with p = 0.026.

Table 3: Comparison of refractive outcomes between low and high astigmatic groups

Characteristics	Low Astigmatism (≤ -1.50D)		High Astigmatism (> -1.50D)		P
	Mean	SD	Mean	SD	
UDVA LogMar	0.004	0.105	0.057	0.099	0.031
CDVA LogMar	-0.03	0.093	0.004	0.098	0.136
Sphere (D)	0.214	0.317	0.087	0.298	0.078
Cylinder (D)	-0.271	0.548	-0.207	0.209	0.366
MRSE (D)	0.093	0.313	-0.015	0.312	0.145
Efficacy index	1.035	0.264	1.082	0.219	0.384
Safety index	1.113	0.235	1.215	0.221	0.057
TIA	0.879	0.335	2.217	0.641	< 0.001
SIA	0.608	0.615	2.011	0.725	< 0.001
DV	0.271	0.548	0.207	0.209	0.366
CI	0.656	0.504	0.896	0.116	0.026
ME	-0.271	0.548	-0.207	0.209	0.366
AE	-2.99	7.265	-1.087	6.735	0.238
IOS	0.344	0.504	0.104	0.116	0.026

Note: UDVA = uncorrected distance visual acuity; CDVA = corrected distance visual acuity; MRSE = manifest refractive spherical equivalent; TIA = target induced astigmatism; SIA = surgically induced astigmatism; DV = difference vector; CI = correction index; ME = magnitude of error; AE = angle of error; IOS = index of success

Figure 1 illustrated the UDVA postoperative in both groups. The UDVA postoperative was better than or equal to 20/20 Snellen in 75.3% (with the low astigmatic group) and in 69.6% (with the high astigmatic group). The UDVA of 20/30 or less in the low astigmatic group was approximately half of that in the high astigmatic group (8.3% and 17.4%, respectively).

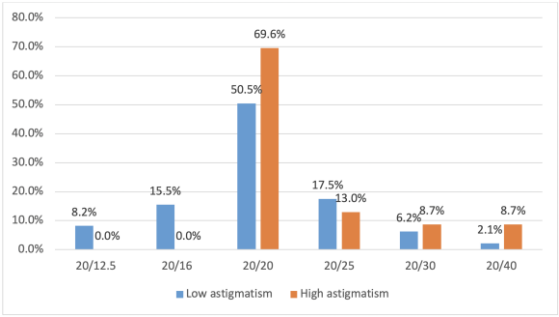

Figure 1: Uncorrected distance visual acuity postoperative

Result of comparison of UDVA between the low astigmatic group and the high astigmatic group was indicated in Table 4. Value of Pearson Chi-Square with 0.575 which meaned that the percentages of UDVA (≥ 20/20 and < 20/20) between two groups were similar.

Table 4: Comparison of Uncorrected distance visual acuity between two groups

UDVA	Low astigmatism (≤ 1.50D)	High astigmatism (> 1.50D)	Pearson Chi-Square
≥ 20/20	73 (75.3%)	16 (69.6%)	0.575
< 20/20	24 (24.7%)	7 (30.4%)	

The correlation between the TIA and the SIA were indicated in Figure 2. This was a high positive correlation. We could see that most of the values were in undercorrection area that suggested the SIA was

less than TIA, and there was an undercorrection in astigmatic treatment.

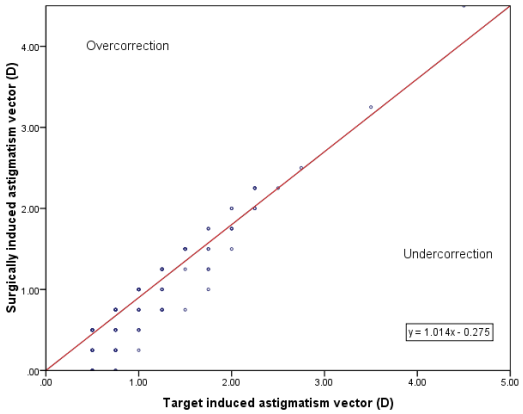

Figure 2: Target induced astigmatism and surgically induced astigmatism

Angle of Error (AE) was showed in Figure 3 and Table 5. The average absolute AE was 6.227 ± 4.758 and 5.348 ± 4.086 degrees (in the low astigmatic and the high astigmatic group). The result was not statistically different with p = 0.375.

Table 5: Average of Angle of Error

Angle of Error (degrees)	Low astigmatism (≤ 1.50D)	High astigmatism (> 1.50D)	p
Arithmetic	-2.99 ± 7.265	-1.08 ± 6.73	0.238
Absolute	6.227 ± 4.758	5.348 ± 4.086	0.375

In the low astigmatic group, 93% of eyes had the AE within ± 15 degrees, and 100% was the rate of the AE within ± 15 degrees in the high astigmatic group. The difference in arithmetic and the absolute mean of the AE were not significantly (p = 0.238 and 0.375, respectively) (Figure 3).

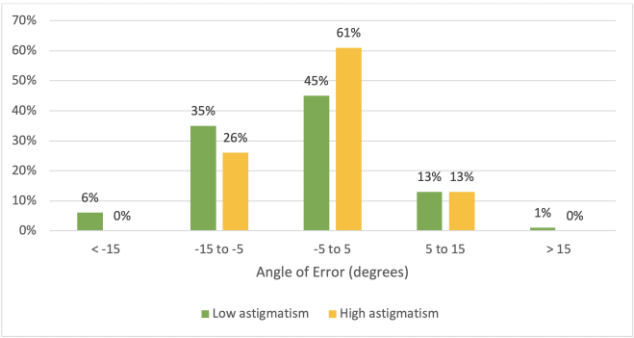

Figure 3: Refractive Astigmatism Angle of Error

There were not any cases which occurred a suction loss or other complications (such as an incomplete lenticule extraction) during the procedure. No eyes of corneal ectasia postoperative were recorded. This study did not also find keratitis after surgery.

Discussion

Some studies indicated that there was a certain rotation of the eye in the sitting and lying position. With the patients undergoing refractive surgery, the preoperative measurement refraction in the sitting position and the surgical intervention in the lying position may exist the rotational eye motions which could lead to reducing the efficacy of laser procedure, especially the eyes with high astigmatism [6]. Nowadays, many modern excimer laser systems have cyclotorsional control function that helps to increase the quality of treatment significantly by LASIK surgery [7]. Through the comparison between the iris images in the sitting and lying position, the laser system automatically analyzes to define the rotational eye. Then, the machine calculates and compensates for cyclotorsional eye motions. In the ReLEx SMILE surgery, Visumax machine has not the cyclotorsional control function that is considered the main limitation of this method. As a result, we would like to evaluate the outcomes of the ReLEx SMILE surgery for the eyes with myopic astigmatism (power of astigmatism ≥ 0.50D). In our study, we distributed the patients to two groups based on the power of astigmatism, which were the low astigmatic group (≤ 1.50D) and the high astigmatic group (> 1.50D). To minimizing the cyclotorsional eyes motions, we attempted to put the patients straight on the bed so that the patient's head aligns with his body, avoiding head tilt.

The outcomes of the ReLEx SMILE in this study was generally very good. In particular, the UDVA postoperative was better than or equal to 20/20 Snellen in 75.3% (with the low astigmatic group) and in 69.6% (with the high astigmatic group). The UDVA of 20/30 or less in the low astigmatic group was approximately half of that in the high astigmatic group (8.3% and 17.4%, respectively). However, when we compared the percentages of UDVA (≥ 20/20 and < 20/20) between the low astigmatic group and the high astigmatic group, we recognized that there was no difference between two groups (p = 0.575). It that means ReLEx SMILE surgery provided good outcomes of UDVA in both two groups which did not depend on the power of astigmatism preoperative. This result was consistent with the study of Zhang et al., who presented the UDVA postoperative of 20/20 Snellen or more was in 79.6% [8]. One another research also showed the UDVA after the ReLEx SMILE surgery two years was better than or equal to 20/20 in 90% [9]. The authors all confirmed that ReLEx SMILE surgery gave good result of visual acuity in patient with astigmatic myopia.

To assess whether this surgery was effective and safe, we based on the efficacy index and the safety index. The efficacy index was the proportion between the UDVA decimal postoperative and the CDVA decimal preoperative, and the safety index was

the proportion between the CDVA decimal postoperative and CDVA decimal preoperative. In our study, the efficacy index was basically 1.035 ± 0.264 with the low astigmatic group and 1.082 ± 0.219 with the high astigmatic group. There was no significant difference in the efficacy index between the two groups (p = 0.384). This index was similar with the result of Lin et al. (1.04 ± 0.20) [5]. Similarly, the safety index of this study was 1.113 ± 0.235 and 1.215 ± 0.221 in the low astigmatic group and the high astigmatic group, respectively, with no significant difference (0.057). This index was also approximately to result of Lin et al., (1.01 ± 0.05) [5]. Another study of Chan et al., showed the efficacy of ReLEx SMILE surgery with 79.6% of eyes had a UDVA of 20/20 or better, and the safety with 57.1% of eyes gained one line of visual acuity, only one eye lost one line, no case lost two or more lines [10]. The outcomes provided evidence to the consideration that ReLEx SMILE surgery was extremely effective and safe in correcting low to moderate astigmatism [10].

The MRSE postoperative was generally good and no statistic difference between two groups (Table 3). Residual astigmatism postoperative (equal to the difference of vector) in the low astigmatic group and the high astigmatic group was 0.271 ± 0.548 and 0.207 ± 0.209D, respectively, with no significant difference (0.366). However, the correction index (CI) and index of success (IOS) [11] were 0.896 and 0.104 (respectively) in the high astigmatic group and significantly higher than those in the low astigmatic group (p = 0.026). This difference may be correlated with the results of the angle of error (AE). In the low astigmatic group, the AE within ± 5 degrees was only accounted in 45%, and 61% in the high astigmatic group. Moreover, 93% of eyes had an AE within ± 15 degrees in the low astigmatism group, and 100% was the rate of the AE within ± 15 degrees in the high astigmatic group (Figure 3). In our results (Table 5), although the difference of the AE was not statistically significant, the lower value of high astigmatic group may occur due to pay special attention to aligning that was occupied less than in the low astigmatic group.

We observed the undercorrection in this study (Figure 2). Several previous researches also showed a trend toward undercorrection [8], [11]. There was a study that compared the astigmatic treatment between two methods (the LASIK and the ReLEx SMILE) indicated excellent results with both techniques. However, an undercorrection postoperative was found in both surgeries in the eyes with high astigmatism (> 2.25 D) that agreed with our results. The high AE values might be the reason for those undercorrections [12].

To compensate for the rotational eye movements, Ganesh introduced a manual technique [13]. They used a pen to mark the horizontal axis of the limbal cornea when the patient sat up straight. After the patient lay down on the operation bed, the docking and suction progress were implemented through the contact glass. The surgeon looked in the microscope eyepiece and corrected the horizontal axis of the centering grid (inside of the microscope eyepiece) to coincide with the marked axis on the patient's eye by manual rotation contact glass. The authors of this study indicated the average cyclotorsion was 5.64 ± 2.55 degrees in 82% of eyes and the rotational contact glass technique compensated well for it. However, this method still existed some drawbacks. The first, the initial marking might be not incorrect. The second, the marking might lead the damage of the cornea, which could make the patients uncomfortable during and after surgery. The third, loss of suction might occur because of the above discomfort or the manual rotation contact glass. The final, the ink marks or the lesions could appear on the cornea might result due to the black spots after laser performance.

However, we did not implement corneal marking before surgery because we had only four eyes with real high astigmatism (≥ 2.50D) in this study. Therefore, we have just aligned exactly the patient's body and head, central fixation of eyes, we have achieved good astigmatic correction.

In conclusion, although the Visumax machine has not any modern eye-tracking systems as well as the cyclotortional control function, the ReLEx SMILE surgery still has had high safety and efficacy index. The most important in treatment for myopic astigmatism undergoing SMILE surgery is to carefully align the patient's body and head, central fixation of eyes during the procedure.

Results of the ReLEx SMILE surgery might be improved with cyclotorsional control systems in the newer generations in the future.

Ethical approval

Our study was accepted by the institutional ethics committee of the Vietnam National Institute of Ophthalmology. All patients understood and voluntarily participated in this study.

References

1. Sekundo W, Kunert KS, Blum M. Blum, Small incision corneal refractive surgery using the small incision lenticule extraction (SMILE) procedure for the correction of myopia and myopic astigmatism: results of a 6 month prospective study. Br J Ophthalmol. 2011; 95(3):335-9. https://doi.org/10.1136/bjo.2009.174284 PMid:20601657

2. Ivarsen A, Asp S, Hjortdal J. Safety and complications of more than 1500 small-incision lenticule extraction procedures.

Ophthalmology. 2014; 121(4):822-8. https://doi.org/10.1016/j.ophtha.2013.11.006 PMid:24365175

3. Kim JR, et al. Efficacy, predictability, and safety of small incision lenticule extraction: 6-months prospective cohort study. BMC Ophthalmol. 2014; 14:117. https://doi.org/10.1186/1471-2415-14-117 PMid:25280533 PMCid:PMC4192335

4. Denoyer A, et al. Dry eye disease after refractive surgery: comparative outcomes of small incision lenticule extraction versus LASIK. Ophthalmology. 2015; 122(4):669-76. https://doi.org/10.1016/j.ophtha.2014.10.004 PMid:25458707

5. Lin F, Xu Y, Yang Y. Comparison of the visual results after SMILE and femtosecond laser-assisted LASIK for myopia. J Refract Surg. 2014; 30(4):248-54. https://doi.org/10.3928/1081597X-20140320-03 PMid:24702576

6. Chernyak DA. Cyclotorsional eye motion occurring between wavefront measurement and refractive surgery. J Cataract Refract Surg. 2004; 30(3):633-8. https://doi.org/10.1016/j.jcrs.2003.08.022 PMid:15050260

7. Prakash G, et al. Comparison of laser in situ keratomileusis for myopic astigmatism without iris registration, with iris registration, and with iris registration-assisted dynamic rotational eye tracking. J Cataract Refract Surg. 2011; 37(3):574-81. https://doi.org/10.1016/j.jcrs.2010.11.025 PMid:21333879

8. Zhang J, et al. Vector analysis of low to moderate astigmatism with small incision lenticule extraction (SMILE): results of a 1-year follow-up. BMC Ophthalmol. 2015:15(1):8. https://doi.org/10.1186/1471-2415-15-8 PMid:25618419 PMCid:PMC4328987

9. Kobashi H, et al. Two-years results of small-incision lenticule extraction and wavefront-guided laser in situ keratomileusis for Myopia. Acta Ophthalmol. 2018; 96(2):e119-e126. https://doi.org/10.1111/aos.13470 PMid:28631305

10. Chan TC, et al. Vector analysis of astigmatic correction after small-incision lenticule extraction and femtosecond-assisted LASIK for low to moderate myopic astigmatism. Br J Ophthalmol. 2016; 100(4):553-9. https://doi.org/10.1136/bjophthalmol-2015-307238 PMid:26206791

11. Khalifa MA, et al. Vector analysis of astigmatic changes after small-incision lenticule extraction and wavefront-guided laser in situ keratomileusis. J Cataract Refract Surg. 2017; 43(6):819-824. https://doi.org/10.1016/j.jcrs.2017.03.033 PMid:28732617

12. Zhang J, Wang Y, Chen X. Comparison of moderate-to high-astigmatism corrections using WaveFront-guided laser in situ Keratomileusis and small-incision Lenticule extraction. Cornea. 2016; 35(4):523-30. https://doi.org/10.1097/ICO.0000000000000782 PMid:26890662

13. Ganesh S, Brar S, Pawar A. Results of Intraoperative Manual Cyclotorsion Compensation for Myopic Astigmatism in Patients Undergoing Small Incision Lenticule Extraction (SMILE). J Refract Surg. 2017; 33(8):506-512. https://doi.org/10.3928/1081597X-20170328-01 PMid:28787514

ID Design Press, Skopje, Republic of Macedonia
Open Access Macedonian Journal of Medical Sciences. 2019 Dec 30; 7(24):4278-4282.
https://doi.org/10.3889/oamjms.2019.374
eISSN: 1857-9655
Basic and Clinical Medical Researches in Vietnam

Assessing the Status of Filtering Blebs at 5 Year Post-Trabeculectomy

Bui Thi Van Anh[1], Nguyen Thai Dat[1], Anh Tuan Vu[2], Nguyen Trung Hieu[3], Do Quyet[4], Than Van Thai[5], Vu Thi Nga[6], Toi Chu Dinh[7], Nguyen Duy Bac[4*]

[1]Vietnam National Institute of Ophthalmology, Hanoi, Vietnam; [2]Hanoi Medical College, Hanoi, Vietnam; [3]Ninhbinh Province Eye Hospital, Ninh Binh, Vietnam; [4]Vietnam Military Medical University (VMMU), Hanoi, Vietnam; [5]NTT Hi-tech Institute, Nguyen Tat Thanh University, Ho Chi Minh City, Vietnam; [6]Institute for Research and Development, Duy Tan University, 03 Quang Trung, Danang, Vietnam; [7]Department of Human and Animal Physiology, Faculty of Biology, Hanoi National University of Education, Hanoi, Vietnam

Citation: Anh BTV, Dat NT, Vu AT, Hieu NT, Quyet D, Thai TV, Nga VT, Dinh TC, Bac ND. Assessing the Status of Filtering Blebs at 5 Year Post- Trabeculectomy. Open Access Maced J Med Sci. 2019 Dec 30; 7(24):4278-4282.
https://doi.org/10.3889/oamjms.2019.374

Keywords: Filtering bleb; OCT anterior; Trabeculectomy

***Correspondence:** Nguyen Duy Bac. Vietnam Military Medical University (VMMU), Hanoi, Vietnam. E-mail: nguyenduybac@vmmu.edu.vn

Received: 01-Jul-2019; **Revised:** 20-Nov-2019; **Accepted:** 21-Nov-2019; **Online first:** 20-Dec-2019

Funding: This research did not receive any financial support

Competing Interests: The authors have declared that no competing interests exist

Abstract

BACKGROUND: Glaucoma is a common cause of blindness in the world as well as in Vietnam. It is treated by many different methods but trabeculectomy is still the most popular and highly effective surgical method to treat this condition.

AIM: To analyze the status of 5 years filtering blebs following trabeculectomy and to explore multiple factors associated with filtering blebs.

METHODS: This is a retrospective, cross-sectional descriptive study. Eyes had been performed trabeculectomy for 5 years were included in these results. The filtering blebs were assessed using slit lamp and OCT. the OCT captured bleb area to evaluate fluid subconjunctival spaces, thickness and height of bleb and to evaluate the related factors

RESULTS: A group of 106 primary glaucoma eyes of 97 patients (88 patients with 1 eye, 9 patients 2 eyes) had been performed trabeculectomy for 5 years were taken OCT anterior image. The proportion of female patients is 1.5 times that of male patients. IOP was controlled with or without topical medication in all eyes. The filtering bleb had a high echo reflection, which accounted for 42.5%, the average echo reflection was 38.6%, the low echo reflection response of 18.9%. 66% of the eyes had the aqueous space under the conjunctiva, 65.1% have the aqueous space under sclera flap, the average height of the bleb on OCT was 0.4 mm ± 0.3 mm. Young patients often have a higher rate of bleb fibrosis and loss of function than older patients

CONCLUSION: OCT is capable of assessing the function of bleb. After 5 years of trabeculectomy, on the OCT image, most cases of blebs are maintaining drainage function.

Introduction

Glaucoma is a common cause of blindness in the world as well as in Vietnam. In most countries, glaucoma is the second-leading cause of blindness and a dangerous threat to public health. The disease has many different pathogenesis and pathophysiology mechanisms and is treated with many different methods but trabeculectomy is still the most popular and highly effective surgical method to treat glaucoma [1], [2]. The aim of the surgery is to create a pathway which allows the aqueous humor to drain from the anterior chamber into an area underneath the conjunctiva where it creates a filtering bleb and subsequently absorbed into the conjunctival capillary system. However, with time, the effect of lowering pressure of the surgery tends to decrease. According to Ehrnooth P, the rate of IOP below 21mmHg after 1 year of trabeculectomy is 82%, after 2 years is 70%, after 3 years is 64%, after 4 years is 52% [3]. Studies by many authors show that the cause of failure of PT has many reasons, but mainly the increase in fibrosis after surgery causes failure of filtering bleb. The structural manifestations of bleb indicate the ability of fluid to pass through the fistula. So that assessment of bleb manifestations can predict its drainage function.

Beside of clinical assessment, OCT images of anterior part of the eyeball allows to accurately record and measure the internal structures of bleb such as: the thickness of the bleb wall, the echo reflection inside of the bleb, the aqueous space subconjunctival or under the sclera flap, the scleral flap thickness, aqueous pathway under the sclera flap and the fistula. This is a non-invasive examination that can help doctors clearly assess the condition of bleb as well as determine the cause of failure of filtration surgery. There are many filtrating bleb classification system but Zang Yi 'one is a clear, complete and easy to use in practice [4], [5].

According to Zhang Yi, there are 4 types of filtering bleb [4]: 1). Diffuse bleb: bleb function. There are several microcapsules under the conjunctiva with low or moderate echogenicity gaps. These blebs have a thick conjunctiva, a fluid space above sclera flap, an aqueous pathway under sclera flap and a visible fistula; 2) Cystic bleb: also a bleb with function. The walls of the scar are relatively thin (usually below 0.2 mm), varying in height and are composed of a wide aqueous cavity or some small or medium space above sclera flap, some of which are fused with the space subconjunctiva. The fluid fistula under sclera flap is clearly visible; 3) Encapsulated bleb: is a non-functional bleb in which the fluid space above sclera flap is surrounded by tissues with high echogenicity. The tissue of the sclera and conjunctiva is not clearly distinguished, may even stick (the entire scar wall is thickened). The fluid cavity on the sclera is surrounded by dense connective tissue with high echogenicity, aqueous pathway under the sclera flap and fistula are usually very thin; and 4) Flattened bleb: is a non-functional bleb. Flat blebs are similar to an encapsulated bleb but there is no aqueous space under the conjunctiva or above the sclera flap. The whole scar is low, the wall is thick. Conjunctiva and sclera are intertwined, with high echogenicity, similar to the echogenicity of the sclera. The aqueous pathway under the sclera flap is often not visible, although openings are visible.

Therefore, we conducted the study to investigate the bleb of trabeculectomy on the OCT image taken 5 years after surgery.

Materials and Methods

A retrospective, cross-sectional descriptive study was conducted on 106 eyes of 97 patients diagnosed with primary glaucoma who had been performed trabeculectomy at the Glaucoma department – Vietnam National Institute of Ophthalmology from September 2008 to March 2009. Among them, 97 patients had unilateral trabeculectomy and 9 patients had bilateral trabeculectomy.

Selection criteria

Primary glaucoma eyes which were performed trabeculectomy with or without anti-metabolic drugs. The study ruled out the patients who had trabeculectomy more than one-time, combined phaco-trabeculectomy, patients with a history of trauma or other pathological treatment surgery of the eye.

The protocol included

Gathering all medical records of patients in the selected subjects, inviting the patients to re-examine, assessing the functional and physical condition, then all patients will be taken OCT to assess filtering blebs. During OCT images were taken, the patients were asked to look down, the photographer gently pulled the upper eye lash to reveal the limbus, filtering bleb and conjunctival area, avoiding pressing on the eyeball and the bleb. The first slice was directly taken through the bleb center, the second horizontal slice was taken passed through the center of the bleb, parallel to the cornea limbus [6], [7].

Capturing and observing filtering blebs

The echogenicity within filtering blebs, the sub conjunctiva aqueous space, the fluid cavity and pathway under sclera flap, the fistula were recorded. Measuring the height, width, the wall thickness of the blebs was calculated on OCT images.

Clinical bleb assessment is performed by slit lamp examination: - Height of blebs was recorded with flattened, low, medium and high performance; - The diffuse of blebs were recorded and classified to less than 1 hour, from 1 hour to 2 hours, from 2 hours to 4 hours, over 4 hours; - Blood vessels were observed on the surface of bleb and were classified to no blood vessels, little blood vessels, average blood vessels, many blood vessels and whether there is congestion or not; - Seidel test: The rate of Seidel negative (blebs had no drainage fluid), Seidel positive within 5 seconds, Seidel positive after 5 seconds (those had drainage fluid); and - In addition, we noted the cases with excessively large filtering blebs, blebs with thin walls with a risk of wound leakage.

General clinical assessment based on classification of Buskirk (1992) [8]: - Good bleb: diffuse and avascular blebs with the presence of small micro- cysts intra conjunctival epithelium; - Moderate bleb: diffuse blebs with many blood vessels on the surface or tend to stick at the bleb margin; and - Bad bleb: Excessively large filtering blebs, bleb fibrosis, conjunctiva lacks mobility, presence of many blood vessels on the surface of the blebs.

The OCT images were taken and filtering blebs were evaluated

The height of bleb measured at highest axis and recorded with less than 1 mm, from 1 – 2 mm and over 2 mm. The echogenicity of blebs was divided to low, medium high echo reflection. Status of fluid space under the conjunctiva or under sclera flap was recoded as visible or invisible. The fluid pathway below the sclera flap and the fistula of sclerectomy was also recorded as visible or invisible. In overall, the blebs were classified into Type D, Type C, Type E, Type F according to Zhang Yi [4].

Results

Demographic characteristics

The average age of the study group is 60.27 ± 9.13, majority of patients aged 55 and over. Of the 97 patients in the study group, there were 39 males and 58 females.

The average intraocular pressure before surgery was 30.3 ± 4.1 mmHg, the IOP level from 26 – 32 mmHg accounted for the highest rate (62.3%). At the time of re-examination, the average intraocular pressure was 19.97 ± 3.3 mmHg with/without glaucoma eye drops, none of which had IOP above 32 mmHg.

In 106 primary glaucoma eyes, there were 89 angle-closure glaucoma (83.9%) and 17 open-angle glaucoma eyes (16.1%). Only 18 (PACG and POAG) eyes were at the primary stage with no glaucomatous optic damages or glaucomatous visual field damages identified. 21/106 eyes were applied 5FU or MMC during the operation. 81.1% had more than 1 anti-glaucoma drop before surgery.

Filtering bleb status after 5 years of surgery

Most of cases had medium size bleb. The proportion of flat blebs was 23.6% and very high blebs accounted for 11.3%. The width of the blebs is mainly 2 to 4 hours (79/106 eyes). The number of eyes with a width of bleb smaller than 1 hour or larger more than 4 hours was very low. 23.6% of eyes had moderate vessels on the bleb surface, 58.5% had few, 6.6% had many blood vessels and 11.3% avascular on the bleb surface. All eyes in the study resulted in a negative Seidel test.

Clinically, the number of eyes with flat fibrous blebs accounted for 44.3% (Figure 1), followed by diffuse blebs and those with small microcysts, accounting for the lowest percentage was capsule-shaped bleb. Besides, we have recorded 7 excessively large blebs, these blebs have thin walls, high roughness, great width.

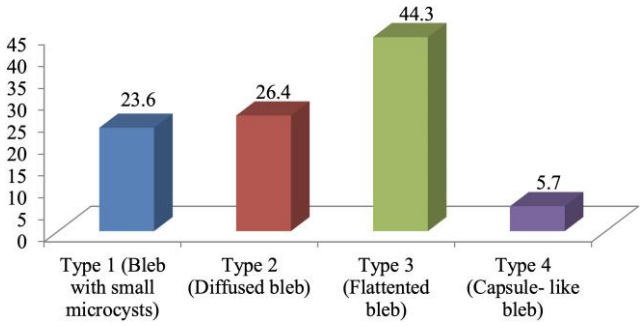

Figure 1: Clinical classification of filtering blebs

Assessing filtering bleb status on OCT

In our study, the rate of bleb with high echogenicity accounted for the highest rate (42.5%), then the bleb had an average echogenicity (38.6%), the lowest was the blebs with the least echo-genecity (18.9%). There were 66% of the eyes which showed visible subconjunctival aqueous spaces, 34% of the eyes showed no aqueous accumulation. 82.1% of cases had aqueous space under sclera flap, 17.9% had blebs without aqueous cavity under the sclera flap.

Fluid pathway under the sclera flap was visible in 69 eyes (accounting for 65.1%), 85/106 of cases had visible fistula while the fistula was not observed in 21eyes (accounting for 34.9%). 61.3% of the eyes had bleb height less than 1 mm; 38.7% were 1 to 2 mm and none of eyes had big bleb with the height more than 2 mm

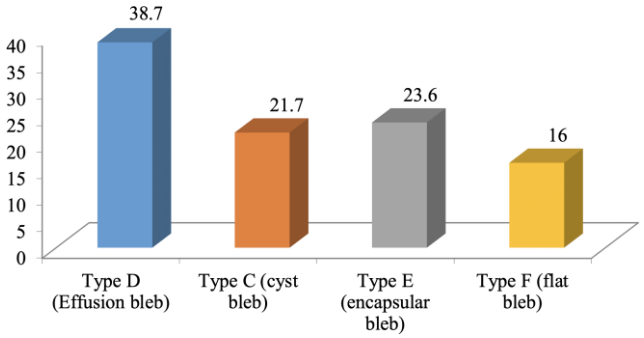

Figure 2: Classification of filtering bleb on OCT

The bleb classification on OCT according to Zhang Yi is described according to the above chart [4]. Type D is the diffuse bleb, which accounts for the highest rate of 38.7%, type C is the bleb with small microcysts that accounts for 21.7%, type E is capsule-like bleb, accounting for 23.6%, type F is the flat bleb, accounting for 16%.

Factors related to blebs

At the age more than or equal to 55, the percentage of eyes with type D was 47.3%, much

higher than the age less than 55, which was 18.8%. Meanwhile, the percentage of eyes with type E blebs at age less than 55 is 40.6%, much higher than those with type E which is 16.2%.

Table 1: IOP at the time of re-examination and bleb status IOP/re- examination

	Type C		Type D		Type E		Type F		Total	
	No of eyes	Rate (%)	No of eyes	Rates (%)	No of eyes	Rate (%)	No of eyes	Rate (%)	No of eyes	Rate (%)
14 - 25 mmHg	23	23.2	41	41.4	22	22.2	13	13.1	99	100
26 - 32 mmHg	0	0	0	0	3	42.9	4	57.1	7	100
Total	23	21.7	41	38.7	25	23.6	17	16.0	106	100
P < 0.01										

P value were determined by Chi-square test.

At the time of re-examination, there were 99/106 eyes with IOP from 14 mmHg to 25 mmHg and 7 eyes with IOP from 26 mmHg to 32 mmHg (Maclakov tonometer). In IOP controlled group, the rate of type D accounted for the highest rate (41/99 eyes), then the eye had type C (23/99 eyes), followed by the eyes in type E (22/99 eyes), finally the eyes of type F had the lowest rate (13/99 eyes) (Table 1).

On the contrary, uncontrolled IOP group, the rate of type F accounted for the highest proportion (4/7 eyes), followed by those with type E (3/7 eyes), whereas no eye in this group had blebs of type C and type D.

Table 2: Anti-metabolite application and blebs status

Anti-metabolic application	The bleb classification on OCT								Total	
	Type C		Type D		Type E		Type F			
	Number of eyes	Rate (%)	Number of eyes	Rate (%)	Number of eyes	Rate (%)	Number of eyes	Rate (%)	Number of eyes	Rate (%)
Yes	13	61.9	4	19.0	4	19.0	0	0	21	100
No	10	11.8	37	43.5	21	24.7	17	20.0	85	100
Total	23	21.7	41	38.7	25	23.6	17	16.0	106	100
p < 0.01										

P values were determined by Chi-square test.

5FU or MMC had been applied during operation in 21 eyes, in which the number of type C blebs accounted for the highest percentage of 61.9% (13/21), followed by the number of type D and type E all accounted for the proportion 19% (4/21), no eye has bleb in type F. 85 eyes were not applied anti-metabolic drugs. In this group, the number of eyes with type D had the highest rate of 43.5% (37/85), followed by the type E 24.7% (21/85), type F accounted for 20% (17/85), the lowest was Type C accounted for 11.8% (10/85) (Table 2).

Discussion

Most blebs can spread from 2-4 hours, number of blebs which spread under 1 hour is less, usually only seen on very fibrous, flattened eyes, sometimes with these eyes must be examined carefully to find out conjunctival wound. The blebs spread > 4 hours, which is more common in patients with anti-metabolic drugs, is also very small number. In our study, there were 7 cases of excessively large blebs causing discomfort for patients and sometimes spreading over the edge of the upper limbus, leading a risk of leakage and being ruptured. Good functional blebs often spread, flattened, not too stretch, no vessels on the surface, many microcapsules are adjacent to the conjunctival epithelium. In contrast, poorly functioning blebs are located blebs, many blood vessels, conjunctival fibrosis anchored to sclera underneath or over stretch. In fact, the blebs that function are not necessarily complete avascular but still have a few blood vessels on the surface of the bleb, but these blood vessels are small and not dense. That is why the number of blebs with blood vessels is the lowest, not the avascular blebs [6], [7].

With the Visante-OCT machine, the image inside the bleb will be clearly observed thanks to the high resolution. In OCT image, type D blebs (diffuse blebs) and type C (blebs with microcysts) usually have low or moderate echogenicity found in homogeneous tissue as a liquid, E-type blebs (capsule-like blebs) and F-type blebs (flat blebs) often have high echogenicity. In this study, of the 61 blebs with low and medium echogenicity, up to 43 blebs in type D and type C, accounting for 70.5% are functional blebs. The rate of low echogenicity was less than those in studies of Leung CK, Nghiem Thi Hong Hanh (2010) due to longer follow up (Leung CK study in 12 months, Nghiem Thi Hong Hanh's study in 26 months) [6], [9]. The longer the time after surgery, the more fibrosis the bleb, so the higher echogenicity inside the bleb.

Besides, in the functional blebs, which means that the pathway for aqueous humor is created, IOP were well controlled, a good bleb was usually highly visible to see the fluid pathway below the sclera flap [10], [11]. In 106 research eyes, 69 eyes have bleb seeing the fluid under the sclera flap, accounting for 65.1%, of which 58/69 eyes are blebs in type D and type C (accounting for 84%), 11/69 eyes are blebs belonging to type E (accounting for 16%), no bleb of type F, $p < 0.01$. In our study, there was a significant higher rate of the eye with visible fluid pathway under the scleral flap than the Leung CK study [9] probably because this author used the Stratus-OCT which is more limited about depth penetration than the Visante OCT machine we used in the study. Thus, the age group ≥ 55 has the rate of blebs of type D and type C (the blebs that were still functional), accounting for a high proportion (67.6%). On the contrary, at the age of < 55, the rate of type E blebs and type F blebs (which were not functional) is higher than the rate of type D and type C (functional blebs). This difference has statistical significance with $p < 0.05$. This is also understandable because in the elderly, the fibrosis after surgery is always reduced compared to young people.

In the study group, Of the 21 eyes had anti-metabolic application up to 17/21 eyes had blebs of type D and type C accounted for 81%, only 19% type

E and type F. Meanwhile, in the eyes that do not use anti-metabolite, the rate of type D and type C is 55.3%. This difference is statistically significant with $p < 0.01$. Thus, anti-metabolic application with trabeculectomy increased markedly the rate of bleb function (type D and type C). In histopathological studies, it has also been shown that anti-metabolite has the effect of inhibiting fibroblast proliferation, thus improving the hydrological drainage efficiency of bleb after trabeculectomy [12], [13], [14].

At the time of re-examination, in IOP controlled group, 64.6% of cases had blebs belonged to type D and type C and 35.4% type E and type F was statistically significant difference ($p < 0.01$) comparing to 100% blebs belonged to type E and type F in uncontrolled IOP group. Our results are similar to Zhang Yi's study, with 72% eyes was Type F in goup IOP uncontrolled [4], this result is similar to the study by Weizer JS [15].

In conclusion, five years after trabeculectomy for primary glaucoma treatment, 93% of blebs in these cases were maintaining the function of lowering IOP, 65.1% blebs had low and medium echogenicity, 74.5% bleb with a width of 2 to 4 hours zones and a few blood vessels, most of these blebs on OCT examination still observe the cavity under the conjunctiva, the fluid pathway under the sclera flap.

Young patients often have a higher rate of bleb fibrosis and loss of function than older patients. Anti-metabolite application increase IOP controlled but also increase the the excessively large blebs. The uncontrolled IOP eyes use to have its bleb belong to type E or type F on OCT.

Acknowledgement

We would like to acknowledge the support of many colleagues from the Departments of Glaucoma, Vietnam National Institute of Ophthalmology.

References

1. Kanski JJ. The glaucomas: Clinical Ophthalmology. A systematic approach. Oxford: Butterworth-Heinemann, 1994.

2. Shaarawy T, Flammer J. Trabeculectomy - The golden standard. Glaucoma Therapy Current Issues and Controversies. London: Martin Dunitz, 2004. https://doi.org/10.3109/9780203488911

3. Ehrnrooth P, et al. Long-term outcome of trabeculectomy in terms of intraocular pressure. Acta Ophthalmol Scand. 2002; 80(3):267-71. https://doi.org/10.1034/j.1600-0420.2002.800307.x PMid:12059864

4. Zhang Y, et al. Evaluating subconjunctival bleb function after trabeculectomy using slit-lamp optical coherence tomography and ultrasound biomicroscopy. Chin Med J. 2008; 121(14):1274-9. https://doi.org/10.1097/00029330-200807020-00005 PMid:18713546

5. Yamamoto T, Sakuma T, Kitazawa Y. An ultrasound biomicroscopic study of filtering blebs after mitomycin C trabeculectomy. Ophthalmology. 1995; 102(12):1770-6. https://doi.org/10.1016/S0161-6420(95)30795-6

6. Hường, Đ.L., Khảo sát sự phù hợp về kết quả khám đánh giá sẹo bọng sau mổ cắt bè củng mạc bằng đèn khe và bằng máy Visante OCT. Tạp chí y học thực hành, 2012. 810:24-27.

7. Izatt JA, et al. Micrometer-scale resolution imaging of the anterior eye in vivo with optical coherence tomography. Arch Ophthalmol. 1994; 112(12):1584-9. https://doi.org/10.1001/archopht.1994.01090240090031 PMid:7993214

8. Van Buskirk EM. Mechanisms and management of filtration bleb failure. Aust N Z J Ophthalmol. 1992; 20(3):157-62. https://doi.org/10.1111/j.1442-9071.1992.tb00934.x PMid:1449767

9. Leung CK, et al. Analysis of bleb morphology after trabeculectomy with Visante anterior segment optical coherence tomography. Br J Ophthalmol. 2007; 91(3):340-4. https://doi.org/10.1136/bjo.2006.100321 PMid:17005548 PMCid:PMC1857643

10. Kojima S, et al. Filtration bleb revision guided by 3-dimensional anterior segment optical coherence tomography. J Glaucoma. 2014; 23(5):312-5. https://doi.org/10.1097/IJG.0b013e3182741ee6 PMid:23377583

11. Mastropasqua R, et al. Anterior segment optical coherence tomography imaging of conjunctival filtering blebs after glaucoma surgery. Biomed Res Int. 2014; 2014:610623. https://doi.org/10.1155/2014/610623 PMid:25136603 PMCid:PMC4127298

12. Heuer DK, et al. 5-Fluorouracil and glaucoma filtering surgery. III. Intermediate follow-up of a pilot study. Ophthalmology. 1986; 93(12):1537-46. https://doi.org/10.1016/S0161-6420(86)33542-5

13. Megevand GS, et al. The effect of reducing the exposure time of mitomycin C in glaucoma filtering surgery. Ophthalmology. 1995; 102(1):84-90. https://doi.org/10.1016/S0161-6420(95)31049-4

14. Mermoud A, Salmon JF, Murray AD. Trabeculectomy with mitomycin C for refractory glaucoma in blacks. Am J Ophthalmol. 1993; 116(1):72-8. https://doi.org/10.1016/S0002-9394(14)71747-7

15. Weizer JS, et al. Bleb morphology characteristics and effect on positional intraocular pressure variation. Ophthalmic Surg Lasers Imaging. 2010; 41(5):532-7. https://doi.org/10.3928/15428877-20100726-06 PMid:20795573

ID Design Press, Skopje, Republic of Macedonia
Open Access Macedonian Journal of Medical Sciences. 2019 Dec 30; 7(24):4283-4286.
https://doi.org/10.3889/oamjms.2019.375
eISSN: 1857-9655
Basic and Clinical Medical Researches in Vietnam

Ocular Biometrics of Vietnamese Young Adults with Myopia

Hien Thi Thu Nguyen[1], Dung Thi Thanh Nguyen[2], Dong Ngoc Pham[1], Anh Phuong Tran[1], Do Quyet[3], Than Van Thai[3], Vu Thi Nga[4], Nguyen Duy Bac[5*]

[1]Division of Refraction, Vietnam National Institute of Ophthalmology, Hanoi, Vietnam; [2]Department of Ophthalmology, Thai Nguyen Medical University, Thai Nguyen, Vietnam; [3]NTT Hi-tech Institute, Nguyen Tat Thanh University, Ho Chi Minh City, Vietnam; [4]Institute for Research and Development, Duy Tan University, 03 Quang Trung, Danang, Vietnam; [5]Vietnam Military Medical University (VMMU), Hanoi, Vietnam

Citation: Thi Thu Nguyen H, Nguyen DTT, Ngoc Pham D, Tran AP, Quyet D, Thai TV, Nga VT, Bac ND. Ocular Biometrics of Vietnamese Young Adults with Myopia. Open Access Maced J Med Sci. 2019 Dec 30; 7(24):4283-4286.
https://doi.org/10.3889/oamjms.2019.375

Keywords: Myopia; Axial length; Central cornea thickness; Cornea refraction; Anterior chamber depth; Spherical equivalent refraction

***Correspondence:** Nguyen Duy Bac. Vietnam Military Medical University (VMMU), Hanoi, Vietnam. E-mail: nguyenduybac@vmmu.edu.vn

Received: 02-Jul-2019; **Revised:** 20-Nov-2019; **Accepted:** 21-Nov-2019; **Online first:** 20-Dec-2019

Funding: This research did not receive any financial support

Competing Interests: The authors have declared that no competing interests exist

Abstract

BACKGROUND: Myopia is most prevalent type of refraction error. In some Asian countries, the prevalence of myopia can be 80 – 90% in the population aged 17 – 18.

AIM: To analyze the correlation between ocular biometric indices and refraction status in Vietnamese young myopes.

METHODS: A prospective cross – section study was conducted in young myopes. Data on axial length, central cornea thickness, corneal topography & anterior chamber depth and spherical equivalent were collected. Independent Sample T Test and ANOVA test were used to compare between groups. The correlations between ocular biometry and myopic spherical equivalent refraction were examined by Pearson Correlation with the level of significance $p < 0.05$.

RESULTS: Totally, 418 eyes from 209 patients were recruited. The average axial length, central cornea thickness, cornea refraction & anterior chamber depth were 25.68 ± 1.09 mm, 539.78 ± 32.665 μm, 43.16 ± 1.369 D, 3.30 ± 0.243 mm, respectively. The correlation between axial length and spherical equivalent refraction (SER) was high ($r = - 0.742$, $p < 0.0001$) while those between central cornea thickness and cornea refraction were negligible ($r = - 0.107$, $p = 0.029$; $r = -0.123$, $p = 0.012$; respectively). There was no correlation between anterior chamber depth and spherical equivalent refraction ($r = 0.019$, $p = 0.697$).

CONCLUSION: Among ocular biometric indices, axial length was significantly correlated with spherical equivalent of young adult patients.

Introduction

Refraction error is one among leading preventable blindness causes all over the world [1]. In "VISION 2020: The Right to Sight: A Global Initiative to Eliminate Avoidable Blindness", according to World Health Organization, refraction errors ranks among top five avoidable blindness causes globally [2]. Myopia is most prevalent type of refraction error, and it is anticipated that myopia will account for 50% of the world population by 2050 [3]. In some Asian countries, the prevalence of myopia can be 80 – 90% in the population aged 17 – 18 [4].

Ocular biometric indices including axial length (AL), anterior chamber depth (ACD), central cornea thickness (CCT) and cornea refraction (CR) are crucial in evaluating and treating myopia. There have had some studies concerning the correlation between these indices and the refraction status [5], [6]. However, ocular biometry can vary among ethnic groups [7], [8], [9], which may make an impact on this relation. For understanding of ocular biometry in Asia and around the world, we conducted this study to examine the correlation between ocular biometric indices and the refraction status in a Vietnamese young population with myopia.

Materials and Methods

This was a prospective cross – section study carried out in DND International Eye Hospital from October, 2016 to September, 2017. In the current

study, we recruited 418 eyes from 209 participants aged from 18 to 30 and diagnosed with myopia (> 0.5 D). Myopia severity was classified in three stages: low (> 3D), moderate (3D - 6D) and high (> 6D) [10]. Patients with any anterior or posterior segments abnormalities, ocular motility disorders and lid diseases were excluded from the study.

Each patient underwent a through history taking and comprehensive examination process. Auto-refraction measurement (Nidek autorefractor), Cyclogyl 1% retinoscopy and subjective refraction assessment were performed by qualified refractionists. Slit – lamp, fundus examination and B – ultrasound investigation were carried out by registered ophthalmologists to rule out any ocular diseases. IOL master 500 from Zeiss and SCHWIND Sirius - Topography with Scheimpflug camera were employed to evaluate the AL ACD, CCT and CR.

Independent Sample T Test and ANOVA test were used to compare means of groups. Pearson correlation was applied to analyze the correlation between AL, ACD, CCT and CRand myopic spherical equivalent refraction (level of significance, $p < 0.05$). Data was analyzed by SPSS version 20.0.

Results

We recruited 418 eyes from 209 patients for the current study. Table 1 gives information on some main features of the study population. The majority of participants were female (56%). 77% of patients were in the 18 – 23 age group (undergraduated). The number of patients with moderate myopia accounted for 58.1 % of the study population (58.1%). Nearly 95% of participants had used spectacles before whereas approximately 15% of them worn soft contact lens.

Table 1: Demographic characteristics of study population

Charateristics	Mean ± Standard deviation
No. Gender (men/women)	92 / 117
Age	21.33 ± 3.196
No. Age group (18 – 23 / 24 – 30)	161 / 48
SER	- 4.85 ± 1.99
No. Myopia severity (low / moderate / high)	82 / 243 / 93
No. Treatment (spectacle / soft contact lens / none)	198 / 32 / 11

Table 2 shows the calculation of different ocular biometric indices by myopia classification. The average AL, CCT, CR and ACD were 25.68 ± 1.09 mm, 539.78 ± 32.665 µm, 43.16 ± 1.369D and 3.30 ± 0.243 mm, respectively. The AL of low myopia group was significantly shorter than that of moderate group ($p < 0.0001$), and the AL of high group was significantly higher than that of moderate group ($p < 0.0001$). Central cornea of low myopia group was significantly thinner than that of the moderate group ($p < 0.05$). CR of the group with low myopia was significantly higher than that of the high myopia group ($p < 0.05$). There was no difference among three groups in terms of ACD ($p > 0.05$).

Table 2: Ocular biometric indices and myopia classification

Index	Myopia severity		
	Low n = 82	Moderate n = 243	High n = 93
AL	24,61 ± 0,85 mm	25,63 ± 0.78 mm	26,79 ± 0,93 mm
CCT	530,24 ± 35,56 µm	541,76 ± 32,30 µm	539,78 ± 32,67 µm
CR	43.46 ± 1.51 D	43.15 ± 1.38 D	42,93 ± 1.15 D
ACD	3.34 ± 0.27 mm	3.29 ± 0.22 mm	3.31 ± 0.28 mm

The correlation between myopic SER and a variety of ocular biometric indices was studied (Figure 1). There was a significant correlation between the refraction status and AL ($r = - 0.742$, $p < 0.001$), which implies the equation SER = - 1.358 * AL + 30.042. The correlation between the refraction status and CCT & CR was negligible ($r = -0.107$, $p < 0.05$; $r = 0.123$, $p < 0.05$; respectively) while there was no correlation between the refraction status and ACD ($r = 0.019$, $p > 0.05$) (Figure 1).

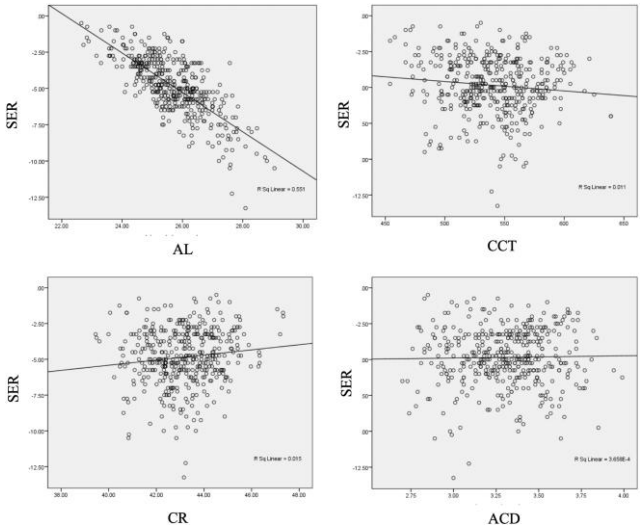

Figure 1: The correlation between ocular biometric indices and refraction status

Table 3 gives information about the correlation between myopic SER and the ocular biometry by myopia classification. AL significantly correlated with the refraction status across all stages of myopia. CCT only significantly correlated with the refraction status in the group with low myopia. There was no significant correlation between the refraction status and remains.

Table 3: The correlation between the ocular biometry and myopia severity

Myopia severity	Low n = 82	Moderate n = 243	High n = 93
SER & AL	r = - 0.380 p = 0.000	r = - 0.428 p = 0.000	r = - 0.595 p = 0.000
SER & CCT	r = -0.240 p = 0.030	r = 0.019 p = 0.770	r = 0.116 p = 0.226
SER & CR	r = 0.006 p = 0.960	r = 0.001 p = 0.987	r = 0.129 p = 0.218
SER & ACD	r = - 0.189 p = 0.090	r = - 0.063 p = 0.329	r = 0.120 p = 0.250

Discussion

The current study examined the correlation between ocular biometric indices and the refraction status. To the best of our knowledge, the present study provides the first comprehensive assessment of the ocular biometry in Vietnamese young patients with myopia.

In this study, we found that the average AL was 25.68 ± 1.09 mm, which was similar to other studies in myopic population. [11], [12], [13]. There was the significant difference in AL among stages of myopia, and this was consistent with previous researches [12], [13], [14]. AL strongly affects the refraction status because its elongation leads to the progression of myopia. CCT in our study was 539 ± 36.74 μm, which was higher than that of Chang et al., (533 ± 29 μm) [15] and tied with those of Kadhim and Farhood [16] (543.95 ± 32.58 μm) and Kawesch (548 ± 33 μm) [17]. CCT plays a key role in the surgical plan or refractive surgeons. Any candidate without enough residual stromal bed will be eligible for other approaches such as Ortho – keratology or Phakic ICL. In the current study, CR was 43.16 ± 1.369 D, which was consistent with other authors [16, 18]. Cornea holds two – third of the refraction power of the whole eye globe; hence appropriate interventions on CR can be supportive to myopia treatment. ACD is very critical in Phakic ICL surgery for patients with high myopia or thin cornea. Phakic ICL is contraindicated in any candidates with shallow anterior chamber (ACD < 3 mm). In the present study, ACD was shorter than findings of other studies [5], [12], [19], [20].

Not surprisingly, there was the significance correlation between the refraction status and AL in general ($r = -0.742$, $p < 0.001$) and in each stage of myopia progression. This means that the higher AL is, the worse myopia gets and is consistent with other studies [6], [11], [12], [15], [21], [22]. Some researches indicated that AL ≥ 26.5 mm was a risk factor of pathological changes in myopia such as lattice degeneration, retinal detachment, choroidal neovascularization, and retinal atrophy [23], [24]. Hence, because of the predictive value, identifying AL in examining myopic patients is very important to the prevention of high myopia complications.

Our result that the correlation between CCT and the refraction status was negligible ($r = - 0.107$, $p < 0.05$) was similar to that of male patients in the study of Suzuki et al., (right eye: $r = - 0.080$, $p < 0.001$; left eye: $r = -0.039$, $p = 0.036$; no correlation in female participants) [25]. This can be inferred that CCT is an independent factor and not correlated with myopic status [6], [26], [27].

Our analysis demonstrated that the correlation between CR and the refraction status was negligible ($r = 0.123$, $p < 0.05$). This was consistent with studies of Chen in 2009 [6] and Zeng in 2015 [28]. We also found no correlation between ACD and the refraction status ($r = 0.019$, $p > 0.05$) while other studies [5], [6], [21] revealed that this correlation was significant.

There are certain strong and weak points of our study. The time for data collection was limited, so we could not increase the sample size. However, we used modern equipment with cutting – edge technologies; hence, our findings were reliable.

In conclusion, among 4 ocular biometric indices examined, AL significantly correlated with myopia status. This factor plays a vital role in the diagnosis, management and prediction of myopia.

Ethics Approval

This prospective study strictly obeys the tenets of Declaration of Helsinki and was approved by Hanoi Medical University Ethics Committee.

Informed Consent

Informed consents were collected from participating patient(s) for their anonymized information to be reported in the study.

References

1. Flaxman SR, et al. Global causes of blindness and distance vision impairment 1990-2020: a systematic review and meta-analysis. Lancet Glob Health. 2017; 5(12):e1221-e1234.

2. Pizzarello L, et al. VISION 2020: The Right to Sight: A Global Initiative to Eliminate Avoidable Blindness. Archives of Ophthalmology. 2004; 122(4):615-620. https://doi.org/10.1001/archopht.122.4.615 PMid:15078680

3. Holden BA, et al. Global Prevalence of Myopia and High Myopia and Temporal Trends from 2000 through 2050. Ophthalmology. 2016; 123(5):1036-1042. https://doi.org/10.1016/j.ophtha.2016.01.006 PMid:26875007

4. Dayan YB, et al. The Changing Prevalence of Myopia in Young Adults: A 13-Year Series of Population-Based Prevalence Surveys. Investigative Ophthalmology & Visual Science. 2005; 46(8):2760-2765. https://doi.org/10.1167/iovs.04-0260 PMid:16043848

5. Hosny M, Alió JL, Claramonte P, Attia WH, Pérez-Santonja JJ. Relationship between anterior chamber depth, refractive state, corneal diameter, and axial length. Journal of Refractive Surgery. 2000; 16(3):336-40.

6. Chen MJ, et al. Relationship between central corneal thickness, refractive error, corneal curvature, anterior chamber depth and axial length. Journal of the Chinese Medical Association. 2009; 72(3):133-137. https://doi.org/10.1016/S1726-4901(09)70038-3

7. Ip JM, et al. Ethnic differences in refraction and ocular biometry in a population-based sample of 11-15-year-old Australian children. Eye. 2008. 22(5):649-56. https://doi.org/10.1038/sj.eye.6702701 PMid:17277756

8. Chua J, et al. Ethnic differences of intraocular pressure and central corneal thickness: the Singapore Epidemiology of Eye Diseases study. Ophthalmology. 2014; 121(10):2013-2022. https://doi.org/10.1016/j.ophtha.2014.04.041 PMid:24950592

9. Wang, D., et al., Ethnic differences in lens parameters measured by ocular biometry in a cataract surgery population. PloS one. 2017; 12(6):e0179836-e0179836. https://doi.org/10.1371/journal.pone.0179836 PMid:28654694 PMCid:PMC5487046

10. Flitcroft DI, et al. IMI - Defining and Classifying Myopia: A Proposed Set of Standards for Clinical and Epidemiologic Studies. Invest Ophthalmol Vis Sci. 2019; 60(3):M20-m30. https://doi.org/10.1167/iovs.18-25957 PMid:30817826 PMCid:PMC6735818

11. Llorente L, et al. Myopic versus hyperopic eyes: axial length, corneal shape and optical aberrations. Journal of Vision. 2004; 4(4):5-5. https://doi.org/10.1167/4.4.5 PMid:15134476

12. Carney LG, Mainstone JC, Henderson BA. Corneal topography and myopia. A cross-sectional study. Investigative Ophthalmology & Visual Science. 1997; 38(2):311-320.

13. Tekiele BC, Semes L. The relationship among axial length, corneal curvature, and ocular fundus changes at the posterior pole and in the peripheral retina. Optometry (St. Louis, Mo.). 2002; 73(4):231-6.

14. Cegarra MJ, et al. Consolidating the anatomical relationship between ocular axial length and spherical equivalent refraction. European Journal of anatomy. 2014; 5(3):145-150.

15. Chang SW, et al. The cornea in young myopic adults. The British Journal of Ophthalmology. 2001; 85(8):916-920. https://doi.org/10.1136/bjo.85.8.916 PMid:11466244 PMCid:PMC1724084

16. Kadhim YJ, Farhood QK. Central corneal thickness of Iraqi population in relation to age, gender, refractive errors, and corneal curvature: a hospital-based cross-sectional study. Clinical Ophthalmology (Auckland, N.Z.). 2016; 10:2369-2376. https://doi.org/10.2147/OPTH.S116743 PMid:27932859 PMCid:PMC5135410

17. Kawesch GM, Kezirian GM. Laser in situ keratomileusis for high myopia with the VISX star laser. Ophthalmology. 2000; 107(4):653-61. https://doi.org/10.1016/S0161-6420(99)00148-7

18. Baradaran-Rafii A, et al. Accuracy of Different Topographic Instruments in Calculating Corneal Power after Myopic Photorefractive Keratectomy. Journal of Ophthalmic & Vision Research. 2017; 12(3):254-259. https://doi.org/10.4103/jovr.jovr_74_16 PMid:28791056

19. McBrien NA, Adams DW. A longitudinal investigation of adult-onset and adult-progression of myopia in an occupational group. Refractive and biometric findings. Investigative ophthalmology & visual science. 1997; 38(2):321-33.

20. Hashemi H, et al. Anterior Chamber Depth Measurement With A-Scan Ultrasonography, Orbscan II, and IOLMaster. Optometry and Vision Science. 2005; 82(10):900-904.

21. Touzeau O, et al. Correlation between refraction and ocular biometry. Journal francais d'ophtalmologie. 2003; 26(4):355-363.

22. Olsen T, et al. On the ocular refractive components: the Reykjavik Eye Study. Acta Ophthalmologica Scandinavica. 2007; 85(4):361-366. https://doi.org/10.1111/j.1600-0420.2006.00847.x PMid:17286626

23. Xu L, et al. Definition of high myopia by parapapillary atrophy. The Beijing Eye Study. Acta Ophthalmol. 2010; 88(8):e350-1. https://doi.org/10.1111/j.1755-3768.2009.01770.x PMid:19900199

24. Jonas JB, Xu L. Histological changes of high axial myopia. Eye (London, England). 2014; 28(2):113-117. https://doi.org/10.1038/eye.2013.223 PMid:24113300 PMCid:PMC3930258

25. Suzuki S, et al. Corneal Thickness in an Ophthalmologically Normal Japanese Population. Ophthalmology. 2005; 112(8):1327-1336. https://doi.org/10.1016/j.ophtha.2005.03.022 PMid:15964631

26. Ortiz S, et al. Relationships between central and peripheral corneal thickness in different degrees of myopia. Journal of Optometry. 2014; 7(1):44-50. https://doi.org/10.1016/j.optom.2013.03.005 PMid:24646900 PMCid:PMC3938742

27. Fam HB, et al. Central corneal thickness and its relationship to myopia in Chinese adults. Br J Ophthalmol. 2006; 90(12):1451-3. https://doi.org/10.1136/bjo.2006.101170 PMid:16916878 PMCid:PMC1857527

28. Zeng J, et al. Correlation of axial length and corneal curvature with diopter in eyes of adults with anisometropia. International Journal of Clinical and Experimental Medicine. 2015; 8(8):13639-13643.

ID Design Press, Skopje, Republic of Macedonia
Open Access Macedonian Journal of Medical Sciences. 2019 Dec 30; 7(24):4287-4291.
https://doi.org/10.3889/oamjms.2019.376
eISSN: 1857-9655
Basic and Clinical Medical Researches in Vietnam

Penetrating Keratoplasty for Keratoconus in Vietnamese Patients

Le Xuan Cung[1], Duong Mai Nga[1], Nguyen Dinh Ngan[2], Nguyen Xuan Hiep[1], Do Quyet[2], Than Van Thai[3], Vu Thi Nga[4], Toi Chu Dinh[5], Nguyen Duy Bac[2*]

[1]Vietnam National Institute of Ophthalmology, Hanoi, Vietnam; [2]Vietnam Military Medical University (VMMU), Hanoi, Vietnam; [3]NTT Hi-tech Institute, Nguyen Tat Thanh University, Ho Chi Minh City, Vietnam; [4]Institute for Research and Development, Duy Tan University, 03 Quang Trung, Danang, Vietnam; [5]Department of Human and Animal Physiology, Faculty of Biology, Hanoi National University of Education, Hanoi, Vietnam

Citation: Cung LX, Nga DM, Ngan ND, Hiep NX, Quyet D, Thai TV, Nga VT, Dinh TC, Bac ND. Penetrating Keratoplasty for Keratoconus in Vietnamese Patients. Open Access Maced J Med Sci. 2019 Dec 30; 7(24):4287-4291.
https://doi.org/10.3889/oamjms.2019.376

Keywords: Keratoconus; Penetrating keratoplasty; Donor-recipient disparity

***Correspondence:** Nguyen Duy Bac. 108 Military Central Hospital, 1 Tran Hung Dao, Hai Ba Trung, Ha Noi, Vietnam. E-mail: nguyenduybac@vmmu.edu.vn

Received: 02-Jul-2019; **Revised:** 20-Nov-2019; **Accepted:** 21-Nov-2019; **Online first:** 20-Dec-2019

Funding: This research did not receive any financial support

Competing Interests: The authors have declared that no competing interests exist

Abstract

BACKGROUND: Keratoconus is an ectatic corneal disorder that can impair the visual acuity. Up to now, penetrating keratoplasty (PK) remains the most common surgical procedure to treat severe keratoconus. In Vietnam, most keratoconus patients come to visit doctor at severe stage and were treated by PK, so we conduct this study.

AIM: To evaluate the results of PK for keratoconus in Vietnamese patients.

METHODS: This was a retrospective study of 31 eyes with keratoconus who underwent PK in VNIO from January 2005 to December 2014.

RESULTS: The average visual acuity was 0.86 ± 0.37 logMAR (20/145). In the group of patients without amblyopia, best spectacle-corrected visual acuity of 20/60 or better was recorded in 75.9% of eyes and 93.1% of eyes achieved a best corrected visual acuity with hard contact lenses of 20/40 or better. Mean postoperative corneal power was 43.8 ± 4.5D. Mean corneal astigmatism was 5.9 ± 2.7D. 94.6% of grafts remained clear. Posterior subcapsular cataract developed in 22.6% of eyes. Graft rejection was recognized in 12.9% of eyes.

CONCLUSION: PK is an effective procedure with high rate of graft survival for keratoconus patients. However, patients should be aware of the necessary of optical correction to gain the best VA after surgery.

Introduction

Keratoconus is a noninflammatory ectatic corneal disorder characterized by localized cornical protrusion owing to thinning of the corneal stroma. This condition can lead to high myopia, irregular astigmatism, and impairment of visual acuity (VA) [1]. The treatment of keratoconus depends on its severity, including spectacle, contact lens, intracorneal rings, collagen cross-linking and keratoplasty [2]. In recent years, deep anterior lamellar keratoplasty (DALK) has been selected to treat this disease as an alternative to PK by some surgeons [3], [4]. However, DALK is a difficult and long-time surgery, especially in patients with acute hydrops or corneal scar. Therefore, PK remains the most popular surgical procedure in the severe stage.

About 10-20% of keratoconus patients require PK for corneal scar, contact lens intolerance, or unsatisfaction with best-corrected visual acuity (BCVA) [1], [5]. Previous studies have noted that keratoconus is one of the common indications for corneal transplantation all over the world. The successful rate of PK for keratoconus is higher than other diseases. After 5 to 12 years, the graft survival rate is more than 90% [6], [7], [8].

In Vietnam, keratoconus is a rare disease and was well described in 2014 [9]. PK has been performed to treat patients with advanced keratoconus over the past fifteen years. This condition accounts for 1.4% of all PK operations [10]. This study was conducted to evaluate the outcomes of PK in Vietnamese patients with keratoconus.

Materials and Methods

All keratoconus patients who underwent PK at Vietnam National Institute of Ophthalmology (VNIO) between January 2005 and December 2014 were enrolled in this retrospective study.

PK surgeries were done under general anaesthesia. We used hand-held trephine to punch in the corneas. The host diameter ranged from 7.0 to 8.0 mm, and the donor diameter was same-size or 0.5 mm larger. The PK technique was 16-bite interrupted suture or a combined 8-bite interrupted suture and a 16-bite running suture. Postoperative treatment consisted of topical antibiotic and steroids 4 times per day. Steroids were tapered after one month and discontinued after 1 year.

Medical records were reviewed for demographic data, pre-and postoperative VA, keratometry, ocular conditions and general diseases associated with keratoconus, surgical technique, intraoperative and postporative complications such as graft rejection episodes, infection, trauma, and the requirement of glaucoma surgery or cataract surgery. After that, patients were recalled for the last follow-up examination. Patients who did not come for the last examination were excluded.

At the last follow-up examination, VA, BSCVA, and BCVA with hard contact lens were noted. The Icare tonometer was utilized to mesure the intraocular pressure. Patients were examined on the slit lamp to evaluate the graft clarity and other ocular conditions. Corneal topography was measured with the OPD-Scan III topographer. Two topographic indices were calculated and registered: average K-value and corneal astigmatism.

Statistical analysis

SPSS 16.0 was utilized to analysed the data. Chi-square test was applied to compare the difference of grouping variables. Fisher's exact test was the alternative algorithm to Chi-square test when the number of data was small. We used t-test to compare continous variables.

Results

From January 2005 to December 2014, there were 31 eyes of 28 keratoconus patients underwent PK. Mean age at the time of surgery was 20.4 ± 8.4 (range 8-58 yrs). There were 24 males (85.7%) and 4 females (14.3%) ($p < 0.001$). Preoperative VA of all patients was less than 20/200. Of all 31 eyes, 28 eyes (90.3%) had the VA less than count finger (CF) 3 m. Indications for PK involved corneal scar (54.8%), corneal hydrops (25.8%), unsatisfactory best corrected visual acuity (19.4%).

Recipient trephine size ranged from 7.0 to 8.0 mm. The most common host diameter was 7.0 mm (15 eyes). Donor-recipient disparity was 0.5 mm in 17 eyes (54,8%) and 0 mm in 14 eyes (45.2%). Suture technique was interrupted sutures in 28 eyes (90.3%) and combined sutures in 3 eyes (9.7%).

Visual Outcome

Of all 31 eyes, 2 eyes had amblyopia with the BCVA less than 20/200. The first patient was diagnosed keratoconus at the age of 2 years and underwent PK at 8 years old. His post-op BCVA was 20/160. The second patient had congenital cataract combined with nystagmus. He had undergone ECCE combined with IOL implantation 6 years before PK. At the last examination, the VA was CF 2.5 m and didn't improve with pinhole. In the group of 29 eyes without amblyopia, mean UCVA and BSCVA at the last examination was 0.86 ± 0.37 logMAR (20/145) and 0.43 ± 0.18 logMAR (20/54) ($p = 0.024$), respectively. Hard contact lenses were fitted in 27 eyes, and the average BCVA was 0.09 ± 0.1 (20/25).

Table 1: Visual outcome at the last visit

VA		UCVA	BSCVA	BCVA with HCL*
< CF 3m	n	2	0	0
	%	6.9	0	0
CF 3m - < 20/200	n	5	0	0
	%	17.2	0	0
20/200 - < 20/60	n	15	7	0
	%	51.7	24.1	0
20/60 - < 20/40	n	7	12	0
	%	24.1	41.4	0
≥ 20/40	n	0	10	27
	%	0	34.5	93.1
Total	n	29	29	29

*BCVA with HCL was not performed in 2 eyes of the non-amblyopia group, including 1 eye had corneal scar and 1 eye was being performed suture removal.

Table 1 show that the majority of patients had UCVA ranged from 20/200 to 20/60 (51.7%). Mean BSCVA at the final follow-up was at least 20/60 in 75.9% of the group without amblyopia. BCVA with hard contact lens of 20/40 or better was recorded in 27 eyes (93.1%) of this group including 14 eyes had BCVA of 20/25 or better.

Refractive outcome

Corneal topography could not be measured in 2 eyes due to nystagmus and corneal scar. Mean keratometry of the remaining 29 eyes at the last visit was 43.8 ± 4.5D (range 32-52.25D). Of 29 eyes, 51.7% (15 eyes) had the keratometry in the normal range (40-44D). Corneal astigmatism was high with the average result of 5.9D (SD 2.7D, range 1-11.5D), and overall, 75.9% (22 eyes) had the corneal astigmatism more than 4D. There were 2 eyes had corneal astigmatism more than 10D. There were only 3

eyes (10.3%) had corneal astigmatism less than 2D.

Graft survival outcome

The rate of clear graft after PK was very high. A total of 94.6% (29 of 31 grafts) of the examined eyes had a clear graft. 1 eye had opaque graft after PK 43 months. 1 eye had corneal scar due to keratitis 1 month postoperatively.

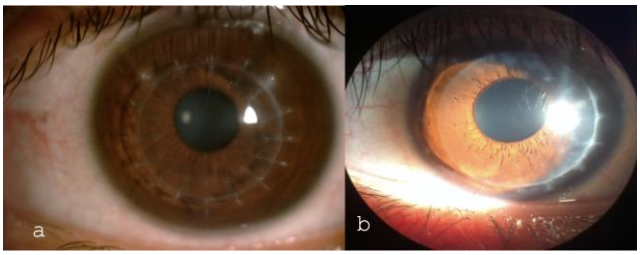

Figure 1: Clear grafts after PK (a.8.8yrs; b.27months)

Complications

Graft rejection was recorded in 4 eyes (12.9%). However, there was no case of graft rejection cause graft failure. Secondary glaucoma occurred in 2 eyes (6.5%) due to prolonged topical corticosteroid therapy to treat graft rejection.

Table 2: Complications after PK

Complication	n	Percentage (%)
Loose suture	9	29.0
Corneal neovascularization	8	25.8
Posterior subcapsular cataract	7	22.6
Graft rejection	4	12.9
Secondary glaucoma	2	6.5
Keratitis	1	3.2

Of the 2 glaucoma eyes, 1 eye required trabeculetomy 10 months after PK because the IOP had not been controlled by 4 types of topical antiglaucoma eyedrops. There was 1 eye developed bacterial keratitis on the graft 1 month postoperatively, leading to graft failure due to corneal scar.

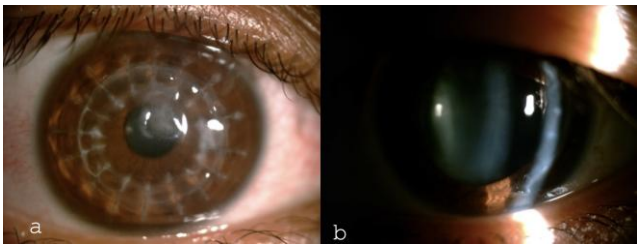

Figure 2: Complications after PK; A) Corneal scar; B) Posterior subcapsular cataract

Discussion

Keratoconus is a progressive disease characterized by paracentral or central thinning, and ectasia of the cornea. This disease often appears in the second decade of life and progresses at a variable rate. It causes severe myopia and irregular astigmatism. Keratoconus patients who underwent keratoplasty are very young because this disease often occurs at puberty.

In our study, most patients were male, which is similar to the results of some other authors [11], [12], [13]. The recent studies indicate that keratoconus is more common in men than women due to the combination of this disease and vernal conjunctivitis, a common disease in men [14]. Furthermore, this disease also progresses faster in men [15]. These findings contribute to explain that male patients tend to have to undergo keratoplasty than women.

Corneal scar was the leading indication for keratoplasty in our study, which account for the proportion of 54.8%. However, the main indication of surgery in Lim's study was contact lens intolerance (51.6%) [8]. The indications for PK in patients with keratoconus vary greatly in different studies. In Vietnam, almost keratoconus patients were discovered in severe stage, and most of them have corneal scars [9]. Therefore, they could not be treated by hard contact lens, collagen cross-linking or intrastromal ring implantation. Penetrating keratoplasty was a good treatment for them.

Postoperative VA is the most important criteria when assessing the success of PK in terms of eye function. Before surgery, almost patients had VA less than CF 1 m. The average VA was 1.94 ± 0.14 logMAR. Postoperatively, the patients' VA was improved significantly. The average UCVA was 0.86 ± 0.37 logMAR (20/145). The BCVA with hard contact lens of 29 eyes without amblyopia in our study was 20/27. This result is similar to the results of previous studies, with the BCVA ranged from 20/25 to 20/32 [7], [8], [11], [13].

For patients with PK, postoperative corneal astigmatism is still a big problem to overcome. Although the postoperative VA is improved significantly, most patients need to wear glasses or hard contact lens to gain the best VA. Wearing a hard contact lens is a non-surgical method, which is often selected to help patients achieve good VA after keratoplasty. It helps to correct corneal astigmatism and refractive deflection. In our study, the BSCVA of 22 non-amblyopia eyes (75.9%) was at least 20/60. 93.1% (27 eyes) of the non-amblyopia group had the BCVA of 20/40 or better with hard contact lens, including 14 eyes had BCVA of 20/25 or better.

Preoperative corneal refraction could not be measured in 26 eyes due to corneal scars, corneal hydrops and over-refraction. After surgery, there were

29 eyes which could be measured corneal topography with the average keratometry of 43.8 ± 4.5 D (range 32-52.25 D). Similar results were found in some previous studies [11], [16]. We could not measure topography in one eye with nystagmus and one eye with corneal scar.

With an average postoperative follow-up of 49.5 months, the rate of clear grafts was 94.6%. PK remains the main surgical procedure to treat severe keratoconus. The result of the other studies has shown that this is a high successful treatment method with the rate of clear grafts is about 95% after 2-5 years [8], [11], [17]. Although the cause of graft failure varies in different studies, the overall survival rate of the graft is still very high because the surgery is performed on the eye without inflammation and neo-vessel. In our study, the rate of graft rejection was 12.9% (4 eyes). Some studies of other authors shown the same result, which had the rate of graft rejection ranging from 4.3-31% [6], [18], [19], [20]. However, all cases of graft rejection were detected and treated promptly with topical and oral corticosteroids, so none of them led to graft failure.

In conclusion, keratoconus is a rare corneal degeneration that causes severe visual impairment. It usually occurs in young patients. In the severe stage, patients with keratoconus will require keratoplasty. PK is indicated for not only optical purpose for restoring VA, but also tectonic purpose for restoring the corneal integrity in terms of corneal thickness and shape. Patients with keratoconus can achieve good VA and a high rate of survival graft postoperatively. We propose that PK should be indicated in keratoconus patients with corneal scars. In some developing countries where advanced techniques as DALK or intracorneal ring implantation are not available, PK also should be considered in patients who have poor vision with spectacles or contact lens intolerance. However, some patients need to wear spectacles or hard contact lens to gain the best VA after PK.

Acknowledgement

We would like to acknowledge the support of all colleagues from Cornea Department and other colleagues from Vietnam National Institute of Ophthalmology.

Ethics in Research

Research subjects voluntarily participate in the research, patients' information is confidentiality. Research is only contributed to the vision of patients. Research subjects have the right to end the study at any time.

Informed Consent

All patients agreed and signed an informed consent form before surgeries.

References

1. Rabinowitz YS. Keratoconus. Survey of Ophthalmology. 1998; 42(4):297-319. https://doi.org/10.1016/S0039-6257(97)00119-7

2. Vazirani J, Basu S, Keratoconus: current perspective. Clinical Ophthalmology. 2013; 7:2019-30. https://doi.org/10.2147/OPTH.S50119 PMid:24143069 PMCid:PMC3798205

3. Kubaloglu A, Sari ES, Unal M. Long-term results of deep anterior lamellar keratoplasty for the treatment of keratoconus. Am J Ophthalmol. 2011; 151(5):760-767. https://doi.org/10.1016/j.ajo.2010.11.020 PMid:21333267

4. MacIntyre R, et al. Long-term outcomes of deep anterior lamellar keratoplasty versus penetrating keratoplasty in Australian keratoconus patients. Cornea. 2014; 33(1):6-9. https://doi.org/10.1097/ICO.0b013e3182a9fbfd PMid:24270676

5. Lass, JH, et al. Clinical management of keratoconus. A multicenter analysis. Ophthalmology. 1990; 97(4):433-45. https://doi.org/10.1016/S0161-6420(90)32569-1

6. Niziol LM, et al. Long-term outcomes in patients who received a corneal graft for keratoconus between 1980 and 1986. Am J Ophthalmol. 2013; 155(2):213-219. https://doi.org/10.1016/j.ajo.2012.08.001 PMid:23111176

7. Al-Mohaimeed MM. Penetrating Keratoplasty for Keratoconua: Visual and Graft Survival Outcomes. International Journal of Health Sciences. 2013; 7(1):58-63. https://doi.org/10.12816/0006023 PMid:23559907 PMCid:PMC3612418

8. Lim L, Pesudovs K, Coster DJ. Penetrating keratoplasty for keratoconus: visual outcome and success. Ophthalmology. 2000; 107(6):1125-31. https://doi.org/10.1016/S0161-6420(00)00112-3

9. Lê Xuân Cung, T.K.M.H., Phạm Ngọc Đông,, Đặc điểm lâm sàng bệnh giác mạc hình chóp. Tạp chí Nghiên cứu Y học, 2014. 88(3):49-54.

10. Phạm Ngọc Đông, T.N.H., Lê Xuân Cung,, Đặc điểm bệnh nhân được ghép giác mạc tại Bệnh viện Mắt Trung ương trong giai đoạn 2002-2011. Tạp chí Nghiên cứu Y học, 2013. 85(5):24-30.

11. Javadi MA, et al. Outcomes of penetrating keratoplasty in keratoconus. Cornea. 2005; 24(8):941-6. https://doi.org/10.1097/01.ico.0000159730.45177.cd PMid:16227837

12. Sharif KW, Casey TA. Penetrating keratoplasty for keratoconus: complications and long-term success. Br J Ophthalmol. 1991; 75(3):142-6. https://doi.org/10.1136/bjo.75.3.142 PMid:1826453 PMCid:PMC1042291

13. Brierly SC, Izquierdo LJ, Mannis MJ. Penetrating keratoplasty for keratoconus. Cornea. 2000; 19(3):329-32. https://doi.org/10.1097/00003226-200005000-00014 PMid:10832693

14. Abu Ameerh MA, Al Refai RM, Al Bdour MD. Keratoconus

patients at Jordan University Hospital: a descriptive study. Clin Ophthalmol. 2012; 6:1895-9. https://doi.org/10.2147/OPTH.S38287 PMid:23204831 PMCid:PMC3508743

15. Fan Gaskin, et al. The Auckland keratoconus study: Identifying predictors of acute corneal hydrops in keratoconus. Clinical and Experimental Optometry. 2013; 96(2):208-213. https://doi.org/10.1111/cxo.12048 PMid:23432147

16. Troutman Richard C, Lawless Michael A. Penetrating Keratoplasty for Keratoconus. Cornea. 1987; 6(4):298-305. https://doi.org/10.1097/00003226-198706040-00013 PMid:3319412

17. Pramanik S, et al. Extended long-term outcomes of penetrating keratoplasty for keratoconus. Ophthalmology. 2006; 113(9):1633-8. https://doi.org/10.1016/j.ophtha.2006.02.058 PMid:16828503

18. Olson RJ, et al. Penetrating keratoplasty for keratoconus: a long-term review of result and complications. J Cataract Ref Surg. 2000; 26:987-91. https://doi.org/10.1016/S0886-3350(00)00430-2

19. Fukuoka S, et al. Extended long-term results of penetrating keratoplasty for keratoconus. Cornea. 2010; 29(5):528-30. https://doi.org/10.1097/ICO.0b013e3181c29705 PMid:20299971

20. Duman F, et al. Indications and Outcomes of Corneal transplantation in Geriatric Patients. Am J Ophathalmol. 2013; 156(3):600-607. https://doi.org/10.1016/j.ajo.2013.04.034 PMid:23769195

ID Design Press, Skopje, Republic of Macedonia
Open Access Macedonian Journal of Medical Sciences. 2019 Dec 30; 7(24):4292-4296.
https://doi.org/10.3889/oamjms.2019.377
eISSN: 1857-9655
Basic and Clinical Medical Researches in Vietnam

Dry Eyes Status on Des Scale and Related Factors in Outpatients at Vietnam National Institute of Ophthalmology

Bui Thi Van Anh[1], Pham Thanh Thuy[1], Nguyen Thi Bich Ngoc[1], Nguyen Thi Thu Hien[1], Pham Hai Yen[1], Do Quyet[2], Than Van Thai[3], Vu Thi Nga[4], Nguyen Duy Bac[2*]

[1]Vietnam National Institute of Ophthalmology, Hanoi, Vietnam; [2]Vietnam Military Medical University (VMMU), Hanoi, Vietnam; [3]NTT Hi-tech Institute, Nguyen Tat Thanh University, Ho Chi Minh City, Vietnam; [4]Institute for Research and Development, Duy Tan University, 03 Quang Trung, Danang, Vietnam

Citation: Anh BTV, Thuy PT, Ngoc NTB, Hien NTT, Yen PH, Quyet D, Thai TV, Nga VT, Bac ND. Dry Eyes Status on Des Scale and Related Factors in Outpatients at Vietnam National Institute of Ophthalmology. Open Access Maced J Med Sci. 2019 Dec 30; 7(24):4292-4296. https://doi.org/10.3889/oamjms.2019.377

Keywords: Dry eyes; Quality of life; OSDI, DES questionnaire

***Correspondence:** Nguyen Duy Bac. Vietnam Military Medical University (VMMU), Hanoi, Vietnam. E-mail: nguyenduybac@vmmu.edu.vn

Received: 02-Jul-2019; **Revised:** 20-Nov-2019; **Accepted:** 21-Nov-2019; **Online first:** 20-Dec-2019

Funding: This research did not receive any financial support

Competing Interests: The authors have declared that no competing interests exist

Abstract

BACKGROUND: Dry eye (DE) can effect on quality of life by pain, inability to perform certain activities that require prolonged attention (driving, reading,…) and productivity at work and finally effect to Q0L associated with DE. OSDI is scale questionnaire is created team to measure the quality of life related to ocular surface disease.

AIM: To describe the dry eye disease according to OSDI scale and related factors of this disease.

METHODS: A cross-sectional descriptive study was carried out on outpatients (≥ 16-year-old) who were examined and diagnosed with dry eyes at Vietnam National Institute Of Ophthalmology from April to July 2018. Data was collected using the OSDI questionnaire.

RESULTS: The average age of participants was 44.6 years; 80.9% of patients were female; 39.9% were identified having mild dry eye. The related factors have been identified that associated with severe dry eye, including age OR = 1.03 (95%CI: 1.01-1.05, p = 0.005), binocular good vision OR = 0.11 (95%CI: 0.05-0.23; p < 0.0001), medical history OR = 17.09 (95%CI: 2.24-130.25; p < 0.0001), chronic conjunctivitis OR = 0.36 (95%CI: 0.14-0.91; p = 0.027), refractive errors OR = 0.14 (95%CI: 0.04-0.48; p < 0.0001), Sjogren's syndrome OR = 31.13 (95%CI: 7.08-136.76; p < 0.0001).

CONCLUSION: Several related factors have been identified associated with severe dry eye, including: age, binocular good vision, medical history, chronic conjunctivitis, refractive errors, Sjogren's syndrome.

Introduction

Dry eye (DE) is an increasing public health issue which causes the discomfort and visual disturbance and which affects the quality of life, including physical, psychological and social aspects, daily activities and labor productivity.

"*Dry eye* is a multifactorial disease of the ocular surface characterized by a loss of homeostasis of the tear film, and accompanied by ocular symptoms, in which tear film instability and hyperosmolarity, ocular surface inflammation and damage, and neurosensory abnormalities play etiological roles" [1]. It is the most common ocular surface disease over the world with the prevalence from 4.4% to 50% in the older and middle-aged patients [2], [3]. In the US, it is estimated from the largest studies that dry eye can affect around 5 million people over 50 years old [4]. Many studies have shown that this disease "is a major cause of visual disturbance which can degrade the quality of daily life and affect health status" [5], [6]. On the other hand, the prevalence of DE is increasing due to the growing demands of modern life styles such as using computers, air conditioning and longevity in the last few years, which are considered as causes of dry eye. Many studies have shown that dry eye can effect on quality of life by pain, uneasy to perform certain activities that require prolonged attention (driving, reading, ...) and reducing productivity at work. Currently, therefore, the main goal of treating dry eyes is to improve eye comfort and maintain the quality of life for patients [7]. This is the main motivation for both patients and society in general and raising awareness about dry eyes in society through educational activities

In recent years, there are many questionnaires used to assess the condition of patients with dry eyes. The tools to measure QoL help

to prove scientifically about the impact of health on QoL. Some tools are widely used such as and SF-36 (Medical Outcomes Study Short Forms) and QOWBS (Quality of Well-Being Scale)… However, each of the different diseases has different characteristics, so that the questionnaire for measurement quality of life in different diseases is often developed by researchers with special tools. OSDI is the most commonly tool for frequency and severity assessment of DE in clinical. The scale consists of 12 questions divide into three categories: ocular symptoms, visual function disturbances, and environmental factors. The severity of symptoms on Likert scale is recorded on a 4-point from 1 to 4 points, the higher the score, the higher the Q_0L effect. If the frequency scale is zero, the scale score is also 0. We believe the score represents the burden of patients and is more exact to evaluate the severity of the disease [7], [8], [9].

In the world, there have been many studies on the quality of life on people with dry eye disease in different aspects. However, there are very few studies about this issue in Vietnam until now. We think that this issue is very important because it provides information related to DE in the aspect of quality of life. It also provides reccommendations for ophthalmologists to pay more attention to the complaints in patients with dry eye and enables doctors to understand the patient's needs and offer a better treatment. Therefore, we carried out this study.

Materials and methods

Patient

Subjects included 175 DE outpatients who were examined in Vietnam National Institute of Ophthalmology (VNIO) from April 2018 to July 2018.

Selection criteria: Participants included DE outpatients with the age from 16 to 72 of years. Criteria of dry eye diagnosing include: OSDI > 12 points; 2 out of 3 positive dry eye tests (BUT test ≤ 5 s, Schirmer test ≤ 5 mm, Fluorescein or Rose Bengal staning).

Exclusion criteria: Patients who do not agree to participate in the study or are unable to respond (mental patients, language problems).

Research design

A cross-sectional descriptive study was conducted. Data were collected by direct interview with patients using OSDI questionaires. OSDI (Ocular surface Disease Index) questionaire was used to evaluate and diagnose dry eye status. The questions in scale were grouped into 3 groups: ocular symptoms (Eyes that are sensitive to ligh, Eyes that feel gritty, Painful or sore eyes, Blurred vision, Poor vision), visual disturbance (reading, driving at night, working with a computer or banking machine (ATM), watching TV), and environmental factors (windy condition, Places or areas with low humidity (very dry), Areas that are air conditioned). OSDI score was calculated and classified into Normal: (0-12 points); Mild (13-22 points); Moderate (23-32 points); Severe (33-100 points) (Figure 1) [7].

OSDI (Ocular Surface Disease Index)

Patient name: **Date of birth:** **Patient ID:**

Have you experienced any of the following during the last week?

	All of the time	Most of the time	Half of the time	Some of the time	None of the time	
1. Eyes that are sensitive to light?	☐	☐	☐	☐	☐	
2. Eyes that feel gritty?	☐	☐	☐	☐	☐	
3. Painful or sore eyes?	☐	☐	☐	☐	☐	
4. Blurred vision?	☐	☐	☐	☐	☐	
5. Poor vision?	☐	☐	☐	☐	☐	

Have you problems with your eyes limited you in performance any of the following during the last week?

	All of the time	Most of the time	Half of the time	Some of the time	None of the time	No Answer
6. Reading?	☐	☐	☐	☐	☐	☐
7. Driving at night?	☐	☐	☐	☐	☐	☐
8. Working with a computer or bank machine (ATM)?	☐	☐	☐	☐	☐	☐
9. Watching TV?	☐	☐	☐	☐	☐	☐

Have your eyes felt uncomfortable in any of the following situations during last week?

	All of the time	Most of the time	Half of the time	Some of the time	None of the time	No Answer
10. Windy conditions?	☐	☐	☐	☐	☐	☐
11. Places or areas with low humidity (very dry)?	☐	☐	☐	☐	☐	☐
12. Areas that are air conditioned?	☐	☐	☐	☐	☐	☐

Figure 1: https://www.collinsoptometrists.com.au/wp-content/uploads/2016/01/OSDI-questionaire.pdf; Data entry and analysis using Epidata 3.0 and SPSS 16.0

Results

General information of research subjects

The study was conducted on 178 subjects and the average age of participants was 44.6 years, standard deviation was 14.65 years with a range between 16 and 72 years of age.

A number of demographic information was collected in our study including educational level, ethnic, occupation, geography and monthly average income. The majority of subjects have professional education of high school or lower (61.8%); 98.3% of subjects were Kinh people. The occupation of the subjects was distributed unevenly: the highest proportion in the farmer group (37.6%), followed by the office staff (25.3%); other occupations (19.7%), business (13.5%) and lowest proportion in worker group (3.9%). There was no stastically significant difference between geography groups. The majority of

research subjects had monthly average income per capita less than 5 million VND (63.5%).

Table 1: Social – demographic information (n = 178)

Characteristics		Number (n)	Proportion (%)
Age	16-39	62	38.4
	40-59	78	43.7
	≥ 60	38	21.3
Sex	Male	34	19.1
	Female	144	80.9
Highest professional/ educational level	Secondary school	14	7.9
	High school	96	53.9
	College	28	15.7
	University	36	20.2
	Postgraduate	4	2.2
Ethnic	Kinh	175	98.3
	Others	3	1.7
Ocupation	Officer	45	25.3
	Worker	7	3.9
	Farmer	67	37.6
	Business	24	13.5
	Others	35	19.7
Geography	Rural	89	50
	Mountain region	01	0.6
	Urban	88	49.4
Monthly average income per capita	< 5 millions VND	113	63.5
	≥ 5 million VND	65	36.5

In our study, the majority of patients had good visual acuity with pinhole or glasses (50% of right eyes and 52.2% of left eyes), followed by morderate vision (25.8% of right eyes and 27.5% of left eyes) and low and blind vision (24.2% of right eyes and 20.3% of left eyes).

Characteristic of medical history

Among 178 of research subjects, 87.6% had at least one type of medical history Types of medical history included arthritis (30.3%), allergic diseases (25.8%), Sjogrens's syndrome (20.5%), chronic conjunctivitis (17.4%), refractive errors (15.5%), hypertension (5.2%), diabetes (1.3%) and other autoimmune diseases (1.9%), (Table 2).

Table 2: Medical history of patients (n = 178)

Medical history		Number (n)	Proportion (%)
Medical history	Yes	156	87.6
	No	22	12.4
Chronic conjunctivitis	Yes	27	17.4
	No	128	82.6
Refractive error	Yes	24	15.5
	No	131	84.5
Allergic diseases	Yes	40	25.8
	No	115	74.2
Diabetes	Yes	2	1.3
	No	152	98.7
Hypertension	Yes	8	5.2
	No	147	94.8
Sjogren's syndrome	Yes	32	20.6
	No	123	79.4
Athritis	Yes	47	30.3
	No	108	69.7
Other autoimmune diseases	Yes	3	1.9
	No	152	98.1
Chronic conjunctivitis	Yes	31	19.9
	No	125	80.1

Description of quality of life related vision according OSDI

According to Figure 1, regarding to the discomfort of ocular surface symptom the majority of patients complained of light sensitivity (41.1%), gritty sensation (31.5%), eye pain (43.3%), blurred vision and poor vision (29.8%).

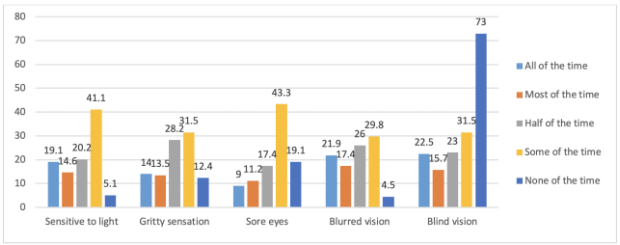

Figure 1: Symptoms of discomfort of ocular surface

On the other hand, most of patients with the symptoms of blurred vision and poor vision experienced this condition all of the time (73.0%). The mean OSDI score of discomfort of ocular surface symptom group was 48.6 ± 26.15.

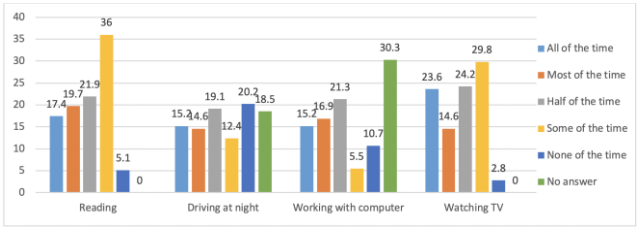

Figure 2: Symptoms of visual disturbance

According to Figure 2, regarding to visual disturbance, among patients had discomfort feeling when reading and watching TV, these symptoms occurred occasionally with the rate of 36% and 29.8% respectively. The majority of participants were farmer, therefore most of them had no answer for the question "when working with a computer or bank machine (30.3%). In patients with discomfort when driving at night, the proportion of disturbance frequency level seemed to be equal. The mean OSDI score of visual disturbance symptom group was 43.64 ± 25.29.

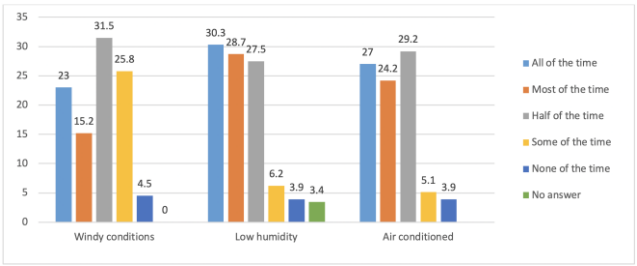

Figure 3: Symptoms of dry eyes related environmental condition

Most of participants answered that they felt uncomfortable at the frequency "half of time" in the windy conditions (31.5%) and areas that are air conditioned (29.2%). In the condition of low humidity (very dry), the prevalence of participants felt uncomfortable at the frequency "all of the time", "most of the time" and "half of the time" was 30.3%, 28.7% and 27.5% respectively. The mean OSDI in the goup of activated symptoms due to environmental factors was 53.37 ± 28.81.

Table 3: Dry eye severity according OSDI scale

Severity	Number (n)	Proportion (%)
Mild (13-22 points)	14	7.9
Morderate (23-32 points)	93	52.2
Severe (33 – 100 points)	71	39.9
Total	178	100

In our study, moderate dry eye accounted for the highest proportion in 3 groups (52.2%), followed by severe dry eye (39.9%) and the lowest was mild dry eye (7.9%), (Table 3).

The relationship between some social-demographic factors and severe dry eye

Age was one of related factors of dry eye (OR 1.03 (95%CI 1.01 – 1.05). The prevalence of dry eye in the group having higher educational level (above high school) was 58.8%, lower than that of the group having lower educations level (60.9%).

Table 4: The relationship between some social-demographic factors and severe DE

Factors		Yes		No		OR 95%CI	P
		n	%	n	%		
Age						1.03 (1.01 – 1.05)	0.005*
Sex	Male	12	35.3	22	64.7	1.27(0.59 – 2.77)	0.543
	Female	59	41	85	59		
Educational level higher than high school	Yes	28	41.2	40	58.8	1.09 (0.59 – 2.02)	0.782
	No	43	39.1	67	60.9		
Occupation	Others	24	36.4	42	63.6		
	Officer	21	46.7	24	53.3	1.53(0.71-3.31)	0.279
	Farmer	26	38.8	41	61.2	1.11(0.55-0.24)	0.771
Binocular good vision	Yes	13	15.3	72	84.7	0.11(0.05- 0.23)	0.0001*
	No	58	62.4	35	37.6		

OR: odds ratio; 95% CI: confident interval; *: p < 0.05; P values were determined by Anova test.

The highest prevalence of severe dry eye by occupation was in farmer group (46.7%), followed by the farmer group (38.8%) and the lowest in other occupations (36.4%), (Table 4).

Table 5: The relationship between severe dry eye and medical history

Risk factors		Yes		No		OR 95%CI	p
		N	%	n	%		
Medical history	Yes	70	44.9	86	55.1	17.09	0.0001*
	No	1	45	21	95.5	2.24 – 130.25	
Chronic conjunctivitis	Yes	7	25.9	20	74.4	0.36	0.027*
	No					0.14 – 0.91	
Refractive error	Yes	3	12.5	51	87.5	0,14	0.0001*
	No	67	51.1	64	48.9	0.04 – 0.48	
Allergic diseases	Yes	13	32.5	27	67.5	0.49	0.062
	No	57	49.6	58	50.4	0.23-1.04	
Diabetes	Yes	1	50	1	50	1.2	1
	No	69	45.4	83	54.6	0.07-19.59	
Hypertension	Yes	5	62.5	3	37.5	2.1	0.47
	No	65	14.2	82	55.8	0.48-9.13	
Sjogren's syndrome	Yes	30	93.8	2	6.3	31.13	0.0001*
	No	40	32.5	83	67.5	7.08-136.76	
Athritis	Yes	22	46.8	25	53.2	1.1	0.786
	No	48	44.4	60	55.6	0.55-2.19	
Other autoimmune diseases	Yes	3	100	0	0	0.44	0.09
	No	67	44.1	85	55.9	0.37-0.53	

OR: odds ratio; 95% CI: confident interval; *: p < 0.05; P values were determined by Anova test.

We did not find any statistically significant relationship between severe DE disease and group of medical history including allergy, diabetes, hypertension, arthritis and other autoimmune diseases (Lupus) (p > 0.05). On the other hand, medical history of chronic conjunctivitis, refractive errors, Sjogren's syndrome was shown to be statistically significant association with severe dry eye disease (p < 0.05) (Table 5).

Discussion

General information of research subjects

The mean age of participants was 44.6 years and the 40-59 age group comprised the most patients among the 3 age groups (43.7%). This characteristic is similar to a study of Alyscia Cheema [8]. DE disease can occur at any age. This study revealed the significant and important effects of dry eye disease on individual health as a public health problem. The prevalence of dry eye symptoms increased with age (p < 0.05); it is consistent with the research of BOSS [9]. The proportion of female participated in our study (80.9%) was higher than of male (19.1%). It is similar to the results of previous epidemiological studies of this disease [10], [11], [12].

Among the dry eye patients, the ratio of low education, low income was higher than the others rest. In fact, people with low educational level, low average income often work in bitter environmental conditions such as overheat, cold or outdoor sunny windy conditions. That is the cause for faster evaporation of tear film, more susceptible blepharitis which affects the adhesion forces of tear film on the corneal surface leads to DE disease. The percentage of mountainous patients who suffer from DE is very low. This may be due to not only the difficulty of mountainous people to seek medical care but also cool moist environment in the living area. Fresh climate in mountainous areas may significantly reduce the rate of DE in people living here.

More than half of our patients had good correction vision. This seems to be suitable because DE disease often insignificantly reduces the visual acuity by altering the tear film layer, not impairing the transparent environment such as cornea, lens.

Description of quality of life (QoL)related vision according OSDI

The symptoms of ocular surface with high scores and frequent occurrences make a significant impact on the QoL of patients with DE. The mean OSDI score of discomfort of ocular surface symptom group was 48.6 ± 26.15 and 73% of patients felt uncomfortable all the time. The visual disturbance was observed with 4 activities: reading, driving, working with computer and watching TV. OSDI score regarding to these categories was also less than half of the normal person (43.64). The average score of

DE increased under the influence of dry, windy and low humidity environments. Therefore, to reduce the effects of DE on the QoL of patients, it is necessary to limit dry, low humidity and windy conditions in living environment (Figure 3).

Related factors with severe DE

In logistic regression analysis with univariate model, we found an association between age and severe dry eye condition ($p < 0.05$). When the age increased by one year, the risk of severe dry eye increased by 1.03 times. This can be explained by hormonal changes at older age which leads to hyposecretion of many exocrine glands of the body (including glands responsible for tear film secretion). This condition can cause the symptoms of dry eyes. Also, the effect of hormonal factors on women also makes the prevalence of severe dry eye in women higher than that of men in our study (64.7% in women compared to 59% in men) (Table 5).

There is a stastically difference in the prevalence of severe dry eye between education levels and occupations ($p < 0.05$).

On the other hand, the variations of age and binocular good vision were shown to have a statistically significant with severe dry eye disease ($p < 0.05$). The group with binocular good vision had lower risk (0.11 times) of dry eye disease than the group without binocular good vision.

People with a history of refractive errors are at lower risk of DE than other people due to regular examination and appropriate treatment. Sjogren's syndrome is an autoimmune disease characterized by dry mouth and signs of dry eyes due to functional impairment of exocrine glands [13]. This syndrome is the second most common autoimmune disease after rheumatoid arthritis [11]. In our study, we have not found an association with allergic diseases, arthritis. This result is similar to the study of Biljana and colleagues [6]. We also have not found the association between dry eyes and contact lenses wearees, other autoimmune diseases (Lupus), thyroid disease because the number of each type of medical history in our study was only 1-2 people [14], [15].

In conclusion, this is one of the first studies on the quality of life of patients with dry eye in Vietnam. The main result includes: dry eyes have a significant impact on visual function and it reduces the quality of daily life of patients. The factors that have been shown to be associated with severe dry eye include age, binocular good vision, medical history, chronic conjunctivitis, refractive errors, Sjogren's syndrome.

References

1. Pflugfelder S, Bauerman R, Stern ME, editors. Dry eye and ocular surface disorders. Taylor & Francis US, 2004:1-428. https://doi.org/10.1201/b14144

2. Lee AJ, Lee J, Saw SM, Gazzard G, Koh D, Widjaja D, Tan DT. Prevalence and risk factors associated with dry eye symptoms: a population based study in Indonesia. Br J Ophthalmol. 2002; 86(12):1347-51. https://doi.org/10.1136/bjo.86.12.1347 PMid:12446361 PMCid:PMC1771386

3. Moss SE, Klein R, Klein BE. Prevalence of and risk factors for dry eye syndrome. Arch Ophthalmol. 2000; 118(9):1264-8. https://doi.org/10.1001/archopht.118.9.1264 PMid:10980773

4. Schaumberg DA, Sullivan DA, Buring JE, Dana MR. Prevalence of dry eye syndrome among US women. Am J Ophthalmol. 2003; 136(2):318-26. https://doi.org/10.1016/S0002-9394(03)00218-6

5. Paulsen AJ, Cruickshanks KJ, Fischer ME, Huang GH, Klein BE, Klein R, Dalton DS. Dry eye in the beaver dam offspring study: prevalence, risk factors, and health-related quality of life. Am J Ophthalmol. 2014; 157(4):799-806. https://doi.org/10.1016/j.ajo.2013.12.023 PMid:24388838 PMCid:PMC3995164

6. Miljanovic B, Dana R, Sullivan DA, Schaumberg DA, et al. Impact of dry eye syndrome on vision-related quality of life. Am J Ophthalmol. 2007; 143(3):409-15. https://doi.org/10.1016/j.ajo.2006.11.060 PMid:17317388 PMCid:PMC1847608

7. Lemp MA. Recent developments in dry eye management. Ophthalmology. 1987; 94(10):1299-304. https://doi.org/10.1016/S0161-6420(87)80015-5

8. Cheema A, Aziz T, Mirza SA, Siddiqi A, Maheshwary N, Khan MA. Sodium hyaluronate eye drops in the treatment of dry eye disease: an open label, uncontrolled, multi-centre trial. Journal of Ayub Medical College Abbottabad. 2012; 24(3-4):14-6.

9. Baudouin C, Creuzot-Garcher C, Hoang-Xuan T, Rigeade MC, Brouquet Y, et al. Severe impairment of health-related quality of life in patients suffering from ocular surface diseases. J Fr Ophtalmol. 2008; 31(4):369-78. https://doi.org/10.1016/S0181-5512(08)71431-1

10. Sakane Y, Yamaguchi M, Yokoi N et al. Development and validation of the Dry Eye-Related Quality-of-Life Score questionnaire. JAMA Ophthalmol. 2013;131(10):1331-8. https://doi.org/10.1001/jamaophthalmol.2013.4503 PMid:23949096

11. Le Q, Zhou X, Ge L, Wu L, Hong J, Xu J. Impact of dry eye syndrome on vision-related quality of life in a non-clinic-based general population. BMC Ophthalmol. 2012; 12(1):22. https://doi.org/10.1186/1471-2415-12-22 PMid:22799274 PMCid:PMC3437197

12. Uchino M, Schaumberg DA. Dry Eye Disease: Impact on Quality of Life and Vision. Curr Ophthalmol Rep. 2013; 1(2):51-57. https://doi.org/10.1007/s40135-013-0009-1 PMid:23710423 PMCid:PMC3660735

13. Fox RI, Michelson P, Casiano CA, et al. Sjogren's syndrome. Clin Dermatol. 2000; 18(5):589-600. https://doi.org/10.1016/S0738-081X(00)00135-8

14. Markoulli M, Kolanu S. Contact lens wear and dry eyes: challenges and solutions. Clin Optom (Auckl). 2017; 9:41-48. https://doi.org/10.2147/OPTO.S111130 PMid:30214359 PMCid:PMC6095561

15. Resch MD, Marsovszky L, Németh J, Bocskai M, Kovács L, Balog A. Dry eye and corneal langerhans cells in systemic lupus erythematosus. J Ophthalmol. 2015; 2015:543835. https://doi.org/10.1155/2015/543835 PMid:25893112 PMCid:PMC4393942

ID Design Press, Skopje, Republic of Macedonia
Open Access Macedonian Journal of Medical Sciences. 2019 Dec 30; 7(24):4297-4300.
https://doi.org/10.3889/oamjms.2019.378
eISSN: 1857-9655
Basic and Clinical Medical Researches in Vietnam

Evaluation of Anterior Chamber Depth and Anterior Chamber Angle Changing After Phacoemulsification in the Primary Angle Close Suspect Eyes

Anh Tuan Vu[1], Van Anh Bui[2], Hai Long Vu[1], Do Quyet[3], Than Van Thai[4], Vu Thi Nga[5], Toi Chu Dinh[6], Nguyen Duy Bac[3*]

[1]Deparment of Ophthalmology, Hanoi Medical University, Hanoi, Vietnam; [2]Vietnam National Institute of Ophthalmology, Hanoi, Vietnam; [3]Vietnam Military Medical University (VMMU), Hanoi, Vietnam; [4]NTT Hi-tech Institute, Nguyen Tat Thanh University, Ho Chi Minh City, Vietnam; [5]Institute for Research and Development, Duy Tan University, 03 Quang Trung, Danang, Vietnam; [6]Department of Human and Animal Physiology, Faculty of Biology, Hanoi National University of Education, Hanoi, Vietnam

Citation: Vu AT, Bui VA, Vu HL, Quyet D, Thai TV, Nga VT, Chu Dinh T, Bac ND. Evaluation of Anterior Chamber Depth and Anterior Chamber Angle Changing After Phacoemulsification in the Primary Angle Close Suspect Eyes. Open Access Maced J Med Sci. 2019 Dec 30; 7(24):4297-4300.
https://doi.org/10.3889/oamjms.2019.378

Keywords: Angle closure suspect; Anterior chamber depth

***Correspondence:** Nguyen Duy Bac. Vietnam Military Medical University (VMMU), Hanoi, Vietnam. E-mail: nguyenduybac@vmmu.edu.vn

Received: 10-Jul-2019; **Revised:** 20-Nov-2019; **Accepted:** 21-Nov-2019; **Online first:** 20-Dec-2019

Funding: This research did not receive any financial support

Competing Interests: The authors have declared that no competing interests exist

Abstract

BACKGROUND: Phacoemulsification surgery has the ability to deeply alter the segment anterior morphology, especially in eye with shallow anterior chamber (AC), narrow anterior chamber angle (ACA). However, the changes of anterior chamber depth (ACD) and ACA on the close angle suspect eyes after phacoemulsification have not been mentioned in many studies. So, we conduct this research.

AIM: To evaluate the alteration in the ACA and ACD after phacoemulsification in the close angle suspect eyes.

METHODS: Interventional study with no control group. Subjects were the primary angle closure suspect (PACS) eyes, that were operated by phacoemulsification with intraocular lens (IOL) at Glaucoma Department of VNIO from December 2017 to October 2018.

RESULTS: 29 PACS eyes with cataract were operated by phacoemulsification with intraocular lens. After 3 months of monitoring, the average ACD augmented from 2.082 ± 0.244 to 3.673 ± 0.222 mm. AOD500 increase from 0.183 ± 0.088 to 0.388 ± 0.132 µm, AOD750 increased from 0.278 ± 0.105 to 0.576 ± 0.149 µm. The TISA500 enlarged from 0.068 ± 0.033 to 0.140 ± 0.052 mm^2, TISA750 enlarged from 0.125 ± 0.052 to 0.256 ± 0.089 mm^2 at the third month ($p < 0.01$).

CONCLUSION: Phacoemulsification surgery increases the ACD and enlarged the angle in the PACS eyes.

Introduction

There have been many studies showing that lens extraction and intraocular lens implantation, especially phacoemulsification surgery in cataract patients can increase the ACD, widening the angle and solving the pupil blockade to increase the aqueous humour outflow [1], [2], [3]. Therefore, phacoemulsification surgery is considered an angle-closure glaucoma treatment method and has a preventive effect on the eyes with narrow AC [4].

Anterior segment optical coherence tomography (AS-OCT) is a non-contact and non-invasive imaging technique that provides high quality images and it offers rapid and easy calculable of anterior segment, especially angle irido-corneal and AC [5].

There have been many studies on images of anterior segment by AS-OCT have shown that after phacoemulsification surgery AC was deeper, ACA was wider on the normal eye group, primary angle closure glaucoma (PACG) group and primery open angle glaucoma (POAG) group.

Altan (2004) studied 53 nonglaucomatous eyes, the results showed that before surgery the

average IOP was 15.1 ± 2.8 mmHg decreased to 13.3 ± 2.7 mmHg after surgery 3 months; Preoperative ACD mean was 3.06 ± 0.49 mm, increased to 3.70 ± 0.36 mm 3 months postoperative (P < 0.05) [1].

The study by Martha Kim (2012) [6] performed phacoemulsification surgery on both PACG and POAG, which showed mean ACD results of PACG groups enlarged from 1.63 ± 0.23 mm to 3.65 ± 0.19; ACD of POAG also enlarged from 2.62 ± 0.47 mm to 3.93 ± 0.26 mm on the second day after surgery (p < 0.001). The ACA in the nasal and temporal quadrants both increased twice in PACG and 1.5 times in POAG.

However, the changes of AC and ACA on the close angle suspect eyes after phacoemulsification have not been mentioned in many studies. So, we conducted this research with the aim to evaluate changes in the ACA and ACD after phacoemulsification surgery in PACS eyes using AS-OCT.

Materials and Methods

This interventional study was performed in the Glaucoma Department of Vietnam institute of ophthalmology, between December 2017 and October 2018. The research was carried out in accordance with the tenets of the Declaration of Helsinki.

We conducted the research on 29 eyes of 25 cataract patients with close angle suspect (The eye has at least 3 quadrants angles at grade 2 according to the Shaffer classification on gonioscopy without indentation and eye in the primary position, with normal intraocular pressure (IOP), normal optic disc and visual fields and ACA under 25° on both nasal and temporal angle quadrants on AS-OCT images). All patients underwent preoperative evaluation including visual acuity testing, slit lamp examination, gonioscopy, Goldmann applanation tonometry and indirect fundoscopy. IOL was calculated by IOLMaster 500 (Zeiss Meditec, Dublin, CA, USA).

Surgeries were performed by one surgeon (ATV). Surgical technique involving phacoemulsification and aspiration through a 2.2 mm temporal clear corneal incision then acrylic hydrophobic IOL was implanted in the capsular bag. Patients with surgical complication which required other surgical approaches were excluded.

AS-OCT (Visante, Zeiss Meditec, Dublin, CA, USA) was carried out 1 day before surgery, and 1 and 3 months after surgery. One examiner achieved all images under indistinguishable lighting conditions. The following parameters were measured: - Central ACD, described the distance from the back surface of the cornea to the front of the lens in the center; - Angle opening distance at 500 µm or 750 µm (AOD500/750) – measured by the length of the line perpendicular between a point 500µm or 750 µm from the scleral spur and the opposing iris; and - Trabecular iris space area (in mm^2) up to 500 µm or 750 µm (TISA500/750) – the area of the quadrilateral define by the AOD 500 or 750, the corneal endothelium, trabecular meshwork and anterior iris surface.

Data are presented as mean values ± standard deviation of the mean. Differences between preoperative and postoperative measurements were evaluated using Friedman test. All results were well thought out significant at $p < 0.05$.

Results

Ours study include 29 eyes of 25 patients; 4 male (16%) and 21 females (84%). The mean age was 70.28 ± 8.95 years, from 47 to 88 years old. All patients were making a diagnosis with senile cataract and narrow angle.

Table 1: Alterations of anterior chamber depht (ACD)

ACD (mm)	$\bar{X} \pm SD$	p*
Preoperative	2.082 ± 0.244	
1 months postoperative	3.620 ± 0.307	
3 months postoperative	3.673 ± 0.222	
ACD difference after surgery 1 month	1.538 ± 0.312	0.000
ACD difference after surgery 3 month	1.592 ± 0.293	0.000
ACD difference between 1 month and 3 months	0.054 ± 0.186	0.131

* Friedman test, comparing before and after surgery.

After surgery, the AC was notably profounder in all postoperative periods. The mean expansion in ACD postoperative was 1.538 ± 0.312 mm after 1 month, and was 1.592 ± 0.293 mm after 3 months, about 73% profounder than before surgery. But the difference of ACD between 1 month and 3 months postoperative is not statistically significant (p = 0.131) (Table 1).

Table 2: Changes in angle opening distance (AOD)

AOD (µm)	AOD500	p*	AOD750	p*
Before surgery	0.183 ± 0.088		0.278 ± 0.105	
1 months after surgery	0.370 ± 0.090		0.569 ± 0.108	
3 months after surgery	0.388 ± 0.132		0.576 ± 0.149	
AOD difference after surgery 1 month	0.187 ± 0.080	0.00	0.291 ± 0.127	0.00
AOD difference after surgery 3 month	0.205 ± 0.108	0.00	0.298 ± 0.149	0.00
AOD difference between 1 month and 3 months	0.018 ± 0.074	0.204	0.007 ± 0.083	0.654

*Friedman test.

Angle opening distance were also significantly augmented. AOD500 average was 0.183 ± 0.088 µm before surgery. One month after surgery mean AOD500 was 0.370 ± 0.090 µm and 0.388 ± 0.132 µm at the third month. AOD750 also augmented from 0.278 ± 0.105 µm to 0.569 ± 0.108 µm at the first month and 0.576 ± 0.149 µm at the third month. However, the change in AOD500 and AOD750 at 1

month and 3 months postoperative is not statistically significant (p > 0.05) (Table 2).

Table 3: Changes in trabecular iris space area (TISA)

TISA (mm^2)	TISA500	p*	TISA750	p*
Before surgery	0.068 ± 0,033		0.125 ± 0.053	
1 months after surgery	0.132 ± 0,038		0.248 ± 0.058	
3 months after surgery	0.140 ± 0,052		0.256 ± 0.089	
TISA difference after surgery 1 month	0.064 ± 0,023	0.00	0.123 ± 0.042	0.00
TISA difference after surgery 3 month	0.072 ± 0,040	0.00	0.132 ± 0.07	0.00
TISA difference between 1 month and 3 months	0.009 ± 0,026	0.087	0.008 ± 0.049	0.373

*Friedman test.

Trabecular iris space area increased roughly 2 times after surgery 1 month in both the temporal and nasal angle (p < 0.001). But the difference of TISA500 and TISA750 at 1 month and 3 months postoperative is not statistically significant (p > 0.05) (Table 3).

Discussion

Recent developments in morphological evaluation of angle irido-cornean, specifically by means of AS-OCT, have exposed that all indicators of the width of angle are increased after lens extraction on all subjects, especially in Asians patients [3].

Lens volume expansions when age increases and the anterior lens surface move toward the cornea [7]. Therefore, almost cataractous lenses are thicker than normal lenses [8]. After cataract extraction and replaced the thinner intraocular lens the iris to back out, extending the anterior chamber and angle irido-cornean.

In this study, we only selected patients at risk of angle closure, so ACD was lower than other studies [9]. The average of ACD before surgery only was 2.082 ± 0.244 mm, but 1 month after surgery ACD was measured at 3.620 ± 0.307 mm. This depth is equivalent to the postoperative ACD value on the senile cataract in normal eye [10], [11].

Among 25 study patients, the rate of women was 5.25 times higher than men. This ratio is also consistent with epidemiology of closed angle glaucoma because the anterior chamber in women are shallower than men, and the average life expectancy for women is higher than for men.

Similar to ACD, the indicators of the AC width are significantly increased at first and third postoperative month, statistically significance with p < 0.001. Many researches have shown that the lens plays an important role in primary angle closure [7]. ACA closure is generally established in eyes with a shallow AC, narrow angle. Studies have revealed an important lens participation in these eyes [12], [13]. One of the mechanisms of angle closure is said to be an augmented lens volume. Also, it has been proclaimed that lens curvature might have a bigger role in angle closure than an enlarged diameter of the lens. A continuous increase in lens volume and lens curvature are suspected to be related to the pathogenesis of angle closure particularly in women in the 3rd or 4th decade.

Therefore, lens removal has special effects on the treatment and prevention of PACG [6]. There are studies that demonstration a diminution in the IOP up to 8,5 mmHg [4] after phacoemulsification. In close angle and close angle suspect eyes, lens removal can enlarge the angle, extend the anterior chamber, and reduce the irido-trabecular contact. This attribute has been related with a stable reduction in the IOP. Some studies have also displayed a diminution in peripheral anterior synechiae after phacoemulsification surgery [14].

Pereira [2] found significant intensify in the ACA opening after cataract extraction. There was a exceptional correlation between the ACA preoperative values and after surgery alterations: "*the shallower the preoperative AC, the greater the postoperative deepening; the narrower the preoperative angle, the greater the postoperative opening of the angle"*.

In ours study, the indicators of anterior chamber angle AOD500, AOD750, TISA500, TISA750 all increased approximate 2 times after surgery. This result is completely consistent with the others studies, the change of the ACA after cataract extraction on angle-closure glaucomatous eyes [9], [10]. Even on normal eyes and open-angle glaucoma, phacoemulsification surgery also extends the ACA but with a smaller margin compare with closed-angle glaucoma [4]. Amount alteration on these parameters was always lesser in the open angle glaucoma against angle close group [6]. The study of Nonaka (2005) on 13 eyes were taken phacoemulsification in 27 eyes residual angle closure after laser peripheral iridotomy. Before surgery, all eyes are positive or suspected positive responses to the prone position test in the dark room. After surgery all eyes becames negative with that test and IOP lowered 4.5 mmHg compared to before surgery.

In conclusion, through studying 29 eyes on 25 PACS patients by AS-OCT machine, we found that phacoemulsification surgery and foldable intraocular lens *increases the ACD and widens the ACA of the PACS eyes*. Results of this research suggest that phacoemulsification might be considered as an effective treatment option for patients at risk of angle-closure glaucoma.

Acknowledgement

We would like to acknowledge the support of many colleagues from Glaucoma Departments of Vietnam Institute of Ophthalmology. We gratefully

acknowledge the help of the statisticians from Hanoi Medical University.

References

1. Altan C, et al. Anterior chamber depth, iridocorneal angle width, and intraocular pressure changes after uneventful phacoemulsification in eyes without glaucoma and with open iridocorneal angles. J Cataract Refract Surg. 2004; 30(4):832-8. https://doi.org/10.1016/j.jcrs.2003.08.023 PMid:15093646

2. Pereira FA, Cronemberger S. Ultrasound biomicroscopic study of anterior segment changes after phacoemulsification and foldable intraocular lens implantation. Ophthalmology. 2003; 110(9):1799-806. https://doi.org/10.1016/S0161-6420(03)00623-7

3. Garudadri CS, Chelerkar V, Nutheti R. Nutheti, An ultrasound biomicroscopic study of the anterior segment in Indian eyes with primary angle-closure glaucoma. J Glaucoma. 2002; 11(6):502-7. https://doi.org/10.1097/00061198-200212000-00009 PMid:12483095

4. Poley BJ, et al. Intraocular pressure reduction after phacoemulsification with intraocular lens implantation in glaucomatous and nonglaucomatous eyes: evaluation of a causal relationship between the natural lens and open-angle glaucoma. J Cataract Refract Surg. 2009; 35(11):1946-55. https://doi.org/10.1016/j.jcrs.2009.05.061 PMid:19878828

5. Leung CK, Weinreb RN. Anterior chamber angle imaging with optical coherence tomography. Eye. 2011; 25(3):261-7. https://doi.org/10.1038/eye.2010.201 PMid:21242985 PMCid:PMC3178313

6. Kim M, et al. Anterior chamber configuration changes after cataract surgery in eyes with glaucoma. Korean J Ophthalmol. 2012; 26(2):97-103. https://doi.org/10.3341/kjo.2012.26.2.97 PMid:22511835 PMCid:PMC3325628

7. Dubbelman M, Van der Heijde GL, Weeber HA. The thickness of the aging human lens obtained from corrected Scheimpflug images. Optom Vis Sci. 2001; 78(6):411-6. https://doi.org/10.1097/00006324-200106000-00013 PMid:11444630

8. Williams DL. Lens morphometry determined by B-mode ultrasonography of the normal and cataractous canine lens. Vet Ophthalmol. 2004; 7(2):91-5. https://doi.org/10.1111/j.1463-5224.2004.04005.x PMid:14982588

9. Kim M, et al. Changes in anterior chamber configuration after cataract surgery as measured by anterior segment optical coherence tomography. Korean J Ophthalmol. 2011; 25(2):77-83. https://doi.org/10.3341/kjo.2011.25.2.77 PMid:21461218 PMCid:PMC3060397

10. Nolan WP, et al. Changes in angle configuration after phacoemulsification measured by anterior segment optical coherence tomography. J Glaucoma. 2008; 17(6):455-9. https://doi.org/10.1097/IJG.0b013e3181650f31 PMid:18794679

11. Chang DH, Lee SC, Jin KH. Changes of Anterior Chamber Depth and Angle After Cataract Surgery Measured by Anterior Segment OCT. J Korean Ophthalmol Soc. 2008; 49(9):1443-1452. https://doi.org/10.3341/jkos.2008.49.9.1443

12. Nonaka A, et al. Angle widening and alteration of ciliary process configuration after cataract surgery for primary angle closure. Ophthalmology. 2006; 113(3):437-41. https://doi.org/10.1016/j.ophtha.2005.11.018 PMid:16513457

13. Zhuo YH, et al. Phacoemulsification treatment of subjects with acute primary angle closure and chronic primary angle-closure glaucoma. J Glaucoma. 2009; 18(9):646-51. https://doi.org/10.1097/IJG.0b013e31819c4322 PMid:20010241

14. Lai JS, Tham CC, Chan JC. The clinical outcomes of cataract extraction by phacoemulsification in eyes with primary angle-closure glaucoma (PACG) and co-existing cataract: a prospective case series. J Glaucoma. 2006; 15(1):47-52. https://doi.org/10.1097/01.ijg.0000196619.34368.0a PMid:16378018

15. Nonaka A, et al. Cataract surgery for residual angle closure after peripheral laser iridotomy. Ophthalmology. 2005; 112(6):974-9. https://doi.org/10.1016/j.ophtha.2004.12.042 PMid:15885784

ID Design Press, Skopje, Republic of Macedonia
Open Access Macedonian Journal of Medical Sciences. 2019 Dec 30; 7(24):4301-4305.
https://doi.org/10.3889/oamjms.2019.379
eISSN: 1857-9655
Basic and Clinical Medical Researches in Vietnam

Evaluation of Phacoemulsification Cataract Surgery Outcomes After Penetrating Keratoplasty

Le Xuan Cung[1], Do Thi Thuy Hang[1], Nguyen Xuan Hiep[1], Do Quyet[2], Than Van Thai[3], Vu Thi Nga[4], Nguyen Duy Bac[2], Dinh Ngan Nguyen[2*]

[1]Vietnam National Institute of Ophthalmology, Hanoi, Vietnam; [2]Vietnam Military Medical University (VMMU), Hanoi, Vietnam; [3]NTT Hi-tech Institute, Nguyen Tat Thanh University, Ho Chi Minh City, Vietnam; [4]Institute for Research and Development, Duy Tan University, 03 Quang Trung, Danang, Vietnam

Citation: Cung LX, Hang DTT, Hiep NX, Quyet D, Thai TV, Nga VT, Bac ND, Nguyen DN. Evaluation of Phacoemulsification Cataract Surgery Outcomes After Penetrating Keratoplasty. Open Access Maced J Med Sci. 2019 Dec 30; 7(24):4301-4305. https://doi.org/10.3889/oamjms.2019.379

Keywords: Complicated Cataract; Corneal graft; Penetrating Keratoplasty; Phacoemulsification

***Correspondence:** Dinh Ngan Nguyen. Vietnam Military Medical University (VMMU), Hanoi, Vietnam. E-mail: ngan.ophthal@gmail.com

Received: 10-Jul-2019; **Revised:** 20-Nov-2019; **Accepted:** 21-Nov-2019; **Online first:** 20-Dec-2019

Funding: This research did not receive any financial support

Competing Interests: The authors have declared that no competing interests exist

Abstract

BACKGROUND: Cataract is one of the reasons which causes impaired visual acuity (VA) of the eyes after penetrating keratoplasy (PK), which can be treated by cataract surgery after PK or triple procedure. Cataract surgery after PK has advantages that parameters of the eyes such as axial length, anterior chamber depth (ACD) as well as corneal curvature are stabilized after removing all sutures postoperatively, and intraocular lens (IOL) power can be calculated correctly. Therefore, postoperative VA will be improved significantly. In Vietnam, there have not been any study about cataract surgery after PK, therefore we conduct this research.

AIM: To evaluate the outcomes of phacoemulsification cataract surgery following primary PK.

METHODS: Non-randomized controlled intervention study. Ninteen eyes (19 patients) that underwent phacoemulsification plus IOL insertion after initial PK in Cornea department, Vietnam National Institute of Ophthalmology, from December 2013 to September 2014.

RESULTS: All patients presented with reduced VA, including 17 eyes (89.9%) with VA ≤ 20/200, mean astigmatism was 7.9 ± 1.0 D. Clear corneal grafts in 16 eyes while corneal opacity was seen in 3 eyes. All eyes with cataract were diagnosed from grade 2. After cataract surgery, improved VA > 20/200 was achieved in 72.22% of cases. There was a markable reduce of postoperative astigmatism with 1.8 ± 0.8 D ($p < 0.05$). However, the immunologic graft reaction was presented in one eye, and two edematous corneas also reported after cataract surgery. After treatment, there was one cornea achieved its clarity.

CONCLUSION: Phacoemulsification cataract surgery following initial PK showed good outcomes with improved postoperative VA, reduced astigmatism, and the ultimate graft survival rate was high.

Introduction

Cataract is considered as one of the reasons that cause impaired VA of the eyes after penetrating keratoplasy (PK). It could be occurred before or after the initial PK. There are several reasons which cause postoperative cataract, that is an accelerated pre-existing cataract, steroid-induced cataract or corneal graft rejection [1], [2]. However, whenever penetrating keratoplasty is considered and cataract is present, one must decide whether to remove the cataract at the same time as corneal transplantation. The arguments suggested that an advantage of a triple procedure (which performing PK, extracapsular cataract extraction as well as intraocular lens (IOL) implantation as one-stage surgery) are less expense for one combined procedure [3], less damage to the endothelium of the transplanted cornea from subsequent cataract surgery and faster visual improvement [4], [5]. However, a triple procedure has some potential intraoperative complications that encountered during the open-sky technique, for example, expulsive hemorrhage, IOL implantation failure due to posterior capsule rupture, prolapse of the vitreous body [6], [7]. Particullarly, the main drawback of this procedure is that intraocular lens (IOL) power calculation could not performed accurately, resulting in a high degree of myopia or hyperopia postoperatively [8], [10]. The reason is that axial length, ACD and corneal curvature could be considerably changed after keratoplasty, affecting the accurate biometric information. Therefore, the postoperative keratometric readings can only be estimated, and estimates can be quite inaccurate. This drawback will be fixed by cataract surgery after PK when all these parameters have been stabilized after removing all sutures, and IOL power can be

calculated correctly. Corneal astigmatism can be reduced with corneal incisions placed in the steepest meridian in cataract surgery. Therefore, postoperative VA will be improved significantly. However, cataract surgery after initial PK is a difficult surgical procedure which requires experienced surgeons to do. The aim of our study is to assess the phacoemulsification cataract surgery outcomes after primary PK in Corneal Department – VNIO.

Patients and Methods

Patients

This study got an approvement from the Scientific Board of VNIO. Patients received phacoemulsification and IOL implantation who underwent a primary PK were included. 19 eyes (19 patients) were included in this study and they all signed an informed consent forms before surgeries. All phacoemulsification cataract surgeries were performed from December 2013 to September 2014 at the Cornea department, VNIO.

Methods

It was a non-randomized controlled intervention study. Patients were asked about their medical records and medical history was collected as well. Patients were examined by a complete ophthalmic examination, such as VA by the standard Snellen chart, IOP measurement with applanation tonometry, slit-lamp biomicroscopy, fundus examination after dilating pupil, A-scan ultrasound for axial length, and keratometric readings measured by topography. Preoperative evaluations including the status of the corneal graft (clear, edema, endothelial decompensation, endothelial immunological rejection, corneal incision), anterior chamber, iris, pupil shape, and the grades of cataract. IOL power calculation used the SRK/T formula and targeted emmetropia.

Keratoplasty

All PKs were performed under general anesthesia. The donor corneas for the PKs taken from our eye bank and imported from CorneaGens eye bank. We used the endothelial punch to prepare the corneal donors and Teflon block with a diameter of 0.50 mm that greater than the recipient bed. Recipient corneas were trephined using handle corneal trephines. 16-bite interrupted sutures using 10-0 nylon were placed. Then we made the suture adjustment to reduce the corneal astigmatism post operation.

Cataract Surgery

Nuclear hardness was defined using the Emery-Little lens opacities classification system. Topical anesthesia with 2% Alcain was administered three times before performing the surgery. Making main corneal incision by using a 2.8 mm knife, and the position of corneal incision was in the steepest meridian to reduce astigmatism. Then, the next step is to put a viscoelastic agent into anterior chamber, followed by making the second incision in a position of 90 degrees away from the main incision on cornea. A continuous curvilinear capsulorhexis is made about 6 mm using a rhexis forceps and after that, injecting BSS during hydro dissection to isolate the lens cortex from the capsule. After that, to sculpt the nucleus using Phaco tip, and the energy using for phacoemulsification is often low not to cause endothelial damage. Then, IOL implantation in the capsular bag will be done, followed by hydration of the corneal incision with BSS or 10-0 nylon suture, if needed. Topical antibacterial and steroid eyedrop were administered four times per day, then it was tapered over several months.

Postoperative examination

Patients will be evaluated on the first postoperative day, one week, one, three and six-month postoperation. At each follow-up visit, operated eyes were examined: VA, IOP, refractive error, astigmatism, corneal graft clarity, graft rejection signs, infection, IOL centeration in the capsular bag and posterior capsule's status. Good results will be corneal graft clarity, stable in-the-bag IOL, posterior capsule clarity, improved VA. Moderate results are blurry graft, stable in-the-bag IOL, posterior capsule clarity or light posterior capsular opacity, little increased VA or unchanged VA. Bad results are graft edema, IOL dislocation, severe posterior capsular opacity, reduced vision compared with pre-op VA.

Results

There were 19 eyes of 19 patients had phacoemulsification plus IOL implantation after original PK. The mean age in our study group was 49.3 ± 17.4 years old, patients aged over 50 accounted for the highest rate (57.95) and the ratio of male/female was the same.

Table 1 shows the preoperative VA. Of 19 eyes included in the study, VA ≤ 20/200 accounted for 89.9%.

Table 1: Preoperative VA

VA	Countfinger (CF) < 3m	CF 3 m – 20/200	> 20/200
Eye	13	4	2

Preoperative IOP was all normal, ranged from 12.05 ± 1.6 mmHg, using Icare tonometer. The mean keratometric was highest at 41.67 D and lowest at 29.48 D. The mean preoperative astigmatism was 7.9 ± 1.0 D with the highest was 12 D, and the lowest was 2.2 D. Characteristics of cataract in pre-op examination showed 4 eyes had complete cataract due to herpes simplex keratitis and 3 eyes had therapeutic keratoplasty.

Table 2: Postoperative VA

VA Time	CF < 3m (n, %)	CF 3m – < 20/200 (n, %)	20/200-20/100 (n, %)	> 20/100 (n, %)	Total (n, %)
Pre-op	13 (68.42%)	4 (21.05%)	2 (10.53%)	0 (0%)	19 (100%)
1st pre-op day	6 (31.58%)	3 (15.79%)	6 (31.58%)	4 (21.05%)	19 (100%)
1-week post-op	3 (15.79%)	4 (21.05%)	9 (47.37%)	3 (15.79%)	19 (100%)
1-month post-op	6 (31.58%)	1 (5.26%)	7 (36.84%)	5 (26.32%)	19 (100%)
3 months post-op	2 (11.11%)	3 (16.67%)	7 (38.89%)	6 (33.33%)	18 (100%)
6 months post-op	2 (25%)	1 (12.5%)	4 (50%)	1 (12.5%)	8 (100%)

Besides, a majority of eyes identified nuclear sclerosis cataract (57.9%). This suggests that age-related cataract also plays a vital role in cataract development after keratoplasty. Regarding postoperative VA, all data showed in Table 2. It is clear in the table 2, VA showed improvement gradually and reached the best vision after 3 months (72.22% cases had VA ≥ 20/200) (Table 2 and Table 3).

Table 3: Corneal graft status

Time Graft	1 week post-operation (n, %)	1 month post-operation (n, %)	3 months post-operation (n, %)	6 months post-operation (n, %)
Corneal clarity	17 (89.47%)	16 (84.21%)	16 (88.88%)	8 (100%)
Edema	2 (10.53%)	2 (10.53%)	1 (5.56%)	0
Immunological rejection	0	1 (5.26%)	1 (5.56%)	0
Infection	0	0	0	0
Total (%)	19 (100%)	19 (100%)	18 (100%)	8 (100%)

The first week post-operation, 1-month post-operation and 3 months post-operation, corneal clarity was noted in 17 eyes, 16 eyes, 16 eyes, respectively (Figure 1).

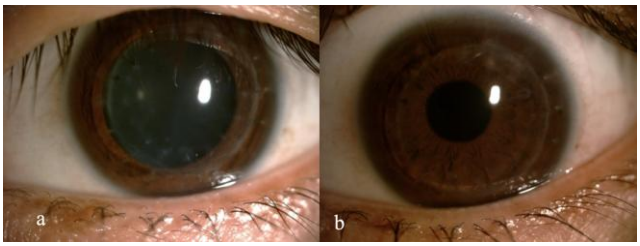

Figure 1: Cataract in PK eye; A) before cataract surgery; B) after cataract surgery

After 6 months post-operation, there were 8 eyes remaining the corneal clarity. According to Table 3, at the presentation of the first postoperative week, there was one eye had endothelial immunological rejection because the patient could not follow the treatment, stop using steroid eyedrop for one week (Figure 2). There were two edematous corneas from the 1st post-op day to 3 months follow-up visit. Then, after treatment, the graft status of this eye was back to corneal clarity, improved vision, while the other eye had endothelial decompensation. IOL position in all examinations was in the capsular bag.

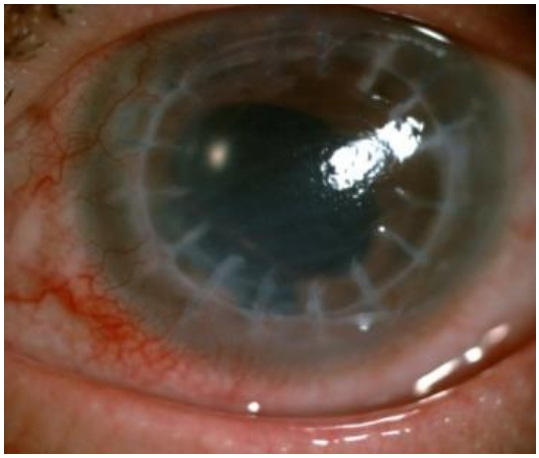

Figure 2: Corneal graft rejection after cataract surgery

We reported 2 of 19 eyes, 4 of 19 eyes and 3 eyes had the posterior capsular opaque in the first-month post-operation, 3 months post-operation and 6 months post-operation, respectively. However, the posterior capsular opaque only happened slightly, and it is no need to do YAG laser posterior capsulotomy. The reduced astigmatism was 1.8 ± 0.8 D postoperatively, and it shows statistically significant difference.

Table 4: Comparison of astigmatism

Astigmatism	$\overline{X}$ ± SD	p
Pre-op Astigmatism	7.9 ± 1.0	< 0.05
Post-op Astigmatism	6.1 ± 0.6	

Note: P values were determined by T-test.

The Table 4 shows the post-operative astigmatism was decreased to 1.8 ± 0.8D. The result was statistically significant difference with $p < 0.05$.

Discussion

Cataract is an age-related disease considered as a leading cause of blindness worldwide. Apart from age-related factor, corneal transplantation can also cause the cataract formation significantly after surgery. Rathi VM studied on 184 eyes underwent PK as the first surgery, reported that 45 eyes developing cataract a few years later, accounted for 24.45% of cases. Particularly, of 45 eyes, 31 had cataract in their first corneal transplantation year [1]. Therefore, cataract surgery is an essential requirement to provide better vision for transplanted eyes.

Regarding cataract surgery outcomes, final VA is an important criterion. In our preoperative evaluation, there were 17 of 19 eyes (89.47%) had the

VA ≤ 20/200, 13 of which considered profound visual impairment with VA of counting fingers lower than the distance at 3 meters. These data showed remarkably very inferior vision of all patients before cataract surgery.

After compared with the high rate of postoperative refractive error in a triple procedure, we performed cataract surgery after PK to achieve better refraction outcomes. In our findings, with the stabilization of keratometric readings after removing all sutures, we had a reliable calculation of IOL powers. The mean keratometric reading was 41.76 D. However, there were only two eyes had keratometric readings ranged from 40 – 44 D. Given the majority of keratometric readings in transplanted eyes were not identified in the normal range (40 – 44 D), our study showed similar findings with a study of Dietrich T, Duran JA [11], [12]. These findings support the benefits of phacoemulsification cataract surgery after initial PK (2-stage procedure), compared with PK combined with extracapsular cataract extraction and IOL insertion (a triple procedure). In previous studies, there was a high astigmatism generally observed after a triple procedure [9], [13] up to 17.0 D in a study of Mohammad-Ali Javadi [14].

Because of the accurate IOL powers calculation using keratometric readings of the transplanted clear cornea in a 2-stage procedure, this technique is preferred in terms of better postoperative refraction. This is also the main drawback of a triple procedure in an attempt to achieve optimal postoperative target refraction. Additionally, in our study, the mean astigmatism was 6.35 D (ranged from 2.2 D to 12 D). Based on corneal topography, we reduced corneal curvature by placing a corneal incision in phacoemulsification surgery at the highest refractive meridian, thereby reducing astigmatism. This is a significant benefit of a 2-step procedure compared with a triple procedure.

In our study, there was no dislocation of the inserted IOL or endophthalmitis was documented. At the first postoperative day, the uncorrected VA was 20/200 or even better that noted in 10 of 19 eyes (52.6%). This VA increased gradually over time. VA in 13 of 18 eyes stabilized completely after 3 months follow-up, in which 6 eyes had VA of above 20/100. Binder's study reported the similar result of VA, that is VA in 19 of 33 eyes (57%) was 20/100 or better [15]. Hsiao CH showed the similar result in 22/24 eyes (81%) [16]. Some authors reported higher results such as Nagra PK with 13/29 eyes achieving 20/70 VA or better, Geggel HS 's study with 91% (20/22) eyes was 20/100 or better. The explanation for the difference between our results and other studies is that the majority of corneal grafts in other studies was optical transplantation, while our PKs were therapeutic keratoplasty.

Postoperative astigmatism reduced 1.8 ± 0.8 D in comparison with preoperative values, and this indicated statistically significant difference ($p < 0.05$). Our finding of astigmatism is similar to other reports, that are HsiaoC (1.55 ±1.3 D) [16], Shi WY (1,0D) [17], Geggel HS (1.96 D) [18], FeiziS (3.03 D) ($P < 0.05$) [19], Nagra PK (2.77 ± 2.36 D), Dietrich T (3.3 ± 2.1 D) [11]. The reduced postoperative astigmatism in our study was partly due to the selection of the corneal incision at the steepest meridian, and the removal of sutures at the time of follow-up visits as well. The study of Kamal A. M. Solaiman conducted from 2014 – 2017 also reported the similar result to our study with better visual outcomes. Therefore, even though a triple approach using a standard keratometry value, or keratometry values in the fellow normal eye still has the major drawback of refraction [4], [5], [20].

In postoperative evaluation, we found 17 eyes (89.47%) had clear corneal grafts, while two eyes presented graft edema. There were two edematous corneas experienced difficulties during cataract surgery due to scarring, vascularization and pupil posterior synechia, causing a prolonged time of surgery. After treatment, these two eyes were stable without any presence of endothelial decompensation. Unfortunately, one eye had graft rejection episodes resulting in corneal opacity, while other grafts showed graft transparency at the last visit.

To control postoperative intraocular inflammation after corneal transplantation is essential to maintain the graft clarity and prepare well for the cataract surgery later. Once postoperative inflammation is controlled well, the situation of capsular adhesions and pupillary membranes hardly happens. Phacoemulsification cataract surgery had some difficulties due to the tough observation through scarring transplanted eyes, irregular corneal astigmatism or unstable anterior chamber, pupil posterior synechia or even contracted pupil. The phacoemulsification cataract surgery with IOL implantation was successfully done with no complications in all our patients. A study of Binder P.S also presented a similar outcome with 100% cases that in-the-bag IOL successfully inserted. posterior capsular Opaque presented in 4 of 19 eyes (21.05%), 2 of which showed early opaque in 1-month post-op. However, there were no cases needed YAG laser posterior capsulotomy.

In summary, the findings in our study showed the remarkable safety and efficacy of phacoemulsification cataract surgery after initial PK. IOL stayed safely in the capsular bag, and the rate of posterior capsular opaque was not significant. Reduced astigmatism leads to significant visual improvement, and the ultimate graft survival rate was good. However, we need to do long-term follow-up examinations for patients to identify more accurate long-term outcome.

Acknowledgement

We would like to acknowledge the support of all colleagues from Cornea Department and other colleagues from Vietnam National Institute of Ophthalmology.

Ethics in Research

Research subjects voluntarily participate in the research, patients' information is confidentiality. Research is only contributed to the vision of patients. Research subjects have the right to end the study at any time.

Informed Consent

All patients agreed and signed an informed consent form before surgeries.

Reference

1. Rathi VM, Krishnamachary M, Gupta S. Cataract formation after penetrating keratoplasty. Journal of cataract and refractive surgery. 1997; 23(4):562-4. https://doi.org/10.1016/S0886-3350(97)80214-3

2. Na KS, Chung SK. Cataract Formation after Penetrating Keratoplasty. J Korean Ophthalmol Soc. 2007; 48(12):1636-42. https://doi.org/10.3341/jkos.2007.48.12.1636

3. Lee JR, Dohlman CH. Intraocular lens implantation in combination with keratoplasty. Annals of ophthalmology. 1977; 9(4):513-8.

4. Shimmura S, Ohashi Y, Shiroma H, Shimazaki J, Tsubota K. Corneal opacity and cataract: triple procedure versus secondary approach. Cornea. 2003; 22(3):234-8. https://doi.org/10.1097/00003226-200304000-00010 PMid:12658089

5. Oie Y, Nishida K. Triple procedure: cataract extraction, intraocular lens implantation, and corneal graft. Current opinion in ophthalmology. 2017; 28(1):63-6. https://doi.org/10.1097/ICU.0000000000000337 PMid:27820748

6. Baca LS, Epstein RJ. Closed-chamber capsulorhexis for cataract extraction combined with penetrating keratoplasty. Journal of cataract and refractive surgery. 1998; 24(5):581-4. https://doi.org/10.1016/S0886-3350(98)80249-6

7. Malta JB, Banitt M, Musch DC, Sugar A, Mian SI, Soong HK. Long-term outcome of combined penetrating keratoplasty with scleral-sutured posterior chamber intraocular lens implantation. Cornea. 2009; 28(7):741-6. https://doi.org/10.1097/ICO.0b013e31819bc31f PMid:19574915

8. Acar BT, Buttanri IB, Sevim MS, Acar S. Corneal endothelial cell loss in post-penetrating keratoplasty patients after cataract surgery: Phacoemulsification versus planned extracapsular cataract extraction. Journal of Cataract & Refractive Surgery. 2011; 37(8):1512-6. https://doi.org/10.1016/j.jcrs.2011.03.039 PMid:21782095

9. Davis EA, Azar DT, Jakobs FM, Stark WJ. Refractive and keratometric results after the triple procedure: experience with early and late suture removal. Ophthalmology. 1998; 105(4):624-30. https://doi.org/10.1016/S0161-6420(98)94015-5

10. Shimmura S, Ohashi Y, Shiroma H, Shimazaki J, Tsubota K. Corneal Opacity and Cataract: Triple Procedure Versus Secondary Approach. Cornea. 2003; 22(3):234-8. https://doi.org/10.1097/00003226-200304000-00010 PMid:12658089

11. Dietrich T, Viestenz A, Langenbucher A, Naumann GO, Seitz B. [Accuracy of IOL power prediction in cataract surgery after penetrating keratoplasty--retrospective study of 72 eyes]. Klinische Monatsblatter fur Augenheilkunde. 2011; 228(8):698-703. https://doi.org/10.1055/s-0029-1245640 PMid:21117018

12. Duran JA, Malvar A, Diez E. Corneal dioptric power after penetrating keratoplasty. The British journal of ophthalmology. 1989; 73(8):657-60. https://doi.org/10.1136/bjo.73.8.657 PMid:2669941 PMCid:PMC1041840

13. Viestenz A, Seitz B, Langenbucher A. Intraocular lens power prediction for triple procedures in Fuchs' dystrophy using multiple regression analysis. Acta ophthalmologica Scandinavica. 2005; 83(3):312-5. https://doi.org/10.1111/j.1600-0420.2005.00418.x PMid:15948783

14. Javadi MA, Feizi S, Moein HR. Simultaneous penetrating keratoplasty and cataract surgery. Journal of ophthalmic & vision research. 2013; 8(1):39-46.

15. Binder PS. Intraocular lens implantation after penetrating keratoplasty. Refractive & corneal surgery. 1989; 5(4):224-30.

16. Hsiao CH, Chen JJ, Chen PY, Chen HS. Intraocular lens implantation after penetrating keratoplasty. Cornea. 2001; 20(6):580-5. https://doi.org/10.1097/00003226-200108000-00005 PMid:11473156

17. Shi WY, Zeng QY, Li SW, Xie LX. [Cataract extraction and intraocular lens implantation after high-risk penetrating keratoplasty]. [Zhonghua yan ke za zhi] Chinese journal of ophthalmology. 2003; 39(11):678-82.

18. Geggel HS. Intraocular lens implantation after penetrating keratoplasty. Improved unaided VA, astigmatism, and safety in patients with combined corneal disease and cataract. Ophthalmology. 1990; 97(11):1460-7. https://doi.org/10.1016/S0161-6420(90)32387-4

19. Feizi S, Zare M, Einollahi B. Simultaneous phacoemulsification and graft refractive surgery in penetrating keratoplasty eyes. ISRN ophthalmology. 2011; 2011:495047. https://doi.org/10.5402/2011/495047 PMid:24527227 PMCid:PMC3912586

20. Gruenauer-Kloevekorn C, Kloevekorn-Norgall K, Duncker GI, Habermann A. Refractive error after triple and non-simultaneous procedures: is the application of a standard constant keratometry value in IOL power calculation advisable? Acta ophthalmologica Scandinavica. 2006; 84(5):679-83. https://doi.org/10.1111/j.1600-0420.2006.00705.x PMid:16965501

ID Design Press, Skopje, Republic of Macedonia
Open Access Macedonian Journal of Medical Sciences. 2019 Dec 30; 7(24):4306-4310.
https://doi.org/10.3889/oamjms.2019.380
eISSN: 1857-9655
Basic and Clinical Medical Researches in Vietnam

Clinical and Microbiological Features of Pediatric Endopthalmitis After Open Globe Injury in the North of VietNam

Tham Truong Khanh Van[1], Do Nhu Hon[2], Nguyen Thi Ngoc Anh[1], Bui Thị Van Anh[1], Do Quyet[3], Than Van Thai[4], Vu Thi Nga[5], Nguyen Duy Bac[3*]

[1]Vietnam National Institute of Ophthalmology, Hanoi, Vietnam; [2]Vienam Ophthalmology Society, Hanoi, Vietnam; [3]Vietnam Military Medical University (VMMU), Hanoi, Vietnam; [4]NTT Hi-tech Institute, Nguyen Tat Thanh University, Ho Chi Minh City, Vietnam; [5]Institute for Research and Development, Duy Tan University, 03 Quang Trung, Danang, Vietnam

Citation: Van TTK, Hon DN, Anh NTN, Anh BTV, Quyet D, Thai TV, Nga VT, Bac ND. Clinical and Microbiological Features of Pediatric Endopthalmitis After Open Globe Injury in the North of Viet Nam. Open Access Maced J Med Sci. 2019 Dec 30; 7(24):4306-4310. https://doi.org/10.3889/oamjms.2019.380

Keywords: Clinical; Microbiological characteristics; Pediatric posttraumatic endophthalmitis

***Correspondence:** Nguyen Duy Bac. Vietnam Military Medical University (VMMU), Hanoi, Vietnam. E-mail: nguyenduybac@vmmu.edu.vn

Received: 12-Jul-2019; **Revised:** 20-Nov-2019; **Accepted:** 21-Nov-2019; **Online first:** 20-Dec-2019

Funding: This research did not receive any financial support

Competing Interests: The authors have declared that no competing interests exist

Abstract

BACKGROUND: Pediatric endophthalmitis after open-globe injury had its clinical features, microbiological profile different from those in aldults. In Viet Nam, there was no report on the clinical and microbiological characteristics of pediatric posttraumatic endophthalmitis. Therefore, we conduct this study.

AIM: To describe clinical features, ultrasound results, gram stain and culture results of endophthalmitis in pediatric open globe injuries.

METHODS: Prospective non-controlled study. Case series of 30 eyes presenting with post-traumatic endophthalmitis between 2015 and 2016 were reviewed.

RESULTS: Mean age was 8.03 ± 3.99 years. Metallic and organic etiologies were the most common causes for injuries (n = 11). 27 cases had penetrating corneal trauma. Dense opaque vitreous was seen in 25 eyes. Retinal necrosis < 1 quadrant and chorioretinal abscess > 1 quadrant were the most common fundus lesions. Dense vitreous opacity on ultrasound was most common (n = 28). Gram stain bacteria positivity was 93.3%, gram-positive was isolated in 63.3%. Vitreous samples were more often positive than aqueous (P = 0,002).

CONCLUSION: Posttraumatic endophthalmitis in children is more common in boys aged 6-10 years and most often caused by injury with metallic and organic matters. Culture results were very low. Vitreous samples were more often positive than aqueous. Gram-positive bacteria were the most common causative organism.

Introduction

Post-traumatic endophthalmitis is one of the severe complications of open globe injuries. It is the infection of the intraocular tissues and intraocular fluids, including hypopyon, vitreous cavity, retina, and the uvea. The pathogens enter intraocular cavities through a corneal wound and/or scleral wound. Post-traumatic endophthalmitis is usually acute with clinical manifestations mainly with symptoms: hypopyon, loss of red pupil reflex, and progressive vitritis. The disease causes intraocular structure damages leading to visual impairment, and severe cases may even require enucleation. Endophthalmitis was estimated at 5%-14% of cases of open globe injuries [1], [2]. In children, according to some recent studies, this rate is much higher. The prevalence of post-traumatic endophthalmitis in children could increase up to 54.1% of all open globe injury cases [3]. In a study by Thordsen et al., post-traumatic endophthalmitis was the most common cause of pediatric endophthalmitis [4]. Regarding pediatric open globe injury, endophthalmitis is considered as the most severe complications. It can occur in very diverse circumstances and causes sight-threatening leading to blindness in many children. On the other hand, because of the physiological characteristic of the age group, the disease situation is complicated with the strong inflammation reaction, the diagnosis and treatment are much difficult with a high sequelae rate. Early diagnosis and treatment can improve prognosis, but it is often delayed because the children do not cooperate well during the examination, the symptoms

of endophthalmitis were covered by signs of open globe injury, and their parents/ guardian do not notice a pain, red eye or visual loss. There are many reports of post-traumatic endophthalmitis, but few reports on the pediatric group. Most of these reports focus on the outcome and factors that influenced it. In Viet Nam, there are some studies of post-traumatic endophthalmitis, but all of them have executed on both adults and children [1], [5], [6], [7]. However, pediatric endophthalmitis after open-globe injury had its clinical features, microbiological profile such as the late hospital presentation leading to delayed primary repair, lack of information about the nature of injury. The spectrum of pathogens seems different from those in adults. Staphylococcus epidermis and Bacillus species are the two most common organisms which cause post-traumatic endophthalmitis, whereas Streptococci are the preference pathogen in children [2], [8]. It is necessary to conduct a separate research on children to understand further accurate clinical data and microbiological characteristics. Therefore, this study aims to identify the clinical and microbiological features of post-traumatic endophthalmitis in children.

Material and Methods

It is a descriptive prospective, single-center, interventional case series analysis on 30 eyes of 30 patients under 16 years, diagnosed and treated endophthalmitis following open globe injuries in Vietnam National Institute of Ophthalmology from August 2015 to August 2016. The exclusion criteria were a history of any ocular surgeries up to 3 months prior to trauma, sepsis, or any systemic sources of infection. Informed consents were obtained from parents or guardians of all participating subjects, the epidemiological data of each patient was documented including age, gender, type and mode of trauma, initial visual acuity, the interval between the trauma and the closure of the wound. Regarding pre-school children, visual acuity was evaluated with Allen card test. All patient underwent comprehensive ophthalmic examinations in which some cases needed to be examined under general anesthesia if they were unable to cooperate with the examination. Clinical examination will detect the following lesions: location and size of the wound, corneal edema, hypopyon, lens the rupture of lens, vitreous opacity grade and retinal lesions such as vessel occlusion, retinal necrosis, retinal abscess through microscopic examination or observation during surgery. Ultrasound was only performed in case an initial surgery was done to close the wound. Plain-film radiology or orbit CT scan should be done when suspected of intraocular foreign body (IOFB). An aqueous or/and the vitreous tap was carried out in all patients, then Gram stain or wet mount preliminarily identifies the microorganisms and culture isolated into appropriate environments to identify the causative agents.

Evaluation criteria: Wound locations were cornea, sclera, and corneosclera. There were three wound sizes including < 5 mm, 5-10 mm, > 10 mm. Associated lesions consisted of lens rupture, IOFB, retinal detachment, retinal tear, and choroidal detachment. The fundus lesions such as vessel occlusion, retinal necrosis, and retinal abscess were documented in quadrants. Vitreous opacity had five grades clinically based on the visibility of retinal details: 1. All the retinal blood vessels are well visible; 2. Only are observed the retinal blood vessels in the 2nd division or above; 3. Only is still observed the large root vessels; 4. All the retinal blood vessels are not visible but the red reflex; and 5. Absent reflex due to dense pus on the vitreous cavity. On ultrasound, the vitreous opacity had three grades: 1. Scatter small dots opacities ≤ 2 mm small; 2. Spreading opacity with dots/ areas, in which a large turbid glass with 3-8 mm, spreading; and 3. Dense opacity.

Microbiological results are divided into groups of microorganisms: Gram (+) bacteria, Gram (-) and fungi.

The statistical analysis of our data was analysed with the SPSS program version 20.0 (SPSS Inc, Chicago, IL, USA).

Results

The mean age of our patients was 8.03 ± 3.99 (ranging from 2 years to 15 years). Children aged 1-3 years old, 3-6 years old, and 10-15 years old accounted for 10%, 20% and 26.7% of cases, respectively. Notably, primary school-aged 6-10 years is the most common age group in the study, with 43.3% of cases. The number of male children is higher than that of female children with a ratio of 6.5 / 1 (P = 0.000).

Rural trauma is one of the common risk factors causing endophthalmitis after open-globe injuries. The proportion of injuries occurring in rural areas accounts for the majority (76.7% of cases), only 23.3% of injuries occur in urban areas; the difference is statistically significant (P = 0.003) (Table 1).

Table 1: Baseline characteristics

The mean age	8.03 ± 3.99
The most common age group	6-8 years old (43.4%)
Male/Female children ratio	6.5 / 1
Rural trauma / Urban trauma	76.7% / 23.3%

Corneal wounds occupy the highest rate, with 90%. 80% of injuries are less than 5 mm in size (Table 2). Five children had a wound length of 5-10 mm (16.7%) and one child with a corneal wound over 10 mm (3.3%). There is no perforating and rupture

wound in our study. 50% of the eyes had the iris prolapse; only 26.7% of eyes did not have intraocular tissue incarceration.

Table 2: Clinical characteristic lesions

Characteristics		Number of eyes (n = 30)	Ratio (100%)
Cornea	Edema	27	90
	Abscess	3	10
Hypopyon		28	93,3
Vitreous opacity	Grade 4	5	16.7
	Grade 5	25	83.3
Vessel occlusion	≤ 1 quadrant	21	70
	> 1 quadrant	9	30
	No	3	10
Retinal necrosis	≤ 1 quadrant	26	86.7
	> 1 quadrant	1	3.3
	No	2	6.7
Retinal abscess	≤ 1 quadrant	12	40
	> 1 quadrant	16	53.3
Retinal detachment		6	20

The leading cause was sharp metal objects (36.7%) such as knives, scissors, nails ... and wood (36.7%) such as wooden sticks, tree branches ... Other causes included animals (fish and stork) bites (10%), plastic toy (6.6%). The remaining three children (10%) could not identify traumatic cause because the children did not remember, and the family members were not present when the child was injured.

The average interval between injury and closure repair was 31.88 ± 30.96 hours (ranging from 3 hours to 120 hours). 60% of the wound was repaired early in the first 24 hours, 30% were closed within 24-72 hours, 10% were delayed after 72 hours.

Visual acuity at presentation was very low: 70% of eyes had VA of LP (+) to HM, VA better than HM accounted for only 6.6% (n = 2). There was no eye with no light perception and only 1 eye with VA better than 20 / 200. Visual acuity could not be tested in 23.4% of eyes due to children's non-cooperation.

Penetrating wound without IOFB accounted for the highest percentage of 93.4% (28 eyes). The IOFB was detected in 2 cases, in which there was one case of metal located in the anterior segment, causing cataract rupture (3.3%). In the other case, the wooden piece was in the vitreous cavity (3.3%).

The infection in anterior chamber expressed by corneal edema and abscess. 90% of eyes presented corneal edema, 10% of eyes (n = 3) appeared corneal abscess. 93.3% of the children in the study had hypopyon with different levels from a little to filling all anterior chamber.

We recorded vitreoretinal lesions and associated lesions by microscopic examination or observation during surgery with intraocular endocamera. Our research has 83.3% of children with vitreous opacity of grade 5. Vascular occlusive inflammation was seen in all patients; retinal necrosis occurs in 90% of cases. However, the area of vascular occlusive inflammation and retinal necrosis is usually less than a quadrant (70% and 86.7%). 10% of cases do not suffer from retinal necrosis. In contrast, retinal abscesses tend to spread over one quadrant in 53.3% of cases. The difference between retinal necrosis and the retinal abscess was statistically significant (p = 0.006). Retinal tears and retinal dialysis were seen in 12 cases (40%).

Endophthalmitis after open globe injury is mostly accompanied by lens rupture with the rate of 63.3% of cases (n = 19), 13.3% of cases (n = 4) had cataract with intact anterior capsule, 23.3 % (n = 7) of cases had clear lens.

Evaluating during surgery and on ultrasound, we also reported that 20% of cases (n = 6) had a retinal detachment.

Some associated factors have been reported to have a greater risk of post-traumatic endophthalmitis. They are retained IOFB, the rupture of lens, delayed timing of initial repair surgeries more than 24 hours, large wound sized over 10 mm and rural trauma. The number of patients with two risk factors accounted for the highest proportion of 46.7%, followed by the case of 1 risk factor (33.3%). There is one eye with all five risk factors. Two children had endophthalmitis without any risk factors.

Microbiological characteristics

In all cases, we collected aqueous or/and vitreous sample for direct wet mount and direct microscopic then a culture to isolate bacteria/ fungi (Table 3). The microorganism was found in 93.3% (n = 28) of eyes with direct wet mount or direct microscopic. Two eyes (6.7%) had negative microbiological results, but the clinical manifestations of acute infections as well as dense vitreous opaque on ultrasound B helped diagnose endophthalmitis.

Table 3: Microbiological results

Microbiological results	Number of eyes (n)	Ratio (%)
Gram-positive Cocci	8	26.7
Gram-positive Bacilli	11	36.7
Gram-negative Bacilli	9	30
Fungii	5	16.7
Negative	2	6.7

Gram-positive was accounted for 63.3% (n = 19) of cases, followed by Gram-negative bacteria with 30%. Fungii was identified in 16.7%. In the bacteria group, Bacilli got the highest rate (66.7%) followed by Cocci at 26.7%. In which, 16.7% had multiple organisms found.

Our study has only 1 case (3.3%) that successfully cultured, isolated Pneumococci from both aqueous and vitreous samples.

In our study, only 13 cases were tested for microbiology from both aqueous and vitreous samples. The positive rate in aqueous and vitreous samples were 92.3% and 100% respectively. Statistical tests showed that the ability to detect microorganism of the aqueous sample is lower than that of the vitreous sample with P = 0.002.

Discussion

The average age in our study is similar to the reports of Alfaro, Rishi, Sheng, and Jin respectively, 8, 9.2, 7 and 7.84 years old [9], [10], [11], [12]. The primary age group from 6 to 10 years of age accounts for the highest proportion, similar to the results of some recent studies [12], [13], [14]. Because the percentage of boys with penetrating eye is higher than that of girls, the rate of boys with endophthalmia after penetrating eye also was higher than that of girls [3], [10], [11], [12], [14], [15]. Our report shows that the number of injuries occurring in rural areas was a majority; this result was similar to other reports [3], [13]. The reason for this difference was that compared to the city, rural children were likely to lack of the supervision or care of their parents and teachers, while they were exposed to many agents, especially sharp objects in the environment that contaminated with soil and sand (bamboo sticks, twigs, pieces of metal).

Moreover, their parents did not fully understand how to prevent these accidents. Therefore, it explains the reason for the increased incidence of ocular injuries in rural areas.

In our study, the pure corneal tear wound occupied the majority of cases. Reports of endophthalmitis after penetrating eye injuries in children of Junejo (2010) and Wu (2016), Sheng (2017), have similar results with the percentage of corneal tear injuries being respectively 62.7%, 86, 7% and 81.4% [11], [13], [14].

Traumatic agents are mainly sharp metal objects (36.7%) such as knives, scissors, nails, and plant agents (36.7%) such as wooden sticks, twigs. Narang and Wu, Sheng, Jin, Zhang also indicated that the cause of injury is mainly metal agents, especially in the report of Sheng, the primary etiology was syringe needle [3], [11], [12], [14], [15]. In contrast, Rishi studied 143 children with endophthalmitis after penetrating eye injury in India found that organic agents such as broomsticks and pencils accounted for the highest proportion with 55.3%, while that sharp metal objects accounted for only 10% of cases [10]. We believed that the rate of plant agents in our study and those of Indian authors such as Narang and Rishi is probably higher than other studies because the rate of children living in rural areas is quite higher while these agents are mainly seen in rural injuries.

The delay in primary repair of the wound was considered as one of the most risk factors for endophthalmitis. Especially, closing the wound after 24 hours after the injury is one of the factors that increase the risk of endophthalmitis after penetrating eye injuries. In our study, 40% of injured eyes were closed after 24 h which is similar to the study of Junejo and Zhang that 46.6% and 53.3% of children came to the hospital after 24 hours [13], [15]. Alfaro (1995) reported an average time from injury to the primary repair higher than our study of 4 days and this time in the report of Sheng (2017) was 9.3 days [9], [11]. In a series of other authors about the pediatric open-globe injury, there was also a high rate of patients who had primary repair late after 24 hours and who got endophthalmitis [16], [17], [18].

The initial VA was very low in our series. The eyes with VA of LP to HM accounted for 70% (n = 21) and VA better than HM was only 6.6% (n = 2). Meanwhile, only 3.3 % of cases had a presenting VA of 20/200 or more. This result was similar to other reports about pediatric endophthalmitis posttraumatic. Wu also showed that the majority of children had very low initial VA, with 73.3% of cases with VA of LP to HM [7]. Junejo reported that, 51.2% patients had VA of LP to HM, 16.3% was NLP or not co-operated; Sheng had 78% of eyes with initial VA < 5 / 200 in which 9.9% was NLP, 25.5% was LP and 25.6% was HM and 67.1% of eyes in Zhang's report had VA at presentation of LP to HM [11], [13], [15].

In the anterior segment, the infection status is evaluated by the corneal edema and hypopyon. In our study, 90% of eyes had corneal edema, and 10% of eyes (n = 3) appeared corneal abscess, which is a sign of particularly severe infection of endophthalmitis. Rishi's study (2016) found that 15% of eyes with corneal abscess and all these eyes had poor treatment outcome at the last visit of follow-up examinations. Rishi also identified this as one of the factors that increased the rate of cases with treatment failure (P = 0.04) [10]. Our research showed that 93.3% of children had hypopyon at varying degrees from very little to all anterior chamber occupied. This result was similar to some recent studies [3], [9], [13]. However, Wu's study only observed 60% of eyes with hypopyon, and in Rishi's study this rate is only 31% [10], [14].

In our study, most cases were accompanied by cataract (63.3%) similar to other authors like Narang, Wu, Sheng [3], [11], [14]. However, Rishi and Junejo showed that the cataract rate was significantly lower at 35% and 27.9%, respectively [10], [13].

When evaluating during surgery and on ultrasound, we also recorded 20% of cases (n = 6) with retinal detachment, similar to the reports of Rishi, Sheng [10], [11]. The presence of retinal and choroidal detachment made the condition of endophthalmitis after penetrating eye more severe, and the treatment outcome was worse.

Specimens were sent to microbiological workup after taking from two procedures: aqueous tap (n = 13) and vitreous tap (n = 30). Of 30 specimens from vitreous, Gram (+) found in 63.3% (n = 19), followed by Gram (-) bacteria in 30%. The results are similar to many other studies. However, the Fungii rate in our study was higher, with the rate of 16.7% [9], [10], [11], [14], [15], [17]. In the bacteria group, bacilli were detected with the highest rate (66.7%),

and the Cocii was 26.7%. This result was quite different from most other study in which the main causes were Cocii (streptococcus and Streptococcus) [3], [9], [10], [11], [12], [13], [14], [15], [17]. We supposed that, in our series, the majority of injuries occurred in the rural areas where many infected wounds were caused by twigs, wooden sticks… which contained a variety of bacilli organism. Multiple pathogens were found in 16.7% of vitreous tap specimens. This ratio was quite different between studies, the multiple pathogens rate in studies of Alfaro, Wu, Rishi and Zhang were respectively 33.3%, 13.3%, 7.3% and 18.4% [9], [10], [14], [15]. Multiple pathogens were considered as risk factors causing the poor prognosis of endophthalmitis after penetrating eye injury in children.

In many reports, the positive isolated rate of culture according to studies in developed countries was about from 41% to 75% [9], [10], [13], [14], [17], [19]. However, Narang (2004) and colleagues reported only 27% of positive cultures [3]. In our series, organism isolated in only 1 case (3.3%) was identified as Streptococcus Pneumonia from both aqueous and vitreous samples. Thus, the positive culture rate in our study was much lower than in other studies in the world. Some reasons are a small number of available organisms or a history of long-time using an antibiotic (frequent in Viet Nam) or our technique of taking samples or culture can affect our results Statistical analysis showed that, the aqueous samples had lower rate of bacteria positive than that of vitreous with P = 0.002. These results were similar to the study of Cornut in 17 cases of posttraumatic endophthalmitis [20]. The reports of Melo and Do Tan on endogenous bacterial endophthalmitis also showed a much higher rate of detecting pathogenic bacteria in vitreous specimens than aqueous specimens [21], [22].

In conclusion, pediatric endophthalmitis after open globe injuries had a higher incidence in children of primary school age boys with predominantly corneal laceration and the leading cause was sharp metal objects. It damages both anterior and posterior segments. Even 60% of wounds were closed within 24 hours, clinical and ultrasound features were very severe with very low presenting visual acuity. Gram-positive bacteria were the major causes but Bacillii were the highest pathogen detected in pediatric endophthalmitis following open-globe trauma in the North of Viet Nam.

Reference

1. Thong LM, et al. Endophthalmitis post-traumatic: microbiological pathogen, risk factors and the outcome. Ho Chi Minh Medical Journal. 2002; 6:8-12.

2. Bhagat N, Nagori S, Zarbin M. Post-traumatic Infectious Endophthalmitis. Surv Ophthalmol. 2011; 56(3):214-51. https://doi.org/10.1016/j.survophthal.2010.09.002 PMid:21397289

3. Narang S, et al. Paediatric open globe injuries. Visual outcome and risk factors for endophthalmitis. Indian J Ophthalmol. 2004; 52(1):29-34.

4. Thordsen JE, Harris L, HUBBARD III GB. Pediatric endophthalmitis. A 10-year consecutive series. Retina. 2008; 28(3):S3-7. https://doi.org/10.1097/IAE.0b013e318159ec7f PMid:18317341

5. ND, S. The outcomes of pars plana vitrectomy for treatment of Pediatric post-traumatic endophthalmitis. Hanoi Medical University: Hanoi, 1999.

6. Hon DN, YNTT, Kham PD, Phuc HT. The outcomes of endophthalmitis due to ocular penetrating injuries. Vietnamese Journal of Ophthalmology:9-15.

7. DN T. Investigate microbiological factors cause endophthalmitis due to ocular penetrating injuries. Hanoi Medical University, 2008.

8. Bansal P, Venkatesh P, Sharma Y. Posttraumatic Endophthalmitis in children: Epidemiology, Diagnosis, Management, and Prognosis. Semin Ophthalmol. 2018; 33(2):284-292.

9. Alfaro DV, et al. Paediatric post-traumatic endophthalmitis. Br J Ophthalmol. 1995; 79(10):888-91. https://doi.org/10.1136/bjo.79.10.888 PMid:7488575 PMCid:PMC505288

10. Rishi E, et al. Post-traumatic endophthalmitis in 143 eyes of children and adolescents from India. Eye. 2016; 30(4):615-20. https://doi.org/10.1038/eye.2016.9 PMid:26869162 PMCid:PMC5108555

11. Sheng Y, et al. Pediatric Posttraumatic Endophthalmitis in China for Twenty Years. J Ophthalmol. 2017; 2017:5248767. https://doi.org/10.1155/2017/5248767 PMid:28191348 PMCid:PMC5278213

12. Jin W, et al. Efficacy and Safety of 23-Gauge Pars Plana Vitrectomy/Silicone Oil Tamponade Combination for Treatment of Pediatric Post-Traumatic Endophthalmitis. Curr Eye Res. 2017; 42(8):1143-1148. https://doi.org/10.1080/02713683.2017.1297460 PMid:28441071

13. Junejo SA, Ahmed M, Alam M. Endophthalmitis in paediatric penetrating ocular injuries in Hyderabad. J Pak Med Assoc. 2010; 60(7):532-5.

14. Wu H, et al. Pediatric posttraumatic endophthalmitis. Graefes Arch Clin Exp Ophthalmol. 2016; 254(10):1919-1922. https://doi.org/10.1007/s00417-016-3330-1 PMid:27067874

15. Zhang M, et al. Pediatric Infectious Endophthalmitis: A 271-case Retrospective Study at a Single Center in China. Chin Med J. 2016; 129(24):2936-2943. https://doi.org/10.4103/0366-6999.195473 PMid:27958225 PMCid:PMC5198528

16. Al Wadeai EA, et al. Epidemiological Features of Pediatric Ocular Trauma in Egypt. J Ophthalmol. 2016; 2016:7874084. https://doi.org/10.1155/2016/7874084 PMid:27800177 PMCid:PMC5069374

17. Sul S, et al. Pediatric open-globe injuries: clinical characteristics and factors associated with poor visual and anatomical success. Graefes Arch Clin Exp Ophthalmol. 2016; 254(7):1405-10. https://doi.org/10.1007/s00417-015-3087-y PMid:26143290

18. AlDahash F, et al. Pediatric open-globe injury in a university-based tertiary hospital. Eur J Ophthalmol. 2018:1120672118818013. https://doi.org/10.1177/1120672118818013 PMid:30539664

19. Chhabra S, et al. Endophthalmitis after open globe injury: microbiologic spectrum and susceptibilities of isolates. Am J Ophthalmol. 2006; 142(5):852-4. https://doi.org/10.1016/j.ajo.2006.05.024 PMid:17056367

20. Cornut PL, et al. A multicentre prospective study of post-traumatic endophthalmitis. Acta Ophthalmol. 2013; 91(5):475-82. https://doi.org/10.1111/j.1755-3768.2011.02349.x PMid:22313810

21. D T. Research on the result of vitrectomy with silicon oil tamponade in treatment of bacterial endogenous endophthalmitis. Hanoi Medical University, 2012.

22. Melo GB, et al. Microbial profile and antibiotic susceptibility of culture-positive bacterial endophthalmitis. Eye. 2011; 25(3):382-7; quiz 388. https://doi.org/10.1038/eye.2010.236 PMid:21336253 PMCid:PMC3171783

ID Design Press, Skopje, Republic of Macedonia
Open Access Macedonian Journal of Medical Sciences. 2019 Dec 30; 7(24):4311-4315.
https://doi.org/10.3889/oamjms.2019.381
eISSN: 1857-9655
Basic and Clinical Medical Researches in Vietnam

Bullous Keratopathy Secondary to Anterior Chamber Angle Foreign Body

Pham Ngoc Dong[1], Nguyen Thi Nga Duong[1], Le Xuan Cung[1], Duong Nguyen Viet Huong[2], Nguyen Dinh Ngan[3], Chu Dinh Thien[4], Do Quyet[3], Nguyen Duy Bac[3*]

[1]Vietnam National Institute of Ophthalmology, Hanoi, Vietnam; [2]Ho Chi Minh University of Medicine and Pharmacy, Ho Chi Minh City, Vietnam; [3]Vietnam Military Medical University (VMMU), Hanoi, Vietnam; [4]Institute for Research and Development, Duy Tan University, 03 Quang Trung, Danang, Vietnam

Citation: Dong PN, Duong NTN, Cung LX, Huong DNV, Ngan ND, Thien CD, Quyet D, Bac ND. Bullous Keratopathy Secondary to Anterior Chamber Angle Foreign Body. Open Access Maced J Med Sci. 2019 Dec 30; 7(24):4311-4315. https://doi.org/10.3889/oamjms.2019.381

Keywords: Foreign body in the chamber angle; Bullous keratopathy; Corneal edema

***Correspondence:** Nguyen Duy Bac. Vietnam Military Medical University (VMMU), Hanoi, Vietnam. E-mail: nguyenduybac@vmmu.edu.vn

Received: 16-Aug2019; **Revised:** 20-Nov-2019; **Accepted:** 21-Nov-2019; **Online first:** 20-Dec-2019

Funding: This research did not receive any financial support

Competing Interests: The authors have declared that no competing interests exist

Abstract

BACKGROUND: Penetrating ocular trauma with intraocular foreign body is a serious injury often resulting in loss of vision. Anterior chamber foreign bodies account for a considerable portion of all cases of all intraocular foreign bodies (up to 15%); however, they can be missed due to inconspicuous location.

CASE REPORT: We report two cases of retained intraocular foreign bodies in the iridocorneal angle that was missed at the first ophthalmic examination. They were only discovered when complications occurred, such as corneal edema and increased intraocular pressure. In the case whereby the foreign body was taken out early, corneal damages were reversible. However, in the case whereby the foreign body was taken out late, endothelial damage was irreversible and endothelial transplantation was needed.

CONCLUSION: Regarding trauma patients, a careful examination should be performed to discover foreign bodies in the iridocorneal angle. If local peripheral corneal edema occurred, attention should be paid to the trauma history and to timely discovery of the foreign body. This will prevent any irreversible corneal damages.

Introduction

Intraocular foreign bodies present commonly in penetrating ocular trauma. Large foreign bodies with conspicuous entry sites are often detected at the first ophthalmic examination. However, in the case of small foreign bodies locating at the anterior chamber angle, they may not be detected or removed promptly. Thus, in patients with an unclear history of trauma and insignificant symptoms, intraocular foreign bodies may be missed [1], [2].

Anterior chamber foreign bodies can be asymptomatic and only manifest after many years with various complications such as corneal edema, anterior uveitis, cataract, and endothelial decompensation, etc. Late diagnosis and management of a retained intraocular foreign body may lead to complications that affect the structure and function of the penetrating eye [3].

Intraocular foreign bodies' surgical management depends largely on the origin, location, nature of the foreign material, structural and functional damages. It is advised not to remove the foreign body if it is small and does not affect visual acuity [4], [5].

In this article, we report two cases of a retained intraocular foreign body at the iridocorneal angle that were missed at the first ophthalmic examination, and were only discovered when severe complications occurred, such as corneal edema and increased intraocular pressure.

Case Reports

Case N$^{o.}$ 1

A 35-year-old man presented with a history of traffic accident. His left eye had a penetrating ocular wound and retinal detachment. The wound was closed promptly. Unfortunately, the eye globe gradually shrunk and lost its function due to severe injury and complications (Figure 1 and Figure 2).

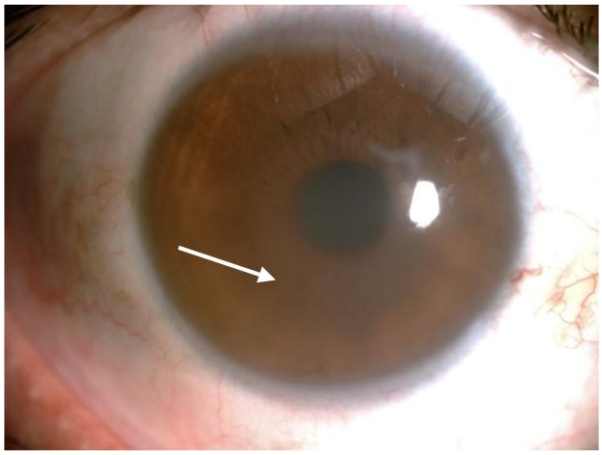

Figure 1: Inferior corneal edema and paracentral corneal scarring

One month after the accident, inferior corneal edema, increased intraocular pressure, and decreased vision (20/200) developed in his right eye. After being treated with topical steroids and glaucoma medications, the cornea became clear and intraocular pressure was well controlled. However, it relapsed after one to two months when medications were stopped.

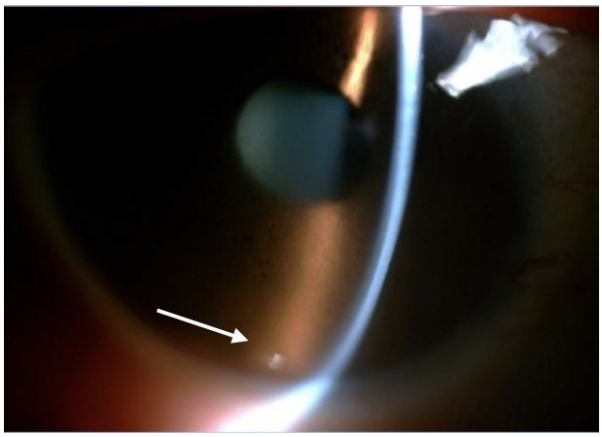

Figure 2: Glass-like foreign body at 6 o'clock (arrow)

At the time of examination, the cornea was clear; on detailed anterior chamber examination, a small glass-like foreign body at 6 o'clock of the inferior iridocorneal angle was detected. In the paracentral cornea, small corneal scarring was observed, this may be the foreign body's point of entry. Consequently, the intraocular foreign body (a piece of glass at 1 × 2 mm) was removed in the operating room. After surgery, corneal edema and increased intraocular pressure disappeared completely without any medications. Visual acuity was 20/40.

Case N$^{o.}$ 2

A 56-year-old woman presented at our department complaining of blurred vision, glare, grittiness and epiphora in her left eye, which first occurred 4 months ago. She had been diagnosed with keratitis at the provincial eye hospital and was treated with topical steroids, nonsteroidal anti-inflammatories and artificial tears. There was no improvement and the symptoms worsened. She had strabismus surgery done in both eyes 20 years ago. Other personal and familial history was unremarkable.

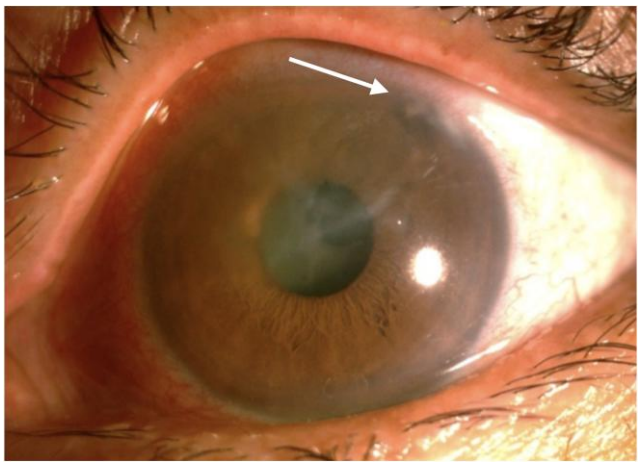

Figure 3: Superior corneal edema and corneal scarring at 1 o'clock

On clinical examination, her best-corrected visual acuity was 20/80 in the right eye and counting finger at 0.3 m in the left eye. Intraocular pressure was 17 mmHg in both eyes.

The left eye experienced irritation, epiphora, and redness. Slit lamp examination revealed central stromal edema, diffuse epithelial microcystic edema, corneal epithelial erosion, Descemet's membrane thickening and peripheral corneal scarring at the 1 o'clock meridian. Gonioscopic examination revealed a retained 1 x 1 mm foreign body located at 1 o'clock in the anterior chamber angle, on the surface of the iris and surrounded by pigments. The iris and pupil were normal. Grade 3 nuclear cataract was observed. Failure to examine the vitreous body and the fundus was due to corneal edema and cataract. The right eye was normal and only had a grade 3 nuclear cataract.

The presence of the anterior chamber foreign body was confirmed by ultrasonic biomicroscopy. It also showed vitreous opacities and no retinal detachment in both eyes.

The patient was finally diagnosed with bullous

keratopathy secondary to anterior chamber foreign body, with peripheral corneal scarring at 1 o'clock in the left eye, and nuclear cataract in both eyes (Figure 3 and Figure 4).

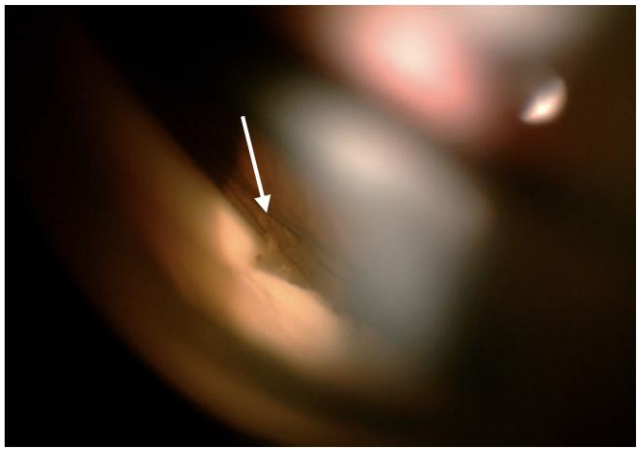

Figure 4: Tube-like anterior chamber foreign body, behind corneal scarring (arrow)

The tube-like anterior chamber foreign body suggested the structure of a glaucoma drainage device but the patient had neither been diagnosed with glaucoma nor undergone any glaucoma drainage surgery. On the other hand, the corneal scarring may be the foreign body's entry site. Thorough history taking revealed a penetrating ocular trauma in her left eye caused by a bamboo branch one year ago. At the first ophthalmic examination after trauma, the symptoms were transient, and insignificant; which spontaneously disappeared after one day and only manifested 6 months after the injury.

The foreign body was removed surgically with foreign body forceps, through a clear corneal incision at 11 o'clock (Figure 5).

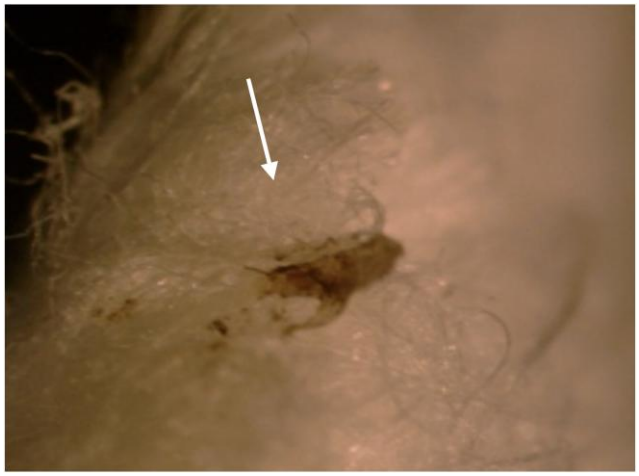

Figure 5: Plastic foreign body (arrow)

The foreign body was plastic with rolled edges and measured about 1.0 x 0.5 mm in size. Due to nuclear cataract in both eyes, phacoemulsification was also performed and then followed by intraocular lens insertions. Unfortunately, 4 months after the surgery, symptoms and signs of bullous keratopathy still existed and progressed worse. Thus, Descemet Stripping Automated Endothelial Keratoplasty was performed to replace the damaged endothelium. After keratoplasty, the graft and recipient cornea became clearer and symptoms and signs disappeared completely. Her best corrected vision was 20/40 (Figure 6).

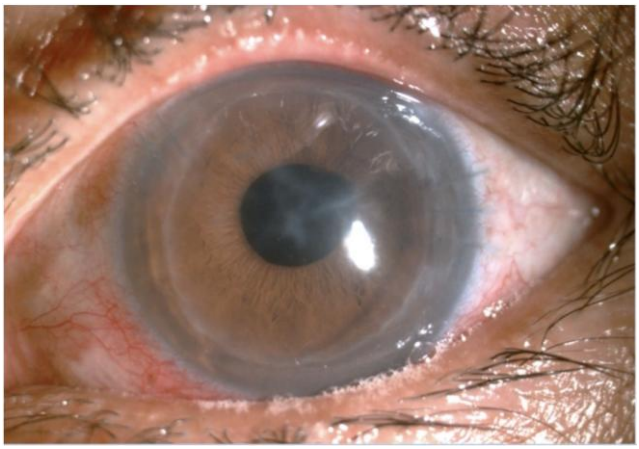

Figure 6: After foreign body removal and endothelial keratoplasty

Discussion

Penetrating ocular trauma is a common injury in ophthalmic emergency, which can result in structural and functional damage to the affected eye. Intraocular foreign bodies take up 40%-53% of penetrating ocular trauma and open globe injuries. In these cases, the prevalence of anterior chamber foreign bodies is about 15% [1]. The velocity of entry, and the size of the foreign body will determine the location at which a foreign body comes to rest. Small non-metallic foreign bodies generally have a lower velocity compared to metallic. Once they have penetrated the cornea, they tend to remain in the anterior chamber. Clinical manifestations and course of progress can vary, depending on the foreign body's composition, shape, and reaction to adjacent structures. In patients with a clear history of penetrating ocular trauma and significant symptoms, the diagnosis of intraocular foreign bodies is often confirmed at the first visit. However, intraocular foreign bodies can be missed by both the doctor and the patient due to its unapparent presence and absence of symptoms [4].

In the first patient, localized corneal edema occurred episodically with increased intraocular pressure. Treatment with medications to control inflammatory reaction and intraocular pressure only had temporary effects and it relapsed after

medications were stopped. However, corneal edema and high intraocular pressure completely disappeared after the foreign body's removal.

The second patient's history revealed a previous penetrating ocular injury caused by a bamboo branch. At the first ophthalmic examination after injury, symptoms were transient and insignificant. She presented in the first visit with grittiness, irritation and epiphora, which developed 6 months after trauma. Only when the anterior chamber foreign body was detected by gonioscopy, we found out about the history of trauma by thorough history taking. Before coming to our service, the patient was diagnosed with keratitis and managed accordingly at another eye hospital. The reason for this late discovery was that the small foreign body could have been hidden by corneal scarring. There was also no inflammatory response in the anterior chamber, which made it clinically undetectable. Thus, gonioscopic examination plays an important role in detecting intraocular foreign bodies in patients with doubtful history of penetrating trauma, peripheral corneal scarring near the limbus and localized corneal edema. Many authors have also emphasized the importance of gonioscopy to assess anterior chamber damage and identify the retained intraocular foreign bodies in penetrating ocular trauma [4], [6]. Anterior chamber foreign bodies can cause endothelial damage due to their sudden shifting or repeated small movements and mechanical contacts between them and the corneal endothelium [1], [7], [8], [9]. Furthermore, due to the endothelium's ability to compensate, patients may be asymptomatic for a long period of time. Thus, the anterior chamber foreign body can be easily missed. The existence of an anterior chamber foreign body may result in corneal edema and severe conditions such as endothelial decompensation.

Acher et al., reported ten cases of non-metallic anterior chamber foreign bodies, in which seven cases caused by glass foreign bodies, two cases of wooden and the rest of plastic material. The most common complication was corneal edema, which may not develop until months or even years (up to 20 years) after the original injury. There was one case whereby the foreign body was removed one year after trauma, and corneal edema consequently progressed to bullous keratopathy [1].

In our first case, corneal edema and increased intraocular pressure occurred one month after injury and only completely disappeared after the foreign body's removal. The second case presented with significant symptoms six months after the trauma but was diagnosed and treated as viral keratitis for a long time. Thus, although the foreign body was taken out, severe bullous keratopathy resulted in decompensation of the cornea and the need for keratoplasty. Similarly, Zengin et al., also reported a case that was treated as herpetic stromal keratitis and the history of ocular injury was not found out until the foreign body was detected by careful gonioscopic examination [7]. These interesting cases showed that the anterior chamber foreign body should be kept in mind as a differential diagnosis, and we should pay more attention to look for and detect it.

In conclusion, anterior chamber foreign body is a cause of decompensation of the corneal endothelium. Patients may be asymptomatic for a long period of time and corneal edema may not develop until the cornea has decompensated. Our cases highlighted the need to have a careful examination to detect intraocular foreign bodies, especially those located in the anterior chamber, based on the history of the ocular trauma. In patients with localized corneal edema near the limbus, thorough history taking and careful examination are necessary to diagnose the intraocular foreign body and manage promptly, which can minimize corneal lesions, and decrease the risk of complications such as endothelial damage, increased intraocular pressure, and loss of vision.

Ethics Approval

All procedures performed in studies involving human participants were in accordance with the ethical standards of the institutional and/or national research committee and with the 1964 Helsinki declaration and its later amendments or comparable ethical standards.

Informed Consent

Informed consents were collected from participating patient(s) for their anonymized information to be reported in the study.

References

1. Archer DB, Davies MS, Kanski JJ. Non-metallic foreign bodies in the anterior chamber. Br J Ophthalmol. 1969; 53(7):453-6. https://doi.org/10.1136/bjo.53.7.453 PMid:5804029 PMCid:PMC1207449

2. Pujar, Chandrakant M, Narayan et al. Journal of Evolution of Medical and Dental Sciences. 2015; 4:2223-2227. https://doi.org/10.14260/jemds/2015/320

3. Iqbal M. Retained Intraocular Foreign Body. Pak J Ophthalmol. 2010; 26(3):158-161.

4. Griffiths ML, Lee GA. Retained intraocular foreign body. Clin Exp Optom. 2004; 87(1):34-6. https://doi.org/10.1111/j.1444-0938.2004.tb03144.x PMid:14720119

5. Anil MS, Nicholson AD, Murade SM, et al. Clinical presentations

and outcomes following ocular injury with intraocular foreign bodies. Sudanese Journal of Ophthalmology. 2015; 7:35-40. https://doi.org/10.4103/1858-540X.169384

6. Loporchio D, Mukkamala L, Gorukanti K, Zarbin M, Langer P, Bhagat N. Intraocular foreign bodies: A review. Surv Ophthalmol. 2016; 61(5):582-96. https://doi.org/10.1016/j.survophthal.2016.03.005 PMid:26994871

7. Han ER, Wee WR, Lee JH, Hyon JY. A case of retained graphite anterior chamber foreign body masquerading as stromal keratitis. Korean J Ophthalmol. 2011; 25(2):128-31. https://doi.org/10.3341/kjo.2011.25.2.128 PMid:21461226 PMCid:PMC3060390

8. Zengin MO, Çinar E, Tuncer I, et al. A presenting as Retained Iridocorneal Angle Foreign Body Resembling to Disciform Keratitis A Case Report. Journal of Glaucoma-Cataract. 2015; 10(1):55-57.

9. Panahibazaz M, Zamani M, Borna F. Huge Bullous Keratopathy following Trauma. J Ophthalmic Vis Res. 2010; 5(4):278-9.

ID Design Press, Skopje, Republic of Macedonia
Open Access Macedonian Journal of Medical Sciences. 2019 Dec 30; 7(24):4316-4318.
https://doi.org/10.3889/oamjms.2019.382
eISSN: 1857-9655
Basic and Clinical Medical Researches in Vietnam

Surpass Flow-Diverter in the Treatment of Two Wide-Neck Aneurysms in the Scheme of an Arteriovenous Malformation Patient: A Case Study

Dang Duc Phuc[1], Do Duc Thuan[1], Pham Dinh Dai[1], Dang Minh Duc[1], Nguyen Quang Anh[2,3], Nguyen Thi Nga[4], Chu Dinh Toi[5], Dao Viet Phuong[6], Duy Ton Mai[6,*]

[1]Department of Stroke, Military Hospital 103, No 261 Phung Hung Street, Ha Dong District, Hanoi, Vietnam; [2]Radiology Center, Bach Mai Hospital, Hanoi, Vietnam; [3]Faculty of Radiology, Hanoi Medical University, Hanoi, Vietnam; [4]Institute for Research and Development, Duy Tan University, 03 Quang Trung, Danang, Vietnam; [5]Faculty of Biology, Hanoi National University of Education, Hanoi, Vietnam; [6]Emergency Department, Bach Mai Hospital, Hanoi, Vietnam

Citation: Duc DP, Thuan DD, Dai PD, Duc DM, Quang Anh N, Nga NT, Toi CD, Viet PD, Mai DT. Surpass Flow-Diverter in the Treatment of Two Wide-Neck Aneurysms in the Scheme of an Arteriovenous Malformation Patient: A Case Study. Open Access Maced J Med Sci. 2019 Dec 30; 7(24):4316-4318. https://doi.org/10.3889/oamjms.2019.382

Keywords: Wide-neck aneurysm; Arteriovenous malformation; Surpass flow-diverter stent

***Correspondence:** Duy Ton Mai. Emergency Department, Bach Mai Hospital, Hanoi, Vietnam. E-mail: BsTonbvbachmai@gmail.com

Received: 16-Aug2019; **Revised:** 20-Nov-2019; **Accepted:** 21-Nov-2019; **Online first:** 20-Dec-2019

Funding: This research did not receive any financial support

Competing Interests: The authors have declared that no competing interests exist

Abstract

BACKGROUND: The cerebral arterial aneurysm, especially in the circumstances of ateriovenous malformation (AVM), has higher risk of rupture than normal isolated aneursym. Therefore, the treatment strategy needs to be plan very carefully in such case.

CASE PRESENTATION: We report a patient with 2 wide-neck aneurysms located in the feeding artery of the arteriovenous malformation and he, then, was treated by using Surpass stent (flow-diverter) to eliminate the aneurysms.

CONCLUSION: In our case, multiple wide-neck aneurysms in combination with low risk unruptured AVM, using long Surpass stent-diversion is an effective way to eliminate all the aneurysms in the main feeding artery while still preserving the AVM anatomy.

Introduction

Cerebral arteriovenous malformation (AVM) is a brain vascular abnormality with incidence ranging from 0.89 – 1.34 case/100.000 people/year [1]. In this circumstance, the aneurysms associated with the AVM always has higher risk of rupture than the isolated ones [2], [3], [4], [5]. This is due to the high-flow in the feeding arteries of the AVM. In our case study, we want to report an AVM-patient having 2 wide-neck aneuryms in his feeding artery of right middle cerebral artery (MCA) which was treated later by Surpass stent flow-diverter (Stryker). The rate of multiple aneurysms normally in case of subarachnoid hemorrhage ranged from 7%-45% in some previous studies [6], [7], [8], [9], [10], [11]. Additionally, aneurysms with wide-neck are defined by neck diameters greater than 4 mm or dome-to-neck ratios less than 2 and are the most difficult to treat with the endovascular method. With the appearance of flow-diverter recently, these wide-neck aneurysms can be treated in an easier way with a low rate of recurrence and complications [12].

Case Presentation

A female patient, 56 years old, was hospitalized due to slight to mild headache for a long time. A base-line CT-Scanner revealed a right parietal lesion with hyperdensity and calcification (Figure 1A) that suggested a brain AVM. Digital subtraction angiography (DSA) then confirmed the AVM diagnosis in combination with multiple aneurysms of the right ICA, the main feeding artery. The malformation size was 5x5x4 cm and its venous drained into the superior sagittal sinus (SSS) (Figure 1B). The Spetzler Martin score was 3. The first aneurysm located at the bifurcating terminal of M1 (size: 12 x 7 mm; neck: 8.3 mm) meanwhile the second aneurysm (size: 4 x 4.2 mm; neck: 3 mm) was at the M2 segment and 25 mm further from the previous one. Both aneurysms need to be treated, especially the first due to their high risk of rupture.

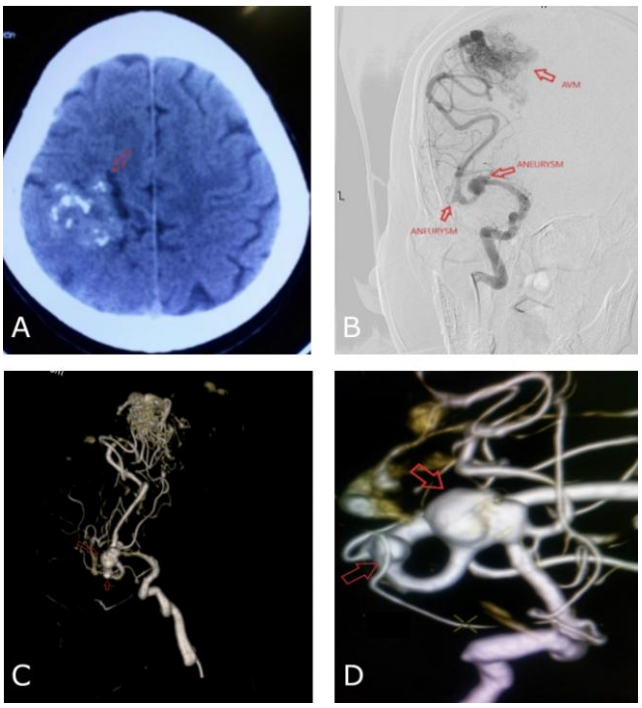

Figure 1: Fifty six year old female patient admitted to hospital due to slight headache; A) Base-line CT Scanner image showed heterogeneous hyperdensity of the right parietal lesion; B) DSA revealed the AVM with main feeding artery from right MCA; C) and D) Morphology and location of two MCA aneurysms

Dual antiplatelet therapy (DAPT) including clopidogrel 75mg/day and aspirin 100 mg/day was indicated for this patient in 5 days. The antiplatelet resistance test with ADP later showed good result of 28%. The procedure was performed under general anesthesia. Long sheath Neuron MAX 6F was placed from groin puncture to the cavernous segment of right ICA. We advanced the AXS Catalyst-5 Distal Access Catheter co-axial to the M2 segment, 10 mm further from second aneurysm location. A 4/50 Surpass flow-diverter was deployed from this point upstream to the M1 segment to cover both aneurysms neck.

Figure 2 showed good result of stent position and coverage post deployment; no thrombus but slight vasospasm seen at M1 segment closed to the proximal part of flow-diverter. This condition was solved by 15 mins infusing solution of Natriclorid 0,9% 500 ml + heparin 5000 UI + 1,5 mg nimodipine through theLong Sheath. The final angiography showed normal contrast material through carotid vessel system.

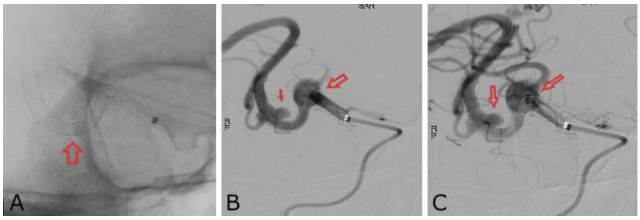

Figure 2: Angiography result during procedure; A) Surpass 4/50 after deployment: good aneurysm neck coverage and no stenosis inside stent; B) and C) Good result post flow-diversion placement with contrast material remained inside both aneurysm

Patient was discharged after 1 week and the modified Rankin scale (mRS) was 0. She was prescribed to continuously use DAPT for 6 months and followed by aspirin 100 mg daily for the rest of life.

Discussion

The normal hemorrhagic risk for unruptured AVM is low (about ~ 1.3%) meanwhile this risk of unruptured aneuryms with diameter ≥ 12 mm, according to Williams L.N. et al., is higher and need to be treated as soon as possible [13], [14]. Additionally, this patient had superficial drainage venous system (lower rate of bleeding) so that we strategized that 2 wide-neck aneurysms in the high-flow feeding MCA should be our treatment priority.

Considering between two kinds of intervention including ballon assisted-coiling or flow-diverter, we chose stent diversion because it could help to treat both wide-neck aneurysms in one phase with high rate of success and less complications [15], [16]. Akgul E. reported his case using 1 Surpass stent to treat 3 aneurysms in 2016 [17]. In our patient, to cover 2 aneurysms with 25 mm of distance between them, we needed the length of stent ≥ 50 mm. Among these available flow-diverter stents in Vietnam, only Surpass and FRED adequated this length. Moreover, with good coverage and delievery system (3.7F delivery catheter/outer catheter in combination with pusher catheter), Surpass stent was reported to have easier procedural deployment compared to other systems [18]. Therefore, surpass 4/50 was our first option in

this case. The good result post-operation showed that it was a good choice.

In conclusion, the unruptured aneurysms related to AVM have the higher risk than normal isolated one due to high-flow of main feeding artery. We need to consider the bleeding risk of both AVM and aneurysm to identify which one is our first treatment goal. In our case, multiple wide-neck aneurysms in combination with low risk unruptured AVM, using long Surpass stent-diversion is an effective way to eliminate all the aneurysms in the main feeding artery while still preserving the AVM anatomy.

Ethical Statements

This study was approved by a local Ethics Committee of Military Hospital 103.

Informed Consent

The patient has agreed in writing for using her medical data in scientific publications.

Reference

1. Laakso A, Hernesniemi J. Arteriovenous Malformations: Epidemiology and Clinical Presentation. Neurosurgery Clinics of North America. 2012; 23(1):1-6. https://doi.org/10.1016/j.nec.2011.09.012 PMid:22107853

2. Stapf C, et al. Concurrent arterial aneurysms in brain arteriovenous malformations with haemorrhagic presentation. Journal of Neurology, Neurosurgery & Psychiatry. 2002; 73(3):294-298. https://doi.org/10.1136/jnnp.73.3.294 PMid:12185161 PMCid:PMC1738025

3. Abla AA, et al. The natural history of AVM hemorrhage in the posterior fossa: comparison of hematoma volumes and neurological outcomes in patients with ruptured infra-and supratentorial AVMs. Neurosurgical focus. 2014; 37(3):E6. https://doi.org/10.3171/2014.7.FOCUS14211 PMid:25175444 PMCid:PMC4425310

4. Platz J, et al. Frequency, risk of hemorrhage and treatment considerations for cerebral arteriovenous malformations with associated aneurysms. Acta neurochirurgica. 2014; 156(11):2025-2034. https://doi.org/10.1007/s00701-014-2225-3 PMid:25246143

5. Thompson RC, et al. The Management of Patients with Arteriovenous Malformations and Associated Intracranial Aneurysms. Neurosurgery. 1998; 43(2):202-211. https://doi.org/10.1097/00006123-199808000-00006 PMid:9696071

6. Solander S, et al. Endovascular treatment of multiple intracranial aneurysms by using Guglielmi detachable coils. Journal of neurosurgery. 1999; 90(5):857-864. https://doi.org/10.3171/jns.1999.90.5.0857 PMid:10223451

7. Ellamushi, H.E., et al., Risk factors for the formation of multiple intracranial aneurysms. Journal of neurosurgery. 2001; 94(5):728-732. https://doi.org/10.3171/jns.2001.94.5.0728 PMid:11354403

8. Jeon P, et al. Treatment of multiple intracranial aneurysms with 1-stage coiling. American Journal of Neuroradiology. 2014; 35(6):1170-1173. https://doi.org/10.3174/ajnr.A3821 PMid:24371032

9. Oh K, Lim YC Single-session coil embolization of multiple intracranial aneurysms. Journal of cerebrovascular and endovascular neurosurgery. 2013; 15(3):184-190. https://doi.org/10.7461/jcen.2013.15.3.184 PMid:24167798 PMCid:PMC3804656

10. Inagawa T. Incidence and risk factors for multiple intracranial saccular aneurysms in patients with subarachnoid hemorrhage in Izumo City, Japan. Acta neurochirurgica. 2009; 151(12):1623. https://doi.org/10.1007/s00701-009-0479-y PMid:19669689

11. Kaminogo M, Yonekura M, Shibata S. Incidence and outcome of multiple intracranial aneurysms in a defined population. Stroke. 2003; 34(1):16-21. https://doi.org/10.1161/01.STR.0000046763.48330.AD PMid:12511744

12. Lubicz B, et al. Flow-Diverter Stent for the Endovascular Treatment of Intracranial Aneurysms. Stroke. 2010; 41(10):2247-2253. https://doi.org/10.1161/STROKEAHA.110.589911 PMid:20798369

13. Kim H, et al. Untreated brain arteriovenous malformation: patient-level meta-analysis of hemorrhage predictors. Neurology. 2014; 83(7):590-7. https://doi.org/10.1212/WNL.0000000000000688 PMid:25015366 PMCid:PMC4141996

14.Williams LN, Brown RD. Management of unruptured intracranial aneurysms. Neurology: Clinical Practice. 2013; 3(2):99-108. https://doi.org/10.1212/CPJ.0b013e31828d9f6b PMid:23914319 PMCid:PMC3721237

15. Rouchaud A, et al. Endovascular Treatment of Ruptured Blister-Like Aneurysms: A Systematic Review and Meta-Analysis with Focus on Deconstructive versus Reconstructive and Flow-Diverter Treatments. American Journal of Neuroradiology. 2015; 36(12):2331-2339. https://doi.org/10.3174/ajnr.A4438 PMid:26381557

16. Wakhloo AK, et al. Surpass flow diverter in the treatment of intracranial aneurysms: a prospective multicenter study. American Journal of Neuroradiology. 2015; 36(1):98-107. https://doi.org/10.3174/ajnr.A4078 PMid:25125666

17. Akgul E, et al. A Patient with Eight Intracranial Aneurysms: Endovascular Treatment in Two Sessions. Case reports in neurological medicine. 2016; 2016. https://doi.org/10.1155/2016/9637905 PMid:27668108 PMCid:PMC5030425

18. Rajah G, Narayanan S, Rangel-Castilla L. Update on flow diverters for the endovascular management of cerebral aneurysms. Neurosurg Focus. 2017; 42(6):E2. https://doi.org/10.3171/2017.3.FOCUS16427 PMid:28565980

ID Design Press, Skopje, Republic of Macedonia
Open Access Macedonian Journal of Medical Sciences. 2019 Dec 30; 7(24):4319-4323.
https://doi.org/10.3889/oamjms.2019.383
eISSN: 1857-9655
Basic and Clinical Medical Researches in Vietnam

HMU Fluorinze Mouthwash Enhances Enamel Remineralization: An In Vitro Study

Vo Truong Nhu Ngoc[1], Kimberly Mathieu Coulton[2], Nguyen Thu Tra[1], Nguyen Ha My[1], Phi Thi Quynh Huong[1], Tong Minh Son[1], Le Quynh Anh[1], Luu Quang Thuy[3], Tran Tuan Anh[4], Thien Chu Dinh[5], Chu Dinh Toi[6*]

[1]School of Odonto Stomatology, Hanoi Medical University, Hanoi, Vietnam; [2]School of Dentistry, Faculty of Medicine and Health, University of Sydney, Australia; [3]Viet Duc Hospital, Hanoi, Vietnam; [4]Becamex International Hospital, Thuan An, Binh Duong, Vietnam; [5]Institute for Research and Development, Duy Tan University, 03 Quang Trung, Danang, Vietnam; [6]Department of Human and Animal Physiology, Faculty of Biology, Hanoi National University of Education, Hanoi, Vietnam

Citation: Ngoc VTN, Mathieu Coulton KM, Tra NT, My NH, Huong PTQ, Son TM, Anh LQ, Thuy LQ, Anh TT, Chu Dinh T, Dinh Toi C. HMU Fluorinze Mouthwash Enhances Enamel Remineralization: An In Vitro Study. Open Access Maced J Med Sci. 2019 Dec 30; 7(24):4319-4323.
https://doi.org/10.3889/oamjms.2019.383

Keywords: Enamel remineralization; HMU Fluorinze; Mouthwash

***Correspondence:** Chu Dinh Toi. Department of Human and Animal Physiology, Faculty of Biology, Hanoi National University of Education, Hanoi, Vietnam. E-mail: chudinhtoi@hnue.edu.vn

Received: 03-Sep-2019; **Revised:** 20-Nov-2019; **Accepted:** 21-Nov-2019; **Online first:** 20-Dec-2019

Funding: This research did not receive any financial support

Competing Interests: The authors have declared that no competing interests exist

Abstract

BACKGROUND: Fluoride therapy has long been used extensively to prevent dental caries. Fluoride appears in a variety of dental care products such as mouth rinses, dentifrices, gels, etc. HMU Fluorinze is the first mouthwash containing fluoride in Vietnam.

AIM: This research was conducted to evaluate the efficacy of HMU Fluorinze mouthwash on remineralizing enamel in laboratory conditions.

METHODS: 20 third molar teeth were cleaned and covered with nail polish, except for a 3 x 3 mm square on their buccal surfaces. These teeth underwent two steps: demineralization using Coca-cola and remineralization for 20 daysusing standard calcifying solution (control group) and standard calcifying solution + HMU Fluorinze mouthwash 2 times/day (experimental group). The index measured of enamel structure after demineralization and remineralization was assessed by a DIAGNOdent pen 2190.

RESULTS: The indices measured of the control group and experimental group at baseline were 3.65 ± 0.76 and 3.35 ± 0.64 respectively. After demineralization the control group measured 21.78 ± 4.48 and the experimental group, 20.25 ± 2.26. Following remineralization, the control group scores were 6.30 ± 1.03 and the experimental group, 3.90 ± 1.24, demonstrating statistical significance ($p < 0.01$) between the two groups. After 20 days, the results for the experimental group did not differ from the original results ($p = 0.272$), in contrast with the control group ($p < 0.01$).

CONCLUSION: Results show that HMU Fluorinze mouthwash is better at remineralizing than standard calcifying solution.

Introduction

Historically, fluoride therapy has been used extensively to prevent dental caries. The fluoride ions replace hydroxyl elements leading to more stable enamel crystals [1]. Alternatively, it was observed that low levels (1 ppm or lower) of fluoride in a dissolved liquid can decrease and even inhibit enamel demineralisation [2] as well as increase mineralization [3]. Fluoride pathways originate from many different products containing fluoride. Patients at high risk of caries are frequently advised to use a mouthwash and brush-on gel at home, as an adjunct to brushing with a fluoride dentifrice [4]. Rinses containing 100 ppm F or 230 ppm F (0.05% sodium fluoride) are as available over-the-counter and recommended to be used less than three times a day [5].

The re-mineralization effect of fluoride mouthwash on dental enamel and the prevention of

tooth decay have been proven [5], [6], [7]. A meta-analysis study combining the results of 35 trials showed that, on average, there was a reduction of 27% in decayed, missing and filled surfaces on permanent teeth exposed to fluoride mouthwashes compared to those that were not [5]. Another experimental study conducted by Faller RV et al., (2011) demonstrated the ability to prevent tooth decay and remineralization of four fluoride mouthwash products (100 ppm) from ACT, Listerine, and Crest brands [6]. This research showed that treating with any mouthwash had significantly higher concentration of fluoride absorption than using water alone as a rinse. Phan Bhongsatiern et al., (2019) conducted a study comparing the remineralization effect of sodium fluoride (NaF) mouthwash and NaF gel with toothpaste on early tooth lesions. The average amount of mineral absorption from NaF mouthwash and NaF gel is similar, and both greater than that of NaF toothpaste [7].

Most mouthwash brands sold in Vietnam are imported from overseas, with the exception of a few domestic products such as Dr. ECA solution, which has been proved to treat gingivitis [8], and more recently, HMU Fluorinze mouthwash. HMU Fluorinze is a solution developed by Hanoi Medical University that is less expensive than imported products; however, its effectiveness has not yet been demonstrated. Therefore, the aim of this study is to evaluate the effects of HMU Fluorinze mouthwash on enamel remineralization.

Materials and Methods

Twenty human third molar teeth, extracted from people from 18 to 25 years old, due to complications or for orthodontic reasons, were used in this research. The teeth selected for the study were those that were intact with pulpal vitality at the time of extraction. Teeth that were broken, partially cracked or identified as having a loss of enamel or an enamel defect were excluded from the study.

Ethical research

The teeth used in this study were collected with consent from patients. This *in vitro* study was approved by High Technique Center, School of Odonto-Stomatology, Hanoi Medical University.

Preparation

The selected teeth were cleaned with a prophy cup and polishing gel using a slow-speed handpiece, then rinsed under water. The teeth were immersed in a formol solution and stored in the refrigerator for preservation. The investigators covered the surfaces of each tooth, except for a 3 x 3 mm window on the buccal surfaces, with an acid-resistant layer (nail varnish). The teeth were labelled respectively and stored in saline solution.

Figure 1: Experimental teeth and control teeth have been labeled

Demineralization

The teeth were immersed in Coca-cola for 20 minutes to demineralize the exposed buccal surfaces of the teeth. Coca-cola the teeth were thoroughly rinsed with water and dried for 1 minute. A DIAGNOdent pen 2190 was used to measure the index before and after demineralization of all teeth.

Remineralization

The four corners of each exposed buccal square were used as reference points. All teeth were randomly divided into two groups. The control group (Group A) was exposed to a standard calcifying solution containing 1,5 mM/L calcium, 0.9 mM/L phosphate and 20 mM/L cacodylate with a pH of 7 for twenty days at 37°C. The calcifying solution (30 ml/tooth) was changed out daily. The experimental group (Group B) received the identical treatment except that a 0.05% NaF solution (HMU Fluorinze mouthwash) was added to the solution twice daily at 8 am and 4 pm, followed by a two-minute rinse with distilled water. At the end of the twenty-day period, the extent of enamel demineralization from the four corners of exposed buccal squares were assessed using the DIAGNOdent pen.

Statistics

The data was analyzed using SPSS 20.0. Pair T-test was used to analyse the difference between demineralization and remineralization stages. The difference between exeperimental and control groups was investigated using independent T-test. $P \leq 0.05$ was established as statistical significance.

Results

At baseline, the mineralization value of the control group was 3.65 ± 0.76 and that of the experimental group was 3.35 ± 0.64. There was no significant difference between the two groups (p = 0.35) (Table 1).

Table 1: Baseline mineralized value

Group	N	max	min	$\bar{x}$	SD	p
Experimental group	15	5	2	3.35	0.64	
Control group	15	6	2	3.65	0.76	0.35

After demineralization, the DIAGNOdent pen value of the experimental group (20.55 ± 2.26) and the control group (21.78 ± 4.89) produced similar results (p = 0.48) (Table 2).

Table 2: Mineralized value after demineralization

Group	n	$\bar{x}$	SD	p
Experimental group	15	20.55	2.26	0.48
Control group	15	21.78	4.89	

Differences between these two groups were first identified after remineralization, as shown in Table 3. The index measured for the experimental group and that of the control were 3.90 ± 1.24 and 6.30 ± 1.03 respectively, with a statistical significance of p < 0.01.

Table 3: Mineralized value after remineralization

Group	n	$\bar{x}$	SD	p
Experimental group	15	3.90	1.24	0.000
Control group	15	6.30	1.03	

To compare the measured DIAGNOdent pen values after mineral deposition and post-remineralization, the results in both groups indicated a statistically meaningful difference (p < 0.01), shown in Table 4.

Table 4: Compared mineralized value after demineralization to after treatment

	Group	n	Mean	SD	p
Demineralization-Remineralization	Experimental group	15	16.65	2.59	0.000
	Control group	15	15.47	4.96	0.000

However, the value following mineralization in the control group was significantly more compared with the initial mineralized value (p < 0.01), whereas the group using HMU Fluorinze mouthwash after 20 days did not differ from the original results (p = 0.272) (Table 5).

Table 5: Compared mineralized value after remineralization to the initial period

	Group	n	Mean	SD	p
Remineralization-Beginning	Experimental group	15	0.55	1.49	0.272
	Control group	15	2.65	1.48	0.000

Discussion

In order to create tooth enamel surface lesions similar to dental caries, many authors have used the pH cycle, an experimental method whereby tooth enamel is successively immersed in a demineralizing and then a remineralizing solution, repeating for a certain period of time to form a closed circle. The duration of immersion and the repetitive process between cycles depends on the author and the research purpose [9]. However, the pH cycle requires a solution that has a strict mixing method, which is only available in the laboratory with the appropriate facilities and materials. For the purposes of this study, the mixing portion of the pH cycle was not possible. In this study, the enamel demineralization was performed by Coca-cola immersion (pH = 2.52) for 20 minutes [10, 11].

According to Neel et al., 2016, Coke may lead to demineralization in all, the outermost surface, subsurface and superficial demineralisation. Erosion begins when the acids in soft drinks encounter the tooth enamel, which is the outermost protective layer on your teeth. Their effect is to reduce the surface hardness of the enamel. Moreover, they also effect on the surface and subsurface erosion [12], [13].

The teeth for this research were the extracted teeth of people from 18 to 25 years old, the age group that found a percentage no carbonated soft drink consumption of 20.3%, less than once a day 44.7%, once a day 25.4% and two or more times a day 9.6% [14].

In this experimental study, the investigators used the tooth decay evaluation device, the DIAGNOdent pen 2190, which is a reliable tool for detecting the detection and extent of surface lesions [15]. The principle of using a laser beam for diagnosis relies on the fact that an altered mineralized surface irradiated by a longitudinal light wave emits fluorescent radiation. Diagnodent is a diagnostic device that has a probe that emits light directed on the mineralized surface to be examined. If this surface has some form of structural change, it will emit a fluorescent light that is captured back by the probe and the device will display values ranging from 0 to 99 [16], [17].

The results show that the values measured by the DIAGNOdent for the control group were 3.65 ± 0.76, the research group were 3.35 ± 0.64, demonstrating that all teeth were without enamel damage. After demineralizing with by Coca-cola for 20 minutes, the DIAGNOdent pen value measured by the control group was 21.78 ± 4.89 andthe research group, 20,55 ± 2,26, indicating all teeth were affected. White spots equivalent to clinical a code of 1-2 according to the International Caries Detection and Assessment System (ICDAS). The difference in means between the two groups was not statistically

significant ($p > 0.05$). After 20 days of remineralization, the DIAGNOdent pen value of the control group was 6.30. ± 1.03, the experimental group was 3.90 ± 1.24, all corresponding to that of a sound tooth with a clinical ICDAS code of 0-1. The difference between the experimental and control groups was statistically noticeable ($p < 0.001$). This shows that the mouthwash solution containing Fluoride is more effective at re-mineralizing than the remineralizing solution alone.

Comparing the values of the two groups after post-mineralization with the initial values, the difference in the control group was 18.13 ± 4.48 and the research group was 17.20 ± 2.49 ($p < 0.001$). This result shows the damaging effect of Coca-cola on enamel minerals. Following remineralization, the mineralization value in the control group was 15.48 ± 4.96 and the experimental group, 16.65 ± 2.59, demonstrating a statistically significance difference. ($p < 0.001$). These measured results of the two groups after remineralization comparing to initial value, this difference in the control group was 2.65 ± 1.48 ($p < 0.001$) and the experimental group is 0.55 ± 1.49 ($p > 0.05$). It suggests that if only using a solution with a mineral composition, the enamel lesions will be recovered but will not reach the initial value before mineral destruction. It is suggested that using mouthwash containing Fluoride may recover mineralization level to baseline.

In 2003, Krithikadatta performed a comparison of the re-mineralization efficiency of three Fluoride-containing products, resulting in NaF mouthwash 0.05% treatment of 18.6 ± 0.9 and after 30 days treatment of 10.47 ± 4.1 [18]. The difference between the two time points demonstrated statistical significance, and showed that NaF mouthwash 0.05% was effective in re-mineralizing tooth enamel. the results of this study are also consistent with the results of the Bahrololoomi et al., study in 2013 investigating toothpaste containing 1450 ppm fluoride using the DIAGNOdent pen 2190 to measure mineralized values [19]. Initial value results were 4.04 ± 2.39; after mineral depletion, 11.38 ± 5.95 and following mineral reclamation, 5.48 ± 2.48.

In conclusion, HMU Fluorinze mouthwash demonstrated enamel remineralization; however, the results were not statistically significant for all groupings and comparisons. Further research is required to confirm the remineralization effectiveness of mouthwashes containing fluoride.

Acknowledgements

The authors thank the patients for their agreement to use their teeth for research, the doctors and technicians at 69 Institute for making templates, Decotra joint stock company for mouthwash supply and School of Odonto-Stomatology, Hanoi Medical University for research funding.

References

1. Rošin-Grget K, Peroš K, Šutej I. The cariostatic mechanisms of fluoride. J Acta medica academica. 2013; 42(2):179. https://doi.org/10.5644/ama2006-124.85 PMid:24308397

2. Margolis H, Moreno E. Physicochemical perspectives on the cariostatic mechanisms of systemic and topical fluorides. Journal of dental research. 1990; 69(2):606-613. https://doi.org/10.1177/00220345900690S119 PMid:2179321

3. Brown W, Gregory T, Chow L. Effects of fluoride on enamel solubility and cariostasis. J Caries research. 1977; 11(1):118-141. https://doi.org/10.1159/000260298 PMid:318567

4. Weyant RJ, et al. Topical fluoride for caries prevention: executive summary of the updated clinical recommendations and supporting systematic review. J Am Dent Assoc. 2013; 144(11):1279-91. https://doi.org/10.14219/jada.archive.2013.0057 PMid:24177407 PMCid:PMC4581720

5. Marinho VC, et al. Fluoride mouthrinses for preventing dental caries in children and adolescents. J Cochrane Database of Systematic Reviews. 2016; (7). https://doi.org/10.1002/14651858.CD002284.pub2 PMid:27472005 PMCid:PMC6457869

6. Faller R, Casey K, Amburgey J. Anticaries potential of commercial fluoride rinses as determined by fluoridation and remineralization efficiency. The Journal of clinical dentistry. 2011; 22(2):29-35.

7. Bhongsatiern P, et al. Adjunctive use of fluoride rinsing and brush-on gel increased incipient caries-like lesion remineralization compared with fluoride toothpaste alone in situ. J Acta Odontologica Scandinavica. 2019:1-7. https://doi.org/10.1080/00016357.2019.1582796 PMid:30905242

8. Vo TNN, et al. Efficacy of electrochemically activated water solution in gingivitis treatment. Journal of Pharmaceutical Investigation. 2019; 49(3):323-329. https://doi.org/10.1007/s40005-018-00419-7

9. Nakata T, et al. Effect of a calcium phosphate and fluoride paste on prevention of enamel demineralization. J Dental materials journal. 2017:2016-347.

10. Van Eygen I, Vannet BV, Wehrbein H. Influence of a soft drink with low pH on enamel surfaces: an in vitro study. Am J Orthod Dentofacial Orthop. 2005; 128(3):372-7. https://doi.org/10.1016/j.ajodo.2004.03.036 PMid:16168334

11. Frank C. What Does Soda Do to Your Teeth? 2017. Available from: https://www.healthline.com/health/dental-oral-health/what-does-soda-do-to-your-teeth?fbclid=IwAR3Zgl8EqXxZOFdf1oM7QJIolqam7HUoOXczgLdysRdniUphOWp1J3rFeYg.

12. Abou Neel EA, et al. Demineralization-remineralization dynamics in teeth and bone. International journal of nanomedicine. 2016; 11:4743-4763. https://doi.org/10.2147/IJN.S107624 PMid:27695330 PMCid:PMC5034904

13. Torres CP, et al. Surface and subsurface erosion of primary enamel by acid beverages over time. J Brazilian Dental Journal. 2010; 21:337-345. https://doi.org/10.1590/S0103-64402010000400009 PMid:20976385

14. Pengpid S, Peltzer K. High carbonated soft drink consumption is associated with externalizing but not internalizing behaviours among university students in five ASEAN states. Psychol Res Behav Manag. 2019; 12:585-592. https://doi.org/10.2147/PRBM.S209611 PMid:31534377

PMCid:PMC6681160

15. Sinanoglu A, Ozturk E, Ozel E. Diagnosis of occlusal caries using laser fluorescence versus conventional methods in permanent posterior teeth: a clinical study. Photomedicine and laser surgery. 2014; 32(3):130-137. https://doi.org/10.1089/pho.2013.3625 PMid:24456171

16. Carvalho FBD, et al. Use of laser fluorescence in dental caries diagnosis: a fluorescence x biomolecular vibrational spectroscopic comparative study. J Brazilian Dental Journal. 2013; 24:59-63. https://doi.org/10.1590/0103-6440201302123 PMid:23657415

17. Kouchaji C. Comparison between a laser fluorescence device and visual examination in the detection of occlusal caries in children. The Saudi dental journal. 2012; 24(3-4): p. 169-174. https://doi.org/10.1016/j.sdentj.2012.07.002 PMid:23960547

PMCid:PMC3729294

18. Krithikadatta J, et al. Remineralisation of occlusal white spot lesion with a combination of 10% CPP-ACP and 0.2% sodium fluoride evaluated using Diagnodent: a pilot study. J Oral health. 2013; 11(2):191-196.

19. Bahrololoomi Z, Musavi SA, Kabudan M. In vitro evaluation of the efficacy of laser fluorescence (DIAGNOdent) to detect demineralization and remineralization of smooth enamel lesions. Journal of conservative dentistry. 2013; 16(4):362. https://doi.org/10.4103/0972-0707.114360 PMid:23956542 PMCid:PMC3740651

ID Design Press, Skopje, Republic of Macedonia
Open Access Macedonian Journal of Medical Sciences. 2019 Dec 30; 7(24):4324-4328.
https://doi.org/10.3889/oamjms.2019.384
eISSN: 1857-9655
Basic and Clinical Medical Researches in Vietnam

Clinical Characteristics and Histopathology of Idiopathic Epiretinal Membrane in Vietnam

Nguyen Dinh Ngan[1, 2], Nguyen Van Cuong[1], Nguyen Le Trung[1], Dang Tran Dat[3], Hoang Anh Tuan[3], Pham Ngoc Dong[3], Vu Thi Nga[4], Nguyen Duy Bac[5], Cung Le Xuan[3*]

[1]Department of Ophthalmology, 103 Military Hospital, Hanoi, Vietnam; [2]Department of Ophthalmology, Vietnam Military Medical University, Hanoi, Vietnam; [3]Vietnam National Institute of Ophthalmology, Hanoi, Vietnam; [4]Institute for Research and Development, Duy Tan University, 03 Quang Trung, Danang, Vietnam; [5]Vietnam Military Medical University (VMMU), Hanoi, Vietnam

Citation: Ngan ND, Cuong NV, Trung NL, Dat DT, Tuan HA, Dong PN, Nga VT, Bac ND, Le Xuan C. Clinical Characteristics and Histopathology of Idiopathic Epiretinal Membrane in Vietnam. Open Access Maced J Med Sci. 2019 Dec 30; 7(24):4328-4328. https://doi.org/10.3889/oamjms.2019.384

Keywords: Idiopathic epiretinal membrane; iERM; Histopathology

***Correspondence:** Cung Le Xuan. Vietnam National Institute of Ophthalmology, Hanoi, Vietnam. E-mail: cungvienmat@gmail.com

Received: 03-Sep-2019; **Revised:** 20-Nov-2019; **Accepted:** 21-Nov-2019; **Online first:** 20-Dec-2019

Funding: This research did not receive any financial support

Competing Interests: The authors have declared that no competing interests exist

Abstract

BACKGROUND: Idiopathic epiretinal membrane (iERM) is an avascular proliferation of different types of cells between the posterior vitreous cortex and the internal limiting membrane. That causes visual impairment including blurry, distortion, scotoma. Many studies of iERM were done to describe the clinical characteristics and investigate the histopathology of this disease. Nonetheless, there has not been a study of iERM histopathology in Vietnam.

AIM: To describe clinical characteristics and histopathological results of idiopathic retinal membrane and the association between them.

METHODS: A cross sectional decriptive study of 35 iERMs (33 patients) in Vietnam National Institute of Ophthalmology (VNIO).

RESULTS: High morbidity incidence was in group age >50 years (32/35), female gender (26/35), limited movement works (27/35), and high educational levels (28/35). Distortion was the highest (77.14%), scotoma and floater was less frequent (28.5%, 45.7%). Macular edema in all cases and PVD and exudate were high frequent (65.7%, 62.8%). Symptom duration was 8.2 ± 4.7 months, (1-21 months). Mean of central macular thickness was 468.51 ± 97.24 µm (656-274 µm). Six types of cell were detected, including glial cell (35/35), fibroblast (23/35), myofibroblast (23/35), macrophage (13/35), lymphocyte (5/35) and neutrophil (2/35). The number of cell types in one sample ranged from 1-5 types (2.85 ± 1.28 cell types). Number of cell types were correlated to symptom duration ($r = 0.47$, $p = 0.004$, Pearson's test) and central macular thickness ($r = 0.72$, $p < 0.001$, Pearson's test).

CONCLUSION: There were 6 types of cells in iERM. Glial cell was the most frequent cell, inflammatory cells (macrophage, lymphocyte, neutrophil) was also detected. The number of cell types was stastitically correlated to symptom duration and CMT.

Introduction

Epiretinal membrane (ERM) is described as cellophane maculopathy or macular pucker, which is also a proliferation of avascular cellular between the posterior vitreous membrane and internal limiting membrane (ILM), it causes visual impairments, primarily due to the mechanical distortion of the macular area [1], [2], [3]. Idiopathic epiretinal membrane (iERM) is an ERM in cases there is not any causative factors or ocular pathology was found and its pathophysiology has remained unclear. That membrane contracts to the layers of retina, that due to changing of retinal surface to most of its layers, and causes macular edema [2].

There have been many studies about clinical characteristics and histopathology of the iERM to investigate the pathogenesis of this disease. Clinical characteristics include risk factors, symptom durations, visual impairment such as blurry, distortion, scotoma; and retinal structure change that was

observed by OCT (Optical Coherence Tomography) as central macular thickness (CMT), macular volume (MV) [1], [3], [4], [5]. In histopathology, two components of iERM were usually detected: the proliferative cells (origin or deprivation) and extracellular matrix (collagen, fibronectin) [2], [6], [7], [8], [9]. The proliferative cells were the most important component that formed extracellular matrix, thus always were the main investigated subjects in studies. Some types of cells were often found in iERM, such as glial cell, hyalocyte, retinal pigment epithelium (RPE) cell, macrophage, fibroblast, myofibroblast, and inflammatory cells (macrophage, lymphocyte, neutrophil). The glial cells were the most frequent cells in iERMs which caused a little traction while myofibroblasts were cell type caused significant traction to the retina. Glial cells were included three types of cells: muller cells, astroglia, microglia. These cells formed supported structures that stretched across full thickness of the retina, and were also at the limits of the retina at the OLM and ILM [2]. By using immunohistochemistry, glial cell was proven able to differentiate to other cells (macrophages, fibroblasts, myofibroblasts). On the other side, myofibroblasts (the major cell type in traction iERMs) did not appear in normal human retina. They could be differentiated from Muller cell, hyalocyte or RPE cell [2], [6], [8]. Others cells such as hyalocyte, RPE were only detected in some recent study using immunochemistry. Inflammatory cells were recently detected in iERM, that suggested the inflammatory mechanism in iERM formation [6].

These diversities of the cell types and the cell density in iERMs may be explained by different methods of histopathology (including chemical staining such as Hematoxylin Eosin (HE), Periodic Acid Schiff (PAS), immune marker staining such as immunocytochemistry, immunohistochemistry or detecting by transmission electron microscopy) and small sample sizes of researches (often less than 20 cases) [6], [8], [10]. The other difficult factor for histopathology of iERM was the small size of membrane sample after peeling that was not enough for analyzing. In Viet Nam, the number iERM cases has increased, but there were only few researches about clinical characteristics of iERM based on examinations and OCT imaging. Thus, we did this study to describe clinical characteristics and histopathological results of idiopathic retinal membrane and association between them.

Material and Methods

A cross sectional descriptive study was done in 35 iERM eyes (33 patients) whom were treated with vitrectomy and membrane peeling in Department of Vitreous and Retina, Vietnam National Institute of Ophthalmology (VNIO) from 7/2016-12/2016. The size requirement of the iERM specimens was more than 2 x 2 mm. Then these specimens were histopathologically tested in pathology laboratory of VNIO and were rechecked in laboratory of 103 Military hospital.

Patients with iERM were diagnosed on clinical and OCT at stage 1 or 2 (Gass J.D 1993) [11]. Patients marked the checklist about history of diseases, then an across retinal section image was done by OCT (RTVue-100 Fourier-Domain Optical Coherence Tomography, Optovue, Inc.) to measure CMT, macular volume (MV). After that, 23 G vitrectomy with 3 ways through parsplana trocar with BIOM system was done to obtain the retinal membrane [12]. The epiretinal membrane was stained by Trypan blue (0.5 mL, 0.25%; Fluoron GmbH, Neu-Ulm, Germany) [13]. Then, the membrane was peeled by intraocular forceps, the epiretinal membrane was fixed immediately in 0.9% saline solution to transported to histopathological laboratory. These specimens were flattened on the antiseptic glass slide and dried in alcohol solution several times with decreasing alcohol concentration (100%, 90%, 80%, 70%). Afterwards, that were stained with Hematoxylin-Eosin Y 1% solution in 10 minutes and re-washed with distilled water within 5 minutes. The fixed specimens were checked by optical microscope with different magnifications (x 100, x 200, x 400). The cell density and cell type were identified based on the cell morphology by a histopathologist. A density of cells in specimen was classified to be dense and sparse. The dense density specimens were that there were 10 or more cells in a field with the magnification x 400. The other specimens were sparse density [2].

Statistical analysis

According to statistical methods Medicine by Excel and SPSS 16.0 program (SPSS, Inc., Chicago, IL, USA). In the analysis, the value of $p < 0.05$ as statistically significant.

Results

Clinical characteristics

Thirty-five eyes with iERM of 33 patients (9 men, 24 women) were collected in our study. The ages of our patients were from 38 to 76 years old and two third cases (22 patients) were more than 50 years old. Most of studied cases (25 patients) have limited movement works (who spends more time for sitting than moving) and 26 patients have high educational level (beyond high school).

Distortion was the highest ratio in each group of visual acuity and overall (77.1%). Scotoma and floater are less frequent (28.5%, 45.7%). In patients with high visual acuity (> 20/100), the symptoms were

easier to be realized (Table 1).

Table 1. Distribution of symptom by visual acuity

Visual acuity	Distortion	Scotoma	Floater
≤ 20/100 (n = 25)	17 (68.4%)	3 (8.6%)	7(28.1%)
20/100 – 20/40 (n = 9)	9 (100%)	7 (77.3%)	8 (88.4%)
≥ 20/40 (n = 1)	1 (100%)	0	1 (100%)
Total	27 (77.1%)	10 (28.5%)	16 (45.7%)

ME were in all of cases (100%), PVD and exudate were high frequent in iERM (65.7% and 62.8% respectively). There was only one case of RH in our study group (Table 2).

Table 2: Distribution of signs by iERM grade

Grade	ME	PVD	RH	Exudate
1 (n = 6)	*6 (100%)*	3 (50 %)	0 (0%)	4 (66.6%)
2 (n = 29)	*29 (100%)*	20 (68.9%)	1 (2.4%)	18 (62.1%)
Total	*35 (100%)*	23 (65.7%)	1 (2.8%)	22 (62.8%)

ME: macular edema; PVD: posterior vitreous detachment; RH: retinal hemorrhage.

Up to surgery time, symptom duration was from 1 to 21 months (8.2 ± 4.7 months). Mean of CMT was 468.51 ± 97.24 µm (656-274 µm). The details of distribution of symptom duration and central macular thickness in study patients were shown in Figure 1, and Figure 2.

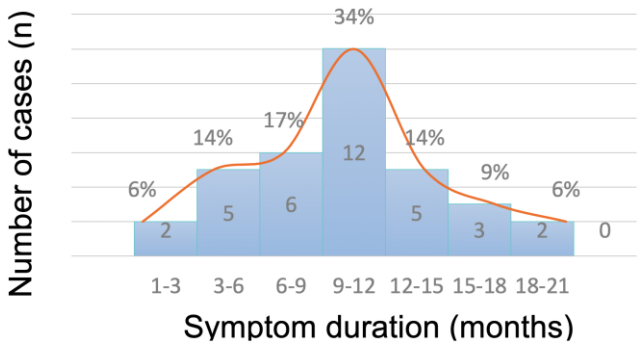

Figure 1: Distribution of symptom duration of iERM

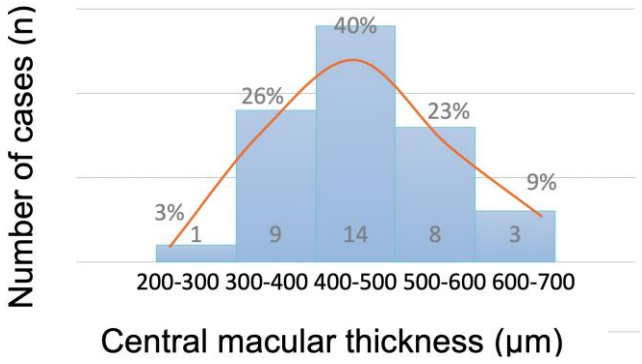

Figure 2: Distribution of central macular thickness in OCT

Histopathological results

There were 12 cases with sparse density A) and 23 cases with dense density B) (Figure 3).

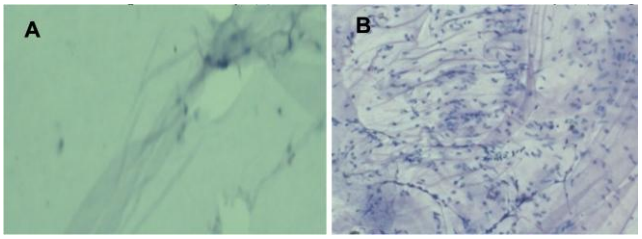

Figure 3: A) sparse density; B) dense density

The number of cell types ranged from 1 to 5 types of cells in one sample (average 2.8 ± 1.2 types of cells). There were statistically a greater number of cell types in dense density group (4.7 ± 2.1) than sparse density group (2.2 ± 1.1) (p = 0.02).

There were 6 types of cells in iERMs samples, including glial cell, contractile cells (myofibroblast, fibroblast), inflammatory cells (macrophage, lymphocyte, neutrophil) (Figure 4).

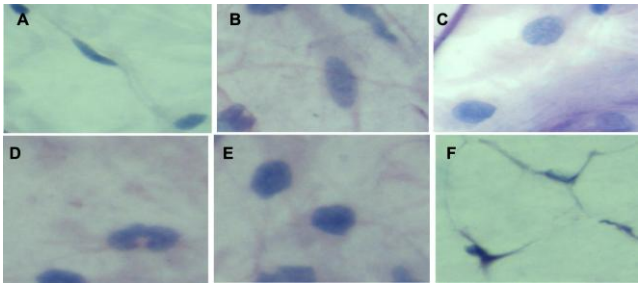

Figure 4: The cell types in our study sample; A) fibroblast; B) myofibroblast; C) macrophage; D) neutrophil; E) lymphocyte; F) glial cell

Glial cell was the most popular cell type (35/35 samples) that must have proved the important role of this cell in the mechanism of iERM. Fibroblast was the second frequent type of cell in 23 specimens (65.7%). Myofibroblasts was detected in 23 cases (65.7%). Macrophage was detected in 13 cases (37.2%). Lymphocyte was detected only in 5 cases (16.7%). Neutrophil was detected in only 2 cases in our study. The cells of connective tissue (glial cell, fibroblast, myofibroblast) were the main part of iERM which were detected in most samples. Otherwise, the inflammatory cells (macrophage, lymphocyte, neutrophil) just appeared in few samples with high number of cell types (from 3 cell types in a sample) (Table 3).

Table 3: Distribution of cell types in a sample

	Number of cell types in a sample				
Cell type	1 (n = 7)	2 (n = 7)	3 (n = 8)	4 (n = 10)	5 (n = 3)
Glial cell	7	7	8	10	3
Fibroblast	0	6	6	8	3
Myofibroblast	0	6	7	8	2
Macrophage	0	0	2	9	2
Lymphocyte	0	0	0	2	3
Neutrophil	0	0	0	0	2

Association between clinical characteristics and histopathology

We had looked for the association between histopathology and some of symptoms and sign of

iERMs in our patients. We found that number of cell types in a sample correlated to symptom duration (r = 0.47, p = 0.004, Pearson's test) and to central macular thickness was statistically significant (r = 0.72, p < 0.001, Pearson's test) (Figure 5).

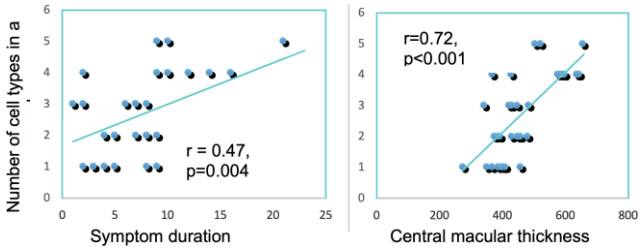

Figure 5: Association between number of cell types in a sample and symptom duration and central macular thickness

Discussion

The distortion was the most frequent iERM symptoms (77.1%) in our patients. This symptom is a manifestation of macular edema as a result of ERM. When the ERM contracted to the layers of macular, it changed the macular structure and made the fluid appear in the extra layers. Thus, after peeling this membrane, the distortion was standard criteria to assessment of surgery outcome [4]. There was macular edema in OCT images in all 35 eyes of our study, so the distortion was more specific symptom than others such as floater, scotoma or blurry and may be used for screening ERM. However, this symptom depends crucially on visual acuity, there were all ten eyes (100%) with visual acuity above 20/200 having the symptom of distortion, but there were only 17 eyes (68.4%) in poor vision group (visual acuity was lower than 20/200).

The manifestation of macular edema in higher level is scotoma. When the edema lasted long time and the function of retinal photoreceptor cells was damaged, the symptom of scotoma appeared. The other reason of scotoma in ERM is the thick membrane over the retina. If the scotoma was in the center or enlarged, visual acuity also decreased making difficult to clinically detect this symptom. This characteristic explained why there were only 10 eyes (28,5%) having scotoma in our study, and most of them (7 eyes) was in group with visual acuity from 20/200 to 20/40.

Central macular thickness (CMT) is quantitative measure of macular edema in OCT. It was an important factor in the pathophysiology of iERM and directly affected vision and other visual functions [5]. In our study, the average of CMT (468.51 µm) was higher than previous studies, which can be explained by the fact that all iERM eyes had been prepared to operate and were in severe stage of disease [14].

In this study, 6 cell types were detected, including glial cell (35/35), fibroblast (23/35), myofibroblast (23/35), macrophage (13/35), lymphocyte (5/35) and neutrophil (2/35). Glial cells was most frequent detected, its collagen was also the important formation of iERM [15]. The importance of these cells in iERM formation had been proven by many researches [16], [17], [18],[15]. However, the subtype of glial cells (Müller cells, astrocytes...) that was the major cell type in iERMs have been controversial. A recent study that used immunohistochemical staining for glutamine synthetase (GS) (expressed specifically in Müller cells and did not appear in astrocytes) on surgically excised iERMs showed the characteristics of continuous, isodense pattern of immunoreactivity for GS. This result proved that Müller cell was the predominant cell type for iERM formation [15]. Using HE staining, this study did not find any other cells such as hyalocyte, astrocyte, retinal pigment epithelium. Fibroblast and myofibroblast which could produce fibril forming the membrane and cause significant traction to the retina were also major component cell in iERMs [6], [8]. These cells that normally did not appear in retina might be differentiated from hyalocytes, glial cell – normal cell in retina. In our study, there were 27 samples in 35 iERMs having this contractile cell (myofibroblast, fibroblast or both of them). This result explained why the CMT in OCT of the study eyes was higher than that in previous studies.

Inflammatory cells (macrophage, lymphocyte, neutrophil) were detected in 14 samples. When comparing the iERMs with inflammatory cell to the sign of retinal hard exudate, we found the significantly statistic correlation ($p < 0.05$, Chi-Square test). Hard exudative was lipoprotein structure that appeared intra retina as a consequence of increased retinal vascular permeability in inflammation. There were 22 eyes with retinal hard exudate with twelve iERMs having inflammatory cell, that may demonstrate the role of inflammation in iERMs mechanism. Some studies also proved the inflammation mechanism in pathophysiology of iERMs [6].

Number of cell types in a sample was different in studies, it ranged from 2 to 4 cell types in Bu S.C. research (2014), 2-3 cell types in Wang L.C. research (2015), 1-4 cell types in Marie Ueki [2], [19], [20]. This difference may be explained due to the method of histopathology. Most studies used HE staining to classified the type of cells and used immunohistochemistry to re-confirm. However, the identification of cells using immunohistopathology method depended on available specific marker and usually used to find out the cell origin. Some specific markers that were often used were glial fibrillary acidic protein (GFAB), vimentin, cellular retinaldehyde-binding protein (CRDLBP), Kir4.1, CD 45, CD 64, CD 168, pan cytokeratin, neurofilament [2], [6], [6], [17]. The cell types in iERM sample could be divided to 3

groups: the original glial cells, the secondary cells (fibroblast and myofibroblast) and others, and inflammatory cells. In our study, using HE staining images identification, there were 6 cell types and maximum 5 cell types in a sample. Looking for the association between histopathology results and some signs and symptoms, we only found the correlation between number cell type and symptom duration ($r = 0.47$, $p = 0.004$, Pearson's test), and CMT ($r = 0.72$, $p < 0.001$, Pearson's test).

The cell types in iERMs of the study were only identified by the cell morphology in HE staining, so it may not be very accurate in cell type classification and origin. The immunohistochemistry should be used to recognize exactly the origin and the type of cells.

In conclusion, our study found that the most frequent symptom of iERM was distortion and the CMT was 468.51 ± 97.24 µm (656-274 µm). In histopathology result, the cell density was higher in dense group (> 10 cells/field 40 x). There were 6 different cell types, including glial cell (35/35), fibroblast (23/35), myofibroblast (23/35), macrophage (13/35), lymphocyte (5/35) and neutrophil (2/35). The number of cell types in a sample was from 1 to 5 and it correlated to CMT and symptom duration.

Ethical approval

All procedures performed in studies involving human participants were in accordance with the ethical standards of institutional and/or national research committee and with the 1964 Helsinki declaration and its later amendments or comparable ethical standards. This study was approved by the institutional ethical review board of Vietnam National Institute of Ophthalmology.

Informed Consent

Informed consents were obtained from the patients included in the study.

Reference

1. Folk JC, Adelman RA, Flaxel CJ, Hyman L, Pulido JS, Olsen TW. Idiopathic epiretinal membrane and vitreomacular traction Preferred Practice Pattern® Guidelines. Ophthalmology. 2016; 123(1):P152-81. https://doi.org/10.1016/j.ophtha.2015.10.048 PMid:26578445

2. Bu SC, et al. Idiopathic epiretinal membrane. Retina. 2014; 34(12):2317-2335. https://doi.org/10.1097/IAE.0000000000000349 PMid:25360790

3. Appiah AP, Hirose T, Kado M. A review of 324 cases of idiopathic premacular gliosis. American journal of ophthalmology. 1988; 106(5):533-535. https://doi.org/10.1016/0002-9394(88)90581-8

4. Arimura E, et al. Retinal contraction and metamorphopsia scores in eyes with idiopathic epiretinal membrane. Investigative ophthalmology & visual science. 2005; 46(8):2961-2966. https://doi.org/10.1167/iovs.04-1104 PMid:16043872

5. Watanabe K, et al. Outer retinal morphology and visual function in patients with idiopathic epiretinal membrane. JAMA ophthalmology. 2013; 131(2):172-177. https://doi.org/10.1001/jamaophthalmol.2013.686 PMid:23411882

6. Joshi M, Agrawal S, Christoforidis JB. Inflammatory mechanisms of idiopathic epiretinal membrane formation. Mediators of inflammation. 2013; 2013. https://doi.org/10.1155/2013/192582 PMid:24324293 PMCid:PMC3844245

7. Kampik A, et al. Ultrastructural features of progressive idiopathic epiretinal membrane removed by vitreous surgery. American journal of ophthalmology. 1980; 90(6):797-809. https://doi.org/10.1016/S0002-9394(14)75195-5

8. Kohno R, et al. Possible contribution of hyalocytes to idiopathic epiretinal membrane formation and its contraction. British Journal of Ophthalmology. 2009; 93(8):1020-1026. https://doi.org/10.1136/bjo.2008.155069 PMid:19429593

9. Smiddy WE, et al. Idiopathic epiretinal membranes: ultrastructural characteristics and clinicopathologic correlation. Ophthalmology. 1989; 96(6):811-821. https://doi.org/10.1016/S0161-6420(89)32811-9

10. Smiddy WE, et al. Histopathology of tissue removed during vitrectomy for impending idiopathic macular holes. American journal of ophthalmology. 1989; 108(4):360-364. https://doi.org/10.1016/S0002-9394(14)73301-X

11. Gass JDM, Blodi BA. Idiopathic juxtafoveolar retinal telangiectasis: update of classification and follow-up study. Ophthalmology. 1993; 100(10):1536-1546. https://doi.org/10.1016/S0161-6420(93)31447-8

12. De Bustros S, et al. Vitrectomy for idiopathic epiretinal membranes causing macular pucker. British Journal of Ophthalmology. 1988; 72(9):692-695. https://doi.org/10.1136/bjo.72.9.692 PMid:3179258 PMCid:PMC1041558

13. Yoon HS, et al. Ultrastructural features of tissue removed during idiopathic macular hole surgery. American journal of ophthalmology. 1996; 122(1):67-75. https://doi.org/10.1016/S0002-9394(14)71965-8

14. Massin P, et al. Optical coherence tomography of idiopathic macular epiretinal membranes before and after surgery. American journal of ophthalmology. 2000; 130(6):732-739. https://doi.org/10.1016/S0002-9394(00)00574-2

15. Messmer EM, Heidenkummer HP, KampikA. Ultrastructure of epiretinal membranes associated with macular holes. Graefe's archive for clinical and experimental ophthalmology. 1998; 236(4):248-254. https://doi.org/10.1007/s004170050072 PMid:9561355

16. Wiznia RA. Posterior vitreous detachment and idiopathic preretinal macular gliosis. American journal of ophthalmology. 1986; 102(2):196-198. https://doi.org/10.1016/0002-9394(86)90144-3

17. Kampik A. Pathology of epiretinal membrane, idiopathic macular hole, and vitreomacular traction syndrome. Retina. 2012; 32:S194-S199. https://doi.org/10.1097/IAE.0b013e31825bc20a PMid:22929320

18. Dugas B, et al. Idiopathic epiretinal macular membrane and cataract extraction: combined versus consecutive surgery. American journal of ophthalmology. 2010; 149(2):302-306. https://doi.org/10.1016/j.ajo.2009.09.011 PMid:20103056

19. Ueki M, Morishita S, Kohmoto R, Fukumoto M, Suzuki H, Sato T, Kobayashi T, Kida T, Oku H, Ikeda T, Shibayama Y. Comparison of histopathological findings between idiopathic and secondary epiretinal membranes. International ophthalmology. 2016; 36(5):713-8. https://doi.org/10.1007/s10792-016-0194-7 PMid:26857724

20. Wang LC, et al. Assessment of retinal pigment epithelial cells in epiretinal membrane formation. Journal of the Chinese Medical Association. 2015; 78(6):370-373. https://doi.org/10.1016/j.jcma.2015.01.003 PMid:25708821

ID Design Press, Skopje, Republic of Macedonia
Open Access Macedonian Journal of Medical Sciences. 2019 Dec 30; 7(24):4329-4332.
https://doi.org/10.3889/oamjms.2019.385
eISSN: 1857-9655
Basic and Clinical Medical Researches in Vietnam

Saprochaete Capitata Infection in an 80–Year Old Chronic Obstructive Pulmonary Disease (COPD) Patient: A Case Report

Pham Ngoc Duan[1, 2], Nguyen Nhu Hung[3], Phong Tran Nhu[4], Chu Dinh Thien[5], Quang Canh Tran[6*]

[1]Department of Parasitology, Hanoi Medical University, Hanoi, Vietnam; [2]Department of Microbiology and Parasitology, Hanoi Medical University Hospital, Hanoi, Vietnam; [3]Department of Microbiology, 74 Hospital, Phuc Yen, Vinh Phuc, Vietnam; [4]Faculty of Nursing, Dainam University, Hanoi, Vietnam; [5]Institute for Research and Development, Duy Tan University, 03 Quang Trung, Danang, Vietnam; [6]Center for Hygiene and Food Safety, Haiduong Medical Technical University, Hai Duong, Vietnam

Citation: Duan PN, Hung NN, Nhu PT, Thien CD, Tran QC. Saprochaete Capitata Infection in an 80–Year Old Chronic Obstructive Pulmonary Disease (COPD) Patient: A Case Report. Open Access Maced J Med Sci. 2019 Dec 30; 7(24):4329-4332. https://doi.org/10.3889/oamjms.2019.385

Keywords: Saprochaete capitata; COPD; Fluconazole

***Correspondence:** Quang Canh Tran. Center for Hygiene and Food Safety, Haiduong Medical Technical University, Hai Duong, Vietnam. E-mail: tranquangcanh68@gmail.com

Received: 04-Sep-2019; **Revised:** 20-Nov-2019; **Accepted:** 21-Nov-2019; **Online first:** 20-Dec-2019

Funding: This research did not receive any financial support

Competing Interests: The authors have declared that no competing interests exist

Abstract

BACKGROUND: The fungal disease caused by invasive fungus *Saprochaete capitata* is becoming an increasingly popular infection. Fungal pathogens mainly occur in patients with immunocompromised disorders such as hematologic malignancies, acute myeloid leukemia, transplant patients.

CASE REPORT: In this study, we presented a COPD patient infected with *S. capitata*. At the first check, the patient showed cough, dyspnea, chest pain on both sides. The clinical laboratory test result was characterized with high White blood cell (12.8 G/L), HIV negative. The X ray showed bronchitis and emphysema. Bronchoscopy illustrated bronchial mucositis. CT scanner demonstrated pneumonia with fuzzy nodular lesions and thick interstitial organization in both lungs. The patient was treated with ciprofloxacin 800 mg/day; cefuroxime 2250 mmg/day. However, the fever appeared 2 weeks thereafter. The *S. capitata* was discovered in the bronchial fluid. The patient was then treated with fluconazole 400 mg/day for 14 days. At the end of treatment, all signs and symptoms of *S. capitata* infection disappeared and the patient recovered.

CONCLUSION: This case study showed that *S. capitata* infection can occur in the COPD patients and fluconazole is a pertinent drug for treatment of the infection.

Introduction

Candida and *Aspergillus* spp. are mainly the causes of invasive fungal infections in hospitals. However, infection with rare fungal pathogens has become more popular in recent years. Infections caused by *Saprochaete capitata* are one of the emerging diseases. *S. capitata*, previously known as *Geotrichum capitatum, Trichosporon capitatum, Blastoschizomyces capitatus, Dipodascus capitatus*, is a non-fermentative, urease-negative ascomycetous yeast classified in Saccharomycetaceae family [1], [2], [3], [4], [5], [6], [7]. *S. capitata* fungus grows well in the Saboraud agar, their colonies are similar to yeast, but their morphology characterizes with long and short segments with different sizes. This fungus is mainly found in natural environments such as soil, sand and wood pulp [8]. In addition, it has also been found in poultry feces, gastrointestinal tract, respiratory tract, and is a part of the normal microflora of human skin [9]. They are known as the fungi that live in the respiratory tract and digestive tracts of humans, they are invasive pathogens like other yeast species [10].

S. capitata infection is mainly seen in patients with neutrophil leukemia (87%), more rarely in patients with other non-hematological diseases such as diabetes, neuralgia, organ transplantation and inflammations [11] (Table 1). In this report, we described a case of fungal infection caused by *S. capitata* in COPD patients.

Table 1: Some report cases cause by *Saprochaete capitata*

No.	Case	Age	Symptoms/ problems	Treatment	References
1	Acute myeloid leukemia	41	Erythema, high fever	caspofungin and liposomal amphotericin B	[12]
2	Kidney transplant	82	hypertensive nephrosclerosis	liposomal amphotericin B	[13]
3	Burkitt lymphoma	74	fever and central nervous system	fluconazole and caspofungin	[12]
4	Acute myeloid leukemia	57	Fever, diarrhoea and skin rash	levofloxacin fluconazole	[14]
5	Pneumonia, asthama	86	shortness of breath, productive cough and fatigue	itraconazole	[15]

Clinical Case

An 80-year-old man was diagnosed with COPD and Gout 10 years ago. The patient came to the hospital with productive cough, dyspnea, chest pain on both sides a week before. Examination revealed symptoms including vesicular breathing, coarse crackle and wheeze in both lungs, no hypertension, non-diabetic, no fever. The laboratory blood test results were: Red blood cell 4.36 T/L, hematocrit 138 g/l, White blood cell 12.8 G/L (Lymphocyte 17.4% and Granulocyte 74.1%), HIV negative, Genxpert DPG (-), AFB (-). The X-ray showed bronchitis and emphysema. Bronchoscopy illustrated bronchial mucositis (Figure 1).

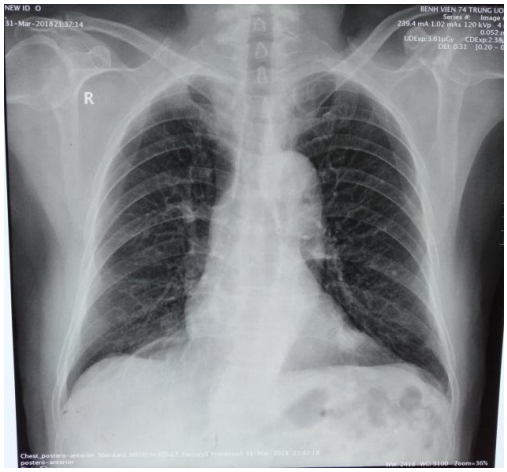

Figure 1: X – ray of patient before treatment

CT scanner demonstrated the pneumonia with fuzzy nodular lesions and thick interstitial organization in both lungs (Figure 2). The patient was treated with ciprofloxacin 800mmg/day; cefuroxime 2250 mmg/day; ventolin 40mg/ day; pulmicort 500mg; salbutamol 16mg/ day.

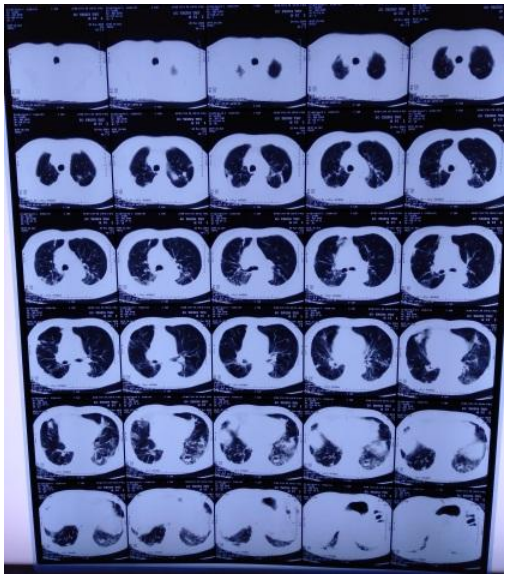

Figure 2: CT scan of the patient before treatment

After 2 weeks, cough and shortness of breath decreased, fever, however, developed. The patient was then treated with methylprednisolon 40 mg per day for 7 days. After the cease of drug, fever again developed. Therefore, the patient was treated with raxadin 2000 mmg + moxifloxacin 400 mmg + doxycyclin 1000 mmg per day for another 7 days. The patient was still feverish, tired, screeching and snoring was in both sides of the lung. The phlegm of patient was sampled and cultured to find fungi. *S. capitate* was detected by semi-automatic Vitek system (Figure 3 and 4), the blood cultured showed negative.

Figure 3: Saprochaete capitata on SAB media at 72 hour at 37°C

After 14 days of treatment with fluconazol 400 mg per day, the patient recovered and all the symptoms disappeared. The phlegm cultured showed negative.

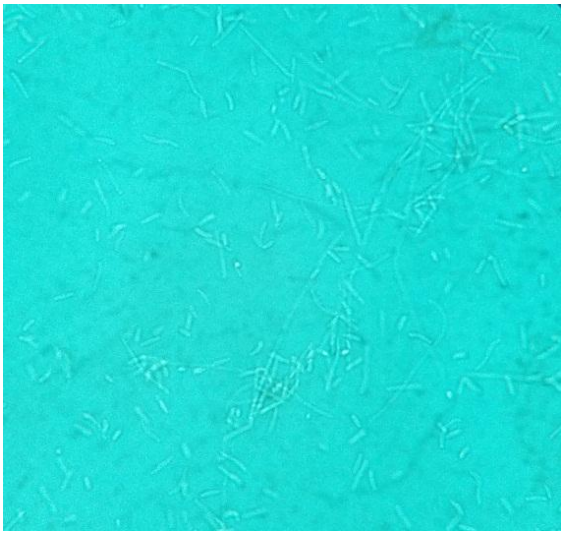

Figure 4: Saprochaete capitata staining with lactophenol cotton blue under microscope (X 400)

Discussion

Saprochaete capitata has determined considerable taxonomic evaluation [16]. Evaluation of this fungus under microscopy showed the septal pores and cell wall structurewith lots of arthroconidia and few blastoconidia [1]. In our case, *S. capitata* grow well on the Saboraud agar at 37°C, the colonies are similar to those of yeast. However, it is, with different dimensions of segments under microscope (Figure 4), similar to the filamentous fungi. Conventionally, detection of these fungi in the culture medium basing on their morphology is an important diagnosis. Using automatic or semi-automatic system may be a great choice. The Vitek 2 system version 07.01 was used to confirm *S. capitata*. This system has been shown to possess an accuracy rate of 98%. Besides, D 32C (bioMérieux), and RapID Yeast Plus (Innovative Diagnostic Systems) systems also were applied to diagnosis of this fungus [17], [18]. Unfortunately, their mophology is very similar to that of *S. clavata* [17].

S. capitata infection is becoming an emerging disease, particularly in immunocompromised such as haematological malignancies, asscociated cancer and onychomycosis [19]. Factors such as extended neutropenia, active chemotherapy, broad-spectrum antibiotics use and reduced local defense system by breaking down the skin and mucosa were mainly beneficial factors for this infection [20]. The haematological malignancy including acute leukemia is the disease in the most popular patients and estimated incidence is around 0.5% [1], [21]. Extremely, all of breaking through infections with acute leukemia developed in patients who were in intentive chemotherapy [1]. Moreover, broad spectrum antibiotic was used for treatment of all patients who developed neutropenic fever. The 30-day mortality is 30 days it related with invasive disease ranges from 60 – 80% [1]. In this case, the patient was treated with two antibioticsfor 14 days. The symptoms decrease at the end of antibiotic treatment. However, the patient appeared fever in the afternoon. This case indicates the antibiotics ciprofloxacin and cefuroxime are not really effective with S. capitata. Positive blood culture was found in almost of case infection with 77.3%. While our case showed negative in blood culture. The pneumonia in S. capitata usually associated in haematological malignancies or multiple diseases. It could make the infection becomes more severse [15].

The in vitro study of susceptibility *S. capitata* is quite weak. Published literature showed that *S. capitata* is susceptible to flucytosine (MIC values 0.25-0.5 mg/mL), itraconazole (MIC values 0.12-0.50 mg/mL), voriconazole (MIC values 0.25-0.5 mg/mL) and posaconazole (MIC values 0.03-0.25 mg/mL). However, these organisms are less susceptible to fluconazole with a MIC between 16 and 32 mg/mL in most studies [3], [22], [23]. Amphotericin B was effective in inhibition of these fungus only with high concentration (MIC values 0.5-2.0 mg/mL) [24]. *S. capitata* was demonstrated to intrinsically resist to echinocandins [25]. Girmenia et al. reported that amphotericin B, flucytosine, fluconazole, itraconazole, and voriconazole hadhigh efficacy against *S. capitata* isolates. Other authors indicated that amphotericin B and voriconazole were more potent than other drugs in inhibition of *S. capitata* [23]. In these cases, demonstrated *S. capitata* reduce susceptive to anidulafungin at 8 mg/mL MIC value as expected. Fluconazole is less effective than itraconazole, voriconazole and azoles against *S. capitata*. The data of optimal treatment to *S. capitata* infection is not enough. In this infection indicated use of amphotericin B alone or in combination with flucytosine is a quality treatment. *S. capitata* infection treat with fluconazole and echinocandins were also quite good choice. Breakthrough infections of *S. capitata* reported in neutropenic patients collected echinocandins [7], [26], [27]. In our case, *S. capitata* was effectively treated with fluconazole 400 mg/day per 14 days, but it is need more evidence of MIC value. This case also demonstrates that antibiotic treatment of this infection only reduces some symptoms, but it is unable to thoroughly treat the infection. Identification of fungi is the most important for diagnosis and treatment.

In conclusion, *S. capitata* infected mostly to haematological malignancies patients, also with immunosuppressive and immunocompetent patients. In this case, the COPD patient was infected with *S. capitata*, treated with fluconazole 400 mg/day. The signs and symptoms disappeared after 2 weeks. The MIC of *S. capitata* should be do in the further study.

References

1. Girmenia C, et al. Invasive infections caused by Trichosporon species and Geotrichum capitatum in patients with hematological malignancies: a retrospective multicenter study from Italy and review of the literature. J Clin Microbiol. 2005; 43(4):1818-28. https://doi.org/10.1128/JCM.43.4.1818-1828.2005 PMid:15815003 PMCid:PMC1081342

2. Kremery V, Krupova I, Denning DW. Invasive yeast infections other than Candida spp. in acute leukaemia. J Hosp Infect; 1999; 41(181). https://doi.org/10.1016/S0195-6701(99)90015-4

3. Martino R, et al. Blastoschizomyces capitatus infection in patients with leukemia: report of 26 cases. Clin Infect Dis. 2004; 38(3):335-41. https://doi.org/10.1086/380643 PMid:14727202

4. Pemmaraju N, et al. Disseminated Saprochaete capitata (formerly known as Geotrichum capitatum and Blastoschizomyces capitatus) in a patient with acute myeloid leukemia. Eur J Haematol. 2014; 93(6):543-4. https://doi.org/10.1111/ejh.12303 PMid:24592915

5. Miceli MH, Diaz JA, Lee SA. Emerging opportunistic yeast infections. Lancet Infect Dis. 2011; 11(2):142-51. https://doi.org/10.1016/S1473-3099(10)70218-8

6. Lafayette TC, et al. Dipodascus capitatus (Geotrichum capitatum): fatal systemic infection on patient with acute myeloid leukemia. Rev Soc Bras Med Trop. 2011; 44(5):648-50.

https://doi.org/10.1590/S0037-86822011000500028 PMid:22031088

7. Ozkaya-Parlakay A, et al. Geotrichum capitatum septicemia in a hematological malignancy patient with positive galactomannan antigen: case report and review of the literature. Turk J Pediatr. 2012; 54(6):674-8.

8. Arendrup MC, et al. ESCMID and ECMM joint clinical guidelines for the diagnosis and management of rare invasive yeast infections. Clin Microbiol Infect. 2014; 20(3):76-98. https://doi.org/10.1111/1469-0691.12360 PMid:24102785

9. Bouza E, Munoz P. Invasive infections caused by Blastoschizomyces capitatus and Scedosporium spp. Clin Microbiol Infect. 2004; 10(1):76-85. https://doi.org/10.1111/j.1470-9465.2004.00842.x PMid:14748804

10. Birrenbach T, et al. Emergence of Blastoschizomyces capitatus yeast infections, Central Europe. Emerg Infect Dis. 2012; 18(1):98-101. https://doi.org/10.3201/eid1801.111192 PMid:22261201 PMCid:PMC3310123

11. Cavanna C, et al. Fungemia due to Saprochaete capitata in a non-neutropenic patient hospitalized in an intensive care unit after cardiac surgery. J Mycol Med. 2017; 27(2):281-284. https://doi.org/10.1016/j.mycmed.2017.01.014 PMid:28302347

12. Garcia-Ruiz JC, et al. Invasive infections caused by Saprochaete capitata in patients with haematological malignancies: report of five cases and review of the antifungal therapy. Rev Iberoam Micol. 2013; 30(4):248-55. https://doi.org/10.1016/j.riam.2013.02.004 PMid:23583265

13. Hajar Z, Medawar W, Rizk N. Saprochaete capitata (Geotrichum capitatum), an emerging fungal infection in kidney transplant recipients. J Mycol Med. 2018; 28(2):387-389. https://doi.org/10.1016/j.mycmed.2018.04.005 PMid:29709266

14. Schuermans C, et al. Breakthrough Saprochaete capitata infections in patients receiving echinocandins: case report and review of the literature. Med Mycol. 2011; 49(4):414-8. https://doi.org/10.3109/13693786.2010.535179 PMid:21105848

15. Tanabe MB, Patel SA. Blastoschizomyces capitatus pulmonary infections in immunocompetent patients: case report, case series and literature review. Epidemiol Infect. 2018; 146(1):58-64. https://doi.org/10.1017/S0950268817002643 PMid:29198203

16. De Hoog GS, Smith MT. Ribosomal gene phylogeny and species delimitation in Geotrichum and its telemorphs. Stud Mycol. 2004; 50:489-515.

17. Desnos-Ollivier M, et al. Misidentification of Saprochaete clavata as Magnusiomyces capitatus in clinical isolates: utility of internal transcribed spacer sequencing and matrix-assisted laser desorption ionization-time of flight mass spectrometry and importance of reliable databases. J Clin Microbiol. 2014; 52(6):2196-8. https://doi.org/10.1128/JCM.00039-14 PMid:24696028 PMCid:PMC4042774

18. Kolecka A, et al. Identification of medically relevant species of arthroconidial yeasts by use of matrix-assisted laser desorption ionization-time of flight mass spectrometry. J Clin Microbiol. 2013; 51(8):2491-500. https://doi.org/10.1128/JCM.00470-13 PMid:23678074 PMCid:PMC3719645

19. Savini V, et al. Multidrug-resistant Geotrichum capitatum from a haematology ward. Mycoses. 2011; 54(6):542-3. https://doi.org/10.1111/j.1439-0507.2010.01894.x PMid:20492528

20. Ersoz G, et al. An outbreak of Dipodascus capitatus infection in the ICU: three case reports and review of the literature. Jpn J Infect Dis. 2004; 57(6):248-52.

21. Christakis G, et al. Fatal Blastoschizomyces capitatus sepsis in a neutropenic patient with acute myeloid leukemia: first documented case from Greece. Mycoses. 2005; 48(3):216-20. https://doi.org/10.1111/j.1439-0507.2005.01098.x PMid:15842341

22. D'Antonio D, et al. Emergence of fluconazole-resistant strains of Blastoschizomyces capitatus causing nosocomial infections in cancer patients. J Clin Microbiol. 1996; 34(3):753-5. https://doi.org/10.1128/JCM.34.3.753-755.1996 PMid:8904454 PMCid:PMC228886

23. Girmenia C, et al. In vitro susceptibility testing of Geotrichum capitatum: comparison of the E-test, disk diffusion, and Sensititre colorimetric methods with the NCCLS M27-A2 broth microdilution reference method. Antimicrob Agents Chemother. 2003; 47(12):3985-8. https://doi.org/10.1128/AAC.47.12.3985-3988.2003 PMid:14638517 PMCid:PMC296229

24. Subramanya Supram H, et al. Emergence of Magnusiomyces capitatus infections in Western Nepal. Med Mycol. 2016; 54(2):103-10. https://doi.org/10.1093/mmy/myv075 PMid:26483432

25. Domenico D'Antonio FR, Lacone A, Violante B, Fazii P, Pontieri E, Staniscia T, Caracciolo C, Bianchini S, Sferra R, Vetuschi A, Eugenio Gaudio, Giuseppe Carruba, Onychomycosis Caused byBlastoschizomyces capitatus. J Clin Microbiol. 1999; 37(2927). https://doi.org/10.1128/JCM.37.9.2927-2930.1999 PMid:10449477 PMCid:PMC85415

26. Chittick P, et al. Case of fatal Blastoschizomyces capitatus infection occurring in a patient receiving empiric micafungin therapy. Antimicrob Agents Chemother. 2009; 53(12):5306-7. https://doi.org/10.1128/AAC.00710-09 PMid:19738005 PMCid:PMC2786321

27. Espinel-Ingroff A. In vitro activity of the new triazole voriconazole (UK-109,496) against opportunistic filamentous and dimorphic fungi and common and emerging yeast pathogens. J Clin Microbiol. 1998; 36(1):198-202. https://doi.org/10.1128/JCM.36.1.198-202.1998 PMid:9431946 PMCid:PMC124833

ID Design Press, Skopje, Republic of Macedonia
Open Access Macedonian Journal of Medical Sciences. 2019 Dec 30; 7(24):4333-4336.
https://doi.org/10.3889/oamjms.2019.386
eISSN: 1857-9655
Basic and Clinical Medical Researches in Vietnam

Cone Beam Computed Tomography Application in Finding Ectopic Tooth: A Systemic Analysis and a Case Report

Vo Truong Nhu Ngoc[1], Le Quynh Anh[1], Nguyen Minh Duc[1, 2], Thien Chu Dinh[3], Toi Chu Dinh[4*]

[1]School of Odonto Stomatology, Hanoi Medical University, Hanoi, Vietnam; [2]Division of Research and Treatment for Oral Maxillofacial Congenital Anomalies, Aichi Gakuin University, Nagoya, Japan; [3]Institute for Research and Development, Duy Tan University, 03 Quang Trung, Danang, Vietnam; [4]Department of Human and Animal Physiology, Faculty of Biology, Hanoi National University of Education, Hanoi, Vietnam

Citation: Ngoc VTN, Anh LQ, Duc NM, Chu Dinh T, Chu Dinh T. CONE BEAM COMPUTED TOMOGRAPHY Application in Finding Ectopic Tooth: A Systemic Analysis and a Case Report. Open Access Maced J Med Sci. 2019 Dec 30; 7(24):4333-4336. https://doi.org/10.3889/oamjms.2019.386

Keywords: Ectopic tooth; CBCT; Case report; Maxillary sinus; Orthodontics

***Correspondence:** Toi Chu Dinh. Department of Human and Animal Physiology, Faculty of Biology, Hanoi National University of Education, Hanoi, Vietnam. E-mail: chudinhtoi.hnue@gmail.com

Received: 04-Sep-2019; **Revised:** 20-Nov-2019; **Accepted:** 21-Nov-2019; **Online first:** 20-Dec-2019

Funding: This research did not receive any financial support

Competing Interests: The authors have declared that no competing interests exist

Abstract

BACKGROUND: Nowadays, cone beam computed tomography (CBCT) are commonly used in dentistry with an advantage about significantly lower dose comparing with CT-Scanner. Utilizing CBCT images which are indicated in dentistry like orthodontics can help diagnose diseases beyond dentistry field. One rare phenomenon can be seen in maxillary sinus, which is often overlooked by dentists, is ectopic teeth.

CASE REPORT: This article describes one orthodontic case found accidentally an ectopic tooth in maxillary sinus by inspecting CBCT images.

CONCLUSION: Dentists and oral radiologists should carefully inspect non-dental structures, like maxillary sinus, even its distance from the dentoalveolar region, especially in asymptomatic patients.

Introduction

Nowadays, cone beam computed tomography (CBCT) have been an efficient tool for imaging diagnosis with a variety of dentomaxillofacial applications. Malocclusion and dentomaxillofacial anomalies are the most common indications for CBCT in the age groups of primary and permanent dentition [1]. CBCT provides adequately images about both dental structures, for instance teeth and jaws, and other non-dental structures like maxillary sinus, nasal cavity, and palate. Nevertheless, dentists or oral radiologists occasionally neglected these non-dental structures due to its distance from the dentoalveolar region, especially in asymptomatic patients. Thus, abnormalities and anatomic changes in this region is frequently overlooked. One rare abnormality can be seen in maxillary sinus is ectopic teeth [2], [3], [4]. Ectopic eruption may derive from one of three processes: developmental disturbance, pathological process and iatrogenic activity [5]. Most of these cases are recurrent sinusitis or asymptomatic and are found accidentally by routine examination and radiography like CBCT. This article describes one orthodontic case with recurrent sinusitis, found accidentally an ectopic tooth in maxillary sinus by inspecting CBCT images.

We run 5 keywords: “ectopic tooth in maxillary sinus”, “ectopic teeth in maxillary sinus”, “ectopic tooth in maxillary antrum”, ”ectopic molar in maxillary sinus” and ”ectopic molar in maxillary antrum” via EndNote X9, using Pubmed database, we have had 40 results, from 1972 to 2018.

After reading titles, abstracts, whole articles, we eliminated those articles with non-English language (Chinese), non- molar tooth (canines, incisors), could not find abstracts/ full-text (too old, often before year of 2000) or content not relevant to ectopic tooth, we have had 26 articles described case

reports about ectopic tooth in maxillary sinus (Figure 1).

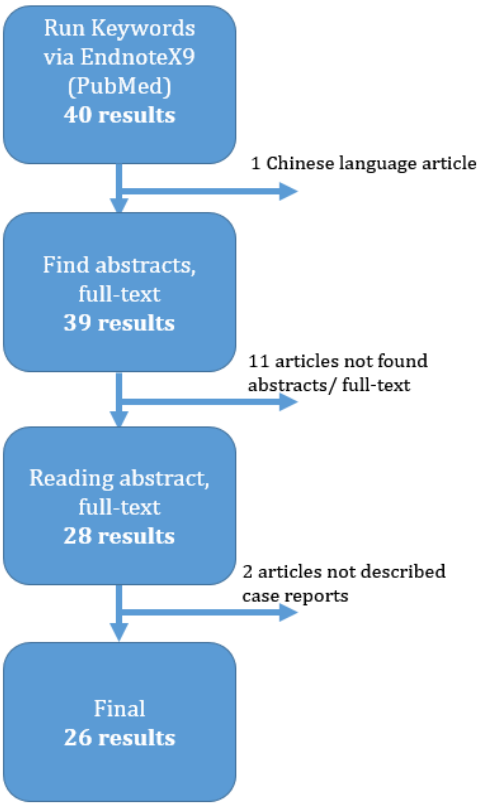

Figure 1: Data Collection

In this review, 33 patients were observed. Compared to the position in maxillary sinus, 16 cases (48.5 %) were on the right and 17 (51.5%) on the left. They are likely located in variable areas of the sinus: antrum, floor, roof, orbital floor, superomedial and anterosuperior aspects, and posterior and anterolateral walls. Among the 33 case reports, the incidence is higher in male (n = 22; 66.7%) compared with female (n = 11; 33.3%).

The age spectrum was relatively wide, varied from 15 to 73 years old. The mean age was 33. According to previous articles, most patients with a dentigerous cyst are likely younger than 20 years [32], [33]**.** However, patients are likely to have the condition for many years before being diagnosed and treated. The dentigerous cyst develops gradually in maxillary sinus for several years without any symptoms. When the sinus space is occupied significantly, symptoms will occur. Therefore, the ectopic teeth might be symptomatic or asymptomatic. There were 4 cases (12.1%) with asymptomatic [6], [12], [18], [19], 13 out of 33 cases observed pain condition, most of them were mild pain. Other symptoms can be found on these patients includes: Swelling (11 cases), purulent rhinorrhea (10 cases). Few more rare symptoms were: decrease in sensation [19], phonatory difficulties [9], and blurred vision [15].

Table 1: Literature review of the dentigerous cyst associated with an ectopic third molar in maxillary sinus

Authors, year	Symptoms	Age (yrs)	Gender	Side of sinus
L. G. F. Lombroni et al., (2018) [6]	Asymptomatic	37	Female	Left
I. L. Liau et al., (2018) [7]	Chronic nasal obstruction, purulent rhinorrhea	63	Male	Right
O. D. Topal et al., (2017) [8]	Swelling, pain in eye, left upper teeth and ear	32	Female	Left
O. L. M. Chagas Junior et al., (2016) [9]	Discomfort, phonatory difficulties.	60	Male	Left
U. A. Aydin et al., (2016) [10]	Pain, feeling of pressure, especially during biting	21	Male	Left
S. H. B. Kang et al., (2015) [11]	Swelling	49	Male	Right
Y. N. Furuya et al., (2015) [12]	Asymptomatic	73	Male	Right
N. M. Touiheme, et al., (2014) [13]	Pain, mucopurulent rhinorrhoea	23	Female	Left
MaMatha N.S et al., (2014) [14]	Foul smelling, salty discharge, Mild pain and slight swelling	17	Male	Left
N. K. Demirtas et al., (2014) [15]	Pain, discomfort, and fullness Blurred vision	19	Male	Right
A. P. Datli et al., (2014) [16]	Chronic sinusitis	41	Male	Right
S. A. O. Bello, et al., (2014) [17]	Swelling, mild pain, discharging sinus	17	Male	Right
S. G. Viterbo et al., (2013) [18]	Asymptomatic	29	Male	Right
S. H. Ramanojam et al., (2013) [19]	Pain and swelling	21	Female	Right
	Heaviness, decrease in sensation	48	Female	Left
	Occasional dull pain	22	Male	Left
	Asymptomatic	26	Male	Left
	Repeated dull pain	24	Male	Left
	Continuous dull pain	32	Female	Right
A. R. Rai et al. (2013) [20]	Watering from the left eye, pain and swelling	46	Female	Left
Y. T. L. Lai, et al., (2013) [21]	-	52	Female	Left
Y. C. Guruprasad et al. (2013) [22]	Swelling, discharge of pus from the nostril	21	Female	Right
S. M. Abdollahifakhim et al., (2013)[23]	Chronic mucopurulent rhinorrhoea	17	Male	Right
V. O. K. Kasat, et al. (2012) [24]	Discharge from upper right posterior region	22	Male	Right
G. N. Thakur et al., (2011) [25]	Cough, recurrent purulent discharge, facial pain	25	Male	Left
L. G. Nisa, et al., (2011) [26]	Dental pain, purulent oral discharge	15	Male	Right
S. K. Mohan et al., (2011) [27]	Recurrent purulent rhinorrhea	28	Female	Right
T. K. Saleem et al., (2010) [28]	Recurrent episodes of haemoptysis	45	Male	Left
M. C. O. Buyukkurt et al., (2010) [29]	Swelling	19	Female	Left
	Swelling	32	Male	Left
	Enlarged soft swelling	30	Male	Left
T. S. Srinivasa Prasad et al., (2007) [30]	Recurrent purulent rhinorrhea	45	Male	Right
S. C. Dagistan et al., (2007) [31]	Multiple missing teeth	37	Male	Right

Case Report

A 15 year-old-male patient came to a Dental Clinic with orthodontic requirement but accompanied with mild pain and recurrent pus discharge from his left maxillary sinus since last 1 year. The symptoms reduced with antibiotics but recurred after 1-2 weeks. Patient also reported about stuffy nose and congestion. There was no history of any systemic disorders or maxillofacial trauma. Extraoral examination revealed no facial swelling (Figure 2A). Intraoral examination showed no carious teeth or abnormality in oral mucosa (Figure 2B).

Patient was indicated CBCT for orthodontic purpose and also maxillary inspecting. CBCT image revealed an ectopic maxillary third molar near the roof of left maxillary sinus with a cystic lesion surrounded. The mucosa of the sinus was thickened suggested the chronic sinusitis condition in CBCT images. (Figure

2C and 2D).

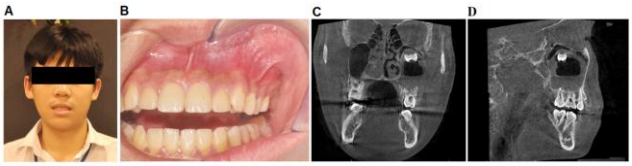

Figure 2: Imaging examination of the patient; Extraoral photo A); Oral mucosa B); Coronal image C); Sagittal image D)

The patient then was referred to an Ears, nose, and throat (ENT) clinic for tooth removal. Caldwell-Luc approaching on the left side were operated under general anesthesia. A vesicular incision was made from tooth 22 to tooth 26. A bony widow was created, 0-degree ENT endoscope revealed an ectopic molar located in the left wall, near the roof of the sinus (Figure 3A), as same as CBCT images. An elevator was used to separate the root from the mucosa then both tooth and surrounded cyst were clipped out by forceps (Figure 3B and 3C). The patient has remained asymptomatic after the operation and 6-month follow-up.

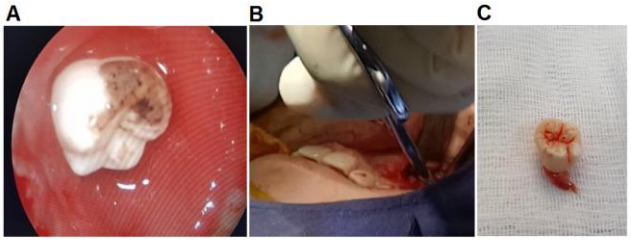

Figure 3: Treatment for the patient; Tooth via ENT endoscope A); Tooth clipped out by forceps B); Post-operation C)

Discussion

Thanks to advantages (low effective dose, short time working…) of cone beam computed tomography (CBCT), imaging diagnosis in dentistry have been easier and more accurate. Effective dose for CBCT values ranged from 13 to 82 μSv, much lower than dose from multi-slice computed tomography (MSCT) (474 to 1160 μSv) [34]. In this case, the patient was indicated CBCT for orthodontic need. Utilizing CBCT images indicated in dentistry like orthodontics requirement for beyond-dentistry field diagnosis bring to patients' great benefits. Nevertheless, dentists or oral radiologists occasionally neglected these non-dental structures, for instance maxillary sinus, due to its distance from the dentoalveolar region, especially in asymptomatic patients. Hence, ectopic teeth are often overlooked in dentistry.

Tooth development results from a complex multistep interaction between the oral epithelium and the underlying mesenchymal tissue. The development begins from the 6th week in utero at the time of maxillary and mandibular dental lamina formation. This ectodermal structure then forms into crowns and roots. Any abnormality occurring in this progress may result in ectopic eruption of teeth [35]. Although there have been reports of teeth in the nasal septum, mandibular condyle, coronoid process, palate and maxillary antrum, ectopic eruption of teeth into other regions instead of the oral cavity is rare. [36]. This article reported an ectopic tooth located in the roof of the left maxillary sinus. According to a review of L.G. Lombron et al., there were 19 cases on the right and 18 on the left maxillary sinus. They occupied different areas of the sinus: antrum, floor, roof, orbital floor, superomedial and anterosuperior aspects, and posterior and anterolateral walls [6].

Teeth removal procedure invading severely into maxilla sinus requires experienced surgeons and dedicated equipment. Hence, interdisciplinary collaboration involved dentistry and ENT is of importance in best health care providing. The patient came to the Dental clinic for orthodontic need but sinusitis condition and an ectopic tooth accidentally found by dentists, treated by otolaryngologists. If there is no well managed for ectopic teeth, they are likely to form a cyst or a tumor. The symptoms may include: facial pain, facial swelling, headache, recurrent purulent rhinorrhea, chronic nasal obstruction, phonatory difficulties. The most popular approaching for teeth removal is Caldwell-Luc operation [6].

In conclusion, utilizing CBCT images indicated in dentistry like orthodontics requirement for beyond-dentistry field diagnosis bring to patients' great benefits. Dentists and oral radiologists should carefully inspect non-dental structures, like maxillary sinus, even its distance from the dentoalveolar region, especially in asymptomatic patients. Ectopic teeth are likely to become a cyst or tumor without well managed. The most popular approaching for teeth removal is Caldwell-Luc operation.

Informed consent

Informed consent was obtained from the patient's parents included in the study. The family read and signed to allow their child as a volunteer to participate in research.

References

1. İşman Ö, et al. Indications for cone beam computed tomography in children and young patients in a Turkish subpopulation. International Journal of Paediatric Dentistry. 2017; 27(3):183-190. https://doi.org/10.1111/ipd.12250 PMid:27452447

2. Erkmen N, Ölmez S, Önerci M. Supernumerary tooth in the maxillary sinus: Case report. Australian Dental Journal. 1998; 43(5):385-386. https://doi.org/10.1111/j.1834-7819.1998.tb00196.x PMid:9973705

3. Gulbranson SH, et al. Squamous Cell Carcinoma Arising in a Dentigerous Cyst in a 16-Month-Old Girl. Otolaryngology-Head and Neck Surgery. 2002; 127(5):463-464. https://doi.org/10.1067/mhn.2002.129039 PMid:12447244

4. Ustuner E, et al. Bilateral maxillary dentigerous cysts: A case report. Oral Surgery, Oral Medicine, Oral Pathology, Oral Radiology, and Endodontology. 2003; 95(5):632-635. https://doi.org/10.1067/moe.2003.123 PMid:12738957

5. Kasat V, Karjodkar F, Laddha R. Dentigerous cyst associated with an ectopic third molar in the maxillary sinus: A case report and review of literature. Contemporary Clinical Dentistry. 2012; 3(3):373. https://doi.org/10.4103/0976-237X.103642 PMid:23293505 PMCid:PMC3532812

6. Lombroni L, et al. Ectopic teeth in the maxillary sinus: A case report and literature review. Indian Journal of Dental Research. 2018; 29(5):667. https://doi.org/10.4103/ijdr.IJDR_347_17 PMid:30409951

7. Liau I, Lynch N, Hearn B, Cheng A. Endoscopically Assisted Modified Caldwell-Luc Approach to Enucleation of Dentigerous Cyst With Ectopic Tooth From the Maxillary Sinus. J Craniofac Surg. 2018; 29(6):e568-e570. https://doi.org/10.1097/SCS.0000000000004346 PMid:29762318

8. Topal Ö, Dayısoylu EH. Ectopic Tooth in the Maxillary Sinus. Turk Arch Otorhinolaryngol. 2017; 55(3):151-152. https://doi.org/10.5152/tao.2017.2308 PMid:29392075 PMCid:PMC5782996

9.Júnior OL, Moura LB, Sonego CL, de Farias EO, Giongo CC, Fonseca AA. Unusual Case of Sinusitis Related to Ectopic Teeth in the Maxillary Sinus Roof/Orbital Floor: A Report. Craniomaxillofac Trauma Reconstr. 2016; 9(3):260-3. https://doi.org/10.1055/s-0036-1581063 PMid:27516844 PMCid:PMC4980138

10. Aydın Ü, Aşık B, Ahmedov A, Durmaz A. Osteoma and Ectopic Tooth of the Left Maxillary Sinus: A Unique Coexistence. Balkan Med J. 2016; 33(4):473-6. https://doi.org/10.5152/balkanmedj.2016.15052 PMid:27606148 PMCid:PMC5001830

11. Kang SH, Bae TH, Kim HK, Kim WS, Kim MK. Immediate reconstruction of the maxillary sinus after resection of preoperatively misdiagnosed unicystic ameloblastoma with an ectopic third molar. J Craniofac Surg. 2015; 26(1):e53-5. https://doi.org/10.1097/SCS.0000000000001072 PMid:25569416

12. Furuya Y, Norizuki Y, Yajima Y. A Case of Simultaneous Ectopic Tooth Extraction and Removal of Migrated Dental Implant from Maxillary Sinus. Bull Tokyo Dent Coll, 2015. 56(4):253-8. https://doi.org/10.2209/tdcpublication.56.253 PMid:26657524

13. Touiheme N, Messary A. Supernumerary ectopic tooth on the maxillary sinus. Pan Afr Med J. 2014; 18:353. https://doi.org/10.11604/pamj.2014.18.353.4912 PMid:25574329 PMCid:PMC4282798

14. Mamatha NS, KriShNaMoorthy B, Savitha JK, Bhai P. Diagnostic CBCT in Dentigerous Cyst with Ectopic Third Molar in the Maxillary Sinus-A Case Report. J Clin Diagn Res, 2014. 8(6):ZD07-9.

15.Demirtas N, Kazancioglu HO, Ezirganli S. Ectopic tooth in the maxillary sinus diagnosed with an ophthalmic complication. J Craniofac Surg. 2014; 25(4):e351-2. https://doi.org/10.1097/SCS.0000000000000795 PMid:25006943

16.Datli A, Pilanci O, Cortuk O, Saglam O, Kuvat SV. Ectopic tooth superiorly located in the maxillary sinus. J Craniofac Surg. 2014; 25(5):1927-8. https://doi.org/10.1097/SCS.0000000000000914 PMid:25119397

17.Bello SA, Oketade IO, Osunde OD. Ectopic 3rd molar tooth in the maxillary antrum. Case Rep Dent. 2014; 2014:620741. https://doi.org/10.1155/2014/620741 PMid:25132999 PMCid:PMC4123483

18.Viterbo S, Griffa A, Boffano P. Endoscopic removal of an ectopic tooth in maxillary sinus. J Craniofac Surg. 2013; 24(1):e46-8. https://doi.org/10.1097/SCS.0b013e31826d07d0 PMid:23348335

19. Ramanojam S, Halli R, Hebbale M, Bhardwaj S. Ectopic tooth in maxillary sinus: Case series. Ann Maxillofac Surg. 2013; 3(1):89-92. https://doi.org/10.4103/2231-0746.110075 PMid:23662268 PMCid:PMC3645620

20. Rai A, Rai NJ, Rai MA, Jain G. Transoral removal of ectopic maxillary third molar situated superiorly to maxillary antrum and posteroinferiorly to the floor of orbit. Indian J Dent Res. 2013; 24(6):756-8. https://doi.org/10.4103/0970-9290.127628 PMid:24552941

21. Lai YT, Luk YS, Fung KH. Anomalous morphology of an ectopic tooth in the maxillary sinus on three-dimensional computed tomography images. J Radiol Case Rep. 2013; 7(2):11-6. https://doi.org/10.3941/jrcr.v7i2.1227 PMid:23705035 PMCid:PMC3661307

22. Guruprasad Y, Chauhan DS, Kura U. Infected dentigerous cyst of maxillary sinus arising from an ectopic third molar. J Clin Imaging Sci. 2013; 3(Suppl 1):7. https://doi.org/10.4103/2156-7514.117461 PMid:24516770 PMCid:PMC3906662

23. Abdollahifakhim S, Mousaviagdas M. Ectopic molar with maxillary sinus drainage obstruction and oroantral fistula. Iran J Otorhinolaryngol. 2013; 25(72):187-92.

24. Kasat VO, Karjodkar FR, Laddha RS. Dentigerous cyst associated with an ectopic third molar in the maxillary sinus: A case report and review of literature. Contemp Clin Dent. 2012; 3(3):373-6. https://doi.org/10.4103/0976-237X.103642 PMid:23293505 PMCid:PMC3532812

25. Thakur G, Nair PP, Thomas S, Ahuja R, Kothari R. Dentigerous cyst associated with ectopic maxillary third molar in maxillary antrum. BMJ Case Rep. 2011; 2011. https://doi.org/10.1136/bcr.02.2011.3873 PMid:22696724 PMCid:PMC3094783

26. Nisa L, Giger R. Images in clinical medicine. Ectopic tooth in the maxillary sinus. N Engl J Med. 2011; 365(13):1232. https://doi.org/10.1056/NEJMicm1101021 PMid:21991896

27.Mohan S, Kankariya H, Harjani B, Sharma H. Ectopic third molar in the maxillary sinus. Natl J Maxillofac Surg. 2011; 2(2):222-4. https://doi.org/10.4103/0975-5950.94488 PMid:22639520 PMCid:PMC3343399

28.Saleem T, Khalid U, Hameed A, Ghaffar S. Supernumerary, ectopic tooth in the maxillary antrum presenting with recurrent haemoptysis. Head Face Med. 2010; 6:26. https://doi.org/10.1186/1746-160X-6-26 PMid:21070657 PMCid:PMC2992486

29.Buyukkurt MC, Omezli MM, Miloglu O. Dentigerous cyst associated with an ectopic tooth in the maxillary sinus: a report of 3 cases and review of the literature. Oral Surg Oral Med Oral Pathol Oral Radiol Endod. 2010; 109(1):67-71. https://doi.org/10.1016/j.tripleo.2009.07.043 PMid:19875313

30. Prasad TS, Sujatha G, Niazi TM, Rajesh P. Dentigerous cyst associated with an ectopic third molar in the maxillary sinus: a rare entity. Indian J Dent Res. 2007; 18(3):141-3. https://doi.org/10.4103/0970-9290.33793 PMid:17687180

31. Dagistan S, Çakur B, Göregen M. A dentigerous cyst containing an ectopic canine tooth below the floor of the maxillary sinus: a case report. J Oral Sci. 2007; 49(3):249-52. https://doi.org/10.2334/josnusd.49.249 PMid:17928734

32. Yamalik K, B.S., Erkmen E, Baris E., Nonsyndromic Bilateral mandibular dentigerous cysts: report of a rare case. Turkiye Klin J Dent Sci. 2007; 13:129-34.

33. Takagi S, Koyama S. Guided eruption of an impacted second premolar associated with a dentigerous cyst in the maxillary sinus of a 6-year-old child. J Oral Maxillofac Surg. 1998; 56(2):237-9. https://doi.org/10.1016/S0278-2391(98)90876-X

34. Loubele M, et al. Comparison between effective radiation dose of CBCT and MSCT scanners for dentomaxillofacial applications. European Journal of Radiology. 2009; 71(3):461-468. https://doi.org/10.1016/j.ejrad.2008.06.002 PMid:18639404

35. Avery JK. Development of the branchial arches, face, and palate. Oral Development and Histology. Thieme Medical Publishers, Inc., New York, 1994:20-41.

36. Goh YH. Ectopic eruption of maxillary molar tooth--an unusual cause of recurrent sinusitis. Singapore Med J. 2001; 42(2):80-1.

ID Design Press, Skopje, Republic of Macedonia
Open Access Macedonian Journal of Medical Sciences. 2019 Dec 30; 7(24):4337-4341.
https://doi.org/10.3889/oamjms.2019.387
eISSN: 1857-9655
Basic and Clinical Medical Researches in Vietnam

Endodontic Retreatment of an Upper First Molar with Bifurcated Palatal Canal Using Preoperative Cone-beam Computed Tomography: A Case Report

Nguyen Thi Chau[1], Vo Truong Nhu Ngoc[1*], Vu Viet Duc[1], Truong Thi Hieu Hanh[1], Thien Chu Dinh[2]

[1]School of Odonto Stomatology, Hanoi Medical University, Hanoi, Vietnam; [2]Institute for Research and Development, Duy Tan University, 03 Quang Trung, Danang, Vietnam

Citation: Chau NT, Ngoc VTN, Duc VV, Hanh TTH, Chu Dinh T. Endodontic Retreatment of an Upper First Molar with Bifurcated Palatal Canal Using Preoperative Cone-beam Computed Tomography: A Case Report. Open Access Maced J Med Sci. 2019 Dec 30; 7(24):4337-4341. https://doi.org/10.3889/oamjms.2019.387

Keywords: Cone-beam computed tomography; Upper first molar; Endodontic retreatment; Bifurcated palatal canal; Second mesiobuccal canal; S-shaped canal

***Correspondence:** Vo Truong Nhu Ngoc. School of Odonto Stomatology, Hanoi Medical University, Hanoi, Vietnam, email: votruongnhungoc@gmail.com

Received: 04-Sep-2019; **Revised:** 20-Nov-2019; **Accepted:** 21-Nov-2019; **Online first:** 20-Dec-2019

Funding: This research did not receive any financial support

Competing Interests: The authors have declared that no competing interests exist

Abstract

BACKGROUND: Anatomic variations in palatal canal morphology in maxillary first molars (MFMs) are relatively rare occurrences. Therefore, omission is common unless clinicians recognize their presence.

CASE REPORT: The aim of this report is to point out new signs that can be viewed as indicators of the existence of additional canals in the palatal root (PR) in this upper first molar endodontic retreatment case. Moreover, the role of preoperative cone-beam computed tomography (CBCT) in both discovering and determining the location of those additional canals will also be discussed.

CONCLUSION: Besides formerly discussed signs that indicate the existence of this canal, clinicians should also pay attention to other signals on periapical radiograph, including the aberrant divergence of a palatal canal at apical third and an unusual lesion occurring laterally in the periapical area of palatal root.

Introduction

For successful endodontic treatment, clinicians should pay attention to anatomic variations in root canal systems besides canal instrumentation and obturation [1]. The canal configurations of maxillary first molars (MFMs) is complex as a result of the presence of additional canals with an extremely high prevalence of the second mesiobuccal (MB2) canal, at over 60% [2], [3], [4], [5]. In contrast, only one single canal, which has one orifice and one foramen, is found in the palatal root (PR) [2], [4]. Nevertheless, there have been reports [6], [7], [8] about cases in which canals split at the last third of the PR are classified type V (1-2 anatomy) according to Vertucci's classification [9]. This means one orifice for the canal and two distinct apical foramina. Ali Nosrat *et al.,* [10] also presented 5 clinical cases involving the treatment of upper first molar whose canal morphology was far from 1-1 anatomy, four out of which, were classified type V.

The omission of root canals with such internal complexities is one of the principal causes of the failure in treating MFM [11]. To uncover the morphology and variations of root canal systems, lots of researches have been carried out with many different approaches; and a combination of techniques such as dental loupes and microscopes, periapical radiographs or CBCT have been employed [2], [12]. Among all of these, CBCT scanning is considered as an ideal tool to easily visualize root canal systems thanks to its ability to produce high-resolution three-dimensional images [8]. However, compliance with the ALARA rule – "*the radiation should be as low as reasonably achievable"* – is essential upon the use of CBCT.

This report presents a clinical case that involved the application of preoperative CBCT in retreatment of upper first molar whose previous

therapeutic attempt had been a failure due to missed S-shaped MB2 canal and bifurcated palatal canal. This work will also review earlier reports on the same issue and point out new signs on two-dimensional images that suggest the existence of additional palatal canals.

Case Report

A 23-year-old male medical student visited our endodontic department due to the dull and persistent pain on his right maxillary first molar (tooth #16) while eating, especially hard food. The dental history showed that the tooth had received previous endodontic treatment and got a porcelain-fused-to-metal (PFM) crown because of asymptomatic irreversible pulpitis 10 months ago. There was also no medical history of systemic diseases or allergy.

The clinical examination revealed: (1) a marginal deficiency at the buccal surface of the crown (Figure 1A); (2) no percussion sensitivity; and (3) a negative result of pulp test. In addition, there were no signs of swelling, sinus tract, abnormal mobility, and pathological periodontal pocket.

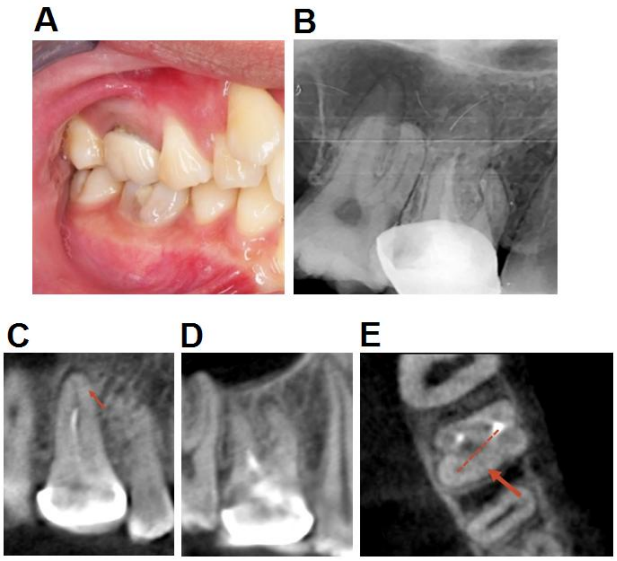

Figure 1: The preoperative examination; A) A marginal deficiency at the buccal surface of the crown; B) The abnormal lesions were indicated in the periapical radiograph; C) A bifurcated palatal canal at the apical third on the coronal slices of CBCT; D) Remaining obturating material in the mesiodistal root; E) Axial slices showed an untreated MB2 orifice which is located along the MB groove, heading 2 mm palatally from the main MB orifice

The periapical radiograph (Figure 1B) of tooth #16 showed abnormal signs: (1) an incomplete endodontic therapy with underfilled obturating materials in the palatal canal; (2) atypically enlarged periodontal ligament that surrounds the J-formed mesiobuccal (MB) root, suggesting the appearance of curved canals; and (3) and a periapical radiolucent lesion towards the distal side in PR and a vague distal divergence of the palatal canal.

To clarify the dubious signs in the periapical film, a CBCT evaluation of high-resolution scanning (Planmeca ProMax 3D Max; Planmeca Oy, Helsinki, Finland) was performed. CBCT scanning were obtained following the parameters: 96 KV (tube voltage), 5 mA (tube current), a field of view (FOV) 80 X 80 mm, and 150 μm voxel size. The result of CBCT images illustrated: - Firstly, there was a branched canal diverging to the mesial side at the last third of the PR (Figure 1C). The precise location and dimension of the apical lesion around this root were determined; Secondly, remaining root-filling material, though unclear on the periapical radiograph at a coronal third of the mesiodistal root, was observed on the sagittal slices (Figure 1D); and Lastly, a second mesiobuccal (MB2) canal was detected on the axial slices. It was located along the MB groove, heading 2mm palatally, from the main MB orifice (Figure 1E).

Based on clinical and radiographical evaluations, the final diagnosis of tooth #16 was symptomatic apical periodontitis after root canal therapy and non-surgical endodontic retreatment was indicated. The retreatment was performed after written consent had been obtained.

First, the PFM crown was removed by Transmetal bur (Dentsply Sirona, Victoria, Australia). The abutment tooth #16 was exposed, displaying temporary filling material and a protruded portion of gutta-percha at the occlusal surface (Figure 2A) which could be the root canal filling material of distobuccal canal poorly obturated with single cone technique. The tooth was then isolated by applying a rubber dam. The Endo Z bur (Dentsply Maillefer, Ballaiges, Switzerland) allowed us to regain direct access to the pulp chamber. During the procedure, a dental loupe with three-time magnification was used to assist in the inspection of the location of orifices. As all intrapulpal materials were removed, it was easier to visualize the pulpal chamber comprising palatal, distobuccal and mesiobuccal orifices. In particular, a conspicuous pink of gutta-percha inside the palatal canal was exposed.

Therefore, the next plan was eliminating the root filling materials using both mechanical and chemical methods (Figure 2B): - Firstly, removed a coronal portion of gutta-percha with a Gates-Glidden drill #3 (Mani, Tochigi, Japan); - Next, put Eucalyptol solvent (Cerkamed, Stalowa Wola, Polska) into the palatal canal within 2 minutes to dissolve the remaining gutta-percha; and Finally, used a C+ file #15 (Dentsply Maillefer) to penetrate into the remaining gutta-percha and remove it.

In the following treatment, the detection of only 3 orifices and the existence of MB2 canal on preoperative CBCT also showed that this canal was omitted in the previous dental treatment and had to be located.

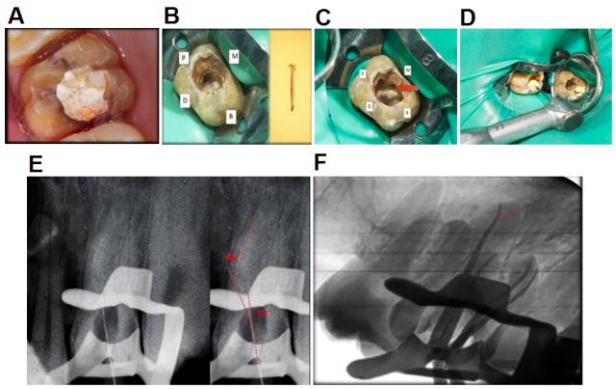

Figure 2: During the procedure; A) The abutment tooth #16 was exposed with temporary filling material and Gutta-percha at the occlusal surface; B) The elimination of filling materials from palatal canal using both mechanical and chemical methods; C) The locating of the MB2 root canal based on CBCT; D) The Glide-Path preparation was carried out with PathFile rotary files; E) S-shaped MB2 canal on the working-length radiograph; (F) The master cone radiograph

MB2 canal was identified based on initial assessments on the axial slices. In sequence, the access cavity was enlarged mesially using the Endo Z bur (Dentsply Maillefer) to enhance the observation of the orifices, making the outline of the access cavity transform into rhombus shape. Then, the dentin layer covering the MB2 orifice was removed following a path that run along the MB groove and headed 2 mm towards the palatal canal from the main MB orifice. This allowed MB2 to be located using DG 16 explorer (Hu-Friedy, Chicago, United States). The MB2 canal at the coronal third was then flared with Gate-Glidden drill #3 (Mani) (Figure 2C). Following the determination of four orifices, the #10 K-files (Dentsply Maillefer), which were initially curved following the canal direction on CBCT images, were applied to negotiate the root canals.

The working-length (WL) of each canal was measured by using Propex II apex locator (Dentsply Maillefer) and then verified through the working-length radiographs. On the confirmation film of MB2's working-length, an S-shaped curvature was revealed and then measured by Schneider's method [13]. The angle of the first curvature portion was 13O while the second one was 42O. (Figure 2E). In the glide-path preparation, the PathFile rotary files (Dentsply Maillefer) were inserted into the root canals corresponding to the ascertained working-length in the following order: Pathfile 13/.02, 16/.02 and 19/.02 (Figure 2D).

At the second appointment, the complete canal preparation was performed with the Protaper Next X1 (17/.04) and X2 (25/.06) rotary file (Dentsply Maillefer). The branched canal in the palatal root is shaped with precurved hand files from size #10/.04 to #30/.04. Throughout the instrumentation, The Intracanal lubricant with 15% EDTA was applied and the canals were then irrigated with sonic-activated sodium hypochlorite 3% between file insertions. Finally, the root canals were flushed with chlorhexidine 2% and rinsed with saline. Utilized intracanal medicament was calcium hydroxide and CavitTM (3MTM ESPE, United States) was applied as a temporary sealing material.

On the next visit, the root canals were filled with the pre-curved ProTaper Next gutta-percha (GP) X2 and evaluated by means of radiographs (Figure 2F). After drying canals, the GP cones were coated with the AH Plus sealer (Dentsply Maillefer) and inserted into the canals to working-length. The obturating procedure was achieved using continuous wave technique with System B-Cordless Obturation (SybronEndo, Orange, CA). The completed obturation process was evaluated through an immediate postoperative radiograph. Finally, the access cavity was directly restored with composite (Surefil SDR and Ceram X universal; Dentsply Sirona). The male patient, eventually, was introduced to the prosthetic department for full crown restoration.

After 6 months of following up, the tooth #16 was asymptomatic as well as complete healing was shown on the radiograph (Figure 3B).

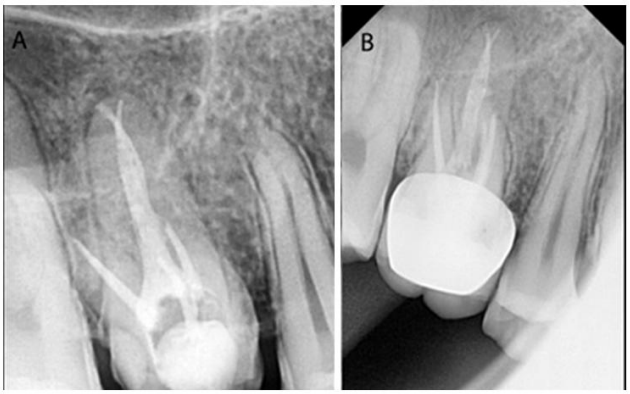

Figure 3: After the procedure; A) Immediate-postoperative image; B) 6-months-follow-up radiograph

Discussion

The case in question represents the root canal retreatment of a right MFM missing MB2 canal with the bifurcated palatal canal. The canal bifurcation is classified as type V (1-2) according to Vertucci's classification [9]. Previous studies have reported rare cases of PR containing more than one root canals in MFM, especially that of the Vertucci type V. In one research conducted by Tian *et al*., [8], CBCT scanning method was applied to study the canal morphology of 1558 MFMs. The findings then revealed statistics on the presence of additional canals, at only 0.7% in the palatal root and an extremely low figure for type V canal anatomy, at 0.05%. As stated in the study done with the same method by Neelakantan *et al., [7],* the

corresponding figures for additional canals and 1-2 canal morphology canal were 9.6% and 1.3% respectively while Vertucci type I (1-1) palatal canal was prevalent in these studies. This indicates that clinicians should carefully examine the existence of bifurcated canals in palatal root through initial radiograph images or clinical inspection besides their typical anatomy (Vertucci type I).

Earlier studies provided two clues about the bifurcation of the palatal canal on periapical radiograph: 1) the unusual diverging gutta-percha on the master cone radiograph or the weird divergence of a master apical hand-file on the working-length film [10], 2) the abnormal divergence of root canal filling material which was obturated previously in palatal canal [10]. In this case, the upper first molar undergoing incomplete endodontic treatment with underfilled obturating material in the palatal canal posed an obstacle to discovering the canal morphology. However, observations of preoperative radiograph showed that the discreet periapical lesion was located on the distal portion of the apical root, suggesting an inflamed canal on that side. Moreover, a distal deviation of the palatal canal at apical third was also disclosed at the film. We supposed that detecting this deviation without gutta-percha point or working-length file was possible because of the canal shaping and cleaning phase in previous treatment. This procedure facilitated the removal of debris, calcified tissues as well as apparently shaped the pathway of the palatal canal. As a consequence, the canal became more radiopaque on the two-dimensional film. This leads to the conclusion that endodontic clinicians should identify both mentioned clues and these following features when determining the possible presence of a bifurcated canal: (1) The aberrant divergence of a palatal canal at apical third on the preoperative radiograph, and (2) An unusual lesion occurring laterally in the periapical area of palatal root.

Once there are signs of the bifurcated palatal canal, clinicians need to re-examine and determine its presence with certainty. On the one hand, according to earlier reports on the case, the canal was only detected after instrumentation with the support of a microscope [6], [10]. More seriously, clinical dentists made a mistake when assuming the palatal root had one canal and one foramen (1-1 anatomy) on the initial periapical film, resulting in failure in the first treatment [10]. On the other hand, the branched canal in the case, which was located at the last third of the PR and barely visible on the two-dimensional radiograph, demonstrated complicated root canal morphology and the need for further examination on the CBCT scan [14]. Therefore, applying preoperative high-resolution CBCT scanning was needed and this method made it possible to confirm the existence and exact position of the bifurcated canal. The use of CBCT not only helped clinically locate additional canals but also avoid complications during canal preparation such as root canal perforation and ledging [15]. In this case, high-resolution CBCT images were taken with the protocol: a FOV 80 x 80 mm, voxel size 150 mm, anode parameters (96 KV and 5 mA). High-resolution scanning mode with voxel size 0.125 mm has been reported to reveal bifurcated canal at apical third of roots as opposed to modes with larger voxel size (0.20 mm and 0.25 mm) [16]. The branched canal located at apical third is likely to be identified under CBCT scanning with a voxel size below 0.20 mm.

The process of canal instrumentation for the type V palatal canal is also worth considering. Ultrasonic irrigation combined with irrigants should be applied in the branched canal at the last third of the root due to the capability of removing smear layer efficiently [17]. Once the blockage at the apical third has disappeared, precurved files can slide down the entire working length easily and the risk of separating instruments will be minimized.

Managing the S-shaped curvature MB2 canal is also a major challenge for clinicians. Besides the application of double flare technique [18], the Ni-Ti rotary files by Dentsply, Pathfiles which prove to be flexible, should be applied to create a smooth glide-path in curved canals before the shaping phase with rotary files. Compared to previous manual stainless steel files, conducting canal preparation with Pathfiles considerably minimize canal defects at curvature portion [19] as well as periapical infections of the root [20]. Thus, glide path preparation with these files enables rotary shaping files to not only eliminate infected tissues more effectively but also contribute to obturating the curved canal more tightly in three-dimensions.

Last but not least, the removal of previous filling material in the retreatment should also be considered. When the palatal canal is poorly obturated with underfilled gutta-percha (GP) using single cone technique, manual removal of GP with rigid C+ file and solvent is the chosen method. By adopting this approach, the risk of excessive enlargement at the coronal third of the canal can be reduced. However, the solvent should be injected into the canal through a small-sized needle to avoid being pushed down to the periapical area.

In conclusion, figures have indicated that the existence of type V palatal canals in MFM is just roughly 1%, which is extremely low. Besides formerly discussed signs that indicate the existence of this canal, clinicians should also pay attention to other signals on periapical radiograph, including the aberrant divergence of a palatal canal at apical third and an unusual lesion occurring laterally in the periapical area of palatal root. In addition, further research should be conducted to determine appropriate parameters on CBCT for identifying the presence of branched canals, which can help lower the risks of treatment failure.

Ethics statement

All study protocols were approved by a local ethics committee of the School of Odonto Stomatology, Hanoi Medical University, and have therefore been performed in accordance with the ethical standards laid down in the 1964 Declaration of Helsinki and its later amendments.

References

1. Weine FS, et al. Canal configuration in the mesiobuccal root of the maxillary first molar and its endodontic significance. Oral Surg Oral Med Oral Pathol. 1969; 28(3):419-25. https://doi.org/10.1016/0030-4220(69)90237-0

2. Kim Y, Lee SJ, Woo J. Morphology of maxillary first and second molars analyzed by cone-beam computed tomography in a korean population: variations in the number of roots and canals and the incidence of fusion. J Endod. 2012; 38(8):1063-8. https://doi.org/10.1016/j.joen.2012.04.025 PMid:22794206

3. Betancourt P, et al. Cone-beam computed tomography study of prevalence and location of MB2 canal in the mesiobuccal root of the maxillary second molar. Int J Clin Exp Med. 2015; 8(6):9128-34.

4. Alavi AM, et al. Root and canal morphology of Thai maxillary molars. Int Endod J. 2002; 35(5):478-85. https://doi.org/10.1046/j.1365-2591.2002.00511.x PMid:12059921

5. Shetty H, et al. A Cone Beam Computed Tomography (CBCT) evaluation of MB2 canals in endodontically treated permanent maxillary molars. A retrospective study in Indian population. J Clin Exp Dent. 2017; 9(1):e51-e55. https://doi.org/10.4317/jced.52716 PMid:28149463 PMCid:PMC5268108

6. Holderrieth S, Gernhardt CR. Maxillary molars with morphologic variations of the palatal root canals: a report of four cases. J Endod. 2009; 35(7):1060-5. https://doi.org/10.1016/j.joen.2009.04.029 PMid:19567335

7. Neelakantan P, et al. Cone-beam computed tomography study of root and canal morphology of maxillary first and second molars in an Indian population. J Endod. 2010; 36(10):1622-7. https://doi.org/10.1016/j.joen.2010.07.006 PMid:20850665

8. Tian XM, et al. Analysis of the Root and Canal Morphologies in Maxillary First and Second Molars in a Chinese Population Using Cone-beam Computed Tomography. J Endod. 2016; 42(5):696-701. https://doi.org/10.1016/j.joen.2016.01.017 PMid:26994598

9. Vertucci FJ. Root canal anatomy of the human permanent teeth. Oral Surg Oral Med Oral Pathol. 1984; 58(5):589-99. https://doi.org/10.1016/0030-4220(84)90085-9

10. Nosrat A, et al. Variations of Palatal Canal Morphology in Maxillary Molars: A Case Series and Literature Review. J Endod. 2017; 43(11):1888-1896. https://doi.org/10.1016/j.joen.2017.04.006 PMid:28673493

11. Nair PN. On the causes of persistent apical periodontitis: a review. Int Endod J. 2006; 39(4):249-81. https://doi.org/10.1111/j.1365-2591.2006.01099.x PMid:16584489

12. Alacam T, et al. Second mesiobuccal canal detection in maxillary first molars using microscopy and ultrasonics. Aust Endod J. 2008; 34(3):106-9. https://doi.org/10.1111/j.1747-4477.2007.00090.x PMid:19032644

13. Schneider SW. A comparison of canal preparations in straight and curved root canals. Oral Surgery, Oral Medicine, Oral Pathology and Oral Radiology. 1971; 32(2):271-275. https://doi.org/10.1016/0030-4220(71)90230-1

14. Patel S, et al. European Society of Endodontology position statement: the use of CBCT in endodontics. Int Endod J. 2014; 47(6):502-4. https://doi.org/10.1111/iej.12267 PMid:24815882

15. Durack C, Patel S. Cone beam computed tomography in endodontics. Braz Dent J. 2012; 23(3):179-91. https://doi.org/10.1590/S0103-64402012000300001 PMid:22814684

16. Ji Y, et al. Could cone-beam computed tomography demonstrate the lateral accessory canals? BMC Oral Health. 2017; 17(1):142. https://doi.org/10.1186/s12903-017-0430-1 PMid:29187181 PMCid:PMC5708093

17. Mozo S, et al. Effectiveness of passive ultrasonic irrigation in improving elimination of smear layer and opening dentinal tubules. J Clin Exp Dent. 2014; 6(1):e47-52. https://doi.org/10.4317/jced.51297 PMid:24596635 PMCid:PMC3935905

18. Reuben J, et al. Endodontic management of a maxillary second premolar with an S-shaped root canal. J Conserv Dent. 2008; 11(4):168-70. https://doi.org/10.4103/0972-0707.48842 PMid:20351976 PMCid:PMC2843539

19. Kim Y, Love R, George R. Surface Changes of PathFile after Glide Path Preparation: An Ex Vivo and In Vivo Study. J Endod. 2017; 43(10):1674-1678. https://doi.org/10.1016/j.joen.2017.04.008 PMid:28689701

20. Dagna A, et al. Comparison of apical extrusion of intracanal bacteria by various glide-path establishing systems: an in vitro study. Restor Dent Endod. 2017; 42(4):316-323. https://doi.org/10.5395/rde.2017.42.4.316 PMid:29142880 PMCid:PMC5682148

ID Design Press, Skopje, Republic of Macedonia
Open Access Macedonian Journal of Medical Sciences. 2019 Dec 30; 7(24):4342-4346.
https://doi.org/10.3889/oamjms.2019.388
eISSN: 1857-9655
Basic and Clinical Medical Researches in Vietnam

Primary Cementless Bipolar Long Stem Hemiarthroplasty for Unstable Osteoporotic Intertrochanteric Fracture in the Elderly Patients

Tran Trung Dung[1, 2], Nguyen Dinh Hieu[3], Le Manh Son[4], Thien Chu Dinh[5], Toi Chu Dinh[6*]

[1]Department of Orthopaedic and Sport Medicine, Saint Paul Hospital, Hanoi, Vietnam; [2]Department of Orthopaedic and Neurosurgery, Hanoi Medical University Hospital, Hanoi, Vietnam; [3]Department of Orthopaedic and Traumatology, E Hospital, Hanoi, Vietnam; [4]Department of Orthopaedic and Traumatology 3, Viet Duc Hospital, Hanoi, Vietnam; [5]Institute for Research and Development, Duy Tan University, 03 Quang Trung, Danang, Vietnam; [6]Department of Human and Animal Physiology, Faculty of Biology, Hanoi National University of Education, Hanoi, Vietnam

Citation: Dung TT, Hieu ND, Son LM, Chu Dinh T, Chu Dinh T. Primary Cementless Bipolar Long Stem Hemiarthroplasty for Unstable Osteoporotic Intertrochanteric Fracture in the Elderly Patients. Open Access Maced J Med Sci. 2019 Dec 30; 7(24):4342-4346. https://doi.org/10.3889/oamjms.2019.388

Keywords: Unstable intertrochanteric fracture; Osteoporotic; Elderly patient; Bipolar long stem hemiarthroplasty; Cementless

***Correspondence:** Toi Chu Dinh. Department of Human and Animal Physiology, Faculty of Biology, Hanoi National University of Education, Hanoi, Vietnam. E-mail: chudinhtoi.hnue@gmail.com

Received: 05-Sep-2019; **Revised:** 20-Nov-2019; **Accepted:** 21-Nov-2019; **Online first:** 20-Dec-2019

Funding: This research did not receive any financial support

Competing Interests: The authors have declared that no competing interests exist

Abstract

BACKGROUND: Intertrochanteric fracture (ITF) is a major part of fracture in femoral head fracture. 95% of ITF are found in elderly patients. Osteosynthese is the preferred method of choice. However, elderly patients had osteoporotic, combined with many of chronic disease conditions that increase the rate of osteosynthese failure. Hemiarthroplasty bipolar long-stem is a surgical method that helps patients relieve pain, facilitate early rehabilitation, limit long-term complications, and improve quality of life for patients.

AIM: The aim of our study is to evaluate the clinical of result of primary cementless bipolar long stem hemiarthroplasty in treatment for unstable ITF in the elderly patients who have severe osteoporosis.

METHODS: Between 01/2016 and 12/2017, 35 patients with ITF type A2.2 and A2.3 (AO) were included in our prospective study. These patients were over 70 years old and treatment by hemiarthroplasty cementless long stem at E hospital and Saint Paul hospital by one group surgeons.

RESULTS: Mean age of studied subjects was 84.29 ± 6.17, the lowest was 71, the highest was 96; ratio male/female was 1/4. Follow-up of 35 patients for at least 6 months showed 88.6% caused by a low-energy injury; Average rehabilitation time was 4.63 ± 1.7 days. The average Harris point at the end was 90.4 ± 4.72.

CONCLUSION: Primary cementless bipolar long stem hemiarthroplasty is one of good choices in treatment unstable ITF in elderly patients with severe osteoporosis helped patients improve the quality of life.

Introduction

ITF is a major part of fracture in femoral head fracture. Ninety-five percent of ITF are found in elderly patients [1]. The most common cause is the poor bone with low energy injury [2]. 90% patients over the age of 70, the mortality rate after fracture from 15%-20%, treatment cost about 10 billion dollars a year [3]. Osteosynthese is the preferred method of choice. However, elderly patients had osteoporotic, combined with many of chronic disease conditions that increased the rate of osteosynthese failure. Won Sik Choy (2010) studied and reported 40 patients with cardiovascular disease and diabetes at the highest percentage of patients in the study 45% and 27.5% [4].

Hemiarthroplasty bipolar long-stem is a surgical method that helps patients to relieve pain, facilitate early rehabilitation, limit long-term complications, and improve quality of life for patients. For more than a decade, many authors have studied and evaluated the result of this surgery. Won Sik Choi (2009) has evaluated in 45 patients with ITF, aged 70 and over, after 2 years follow the average Harris hip score (HHS) at the last time was 80.6 ± 9.3 [4]. That was excellent result with patients osteoporotics have fractures unstable intertrochanterics. The author concluded that “the short-term result of cementless bipolar hemiarthroplasty in elderly patients with unstabe ITF demonstrated satisfactory results” [4].

Materials and Methods

Between 01/2016 to 12/2017, 35 patients with unstable comminuted ITF and osteoporosis (Figure 1) were treated by primary cementless bipolar long stem hemiarthroplasty at E Hospital and Saint Paul Hospital. The track period was 6 months. Average age was 84.29 years (range 71-96). They were included from the AO classification A2.2 in 14 patients and A2.3 in 21 patients. The Singh index was 2 in 27 patients and 3 in 8 patients. Average time from hospitalisation to intervention was 3.4 days. The elderly patients often have many chronic diseases association, including cardiovascular disease, diabetes mellitus, lung disease, and others.

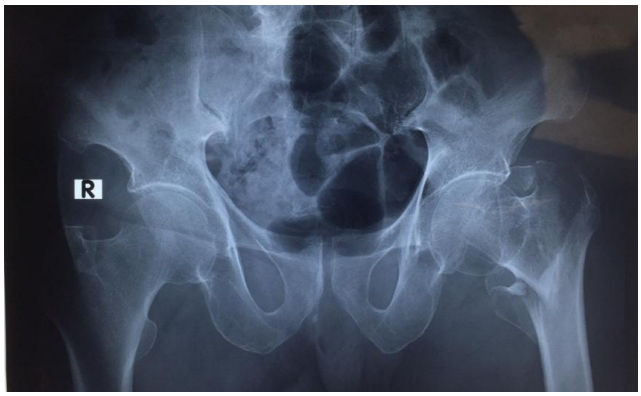

Figure 1: Pre-operative X-ray

Operative technique

Posterior lateral approach was used. Orientation of the prosthesis was made out using the lesser trochanter anatomically and posterior condylar plane. The fracture trochanter was reduced and fixed to the prosthesis with stainless steel wires (Figure 2).

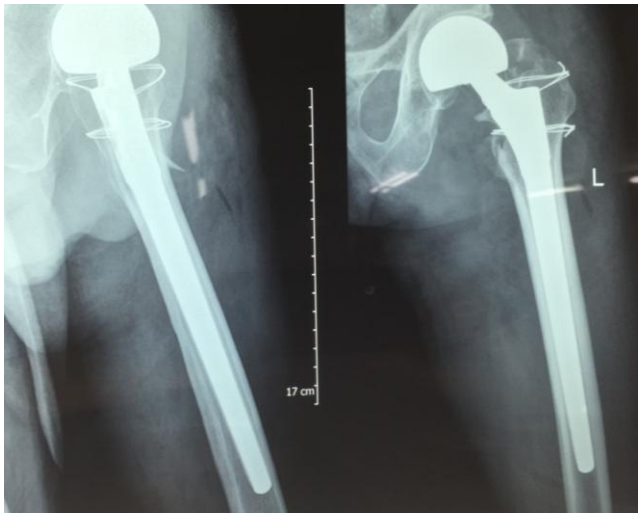

Figure 2: Post-operative x-ray

Pre-operation 12h, we used antibiotic and low-molecular weight heparin (enoxaparin) for the patients. In post-operative phase, we used antibiotic and enoxaparin for 5 days. Non-weight bearing (WB) exercises were stared on the second day after operation, partial WB exercises were stared in 4 post-operation days.

Patients were followed in 1 month, 3 months, and 6 months. Follow-up patients were assessed according to the score of HHS.

Data in our study were analysed and calculated by the medical statistics software SPSS 20.2

Results

Average follow up time was 6 months. Mean age was 84.29 ± 6.17 years (range 71-96). The ratio men/women were ¼. 88.6% were caused by a low-energy injury. Average Singh index was 2.23 ± 0.426. Most patients with chronic disease in which the two groups accounted for the highest rate of cardiovascular disease and diabetes accounted for 40% and 22.9% (Table 1).

Table 1: Accompanied medical diseases

Medical disease	n	%
Respiratory disease	2	5.7
Cardiovascular	14	40
Diabete	8	22.9
Urinary disease	5	14.3
Rheumatology disease	3	8.6
Other	9	25.7

Mean operation time was 64 ± 24.9; mean peri-operative blood transfer was 643.7 ml; mean time rehabilitation was 4.63 days; mean time hospital was 14.69 days.

Complications post-operative was included in 3 patients accounted 8.6% (Table 2). One patient was superficial infection and two others were pulmonary infection. All of them were treated well before being discharged from the hospital.

Table 2: Complication post-operative

Complication	n	%
Superficial infection	1	2.9
Dislocation	0	0
Lung infection	2	5.7
Cardiovascular	0	0
Die	0	0
Total	3	8.6

After 6 months, 22 patients had no pain, 13 had mild pain; 30 patients without aids, 5 patients with crutches; The mean HHS was 90.4 ± 4.72, of which 24 were excellent (68.6%), 10 were very good (28.6%), 1 was good (2.9%) and none show poor results (Table 3).

Table 3: Harris hip score post-operative 6 months

Result	Excellent	Very good	Good	Poor	Total
n	24	10	1	0	35
%	68.6	28.6	2.9	0	100
Average			90.4 ± 4.72		

Discussion

According to the previous researches, the method osteosynthese is prefered with a lot of materiel such as lock plate, DHS plate, Pfna nail, and gamma nail. However, there are many problems are associated with osteosynthese of unstable ITF in senile patients with osteoporotic bone: pseudarthrose, loss of fixation, and cut-out of the lag screw. For earlier WB after operation and to protect the fracture stable, some surgeons have recommended prosthetic replacement, especially with a long stem prosthesis hemiarthroplasty for the treatment of unstable ITF [5], [6], [7].

Our results indicate that a primary partial replacement with long stem prosthesis decrease pain, early rehabilitation, stability of the implant in long time, decrease complications in unstable ITF of femur osteoporosis severe.

Mean time rehabilitation in our study is 4.63 ± 1.7 days. This is a period of early rehabilitation, helps patients to move early, facilitate the process of care, avoid the risk of long-term complications such as pressure sores, pneumonia, urinary tract inflammation. According to Su-Hyun Cho (2014) the average time to partial weight-bearing is 7 days after hemiarthroplasty surgery for patients with fracture intertrochanteric [8]. Shin-Yoon Kim (2005) compared two groups of arthroplasty and osteosynthese with PFNa, showing the average time of rehabilitating exercise in the arthroplasty group was 7.8 ± 1.6 days, while in the group osteosynthese was 8.8 ± 2.9 days [9]. Parvjeet et al., (2009) compared two groups of hemiarthroplasty biplar long stem and osteosynthese with DHS plate, which resulted in an average partial stand-up time of the arthroplasty group was 7 days, while osteosynthese group was 10.1 days. The reason is the hemiarthroplasty bipolar long-stem strengthened the joints and fractures so that the patient could practice early and weight-bearing early [10].

When compared with previous results of osteosynthese, hip replacement surgery gave the same or better results[9], [11], [12], [13]. In the osteoporotic patients, treatement osteosynthese for unstable ITF needed a long time to WB. And this solution has many complications such as loss of fixation, pseudarthrose, and cut-out of the lag screw [14].

Some authors supported the point of view primary hemiarthroplasty to evade these complications of osteosynthese and help the patient have early rehabilitation, early come back to the normal activity before fracture. However, with a canal of osteoporotic femur, the stable fixation of stem into the canal is very poor. And they prefered cemented stem to get an immediate stability of the prosthesis [14]. Though, the intervention with cement rise the risk of embolism and may cause secondary cardiopulmonary complications, particularly in senilepatients with many chronic diseases. With the cementless long stem we can avoid using cement while still ensuring the stability of the fracture. The stem which was used is a tapered round-rectangular stem.It fits into the distal dyaphysis of femur (Figure 2). This method is based on the principle of fixation at the distal of femur which reduces the impact on the level fracture. With this stem, first stability and long-term biologic fixation can be got even in osteoporotic proximal femur with large bone defect [15].

In the study of Rothman, the author has noticed that the problems such as bleeding, and operative time in cementless stems is lower than cemented stems [16].

Deniz et al., (2013) compared two hemiarthroplasty groups: cemented and cementless treatment to fracture intertrochanteric, resulting in HHS of the group cemented higher than the cementless group, however the rate of complications in and after surgery of the group cemented much higher. The ratio of patients who died after surgery during hospital stay was 13% compared to 0% in cementless group with $p < 0.05$ with statistical significance. Therefore, the author still recommends the use arthroplasty cementless, and a method to improve the stability of postoperative joints is using a long stem to fix at the distal of the femoral [13].

Keating (2017) the ratio of patients with general complications (including infection, pneumonia, deep vein thrombosis ...) in the osteosynthese group was 22.73% in the hemiarthroplasty group was 18.01% [17].

Florian Geiger (2007) studied the ratio mortality patients postoperative with osteosynthese group and arthroplasty group, the results as follows: mortality after 1 year in osteosynthese group is 39.8% also in arthroplasty group is 33% [14].

Jaswinder compared two groups including hemiarthroplasty (group 1) and totalarthroplasty (group 2) in the elderly, showing that the HHS on group 2 were higher than that of the group 1. However, the rate of articular dislocation in the group 2 was higher than that of the group 1 (8% vs 0%), while the length of surgery was longer, the cost of surgery was higher. The authors recommend that although total joint replacement should be more effective, the option of hemiarthroplasty should be selected in treatment unstable ITFs in the elderly patients [18].

A study compares between hemiarthroplasty and osteosynthese of Khadoun Sinno in 2010. Result post-operative: for the group arthroplasty time fullWB was earlier than group osteosynthese and the point Harris was higher [19].

Yeesuk Kim followed 161 elderly patients after bipolar hemiarthroplasty with the time average was 3.8 years, the result obtained was positive with an average HHS at the last time was 82 [20]. The author also recommends that bipolar hemiarthroplasty is a good choice for senile patients with osteoporotic unstable ITFs [20].

In the study of Kayali et al., [21], when they compared 2 groups in treatment un stable ITF . group 1 included 42 hemiarthroplasties with group 2 included 45 osteosynthese. And they found that average time rehabilitation of group 1 lower than group 2.

In this study, we obtained excellent and very good about 97% post-operative 6 months, there were no dislocation and loosening. Time rehabilitation was about 4 days. Short- term cementless long stem bipolar seems to give better results than osteosynthese with the death rate, complication, early WB and early return to pre-fracture activities.

In 2011 Young Kyun Lee reported 87 patients with long stem bipolar for unstable intertrochanteric results 14.7 points for the scale Merle d'Aubigné [22], [23]. The author assumed even if the final results were not quite good and good, the long-term hemiarthroplasty method is still an effective method which can be applied for the unstable ITF in senile patients [22].

In our study, there were some restrictions. First, our study had short follow-up. Because a long follow-up study is very difficult for us, and has a few of clinical relevance in senile patients who have a short life and limited activity during their life. Secondly, our study has not compared between osteosynthese and arthroplasty. In addition we have not conducted a collation with cemented procedure. This is because we were afraid of the complications of cemented procedure. We will elaborate further on this matter in our future work reports.

Although these restrictions, we has successfully demonstrated that primary cementless bipolar long stem hemiarthroplasty is a satisfactory indication for elderly patients with unstable ITF of femur osteoporosis severe.

In conclusion, the difficulty is that we cannot say this method is better than internal fixation, but according to the result of our study, cementless bipolar long stem hemiarthroplasty is also a good indication when treating unstable ITF in elderlys patients osteoporotic. The patients have better prognosis, early WB, early rehabilitation, decrease the complications and increase quality of life. In order to better evaluate the effectiveness of this method, research on larger numbers of patients is required, and in the longer term, with more evaluation criteria, this helps to open up ideas for our studies next.

Ethical approval

This is a one of indications to treat unstable ITF in the elderly patients who have severe osteoporosis. This method has been applied in many countries as well as many hospitals in Vietnam, so this study does not require the ethical approval.

Informed consent

The consent and commitment were signed by the patients in the study and their families.

Reference

1. Guyton JL. Fractures of hip - Acetabulum and Pelvis. Campbells operative orthopaedics, 9th Edit (Mosby), 2003:2181-2262.

2. Lindskog DM, Baumgaertner MR. Unstable Intertrochanteric hip Fractures in the Elderly. J. Am Acad Orthop Surg. 2004; 12:179-190. https://doi.org/10.5435/00124635-200405000-00006 PMid:15161171

3. Lorich DG, Geller DS, Nielson JH. Osteoporotic pertrochanteric hip fractures. Management and current controversies. J. Bone Joint Surg Am. 2004; 86:398-410. https://doi.org/10.2106/00004623-200402000-00028

4. Choy WS, Ahn JH, Ko JH, Kam BS, Lee DH. Cementless bipolar hemiarthoplasty for unstable intertrochanteric fractures in elderly patients Clinics in orthopedic surgery. 2010; 2(4):221-226. https://doi.org/10.4055/cios.2010.2.4.221 PMid:21119938 PMCid:PMC2981778

5. Broos PL, et al. Pertrochanteric fractures in the elderly. Is the Belgian VDP prosthesis the best treatment for unstable fractures with severe comminution? Acta Chir Belg. 1991; 91:242-9. https://doi.org/10.1097/00005131-199112000-00010

6. Harwin SF, Stern RE, Kulick RG. Primary Bateman-Leinbach bipolar prosthetic replacement of the hip in the treatment of unstable intertrochanteric fractures in the elderly. Orthopedics. 1990; 13:1131-6.

7. Green S, Moore T, Proano F. Bipolar prosthetic replacement for the management of unstable intertrochanteric hip fractures in the elderly. Clin Orthop Relat. 1987; 224:169-77. https://doi.org/10.1097/00003086-198711000-00024

8. Cho SH, Cho HL, Cho H. Primary Cementless Hip Arthroplasty in Unstable Intertrochanteric Femur Fracture in Elderlys: Short-term Results. Hip Pelvis. 2014; 26(3):157-65. https://doi.org/10.5371/hp.2014.26.3.157 PMid:27536574 PMCid:PMC4971141

9. Kim SY, Kim YG, Hwang JK. Cementless calcar-replacement hemiarthroplasty compared with intramedullary fixation of unstable intertrochanteric fractures: a prospective, randomized study. JBJS.

2005; 87(10):2186-92. https://doi.org/10.2106/00004623-200510000-00005

10. Parvjeet Singh Gulati, et al., Comparative study of treatment of intertrochanteric fractureof femur with long-stem bipolar prosthetic replacement versus dynamic hip screw fixation. Pb Journal of Orthopaedics. 2009; 1:38-40.

11. Little NJ, et al. A prospective trial comparing the Holland nail with the dynamic hip screw in the treatment of intertrochanteric fractures of the hip. J Bone Joint Surg Br. 2008; 8:1073. https://doi.org/10.1302/0301-620X.90B8.20825 PMid:18669966

12. Lihong F, Dang X, Wang K. Comparison between bipolar hemiarthroplasty and total hip arthroplasty for unstable intertrochanteric fractures in elderly osteoporotic patients. PLoS One. 2012; 7(6):e39531. https://doi.org/10.1371/journal.pone.0039531 PMid:22745778 PMCid:PMC3382155

13. Cankaya D, Ozkurt B, Tabak AY. Cemented calcar replacement versus cementless hemiarthroplasty for unstable intertrochanteric femur fractures in the elderly. Ulus Travma Acil Cerrahi Derg. 2013; 19(6):548-53. https://doi.org/10.5505/tjtes.2013.57615 PMid:24347215

14. Geiger F, et al. Trochanteric fractures in the elderly: the influence of primary hip arthroplasty on 1-year mortality. Arch Orthop Trauma Surg. 2007; 127(10):959-66. https://doi.org/10.1007/s00402-007-0423-7 PMid:17899138 PMCid:PMC2111040

15. Keisu KS, Orozco F, Sharkey PF. Primary cementless total hip arthroplasty in octogenarians. Two to eleven-year follow-up. J Bone Joint Surg Am. 2001; 3:359. https://doi.org/10.2106/00004623-200103000-00007 PMid:11263639

16. Rothman RH, Cohn JC. Cemented versus cementless total hip arthroplasty. A critical review. Clin Orthop Relat Res. 1990; 254:153. https://doi.org/10.1097/00003086-199005000-00024

17. Keating JF, et al. The journal of bone and joint surgery. 2017; 88(2):249-260. https://doi.org/10.2106/JBJS.E.00215 PMid:16452734

18. Walia JP, Sansanwal D, Walia SK, Singh S, Gupta AC. Role of primary bipolar arthroplasty or total hip arthroplasty for the treatment of intertrochanteric fracture femur in elderly. Pb Journal of Orthopaedics. 2011; 12(1):5-9.

19. Sinno K, Sakr M, Girard J, Khatib H. The effectiveness of primary bipolar arthroplasty in treatment of unstable intertrochanteric fractures in elderly patients. North American journal of medical sciences. 2010; 2(12):561. https://doi.org/10.4297/najms.2010.2561 PMid:22558568 PMCid:PMC3338223

20. Kim Y, Moon JK, Hwang KT, Choi IY, Kim YH. Cementless bipolar hemiarthroplasty for unstable intertrochanteric fractures in octogenarians. Acta Orthop Traumatol Turc. 2014; 48(4):424-430. https://doi.org/10.3944/AOTT.2014.13.0119 PMid:25230266

21. Kayali C, et al. Treatment for unstable intertrochanteric fractures in elderly patients: internal fiation versus cone hemiarthroplasty. Journal of Orthopaedic Surgery. 2006; 14(3):240-244. https://doi.org/10.1177/230949900601400302 PMid:17200522

22. Lee YK, et al. Cementless bipolar hemiarthroplasty using a hydroxyapatite-coated long stem for osteoporotic unstable intertrochanteric fractures. J Arthroplasty. 2011; 26(4):626-32. https://doi.org/10.1016/j.arth.2010.05.010 PMid:20637559

23. D'Aubigne RM, Postel M. Functional results of hip arthroplasty with acrylic prosthesis. J Bone Joint Surg Am. 1954; 3:451. https://doi.org/10.2106/00004623-195436030-00001

ID Design Press, Skopje, Republic of Macedonia
Open Access Macedonian Journal of Medical Sciences. 2019 Dec 30; 7(24):4347-4350.
https://doi.org/10.3889/oamjms.2019.389
eISSN: 1857-9655
Basic and Clinical Medical Researches in Vietnam

"False Patellar Duplication" Originated from Synovial Osteochondromatosis in Knee Joint: A Rare Case Report

Dung Tran Trung[1, 2], Tung Pham Son[1], Thien Chu Dinh[3], Toi Chu Dinh[4*]

[1]Saint Paul University Hospital, Hanoi, Vietnam; [2]Hanoi Medical University, Hanoi, Vietnam; [3]Institute for Research and Development, Duy Tan University, 03 Quang Trung, Danang, Vietnam; [4]Department of Human and Animal Physiology, Faculty of Biology, Hanoi National University of Education, Hanoi, Vietnam

Citation: Trung DT, Son TP, Chu Dinh T, Chu Dinh T. "False Patellar Duplication" Originated from Synovial Osteochondromatosis in Knee Joint: A Rare Case Report. Open Access Maced J Med Sci. 2019 Dec 30; 7(24):4347-4350.
https://doi.org/10.3889/oamjms.2019.389

Keywords: False patellar duplication; Synovial osteochondromatosis

***Correspondence:** Toi Chu Dinh. Department of Human and Animal Physiology, Faculty of Biology, Hanoi National University of Education, Hanoi, Vietnam. E-mail: chudinhtoi.hnue@gmail.com

Received: 05-Sep-2019; **Revised:** 20-Nov-2019; **Accepted:** 21-Nov-2019; **Online first:** 20-Dec-2019

Funding: This research did not receive any financial support

Competing Interests: The authors have declared that no competing interests exist

Abstract

BACKGROUND: "False patellar duplication" is a situation where there are two pieces in the position of a knee-joint like patella. It can derive from cartilage tumors, soft tissue tumors, or gout tumors, or due to the heterotopic ossification, forming a sub patella in the knee joint.

CASE REPORT: A woman, 57 years old, healthy history, she has hospitalized for right knee joint pain since 2 years. Diagnosis: the synovial osteochondromatosis of the right knee. We decided to conduct and arthroscopy and removal. After 18 months surgery, the patient knee joint is currently good, range of motion (ROM) (-10)°- 0°-160°, Lysholm Knee Scoring Scale 85/100 point.

CONCLUSION: This is the second case in the world and the first case in Vietnam. This is an experience in the process of diagnosis, arthroscopic treatment and differentiation from the "double patellae" status.

Introduction

The synovial osteochondromatosis are a begin metaplasia of the synovial fluid, in which the connective cells have the ability to self-produce cartilages. The relapse rate is high, about 7.1%-39% [8], [9], [14], [13]. The synovial osteochondromatosis are commonly present in the knee joint, accounting for 50%-60%, then in other joints such as hip and shoulder joints, elbows and ankles joints. When the synovial osteochondromatosis in the knee joint have large size, they will limit the knee joints movement, cause pain for patient, limit movement, causing knee joint effusion; making doctors mistakenly think that it is patellar duplication, sub patella, nonunion of patella fracture, ... There have been many cases report of synovial osteochondromatosis in knee joint causing reported deformity, as reported by Tushar Kambale [3], Sunil Kukreja [4], Samir Dwidmuthe [7] , Hugh Mackenzie [5] …. and all authors had to open surgery to remove the cartilage osteochondromatosis.

"Double patellae" or "patellar duplication" means there are two patellae on one knee, this is a very rare case and in the world medical literature, currently only about 15 published cases [12]. When a child, the central cartilage develops into the patella. In some cases, the cartilages divides into another 2, 3 partite (this is very rare) which will develop into the patella, resulting in a "True patella duplication" [2]. "False patellar duplication" is a situation where there are two pieces in the position of a knee joint like patella, in which one is a true patella that originate from the central cartilage, another is a non- patella, but in an adjacent position and we think it is a patella too. It can derive from cartilage tumors, soft tissue tumors, or gout tumors, or due to the heterotopic ossification, forming a sub patella in the knee joint. In the world medical literature, there is only one case of "false patellar duplication" that originated from synovial osteochondromatosis published in 2012 by Yoshiteru Kajikawa [12] and he had to open surgery to

remove the these block, my case is the second case in the world and the first case in Vietnam of false patellar duplication originated from synovial osteochondromatosis that I had arthroscopic treatment and followed for the past 18 months.

Case Report

The patient is a woman, 57 years old, healthy history, no history of right knee joint injury, not detected abnormalities in the right knee joint. She has hospitalized for right knee joint pain for 2 years. According to the patient, she felt an abnormal mass under the right patella 10 years ago. At the beginning, the mass was small that she could only touch but not see. She didn't have pain or feel pain. Gradually it increases the volume, in the last 2 years it has affected her knee joint function: more difficult walking, reduced movement, swollen knees, pain, not hot, no fever. She had many examinations and was diagnosed: right knee osteoarthritis and treated towards the knee joint osteoarthritis. After 2 years, it is not better, movement limit increased so she went to the Saint Paul Hospital for examination.

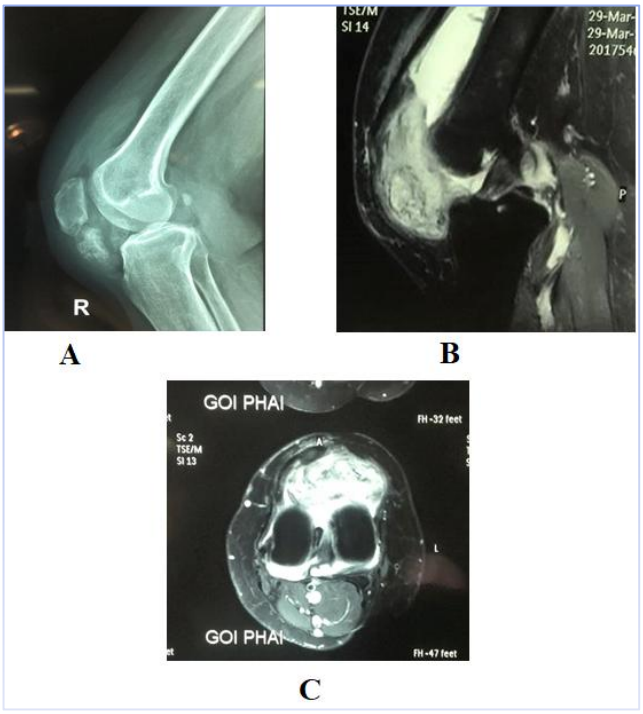

Figure 1: X-ray and MRI before surgery. A. X-ray before surgery; B and C. MRI before surgery

Through the examination, the doctors at the Saint Paul Hospital detected a positive mass of 26mm x 62mm size at the lower patella, with clear boundaries and not existence of penetration or metastasis, swollen knee, ROM 20°-30°-90° degree, Lysholm Knee Scoring Scale 50/100 points, no infection syndrome, leukocyte 4.5 G/l, neutral 58%, X-ray: a mass with calcium deposits in the right lower patella; on MRI film, there is image of knee joint effusion, the thickest is 21 mm, the wall of the synovial fluid is thick with medicine after injection, the lower part of synovial fluid has the structure of 26 mm x 62 mm size, increasing and decreasing uneven signal on T1W and T2W, do not absorb the medicine after the magnetic contrast injection (Figure 1). Diagnosis before surgery: the synovial osteochondromatosis of the right knee.

We decided to conduct an arthroscopy, we may use the" bone cutter shaver blade" if the mass is hard and had an open surgery plan if it was not possible to cut them for arthroscopy removal. We carried out arthroscopy into the knee joint with 2 trocar holes, because cartilage takes up most of the lower inner cavity so our inlet hole must be placed higher than the normal position, from about 1cm to avoid the tumor. When we were checking, we found knee osteoarthritis, femoral condylar offset began to disappear, bilateral meniscus tear, the anterior cruciate ligament and the posterior cruciate ligament are normal with a lot of fluid. A cartilage mass located at the injury, not attached to the patella, derived from the synovial membrane, occupying the entire area of the anterior cavity and the inner cavity in the knee joint, limiting the right knee movement (Figure 2A).

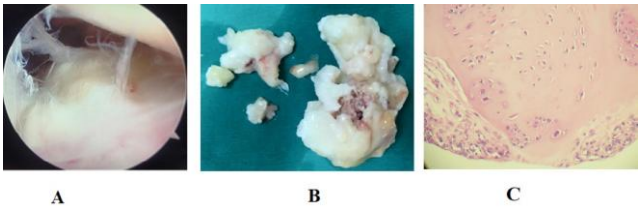

Figure 2: Image in surgery; A) Images in arthroscopy; B) Synovial osteochondromatosis after surgery; C) The anapatthology of synovial osteochondromatosis

We used the bone cutter shaver blade and soft tissue cutter shaver blade, proceeded to clean the knee joint, meniscectomy, repaired the cartilage, cut and planed this cartilage tumor, then used the forceps to hold them out of the knee one after another and send to the anapathology (Figure 2B). After removing all of the masses, we checked the knee joint movement and saw that its movement is good, ROM 0°-5°-120°, we placed the drain and closed the skin. The operation time is 90 minutes. The patient used betalactam antibiotics, anti-inflammatory, analgesics and rehabilitation training on the first day after surgery, withdrew the drain after 2 days and discharged 5 days after surgery. The result of anapathology is synovial osteochondromatosis (Figure 2C). Through regular check-ups after 2 weeks, 1 month, 3 months, 6 months, 12 months, 18 months, the patient knee joint is currently good, ROM (-10)°-0°-160°, without pain while sitting, painful while walking due to the condition of knee osteoarthritis, Lysholm Knee Scoring Scale 85/100 point (Figure 3). We didn't find any signs of relapse of synovial

osteochondromatosis.

Figure 3: Knee function after 18 months of surgery; A) Extending knee posture; B. Flexing knee posture

Discussion

The proportion of congenital "patellar duplication" or "double patella" is extremely low, very rare in the clinical world and in the world medical literature, now only about 15 cases have been published in the world; in which "false patellar duplication" due to the synovial osteochondromatosis, this is the second case published in the world, the first case was published by the Japanese author Yoshiteru Kajikawa [12] in 2012 and he had to open surgery to remove the these block . The "false patellar duplication" has many causes, probably of cartilage tumor, gout tumor, soft tissue tumor or sub patella, sometimes false knee joint of the patella. To know exactly what the "false patellar duplication" is and where it comes from, the best method is surgery to draw the false patella out and send it to the anapathology. However, we based on the question of the disease history, medical history and clinical examination, and we can also determine up to 80% of what the false patella is and where it came from. For example, if the false patella due to gout tumor, the patient has a gout history, this false patella was usually not mobile, has lied next to the bone for a long time; or the false patella originated from cartilage tumors, so these cartilage tumors were often mobile and have appeared for a long time. "False patellar duplication" is usually benign, just lies next to the patella and affects the patella's movement, not malignant, invasive and metastatic. It is for this reason that in the image of X-ray film, the real patella, the femur condyle and the tibia higher head are normal, no secondary injury caused by the "false patellar duplication"; on the contrary, when "false patellar duplication" is malignant, invades the surrounding organs, making the surrounding soft tissues change the nature, the bone part will have the image of bone defect, periosteum reaction, bone deformity, ...

In case the first "false patellar duplication" originates from the synovial osteochondromatosis published by Yoshiteru Kajikawa, the author described the mass behind the patella in large size and there are many smaller cartilage tumors in the joint. Normally, the synovial osteochondromatosis are not rare, but often they are small in size and located in the joints for many years, however, there are some favorable conditions that facilitate the synovial osteochondromatosis to develop, the authors Itaru Tojyo [15] and Seiya Jingushi [11] have found a relation between hormones to the growth factor the synovial osteochondromatosis, which is specifically related to fibroblast growth factor (FGF: FGF-2 and FGF-3). These factors will facilitate the synovial osteochondromatosis to develop, promote cartilage division that makes the cartilage size grow larger than usual.

The false patellar duplication can be located anywhere in the knee joint, either inside or outside the patella, or can come out behind the patella. The authors Eric Yeung and John Ireland reported a case of the false patellar duplication appeared after a 6-year knee joint injury, after the surgery, the author concluded that the mass was bone, limiting movement for injured knee joints. In addition, the most recently in 2017, the author Annemieke [1], has published a case of the false patellar duplication behind the patella due to Multiple Epiphyseal Dysplasia (MED), causing a double layer of patella, that means the true patella lying on the other patella, the author asked to have MRI to accurately assess the level of the compression of the tendon, the patella cartilage and strange thing**s** hidden in the joint before treatment. The author Eric Saupe [6] studied and classified double patella into 3 types, each type has its own characteristics. The first type is that the patella is divided in the lower part, making the patella have 2 pieces: big piece at the top and the small piece at the bottom. The second type is the patella split vertically, a big piece and a small piece on the opposite side. The last type is the third type, the divider line at the upper corner into the big piece at the bottom and the small piece at the top.

The condition of false patellar duplication is largely asymptomatic, but in some cases, it may be the cause of knee joint pain that cannot be explained by other causes, which can cause knee joints movement limitations because they caused joints obstruction or block the movement of the patella and femoral condyle and tibial plateau. In addition, if their size is too large, they can cause patella dislocation, causing joint deformities, joint effusion or joint

stiffness. According to author Goebel [10], the surgery requests was set when the false double patella has complications, depending on the size and nature of that mass that the surgeons should consider arthroscopy surgery or open surgery to remove the mass and send it to the anapathology. The principle is to remove all the masses and correct the complications caused by them. In our opinion, if arthroscopy surgery is possible, it will still be used for arthroscopy surgery for patients to intervene at the minimum incision, avoiding damaging the surrounding parts, shortening the hospitalization time and early rehabilitation training.

In conclusion, this is the second case report of "false double patella" with the cause of the synovial osteochondromatosis in the world and the first case report in Vietnam and Southeast Asia. This status of "false double patella" needs to be distinguished from many other causes such as soft tissue tumors, gout tumor or "congenital double patella". Arthroscopic treatment is the treatment method that is planned because of complications for the patient. After 18 months of follow-up, this patient is now well-traveled, with good knee function and 85/100 points Lysholm Knee Scoring Scale.

Informed consent

The consent and commitment were signed by the patient.

References

1. Milants A, De Maeseneer M, De Mey J. Double-layered patella (DLP) in multiple epiphyseal dysplasia (MED). Journal of the Belgian Society of Radiology. 2017; 101(1). https://doi.org/10.5334/jbr-btr.1219 PMid:30039000 PMCid:PMC5854308

2. J. Gasco J, Del Pino JM, Gomar-Sancho F. Double patella. A case of duplication in the coronal plane. The Journal of bone and joint surgery. British volume. 1987; 69(4):602-3. https://doi.org/10.1302/0301-620X.69B4.3611165

3. Kambale T, Iqbal B, Jain A. A case report of synovial chondromatosis of the knee. Clin Cancer Investig J. 2015; 4:105-7. https://doi.org/10.4103/2278-0513.149065

4. Kukreja S. A Case Report of Synovial Chondromatosis of the Knee Joint arising from the Marginal Synovium. J Orthop Case Reports. 2013; 3(1):7-10. https://doi.org/10.1136/bcr-2013-202186 PMid:24326442 PMCid:PMC3863075

5. Mackenzie H, Gulati V, Tross S. A rare case of a swollen knee due to disseminated synovial chondromatosis: a case report. Journal of medical case reports. 2010; 4(1):113. https://doi.org/10.1186/1752-1947-4-113 PMid:20416049 PMCid:PMC2873448

6. Saupe E. Beitrag zur patella. Fortschr. Rontgenstr.. 1921; 28:37-41.

7. Dwidmuthe S, Sharma M. A Case Report of Primary Synovial Chondromatosis with Bilateral Genu Valgum. J Orthop Case Reports. 2017; 7(5):92-95.

8. Boyer T, Dorfmann H. Arthroscopy in primary synovial chondromatosis of the hip: description and outcome of treatment. J Bone Joint Surg Br. 2008; 90(3):314-8. https://doi.org/10.1302/0301-620X.90B3.19664 PMid:18310752

9. de Sa D, et al. Arthroscopic surgery for synovial chondromatosis of the hip: a systematic review of rates and predisposing factors for recurrence. Arthroscopy. 2014; 30(11):1499-1504.e2. https://doi.org/10.1016/j.arthro.2014.05.033 PMid:25064754

10. Goebel S, Steinert AF, Barthel T. Surgical management of a double-layered patella: a case report. Archives of orthopaedic and trauma surgery. 2009; 129(8):1071-5. https://doi.org/10.1007/s00402-008-0701-z PMid:18677496

11. Jingushi S, et al. Transient exposure of fibroblast growth factor-2 induced proliferative but not destructive changes in mouse knee joints. Connect Tissue Res. 2006; 47(4):242-8. https://doi.org/10.1080/03008200600883146 PMid:16987757

12. Kajikawa Y, Arai Y, Takamiya H, Higuchi T, Mori G, Morisaki S, Kubo T. A double patella-like condition secondary to synovial osteochondromatosis", Sports medicine, arthroscopy, rehabilitation, therapy & technology : SMARTT. 2012; 4(1):31-31. https://doi.org/10.1186/1758-2555-4-31 PMid:22943294 PMCid:PMC3494534

13. Lee JB, et al. Arthroscopic treatment of synovial chondromatosis of the hip. Am J Sports Med. 2012; 40(6):1412-8. https://doi.org/10.1177/0363546512445150 PMid:22539535

14. Marchie A, Panuncialman I, McCarthy JC. Efficacy of hip arthroscopy in the management of synovial chondromatosis. Am J Sports Med. 2011; 39(1):126-31. https://doi.org/10.1177/0363546511414014 PMid:21709042

15. Tojyo I, et al. The expression of fibroblast growth factor receptor-3 in synovial osteochondromatosis of the temporomandibular joint. Arch Oral Biol. 2004; 49(7):591-4. https://doi.org/10.1016/j.archoralbio.2003.12.009 PMid:15126141

ID Design Press, Skopje, Republic of Macedonia
Open Access Macedonian Journal of Medical Sciences. 2019 Dec 30; 7(24):4351-4356.
https://doi.org/10.3889/oamjms.2019.390
eISSN: 1857-9655
Basic and Clinical Medical Researches in Vietnam

Preliminary Result of Arthroscopic Anterior Cruciate Ligament Reconstruction Using Anterior Half of Peroneus Longus Tendon Autograft

Dung Tran Trung[1, 2], Son Le Manh[3], Luan Nguyen Thanh[3], Thien Chu Dinh[4], Toi Chu Dinh[5*]

[1]Department of Orthopaedic and Sport Medicine, Saint Paul Hospital, Hanoi, Vietnam; [2]Department of Orthopaedic and Neurosurgery, Hanoi Medical University Hospital, Hanoi, Vietnam; [3]Department of General Orthopeadic and Trauma, Viet duc Hospital, Hanoi, Vietnam; [4]Institute for Research and Development, Duy Tan University, 03 Quang Trung, Danang, Vietnam; [5]Department of Human and Animal Physiology, Faculty of Biology, Hanoi National University of Education, Hanoi, Vietnam

Citation: Trung DT, Manh SL, Nguyen Thanh L, Chu Dinh T, Chu Dinh T. Preliminary Result of Arthroscopic Anterior Cruciate Ligament Reconstruction Using Anterior Half of Peroneus Longus Tendon Autograft. Open Access Maced J Med Sci. 2019 Dec 30; 7(24):4351-4356. https://doi.org/10.3889/oamjms.2019.390

Keywords: Anterior cruciate ligament; Anterior half peroneus longus tendon

***Correspondence:** Toi Chu Dinh. Department of Human and Animal Physiology, Faculty of Biology, Hanoi National University of Education, Hanoi, Vietnam. E-mail: chudinhtoi.hnue@gmail.com

Received: 08-Sep-2019; **Revised:** 20-Nov-2019; **Accepted:** 21-Nov-2019; **Online first:** 20-Dec-2019

Funding: This research did not receive any financial support

Competing Interests: The authors have declared that no competing interests exist

Abstract

BACKGROUND: Arthroscopic anterior cruciate ligament reconstruction is one of the most successful operations in sports medicine. At present, ligament autografts have been the best method due to good histocompatibility, rapid healing, no cross-contamination, and low cost of treatment. However, autografts do not have infinite amount and are also not always feasible. Anterior half of peroneus longus tenden autograft is likely to become a source of autograft with many advantages. This study aims to evaluate the clinical outcomes of arthroscopic anterior cruciate ligament reconstruction using anterior half of peroneus longus tendon autograft (AHPLT).

AIM: To evaluate the initial outcome of ACL reconstruction arthroscopy by anterior half of peroneus longus tendon.

METHODS: This is a prospective non-controlled case series.

RESULTS: A prospective study on 30 patients (from 9 / 2016 to 01 / 2019) had both ACL and MCL injury who had operated ACL reconstruction using anterior half of peroneus longus tendon autograft (AHPLT) at Department of General Orthopaedic and Trauma, Viet Duc hospital. Our outcome: the year average 35.4 ys, the rate of ACL rupture combined with meniscus injury was 40%. The average diameter AHPLT autograft is 7.0 mm. The function Lysholm scores improved from 59 to 94.27 postoperative 6 months. No difference beetwen the AOFAS scale of preoperative and postoperative.

CONCLUSION: Peroneus longus tendon is recommended to be a safe and practical autograft resource for arthroscopic anterior cruciate ligament reconstruction.

Introduction

Sport injury and vehicle collision are among the most striking problems. In these circumstances, ligaments are the main suffered organ. The graft used for reconstruction surgery requires good biomechanics, rapid healing and easy ability to ligate from the body. Many different kinds of graft have been successfully used in clinical settings [1], [2]. Research about biomechanical features of anterior half of peroneus longus tendon auto-graft began in 1977, mostly for knee ligament reconstruction in general and ACL reconstruction in specific for preserving the function of peroneus longus tendon [3].

In 2012, Jinzhong Zhao did a research about biomechanical features, application of anterior half of peroneus longus and its safety and effectiveness. This study compared the ankle function before and after operation of ligament reconstruction using AOFAS score [4]. It showed that AOFAS score pre- and post-operation was 97.4 ± 2.0 and 97.2 ± 1.6 respectively ($p = 0.85$). Author's conclusion was that it is a good autograft by advantages in bearing force, safety and risk.

Hong-Bin Cao (2012) treated ACL injury by using AHPLT tendons and assessed the clinical

results of ankles function. There were 35 patients suffering from injury requiring surgery following up from January 2006 to December 2009, average age 31.8 (21 to 56 years). Postoperative evaluation includes clinical assessment, Lysholm score, KT 3000 and AOFAS scale. Mean follow-up evaluation time was 55 months of follow-up. Lysholm score is classified as very good in 25 cases, quite good in 3 and poor in 1 case. AOFAS scores are not statistically different ($p > 0.05$). The author concluded that AHPLT is good enough to apply in ACL regeneration and did not affect the ankle joint function [5].

In the study done by Nhan TT in 2016, the research conducted over 61 patients with ACL reconstruction using AHPLT showed that post-op Lysholm score is classified as very good and good in 93.44% of patients (57 / 61 patients) [6]. In another done by Vinh PQ in 2017, the research recruited 150 patients over 18 years of age treated by arthroscopic ACL reconstruction. Results showed that Lysholm score is classified as good in 84.67% of patients and the function of ankle joint (AOFAS scale) before surgery was 97.13 ± 1.92 [7].

These studies demonstrated that the impact of taking AHPLT in ankle was not significant. At Viet Duc Hospital, research about AHPLT application in arthroscopic ACL reconstruction has been conducted, but no research has evaluated the effectiveness of AHPLT in arthroscopic ACL reconstruction. The patients in our research are both ACL and MCL injury. We do not use Hamstring tendon as standard technique for reconstruction because of adding more medial unstability of the knee.Therefore, we conducted this study with two objectives [1]. Clinical symptoms and imaging of patients with ACL injury, and [2]. Evaluate the results of arthroscopic ACL reconstruction by AHPLT.

Material and Method

Thirty patients were diagnosed ACL injury with or without meniscus injury combined with mild and moderate MCL injury. All the patients were treated with conservation of MCL and arthroscopy ACL reconstruction by anterior half of peroneus longus tenden auto-graft in Vietduc hospital from September, 2016 to January,2019 with more than 6 months follow-up.

Subjects

Recruitment criteria: The patient has ACL injury with or without meniscus injury with mild and moderate MCL injury based on MRI and clinical features. The patients agree to take part in the research.

Exclusion criteria: Simple ACL injury or PCL injury or external ligament. Patients with pathological injury of ankle joint and common fibular nerve.

Sample size and place

Thirty patients are appropriate to those criteria. We conducted the prospective non-controlled case series study from September, 2016 to January,2019 at Department of General orthopedic and Trauma, Viet duc hospital.

Surgical technique

The endoscopic surgical instrument ACL reconstruction by anterior half of peroneus longus tendon, fixed the graft by Tightrope with all-inside technique. Exam the patient before surgery: (1) The patients selected for the study will be conducted for clinical examination and follow-up medical records (sample medical records). Record preoperative variables such as Lysholm score, IKDC score, AOFAS score; and (2) Surgical procedure for ACL reconstruction using anterior half of peroneus longus tendon auto-graft through arthroscopy including 4 steps: Step 1: Arthroscopy check the meniscus, treat the meniscus if injury available. Then reconstruct the ACL; Step 2: Take the graft: Skin incision 2-3 cm along the back of fibula and 2cm above the lateral malleolus, the peroneus longus tendon just below it. Separate the peroneus longus tendon at the farthest possible location without damage the upper retinaculum. Split the anterior half and posterior half of peroneus longus tendon and cut the anterior half. Using the surgical instrument to take the graft (Figure 1); Step 3: Preparing the graft: Four-fold the graft. Using tendon frames to stretch the graft with force of about 5 kg (50 – 60 N) for 10 minutes. Put 2 Tight-rope and sew 2 sides of graft on the piece about 2 cm. Measure the diameter and the length of the graft; and Step 4: Take the graft through endoscopy: Through endoscopy drilling tunnel tibial plateau and thigh the diameter of graft. Fix the graft to the tibial and thigh tunnel by Tight-rope. Check again by Lachman test. Maximum stretching the knee to assess the ligament. The post operation rehabilitation has been done by following Karistinos A. and James A. Walker [8]:

- Phrase 1: 6 weeks after surgery.

+ Patella glides and tilts

+ Decrease swelling

+ Quad sets

+ Straight leg raise and short arc quads 90° – 40°

+ Hamstring PRE and move to aquatic therapy after wound is completely healed or a protective waterproof dressing is available

+ Proprioception exercises and prone terminal

knee extensions

- Phrase 2: from 7 weeks to 10 weeks after surgery

+ Bicycle with resistance

+ Leg press, progressive resistive exercises

+ 0^{o}-30^{o} leg extension exercises

+ Increase flexion as fast as possible

-Phrase 3: from 11 weeks to 16 weeks after surgery

+ Full PREs

+ Hamstrings and quads

+ Stair stepper

+ Patient may golf and hike

-Phrase 4: from 17 weeks to 24 weeks after surgery: Transition to Sport and Work

+ No contact or competition

+ Full weight lifting program

+ Advanced balance exercises

+ Begin progressive running program

-Phrase 5: from 6 months to 9 months: Return to play

+ Run up or down stairs

+ Progress cutting, jumping, and sport-specific drills

+ Transition to sport

+ Quad strength and Hamstring strength must be 90% of opposite side

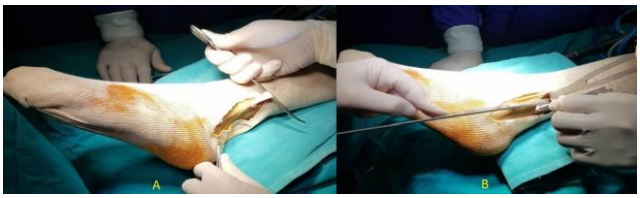

Figure 1: Skin incision to approach AHPLT tendon A) and Tendon stripping B)

Variable research and study tool

Genders, location of knee, and time of injury, clinical features: knee pain, knee instability, Lach-man test, Pivot shift test, Lysholm score, AOFAS score, IKDC score. We used optimal MR360 1.5T MRI scanning system, made in Florida, USA, November 2009, serial 037255, thin cut 1 mm, 256 slice and X-ray machine. Data were analysed by using SPSS software version 22. Frequency and percentage were used to show quanlitative variable and mean and the standard deviation was used to show the quantitative variables.

Results

General characteristics

The average age of research group is 35.4 years old, of which the smallest is 18 years old, the oldest is 51 years old. There are 19 male patients accounting for 63.3%, higher than female with 11 patients occupy 36.7%. The most common cause is sport injury in 12 cases accounting for 40%, 12 cases of daily activities accident accounting for 40%, traffic accident occupy 20% (Figure 2).

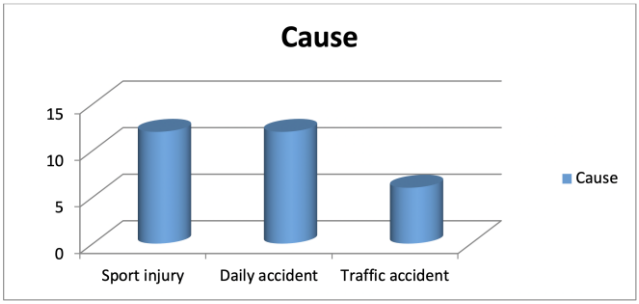

Figure 2: The cause of ACL injury

Common clinical symptoms are knee pain when strongly activities, loosen knee in daily activities, most of the patients have problems when going up and down the stairs. Clinical symptoms are valuable for preoperative diagnosis including Lachman sign, anterior drawer test and Pivot shift test with 82.3%, 100% and 86.7% sensitivity, respectively.

The average length of anterior half of peroneus longus tendon graft is 60 mm, the shortest is 60 mm and the longest is 65 mm. The graft mainly four-fold or three-fold to achieve the shortest length approximately 60 mm. We use All-in-side technique with Tightrope 2 head fixed. The average diameter of the research group is 7.0 mm, the smallest is 6.0 mm, the largest is 8.5 mm.

Through many studies, we found that the average of ACL size ranges from 7-12 mm, in the study group, the diameter of tendon mainly greater than 7mm (22 over 30 patients), just 4 patients were from 6.5 to 7mm. Graft size in ACL reconstruction is an important factor. Magnussen et al., [9] considered 7mm as the minimum graft size to avoid the revision surgery. In a study of 256 patients with hamstring autograft ACL reconstruction, grafts larger than 8.5 mm had a 1.7% revision rate, and grafts between 8.0 and 8.5 mm and 7.5 and 8.0 mm had a revision rate of 6.5% and 6.2%, respectively. In the same study, grafts that ranged from 7.0 to 7.5 mm and 7 mm or less had a revision rate of 11.3% and 33%, respectively.

Preoperative determination of hamstring graft size is challenging. Magnetic resonance imaging and ultrasound scanning have been used to predict hamstring graft sizes with moderate success

[10]. Anthropometric data collection has also been used with more success in the literature [11] though the confidence intervals remain too large for an accurate clinical use.

Clinical post-operative outcome

The stability of knee was evaluated through the results of Lachman sign after surgery: the rate of negative is 90%; level 1 is 10% and no longer level 2,3 (Table 1). Compared to the Lachman before surgery, it was 76.7% in level 2 and level 3 was seen 16.7%.

Table 1: Lachman sign after surgery

Lachman	Negative	Level 1	Level 2	Level 3	Total
n	27	3	0	0	30
Percentage	90%	10%	0%	0%	100%

The stability of knee was evaluated through the results of anterior drawer test postoperation: the rate of negative is 96.7%; level 1 is 3.3% and no longer level 2,3. Compared to the Lachman before surgery, it was 96.7 positive (Table 2).

Table 2: Anterior drawer test after surgery

Anterior drawer test	Negative	Level 1	Level 2	Level 3	Total
N	29	1	0	0	30
Percentage	96.7%	3.3%	0%	0%	100%

These are two methods to determine the displacement of anterior tibial plateau compared with femoral condyle or the instability of knee joint. There was a sinificant improvement before and after surgery.

The percentage of stability knee in our research higher or lower in comparison with other authors may due to the rate of meniscus injury when ACL reconstruction. Because cutting the meniscus also contributes to the instability of knee joint after surgery.

The results of knee recovery following Pivot Shift test after 6 months: negative is 93.3%; level 1 is 6.7%; no longer level 2 and 3 (Table 3). Compared to before surgery, Pivot Shift test: there is 1 patient accounting for 3.3% at level 1; 25 patients occupy 83.3% at level 2; 13.3% at level 3.

Table 3: Pivot Shift test after surgery

Pivot Shift	Negative	Level 1	Level 2	Level 3	Total
n	28	2	0	0	30
Percentage	93.3%	6.7%	0%	0%	100%

This shows a significant improvement before and after surgery.

Twenty-five patients (86.7%) achieved good outcome, 5 patients (13.3%) are medium and no patients achieved bad results (Table 4). The average Lysholm score after surgery of the study group is 95.13 ± 3.98 (highest is 99 and the smallest is 80) compared to Lysholm before surgery is 59 (highest is 69 score, smallest is 56 with statistically significance difference.

Table 4: Lysholm score after sugery

Lysholm score Time	Good	Mediun	Bad	Total
≤ 6 months	10	2	0	12
7 - 11 months	8	1	0	9
≥ 12 months	7	2	0	9
Total	25	5	0	30
Rate %	86.7%	13.3%	0%	100%

In our research, there is no case of infection or deterioration of strength first ray plantar flexion or foot eversion.

Ankle joint function after surgery

The function of ankle joint following AOFAS score before surgery is 97.3 ± 1.67 and after surgery is 97.3 ± 1.54 (smallest is 93 and the highest is 100 scoring). There was no complaint about the weakness of the ankle joint after surgery from the patients in the study. No vascular neurological complications were noted and no cases of ACL rupture recurrence.

Discussion

The average age of the researched patients is 35.4 ± 8.8 years, similar to the average age in previous studies by Nam Anh Ha Tang [12] (32.1 years), and Muoi Le Van [13] (28.73 years). ACL injury can be encountered at all ages, in this study, a large proportion of the patients is in the age group 31 to 40, accounts for 56.7%. This is the age group in which patients usually participate in highly combative sports.

A majority of our patients is male, accounts for 63.3%, or 1.7 times the number of female patients. This result is consistent with studies by other authors, for example, Hoang Anh Dang [14] reported 85.1% of the patients were male. This high proportion can be explained by the tendency of male patients in participating in intense activities, and their need for healthy knees to resume participating in such activities, thus more male patients choose surgery. The most common cause of for ACL injury in our study group is sport injury, accounts for 40%.

The average length of our graft is 60 ± 0.8 (60 – 65) mm, of Khanh Nguyen Manh [15] is 60.3 ± 0.5, and of Nam Anh Ha Tang [12] is 67 ± 2.04 mm. The tendon length in most studies ranged from 61 mm to 69 mm.

The average diameter of our graft is 7.0 ± 0.8 mm, ranging from 6.0 mm to 8.5 mm, most of the grafts (66.7%) have a diameter of 7.0 to 7.5 mm, 16.6% of the grafts have a diameter of 7.5 to 8.0 mm.

Vinh Pham Quang [7] reported an average diameter of 7.5 ± 0.57 mm. Our diameter is smaller because we included more female patients, and our female patients have smaller tendons. Khanh Nguyen Manh [15] reported an average graft diameter of 7.6 ± 0.7 mm. In comparison with other technique, for example, a study by Hoang Anh Dang [14] using semitendinosus-gracilis graft with a diameter of 7.25 mm, our grafts were much larger.

We assessed the stability of the knees using Lachman and Pivot-Shift tests. Lachman test assesses the level of forward movement of the tibial plateau and has high sensitivity. Among 30 patients operated, 27 patients (90%) had a negative Lachman test, only 3 patients had a positive grade 1 result. This result is consistent with Khanh Nguyen Manh [15] who reported a 92.7% negative rate. Pivot-Shift test is used to assess rotational stability of the knee. In our study 93.3% of the patients had a negative result for this test, while 6.7% of the patients had a positive grade 1 result. Khanh Manh Nguyen [15] reported a 100% negative rate, while this rate, as reported by Hoang Anh Dang [14] was 97.6%. Average post-operative Lysholm Knee Score after 6 month for all-inside technique by Nam Anh Ha Tang [12] was 96.9 points, Khanh Nguyen Manh [15] was 96.5 points and Mohammad Mahdi Omidian [16] was 91.5 points. Average AOFAS score at 6 months after the operation was 97.2 ± 1.6 points, ranging from 93 to 100. Among that, very good and good results accounted for 96.7%, moderate result accounted for 3.3% and there was no case with bad result. One patient had an AOFAS score of 88 points because of unadequate postoperative physical therapy for their ankle. The increase in preoperative and postoperative AOFAS score is statistically significant.

Chayanin Angthong (2015) assessed biomechanical and clinical features of the ankle after using peroneus longus graft to reconstruct the ACL. The average follow-up time was 12.8 months. Average preoperative AOFAS score was 97.7 ± 1.1 points and after 13 months of follow-up, the postoperative score was 95.4 ± 12 points (p = 0.09). The author concluded that peroneus longus graft could be selected if more of the graft were needed to reconstruct ACL [3]. The average AOFAS score by Pham Quang Vinh [7] was 97.37 ± 1.67 before the operation, and the postoperative score was 97.3 ± 1.54 (p = 0.88).

Sholahuddin Rhatomy et al., (2019) [17] conducted a research on patients who suffered isolated ACL injury were enrolled and underwent isolated single bundle ACL reconstruction using peroneus longus autograft at pre-operative and 2-years after surgery. Graft diameter was measured intraoperative. Donor site morbidities were assessed with thigh circumference measurement and ankle scoring using AOFAS and FADI. Peroneus longus graft diameter was 8.38 ± 0.68 mm. There was significant difference between pre and 2-years post-operative functional score in IKDC, Lysholm score. Mean of AOFAS was 98.93 ± 3.10 and FADI was 99.79 ± 0.59.

Khajotia and Shakti Chauhan (2018) [18] conducted a research with 25 patients, ranging 18-42 years to evaluate the functional outcome of arthroscopic reconstruction of ACL tear using triple layered PLT autograft and to study its effect on ankle stability. IKDC score was normal or near normal in 21 patients and only 4 patients were rate as abnormal or severely abnormal. Mean IKDC Score was 83.53. Stability of the ACL was assessed using the Lachman test: normal in 18 cases (72%), 1+ laxity in 5 cases (20%), 2+ and 3+ in 1 case (4%) each. Pivot shift was negative in 15 cases (60%), Pivot glide was seen in 9 cases (36%) and gross pivot shift was seen in 1 patient. Partial meniscectomy of the medial meniscus was performed in 5 patients. No patient experienced ankle dysfunction however 2 patients had pressure pain in the region of the graft harvest.

Fu-Dong Shi et al., (2017) [19] utilized peroneus longus tendon as an autograft for ACL reconstruction of patients with ACL rupture and grade III MCL injury. Thirty-eight patients with acute ACL ruptures and grade III MCL injuries were treated with ACL reconstruction with a doubled autologous PLT or quadrupled autologous HT. Knee stability and function was evaluated clinically with the Lachman test and KT-2000 arthometer as well as subjectively with functional scores. Effects on the donor ankle were evaluated by biomechanical testing. For the results of subjective index appraisal at 6 months postoperatively, Lysholm scores between group A (94 ± 6.02) and group B (95 ± 2.35), nor was there a statistical difference of IKDC knee functional score (group A: 89.45 ± 2.89, group B: 90.12 ± 4.56). For the results of ankle functional testing at 12 and 24 months, there were no significant differences in ankle dorsiflexion strength preoperatively (80.92 ± 0.26 N) and postoperatively (80.00 ± 0.57 N at 12 months and 81.46 ± 0.48 N at 24 months postoperatively) of the PLT resected donor ankle, and no marked differences in ankle plantar flexion strength preoperatively (147.96 ± 0.38 N) and postoperatively (147.76 ± 0.25 N at 12 months and 150.22 ± 0.35 N) of the donor ankle.

In conclusion, through the evaluation of the surgery results of 30 patients with ACL rupture were arthroscopic surgery ACL reconstructions, anterior half of peroneus longus tendon may be an alternative, complementing the source of the autologus graft in ACL reconstruction.

Ethical approval

This study is approved by the ethics committee of Hanoi Medical University in Vietnam

Informed consent

The consent and commitment were signed by the patients in the study

References

1. West RV, Harner CD. Graft selection in anterior cruciate ligament reconstruction. The Journal of the American Academy of Orthopaedic Surgeons. 2005; 13(3):197-207. https://doi.org/10.5435/00124635-200505000-00006 PMid:15938608

2. Otis JC. Peroneus Brevis is a More Effective Evertor than Peroneus Longus. Foot and Ankle International. 2004; 25(4):242-6. https://doi.org/10.1177/107110070402500408 PMid:15132932

3. Angthong C, Chernchujit B, Apivatgaroon A, Chaijenkij K, Nualon P, Suchao-in K. The Anterior Cruciate Ligament Reconstruction with the Peroneus Longus Tendon: A Biomechanical and Clinical Evaluation of the Donor Ankle Morbidity. Journal of the Medical Association of Thailand = Chotmaihet thangphaet. 2015; 98:555-60.

4. Zhao J, Huangfu X. The biomechanical and clinical application of using the anterior half of the peroneus longus tendon as an autograft source. The American journal of sports medicine. 2012; 40(3):662-71. https://doi.org/10.1177/0363546511428782 PMid:22174343

5. Cao HB, Liang J, Xin JY. [Treatment of anterior cruciate ligament injury with peroneus longus tendon]. Zhonghua yi xue za zhi. 2012; 92(35):2460-2.

6. Trong NT, Hoang LP, Duong TM. " Evaluation of ACL reconstruction arthroscopy by peroneus longus tendon. 121 Military Hospital. 2016.

7. Quang VP. Anatomical and mechanical feature of peroneus longus tendon - applying ACL reconstruction: Ho Chi Minh medical university; 2017.

8. Paulos L.E KA, Walker J.A. 'Criteria' - Based Rehabilitation of surgically reconstructed and non-surgically treated Anterior Cruciate Ligament injuries. . fourth ed ed. Insall & Scott Surgery of the knee: Churchill Living Stone Elsevier; 2006.

9. Magnussen RA, Lawrence JT, West RL, Toth AP, Taylor DC, Garrett WE. Graft size and patient age are predictors of early revision after anterior cruciate ligament reconstruction with hamstring autograft. Arthroscopy : the journal of arthroscopic & related surgery : official publication of the Arthroscopy Association of North America and the International Arthroscopy Association. 2012; 28(4):526-31. https://doi.org/10.1016/j.arthro.2011.11.024 PMid:22305299

10. Conte EJ, Hyatt AE, Gatt Jr CJ, Dhawan A. Hamstring autograft size can be predicted and is a potential risk factor for anterior cruciate ligament reconstruction failure. Arthroscopy : the journal of arthroscopic & related surgery : official publication of the Arthroscopy Association of North America and the International Arthroscopy Association. 2014; 30(7):882-90. https://doi.org/10.1016/j.arthro.2014.03.028 PMid:24951356

11.Ho SW, Tan TJ, Lee KT. Role of anthropometric data in the prediction of 4-stranded hamstring graft size in anterior cruciate ligament reconstruction. Acta Orthop Belg. 2016; (82):72-7.

12. Tang NAH. Evaluation of ACL reconstruction arthroscopy using Hamstring by all-inside technique Vietnam Orthopedic Association Journal 2013:109-14.

13. Van ML. Evaluation of ACL reconstruction by all-inside tecnique in Da Nang hospital. Vietnam Orthopedic Association Journal 2015:105-10.

14. Dang HA. Research on ACL reconstruction arthoscopy by Hamstring tendon, 2009.

15. Nguyen KM. Preliminary results of ACL reconstruction with all-inside technique. Vietnam Medical Jounal. 2015; 2:136-40.

16. Omidian MM, Sarzaeem MM, Kazemian GH. Arthroscopic Anterior Cruciate Ligament Reconstruction Using Hamstring Tendon Graft: Comparison of All-Inside and Outside-in Techniques. J Orthop Spine Trauma. 2016; 2(1).

17. Rhatomy S, Hartoko L, Setyawan R, Soekarno NR, Zainal Asikin AI, Pridianto D, et al. Single bundle ACL reconstruction with peroneus longus tendon graft: 2-years follow-up. Journal of Clinical Orthopaedics and Trauma. 2019. https://doi.org/10.1016/j.jcot.2019.09.004

18. Khajotia BL, Chauhan S, Sethia R, Chopra BL. Functional outcome of arthroscopic reconstruction of anterior cruciate ligament tear using peroneus longus tendon autograft. International Journal of Research in Orthopaedics. 2018; 4(6):898. https://doi.org/10.18203/issn.2455-4510.IntJResOrthop20184382

19. Shi FD, Hess DE, Zuo JZ, Liu SJ, Wang XC, Zhang Y, et al. Peroneus Longus Tendon Autograft is a Safe and Effective Alternative for Anterior Cruciate Ligament Reconstruction. The journal of knee surgery. 2019; 32(8):804-11. https://doi.org/10.1055/s-0038-1669951 PMid:30206913

ID Design Press, Skopje, Republic of Macedonia
Open Access Macedonian Journal of Medical Sciences. 2019 Dec 30; 7(24):4357-4361.
https://doi.org/10.3889/oamjms.2019.835
eISSN: 1857-9655
Basic and Clinical Medical Researches in Vietnam

The Anatomical Numerical Measurement of Posterior Cruciate Ligament: A Vietnamese Cadaveric Study

Do Van Minh[1, 2], Tran Trung Dung[1, 3*], Ngo Van Toan[4], Nguyen Huy Phuong[1, 2], Vo Sy Quyen Nang[2], Thien Chu Dinh[5]

[1]Hanoi Medical University, Hanoi, Vietnam; [2]Hanoi Medical University Hospital, Hanoi, Vietnam; [3]Saint Paul University Hospital, Hanoi, Vietnam; [4]Viet Duc University Hospital, Hanoi, Vietnam; [5]Institute for Research and Development, Duy Tan University, 03 Quang Trung, Danang, Vietnam

Citation: Minh DV, Dung TT, Toan NV, Phuong NH, Nang VSQ, Chu Dinh T. The Anatomical Numerical Measurement of Posterior Cruciate Ligament: A Vietnamese Cadaveric Study. Open Access Maced J Med Sci. 2019 Dec 30; 7(24):4357-4361. https://doi.org/10.3889/oamjms.2019.835

Keywords: Anatomy; Knee; Posterior cruciate ligament; Femoral footprint; Tibial footprint; Intra-articular posterior cruciate ligament

***Correspondence:** Tran Trung Dung. Hanoi Medical University, Hanoi, Vietnam; Saint Paul University Hospital, Hanoi, Vietnam. E-mail: dungbacsy@dungbacsy.com

Received: 11-Sep-2019; **Revised:** 20-Nov-2019; **Accepted:** 21-Nov-2019; **Online first:** 20-Dec-2019

Funding: This research did not receive any financial support

Competing Interests: The authors have declared that no competing interests exist

Abstract

BACKGROUND: The posterior cruciate ligament (PCL) is crucial to restrain the posterior translation of the tibia. Its anatomical structure is complex. A proper understanding of PCL anatomy may assist surgeon in reconstructing anatomically native PCL.

AIM: To describe the anatomical numerical measurement of the PCL in Vietnamese adults.

METHODS: Twenty-one fresh cadaveric knees were examined. The macroscopic details of the intra-articular PCL, the attachment of the anterolateral bundle (ALB), posteromedial bundles (PMB) to the femur and tibia were analysed. We used a digital camera to photograph the cadaveric specimens and used the ImageJ software to analyse the collected images.

RESULTS: The ALB and PMB length were 35.5 ± 2.78 and 32.6 ± 2.28 mm, respectively. The smallest and the biggest diameter of middle third of the PCL were 5.9 ± 0.71 and 10.0 ± 1.39 mm, respectively. The area of cross section of middle third of the PCL was 53.6 ± 12.37 mm^2. The femoral insertion area of ALB and PMB were 88.4 ± 16.89 and 43.5 ± 8.83 mm^2, respectively. The distance from the central point of femoral ALB, PMB, and total PCL insertion to the Blumensaat line were 5.5 ± 0.91, 11.5 ± 1.98, and 7.6 ± 1.42 mm, respectively. The shortest distance from medial femoral cartilage rim to the central point of femoral ALB, PMB, and total PCL insertion were 7.0 ± 0.79, 7.3 ± 0.95, and 7.8 ± 1.73 mm, respectively. The tibial insertion area of ALB and PMB were 84.5 ± 12.52 and 47.8 ± 6.20 mm^2 respectively. The shortest distance from the posterior cartilage corner of the medial tibial plateau to the central point of ALB, PMB, and total PCL insertion to tibia were 8.5 ± 1.02, 9.4 ± 1.11, and 8.3 ± 1.1 mm, respectively. The central point of tibial PCL insertion was 9.7±1.08 mm below cartilage plane of the medial tibial plateau.

CONCLUSION: This study describes the detailed anatomical measurement of the PCL and its bundles in adults.

Introduction

The posterior cruciate ligament (PCL) is crucial to restrain the posterior translation of tibia. Shelbourne et al., found that 1%-44% of all acute injuries of the knee are PCL injuries [1]. Although non-operative and operative management have been described, the optimal management strategy remains to be determined. In general, non-operative management has been advocated for patient with isolated grade 1 or 2 PCL injuries or for those with grade 3 injuries with non-serious symptoms or low activity requirement. PCL reconstruction is typically indicated for patients with acute or chronic symptomatic grade 3 PCL injuries in whom non-operative management was unsuccessful. Bedi et al., reviewed the literature and reported that PCL reconstruction generally have worse post-operative clinical outcomes than ACL reconstruction [2]. Excellent post-operative clinical outcome of PCL reconstructions depends on appropriate reproduction of the PCL anatomy [2], [3], [4]. Therefore, orthopaedic surgeons pay great attention to the comprehension of anatomical PCL structure. Up to now, there have been little research on numerical anatomical measurement of PCL. The study objective is to measure anatomical sizes of intra-articular PCL and attachment footprints of the

PCL bundles in Vietnamese adults in order to help surgeons to understand the principles of anatomical reconstruction of PCL.

Materials and Method

The study was designed to be a descriptive anatomical study. We studied twenty-one articulated knees. Eight cadaveric knees from 4 donors were dissected in the Anatomy Department of University of Medicine and Pharmacy in Ho Chi Minh city. Thirteen knees from above knee amputation specimens were dissected in Anatomic Pathology, Cytological Pathology and Forensic Medicine Department in Viet Duc University Hospital. We excluded all cadavers with a history of knee surgery or trauma. We exposed 21 articulated knees and confirmed that all of them had intact anterior cruciate ligament (ACL) and PCL without any signs of osteoarthritis. The mean age of the specimens were 44 ± 13.3 years (24-59 years). 21 studied knees, which are composed of 8 right knees and 13 left knees, were from 15 males and 2 females.

All specimens had been only used to study the anatomy of PCL. We removed all adjacent soft tissue and surrounding structures, and isolated the knee by cutting the femur and tibia. The proximal tibia was cut at 2 cm below the anterior tubercle. We cut the distal femur above the intercondylar notch.

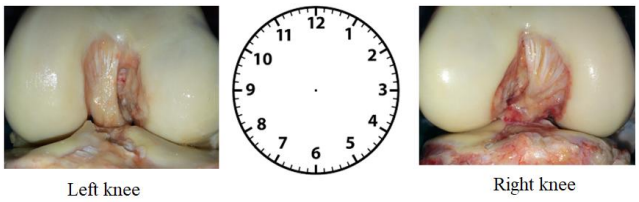

Figure 1: The femoral attachment of PCL when we viewed the knee from the anterior aspect

We removed all tissues except PCL (Figure 1) then cut the femoral intercondyle between the insertion of ACL and PCL to the femur. Next step, we separated 2 bundles of the PCL based on the level of tension and fibre orientations at different position when the knee is flexed. The PCL was marked to divide into an ALB and PMB with a small soft wire (Figure 2). We measured the length of the intra-articular part of ALB when the knee is flexed 90 degrees and the length of the intra-articular part of PMB in extended knee. We measured both the smallest and biggest diameter of the middle PCL.

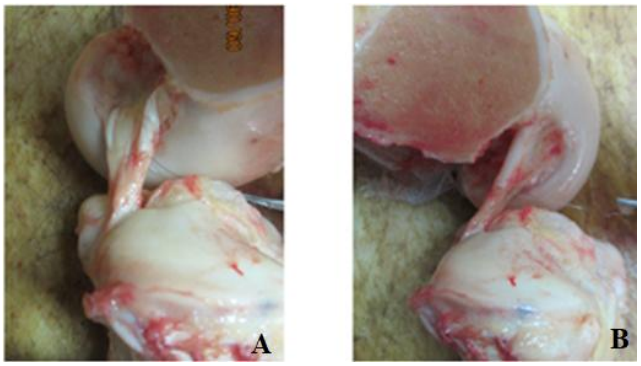

Figure 2: PCL imaging when the knee was full extended (A) and when the knee was flexed at 90 degrees (B)

We separated the body of the PCL into ALB and PMB from the middle part of the ligaments to the femoral and tibial attachment footprints. Two bundles of PCL were removed from the bone and the attachment footprint was marked with ink pen (Figure 3). We photographed the femoral and tibial specimens with a measurement scale using a Canon EOS 70D with macro lens. All the images were perpendicular to the PCL attachment footprint area. The images were transfered into a computer. We performed all measurement and analysis by the use of the ImageJ software (https://imagej.nih.gov/ij/index.html).

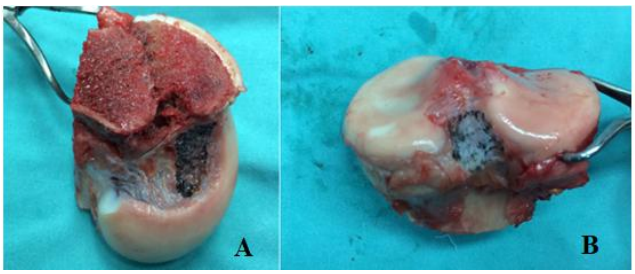

Figure 3: Femoral and tibial footprint of PCL

To define the central point of the native ALB, PMB and total PCL insertion footprint on the femur and tibia, the entire morphed ALB, PMB and total PCL footprint were analysed and best-fit ellipses applied using the ImageJ software. The center of these ellipses were defined as the central point of ALB, PLB and total PCL insertion footprint.

We performed anatomical measurements on the tibial and femoral attachment footprint of ALB, PMB and total PCL. At the femoral site, we measured the distance from the central point of ALB, PMB, and total PCL footprint to the Blumensaat line and the articular cartilage rim of medial femoral condyle. The measure from central point of the ALB, PMB and PCL were perpendicular to the Blumensaat line and articular cartilage rim. We calculated the area of every footprint of attachment to the femur (Figure 4).

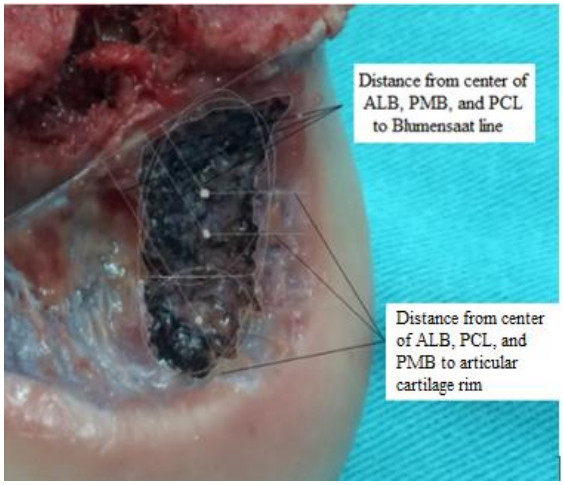

Figure 4: Femoral PCL attachment footprint analysis

At the tibial site, we measured the attachments of ALB, PMB, and PCL on the posterior tibial plan. The area of each tibial attachment footprint was determined. The shortest distance from the central point of tibial ALB, PMB and total PCL footprint to posterior cartilage corner of the medial tibial plateau to were measured (Figure 5). The distance from the articular plane of the medial tibial plateau to the central point of total PCL attachment footprint and to the inferior margin of total PCL attachment footprint were measured.

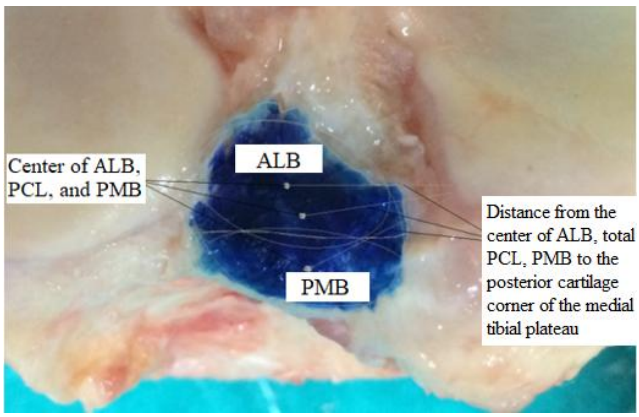

Figure 5: Tibial PCL attachment footprint analysis

Results

The anatomical features of intra-articular PCL

The numerical measurement of intra-articular PCL including the length of the ALB and PMB, the smallest and the biggest diameter of the middle third of the PCL, and the area of cross section of middle third of the PCL were shown in Table 1.

Table 1: Anatomical features of intra- articular PCL

Anatomical index	Mean ± SD	Min- Max
ALB length at 90 degree of knee flexion (mm)	35.5 ± 2.78	31.2-38.8
PMB length at full knee extension (mm)	32.6 ± 2.28	30.1-36.9
Smallest diameter of middle third (mm)	5.9 ± 0.71	5.0-7.6
Biggest diameter of middle third (mm)	10.0 ± 1.39	7.7-12.3
Cross- sectional area of middle third (mm^2)	53.6 ± 12.37	30.7-75.2

The anatomical femoral attachment of PCL

The femoral insertion of PCL presented as an oval shape. The femoral insertion area of PCL and its bundles and the distance from the central point of the femoral ALB, PMB and total PCL footprint to the Blumensaat line and the articular cartilage rim were shown in Table 2.

Table 2: Quantitative measurements on femoral insertion of PCL

Anatomical index	Mean ± SD	Min-Max
ALB footprint (mm^2)	88.4 ± 16.89	60.7-128.3
PMB footprint (mm^2)	43.5 ± 8.83	31.8-61.4
Total PCL footprint (mm^2)	131.9 ± 23.94	95.3-182.0
Distance from the rim of cartilage to the central point of		
ALB (mm)	7.0 ± 0.79	5.1-8.2
PMB (mm)	7.3 ± 0.95	5.9-9.3
Total PCL (mm)	7.8 ± 1.73	5.5-11.1
Distance from Blumenssat line to the central point of		
ALB (mm)	5.5 ± 0.91	4.2-7.4
PMB (mm)	11.5 ± 1.98	7.8-16.2
Total PCL (mm)	7.6 ± 1.42	5.3-11.0

The anatomical tibial attachment of PCL

The attachment of PCL to the tibia is trapezoidal in shape. The tibial PMB footprint is placed distally and medially to the ALB footprint.

The tibial attachment area of PCL and its bundles, the shortest distance from the central point of tibial ALB, PMB and total PCL footprint to posterior cartilage corner of the medial tibial plateau along with the distance from the articular plane of the medial tibial plateau to the central point of total PCL attachment footprint and to the inferior margin of total PCL attachment were shown in Table 3.

Table 3: Quantitative measurements on tibial insertion of PCL

Anatomical index	Mean ± SD	Min-Max
ALB footprint (mm^2)	84.5 ± 12.52	68.8-110.2
PMB footprint (mm^2)	47.8 ± 6.20	37.0-57.3
Total PCL footprint (mm^2)	132.3 ± 16.64	105.8-164.8
Shortest distance from the posterior cartilage corner of the medial tibial plateau to the central point of		
ALB (mm)	8.5 ± 1.02	6.5-10.8
PMB (mm)	9.4 ± 1.11	7.4-11.5
PCL (mm)	8.3 ± 1.1	6.5-10.5
Distance from articular plane of the medial tibial plateau to the central point of PCL attachment footprint (mm)	9.7 ± 1.08	8.1-12.2
Distance from articular plane of the medial tibial plateau to the inferior margin of PCL attachment footprint (mm)	13.6 ± 0.96	11.6-15.5

Discussion

Our study focused on describing the numerical anatomical data of PCL. So far, there is a limited number of reports on the numerical anatomical data of the PCL. As reported by Girgis et al., the

length and width of PCL are about 32-38 mm and 11-13 mm respectively [5]. It is reported by Makris et al., that the PCL length is 38 ± 2 mm when the knee is flexed at 90 degrees, and the middle third anteroposterior diameter and mediolateral diameter of PCL ligament were approximately 5 ± 0.5 mm and 14 ± 0.8 mm respectively [6]. In our evaluation, we noted a shorter intra-articular length of the ALB and PMB, and a smaller diameter of the middle third of the PCL, as compared to other author's findings. Knowledge of the intra-articular length and diameter of PCL is critical for the selection of an appropriate graft size in PCL reconstruction.

According to Amis et al., the footprint of femoral attachment of the PCL to the femur makes a "haft- moon" shape [7]. In our study, all described femoral attachments of the PCL were oval shaped.

Regarding the areas of the PCL attachment to femur, a study by Takahashi et al., on 32 femurs revealed that the mean area of attachment of the ALB and PMB to femur were 58.0 ± 25.4 mm^2 and 64.6 ± 24.7 mm^2, respectively [8]. In this study, measurements were obtained by evaluating photographs integrated with a measure scale, and computer analyses were performed using a MacSCOPE software. By the help of a specific software, Lopes et al., evaluated photos of 20 knees obtained from a specific digital camera equipped with three-dimensional laser. According to this study, the mean femoral attachment areas of ALB, PMB and the PCL were 118.0 ± 23.95 mm^2, 90.0 ± 16.13 mm^2, and 209.0 ± 33.82 mm^2 respectively [9]. Gali et al., photographed 24 knees using Canon EOS Rebel T1i camera with a measure scale, and performed subsequent computer analyses using ImageJ software. As reported by this study, the mean attachment area of the ALB, PMB, and the total femoral attachment area of PCL were 47.13 ± 19.14 mm^2, 40.67 ± 16.19 mm^2, and 87.80 ± 31.42 mm^2 respectively [10]. In our evaluation, the insertion area of ALB was greater than that of PMB. The results of this study were like that of Lopes et al., and Gali et al., but oppose to the findings of Takahashi et al.

There have been several reports about numerical measurements description of the central point of femoral PCL insertion [11]. According to Cosgarea and Jay, the central point of the attachment of the PCL to the femur is described 10 mm behind the cartilage rim of the medial condyle of femur [3]. However, Wind et al., found that this point is 10 mm proximal to this border [12]. According to the study conducted by Takahashi et al., the average measure from the central point of the attachments of ALB and PMB to the Blumensaat line were 4.8 mm and 11.4 mm, and to the anterior cartilage rim were 9.6 mm and 10.6 mm, respectively [8]. As reported by Gali et al., the shortest distance from the edge of the posterior cartilage corner of medial tibial plateau to the central point of ALB and PMB were 5.00 ± 2.06 mm and 5.58 ± 1.64 mm, respectively [10]. In our evaluation, we used two anatomical index that may be clearly view during knee arthroscopy to identify the center of femoral ALB, PMB and total PCL insertion to support surgeon in creating femoral tunel.

Regarding the anatomical tibial footprint of the PCL, it is reported by Harner et al., that the average area of ALB and PMB were 70 ± 26 mm^2 and 62 ± 17 mm^2, respectively [13]. According to the report by Tajima et al., the average areas of attachment of the ALB and PMB were 93.1 ± 16.6 mm^2 and 150.8 ± 31.0 mm^2, respectively [14]. In this study, three-dimensional laser photography was used to evaluate the tibial attachment area of 21 unpaired cadaveric knees, and collected data were analysed with a specific software. Takahashi et al., evaluated photographs integrated with measurement scales of 33 tibias and use MacSCOPE software to analyse collected data, which revealed that the mean area of attachment of the ALB and PMB were 46.7 ± 15.6 mm^2 and 115.8 ± 54.6 mm^2, respectively [8]. Gali et al., photographed 24 knees using Canon EOS Rebel T1i camera equipped with a measurement scale and subsequently analysed their photos using the ImageJ software. According to this study, the mean attachment area of the ALB and PMB were 46.79 ± 14.10 mm^2 and 41.54 ± 9.15 mm^2, respectively. The total area of insertion of PCL to tibia was 88.33 ± 21.66 mm^2 [15]. In our study, the attachment area of ALB was greater as compared to that of PMB.

Few reports on numerical anatomical description of the center of tibial PCL insertion have been done. This point is located 2 – 3 mm below the articular plane, according to the study by Girgis et al., [5]. According to Cosgarea and Jay, it is 10 – 15 mm below the articular plane [3]. According to report by Takahashi et al., the tibial ALB attachment is nearly on the articular plane (that means the tibial PMB attachment center is close to 0 mm), and the central point of the tibial PMB attachment is located 4.6 mm below the articular plane [8]. According to our evaluation, the central point of the tibial PCL footprint is 9.7 ± 1.08 mm below the articular plan. In this study, we described two anatomical index that can clearly view during knee arthroscopy to identify the center of tibial PCL insertion to support surgeon in creating tibial tunnel.

Our study has some limitations. We had a relatively small sample size. Additionally, a three-dimensional view of PCL ligament attachment areas was not possible with the use of photographs taken with a digital camera.

In conclusion, our study described the detail numerical measurements of the intra- articular PCL and attachment footprint of the ALB, PMB, and total PCL in adults. These findings can assist surgeons in performing graft preparation and anatomical tunnel placement in anatomical native PCL reconstruction.

Ethical approval

This study protocol was approved by Ethic Committee of Viet Duc University Hospital.

References

1. Shelbourne KD, Davis TJ, Patel DV. The natural history of acute, isolated, nonoperatively treated posterior cruciate ligament injuries. A prospective study. The American Journal of Sports Medicine. 1999; 27(3):276-83. https://doi.org/10.1177/03635465990270030201 PMid:10352760

2. Bedi A, Musahl V, Cowan JB. Management of Posterior Cruciate Ligament Injuries: An Evidence-Based Review. The Journal of the American Academy of Orthopaedic Surgeons. 2016; 24(5):277-89. https://doi.org/10.5435/JAAOS-D-14-00326 PMid:27097125

3. Cosgarea AJ, Jay PR. Posterior cruciate ligament injuries: evaluation and management. Journal of the American Academy of Orthopaedic Surgeons. 2001; 9(5):297-307. https://doi.org/10.5435/00124635-200109000-00003 PMid:11575909

4. LaPrade CM, Civitarese DM, Rasmussen MT, LaPrade RF. Emerging Updates on the Posterior Cruciate Ligament: A Review of the Current Literature. The American Journal of Sports Medicine. 2015; 43(12):3077-92. https://doi.org/10.1177/0363546515572770 PMid:25776184

5. Girgis FG, Marshall JL, Monajem A. The cruciate ligaments of the knee joint. Anatomical, functional and experimental analysis. Clinical Orthopaedics and Related Research. 1975; (106):216-31. https://doi.org/10.1097/00003086-197501000-00033 PMid:1126079

6. Makris CA, Georgoulis AD, Papageorgiou CD, Moebius UG, Soucacos PN. Posterior cruciate ligament architecture: evaluation under microsurgical dissection. Arthroscopy. 2000; 16(6):627-32. https://doi.org/10.1053/jars.2000.9238 PMid:10976124

7. Amis AA, Gupte CM, Bull AMJ, Edwards A. Anatomy of the posterior cruciate ligament and the meniscofemoral ligaments. Knee Surgery, Sports Traumatology, Arthroscopy. 2006; 14(3):257-63. https://doi.org/10.1007/s00167-005-0686-x PMid:16228178

8. Takahashi M, Matsubara T, Doi M, Suzuki D, Nagano A. Anatomical study of the femoral and tibial insertions of the anterolateral and posteromedial bundles of human posterior cruciate ligament. Knee Surgery, Sports Traumatology, Arthroscopy. 2006; 14(11):1055-9. https://doi.org/10.1007/s00167-006-0192-9 PMid:16897069

9. Lopes OV, Ferretti M, Shen W, Ekdahl M, Smolinski P, Fu FH. Topography of the femoral attachment of the posterior cruciate ligament. The Journal of Bone and Joint Surgery American Volume. 2008; 90(2):249-55. https://doi.org/10.2106/JBJS.G.00448 PMid:18245582

10. Gali JC, Oliveira HCS, Camargo AB, Martins CRB, Silva P, Caetano EB. Anatomical Study and Morphometric Analyses on the Femoral Insertions of the Posterior Cruciate Ligament. Rev Bras Ortop. 2013; 48(2):186-90. https://doi.org/10.1016/j.rbo.2012.04.002 PMid:31211126 PMCid:PMC6565879

11. Narvy SJ, Pearl M, Vrla M, Yi A, Hatch GF, 3rd. Anatomy of the femoral footprint of the posterior cruciate ligament: a systematic review. Arthroscopy. 2015; 31(2):345-54. https://doi.org/10.1016/j.arthro.2014.07.004 PMid:25194165

12. Wind WM. Evaluation and Treatment of Posterior Cruciate Ligament Injuries: Revisited. American Journal of Sports Medicine. 2004; 32(7):1765-75. https://doi.org/10.1177/0363546504270481 PMid:15494347

13. Harner CD, Baek GH, Vogrin TM, Carlin GJ, Kashiwaguchi S, Woo SLY. Quantitative analysis of human cruciate ligament insertions. Arthroscopy: The Journal of Arthroscopic & Related Surgery. 1999; 15(7):741-9. https://doi.org/10.1016/S0749-8063(99)70006-X

14. Tajima G, Nozaki M, Iriuchishima T, Ingham SJM, Shen W, Smolinski P, et al. Morphology of the tibial insertion of the posterior cruciate ligament. The Journal of Bone and Joint Surgery American Volume. 2009; 91(4):859-66. https://doi.org/10.2106/JBJS.H.00991 PMid:19339570

15. Gali JC, Oliveira HCS, Lisboa BCB, Dias BD, Casimiro FG, Caetano EB. Tibial Insertions of the Posterior Cruciate Ligament: Topographic Anatomy and Morphometric Study. Rev Bras Ortop. 2013; 48(3):263-7. https://doi.org/10.1016/j.rbo.2012.06.005 PMid:31214543 PMCid:PMC6565906

ID Design Press, Skopje, Republic of Macedonia
Open Access Macedonian Journal of Medical Sciences. 2019 Dec 30; 7(24):4362-4367.
https://doi.org/10.3889/oamjms.2019.836
eISSN: 1857-9655
Basic and Clinical Medical Researches in Vietnam

Anatomical Study of Femoral Condylar Index in Magnetic Resonance Imaging: Implication to Total Knee Replacement Surgery for Vietnamese People

Dung Tran Trung[1, 2], Phuong Nguyen Huy[2], Tung Pham Son[1], Thien Chu Dinh[3], Toi Chu Dinh[4*]

[1]Saint Paul University Hospital, Hanoi, Vietnam; [2]Hanoi Medical University, Hanoi, Vietnam; [3]Institute for Research and Development, Duy Tan University, 03 Quang Trung, Danang, Vietnam; [4]Department of Human and Animal Physiology, Faculty of Biology, Hanoi National University of Education, Hanoi, Vietnam

Citation: Tran Trung D, Huy PN, Son TP, Chu Dinh T, Chu Dinh T. Anatomical Study of Femoral Condylar Index in Magnetic Resonance Imaging: Implication to Total Knee Replacement Surgery for Vietnamese People. Open Access Maced J Med Sci. 2019 Dec 30; 7(24):4362-4367. https://doi.org/10.3889/oamjms.2019.836

Keywords: Femoral rotation angle; Magnetic resonance imaging of knee joint; Total knee replacement

***Correspondence:** Toi Chu Dinh. Department of Human and Animal Physiology, Faculty of Biology, Hanoi National University of Education, Hanoi, Vietnam. E-mail: chudinhtoi.hnue@gmail.com

Received: 11-Sep-2019; **Revised:** 20-Nov-2019; **Accepted:** 21-Nov-2019; **Online first:** 20-Dec-2019

Funding: This research did not receive any financial support

Competing Interests: The authors have declared that no competing interests exist

Abstract

BACKGROUND: The femoral rotation angle is important element in total knee replacement (TKR).

AIM: To measure this angle, we determine through the axes: the transepicondylar axis (cTEA and sTEA), the posterior condylar axis (PCA), the anteroposterior axis (APA – Whiteside axis).

METHODS: Measuring the angles created by the four axes: cTEA, sTEA, PCA and APA in magnetic resonance imaging (MRI); determining the femoral rotation angle and application TKR.

RESULTS: the angle between APA and cTEA: 90.41° ± 3.35°, the angle between APA and sTEA: 94.47° ± 3.31°, the angle between APA and PCA: 96.40° ± 4.59°, the angle between cTEA and sTEA: 4.00° ± 1.02°, the angle between cTEA and PCA: 6.53° ± 2.55°, the angle between sTEA and PCA: 3.48° ± 1.91°.

CONCLUSION: The angle between sTEA and PCA is the angle that best represents the femoral rotation angle. However, in case of sTEA or PCA is difficult to identify, it can be measure via the APA or cTEA. These angles don't differ by age, gender and place of knee joint.

Introduction

Knee osteoarthritis is a very common disease and one of the biggest causes of disability in the elderly. According to many epidemiology researches, approximately 13% of people over 60 years old has symptom of knee osteoarthritis [4]. There are many treatments for knee osteoarthritis: medicine treatment in combination with rehabilitation, weight reduction, joint arthroscopy, hight tibial osteotomy. Finally, when all the above methods fail, patient suffers severe pain, articular cartilage is destroyed, joint is deformed, mechanical axis is misaligned and knee osteoarthritis is shown clearly on the X-ray scan, then the decision to perform knee replacement is made.

Total knee replacement (TKR) is the surgery method of cutting the damaged articular cartilage and replacing it with artificial joint. The aim of TKR is to repair and to restore the mechanical axis of leg and reduce pain and improve the function of knee joint thanks to the precise placement of artificial joint and balance of soft tissues surrounding knee joint. To do this, the suitable surgical technique is very crucial and the access to well-designed artificial joint is available. The structure of an artificial knee joint set includes femur, tibia and patella, in which the femoral rotation angle is an important element that directly affect the result of the TKR. Many researches show that incorrect femoral rotation angle can lead to complications such as femur and patella pain after surgery, limitation in knee function, wear increment of artificial joint material and so forth. Although clinical reports of TKR usually show good results, the optimal femoral rotation angleis only 75% of cases [9].

Many surgery techniques can determine the femoral rotation angle and while each technique has its own theoretical basis, all of them rely on the anatomical landmarks of femoral condyle and related components. Today, to measure this angle, we determine through the axes: the transepicondylar axis (cTEA và sTEA) [11], the posterior condylar axis (PCA), the anteroposterior axis (APA – Whiteside axis) [2]. The TEA is considered to be the most accurate of the four in reflecting the folding axis of knee joint and it is perpendicular to the mechanical axis. It is difficult to be identified and mark during surgery, thus the PCA is more commonly used [16]. Many researches in Europe and America evaluated that the PCA has an femoral rotation angle of 3^o compared to the TEA, which mean the femoral component external rotation angle is about 3° compared to the knee transverse axis [7], [5]. Currently our country is using this 3° external rotation angle to cut the femoral condyle. However, several researches on Asian races such as Chinese, Korean, and Japanese indicate that this angle varies in a wide range, from 1.7° to 9.7° [15], [17] . Specifically, researches in Japan indicated that the external rotation angle is 5°. This may be due to difference in races, living and working habits in each region. The determination of the femoral rotation angle or the relationship between anatomical landmarks have been researched multiple times through analyzing and measuring on corpses, or using diagnostic imaging tools such as MRI and CT scanner of knee joint. However, there has not been any research on these anatomical axes in Vietnam, causing many difficulties for surgeons during TKR.

Therefore, we decided to conduct this research to measuring the angles created by the four axes: cTEA, sTEA, PCA and APA in MRI; determining the femoral rotation angle and appling in TKR**.**

Materials and Methods

Subjects

Inclusion criteria: All patients with MRI scans of knee taken, above 16 years old, and have all four axes (APA, cTEA, sTEA and PCA) identifiable on axial slices.

Exclusion criteria: Foreign patients, patients under 16-year-old, patients with bone damage or surgical intervention at distal femur detected on MRI scan, and patients with any of the four axes (APA, cTEA, sTEA and PCA) not identifiable on axial slices.

Sample size calculation formula

We use the sample size calculation formula to determine the average value

$N=Z_{(1-\alpha/2)}{}^2.\delta^2/d^2$ [3]

δ : Standard Deviation.

D: Confident limit around the point estimate.

$Z_{(1-\alpha/2):}$ score corresponds to the desired level of statistical significance, usually taken 95%-95% CI, 2-side test Z = 1.96.

So, totally we had 280 patients conform to the requirement for selection.

Method of research

Retrospective research and prospective research using the descriptive cross-sectional method.

Research variables

Age, gender, place of knee, average measurement of 6 angles (APA, cTEA), (APA, sTEA), (APA, PCA), (cTEA, sTEA), (cTEA, PCA), (sTEA, PCA) calculated by age, gender and place of knee.

Tools

GE Optima MR360 1.5 Tesla MRI Scanner, made in Florida, USA, November, 2009, serial code 037255, high definition, 1 mm slice, 256 rows.

Simple Angle Measurement software. It is written using C#, uses Visual Studio 2015 and is designed to measure the angle between predetermined lines, and measures to the nearest 0.01%. This software is completely accurate.

Methods

The angles are measured using the Simple Angle Measurement software, then the data is collected using a uniform research form.

Statistical analysis

STATA 12.0 software to calculate Kruskal Wallis test, T-test.

Reduce errors

For one measurement, taking an average of these three measurements as the result of final research will minimize mistakes, and I use the four-digit figures after the comma. I use the software fully on my machine; therefore, the probability of errors has been greatly reduced.

Results

General characteristics

The age range of most patients participating in the research is 16-45 years old (195/280 patients). The average age of researched patients is 39.78 ± 15.14 (Table 1).

Table 1: Characteristics of age

Age range	Number of patients	Average age of each team	Rate (%)
Age 16-45	195	31.40 ± 7.32	69.64
Age > 45	85	59,00 ± 10.02	30.36
Total	280		100
Average age		39.78 ± 15.14	

In the young patient team, most of them are male, with the ratio between male and female being 2.7/1. In the elderly patient team, the ratio between male and female is 1/2.4. The ratio between male and female ratio of the entire team is 1.5/1 (Figure 1).

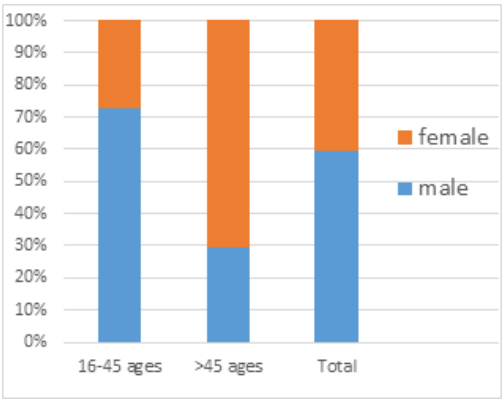

Figure 1: Characteristics of gender

The right knee/left knee ratio in the young patient team, elderly patient team and both teams combined are all approximately 1/1 (Figure 2).

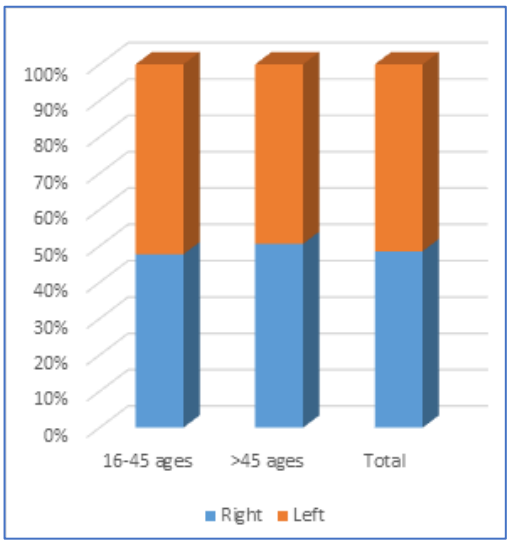

Figure 2: Characteristics of MRI scanning place

The APA and the cTEA are perpendicular to each other. The (sTEA, PCA) angle has an average measurement of 3.48° ± 1.91° (Table 2).

Table 2: Average measurement of anatomical angle (n = 280)

Angle	Average (°)	Smallest angle (°)	Biggest angle (°)
(APA, cTEA)	90.4 ± 3.35	78.68	103.14
(APA, sTEA)	94.47 ± 3.31	83.79	106.44
(APA, PCA)	96.40 ± 4.59	77.07	105.71
(cTEA, sTEA)	4.00 ± 1.02	1.11	7.38
(cTEA, PCA)	6.53 ± 2.55	0.01	13.74
(sTEA, PCA)	3.48 ± 1.91	0.08	13.36

Comparison of average measurement of angles created by 4 anatomical axes: APA, cTEA, sTEA and PCA between the young and the elderly patient teams

The result of analysis shows a relationship between anatomical axes of femoral condyle has no significant statistical difference in both the young and the elderly patient team ($p > 0.05$ in all 6 angles-Kruskal Wallis test) (Table 3).

Table 3: Comparison of average measurement of anatomical angles between the young and the elderly patient teams

Angle	Young patient team (n = 195)	Elderly patient team (n = 85)	p
(APA, cTEA)	90.33°	90.60°	0.21
(APA, sTEA)	94.34°	94.75°	0.13
(APA, PCA)	96.34°	96.54°	0.85
(cTEA, sTEA)	3.94°	4.15°	0.12
(cTEA, PCA)	6.60°	6.38°	0.45
(sTEA, PCA)	3.56°	3.29°	0.25

Discussion

In this research, we researched over 280 knee joints of patients from 16 to 88 years old, the most common age range was from 16 to 45 years old, the working age range. Perhaps because of that, there are many risk factors leading to knee disease such as injury, accident, soft tissue rheumatic syndromes, arthritis, and so forth. Thus, people in this age range should get MRI scanning more often. In the elderly patient team, the number risk factors decrease with the main factor being degeneration, so the patients go for examination less often.

Since this is a team of patients in working age, men often work harder, play more sports, and the male weight index is higher than that of women. Because of that the risk of men suffering from knee-related injuries is higher than that of women. In the elderly patient team, the male/female ratio is 1/2.4, which means women are the majority in this age team. This is reasonable because for women, after menopause, the estrogen level drops rapidly, which cause osteoporosis and osteoarthritis conditions to increase, especially in knee joint. This means more MRI scanning.

Researches by international authors show that the ratio of male patients and female patients is

equal (Figure 1), according to Ye-Yeon Won [17] and Jai Gon Seo [15], or the ratio of male patients is lower than that of female patients, according to Grinffin [7] (Table 4).

Table 4: Characteristics based on gender according to several international authors

Author	Average age	Male ratio	Female ratio	Research sample (n)	References
Ye-Yeon Won	44.7	50%	50%	100	[17]
Jai Gon Seo	68	50%	50%	20	[15]
Griffin	42.8	40%	60%	104	[7]
Andrew Park	64	47%	53%	114	[13]

This is due to customs, practices and labor activities in each region. In Vietnam, men are predominantly heavy workers and most of them also participate in high intensity sport activities, so the risk of them having knee joint disease is higher than that of women. In foreign countries, women are more involved in social activities and the intensity of physical activities is higher than that of Vietnamese women, which means there are more factors that can lead to knee joint injuries. This is the reason leading to the difference of femoral condylar angles between Vietnamese and foreign countries people.

Looking at Figure 2, we see no difference between right knee position and left knee joint position in both young and elderly patient teams, similar to the research result of Anay R. Patel [14], Ye Ye-on Won [17] (right/left knee ratio is 1/1). In researches by international authors, the right/left ratio changes depending on the criteria for selecting patients. However, if patients are selected regardless of diagnosis or only patients with knee joint degeneration are selected, the right/left ratio is usually 1/1. This is due to the fact that joint degeneration usually happens on both knees and rarely on only one knee. The risk element of knee joint injuries for both knees are also the same.

During this research, we found that the APA is perpendicular to the cTEA and nearly perpendicular to the sTEA. Our result are similar to the results of international authors Kobayashi [10] and Adrew Park [13]. The cTEA and the sTEA are very difficult to accurately identify during surgery, as this is the attachment point of ligament lateral internes and is shielded by femoral muscles. Jerosch [8] proved that the change in position selected between surgeons was 22.3 mm at the medial and 13.8 mm at the lateral femoral condyle. When researching the accuracy in determining the femoral condyle in 74 cases of TKR, Kinzel [9] discovered that the TEA was only accurately determined within ± 3° in 75% of the cases when examined by CT scaner after surgery. The deviation stretches in a wide range: from 6° external rotation angle to 11° internal rotation angle, including the TEA not identified during surgery. Thus, determining the cTEA and the sTEA indirectly through the PCA and/or the APA gives higher accuracy and does not cause damage to the muscles in the knee.

In our researches, the (cTEA, sTEA) angle is 4.00° which is similar to the results of Victor J. [16] and Kumar [11]. This angle is mostly unnoticed by surgeons as well as authors, which is because it is made by two axes that are difficult to distinguish clinically. Many authors assume that the sTEA is the approximate axis of the transverse axis rather than the cTEA. Since the cTEA des not coincide with the sTEA and they also create a 4° angle together, this means that the two axes are significantly different in clinical practice, so accurately determining the cTEA is very important. Using the cTEA as the transverse axis of knee may cause mistake and directly affect the results of TKR. In researches by international authors, only 50%-80% of cases managed to identify the sTEA. For the remaining patients, since the sTEA was unidentifiable, they used the cTEA as the transverse axis of knee joint. In our research, the sTEA was only unidentifiable in 8 cases. Since the ratio was very small, we did not count them in this research. This is because we used a GE Optima MR360 1.5 Tesla with 1 mm slice cut so the scans were of high quality and we were able to get the slice we wanted.

The angle created by the cTEA and the sTEA with the PCA is the highest concern of surgeons, in which the sTEA is the approximate axis with the transverse axis of knee. Accurately identifying this axis and using it as a landmark is very important in TKR surgery. Surgeons have tried to find another axis that is more easily identified clinically and has the most accuracy when using it to identify the sTEA. Many authors agree to take the PCA as an indirect axis to determine the sTEA. Many international authors have published the measurement results between these two angles as follows: Victor J. [16] measured of (cTEA, PCA) angle = 6.4°, (sTEA, PCA) angle = 3.1°; Nobuyuki Yoshinno [18] measured the (cTEA, PCA) angle = 6.4°, (sTEA, PCA) angle = 3°; and Jai Gon Seo [7] measured the (cTEA, PCA) angle = 5.3°, (sTEA, PCA) angle = 2.2°, and many others show similar results. In our research, by analyzing 280 MRI scans of knee joint, we found that the (cTEA, PCA) angle = 6.53° ± 2.55° and the (sTEA, PCA) angle = 3.48° ± 1. 91°. The results are quite similar to those of Asian and European authors [6], [13], [1]. This shows that although there are differences in anthropometric indicators, regions and living habits, the PCA always spins about 3° compared to the transverse axis of knee joint, or in other words, the posterior condylar angle is about 3° and the condylar twist angle is about 6°. This has a very important application in TKR, specifically in the cutting of the front and back of the distal extremity of femur, we let the cross-section rotate about 3° apart from the PCA, the transverse axis of knee will ensure the most physiological similarity. However, since the deviation of the (sTEA, PCA) angle between individuals is quite large, from 0.08° to 13.36°, we should evaluate this angle before surgery by using MRI scan of knee to optimize the femoral rotation angle, the femoral rotation angle of each patient will be different.

The measurement results of anatomical angles of young patients are equal to the results of the corresponding anatomical angles of elderly patients ($p > 0.05$ in all 6 angles-Kruskal Wallis test), which is shown in table 3. We found that the APA is perpendicular to the cTEA in both teams and the APA is not perpendicular to the sTEA but creates with that axis an angle of 94°. In 2000, Griffin [7] researched 104 knee joints, in which he also divided the team of patients into young and elderly teams, and his results were exactly the same as the results of our research. This means that the PCA rotated about 3° with the transverse axis and there is no difference between the young and the elderly. In TKR surgery, the PCA will be an important landmark to determine the transverse axis of knee.

Currently, other than the posterior condylar angle, the remaining angles are rarely researched. This is because on one hand these angles have little clinical significance, on the other hand they are also difficult to measure, their values are not high. According to Olcott [12], after comparing four methods of TKR, he determined that the method of using the sTEA is the most accurate, but since it is difficult to be identified during operation, he suggested using the PCA to determine the transverse axis of knee joint. According to Anay R. Patel [14], his research also shows that the relationship between the APA and the TEA is more volatile than the relationship between the TEA and the PCA, he also confirms that the anatomical angle is not affected by age. Therefore, authors focus on researching the angle created by the PCA with the cTEA and the sTEA, while the remaining angles are less researched. We researched all angles created by four anatomical axes of femoral condyle, which are APA, cTEA, sTEA and PCA, and use the result as reference data for research on Vietnamese people to serve the research of later Vietnamese authors.

Through the above analysis, in each team of patients, we found no difference between male and female, as well as right knee and left knee. When comparing the young and elderly patient team, the results of anatomical angles were not different ($p > 0.05$-Kruskal Wallis test), this result is consistent with the research results of European and Asian authors.

In conclusion, the angle between sTEA and PCA is the angle that best represents the femoral rotation angle. However, in cases sTEA or PCA is dificults to identify, it can be measure via the APA or cTEA. The value of the femoral rotation angle is about angle between sTEA and PCA, (sTEA, PCA) angle = 3.48° ± 1.91°. These angles don't differ by age, gender and place of knee joint.

Recommendation: The aim of TKR surgery is to restore the mechanical axis of leg, thus reduce pain and improve function of knee joint. In order to accomplish this, the precise placement of artificial knee joint and balance of the soft tissues surrounding knee joint is required. However, the relationship of anatomical axes of each patient is different. Therefore, through this research as well as researches of other authors around the world, we believe surgeons should evaluate the anatomical values on MRI scans before operation and identify the suitable femoral component external rotation for each patient, at the same time use multiple axes together to achieve the best surgery result.

Ethical approval

Approved by the Ethics Committee of Hanoi Medical University on June 30th, 2016.

Informed consent

The consent and commitment were signed by the patients.

References

1. Chao TW, Geraghty L, Dimitriou P, Talbot S. Averaging rotational landmarks during total knee arthroplasty reduces component malrotation caused by femoral asymmetry. Journal of orthopaedic surgery and research. 2017; 12(1):74. https://doi.org/10.1186/s13018-017-0575-2 PMid:28499396 PMCid:PMC5429545

2. Cho Y, Lee MC. Rotational alignment in total knee arthroplasty. Asia-Pacific Journal of Sports Medicine, Arthroscopy, Rehabilitation and Technology. 2014; 1(4):113-8. https://doi.org/10.1016/j.asmart.2014.08.001

3. Cochran WG. Sampling Techniques, John Wiley & Sons, ed. Edition, 3rd, New York, 1977.

4. Hung NV. Osteoarthritis. Medicine, Medical Publishing, 2012:188-196.

5. Berger RA, et al. Determining the rotational alignment of the femoral component in total knee arthroplasty using the epicondylar axis. Clin Orthop Relat Res. 1993; (286):40-7. https://doi.org/10.1097/00003086-199301000-00008

6. Franceschini V, Nodzo SR, Della Valle AG. Femoral Component Rotation in Total Knee Arthroplasty: A Comparison Between Transepicondylar Axis and Posterior Condylar Line Referencing. J Arthroplasty. 2016; 31(12):2917-2921. https://doi.org/10.1016/j.arth.2016.05.032 PMid:27374639

7. Griffin FM, et al. Anatomy of the epicondyles of the distal femur: MRI analysis of normal knees. J Arthroplasty. 2000; 15(3):354-9. https://doi.org/10.1016/S0883-5403(00)90739-3

8. Jerosch J, et al. Interindividual reproducibility in perioperative rotational alignment of femoral components in knee prosthetic surgery using the transepicondylar axis. Knee Surg Sports Traumatol Arthrosc. 2002; 10(3):194-7. https://doi.org/10.1007/s00167-001-0271-x PMid:12012038

9. Kinzel V, Ledger M, Shakespeare D. Can the epicondylar axis be defined accurately in total knee arthroplasty?. Knee. 2005; 12(4):293-6. https://doi.org/10.1016/j.knee.2004.09.003 PMid:16026698

10. Kobayashi H, et al. Reproducibility of condylar twist angle measurement using computed tomography and axial radiography of the distal femur. Orthop Traumatol Surg Res. 2014; 100(8):885-90. https://doi.org/10.1016/j.otsr.2014.07.025 PMid:25453922

11. Kumar K, Sharma D. A study of anatomy of distal femur pertaining to total knee replacement: an analysis, conclusions and recommendations. Musculoskelet Surg. 2018; 102(1):29-34. https://doi.org/10.1007/s12306-017-0489-5

12. Olcott CW, Scott RD. A comparison of 4 intraoperative methods to determine femoral component rotation during total knee arthroplasty. J Arthroplasty. 2000; 15(1):22-6. https://doi.org/10.1016/S0883-5403(00)91051-9

13. Park A, Nam D, Friedman MV, Duncan ST, Hillen TJ, Barrack RL. Inter-observer precision and physiologic variability of MRI landmarks used to determine rotational alignment in conventional and patient-specific TKA. The Journal of arthroplasty. 2015; 30(2):290-5. https://doi.org/10.1016/j.arth.2014.08.015 PMid:25267537 PMCid:PMC4323956

14. Patel AR, et al. Femoral component rotation in total knee arthroplasty: an MRI-based evaluation of our options. J Arthroplasty. 2014; 29(8):1666-70. https://doi.org/10.1016/j.arth.2014.02.033 PMid:24746490

15. Seo JG, et al. Relationship between mechanical axis-derived and anatomic landmark-derived femoral rotation in TKA: a three-dimensional CT study. J Arthroplasty. 2014; 29(12):2314-8. https://doi.org/10.1016/j.arth.2014.07.017 PMid:25138615

16. Victor J. Rotational alignment of the distal femur: a literature review. Orthop Traumatol Surg Res. 2009; 95(5):365-72. https://doi.org/10.1016/j.otsr.2009.04.011 PMid:19592323

17. Won YY, et al. An additional reference axis for determining rotational alignment of the femoral component in total knee arthroplasty. J Arthroplasty. 2007; 22(7):1049-53. https://doi.org/10.1016/j.arth.2007.02.005 PMid:17920480

18. Yoshino N, et al. Computed tomography measurement of the surgical and clinical transepicondylar axis of the distal femur in osteoarthritic knees. J Arthroplasty. 2001; 16(4):493-7. https://doi.org/10.1054/arth.2001.23621 PMid:11402414

ID Design Press, Skopje, Republic of Macedonia
Open Access Macedonian Journal of Medical Sciences. 2019 Dec 30; 7(24):4368-4371.
https://doi.org/10.3889/oamjms.2019.837
eISSN: 1857-9655
Basic and Clinical Medical Researches in Vietnam

A Rare Colonic Metastasis Case from Hepatocellular Carcinoma

Binh Van Pham[1], Huynh Huu Phan[1], Lam Le Ngo[1], Hang Thi Thuy Nguyen[1], Ky Van Le[1], Thien Chu Dinh[2], Nguyen Duy Bac[3*]

[1]Vietnam National Cancer Hospital, Hanoi, Vietnam; [2]Institute for Research and Development, Duy Tan University, 03 Quang Trung, Danang, Vietnam; [3]Vietnam Military Medical University (VMMU), Hanoi, Vietnam

Citation: Van Pham B, Huu Phan H, Le Ngo L, Nguyen HTT, Le KV, Chu Dinh Y, Bac ND. A Rare Colonic Metastasis Case from Hepatocellular Carcinoma. Open Access Maced J Med Sci. 2019 Dec 30; 7(24):4368-4371. https://doi.org/10.3889/oamjms.2019.837

Keywords: Hepatocelluar carcinoma; GI metastasis; Sigmoid metastasis

***Correspondence:** Nguyen Duy Bac. Vietnam Military Medical University (VMMU), Hanoi, Vietnam. E-mail: nguyenduybac@vmmu.edu.vn

Received: 11-Sep-2019; **Revised:** 20-Nov-2019; **Accepted:** 21-Nov-2019; **Online first:** 20-Dec-2019

Funding: This research did not receive any financial support

Competing Interests: The authors have declared that no competing interests exist

Abstract

BACKGROUND: Hepatocellularcarcinoma (HCC) metastasis include intrahepatic and extrahepatic metastasis. Similar to intrahepatic metastasis, extrahepatic metastases are not unusual in cases with HCC. However, colonic metastasis is infrequent.

CASE REPORT: We describe a clinical case, he was diagnosed with HCC a year ago, treated with TACE (transarterialchemoembolisation), re-examined with abdominal pain and defecation disorder. The tests such as CT scan, colorectal endoscopy, fine needle aspiration (FNA) revealed secondary metastatic lesion of HCC in sigmoid colon. This is the first gastrointestinal (GI) tract metastatic we have encountered.

CONCLUSION: HCC metastases of the colon are rare, especially cases of hematogenous spread. The prognosis of these patients is often very critical. Indications for surgical removal of the lesion may be used if the general situation of patient is acceptable.

Introduction

In the top ten frequent cancers worldwide, the cancers of lung, breast, prostate, colon, nonmelaoma of skin, and stomach are followed by primary liver cancer. On the other hand, primary liver cancer is one of most common causes of death which relative to cancer diseases globally due to its extremely poor prognosis [1]. It is not denying that many patients could not be diagnosed at early stage. Even though surveillance programs for early liver cancer and hepatocellular carcinoma (HCC) have been implemented. Consequently, only 30% of them take advantage of radical treatment such as hepatectomy, liver transplant surgery [2]. Extrahepatic metastasis of HCC is not rare, lung and adrenal are two of typical side. Gastrointestinal (GI) tract metastasis from HCC is not common. Distal colon metastasis is extremely uncommon situation of extrahepatic metastasis. This article aims to present a case of HCC patient with a single colonic metastatic lesion which derive from HCC treated with TACE.

Case Report

The patient was 60 years old; he had been infected hepatitis B virus for 15 years was determined to have HCC in 2018. He received TACE. This man has been reexamined every three months. The result of CT scans and AFP test were normal. He visited our center because tenesmus and left lower quadrant abdominal pain lasting for several days.

Nothing abnormal was found during physical examination. The result of AFP was 9.48 ng/ml. Other laboratory tests were within normal limits. A colonoscopy revealed a mass located in sigmoid colon with intact overlying mucosa so the biopsy

procedure was not performed. CT scan revealed a 50 x 60 mm sized, bulging contoured mass located in sigmoid colon (Figure 1E and 1F). A natural hypodense mass with 39 x 41 mm located in segment IV – VIII of liver (Figure 1A), no enhancement at arterial phase. Several hypervascular lesions located in both lobes (Figure 1B and 1C). An ultra sound – guided FNA biopsy was performed. Result of pathology demonstrated metastasis of carcinoma.

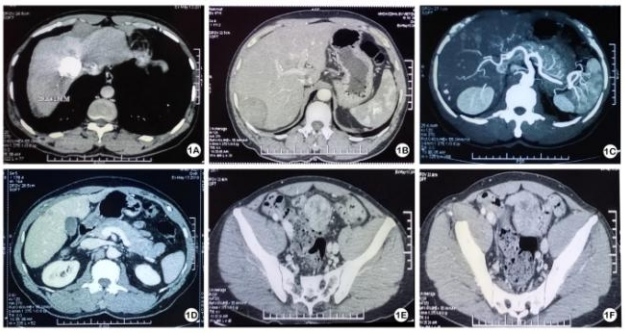

Figure 1: CT scan result: A natural hypodense mass with 39 x 41 mm located in segment IV – VIII

At the multidisciplinary team meeting, we decided that he would undergo surgical treatmet first. The patient underwent anterior resection. He tolerated that surgical procedure without any complication.

Gross examination, the 15 cm rectosigmoid segment with smooth surface mucosa had two well-circumscribed masses measuring 50 x 40 x 35 mm and 15 x 10 x 10 mm and pushing the serosa. The cut surface was tan-yellow. Nine masses ranging from 15 x 10 x 10 mm to 30 x 30 x 20 mm attaching to adipose tissue were removed from the mesentery. They shared similar features with intestinal masses. Histopathological examination showed the tumor found under the mucosa was composed of atypical polygonal cells with irregular hyperchromatic nuclei, prominent nucleoli and clear or eosinophic cytoplasm (Figure 2A). They were arranged in large sheets or trabeculae. Vascular invasion was seen (Figure 2B).

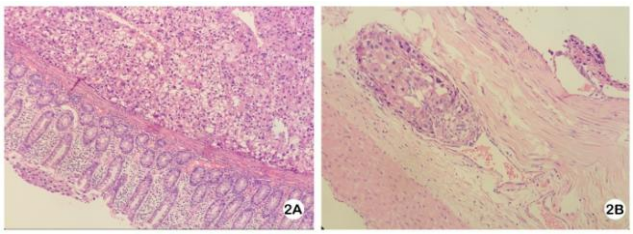

Figure 2: The tumor is in submucosa, was composed of a typical polygonal cells that resemble HCC 2A) and vascular invasion 2B)

Immunohistochemistry staining were utilized. They show the reacting positively for Hepar-1 and Arginase-1 (Figure 3A and B).

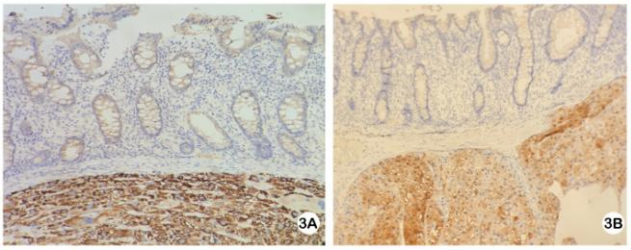

Figure 3: Immunohistochemicalstaiing, the tumor cells were positive for Hepar-1 3A) and Arginase-1 3B)

After completing recovery, he started received HAIC (hepatic arterial infusion chemotherapy). We concluded that the metastasis lesion in sigmoid colon appeared due to the seeding which occurs after some interventional techniques such as TACE. The lesion had been removed completely. On the other hand, there was no evidence of other extrahepatic metastasis. Moreover, the patient did not accept the expense of target therapy. As result, we decided HAIC is convenience therapy for him. The patient had been treated with HAIC-mFP, 3 cycles. The response was quite good. AFP and PIVKA-II were decrease.

Discussion

Currently, liver cancer is classified as the third cause of death due to malignant diseases over the world, approximately 800 000 per year. Liver cancer has particular age, sex and geographic distributions, likely influenced by certain etiologic variables. Histologically, the majority of liver cancer falls into one of two categories: HCC and ICC (intrahepatic cholangiocarcinoma), and cholangiocarcinoma is less common**.** Even though malignant hepatic tumor is more common in developing countries, it is still significantly prevalent in other developed regions such as North America and central Europe [3]. While other cancers, like breast, lung, and colorectal cancer are on the decline, the mortality rate for primary liver cancer has increased in both sexs in recent decades [4]. While hepatitis B is a paving hepatic cancer risk factor in Asia, hepatitis C infection is reason why the incidence of liver cancer is increasing in the US. Furthermore, other significant risk factors include aflatoxin B1 poisoning, diabetes, alcoholicabuse, non-alcoholoc fatty liver disease [5].

Among malignant diseases of the liver, the most frequent is HCC, the direct cause of the disease is unclear, the mechanism of the disease is thought to be a disorder of the DNA structure of the cell nucleus [6]. According the Globocan 2018 data base, the number new HCC cases in Vietnam (both sexes, all ages) is highest (25 335 – 15.4%). As reported by a recently published study on HCC in southern and central Vietnam, statistics show that there were 24

091 patients between 2010 and 2016, with a significant increase over the years (from 2793 cases in in 2010 to 4069 in 2016), men were the majority compared to women, most patients were positive for viral hepatitis (88.3% positive for hepatitis B or hepatitis C and 2.7% simultaneously positive for both of them) [7].

HCC is considered to be a cancer with a very high degree of malignancy, it has the tend to invade the portal vein as well as the liver vein. Therefore, lymph node metastases and distant metastases are also common, about 50% [8], especially for tumors larger than 5 cm in diameter [9]. Most extrahepatic HCC has been observed in cases with advanced stage of disease (stage VIa), as expected [10]. The longer a patient survives, the more risk of extra-hepatic metastases increases and metastases to the lungs, bones, lymph nodes are most common [8].

Signs and symptoms of patients suffering from HCC primarily focused on the manifestation of the primary tumor and the metastatic features later. Recently, the metastatic characteristics of HCC has displayed two alluring new behaviors: the unexpected spread site, and the discovery of the metastatic lesion before the primary tumor is recognized. Metastases to the gastrointestinal tract are rare and mainly reported by clinical case reports. Direct invasion through the adjoining serous tumor due to the excessive growth of a primary tumor is a common mechanism and the invasive organ is often the duodenum, the stomach, jejunum, and colon (anatomical location close to the liver) [11], [12]. Metastases to other parts of the gastrointestinal tract are rarer and have not been adequately explained. Hematogenous dissemination is a hypothesis of distant GI tract metastasis. The explanation of haematogenous spread has been supposed to be the blockage of portal vein come after the vascular was infiltrated. The existence of tumour thrombosis in the portal vein may lead to a reversal of flow, which likely acts as the medium of haematogenous metastasis of HCC to the GI tract [13]. Transarterial embolization (TAE) and TACE can also cause increased portal vein pressure to cause blood clots and reverse flow [12], enabling HCC to invade nearby organs such as the colon or other parts of the digestive tract.

Main local symptoms of colon metastasis from HCC patient are blood in stool, changed defecation pattern, abdominal pain, very similar with primary colorectal cancer. Unfortunately, gastrointestinal endoscopy is easy to confuse metastatic damage of HCC with polyps, mucosal tumors or colorectal ulcers. Sometimes, it is really difficult to identify them through endoscopic examination and performed biopsy, especially the lesions which have intact overlying mucosal. Therefore, immunohistochemistry is considered an effective tool for the differential diagnosis between liver cancer and adenocarcinoma of the colorectal. Hepar-1, Arg-1, GPC-3, p-CEA, BSEP are some popular inmmunohostochemical markers which are available for establishing the diagnosis. As previously study, Hepar-1 and p-CEA are the two most widely used markers for high sensitivity and specificity [14], [15].

Some reports indicate GI metastasis usually could be dectected between 3 months to 8 years from the initial confirmation of HCC [11], [16], [17]. Nasuizaka et al., reported an average survival time of HCC patients with metastatic gastrointestinal tract was 7 months (1-59 months) and only 24.9% lived more than 1 year or more [10]. Another aspect for these patients is whether the treatment to eliminate extrahepatic metastatic lesions is effective, especially in the early cases with good liver function and no portal vein invasion [18]. Although there is too little evidence and insufficient data to prove the effectiveness of surgical treatment, especially for colon metastases in HCC patients, we believe that surgery removes this type of metastatic injury is especially necessary for patients with only a single metastatic lesion and good physical condition.

In conclusion, this article aims to report a patient with HCC who has metastases of sigmoid colon. This is a very rare clinical morphology and is the first case in our clinic. Medical history has noted that HCC's extrahepatic metastases are quite common but colon metastases are very rare. Like other metastatic cases, colon metastasis patients have not delight outcome. Surgery to remove metastatic lesions is thought to be a treatment option especially for patients who had good liver function and acceptable condition.

Ethical approval

This study is approved by the ethics committee of Vietnam National Cancer Hospital

Informed consent

The consent and commitment were signed by the patients in the study

References

1. Bray F, et al. Global cancer statistics 2018: GLOBOCAN estimates of incidence and mortality worldwide for 36 cancers in 185 countries. CA Cancer J Clin. 2018; 68(6):394-424. https://doi.org/10.3322/caac.21492 PMid:30207593

2. Llovet JM, Burroughs A, Bruix J. Hepatocellular carcinoma. Lancet. 2003; 362:1907-1917. https://doi.org/10.1016/S0140-6736(03)14964-1

3. Hashim D, Boffetta PP, La Vecchia C, et al. The global decrease in cancer mortality: trends and disparities. Ann Oncol. 2016; 27:926-33. https://doi.org/10.1093/annonc/mdw027 PMid:26802157

4. Seigel RL, Miller KD, Jemal A. Cancer statistics. CA Cancer J Clin. 2016; 66:7-30. https://doi.org/10.3322/caac.21332 PMid:26742998

5. Makariva-Rusher OV, Altekruse SF, McNeel TS. Population - attributable fractions of risk factors for hepatocellular carcinoma in the United States. Cancer. 2016; 122:1757-65. https://doi.org/10.1002/cncr.29971 PMid:26998818 PMCid:PMC5548177

6. Alison MR. Liver stem cells: implications for hepatocarcinogenesis. Stem Cell Rev. 2005; 1(3):253-60. https://doi.org/10.1385/SCR:1:3:253

7. Nguyen Dinh SH, Do A, Pham TND, et al. High burden of hepatocellular carcinoma and viral hepatitis in Southern and Central Vietnam: Experience of a large tertiary referral center, 2010 to 2016. World J Hepatol. 2018; 10(1):116-123. https://doi.org/10.4254/wjh.v10.i1.116 PMid:29399285 PMCid:PMC5787675

8. Si Ms, Amersi F, Golish SR, Ortiz JA, et al. Prevalence of metastases in hepatocellular carcinoma: risk fartors and impact on survival. Am Surg. 2003; 69:879-885.

9. Yuki K, Hirohashi S, Sakamoto M. Growth and spead of hepatocellular carcinoma. Cancer. 1990; 66:2174-2179. https://doi.org/10.1002/1097-0142(19901115)66:10<2174::AID-CNCR2820661022>3.0.CO;2-A

10. Natsuizaka M, Omura T, Akaike T, et al. Clinical features of hepatocellular carcinoma with extra hepatic metastases. J Gastroenterol Hepatol. 2005; 20:1781-1787. https://doi.org/10.1111/j.1440-1746.2005.03919.x PMid:16246200

11. Chen LT, Chen CY, Jan CM, et al. Gastrointestinal tract involvement in hepatocellular carcinoma: clinical, radiological and endoscopic studies. Endoscopy. 1990; 118-123. https://doi.org/10.1055/s-2007-1012815 PMid:2162757

12. Hu ML, Tai WC, Chuah SK. Gastric metastasis of hepatocellular carcinoma via a possible existing retrograde hematogenous pathway. J Gastroenterol Hepatol. 2010; 25(2):408-412. https://doi.org/10.1111/j.1440-1746.2009.06022.x PMid:19929932

13. Tapuria N, Sinha CK, Michael NG, Fisher PW. Haematogenous metastasis to ascending colon in a patient with hepatocellular carcinoma and autoimmune hepatitis. Eur J Gastroenterol Hepatol. 2007; 19:607-609. https://doi.org/10.1097/MEG.0b013e3281c55f3e PMid:17556911

14. Chu PG, Ishizawa S, Wu E, Weiss LM. Hepatocyte antigen as a marker of hepatocellular carcinoma: an immonohistochemical compariosn to carcinoembryonic antigen, CD10, and alpha - fetpprotein. Am J Surg Pathol. 2002; 26(8):978-988. https://doi.org/10.1097/00000478-200208000-00002 PMid:12170084

15. Fan Z, van de Rijin M, Montgomery K, Rouse RV. Hep Par 1 antibody stain for the differential diagnosis of hepacellular carcinoma: 676 tumors tested using tissue microarrays and conventional tissue sections. Mod Pathol. 2003; 16(2):137-144. https://doi.org/10.1097/01.MP.0000052103.13730.20 PMid:12591966

16. Lin CP, Cheng JS, Lai KH, et al. Gastrointestinal metastasis in hepatocellular carcinoma: radiological and endoscopic studies of 11 cases. J Gastroenterol Hepatol. 2000; 15:536-541. https://doi.org/10.1046/j.1440-1746.2000.02152.x PMid:10847441

17. Park MS, Kim KW, Yu JS, et al. Radiologic findings of gastrointestinal tract involvement in hepatocellular carcinoma. J Comput Assist Tomogr. 2002; 26:95-101. https://doi.org/10.1097/00004728-200201000-00014 PMid:11801910

18. Uka K, Aikata H, Takaki S. Clinical features and prognosis of patients with extrahepatic metastases from hepatocellular carcinoma. World J Gastroenterol. 2007; 13:414-420. https://doi.org/10.3748/wjg.v13.i3.414 PMid:17230611 PMCid:PMC4065897

ID Design Press, Skopje, Republic of Macedonia
Open Access Macedonian Journal of Medical Sciences. 2019 Dec 30; 7(24):4372-4377.
https://doi.org/10.3889/oamjms.2019.838
eISSN: 1857-9655
Basic and Clinical Medical Researches in Vietnam

Transformation Chlorophyll a of *Spirulina platensis* to Chlorin e6 Derivatives and Several Applications

Hoa Thi Hai Bui[1], Tam Thi Pham[1], Hien Thi Thu Nguyen[1], Trung Minh Do[2], Vu Thi Nga[3], Nguyen Duy Bac[2], Vu Thi Bich Huyen[4], Hai Minh Le[5], Quang Canh Tran[6*]

[1]Hanoi Open University, Hanoi, Vietnam; [2]Vietnam Military Medical University, Hanoi, Vietnam; [3]Institute for Research and Development, Duy Tan University, 03 Quang Trung, Danang, Vietnam; [4]Department of Genetics and Biochemistry, Faculty of Biology, Hanoi National University of Education; [5]Vinh University, Nghe An, Vietnam; [6]Center for Hygiene and Food Safety, Haiduong Medical Technical University, Hai Duong, Vietnam

Citation: Bui THH, Pham TT, Nguyen TTH, Trung DM, Nga VT, Bac ND, Huyen VTB, Le MH, Tran QC. Transformation Chlorophyll a of *Spirulina platensis* to Chlorin e6 Derivatives and Several Applications. Open Access Maced J Med Sci. 2019 Dec 30; 7(24):4372-4377. https://doi.org/10.3889/oamjms.2019.838

Keywords: *Spirulina platensis*; Chlorin e6 trimethylester; Photodynamic therapy; Hela cell; Antibacterial

***Correspondence:** Quang Canh Tran. Center for Hygiene and Food Safety, Haiduong Medical Technical University, Hai Duong, Vietnam. E-mail: tranquangcanh68@gmail.com

Received: 23-Sep-2019; **Revised:** 20-Nov-2019; **Accepted:** 21-Nov-2019; **Online first:** 20-Dec-2019

Funding: This study was funded by a project (No. KYTH-86) from the Ministry of Education and Training of Vietnam

Competing Interests: The authors have declared that no competing interests exist

Abstract

BACKGROUND: *Spirulina platensis* contains a large amount of chlorophylls, chlorophyll a, that are starting materials to synthesize functionalized chlorins. Chlorin e6 (Ce6) as well as its derivatives are second generation sensitizers using in photodynamic therapy (PDT) of various cancers. In this study, we transfer chlorophyll a of *S. platensis* to Ce6 derivatives and determine their several applications.

AIM: We aimed to evaluate the effects of Ce6 derivatives to treat cancer cells.

METHODS: Ce6 trimethylester was created from methyl pheophorbide a2 in *S. platensis* provided by the Hidumi Company, Nghe An province, Viet Nam. Hela cells were incubated with Ce6 trimethylester and the irradiated with the diode laser dose of 1.2 J/cm^2/min through the system of filters £ 650 nm. MTT assay and clonogenic assay were used to determine survival rate and cloning efficiency of cells. Antimicrobial effect of Ce6 trimethylester with halogen light were studied with *Propionibacterium acnes* VTCC 0218 and *Staphylococcus aureus* VTCC 0173.

RESULTS: From dry biomass (700 g) of *S. platensis*, after extracting chlorophyll a and methanolysis, 4.2 g of methyl pheophorbide a was obtained. The reaction to give Ce6 trimethylester with 82% yield was performed with potassium hydroxide (KOH) in MeOH/THF/CHCl3. After irradiation with a 650 nm laser at 1.2 J, the cell viability in all samples decreased with Ce6 trimethylester treatment, the survival declining trend of Hela cells treated with Ce6 trimethylester were proportional when concentration of Ce6 trimethylester increased. The rate of colony formation was declined as the concentration of Ce6 trimethylester treated was increased. The growth of both *S. aureus* and *P. acnes* can be inactivated by Ce6 trimethylester PDT. The MIC99 value against *P. acnes* VTCC 0218 and *S. aureus* VTCC 0173 of Ce6 trimethylester with halogen light was 1.25 µg/ml.

CONCLUSION: The Ce6 trimethylester from *S. platensis* cultivated in Viet Nam could be used as a potential photosentizer for photodynamic therapy for treatment of cancer and acne.

Introduction

Spirulina platensis has been used for production nutritional supplements, functional foods, cosmetics as well as other biomaterials [1], [2]. *Spirulina* contains the very large amount of chlorophylls, specially chlorophyll a [3]. Chlorophylls are starting materials to synthesize functionalized chlorins that have the ability to improve the photodynamic activity [4]. Chlorophyll a, as a natural chlorin, is a potential renewable resource to product chlorin photosensitizers [5] which can use for photodynamic therapy to treat cancer. Chlorins, that are a class of tetrapyrroles derived from plant, are potential photosensitizers because they can absorb remarkably strongly in the light with high phototoxic red spectrum [6].

Photodynamic therapy (PDT), is a treatment therapy for cancer, uses some photosensitizers [6]. The photosensitizer molecules have singlet state with two electrons with opposite spins. They are activated by absorption a photon of light with appropriate wavelength to transfer from the excited singlet state to more stable excited triplet state. The photosensitizers in triplet state can participate in photochemical reactions with oxygen to form reactive oxygen species (ROS) which can destroy pathogenic bacteria, tumors,

cancer cells and target tissues [7]. Ce6 that is synthesized readily from natural chlorophyll is a second-generation photosensitizer. It can absorb strongly in the light with red spectrum. Ce6 and its derivatives have the ability to accumulate more effectively in tumors than normal cells, to absorb at longer wavelengths (670 nm) more strongly to be clear faster from organism so they can be used as second generation sensitizers for PDT of various cancers. It was report using in PDT successfully, namely C6-mediated PDT (Ce6-PDT), to treat some various cancer types such as nasopharyngeal cancer, bladder cancer as well as melanoma [8], [9].

Cervical cancer that is caused by infection of the human papilloma virus is the third common cancer in women in the word [10]. This infection of virus persistently causes intraepithelial transformations, following form a cancer if left untreated. The PDT can be an alternative method for the traditional invasive treatment to treat cervical cancer [11], [12].

Therefore, using PDT with Ce6 photosensitizer can be a potential treatment for cervical cancer. In the present study, Ce6 that was obtained from chlorophylls of *S. platensis* cultured in Viet Nam were used to evaluate the effects in Hela cells. Our findings might provide experimental evidence to support Ce6-PDT in treatment for cancerous cervical tumor.

Materials and Methods

Isolation of methyl pheophorbide a2 and transferred it to Chlorin e6 trimethylester

Chlorophyll was extracted and purified from dried *S. platensis* powder provided by the Hidumi Company, Nghe An province, Viet Nam. Isolation of methyl pheophorbide a2 as a mixture of 13^2R:13^2S diastereomers from *S. platensis* was carried out by the method of Bauer D *et al*., (2019) [5]. *Spirulina* powder (700-800 g) was taken into a Sohxlet thimble (length 32.5 cm, diameter 8 cm). Then add acetone (500 ml) Sohxlet thimble to soaks up all the *Spirulina* powder inside the thimble and add liquid nitrogen (2.5 liters) slowly into thimble. The Soxhlet thimble was put in Soxhlet extractor, and let the thimble returned to 10-20°C. Acetone (2.0 liters) was added into extractor. *Spirulina* powder was extracted 24 hours under an Ar atmossphere, 75 extraction cycles. The acetone extract was filtered and distilled vacuum to recover acetone. Then, add CH_2Cl_2 (200 mL) into the concentrated extract container and continue the vacuum distillation to remove the water in the mixture. Methyl pheophorbide a in the mixture was extracted and purified on chromatographic column. The methyl pheophorbide was crystallized to give dark green crystals.

Methyl pheophobide a was transferred to Ce6 trimethylester by two methods: (1) Methylphephorbide a (2.4 g, 2.8 mmol) was dissolved under an Ar atmosphere in degassed dry THF (25 mL) and $CHCl_3$ (125 mL) was added followed by 1 M KOH in MeOH (12 mL) and (2) methylpheophorbide a (186.5 mg, 0.25 mmol) was dissolved under an Ar atmosphere in THF (12 mL) and then MeOH (125 mL) was added followed by $KOCH_3$ in MeOH (2.5 mL 35% solution). Then, they were treated according to method of Bauer D *et al*., (2019) [5].

Hela cell culture

Hela cell line was purchased from Sigma Chemical Company (St Louis). The cells were seeded in 12-well plates containing E'MEM medium (GIBCO, serum-free medium) supplemented with L-glutamine (200 mM), HEPES (1 M), amphotericin B (0.1%), penicillin-streptomycin 200 x and 10% (v/v) FBS. The cells were cultured under a humidified 5% CO_2; at 37°C to achieve ~90% confluency was used in the photodynamic and laser treatment.

Treatment cells with laser light

The cells were incubated with 0.5, 1, 2.5, 5, 10 µg/ml of Ce6 trimethylester in serum-free E'MEM for 2, 4, 6, 8, 10 hours in dark at 37°C in humidified 5% CO_2. After that, the cells were twice washed with RPMI and irradiated with the diode laser dose of 1.2 J/cm^2/1min through the system of filters £ 650 nm. Control cells were incubated with serum-free E'MEM without Ce6 trimethylester for equivalent times. Treatment cells were trypsinized and washed by PBS for measuring the specific fluorescence intensity of Ce6 trimethylester by flow cytometry, determined the cell survival by MTT assay and colony formation assay to evaluate the long-term proliferative potential of Hela cells following photodynamic therapy.

Flowcytometry

The accumulation and removal of Ce6 trimethylester in the cells was studied with the flow fluorometer FACS Canto II (Becton Dickinson, USA). The cell suspension was omitted at the rate 500 cells/s in the flow solution under the argon laser emitting excitation light at wave length 488 nm. The data was analyzed with the use of FACSDiva verion 2.1 sofware.

MTT assay

The cells were trypsinized after being washed by PBS and then was resuspended in E'MEM medium with 10% FBS. 10 µl MTT solution (2 mg/mL) was added and incubated for 4 hours at

37°C in 5% CO_2. The crystals formed were dissolved within one night by addition 25% SDS solution and using a shaker overnight. The result was recorded by microplate reader at wavelength 540 nm. The rate of cells survival (%) was calculated by formula: [1-(OD of treatment cells/OD of control cells)] x 100.

Clonogenic assay

The treatment and trypsinization cells were seed in E'MEM medium with 10% FBS, the experiment was carried out in five replicates. The cells were incubated at 37°C in the environment with 5% CO2 for colony formation. The colonies were dried then stained with Giemsa for 30 minutes; the ones containing more than 50 cells were counted manually. Cloning efficiency was determined by the equation:

$$\text{Relative clone formation rate } (\%) = \frac{\text{colony number of treatment group}}{\text{colony number of control group}} x100\%$$

Antimicrobial effect of TME with halogen light

Propionibacterium acnes VTCC 0218 and *S. aureus* VTCC 0173 from the Vietnam Type Culture Collection were treated with Ce6 and halogen light to determine antimicrobial effect of Ce6. *P. acnes* VTCC 0218 and *S. aureus* VTCC 0173 strains were cultured and treated with TME in condition with or without light irradiation. The bacterial suspensions with concentration 10^6 CFU/ml were added in 96-well microtiter plate containing TME with different concentration and irradiated with halogen light (12 V/50 W; 30,000 lx) for 30 min. Incubation proceeded at 37°C, for 12 h, in optimal aerobic conditions for each bacterial strain. Absorbance at 620 nm of bacterial suspensions after treatment was measured to determine bacterial growth. MIC99 is the TME concentration at which bacterial growth was more than 99% inhibited.

Results

Transformation chlorophyll a of S. platensis to Ce6 derivatives

Ce6 derivatives were obtained by transformation of chlorophyll a using standard protocol described by Bauer D *et al.,* (2019). Briefly, 900 g of dry biomass of *S. platensis* containing more than 0.4% of chlorophyll was subjected into a 10 mm x 38 mm Soxhlet thimble with 400 mL of acetone in addition of nitrogen liquid. The solvent was then refluxed using Soxhlet extractor, under Ar atmosphere for 24 h to ensure 70-75 of deep green chlorophyll extraction cycles. The extract was filtered and acetone was removed by evaporating. The water containing residue was dissolved in 250 mL of CH_2Cl_2 and the water was removed in a rotavapor. The residue was then dried, suspended in 750 mL of dry MeOH and 37.5 mL of H_2SO_4 and stirred at ambient temperature for 20 hours. 500 mL of CH_2Cl_2, 1000 mL of H_2O, 250 mL of saturated NaCl and 350 ml of $NaHCO_3$ were added and the aqueous layer was extracted three times with 250 mL of CH_2Cl_2, washed twice with H_2O, then filtered and evaporated. The red crude extract was dried and dissolved in 35 mL of CH_2Cl_2 and eluted in column chromatography (200 g silica gel, 32–63 mm, 60 Å). The main fraction of methyl pheophorbide a was recovered after elution with CH_2Cl_2 and CH_2Cl_2: acetone (30: 1). The minor fraction of methyl pheophorbide a was obtained by elution with H_2SO_4/MeOH.

The dark green crystal of methyl pheophorbide a was obtained by crystallization from CH_2Cl_2/MeOH (1.5: 10) of the two fractions to form 89: 11 mixture of 132R: 132S diastereomers and the final yield was 4.95 g (0.55% of biomass), mp 226-227°C. TLC (Alox, CH_2Cl_2/Acetone: 10/0.4) Rf = 0.58. IR (KBr): v = 3377 cm^{-1} (w, N-H), 2958 (w), 1734 (s, C- = O, ester), 1701 (s, C = O, ester), 1619 (m, C = C, aromatic), 1556 (w), 1498 (w), 1432 (w), 1365 (w), 1345 (w), 1297 (w), 1213 (s, C-O-C, ester), 1164 (s,br, C-O-C, ester), 1122(w), 1035 (w), 990 (w), 909 (w), 895 (w), 829 (w), 752 (w), 671(w). UV/VIS (THF): λmax (Ɛx10-3) = 321 (21.64), 411 (109.05), 505 (10.39), 535 (9.98), 610 (8.72), 670 (45.55). MS: (EI, 70 eV, direct, T = 200°C): m/z (% rel. intensity) = 606 (100) [M+], 548 (28), 459 (16), 236 (10), 44 (39), 28 (100) [C2H4]+. MS: (ESI, positive, CH_2Cl_2/MeOH 1:10): 607.3 [M + H]+, 629.2 [M + Na]+, 645.2 [M + K]+. MS: (ESI, negative, CH_2Cl_2/MeOH 1:10): 605.2 [M – H]-

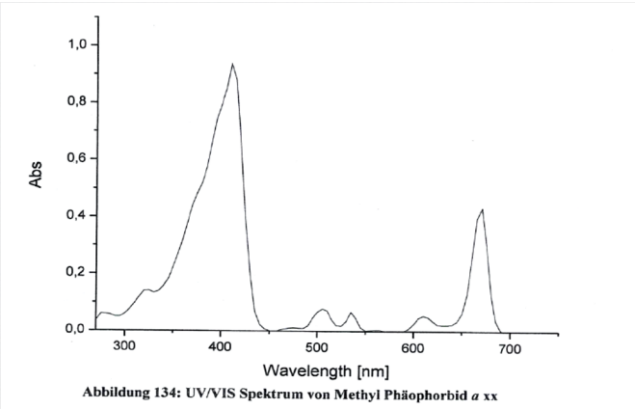

Figure 1: UV/V is spectrum of Methyl pheophobide a in MeOH

The 2.4 g of the first variant (variant A) of methyl pheophorbide a 2 was dissolved in 25 mL dry THF, 125 mL $CHCl_3$ and 12 mL 1 M KOH in MeOH was added. The mixture was stirred and poured into 500 mL ice water. After extraction twice with 100 mL of diethyl ether, the combined organic layer was

washed four times with water and filtered. The solvent was removed and the residue was purified by column chromatography (200 g silica gel, 32 – 63 mm, 60 Å). Blackblue crystals of Ce6 were obtained by crystallization of residue from Acetone/MeOH. Yield 1.84 g (77%), mp 210°C. 186.5 mg of the second variant of methyl pheophorbide a 2 was dissolved in 12 mL of THF, then mixed in dark with 125 mL of MeOH and 2.5 mL of $KOCH_3$ in MeOH 35% for 30 min in ambient temperature. 400 mL of water was added an extraction with 100 mL diethy ether will be carried-out. The organic extracts were washed with water for 4 times and filtered. The solvent was eliminated and the crude product was purified by column chromatography (40 g silica gel, 32–63 mm, 60 Å). The blackblue crystals of Ce6 trimethyester 3 were obtained after crystallization of the fraction from acetone/MeOH. Yield 151 mg (80%), mp (acetone/MeOH) 207 – 208°C. TLC (silica gel, CH_2Cl_2/EtOAc, 7:1): Rf = 0.58. IR (KBr): v = 3298 cm^{-1} (w, N-H), 2953 (m, C-H), 2916 (s, C - H), 1726 (s), 1600 (s), 1440 (m), 1243 (m), 1165 (m), 1063 (m). UV/VIS (MeOH): λmax (ε) = 303 nm (9543), 401 (126760), 501 (21134), 605 (11775), 660 (50134). MS: (EI, 70 eV, T = 200°C): m/z (% rel. intensity) = 638 (100) [M+], 579 (15), 565 (27), 479 (21), 289 (6), 236 (8) MS (DCI, negative, NH_3, 8 mA/sec): m/z (%) 641 (2) 640 (14), 639 (51), 638 (100) MS: (ESI, positive, CH_2Cl_2/MeOH 1:10): 639.2 [M + H]+. MS: (ESI, negative, CH_2Cl_2/MeOH 1:10): 637.3 [M – H]-

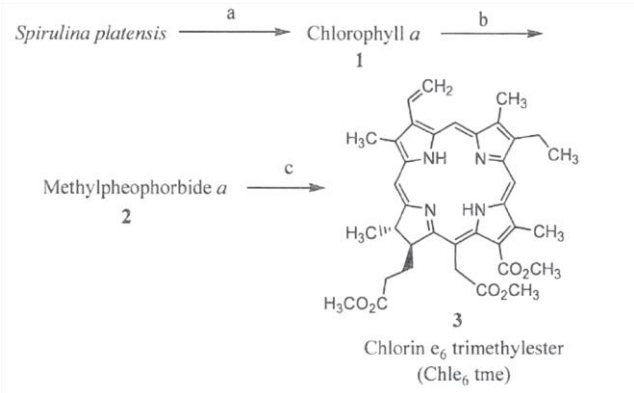

Figure 2: Chlorophyll a extraction from S. platensis and its transformation into Ce6 trimethylester; A) Dry spirulina mass, acetone, N2 (liquid), ca, 60 min, then warm up to room temperature, acetone, reflux, 24 hours; B). H_2SO_4 conc, MeOH, Ar, rt, 20 hours. (c). 1M KOH in MeOH, THF/$CHCl_3$, Ar, rt, 30 min (73%) or KOMe, MeOH, acetone, Ar, rt, 30 min, 85%

Efficacy of Ce6 trimethylester for photodynamic on Hela cells

Cellular uptake of Ce6 trimethylester following various concentration and different incubation times was analyzed based on the fluorescence of Ce6 trimethylester, using fluorescence microscopy and a flow cytometer. In Figure 3, Ce6 trimethylester treated Hela cells had a strong red color, the fluorescence intensity rapidly increased at the few hours after Hela cells were incubated with various concentration of Ce6 trimethylester and reached a relatively high level at 8 hours after incubation. The result in Figure 2 suggested that 4 hours may be the optimal incubation time of Ce6 trimethylester with Hela cells for our experiments. Then, we varied the concentration of each sample from 0.5; 1.0; 2.5; 5 and 10 µg/mL of Ce6 trimethylester and compared the cellular uptake, the cellular uptake of Ce6 trimethylester increased with the concentration, the cells treated with any of Ce6 trimethylester concentrations had higher intensity than untreated control cells.

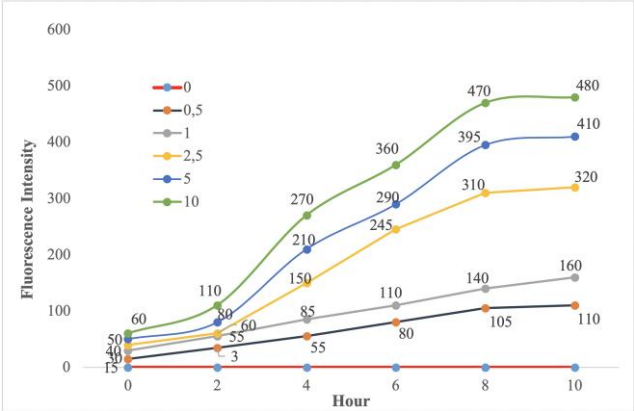

Figure 3: Alterations of Ce6 trimethylester fluorescence intensity in Hela cells at various Ce6 trimethylester concentrations with different incubation time (measured by flow cytometry)

Survival rate of cells was determined by the MTT assay after 8 hours treatment with Ce6 trimethylester (0, 0.5, 1, 2.5, 5, 10 µg/ml, respectively) and the subsequent photodynamic irradiation (Figure 3).

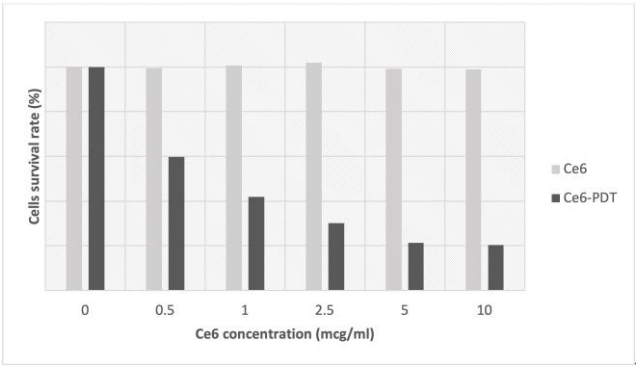

Figure 4: The cell survival rates of Hela cells were assessed by the MTT assay

Hela cells, which was treated with Ce6 trimethylester at corresponding concentrations and without photodynamic irradiation, were used as controls. The results in Figure 3 showed that, different treatment concentrations of Ce6 trimethylester alone could not influence the survival rate of cells. After irradiation with a 650 nm laser at 1.2 J, the cell viability in all samples decreased with Ce6 trimethylester treatment, the

survival declining trend of Hela cells treated with Ce6 trimethylester were proportional when Ce6 trimethylester treatment concentration increased (Figure 4).

Assay of colony formation assay was used to evaluate the ability of proliferation and clonogenicity of single Hela cells following PDT therapy. Following the Ce6 trimethylester treatment at various concentrations, Hela cells without photodynamic irradiation were control groups. The results in Figure 5 showed that the colony formation rate was declined as the Ce6 trimethylester treatment concentration was increased.

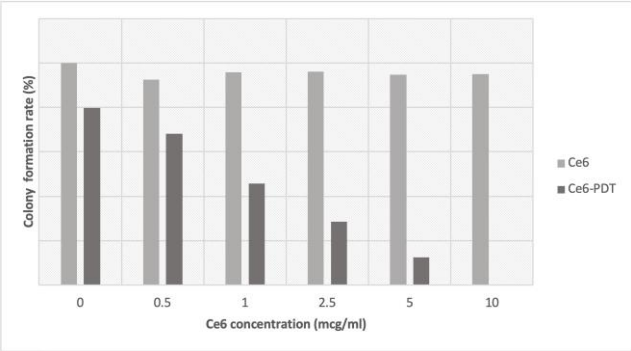

Figure 5: Colony formation assay of Hela after different treatment

Antimicrobial effect of Ce6 trimethylester with halogen light

The antibacterial activity of Ce6 trimethylester with halogen light was tested by the ability of *P. acnes* and *S. aureus* against (Figure 6). TME was prepared at 11 concentrations, include 0.25, 0.5; 0.75; 1.0; 1.25; 1.5; 1.75; 2.0; 2.25; 2.5; 2.75; 3.0 µg/mL. After treatment with TME, halogen light (12 V/50 W, 30000 lx) irradiation had done during 30 min.

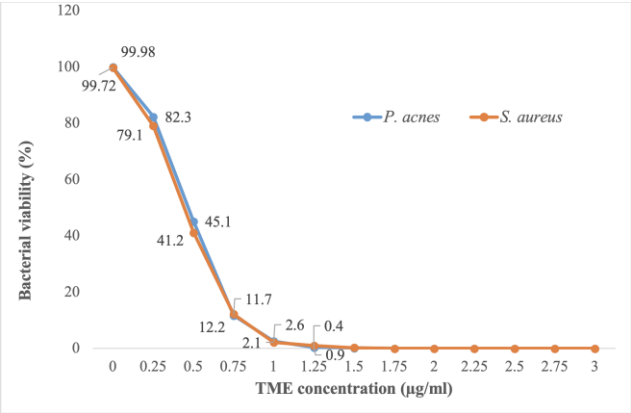

Figure 6: Antimicrobial effect of Ce6 trimethylester using halogen light

The results in Figure 6 indicated that halogen light did not affect the bacterial growth at this condition. The combined treatment TME and halogen light inhibited the growth of bacteria, and this inhibition was dependent on the dose of treatment. The MIC99 value against *P. acnes* VTCC 0218 and *S. aureus* VTCC 0173 of TME with halogen light was 1.25 µg/ml. The results showed that the growth of both *S. aureus* and *P. acnes* can be inactivated by TME PDT.

Discussion

Photodynamic therapy (PDT), which used to treat several diseases (cancers, skin disease, rheumatoid arthritis), includes three essential factors: light, a photosensitizer, and oxygen [13], [14], [15]. These factors are not toxic if they separated; however together they create a photochemical reaction that can generate a highly-reactive product called singlet oxygen [16]. Ce6, as a second generation photosensitizer, is a hydrophilic photosensitizers extracted from porphyrin [17]. It has remarkable characteristics: easy and simple production, selective accumulation ability in target tissues, shorter photosensitizing period,deep penetration into tissues if it is absorbed light having longer wavelength, as well as having minimal side effect [18], [19].

There are three interconnected mechanisms of PDT to treat tumor: (1) direct toxic for the cells of tumors; (2) destroy the vasculature of tumors; and (3) causing a robust inflammatory reaction which can contribute for development of the systemic immunity. These mechanisms have different effects in treatment tumors, which depend on: the dose of photosensitizer used the time interval between photosensitizer administration and light exposure, light flounce rate as well as total light dose. In the present study, the subcellular localization of Ce6 trimethyleste in Hela cells increased with its concentration. These results suggest that the Ce6 trimethylester treatment could inhibit the proliferation of Hela cells as well as decrease the colony formation rate of it, in a dose-dependent manner. In previous report, Ce6 could enhance the production of ROS (reactive oxygen species) and cell apoptosis, inhibit proliferation of the cells, decline abilities of the migration as well as colony formation in SW480 cells. These effects depended on in a Ce6 dose [8].

Antibacterial PDT that used photosensitizer (PS) with laser light may become a potential method to treat acne. Halogen lights that have approximately 35% amount of light emitted falling into the range 600 to 900 nm, emit light spectra similar to sunlight [20] . In this study, we have demonstrated that combination of Ce6 trimethylester and halogen light is a potential method for antibacterial therapy to treat acne. The results showed that Ce6 trimethylester with halogen light has strong antibacterial activity against skin bacteria such as *P. acnes* and *S. aureus in vitro*. With the treatment of 1.25 µg/mL Ce6 with and without irradiation of halogen light, the growth of both *P. acnes* and *S. aureus* were inactivated completely.

In conclusion, the data generated of this study demonstrated that the Ce6 trimethylester obtained from *S. platensis* which was cultivated in Viet Nam could be used as a potential photosentizer for photodynamic therapy for treatment of cancer and acne.

Ethical Approval

All procedures performed in studies involving human participants were in accordance with the ethical standards of institutional and/or national research committee and with the 1964 Helsinki declaration and its later amendments or comparable ethical standards.

References

1. García JL, de Vicente M, Galán B. Microalgae, old sustainable food and fashion nutraceuticals. Microbial Biotechnology. 2017; 10:1017-1024. https://doi.org/10.1111/1751-7915.12800 PMid:28809450 PMCid:PMC5609256

2. Wells ML, Potin P, Craigie JS, Raven JA, Merchant SS, Helliwell KE, et al. Algae as nutritional and functional food sources: revisiting our understanding. Journal of applied phycology. 2017; 29:949-982. https://doi.org/10.1007/s10811-016-0974-5 PMid:28458464 PMCid:PMC5387034

3. de Morais MG, Costa JA. Biofixation of carbon dioxide by Spirulina sp. and Scenedesmus obliquus cultivated in a three-stage serial tubular photobioreactor. Journal of biotechnology. 2007; 129:439-445. https://doi.org/10.1016/j.jbiotec.2007.01.009 PMid:17320994

4. Uliana MP, Pires L, Pratavieira S, Brocksom TJ, de Oliveira KT, Bagnato VS, et al. Photobiological characteristics of chlorophyll a derivatives as microbial PDT agents. Photochem Photobiol Sci. 2014; 13:1137-1145. https://doi.org/10.1039/C3PP50376C PMid:24898703

5. Bauer D, Nghiem HV, Tien DD, Stelten J, Montforts F-P. Functionalization of chlorin e6 trimethylester towards potential amphiphilic photosensitizers for photodynamic therapy. Journal of Porphyrins and Phthalocyanines. 2019; 23:243-250. https://doi.org/10.1142/S1088424618501183

6. Ol'shevskaya V, Savchenko A, Zaitsev A, Kononova E, Petrovskii P, Ramonova A, et al. Novel metal complexes of boronated chlorin e6 for photodynamic therapy. Journal of Organometallic Chemistry. 2009; 694:1632-1637. https://doi.org/10.1016/j.jorganchem.2008.11.013

7. Abrahamse H, Hamblin MR. New photosensitizers for photodynamic therapy. Biochem J. 2016; 473:347-364. https://doi.org/10.1042/BJ20150942 PMid:26862179 PMCid:PMC4811612

8. Li Y, Yu Y, Kang L, Lu Y. Effects of chlorin e6-mediated photodynamic therapy on human colon cancer SW480 cells. International journal of clinical and experimental medicine. 2014; 7(12):4867-4876.

9. Savitskiy V.P., Zorin V.P., M.P. P. Selective phototoxicity of chlorine e6 derivatives toward leukemic cells. Experimental oncology. 2002; 24:142-144.

10. de Freitas LM, Soares CP, Fontana CR. Synergistic effect of photodynamic therapy and cisplatin: a novel approach for cervical cancer. Journal of photochemistry and photobiology B, Biology. 2014; 140:365-373. https://doi.org/10.1016/j.jphotobiol.2014.08.021 PMid:25240426

11. Hass R, Jacobs R, Kaufmann AM, Hillemanns P, Soergel P. Sensitization of immune cells following hexylaminolevulinate photodynamic therapy of cervical intraepithelial neoplasia. Photodiagnosis and photodynamic therapy. 2017; 17:82-86. https://doi.org/10.1016/j.pdpdt.2016.11.006 PMid:27888161

12. Choi MC, Jung SG, Park H, Lee SY, Lee C, Hwang YY, et al. Fertility preservation by photodynamic therapy combined with conization in young patients with early stage cervical cancer: a pilot study. Photodiagnosis and photodynamic therapy. 2014; 11:420-425. https://doi.org/10.1016/j.pdpdt.2014.06.001 PMid:24927981

13. Isakau HA, Parkhats MV, Knyukshto VN, Dzhagarov BM, Petrov EP, Petrov PT. Toward understanding the high PDT efficacy of chlorin e6-polyvinylpyrrolidone formulations: photophysical and molecular aspects of photosensitizer-polymer interaction in vitro. Journal of photochemistry and photobiology B, Biology. 2008; 92:165-174. https://doi.org/10.1016/j.jphotobiol.2008.06.004 PMid:18656379

14. Park JH, Moon YH, Bang IS, Kim YC, Kim SA, Ahn SG, et al. Antimicrobial effect of photodynamic therapy using a highly pure chlorin e6. Lasers in medical science. 2010; 25:705-710. https://doi.org/10.1007/s10103-010-0781-1 PMid:20414708

15. Na JI, Kim SY, Kim JH, Youn SW, Huh CH, Park KC. Indole-3-acetic acid: a potential new photosensitizer for photodynamic therapy of acne vulgaris. Lasers in surgery and medicine. 2011; 43:200-205. https://doi.org/10.1002/lsm.21029 PMid:21412803

16. Dolmans DEJGJ, Fukumura D, Jain RK. Photodynamic therapy for cancer. Nature Reviews Cancer. 2003; 3:380-387. https://doi.org/10.1038/nrc1071 PMid:12724736

17. Mojzisova H, Bonneau S, Vever-Bizet C, Brault D. Cellular uptake and subcellular distribution of chlorin e6 as functions of pH and interactions with membranes and lipoproteins. Biochimica et biophysica acta. 2007; 1768:2748-2756. https://doi.org/10.1016/j.bbamem.2007.07.002 PMid:17692283

18. Kostenich GA, Zhuravkin IN, Zhavrid EA. Experimental grounds for using chlorin e6 in the photodynamic therapy of malignant tumors. Journal of photochemistry and photobiology B, Biology. 1994; 22:211-217. https://doi.org/10.1016/1011-1344(93)06974-8

19. Park H, Na K. Conjugation of the photosensitizer Chlorin e6 to pluronic F127 for enhanced cellular internalization for photodynamic therapy. Biomaterials. 2013; 34:6992-7000. https://doi.org/10.1016/j.biomaterials.2013.05.070 PMid:23777915

20. Hanakova A, Bogdanova K, Tomankova K, Pizova K, Malohlava J, Binder S, et al. The application of antimicrobial photodynamic therapy on S. aureus and E. coli using porphyrin photosensitizers bound to cyclodextrin. Microbiological Research. 2014; 169:163-170. https://doi.org/10.1016/j.micres.2013.07.005 PMid:23899404

ID Design Press, Skopje, Republic of Macedonia
Open Access Macedonian Journal of Medical Sciences. 2019 Dec 30; 7(24):4378-4382.
https://doi.org/10.3889/oamjms.2019.839
eISSN: 1857-9655
Basic and Clinical Medical Researches in Vietnam

Treatment of Anti–NMDA Receptor Encephalitis with Ovarian Teratoma Removal: A Literature Review and Two Case Reports

Nguyen Phuong Tu[1, 2], Pham Ba Nha[1, 2], Nguyen Duy Hung[1, 2], Nguyen Hoang Minh[3*], Hoang Ngoc Anh[2], Thien Chu Dinh[4,5]

[1]Obstetrics and Gynecology Department of Hanoi Medical University, Hanoi, Vietnam; [2]Obstetrics and Gynecology Department in Bach Mai Hospital, Hanoi, Vietnam; [3]Hanoi National Hospital of Odontostomatology, Hanoi, Vietnam; [4]School of Odonto Stomatology, Hanoi Medical University, Hanoi, Vietnam; [5]Institute for Research and Development, Duy Tan University, Danang, Vietnam

Citation: Tu NP, Nha PB, Hung ND, Minh NH, Anh HN, Chu Dinh T. Treatment of Anti–NMDA Receptor Encephalitis with Ovarian Teratoma Removal: A Literature Review and Two Case Reports. Open Access Maced J Med Sci. 2019 Dec 30; 7(24):4378-4382. https://doi.org/10.3889/oamjms.2019.839

Keywords: NMDA encephalitis; Immunoglobulin; Ovarian teratoma

***Correspondence:** Nguyen Hoang Minh. Hanoi National Hospital of Odontostomatology, Hanoi, Vietnam. E-mail: drnguyenhoangminh@gmail.com

Received: 23-Sep-2019; **Revised:** 20-Nov-2019; **Accepted:** 21-Nov-2019; **Online first:** 20-Dec-2019

Funding: This research did not receive any financial support

Competing Interests: The authors have declared that no competing interests exist

Abstract

BACKGROUND: N-methyl-d-aspartate receptor (NMDAR) antibody encephalitis appears common in the world, but the number of clinical cases in Vietnam which were recorded is rare.

CASE REPORT: We describe two new cases of disease in recent years with the aim of contributing to diagnosis and treatment experiences. These cases were noted over the past 3 years with the patients who have been treated at lower levels but have no results. They came to us when symptoms became worse and therefore required prolonged treatment with special intensive care facilities. The atypical and easily confused symptoms are the reasons that make the disease be detected late; leading to a much higher cost of treatment and the complication may appear in the patient. In the past, patients with these manifestations were diagnosed with unexplained encephalitis and severe sequelae or death. Autoimmune encephalitis has many types; NMDA encephalitis associated with ovarian teratoma is the most common autoimmune encephalitis in young women.

CONCLUSION: In conclusion, based on the case report, we hope to contribute some experiences on the diagnosis and the strategy in early treatment. With most female patients at very young age, early treatment to avoid complications will help patients have a quality life and maintain reproductive function.

Introduction

Anti–N-methyl-D-aspartate–receptor (anti – NMDAR) encephalitis is defined as an autoimmune disorder connected with ovarian teratomas [1]. Patients regularly show noticeable psychiatrical signs and unintentional movements and rapidly progress to unresponsiveness with central hypoventilation and dysautonomia [2]. In spite of the fact that the occurrence of anti – NMDAR encephalitis linked with ovarian teratomas is different across studies, it could lead to severe consequences and the health of a person might be under threat. Although the symptoms are very serious but when the tumor is removed, those symptoms improve quickly [2]. The reason why this syndrome was not depicted until 2007 is related to the lack of radiologic discovery and precise laboratory. This explains why the majority of earlier cases likely diagnosed as viral encephalitis [1]. Accordingly, the prognosis is very important, and in many cases, disease can be fatal with irreversible damage to cortical areas in those who suffer delay in diagnosis and medical care. As a result, patients could end up with weakening neuropsychiatric dysfunction or even being death. However, if the antibodies are pathogenic, doctors can determine that their effects on NMDA receptors would be reversible because most of the patients did recover [2]. When studying this antibody based on pharmacological and genetic properties, these antibodies show a relationship between the ability to decline receptor function and the clinical presentation of the disease [3].

The exact diagnosis of the disease is still difficult because the symptoms of the disease are not typical and easily confused with neurological diseases

[4]. Grassroots hospitals will face difficulties to diagnose due to the lack of specific clinical cases and treatment experience. The type of immunotherapy that is often claimed as most effective in controlling the symptoms of the disease still remains a matter of debate. Hence, there is a vital lack of data concerning the optimum treatment of the disease and the cases may show some confounding factors that leading to a delay in diagnosis [3].

Therefore, with the aim of contributing part of the experience in diagnosis anti- NMDAR encephalitis and early treatment, we report cases of two young women with teratoma removal and treatment therapy after surgery, a patient with plasmapheresis and a patient without plasmapheresis.

Case Reports

Case 1

The first patient was an 18-year-old female who had not yet been found any abnormal in medical history. She presented with vomiting, headache, high fever (always over 39,5°C) and acute disorientation for one week, then high fever accompanied with urine incontinence, confusion and dull response. She was admitted with the identification of meningitis-encephalitis since January 7th, 2017 after one day at Thanh Hoa Province General hospital. She was treated by high dose and a combination of intravenous (IV) antibiotic which were Meronem 500 mg and Pamecillin 1 g, antiviral drugs, antimicrobial treatment, solumedrol (Methylprednisolone 1 g), sedative drugs to against brain edema. However, her disease progressed more serve despite having drug treatment. As her Glasgow Coma score was 10, her prognosis had become worsen, therefore, we must open the trachea, support with mechanical breathing. As a result, the patient then fell into unconscious condition.

MRI brain showed a condition of mild posterior hemisphere edema. Her abdominal CT (Computed Tomography) and ultrasound (Figure 1) revealed a 90 x 60 mm ovarian teratoma in the right ovary.

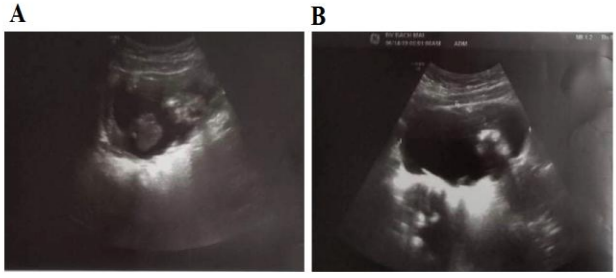

Figure 1: Imaging of the ovarian teratoma on the ultrasound; A) Ovarian teratoma on the vaginal ultrasound imaging; B) Ovarian teratoma on the abdominal ultrasound imaging

After a consultation within the most important departments of the hospital (including neurologists, internists, psychiatrists, intensivists, infectious disease specialists, radiologists, gynecologists and pathologists), we decided to used immunoglobulin therapy and the gynecologist removed the ovarian teratoma by using laparoscopic method at the Obstetrics Department in Bach Mai Hospital. She was treated with intravenous immunoglobulin to against anti-NMDA receptor encephalitis and went through minimal changes in neurologic symptoms. We used Intratect (Immunoglobulin G2,5g) for her with the dose of 20 gr per day on 5 consecutive days. Besides, she also received corticosteroid therapy by IV 5 days after surgery with Methylprednisolone 1 g per day. She experienced a successful surgery (Figure 2). Within 24 hours after surgery, she achieved a remarkable improvement in her cognitive function (the patient could recognize herself, her parents' names, and in few days later she could remember previous events). The result of histopathology showed the present of mature teratoma and nerve tissue. Several days later, she had recovery with good condition and could be discharged.

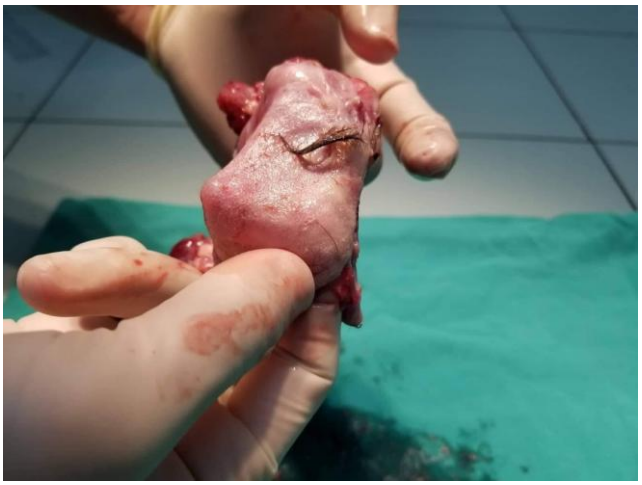

Figure 2: Imaging of the ovarian teratoma after surgery

In conclusion, after 3 months of treatment, the patient was able to resume normal activities, recognize and exercise completely normally, return to school and memory recovers well.

Case 2

The second female patient was 17 years old who has no history of medical or psychiatric problems. She began with headache, memory loss, and intermittent fever (38°C) for 6 days. The patient had high continuous fever during days, the average temperature was over 38.2 Celsius degrees continuously and her mental was affected, such as she spoke all day without determined topics, laughed for whole day then lost appetite. Also, her mother reported to doctor that she had been enduring increasingly memory loss over the past few weeks.

Later, she developed disjointed and unintelligible speech and an irregularly aggressive behavior including shouting at everyone. She was brought to the Hanoi Mental Hospital but the doctors were not sure about the diagnosis and treatment there. Afterwards, she was admitted to the National Hospital of Tropical Diseases and was treated for 4 days before hospitalized in the National Institute of mental health on June 4th with the present of sporadically incoherent language and altered manner. The results of basic tests and initial investigations were normal. Brain CT and MRI (Magnetic resonance imaging) (Figure 3) were checked without findings, Ultrasound and abdominal CT revealed a 61 x 116 mm mass likely an ovarian teratoma.

After 1 week, the mental of the patient got worse, acute confusion and a subjective fever with infectious respiratory organs and two weeks into admission, the patient developed many complications, including severe pneumonia.

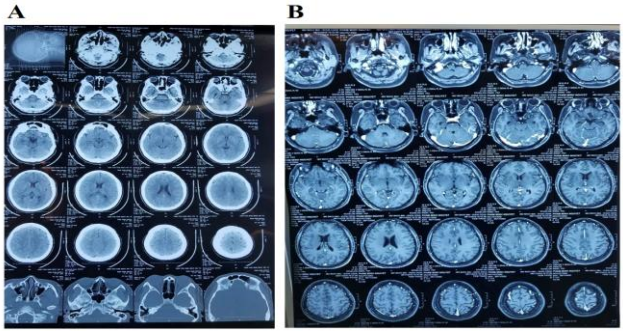

Figure 3: Imaging of the patient on MRI result; A) Imaging of a normal condition; B) Imaging did not show a condition of brain edema

More thorough methods were carried out to analysis and found out the reason. The Electro-encephalograms (EEG) were accomplished and they showed general slower with unspecific characteristics and there was no evidence of abnormal paroxysmal activity. She was given a course of IV solumedrol and antibiotics (high dose and combined three types of antibiotics). We considered to find out the anti – NMDA glutamate receptor antibodies and it was positive. And surgeons removed ovarian mass by laparoscopic cystectomy after one month from the moment she had her first symptoms (Figure 4). In the following days, the patient's condition was fast improving under ongoing corticosteroid therapy with intravenous Methylprednisolone 1 g per day for seven days and followed the routine supportive care. Hence, the histopathology was consistent with mature cystic teratoma. The results verified the appearance of nervous system tissue. The microscopic examination showed the tumor of ovary tissue and the tumor included different embryonal component. The well – differentiated element was cutaneous tissue. The mesodermal comprised of bone and cartilage tissue. In addition, there was a presence of poor differentiated element that contained immature neuroepithelium (amount of immature neuroectoderm occupies ≤ 3 low-power magnification fields).

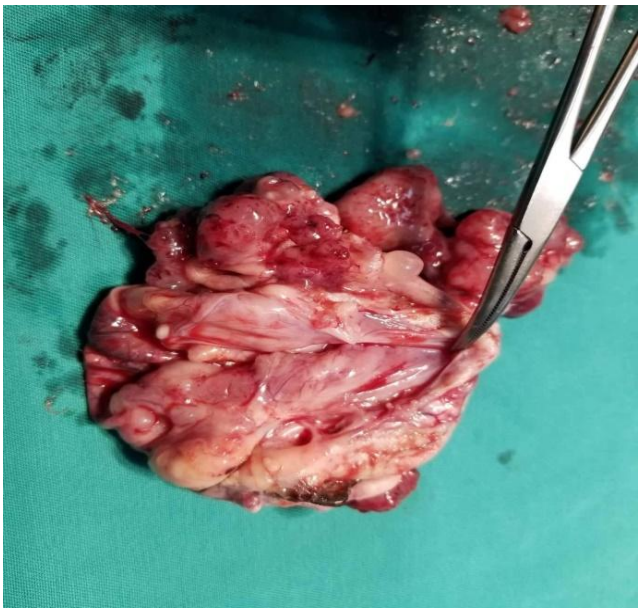

Figure 4: Imaging of the ovarian teratoma after laparoscopic cystectomy. After surgery, the patient had recovered significantly

According to the information above, we created a comparison between two patients (Table 1). The table shows the same symptoms and some basic tests to find out the cause to the disease, it also gives the differences in the treatment of two patients. Thus, it is possible to draw experience in diagnosis and treatment.

Table 1: Comparison between two cases

	Case 1: The 1st Patient	Case 2: The 2nd Patient
Gender	Female	Female
Age	18	17
Medical history	Normal	Normal
First symptoms	Vomiting, headache High fever (> 39 degree) Acute disorientation	Headache Intermittent fever (38 degree) Memory loss Speak and laugh whole day
Late symptoms	Urine incontinence Confusion Dull response	Incoherent speech Abnormally aggressive behavior.
Complication	Hypoxic respiratory failure	Infectious respiratory organ by Pseudomonas bacteremia.
First diagnosis	Meningitis encephalitis	Psychosis
Blood test	Normal	White blood cells increase
Biochemical test	Normal	Normal
Coagulation	Normal	Normal
Urine sediment	Positive for leukocytes	Negative
PCR	HSV: negative Tuberculosis: negative	Fever test: negative Dengue test: negative Tuberculosis: Negative
MRI brain	Mild posterior hemisphere edema	Normal
EEG	Normal	Generalized slowing characteristics
Lumbar puncture	Protein 0,81 g/L Glucose 3,9 mmol/L Pandy: positive	Protein 0,21 g/L Glucose 3,4 mmol/L Pandy: negative
Abdominal CT	90x60 mm teratoma in the right ovary	61x116 mm ovarian teratoma
Anti-NMDA glutamate receptor	Positive	Positive
Treatment	-Immunoglobulin therapy -Laparoscopic cystectomy -Corticosteroid therapy	Laparoscopic cystectomy Corticosteroid therapy
Histopathology	The present of nerve tissue and mature teratoma	The present of nervous system tissue and ovary tissue
Recovery	Recharged after several days	Recharged after two weeks

Discussion

Base on a previous study, Anti-NMDA encephalitis often happens in young women and it is usually combined with ovarian tumors, particularly teratomas [2]. The presence of a tumor in men and children is unusual [3], while in young women, encephalitis is regularly attached with ovarian teratomas [4]. Eventually, the average age of the patients in two cases are very young. The disorder causes a mental condition that appeared with noticeable psychiatric syndrome or, less often, memory decline, accompanied by the level of consciousness, abnormally behavior and unintentional movements. Two patients in this report are very young, one is 17 years old and another is 18 years old, and the first symptoms are the same (high temperature and headache). The derangement is usually beginning with headache, or malaise, then followed by a series of mental symptoms and behavior changes that lead to loss of consciousness around. The patients came in condition the psychiatric symptoms were often the most prominent but they did not respond to anti-psychotics. The patient after suffering psychiatric symptoms may have some complications related to respiratory tract and severe pneumonia appears most often. Hence, we can see that the symptoms of two cases often effected on the particular organs which were responsible for ability to remember, character, movement, autonomic control, which accounts for the unique assemblage of changes related to personality, impairments in perception and motor disorder. With cases of patients who had acute onset of psychiatric symptoms but had no unresponsive to anti-psychotic medication, we should consider that it is due to autoimmune encephalitis and should find out the cause. The progression of these manifestations in a young woman should raise a question in the dysfunction and motivate the search of an ovarian teratoma [5].

When comparing the above two cases, we found that surgical removal of ovarian tumors combined with immunotherapy would bring better results and patients would also recover faster. The first patient, although the symptoms were worse, the time for diagnosis and surgery was later, but thanks to the combination of immunoglobin, the recovery process was faster than the second patient. The analysis suggests that the use of more immunoglobulin is helpful in the postoperative treatment of patients and addition to surgery to remove ovarian tumors. Eliminate of an abnormal ovarian mass accompanied by plasma exchange and using corticosteroids led to a brisk neurological reaction and final full recuperation. In the first case, we required more time to diagnose, and then the patient was operated and was treated with immunotherapy. And in the second case, the fact that we had previous experience so we could diagnose earlier. Therefore, the patient had teratoma ovary was cured sooner. Due to some reasons, the second patient did not have enough condition to be used immunoglobulin but when she had surgery immediately right after diagnosis and was treated with intravenous corticosteroids for post-operative days, she could be eventual full recovered without immunotherapy. Thus, we determine that immunotherapy is frequently efficient, and it has been recommended that brisk excision of the teratoma accelerate recovery [2].

From many researches in the world, the scientists had proved that immune balancing methods eliminating causes and risk factors are the main options and chief supports of treatment plan [3]. Immune methods such as with steroids, plasmapheresis and IV Immuno globulin supports decrease antibody titers. Ovarian teratoma removal results in shorten clinical improvement. Besides, we specify that early tumor excision is the most essential way enabling brisk and full recuperation from anti-NMDAR encephalitis. If we do the operation as soon as possible, we can shorten the duration of the treatment. When comparing the results of treatment between two cases, it is clear that immunotherapy offers much better results. Indeed, the lesson is that we should try to combine both surgical and immunotherapy, not just remove ovarian tumors. In addition, early diagnosis will help patients to avoid severe neurological complications and restore memory faster. In the previous study, scientists indicated that ovarian teratomas accounted for 94% of all neoplasms which are responsible for the creation of anti-NMDAR encephalitis, with clinical improvement after tumor resection [6]. There are several methods of immunosuppressive treatments such as immunoglobulin therapy, intravenous steroids, plasmapheresis therapy or cyclophosphamide but if we just use only immunosuppressant drugs, the disease cannot be cured [7]. In contrast, the removal of ovarian tumor may be curative, so we can notice that all the immunosuppressive methods give the further support for treatment. Moreover, these drugs cost high prices so if the patients do not have the insurance, their hospital fee will be very expensive. When we compare with the results of other patients who have been reported before we see that about 80% of patients have improvement in neurological symptoms after tumor removal and immunosuppressive treatment [3]. However, there has not been any specific study to evaluate the possibility of recurrence, the disease relapses less likely in patients who do not have microscopic germ cell tumors undetectable by imaging [8]. There are even patients who are discovered with ovarian tumor after many years since they have had neurological manifestations. Therefore, after being discharged from the hospital, the patients should be examined at follow up visits to prevent recurrence. In addition, these patients should be checked for their fertility in the future.

In conclusion, Anti-NMDA-R encephalitis can be defined as a diverse syndrome with a broad differential diagnosis, disease manifestations often change but the disease responds quickly if it is treated in the right direction. Definitive diagnosis is confirmed when anti – NMDA-R antibodies are determined in the blood or cerebrospinal fluid [7]. In order to have prompt diagnosis and management, the awareness and communication between medical professionals from the various specialties are necessary, the gynecologists have an important role to make the patients have positive outcome, not only treat the disease by removing the ovarian tumors but also preserve the reproductive function for patients.

Ethical Approval

All procedures performed in studies involving human participants were in accordance with the ethical standards of the institutional and / or national research committee and with the 1964 Helsinki declaration and its later amendments or comparable ethical standards. The reports were approved by the Ethics Committee of Bach Mai hospital.

Informed Consent

The patients and their families agreed to provide the information, the images in writing/publishing this article.

References

1. Day GS, et al. Anti-NMDA-receptor encephalitis: case report and literature review of an under-recognized condition. Journal of general internal medicine. 2011; 26(7):811-816. https://doi.org/10.1007/s11606-011-1641-9 PMid:21318640 PMCid:PMC3138579

2. Dalmau J, et al. Anti-NMDA-receptor encephalitis: case series and analysis of the effects of antibodies. The Lancet. Neurology. 2008; 7(12):1091-1098. https://doi.org/10.1016/S1474-4422(08)70224-2

3. Dalmau J, et al. Clinical experience and laboratory investigations in patients with anti-NMDAR encephalitis. The Lancet. Neurology. 2011; 10(1):63-74. https://doi.org/10.1016/S1474-4422(10)70253-2

4. Uchino A, et al. Pseudo-piano playing motions and nocturnal hypoventilation in anti-NMDA receptor encephalitis: response to prompt tumor removal and immunotherapy. Internal medicine. 2011; 50(6):627-630. https://doi.org/10.2169/internalmedicine.50.4764 PMid:21422691 PMCid:PMC3740121

5. Shimazaki H, et al. Reversible limbic encephalitis with antibodies against the membranes of neurones of the hippocampus. Journal of neurology, neurosurgery, and psychiatry. 2007; 78(3):324-325. https://doi.org/10.1136/jnnp.2006.104513 PMid:17308294 PMCid:PMC2117656

6. Wong D, Fries B. Anti-NMDAR encephalitis, a mimicker of acute infectious encephalitis and a review of the literature. IDCases. 2014; 1(4):66-67. https://doi.org/10.1016/j.idcr.2014.08.003 PMid:26839775 PMCid:PMC4735025

7. Titulaer M. Treatment and prognostic factors for long-term outcome in patients with anti-NMDA receptor encephalitis: an observational cohort study. Lancet Neurol. 2013; 12(2):157-165. https://doi.org/10.1016/S1474-4422(12)70310-1

8. Mann A, Grebenciucova E, Lukas R. Anti- N-methyl-D-aspartate receptor encephalitis: diagnosis, optimal management, and challenges. Ther. Clin. Risk Manag. 2014; 10:517-525. https://doi.org/10.2147/TCRM.S61967 PMid:25061311 PMCid:PMC4085332

ID Design Press, Skopje, Republic of Macedonia
Open Access Macedonian Journal of Medical Sciences. 2019 Dec 30; 7(24):4383-4388.
https://doi.org/10.3889/oamjms.2019.840
eISSN: 1857-9655
Basic and Clinical Medical Researches in Vietnam

Short Tandem Repeats Used in Preimplantation Genetic Testing of B-Thalassemia: Genetic Polymorphisms For 15 Linked Loci in the Vietnamese Population

Dang Tien Truong[1], Ngo Van Nhat Minh[1], Dinh Phuong Nhung[1], Hoang Van Luong[1], Do Quyet[1], Tran Ngoc Anh[1], Trinh The Son[1], Nguyen Thanh Tung[1], Nguyen Thi Thu Ha[2], Duong Thi Phuong Anh[3], Le Hoang[3], Nguyen Le Thuy[3], Nguyen Thi Hoa[3], Nguyen Duy Bac[1], Vu Thi Nga[4], Toi Chu Dinh[5*]

[1]Vietnam Military Medical University, Hanoi, Vietnam; [2]National Institute of Hematology and Blood Transfusion, Hanoi, Vietnam; [3]Tam Anh General Hospital, Hanoi, Vietnam; [4]Institute for Research and Development, Duy Tan University, Danang, Vietnam; [5]Department of Human and Animal Physiology, Faculty of Biology, Hanoi National University of Education, Hanoi, Vietnam

Citation: Truong DT, Minh NVN, Nhung DP, Luong HV, Quyet D, Anh TN, Son TT, Tung NT, Ha NTT, Anh DTP, Hoang L, Thuy NL, Hoa NT, Bac ND, Nga VT, Chu Dinh T. Short Tandem Repeats Used in Preimplantation Genetic Testing of B-Thalassemia: Genetic Polymorphisms For 15 Linked Loci in the Vietnamese Population. Open Access Maced J Med Sci. 2019 Dec 30; 7(24):4383-4388.
https://doi.org/10.3889/oamjms.2019.840

Keywords: Preimplantation genetic testing (PGT); β-thalassemia; Short tandem repeat (STRs); Microsatellite markers

***Correspondence:** Toi Chu Dinh. Department of Human and Animal Physiology, Faculty of Biology, Hanoi National University of Education. E-mail: chudinhtoi@hnue.edu.vn

Received: 25-Sep-2019; **Revised:** 20-Nov-2019; **Accepted:** 21-Nov-2019; **Online first:** 20-Dec-2019

Funding: This research did not receive any financial support

Competing Interests: The authors have declared that no competing interests exist

Abstract

BACKGROUND: β-thalassemia is one of the most common monogenic diseases worldwide. Preimplantation genetic testing (PGT) of β-thalassemia is performed to avoid affected pregnancies has become increasingly popular worldwide. In which, the indirect analysis using short tandem repeat (STRs) linking with HBB gene to detect different β-globin (HBB) gene mutation is a simple, accurate, economical and also provides additional control of contamination and allele-drop-out ADO.

AIM: This study established microsatellite markers for PGT of Vietnamese β-thalassemia patient.

METHODS: Fifteen (15) STRs gathered from 5 populations were identified by in silico tools within 1 Mb flanking the HBB gene. The multiplex PCR reaction was optimized and performed on 106 DNA samples from at-risk families.

RESULTS: After estimating, PIC values were ≥ 0.7 for all markers, with expected heterozygosity and observed heterozygosity values ranged from 0.81 to 0.92 and 0.53 to 0.86, respectively. One hundred percent of individuals had at least seven heterozygous markers and were found to be heterozygous for at least two markers on either side of the HBB gene.

CONCLUSION: In general, a pentadecaplex marker (all < 1 Mb from the HBB gene) assay was constituted for β-thalassemia PGT on Vietnamese population.

Introduction

β-Thalassemia is one of the most common monogenic diseases, accounting for 1.5% of the population [1], concentrated in Central and Southern Asia, the Middle East, Northern Africa and the Mediterranean including Vietnam with the carrier. *HBB* mutations have more than 200 different types which have been knowns [2] lead to insufficient β-globin synthesis. The frequency of Vietnamese carriers ranged from 1.5 to 25.0% depending on ethnic group [3], [4], [5]. PGT-M (Preimplantation genetic testing for monogenic disease) promises to prevent monogenic disease in children born to at-risk couples by avoiding transferring mutation embryos to women *in vitro* fertilization. In which, PGT-M for β-Thalassemia has become the most common application among monogenic disorders.

There have been various studies that established direct or indirect PGT procedure for β-Thalassemia. Among numerous techniques, microsatellite markers such as STRs have provided many advantages in the indirect analysis. STRs are the repetitive DNA fragments of 2-6 bp which structure is highly conservative, inherited through generations and characteristic for each individual. The STRs is also highly diverse and can be amplified by PCR.

Thus, microsatellite markers linking with *HBB* gene has played an essential role in linkage analysis for β-Thalassemia.

Currently, there have been many typical studies on indirect linkage-based PGT for β-thalassemia published in the world. Wen Wang (2009) combined the Nested-PCR method amplifying STR markers and minisequencing method on nine embryos and concluded five unaffected embryos for transferring [6]. Li Fan (2017) used STR markers to perform PGT on WGA products from 147 day-5 embryos and identified 24 non-mutations, 38 carriers, and 18 mutation embryos [7].

Nevertheless, these direct analysis methods have no probability of controlling contamination and ADO phenomenons, which are considered as the main reasons leading to misdiagnosis in PGT. Thus, β-Thalassemia with wide range of gene and variety of mutations is recommended applying with indirect analysis method. These methods were proved to be sensitive, accurate, reliable and rapid to control the pitfalls of PCR-based PGT, including PCR failure, contamination, and ADO.

Despite the preeminence of STRs, the limited number of researches and available markers for the Vietnamese population, this hampers their utility in linkage-based β-Thalassemia PGT. In this study, we developed a multi-marker panel consisting of 15 STRs for Vietnamese β-Thalassemia patients. The data suggested that the STRs set was qualified to perform PGT-M with high heterozygous values, number of heterozygous markers on each individual and the equal distribution of markers on either side of *HBB* gene.

Materials and methods

Control Samples for Method Optimization

One hundred six genomic DNA samples were extracted from blood and amniotic fluid of at-risk families at the Vietnam National Institute of Hematology and Blood Transfusion (NIHBT), Vietnam from 07/2016 to 6/2018. DNA was used either to pre-screen of microsatellite markers or to determine heterozygosity values of them.

Short tandem repeat

Initial selected STRs were identified based on the STR database and Tandem Repeat Finder provided by Gary Benson (http://tandem.bu.edu/trf/trf.html). DNA sequence within 1 Mb upstream and downstream of the *HBB* gene (11p15.4) (genome assembly GRCh37/hg19, Feb 2009, annotation) was extracted from the UCSC Genome Browser. Initial selection criteria for the STRs followed Machado 2009 [8]. The first microsatellite markers were subsequently compared and selected for Vietnamese population based on report from populations of Malaysia, China, and India [9]. Primers were designed by Primer3 Tool. UCSC In-silico PCR with downloaded reference DNA sequence (genome assembly GRCh37/hg19, Feb 2009, annotation) and BLAST from NCBI were used to determine and exclude the primer complementing with Alu and non-specific sequences.

DNA Extraction

DNA was extracted from blood or amniotic fluid by Blood DNA Extraction QIAamp® DNA Mini Kit (Cat No./ID: 51304, QIAGEN) following the optimal instruction from QIAGEN Producer. Purified DNA was qualified and quantified by *NanoDrop One* Spectrophotometer with criteria: OD A260/A280 between 1.7-2.0 and concentration above 10 ng/µl.

PCR amplification

Single PCR: Followed T_m of 15 primers on http://www.operon.com/tools/oligo-analysis-tool.aspx, determined the average theoretical annealing temperature of these 15 primer pairs which is 60°C. Thus, PCR single primer was conducted according to the temperature range set at 55°C-60°C-65°C, and products were analyzed on the agarose gel. Single PCR amplification was performed in a 50 µL reaction volume consisting of 2 µL genomic DNA (concentration: 10-20 ng/µL), 25 µL 2X QIAGEN Multiplex Master Mix, and 0.2 µM of each primer (Table 1). Thermal cycling involved an initial 15 minutes enzyme activation at 95°C, 30 cycles of denaturation at 95°C for 30 seconds, annealing at 60°C for 1 minute 30 seconds, and extension at 72°C for one minute, and a final extension at 60°C for 30 minutes.

Table 1: Singleplex PCR components (Total volume: 50 µL)

Component	Concentrattion	Volume (µL/tube)
HPLC H_2O		21
2X QIAGEN Multiplex MasterMix	1 X	25
Forward primer	0.2 µM	1
Reverse primer	0.2 µM	1
DNA template		2

Multplex PCR optimization

Multiplex PCR was performed at optimal annealing temperature and primer concentrations initially keeping at the same concentration of 0.2 µM. Then, each primer concentration was adjusted based on product signal strength by increasing or decreasing 0.05 µM. The multiplex PCR amplification was performed in 50 µl reaction consisted of 1X QIAGEN Multiplex PCR Master Mix, 0.05-0.4 µM of each primer and 100 ng DNA template; followed the protocol: an

initial 15 min enzyme activation at 95°C, 30 cycles of denaturation at 95°C for 30 seconds, annealing at 60°C for 1 min 30 s at the first cycle and 6 additional seconds for every next cycle, and extension at 72°C for 1 min.

Capillary electrophoresis

The PCR products were fluorescently labeled in a 20 µL mixture consisted of 1X QIAGEN Multiplex MasterMix, 0.2 µM each fluorescent primer with M13 sequences as in Table 2, following cycling condition: an initial denaturation step at 95°C for 15 min, followed by 5cycles of denaturation at 98°C for 45 s, annealing at 60°C for 1 min, and extension at 72°C for 1 min, and a final extension at 72°C for 5 min.

One µL aliquot of fluorescent PCR product was mixed with 8.5 µL of Hi-Di Formamide (Applied Biosystems, Foster City, CA, USA) and 0.5 µL of GeneScan 500 LIZ size standard, denatured at 95°C for 5 minutes, cooled to 4°C, and resolved in ABI 3130XL Fragment Analyzer (Applied Biosystems). Post-electrophoresis analysis was performed using GeneMapper 5.0 software (Applied Biosystems).

Statistical analysis

Allele frequency, PIC, expected heterozygosity (He) and Observed Heterozygosity (Ho) of the 15 microsatellite markers were calculated using Microsoft Excel.

Results

Identification of STR

Fifteen (15) STRs were identified within 1 Mb around the *HBB* gene (6 upstream STRs and nine downstream STRs) (Table 2). HBB4506 located farthest to HBB gene (0.74 Mb) and all other markers were comparatively closer. Thus, all STRs had high linkage to the HBB gene.

Table 2: Information on initial selected STR

No.	STR	Repeat	Size (bp)	Location with HBB gene
1	HBB4506	(AC) n	366-398	Downstream
2	D11S988	(TG) n	103-147	Downstream
3	HBB4677	(AC) n	172-214	Downstream
4	D11S2362	(AAT) n	87-123	Downstream
5	HBB5089	(AC) n	241-265	Downstream
6	D11S1243	(TG) n	220-256	Downstream
7	HBB5138	(AC) n	404-428	Downstream
8	HBB5178	(TG) n	158-192	Downstream
9	HBB5205	(AGAT) n	401-449	Downstream
10	D11S1760	(CA) n	195-241	Downstream
11	HBB5576	(AAGG) n	327-369	Upstream
12	HBB5655	(AC)n(AT) n	272-320	Upstream
13	HBB5820	(AC)n(AG) n	311-331	Upstream
14	HBB5859	(ATCT) n	375-417	Upstream
15	D11S1338	(AC) n	137-157	Upstream

Forward primer had an additional sequence for fluorescent primer M13 were shown in Table 3.

Table 3: Information of primers for STR amplification

STR	Primer	Sequence (5'-3')	T_m (°C)
HBB 4506	B1F*	GTAAAACGACGGCCAGTGGTTTGACATATCTGTGAG GAAG	71.9
	B1R	GTTTCAGCAAGTAAATAGGGCACTG	62.9
D11S988	B2F**	GGTTTTCCCAGTCACGACGGACAAGAGAAAGTTGAA CATACTG	72.3
	B2R	GTTTCCACCATTTAAGATGCCAATAAGC	63.2
HBB 4677	B3F*	GTAAAACGACGGCCAGTGTGTAAAAGGGCCTCTAAT CAG	72.1
	B3R	GTTTCACTGATATACAAATGGCAAAGTG	61.7
D11S236 2	B4F*	GTAAAACGACGGCCAGTGCTTCCCTRATCTGGAATG AACTC	73.2
	B4R	GGGTTTCCCAGTCCTTTTAC	60.4
HBB 5089	B5F**	GGTTTTCCCAGTCACGACCAATTTCCTTTTCTTCTCC CTATAC	71.4
	B5R	GTGAGTCTAGCATTTGTCTTGC	60.8
D11S124 3	B6F*	GTAAAACGACGGCCAGTGCTGCCCTAATTCTGTCTAC C	73.3
	B6R	GTTGTGCACYATGAAGATACAC	59.9
HBB 5138	B7F*	GTAAAACGACGGCCAGTGAGAAATGTCCTTTAGAGA AATACCTTC	71.1
	B7R	GTGGAGAGGAATCTRTTACTG	59.6
HBB 5178	B8F**	GGTTTTCCCAGTCACGACCGTAATTGCTTTCAGTACC ATTTATG	71.2
	B8R	GATGTATTCGTCAACAGATAAATGG	59.7
HBB 5205	B9F**	GGTTTTCCCAGTCACGACCCAGGGTAGGTGACATAT AC	73.3
	B9R	GTAACTCAAAAAATGGGACCCAAAC	61.3
D11S176 0	B10F**	GGTTTTCCCAGTCACGACACCCTGAGTGTCTTCAAAA CTC	72.9
	B10R	GTTTCCAAKACTGCTGCATCATGAC	63.8
HBB 5576	B11F**	GGTTTTCCCAGTCACGACTCCTTCAGGTAAGAAGGA GC	73.3
	B11R	CTTGAAGAGGCTAGGTGC	59.9
HBB 5655	B12F**	GGTTTTCCCAGTCACGACTCATTGTTTTGGTAGGTAC TGAAAG	71.4
	B12R	AGTTGTAGTAAGTTTGTCAGGCTA	59.4
HBB 5820	B13F*	GTAAAACGACGGCCAGTGCTGAGATTATTTATACAGC AACACTTG	71.1
	B13R	GTTTCCAGTTATTGGTTGCTTTAGATTAC	63.3
HBB 5859	B14F**	GGTTTTCCCAGTCACGACCTGTCTATTTCATCTGTCA GCTTC	72.5
	B14R	GTTTAAAGTGTTGGCGTGAGC	60.6
D11S133 8	B15F*	GTAAAACGACGGCCAGTGAAGGACACACAGATTCAC TTAAAG	71.5
	B15R	GCTACTTATTTGGAGTGTGAATTTC	59.7
	T_m means		66.6

* Primer fluorescently labeled with HEX; ** Primer fluorescently labeled with FAM.

Multiplex PCR Optimization

Annealing temperature (T_a) and primer concentration optimization were performed. The results of T_a optimization of 15 primer were shown in Figure 1.

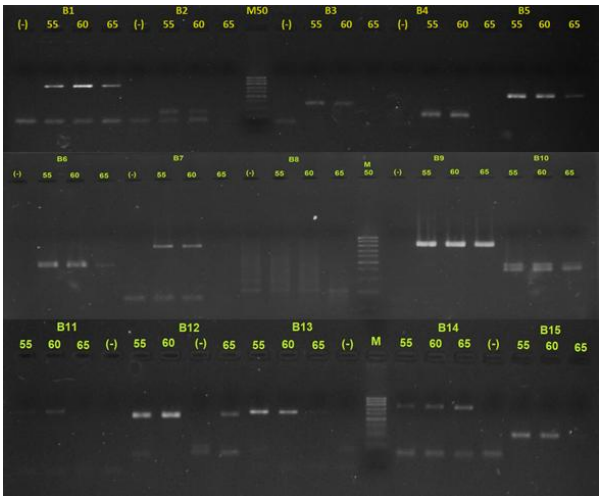

Figure 1: Annealing temperature optimization of 15 STRs. Annealing temperature at 60°C gave clear bands and most uniform signal. The products were electrophoresed on 1% agarose gel, at 120V for 30 minutes. The 10 µl sample was each well

The optimal annealing temperature showed clear bands and fair signals for all 15 primers (Figure 1). We finally concluded that 60°C was the optimal annealing temperature.

After adjusting primer concentrations (0.05-0.4 µM), optimal Multiplex PCR gave clear peaks. The PCR products were fluorescently labeled for capillary electrophoresis (Figure 2).

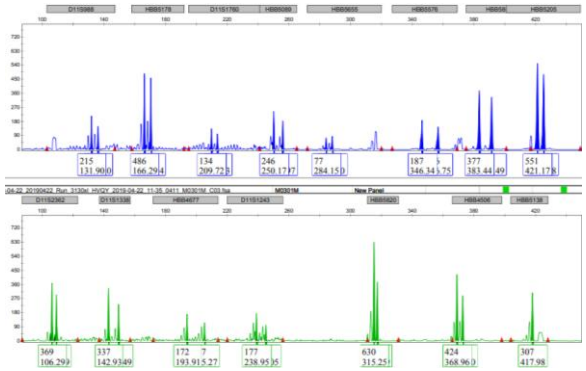

Figure 2: Representative electropherogram of multiplex PCR product after optimization

Polymorphism evaluation

To determine the polymorphism and informativeness of the 15 markers, the allele frequencies, PIC, He, and Ho values of each marker were calculated. Most STRs sequences were successfully amplified in all individuals except D11S1760 (84/106) and HBB5655 (81/106) caused by PCR Failure.

In summary, 270 alleles were observed with 11-28 alleles per marker. Allele frequency ranged from 0.0047 to 0.3255 (Table 4). All marker had PIC values of ≥ 0.7 and among these markers ranged, HBB5178 showed the lowest polymorphism (0.79), and D11S1760 showed the highest polymorphism (0.91).

The data showed that *He* values ranged from 0.81 (HBB5138) to 0.92 (D11S1760), and all markers had *Ho* values of ≥ 0.5, guaranteeing high polymorphic information. The *Ho* values of markers ranged from 0.53 (HBB5655)-0.86 (HBB5205). Thus, HBB5205 was the most informative marker, while HBB5655 was the least informative marker. Furthermore, the number of heterozygous markers of each individual was also counted.

Data showed 100% of individuals had at least seven heterozygous markers (Figure 4). Also, all were observed to be heterozygous for at least two markers on either side of the *HBB* gene (Figure 5). Based on the results, all 15 markers are high in polymorphism and informativeness for the Vietnamese population.

Table 4: Distribution of observed allele frequencies of 15 microsatellite markers

HBB4506		D11S988		HBB4677		D11S2362		HBB5089	
Allele	Frequency	Allele	Frequency	Allele	Frequency	Allele	Frequency	Allele	Frequency
364	0.0094	115	0.0472	173	0.0047	99	0.0048	242	0.0142
369	0.0283	116	0.0236	179	0.0047	101	0.0095	243	0.0425
371	0.0566	120	0.0047	183	0.0283	103	0.0095	244	0.0189
372	0.0047	121	0.0142	184	0.0047	104	0.0429	248	0.0142
373	0.1651	122	0.0283	185	0.2123	105	0.0048	249	0.0236
375	0.0755	123	0.0189	186	0.0283	106	0.1095	250	0.0991
376	0.0047	124	0.2783	187	0.0047	107	0.2048	251	0.1321
377	0.0094	125	0.0142	188	0.0047	108	0.0048	252	0.0519
380	0.1651	126	0.1038	190	0.0142	109	0.219	253	0.0142
381	0.1462	128	0.1274	191	0.0047	110	0.0857	254	0.0472
382	0.066	129	0.0047	192	0.0094	111	0.0095	255	0.0896
383	0.0425	130	0.0472	193	0.0189	112	0.1	256	0.1274
384	0.1509	131	0.0094	194	0.1085	113	0.1095	257	0.283
385	0.0142	132	0.033	195	0.1179	114	0.0095	258	0.0142
386	0.0142	134	0.0189	196	0.0236	115	0.019	259	0.0094
387	0.0047	136	0.0613	197	0.0236	116	0.0286	260	0.0189
388	0.0377	137	0.1132	198	0.0047	118	0.0048	242	0.0142
390	0.0047	138	0.0189	200	0.0189	119	0.0143	243	0.0425
		139	0.0189	201	0.0047	121	0.0095	244	0.0189
		140	0.0047	203	0.0189				
		141	0.0047	204	0.0755				
		143	0.0047	205	0.0566				
				206	0.1321				
				207	0.0472				
				208	0.0047				
				210	0.0142				
				212	0.0047				
				213	0.0047				

D11S1243		HBB5138		HBB5178		HBB5205		D11S1760	
Allele	Frequency	Allele	Frequency	Allele	Frequency	Allele	Frequency	Allele	Frequency
224	0.0047	404	0.0802	164	0.1557	392	0.0047	201	0.0833
235	0.0047	405	0.3208	165	0.1698	409	0.0047	202	0.0476
236	0.0094	406	0.0142	166	0.1179	413	0.0094	203	0.0893
237	0.0094	414	0.0189	167	0.1274	417	0.0802	204	0.0179
238	0.0283	415	0.0047	168	0.0094	418	0.0047	205	0.0476
239	0.0943	416	0.0047	169	0.0142	420	0.0047	206	0.0119
240	0.1415	417	0.0189	170	0.0377	421	0.2311	210	0.1607
241	0.0189	418	0.184	171	0.3255	422	0.0142	211	0.0476
242	0.1651	419	0.1557	172	0.0189	425	0.2358	213	0.006
243	0.1085	420	0.1368	173	0.0094	426	0.0047	214	0.119
244	0.2406	421	0.033	177	0.0047	429	0.2217	215	0.0417
245	0.033	422	0.0142	181	0.0047	430	0.0189	216	0.0238
246	0.066	423	0.0094	183	0.0047	431	0.0283	217	0.006
247	0.0189	424	0.0047			433	0.066	218	0.0893
248	0.0283					435	0.0472	219	0.0357
249	0.0047					437	0.0094	221	0.006
250	0.0189					439	0.0047	222	0.0238
254	0.0047					440	0.0047	226	0.006
						442	0.0047	227	0.0298
								228	0.0714
								230	0.0119
								231	0.0119
								277	0.0119

HBB5576		HBB5655		HBB5820		HBB5859		D11S1338	
Allele	Frequency	Allele	Frequency	Allele	Frequency	Allele	Frequency	Allele	Frequency
330	0.0047	283	0.0123	294	0.0047	374	0.0047	142	0.0047
338	0.0047	284	0.0988	313	0.0047	383	0.283	143	0.1651
339	0.0047	285	0.1049	315	0.1179	384	0.1604	144	0.1274
340	0.0283	286	0.0556	316	0.0991	387	0.0755	145	0.0142
341	0.0094	287	0.0123	317	0.2877	388	0.0472	146	0.0236
342	0.0425	288	0.0679	318	0.0472	391	0.0991	147	0.0047
343	0.1368	289	0.179	319	0.1038	392	0.1226	149	0.033
344	0.0708	290	0.1543	320	0.0094	395	0.0236	150	0.217
345	0.0425	291	0.0247	321	0.0189	396	0.1274	151	0.0377
346	0.0472	292	0.0494	323	0.0047	397	0.0094	152	0.2311
347	0.1415	293	0.0247	324	0.0377	400	0.0472	153	0.0943
348	0.0142	294	0.037	325	0.0472			154	0.033
349	0.0142	315	0.0247	326	0.0142			156	0.0094
350	0.2217	316	0.0864	327	0.0094			157	0.0047
351	0.0047	318	0.0617	328	0.0236				
352	0.0142	325	0.0062	329	0.1274				
353	0.1179			330	0.0283				
354	0.0377			331	0.0094				
357	0.0377			333	0.0047				
360	0.0047								

In general, the study had established a high polymorphic STR panel and relatively close with HBB gene. The panel should be potential to perform PGT for β-thalassemia

Table 5: Observed Heterozygosity, Expected Heterozygous and Polymorphic Information Content values of 15 STRs

Order	Markers	Heterozygous	Total	H_o	He	PIC
1	HBB4506	84	106	0.79	0.883	0.872
2	D11S988	87	106	0.82	0.87	0.86
3	HBB4677	90	106	0.85	0.896	0.888
4	D11S2362	88	105	0.84	0.865	0.851
5	HBB5089	75	106	0.71	0.859	0.847
6	D11S1243	86	106	0.81	0.866	0.853
7	HBB5138	59	106	0.56	0.811	0.789
8	HBB5178	67	106	0.63	0.809	0.785
9	HBB5205	91	106	0.86	0.827	0.805
10	D11S1760	53	84	0.63	0.919	0.914
11	HBB5576	83	106	0.78	0.883	0.873
12	HBB5655	43	81	0.53	0.898	0.89
13	HBB5820	70	106	0.66	0.858	0.846
14	HBB5859	85	106	0.80	0.842	0.825
15	D11S1338	68	106	0.64	0.843	0.824

Discussion

For many years, despite medical advances, the treatment of a β-Thalassemia patient still confronts many obstacles because it is impossible to completely treat the disease. Along with the treatment of individuals with β-Thalassemia, the application of PGT-M to help at-risk couples of having healthy babies is an extensively studied field.

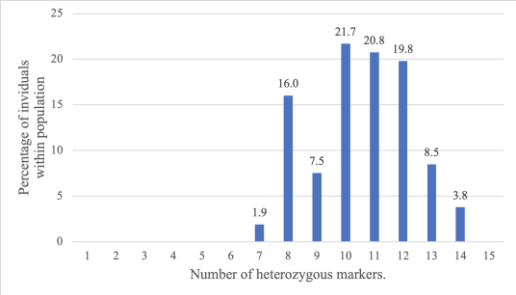

Figure 4: Percentage of individuals for number of heterozygous markers

Direct techniques have been commonly applied in diagnosis. However, for a wide gene such as HBB with a various kind of mutations, direct methods may be ineffective when using Multiplex PCR to simultaneously amplify many mutation sequences, and indirect techniques applying microsatellite markers should be the only option for this situation.

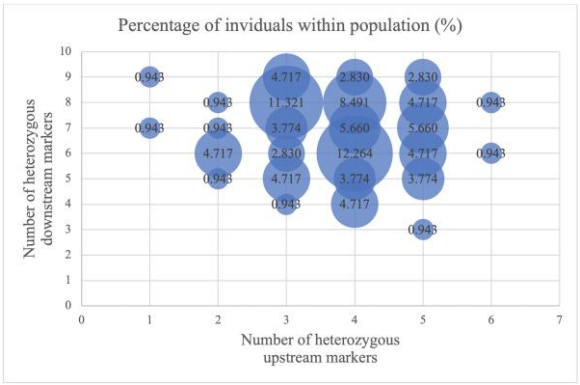

Figure 5: Percentage of individuals heterozygous for different numbers of upstream and downstream flanking microsatellite markers (n = 106)

The application of both direct and indirect techniques will increase the accuracy of the diagnosis. Therefore, linked markers play an essential role in PGT-M β-Thalassemia disease. There have been many studies of microsatellite markers [10], [11], [12], [13], [14], [15], [16], [17], but the number of STRs is still limited, so the detection of new STRs and surveys on different populations are crucial.

In this study, we developed a linked-marker set consisting of 15 STRs used for PGT-M of Vietnamese β-Thalassemia patients. Fifteen published STR located < 1 Mb distance from *HBB* were successfully amplified in one PCR amplification on Vietnamese at-risk individuals with high results in Ho, He and PIC estimation. We observed that 100% individuals were heterozygous for at least 7 of the 15 markers and at least 2 of these heterozygous markers were on either side of *HBB* gene, reliably proving the high polymorphism and informativeness of them in most if not all Vietnamese β-Thalassemia cases.

The studied STRs panel was first established and researched on five populations by Cheng [9]. Our data on Vietnamese cases were consistent with their result and replicated the previous result in the Vietnamese Population Beside the PCR failure happening with D11S1760 (84/106) and HBB5655 (81/106), other STRs were successfully amplified with no contamination and ADO phenomenons. Most previous PGT-M on β-Thalassemia cases included nested-multiplex PCR, however by combining 15 microsatellite markers into a standard multiplex PCR reaction, nested PCR should be removed. For the lack of available published STRs on Vietnamese population, establishment of STR set that compatible with Vietnamese population contributed great support to decline the high rate of Vietnamese β-Thalassemia carriers.

STRs contained different polymorphism and informativeness, but all showed the high values of PIC, Ho, He proving their clinical application. Our method had high sensitivity and specificity along with sufficient contamination and ADO monitoring. Microsatellite markers became a reliable tool when using alone in indirect mutation detection or conjunction with direct mutation detection for more precise diagnosis. Besides, this method required highly trained staffs, accurate instrument, and optimal procedures. Therefore, a particular training program needs carrying out before performing this method.

In addition to the previous study from different populations, the STRs panel continuously showed tremendous potential when applying on various kinds of population. Thus, we suggest applying this STRs panel for PGT in clinical cases.

In conclusion, All 15 STR markers were polymorphic and informative with high Ho, He and PIC. At least 7 of 15 markers were informative for 106 studied individuals, and all were observed to be heterozygous for at least two markers on either side of the HBB gene. Thus, these STRs markerhave significant meaning when applied in PGT-M widely.

Authors' contributions

DTT, NVNM, DPN, HVL, DQ, TNA, TTS, NTT, NTTH, DTPA, NLT, HTH, LH and NDB designed and performed experiments, and collected data and

informed consents. DTT, NVNM, DPN, HVL, DQ, TNA, TTS, NTT, NTTH, DTPA, NLT, HTH, LH, NDB, VTN and DTC analyzed and interpreted the results, and edited and corrected the manuscript. DTT, NVNM, VTN and DTC wrote the manuscript. All authors approved the final manuscript.

Ethical approval

This study is approved by the ethics committee of the Tam Anh General Hospital on 21 April 2018 following the Decision No 59/QĐ/BĐKTA by the director of the Tam Anh General Hospital about the establishment of the ethical committee.

Informed consent

The informed consents were signed by patients and their male partners

References

1. Higgs DR, Engel JD, Stamatoyannopoulos G. Thalassaemia. The lancet. 2012; 379(9813):373-383. https://doi.org/10.1016/S0140-6736(11)60283-3

2. Giardine B, et al. Updates of the HbVar database of human hemoglobin variants and thalassemia mutations. Nucleic Acids Res. 2013; 42(D1):D1063-D1069. https://doi.org/10.1093/nar/gkt911 PMid:24137000 PMCid:PMC3964999

3. Khanh N. The frequency of hemoglobinopathies in Vietnam. Vietnamese J Med. 1993; 8(174):11-16.

4. Fucharoen S, Winichagoon P. Hemoglobinopathies in Southeast Asia: molecular biology and clinical medicine. Hemoglobin. 1997; 21(4):299-319. https://doi.org/10.3109/03630269709000664 PMid:9255610

5. Bowman JE, editor. Distribution and Evolution of Hemoglobin and Globin Loci: Proceedings of the Fourth Annual Comprehensive Sickle Cell Center Symposium on the Distribution and Evolution of Hemoglobin and Globin Loci at the University of Chicago, Chicago, Illinois, USA, October 10-12, 1982. Elsevier Publishing Company; 1983.

6. Yap C, et al. First successful preimplantation genetic diagnosis in Singapore-avoidance of beta-thalassaemia major. Ann Acad Med Singapore. 2009; 38(8):720-3.

7. Fan L, et al. Genetic diagnosis of beta-thalassemia preimplantation using short tandem repeats in human cryopreserved blastocysts. International Journal of Clinical and Experimental Pathology. 2017; 10(7):7586-7595.

8. Machado F, Medina-Acosta E. High-resolution combined linkage physical map of short tandem repeat loci on human chromosome band Xq28 for indirect haemophilia A carrier detection. Haemophilia. 2009; 15(1):297-308. https://doi.org/10.1111/j.1365-2516.2008.01866.x PMid:18752533

9. Chen M, et al. Identification of novel microsatellite markers< 1 Mb from the HBB gene and development of a single-tube pentadecaplex PCR panel of highly polymorphic markers for preimplantation genetic diagnosis of beta-thalassemia. Electrophoresis. 2015; 36(23):2914-2924. https://doi.org/10.1002/elps.201500146 PMid:26331357

10. Rechitsky S, et al. Reliability of preimplantation diagnosis for single gene disorders. Molecular Cellular Endocrinology. 2001; 183:S65-S68. https://doi.org/10.1016/S0303-7207(01)00576-7

11. Rechitsky S, et al. Preimplantation genetic diagnosis with HLA matching. Reproductive BioMedicine Online. 2004; 9(2):210-221. https://doi.org/10.1016/S1472-6483(10)62132-3

12. Fiorentino F, et al. Short tandem repeats haplotyping of the HLA region in preimplantation HLA matching. European Journal of Human Genetics. 2005; 13(8):953. https://doi.org/10.1038/sj.ejhg.5201435 PMid:15886713

13. Kuliev A, et al. Preimplantation diagnosis and HLA typing for haemoglobin disorders. Reproductive BioMedicine Online. 2005; 11(3):362-370. https://doi.org/10.1016/S1472-6483(10)60845-0

14. Fiorentino F, et al. Strategies and clinical outcome of 250 cycles of preimplantation genetic diagnosis for single gene disorders. Human Reproduction., 2005; 21(3):670-684. https://doi.org/10.1093/humrep/dei382 PMid:16311287

15. Kuliev A, et al. Preimplantation genetic diagnosis for hemoglobinopathies. Hemoglobin. 2011; 35(5-6):547-555. https://doi.org/10.3109/03630269.2011.608457 PMid:21910603

16. Zachaki S, et al. Novel and known microsatellite markers within the β-globin cluster to support robust preimplantation genetic diagnosis of β-thalassemia and sickle cell syndromes. Hemoglobin. 2011; 35(1):56-66. https://doi.org/10.3109/03630269.2010.544620 PMid:21250882

17. Durmaz B, et al. Genotyping of β-Globin Gene Mutations in Single Lymphocytes: A Preliminary Study for Preimplantation Genetic Diagnosis of Monogenic Disorders. Hemoglobin. 2012; 36(3):230-243. https://doi.org/10.3109/03630269.2012.675891 PMid:22524255

ID Design Press, Skopje, Republic of Macedonia
Open Access Macedonian Journal of Medical Sciences. 2019 Dec 30; 7(24):4389-4392.
https://doi.org/10.3889/oamjms.2019.841
eISSN: 1857-9655
Basic and Clinical Medical Researches in Vietnam

Lung Volume Reduction Surgery in Patients with Heterogenous Emphysema: Selecting Perspective

Nguyen Truong Giang[1], Trung Nguyen Ngoc[1*], Nguyen Van Nam[1], Nguyen Viet Nhung[2], Ta Ba Thang[3], Dong Khac Hung[3], Nguyen Duy Bac[4], Chu Dinh Toi[5], Pham Ngoc Hung[4, 6]

[1]Department of Cardiothoracic Surgery, Vietnam Military Medical University, Hanoi, Vietnam; [2]Vietnam National Lung Hospital, Hanoi, Vietnam; [3]Department of Pneumology, Vietnam Military Medical University, Hanoi, Vietnam; [4]Department of Training, Vietnam Military Medical University, Hanoi, Vietnam; [5]Department of Human and Animal Physiology, Faculty of Biology, Hanoi National University of Education, Hanoi, Vietnam; [6]Department of Epidemiology, Vietnam Military Medical University, Hanoi, Vietnam

Citation: Giang NT, Nguyen Ngoc T, Nam NV, Nhung NV, Thang TB, Hung DK, Bac ND, Toi CD, Hung PN. Lung Volume Reduction Surgery in Patients with Heterogenous Emphysema: Selecting Perspective. Open Access Maced J Med Sci. 2019 Dec 30; 7(24):4389-4392. https://doi.org/10.3889/oamjms.2019.841

Keywords: Lung volume reduction surgery (LVRS); Heterogenous emphysema; Selecting patient

***Correspondence:** Trung Nguyen Ngoc. Department of Cardiothoracic Surgery, Vietnam Military Medical University, Hanoi, Vietnam. E-mail: Ngoctrungbv103@yahoo.com

Received: 26-Sep-2019; **Revised:** 20-Nov-2019; **Accepted:** 21-Nov-2019; **Online first:** 20-Dec-2019

Funding: This research did not receive any financial support

Competing Interests: The authors have declared that no competing interests exist

Abstract

BACKGROUND: Lung volume reduction surgery (LVRS) was introduced to alleviate clinical conditions in selected patients with heterogenous emphysema. Clarifying the most suitable patients for LVRS remained unclear.

AIM: This study was undertaken to specifically analyze the preoperative factor affecting to LVRS.

METHODS: The prospective study was conducted at 103 Military Hospital between July 2014 and April 2016. Severe heterogenous emphysema patients were selected to participate in the study. The information, spirometry, and body plethysmographic pulmonary function tests in 31 patients who underwent LVRS were compared with postoperative outcomes (changing in FEV1 and CAT scale).

RESULTS: Of the 31 patients, there was statistically significant difference in the outcome of functional capacity, lung function between two groups (FEV1 ≤ 50% and > 50%) (∆FEV1: 22.46 vs 18.32%; p = 0.042. ∆CAT: 6.85 vs 5.07; p = 0.048). Changes of the FEV1 and CAT scale were no statistically significant differences in three groups residual volume. Patients with total lung capacity < 140% had more improved than others (∆FEV1: 23.81 vs 15.1%; p = 0.031).

CONCLUSION: Preoperative spirometry and body plethysmographic pulmonary function tests were useful measures to selected severe heterogenous emphysema patients for LVRS. Patients with FEV1 ≤ 50%, TLC in the range of 100-140% should be selected.

Introduction

Emphysema is an incurable with high prevalence in adults worldwide [1]. It has been treated according to the guideline of GOLD [1]. In severe emphysema, treatment included lung volume reduction (LVR) therapy in accordance with medical treatment to maximize clinically meaningful benefits [2]. Three common LVR therapies were surgery, endobronchial valve, endobronchial coil but each therapy was considered to feasible in selected patients [2]. LVR coil treatment for bilateral lung emphysema resulted in good safety and sustained outcomes with significant clinical improvements [3]. Endobronchial valves for intact interlobar fissures in emphysema improved significantly in lung function [4]. In severe emphysema with selected cases, LVRS has been showed good outcomes [5]. It was more widely used in the treatment of emphysema [6], [7] with selection criteria depended on characteristics of diseases and patients. In most series, LVRS was chosen for patients who had heterogenous emphysema with upper lobes occupying almost that present in about 25 percent of moderate-to-severe patients [8]. Thus, the benefit of LVRS did not generate to all patients. The reason behind this is that LVRS is suitable for selecting patients. It showed effective in patients with bilateral upper lobe heterogeneous emphysema but did not use for the

arbitrary patient [9]. The NETT study pointed out the condition that benefits for LVRS were heterogenous disease, low baseline exercise capacity, and upper lobe predominance [5]. Beyond the NETT selection criteria, more patients with different conditions also can be suitable for LVRS [10]. To get successful outcomes, patient selection and preoperation care were crucial [11].

Clarifying the most suitable patients for LVRS remained unclear. This study, therefore, was undertaken to specifically analyze the preoperative factor affecting to this surgery. This contributed to further refine the selection criteria when LVRS is performed for patients with severe heterogeneous emphysema.

Materials and Method

Patients

This prospective study was conducted at 103 Military Hospital between July 2014 and April 2016. Severe emphysema patients were selected to participate in the study. Patients had inclusion and no exclusion criteria underwent LVRS. Selecting criteria for LVRS showed in Table 1. Indications for LVRS included clinical symptom (severe dyspnea), spirometry (airflow obstruction), and image of emphysema (on chest radiography and computed tomographic (CT) scanning). Any history of childhood asthma/atopy, bronchiectasis, inhalation injury or drug-caused bronchiolitis was excluded from the study.

Table 1: Selecting criteria for LVRS

Inclusion criteria
Age 40-80 years
Severe, heterogeneous emphysema, at CT
Forced expiratory volume in one second ≤ 60% but > 20%
Residual volume ≥ 150%
Total lung capacity ≥ 100%
Resting room PaO2 > 45 mmHg
Quit smoking since at least 4 months

Evaluation before surgery

Six months before performing surgery, all patients stopped cigarettes and six-week before that, a pulmonary rehabilitation program for all patients was required. The final routine evaluation for surgery was managed without abnormal findings [12], [13], [14]. Patients had any contraindications to surgery at that time were excluded such as severe concurrent diseases, pleural scarring, pulmonary-artery hypertension or; using inappropriate glucocorticoids; and failure to complete the requirements above before surgery [5]. Dividing patients into two groups: group 1: 17 patients with FEV1 ≤ 50% before surgery and group 2: 14 patients with FEV1 > 50% before surgery.

Surgical Technique

Choosing a surgical technique depended on the condition of patients [15]. After placing lateral decubitus position, general anesthesia was used with provision for single-lung ventilation. Unilateral thoracoscopic surgery was performed in 6 patients and video-assisted thoracoscopic surgery (VATS) was performed in 25 patients to reduce lung volume. Approximately about 30% of the lung (estimating 30-40 grams) was resected (Figure 1).

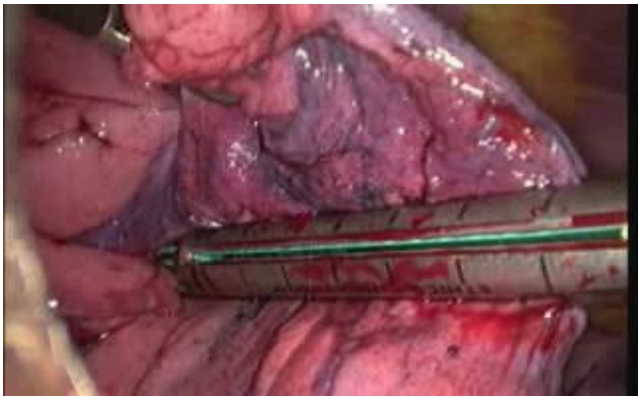

Figure 1: Lung resection in lung volume reduction surgery (LVRS)

Follow-up

Three months after surgery, change FEV1 and CAT scale were compared to evaluate the valuable index for LVRS.

Statistical Analysis

Using SPSS ver. 20.0 software (IBM Corporation, Armonk, NY, USA) to analyze. Descriptive analysis was presented as a means ± standard deviations. Using Student's paired t-test to compare with p-value that considered statistically significant was < 0.05.

Results

Patients' characteristics

Thirty-one patients participated in and completed the study. There were no hospital deaths in all group, no patient died three months after surgery. Preoperative patient's characteristics showed in Table 2. Functional capacity was assessed by the COPD Assessment Test scale (CAT). Spirometry demonstrated FEV1, TLC, and RV. All FEV1 values were less than normal with the mean was 49.46 percent and the lowest value was 23 percent. TLC was only minimally elevated with the value was more than 100 percent. Whereas RV was significantly elevated with patients, the value was more than 150

percent in all patients and the maximum value was 479 percent.

Table 2: Preoperative characteristics

Characteristics	Value
Age (years)	62.13 ± 5.77
Gender (M/F)	31 / 0
CAT scale	18.42 ± 5.57
Forced expiratory volume in one second (FEV1)	
Mean (%)	49.46 ± 12.22
≤ 50%	17
> 50%	14
Geansler index (%)	58.0 ± 11.93
Total lung capacity (TLC)	
Mean	137.29 ± 23.83
Range	106-227
Residual volume (RV)	
Mean	219.25 ± 72.14
Range	153-479

Postoperative outcome

After LVRS, FEV1 significantly increased as a whole. Two groups were compared before surgery and three months after surgery. Detail information showed in Table 3. Changes in FEV1 and CAT scale in group 1 was 22.46% and 6.85. Group 1 had more improved than group 2.

Table 3: Comparison between two groups

Variable	ΔFEV1 *Mean (95% CI)*	ΔCAT *Mean (95% CI)*
FEV1		
≤ 50%	22.46 (7.75 – 37.16)	6.85 (5.84 – 7.4)
> 50%	18.32 (7.55 – 29.10)	5.07 (3.36 – 6.77)
Significance	*p = 0.042*	*p = 0.048*
RV		
150-200%	19.81 (7.33 – 32.28)	5.3 (3.81 – 6.79)
200-250%	29.75 (8.87 – 50.64)	7 (5.11 – 8.88)
> 250%	16.37 (9.90 – 42.73)	6.4 (3.97 – 8.82)
Significance	*p = 0.123*	*p = 0.19*
TLC		
100 – 140%	23.81 (10.21 – 37.41)	5.76 (4.45 – 7.06)
> 140%	15.10 (7.23 – 22.97)	6.27 (4.68 – 7.86)
Significance	*p = 0.031*	*p = 0.6*

Patient with a preoperative RV less than 200%, the mean of change FEV1 was 19.81% and change of CAT scale was 5.3. The FEV1 increased 29.75% for patients with RV from 200 to 250% compared with 16.37% for patients with RV greater than 250% ($p > 0.05$). Preoperative, 10 patients had TLC than 100% and less than 140% of the predicted value. Their postoperative mean FEV1 increased by 23.81% compared with 15.10% changes in patients with preoperative TLC greater than 140% of the predicted value.

Discussion

LVRS showed more benefits in the patient with severe heterogeneous emphysema in terms of many clinical outcomes [16]. One of the key factors to achieve these benefits is selecting the right candidates for surgery. It includes general risk and the emphysema characteristics regarding morphology and function. From morphological perspectives, the diseased regions in emphysema were detected by computed tomography densitometry [17]. It helped to target and treat with segmental approach that was promise method to improve efficacy and safety outcomes.[18] But from functional perspectives, many questions for the selection of ideal candidates for LVRS remained unclear [19].

The core concept of LVRS is resecting non-functional areas to allow improving functional areas [20]. This is why it does not benefit in the case of patients who had airway obstruction. In our study, we reasoned that spirometry and body plethysmographic pulmonary function tests would be valuable factors in selecting patients for LVRS. In patients with highly airway resistance, the expiratory flow seems to not improving in response to LVRS [21], [22]. Vice versa, lung function improved when performing LVRS in patients with less airway resistance [23], [24], [25], [26]. In line with the lung function test, functional capacity assessed by CAT that presented the limitation of activity with moderate-to-severe level [27], [28]. It is valuable indicator to fully evaluate patients after LVRS.

In this study, the measures of clinical outcomes include changing in FEV1 and changing in CAT scale. After LVRS, the apparent improvement in FEV1 and CAT scale has improved quality of life, reduced dyspnea, and increased physical activities. The improvement in clinical outcomes following LVRS best correlates with the activity of respiratory muscle. Patients with FEV1 ≤ 50% have relatively severe obstruction. Meanwhile, patients with FEV1 > 50% of the degree of dyspnea and moderate obstruction, and the improvement was not as obvious as the FEV1 group under 50%. However, the patients who have too low FEV1 face a high risk of complications after surgery, especially those with FEV1 below 20% [29]. In addition, TLC is also a factor in recommending patients for LVRS. In our study, the results showed that TLC patients in the range of 100-140% given better postoperative results than patients with TLC above 140%. High TLC patients exhibit severe emphysema. With these patients, the lung parenchyma was less elastic, reducing perfusion, so LVRS recovery was also worse than that of the small TLC group. Our data showed that it was reasonable to perform LVRS on the patients with FEV1 ≤ 50 and TLC < 140 percent of the predicted value. These findings will optimize evaluating patients with heterogeneous emphysema who consider for LVRS.

In conclusion, preoperative spirometry and body plethysmographic pulmonary function tests were useful measures to selected severe heterogenous emphysema patients for LVRS. Patients with FEV1 ≤ 50%, TLC in the range of 100-140% should be selected.

Ethical approval

This study is approved by the ethics committee of 103 Military Hospital.

Informed consent

The consent and commitment were signed by the patients in the study.

References

1. Vogelmeier CF, et al. Global strategy for the diagnosis, management, and prevention of chronic obstructive lung disease 2017 report. GOLD executive summary. American journal of respiratory and critical care medicine. 2017; 195(5):557-582. https://doi.org/10.1164/rccm.201701-0218PP PMid:28128970

2. van Geffen WH, et al. Surgical and endoscopic interventions that reduce lung volume for emphysema: a systemic review and meta-analysis. Lancet Respir Med. 2019; 7(4):313-324. https://doi.org/10.1016/S2213-2600(18)30431-4

3. Deslee G, et al. Lung volume reduction coil treatment for patients with severe emphysema: a European multicentre trial. Thorax. 2014; 69(11):980-6. https://doi.org/10.1136/thoraxjnl-2014-205221 PMid:24891327 PMCid:PMC4215297

4. Davey C, et al. Bronchoscopic lung volume reduction with endobronchial valves for patients with heterogeneous emphysema and intact interlobar fissures (the BeLieVeR-HIFi study): a randomised controlled trial. Lancet. 2015; 386(9998):1066-73. https://doi.org/10.1016/S0140-6736(15)60001-0

5. National Emphysema Treatment Trial Research Group. A randomized trial comparing lung-volume-reduction surgery with medical therapy for severe emphysema. New England Journal of Medicine. 2003; 348(21):2059-73. https://doi.org/10.1056/NEJMoa030287 PMid:12759479

6. Sharafkhaneh A, Hanania NA, Kim V. Pathogenesis of emphysema: from the bench to the bedside. Proc Am Thorac Soc. 2008; 5(4):475-7. https://doi.org/10.1513/pats.200708-126ET PMid:18453358 PMCid:PMC2645322

7. Minai OA, Benditt J, Martinez FJ. Natural History of Emphysema. Proc Am Thorac Soc. 2008; 5(4):468-74. https://doi.org/10.1513/pats.200802-018ET PMid:18453357 PMCid:PMC2645321

8. Argenziano M, Ginsburg ME. Lung Volume Reduction Surgery. Totowa, New Jersey: Humana Press Inc., 2002. https://doi.org/10.1007/978-1-59259-121-3

9. McKenna Jr RJ, et al. Patient selection criteria for lung volume reduction surgery. J Thorac Cardiovasc Surg. 1997; 114(6):957-64; discussion 964-7. https://doi.org/10.1016/S0022-5223(97)70010-2

10. Caviezel C, et al. Lung volume reduction surgery beyond the NETT selection criteria. J Thorac Dis. 2018; 10(Suppl 23):S2748-s2753. https://doi.org/10.21037/jtd.2018.08.93 PMid:30210828 PMCid:PMC6129809

11. Seadler B, et al. Clinical and Quality of Life Outcomes After Lung Volume Reduction Surgery. Ann Thorac Surg. 2019; 108(3):866-872. https://doi.org/10.1016/j.athoracsur.2019.03.089 PMid:31055037

12. Eda S, et al. The relations between expiratory chest CT using helical CT and pulmonary function tests in emphysema. Am J Respir Crit Care Med. 1997; 155(4):1290-4. https://doi.org/10.1164/ajrccm.155.4.9105069 PMid:9105069

13. Sciurba FC. Preoperative predictors of outcome following lung volume reduction surgery. Thorax. 2002; 57(2):47-52.

14. Zoumot Z, et al. Lung Volume Reduction in Emphysema Improves Chest Wall Asynchrony. Chest. 2015; 148(1):185-95. https://doi.org/10.1378/chest.14-2380 PMid:25654309 PMCid:PMC4493874

15. DeCamp Jr MM, et al. Lung volume reduction surgery: technique, operative mortality, and morbidity. Proc Am Thorac Soc. 2008; 5(4):442-6. https://doi.org/10.1513/pats.200803-023ET PMid:18453353 PMCid:PMC2645317

16. Huang W, et al. Several clinical interests regarding lung volume reduction surgery for severe emphysema: meta-analysis and systematic review of randomized controlled trials. J Cardiothorac Surg. 2011; 6:148. https://doi.org/10.1186/1749-8090-6-148 PMid:22074613 PMCid:PMC3226652

17. Stolk J, et al. Densitometry for assessment of effect of lung volume reduction surgery for emphysema. Eur Respir J. 2007; 29(6):1138-43. https://doi.org/10.1183/09031936.00056206 PMid:17331971

18. Bandyopadhyay S, et al. Segmental approach to lung volume reduction therapy for emphysema patients. Respiration. 2015; 89(1):76-81. https://doi.org/10.1159/000369036 PMid:25500669

19. Russi EW, Bloch KE, Weder W. Functional and morphological heterogeneity of emphysema and its implication for selection of patients for lung volume reduction surgery. Eur Respir J. 1999; 14(1):230-6. https://doi.org/10.1034/j.1399-3003.1999.14a39.x PMid:10489857

20. Gelb AF, et al. Lung function 5 yr after lung volume reduction surgery for emphysema. Am J Respir Crit Care Med. 2001; 163(7):1562-6. https://doi.org/10.1164/ajrccm.163.7.2009048 PMid:11401874

21. Clark SJ, et al. Surgical approaches for lung volume reduction in emphysema. Clin Med. 2014; 14(2):122-7. https://doi.org/10.7861/clinmedicine.14-2-122 PMid:24715121 PMCid:PMC4953281

22. Criner GJ, et al. The National Emphysema Treatment Trial (NETT): Part II: Lessons Learned about Lung Volume Reduction Surgery. Am J Respir Crit Care Med. 2011; 184(8):881-93. https://doi.org/10.1164/rccm.201103-0455CI PMid:21719757 PMCid:PMC3208657

23. Criner GJ, et al. Effect of lung volume reduction surgery on resting pulmonary hemodynamics in severe emphysema. Am J Respir Crit Care Med. 2007; 176(3):253-60. https://doi.org/10.1164/rccm.200608-1114OC PMid:17496227 PMCid:PMC1994220

24. Daniel TM, et al. Lung volume reduction surgery. Case selection, operative technique, and clinical results. Ann Surg. 1996; 223(5):526-33. https://doi.org/10.1097/00000658-199605000-00008 PMid:8651743 PMCid:PMC1235175

25. DeCamp Jr MM, et al. The evaluation and preparation of the patient for lung volume reduction surgery. Proc Am Thorac Soc. 2008; 5(4):427-31. https://doi.org/10.1513/pats.200707-087ET PMid:18453350 PMCid:PMC2645314

26. Dong Khac Hung DK, Ta Ba Thang, Lung reduction therapy in management of chronic obstructive pulmonary disease. Hanoi, Medicine Publisher, 2015.

27. Lee SD, et al. The COPD assessment test (CAT) assists prediction of COPD exacerbations in high-risk patients. Respiratory Medicine. 2014; 108(4):600-608. https://doi.org/10.1016/j.rmed.2013.12.014 PMid:24456695

28. Ghobadi H, et al. The Relationship between COPD Assessment Test (CAT) Scores and Severity of Airflow Obstruction in Stable COPD Patients. Tanaffos. 2012; 11(2):22-6.

29. Fishman A, et al. Patients at high risk of death after lung-volume-reduction surgery. N Engl J Med. 2001; 345(15):1075-83. https://doi.org/10.1056/NEJMoa11798 PMid:11596586

ID Design Press, Skopje, Republic of Macedonia
Open Access Macedonian Journal of Medical Sciences. 2019 Dec 30; 7(24):4393-4398.
https://doi.org/10.3889/oamjms.2019.842
eISSN: 1857-9655
Basic and Clinical Medical Researches in Vietnam

Antibiotic Resistance Profile and Diversity of Subtypes Genes in *Escherichia coli* Causing Bloodstream Infection in Northern Vietnam

Pham Ngoc Hung[1, 2], Do Quyet[3], Kieu Chi Thanh[4], Dinh Cong Pho[5], Tran Viet Tien[6], Quan Anh Dung[5], Do Dieu Linh[7], Ha The Tan[1], Thien Chu Dinh[8], Nguyen Duy Bac[2], Le Van Nam[6*]

[1]Department of Epidemiology, Vietnam Military Medical University, Hanoi, Vietnam; [2]Department of Training, Vietnam Military Medical University, Hanoi, Vietnam; [3]Department of Tuberculosis and Lung Diseases, Military Hospital 103, Vietnam Military Medical University, Hanoi, Vietnam; [4]Department of Hospital Infection Control, Military Hospital 103, Vietnam Military Medical University, Hanoi, Vietnam; [5]Faculty of Medicine, Vietnam Military Medical University, Hanoi, Vietnam; [6]Department of Infectious Diseases, Military Hospital 103, Vietnam Military Medical University, Hanoi, Vietnam; [7]Faculty of Medicine, Hai Phong Medical University, 72A Nguyen Binh Khiem, Hai Phong, Vietnam; [8]Institute for Research and Development, Duy Tan University, 03 Quang Trung, Danang, Vietnam

Citation: Hung PN, Quyet D, Thanh KC, Pho DC, Tien TV, Dung QA, Linh DD, Tan HT, Chu Dinh T, Duy Bac N, Nam LV. Antibiotic Resistance Profile and Diversity of Subtypes Genes in *Escherichia coli* Causing Bloodstream Infection in Northern Vietnam. Open Access Maced J Med Sci. 2019 Dec 30; 7(24):4393-4398. https://doi.org/10.3889/oamjms.2019.842

Keywords: Antibiotic resistance; Escherichia coli (E. coli); ESBL-producing; BSIs (bloodstream infections)

***Correspondence:** Le Van Nam. Department of Infectious Diseases, Military Hospital 103, Vietnam Military Medical University. Hanoi, Vietnam. E-mail: drlenam103@gmail.com

Received: 28-Sep-2019; **Revised:** 20-Nov-2019; **Accepted:** 21-Nov-2019; **Online first:** 20-Dec-2019

Funding: This research did not receive any financial support

Competing Interests: The authors have declared that no competing interests exist

Abstract

BACKGROUND: Evaluating the antibiotic susceptibility and resistance genes is essential in the clinical management of bloodstream infections (BSIs). But there are still limited studies in Northern Vietnam.

AIM: The aim of the study was to determine the antibiotic resistance profile and characteristics of subtypes genes in *Escherichia coli* causing BSIs in Northern Vietnam.

METHODS: The cross-sectional study was done in the period from December 2012 to June 2014 in two tertiary hospitals in Northern Vietnam. Tests were performed at the lab of the hospital.

RESULTS: In 56 *E. coli* strains isolating 39.29 % produced ESBL. 100% of the isolates harbored *blaTEM* gene, but none of them had the *blaPER* gene. The prevalence of ESBL producers and ESBL non-producers in *blaCTX-M* gene was 81.82%, and 73.53%, in *blaSHV* gene was 18.18% and 35.29%. Sequencing results showed three *blaTEM* subtypes (*blaTEM* 1, 79, 82), four *blaCTX-M* subtypes (*blaCTX-M*-15, 73, 98, 161), and eight *blaSHV* subtypes (*blaSHV* 5, 7, 12, 15, 24, 33, 57, 77). Antibiotic resistance was higher in ampicillin (85.71%), trimethoprim/sulfamethoxazole (64.29%) and cephazolin (50%). Antibiotics were still highly susceptible including doripenem (96.43%), ertapenem (94.64%), amikacin (96.43%), and cefepime (89.29%).

CONCLUSION: In *Escherichia coli* causing BSIs, antibiotic resistance was higher in ampicillin, trimethoprim/sulfamethoxazole and cephazolin. Antibiotics was highly susceptible including doripenem, ertapenem, amikacin, and cefepime.

Introduction

Escherichia coli (*E. coli*) took the highest position in causative gram-negative bacterium from bloodstream infection (BSIs) patients in Asia region [1]. It led to severe infections with a high rate of shock and mortality [2]. Currently, the worldwide incidence of *E. coli* BSI is still increasing over time [3] with the overall incidence increased year on year [4] that suggested an increasing burden of disease [5]. The estimation of infections worldwide showed that third-generation cephalosporin-resistant *E. coli* and *K. pneumoniae* caused 6.4 million (interval estimate 3.5-9.2) BSIs and 50.1 million (27.5-72.8) serious infections in 2014[6]. In addition, it was difficult to treat because of the emergence of multi-drug resistance (MDR) of *E. coli* [7]. Thus, evaluating antibiotic susceptibility is essential to decide what types of antibiotics and what appropriate doses that improving treatment efficiency and minimizing the antibiotic resistance rate. Over 20 years, the susceptibility of *E. Coli* BSIs was alarmed with the prevalence of antimicrobial-resistant isolates was increased [8]. In these cases, the patients had a worse prognosis with partial effect on correct empirical treatment [9]. Antimicrobial resistance-related encoding gene in each *E. coli* strain. Extended-spectrum β-lactamases

(ESBLs) was one of the most important genes [10]. It minimized the antibiotic efficiency in treatment [11]. Besides, the ability of inter-transmission within different *E. Coli* strains and transmission between *E. Coli* and other bacteria led to the state of becoming widespread resistance genes around the world. It becomes public-health concern [12] with increasing burden and cost of hospital-acquired infections [13], [14].

In Vietnam, there was one study in Northern Vietnam showed 25.1% of ESBLs among *Enterobacteriaceae* causing BSIs [15] but there are still limited studies in Northern Vietnam. Thus, this study aims to determine the antibiotic resistance profile and characteristics of subtypes genes in *Escherichia coli* causing bloodstream infections in Northern Vietnam.

Materials and Methods

The cross-sectional study was done in the period from 12/2012 to 6/2014 in two tertiary hospitals in Northern Vietnam (National Hospital of Tropical Diseases and 103 Military Hospital). Isolating from hospitalized BSIs patients in two hospitals 56 *E. coli* strains were inoculated in BHI Broth with 20% glycerol after being identified at the labs of these two hospitals.

Antimicrobial susceptibility assessed through MIC test by VITEK®2 Compact (BioMérieux, France and provided by DEKA *Limited Liability Company)* standardized by CLSI [16]. Antibiotics which has been used are *were (with number coding - abbreviation):* amikacin (1-AK), ampicillin (2-AM), ceftazidime (3-CAZ), ciprofloxacin (4-CIP), ceftriaxone (5-CRO), cefazolin (6-CZ), doripenem (7-DOR), ertapenem (8-ETP), cefepime (9-FEP), gentamycin (10-GM), levofloxacin (11-LVX), ampicillin/sulbactam (12-SAM), trimethoprim/sulfamethoxazole (13-SXT), tobramycin (14-TM) , piperacillin/tazobactam (15-TZP).

Using QIAamp DNA Mini Kit (USA) for DNA extraction (including isolation and quantification), we performed the experimental procedure according to manufacturer's instruction. PCR amplification performed in PCR master mix (Invitrogen – USA) that consisted of 200 µM of each dNTPs (dATP, dCTP, dGTP, dTTP), 100 pM primers, 1 U Taq DNA polymerase, 10 mM Tris-HCl, 50 mM KCl, 1,5 mM $MgCl_2$ and 10 µl DNA template. Specific primers for bla_{TEM}, bla_{SHV}, bla_{CTX-M}, bla_{PER} genes showed in Table 1. The experiments were performed using the protocol with 30 cycles that each of them consisted of 3 steps including denaturing (95°C for 30 seconds), annealing (58, 57, 60, 54°C for 30 seconds), elongating (72°C for 1 minute). PCR products were performed electrophoresis, imaged routinely and sequenced. The sequence of PCR products was compared with the original gene's sequence on GenBank to confirm bla_{TEM}, bla_{SHV}, bla_{CTX-M} and bla_{PER} gene.

Table 1: Specific primers for blaTEM, blaSHV, blaCTX-M, blaPER genes

Target gene	Primer	Nucleotide sequence (5' – 3')	Size (bp)	AT (°C)
bla_{TEM}	TEM-F	5' – TGC GGT ATT ATC CCG TGT TG – 3'	300	52.2
	TEM-R	5' – TCG TCG TTT GGT ATG GCT TC – 3'		
bla_{SHV}	SHV-F	5' – TCT CCC TGT TAG CCA CCC TG – 3'	600	51.2
	SHV-R	5' – CCA CTG CAG CAG CTG C – 3'		
bla_{CTX-M}	CTX-M-F	5' – CGA TGT GCA GTA CCA GTA A – 3'	650	60
	CTX-M-R	5' – TTA GTG ACC AGA ATC AGC GG – 3'		
bla_{PER}	PER-F	5' – ATG AAT GTC ATT ATA AAA GC – 3'	933	
	PER-R	5' – TTA ATT TGG GCT TAG GGC AGA A – 3'		

Statistical Analysis

The statistical analysis was conducted using the R language [17]. Graphics also were performed by R language (version 3.5.2). The analysis of such enormous volumes of information in the acquisition of data from 56 strains, each strain companion with subtype genes (three bla_{TEM} subtypes, four bla_{CTX-M} subtypes, eight bla_{SHV} subtypes) and 15 antibiotics with 3 level of resistance (susceptible, intermediate, resistance). For this reason, we used R language to analyze.

Results

Clinical characteristics of the patient in this study showed in Table 2.

Table 2: Clinical characteristics of patients

Age (subgroup)	
16-19	0 (0)
20-29	8 (14.29)
30-39	3 (5.36)
40-49	9 (16.07)
50-59	17 (30.35)
≥ 60	19 (33.93)
Gender	
Male	37 (66.07)
Female	19 (33.93)
History of medical condition	
Cirrhosis	13 (23.21)
Self-report alcoholism	10 (17.86)
Diabetes	8(14.29)
Hypertension	6 (10.71)
Long-term corticosteroid use	4 (7.14)
Renal failure	2 (3.57)
Pregnancy	2 (3.57)
Spinal cord injury	1 (1.79)
Urinary tract stone	1 (1.79)
Heart failure	1 (1.79)
Cancer	1 (1.79)
No	7 (12.5)
Time to hospitalization	
< 5	40 (71.43)
5-14	14 (25.00)
> 14	2 (3.57)

Among 56 *E. coli* strains isolated analyzed, 39.3% strains were identified as producing ESBL. Detail information of sequencing results showed in Table 3 highlighting three bla_{TEM} subtypes (bla_{TEM} 1, bla_{TEM} 79, bla_{TEM} 82), four bla_{CTX-M} subtypes (bla_{CTX-M}-15, bla_{CTX-M}-73, bla_{CTX-M}-98, bla_{CTX-M}-161), and eight bla_{SHV} subtypes (bla_{SHV}-5, bla_{SHV}-7, bla_{SHV}-12, bla_{SHV}-15, bla_{SH} -24, bla_{SHV}-33, bla_{SHV}-57, bla_{SHV}-77).

Table 3: ESBL-producing E. coli strains and ESBL encoding genes

Result	Number of strains (n = 56) Percentage (%)
ESBL-positive	22 (39.29 %)
ESBL-negative	34 (60.71 %)
bla$_{TEM}$	56
TEM-1	34
TEM-79	19
TEM-82	3
bla$_{CTX-M}$	43
CTX-M-15	12
CTX-M-73	11
CTX-M-98	17
CTX-M-161	3
bla$_{PER}$	0
bla$_{SHV}$	16
SHV-5	3
SHV-7	2
SHV-12	6
SHV-15	1
SHV-24	1
SHV-33	1
SHV-57	1
SHV-77	1
bla$_{TEM}$ + *bla*$_{CTX-M}$	32 (57.2 %)
bla$_{TEM}$ + *bla*$_{SHV}$	5 (8.9 %)
bla$_{TEM}$ + *bla*$_{SHV}$ + *bla*$_{CTX-M}$	11 (19.6 %)

The results of gene analysis revealed that 100% of isolates harbored *bla*$_{TEM}$ gene, but none of them had the *bla*$_{PER}$ gene (Table 4). The prevalence of *bla*$_{CTX-M}$ gene of overall strains, ESBL-producing, and non-ESBL-producing were 76.79%, 81.8%, and 73.5%, respectively. The prevalence of *bla*$_{SHV}$ gene among ESBL-producing and non-ESBL-producing strains were 18.2% and 35.3%. More information showed in Table 4.

Table 4: Encoding gene of ESBL subtypes

Gene	ESBL-positive (n = 22)				ESBL-negative (n = 34)			
	(+)		(-)		(+)		(-)	
	n	(%)	n	(%)	N	(%)	n	(%)
bla$_{PER}$			22	100			34	100
bla$_{TEM}$	22	100			34	100		
bla$_{TEM}$ + *bla*$_{CTX-M}$	18	81.82	4	18.18	25	73.53	9	26.47
bla$_{TEM}$ + *bla*$_{SHV}$	4	18.18	18	81.82	12	35.29	22	64.71
bla$_{TEM}$ + *bla*$_{SHV}$ + *bla*$_{CTX-M}$	3	13.64	19	86.36	8	23.53	26	76.47

Figure 1 showed a high prevalence of resistance to ampicillin (AM-85.7% of strains), trimethoprim/sulfamethoxazole (STX-64.3% of strains), cephazolin (CZ-50% of strains), ciprofloxacin (CP-35.7% of strains) and levofloxacin (LVX-35.7% of strains).

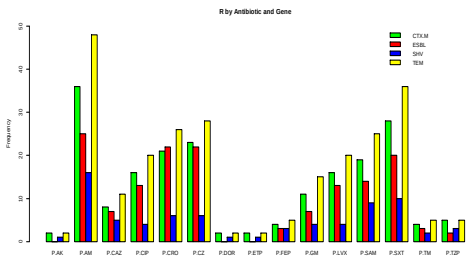

Figure 1: Antibiotic resistance profile; Antibiotics are 1 to 15 following 15 antibiotic have been coded Amikacin (1-AK); Ampicillin (2-AM); Ceftazidime (3-CAZ); Ciprofloxacin (4-CIP); Ceftriaxone (5-CRO); Cefazolin (6-CZ); Doripenem (7-DOR); Ertapenem (8-ETP); Cefepime (9-FEP); Gentamycin (10-GM); Levofloxacin (11-LVX); Ampicillin/Sulbactam (12-SAM); Trimethoprim/sulfamethoxazole (13-SXT); Tobramycin (14-TM); Piperacillin/Tazobactam (15-TZP)

Figure 2 showed highly active antibiotics such as doripenem (DOR-96.4% of strains), ertapenem (ETP-94.6% of strains), amikacin (AK-96.4% of strains), and cefepime (PEP-89.3% of strains). In each antibiotic, detail information of genes was shown.

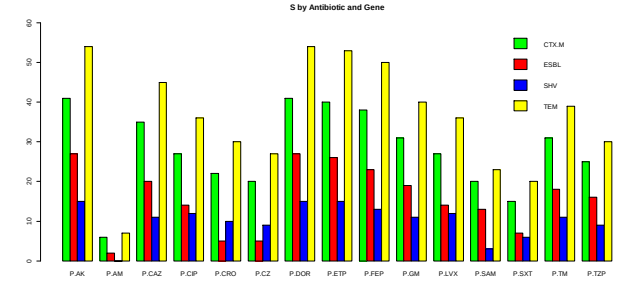

Figure 2: Antibiotic sensitivity profile; Antibiotics are 1 to 15 following 15 antibiotic have been coded Amikacin (1-AK); Ampicillin (2-AM); Ceftazidime (3-CAZ); Ciprofloxacin (4-CIP); Ceftriaxone (5-CRO); Cefazolin (6-CZ); Doripenem (7-DOR); Ertapenem (8-ETP); Cefepime (9-FEP); Gentamycin (10-GM); Levofloxacin (11-LVX); Ampicillin/Sulbactam (12-SAM); Trimethoprim/sulfamethoxazole (13-SXT); Tobramycin (14-TM); Piperacillin/Tazobactam (15-TZP)

Figure 3 showed that in patients who carried gene had high rate of antibiotic resistance with the main antibiotics were ceftazidime (3-CAZ), cefazolin (6-CZ), doripenem (7-DOR), gentamycin (10-GM), levofloxacin (11-LVX), ampicillin/sulbactam (12-SAM), trimethoprim/sulfamethoxazole (13-SXT) in line with *bla*$_{CTX-M}$ gene with the same allocation. Tobramycin (14-TM) with intermediate response had *bla*$_{SHV}$ and *bla*$_{TEM}$ as main genes. Figure 3 supported Figures 1 and 2 to visualize the association between gene and antibiotic resistance.

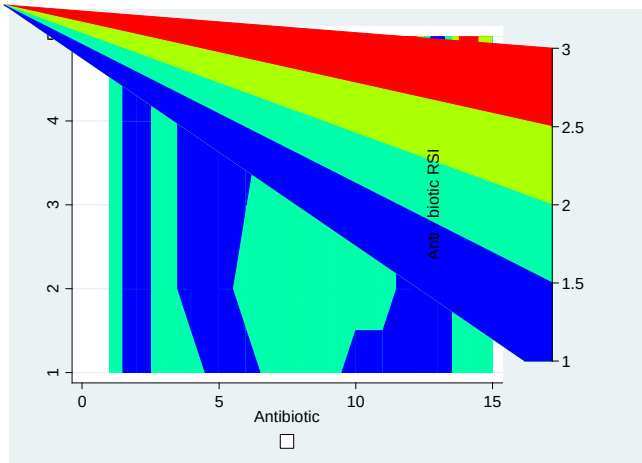

Figure 3: The antibiotic resistance level with genes. Gen antibiotic is 1 to 5 following CTX-M gene, ESBL gene, PER gene, SHV gene and TEM gene; Anti – biotic RSI is 1 to 3 following R (resistance), S (sensitive), I (intermediate); Antibiotics are 1 to 15 following 15 antibiotic have been coded Amikacin (1-AK), Ampicillin (2-AM), Ceftazidime (3-CAZ), Ciprofloxacin (4-CIP), Ceftriaxone (5-CRO), Cefazolin (6-CZ), Doripenem (7-DOR), Ertapenem (8-ETP), Cefepime (9-FEP), Gentamycin (10-GM), Levofloxacin (11-LVX), Ampicillin/Sulbactam (12-SAM), Trimethoprim/sulfamethoxazole (13-SXT), Tobramycin (14-TM) , Piperacillin/Tazobactam (15-TZP)

Table 5 clarified the detail of antibiotic resistance with the ESBL gene. While ESBL-positive strains were highly resistant to ampicillin (AM), ceftriaxone (CRO), cephazolin (CZ), and trimethoprim/sulfamethoxazole (SXT) at the rate of 100%, 100%, 100%, and 81.8%, respectively, ESBL-negative strains had a lower prevalence of resistance to these agents at the rate of 76.5%, 11.8%, 17.7%, and 53%, respectively. Both groups were susceptible to doripenem (DOR), ertapenem (ETP), and amikacin (AK) at the rate of more than 90%.

Table 5: The antibiotic resistance profile of ESBL subtype

Antimicrobial Agents	ESBL-positive (n = 22)			ESBL-negative (n = 34)		
	S (%)	I (%)	R (%)	S (%)	I (%)	R (%)
Ampicilin			22 (100)	7 (20.59)	1 (2.94)	26 (76.47)
Ceftriaxone			22 (100)	30 (84.24)		4 (11.76)
Cephazolin			22 (100)	27 (79.41)	1 (2.94)	6 (17.65)
Trimethoprim/ sulfamethoxazole	4 (18.18)		18 (81.82)	16 (47.06)		18 (52.94)
Ampicilin/sulbactam	10 (45.45)		12 (54.55)	13 (38.24)	8 (23.53)	13 (38.24)
Ciprofloxacin	11 (50)		11 (50)	25 (73.53)		9 (26.47)
Levofloxacin	11 (50)		11 (50)	25 (73.53)		9 (26.47)
Piperacilline/ Tazobactam	11 (73.33)	2 (13.33)	2 (13.33)	19 (82.61)	1 (4.35)	3 (13.04)
Ceftazidime	15 (68.18)		7 (31.82)	30 (88.24)		4 (11.76)
Cefepime	18 (81.82)	1 (4.55)	3 (13.64)	22 (94.12)		2 (5.88)
Doripenem	22 (100)			32 (94.12)		2 (5.88)
Ertapenem	21 (95.45)	1 (4.55)	1 (4.55)	32 (94.12)		2 (5.88)
Amikacin	22 (100)			32 (94.12)		2 (5.88)
Gentamycin	15 (68.18)		7 (31.82)	25 (73.53)	1 (2.94)	8 (23.53)
Tobramycin	14 (63.64)	5 (22.73)	3 (13.64)	25 (73.53)	7 (20.59)	2 (5.88)

Discussion

ESBL-producing *E. coli* is common genotypes and its incidence varies from region to region. ESBLs are typically inhibitor-susceptible B-lactamases that are encoded by mobile genes with the bla_{CTX-M}, bla_{SHV}, and bla_{TEM} families were the most frequently. In our study, among 56 *E. coli* strains have been analyzed, 39.3% strains were identified as ESBL-producing. Our finding is higher than that of study in Northern, Vietnam (25.1% of strains produced ESBL among *Enterobacteriaceae*) [15]. Comparing with other countries, it is higher than Singapore (33%) [18], Chile (23.8%) and Brazil (12.8%) but lower than that of India (60%), Hong Kong (48%) [18] Mexico (48.4%) [19]. All cases with ESBL-producing *E. Coli* had bla_{TEM} gene and the 100% resistance to ampicillin was found that in line with the present study [20].

Our results about bla_{CTX-M} gene also corroborated another study that reported bla_{CTX-M} bla (beta-lactamase) gene was common in all the ESBL isolates [21]. This result is also in agreement with study Gurntke et al., of that among 19% ESBL-positive cases, bla_{CTX-M}-15 was the most common genotypes (60%), followed by bla_{SHV}-5 (27%) [22]. Other studies showed the same results with bla_{CTX-M}-14 (48% of the isolates) were the most frequent ESBL [11], [23]. It was observed that the predominant of subtypes bla_{CTX-M} gene was diverse from study to study. Analyzing 552 isolates from BSIs that resistance to third-generation cephalosporin showed more detail with bla_{CTX-M}-15 (50%), bla_{CTX-M}-14 (14%), bla_{CTX-M}-27 (11%) and bla_{CTX-M}-101 (5%) [24].

ESBL-producing *E. Coli* in BSIs have been shown a substantial increase in the 21st century [25]. Besides that, its burden was growing worldwide [26]. Finding the appropriate therapy became crucial and carbapenems emerged as 'best therapy' for ESBL-producing bacteria [25]. But in the time of antibiotics and resistance becoming popular, *E. Coli* also starts resistance to carbapenem that leading a high financial burden and increased mortality [27].

The knowledge of antibiotic resistance profile is key in clinical practice. The high rate of resistance to some routine antibiotic agents which were commonly used in most hospitals in our area was provided in this study. The results also showed that amikacin and carbapenems (doripenem and ertapenem) emerged as choices for empiric therapy instead. Sinha et al., showed similar findings with high prevalence of ESBL-positive, high rate of resistance to ampicillin (86%), ceftriaxone (80.6%), and fluoroquinolones (80%) and the clear choice for empirical treatment were carbapenems in these cases [21].

Knowing the risk factors of antibiotic resistance is crucial for management strategy. The time before hospitalization was an only independent risk factor among ESBL in BSIs [28] while previous use of oxyimino-beta-lactams was the only modifiable risk factor among nosocomial BSIs [11]. In our study, ESBL encoding genes showed high correlation with antibiotic resistance.

While ESBL-positive strains were highly resistant to ampicillin, ceftriaxone, cephazolin, and trimethoprim/sulfamethoxazole at the rate of 100%, 100%, 100%, and 81.8%, respectively, ESBL-negative strains showed a lower prevalence of resistance to these agents at the rate of 76.5%, 11.8%, 17.7%, and 53%, respectively. Both groups were susceptible to doripenem, ertapenem, and amikacin at the rate of more than 90%. This finding was similar to the study in Finland from 1999 to 2013 that showed most (88%) of the isolates reported as non-susceptible to third-generation cephalosporins had ESBL phenotype [29].

In conclusion, in *Escherichia coli* causing bloodstream infections, antibiotic resistance was higher in ampicillin, trimethoprim/sulfamethoxazole and cephazolin Antibiotics was highly susceptible including doripenem, ertapenem, amikacin, and cefepime.

Ethical approval

This study is approved by the ethics committee of National Hospital of Tropical Diseases and Military Hospital 103.

Ethical considerations

The protocol was approved by the Ethics Committee of both National Hospital of Tropical Diseases and 103 Military Hospital. The study was in line with the Declaration of Helsinki. Written informed consent has been provided to all participants with full explanation. After that, the blood samples were collected.

Informed consent

The consent and commitment were signed by the patients in the study.

Reference

1. Mehl A, et al. Trends in antimicrobial resistance and empiric antibiotic therapy of bloodstream infections at a general hospital in Mid-Norway: a prospective observational study. BMC Infect Dis. 2017; 17(1):116. https://doi.org/10.1186/s12879-017-2210-6 PMid:28148226 PMCid:PMC5288893

2. Russo TA, Johnson JR. Medical and economic impact of extraintestinal infections due to Escherichia coli: focus on an increasingly important endemic problem. Microbes Infect. 2003; 5(5):449-56. https://doi.org/10.1016/S1286-4579(03)00049-2

3. de Kraker ME, et al. The changing epidemiology of bacteraemias in Europe: trends from the European Antimicrobial Resistance Surveillance System. Clin Microbiol Infect. 2013; 19(9):860-8. https://doi.org/10.1111/1469-0691.12028 PMid:23039210

4. Vihta KD, et al. Trends over time in Escherichia coli bloodstream infections, urinary tract infections, and antibiotic susceptibilities in Oxfordshire, UK, 1998-2016: a study of electronic health records. Lancet Infect Dis. 2018; 18(10):1138-1149. https://doi.org/10.1016/S1473-3099(18)30353-0

5. Gagliotti C, et al. Escherichia coli and Staphylococcus aureus: bad news and good news from the European Antimicrobial Resistance Surveillance Network (EARS-Net, formerly EARSS), 2002 to 2009. Euro Surveill. 2011; 16(11). https://doi.org/10.2807/ese.16.11.19819-en PMid:21435327

6. Temkin E, et al. Estimating the number of infections caused by antibiotic-resistant Escherichia coli and Klebsiella pneumoniae in 2014: a modelling study. Lancet Glob Health. 2018; 6(9):e969-e979. https://doi.org/10.1016/S2214-109X(18)30278-X

7. Allocati N, et al. Escherichia coli in Europe: an overview. Int J Environ Res Public Health. 2013; 10(12):6235-54. https://doi.org/10.3390/ijerph10126235 PMid:24287850 PMCid:PMC3881111

8. Schlackow I, et al. Increasing incidence of Escherichia coli bacteraemia is driven by an increase in antibiotic-resistant isolates: electronic database study in Oxfordshire 1999-2011. J Antimicrob Chemother. 2012; 67(6):1514-24. https://doi.org/10.1093/jac/dks082 PMid:22438437

9. Peralta G, et al. Impact of antibiotic resistance and of adequate empirical antibiotic treatment in the prognosis of patients with Escherichia coli bacteraemia. J Antimicrob Chemother. 2007; 60(4):855-63. https://doi.org/10.1093/jac/dkm279 PMid:17644532

10. Sidjabat HE, Paterson DL. Multidrug-resistant Escherichia coli in Asia: epidemiology and management. Expert Rev Anti Infect Ther. 2015; 13(5):575-91. https://doi.org/10.1586/14787210.2015.1028365 PMid:25805210

11. Rodriguez-Bano J, et al. Risk factors and prognosis of nosocomial bloodstream infections caused by extended-spectrum-beta-lactamase-producing Escherichia coli. J Clin Microbiol. 2010; 48(5):1726-31. https://doi.org/10.1128/JCM.02353-09 PMid:20181897 PMCid:PMC2863889

12. Pitout JD, Laupland KB. Extended-spectrum beta-lactamase-producing Enterobacteriaceae: an emerging public-health concern. Lancet Infect Dis. 2008; 8(3):159-66. https://doi.org/10.1016/S1473-3099(08)70041-0

13. Patil A, Krishna BV, Chandrasekhar MR. Increasing burden of hospital acquired infections: resistance to cephalosporin antibiotics among klebsiella and Escherichia coli. J Indian Med Assoc. 2011; 109(3):158-60.

14. Tumbarello M, et al. Costs of bloodstream infections caused by Escherichia coli and influence of extended-spectrum-beta-lactamase production and inadequate initial antibiotic therapy. Antimicrob Agents Chemother. 2010; 54(10):4085-91. https://doi.org/10.1128/AAC.00143-10 PMid:20660675 PMCid:PMC2944559

15. Dat VQ, et al. Bacterial bloodstream infections in a tertiary infectious diseases hospital in Northern Vietnam: aetiology, drug resistance, and treatment outcome. BMC Infect Dis. 2017; 17(1):493. https://doi.org/10.1186/s12879-017-2582-7 PMid:28701159 PMCid:PMC5508750

16. Clinical and Laboratory Standards Institute. Performance standards for antimicrobial susceptibility testing of anaerobic bacteria: informational supplement. Clinical and Laboratory Standards Institute (CLSI); 2009.

17.Team RC. R: A language and environment for statistical computing; 2013.

18. Hsueh PR, et al. Consensus review of the epidemiology and appropriate antimicrobial therapy of complicated urinary tract infections in Asia-Pacific region. J Infect. 2011; 63(2):114-23. https://doi.org/10.1016/j.jinf.2011.05.015 PMid:21669223

19. Gales AC, et al. Antimicrobial resistance among Gram-negative bacilli isolated from Latin America: results from SENTRY Antimicrobial Surveillance Program (Latin America, 2008-2010). Diagn Microbiol Infect Dis. 2012; 73(4):354-60. https://doi.org/10.1016/j.diagmicrobio.2012.04.007 PMid:22656912

20. Waltner-Toews RI, et al. Clinical characteristics of bloodstream infections due to ampicillin-sulbactam-resistant, non-extended-spectrum-beta-lactamase-producing Escherichia coli and the role of TEM-1 hyperproduction. Antimicrob Agents Chemother. 2011; 55(2):495-501. https://doi.org/10.1128/AAC.00797-10 PMid:21135189 PMCid:PMC3028797

21. Sinha R, Kamath S, M Shenoy S. Association of Risk Factors, Antimicrobial Resistance Trends and Occurrence of blaTEM, bla SHV and blaCTX M in Escherichia coli Causing Bacteremia. Infect Disord Drug Targets. 2016; 16(2):95-100. https://doi.org/10.2174/1871526516666151228105150 PMid:26707079

22. Gurntke S, et al. Molecular epidemiology of extended-spectrum beta-lactamase (ESBL)-positive Klebsiella pneumoniae from bloodstream infections and risk factors for mortality. J Infect Chemother. 2014; 20(12):817-9. https://doi.org/10.1016/j.jiac.2014.08.012 PMid:25224765

23. Pitout JD. Infections with extended-spectrum beta-lactamase-producing enterobacteriaceae: changing epidemiology and drug treatment choices. Drugs. 2010; 70(3):313-33. https://doi.org/10.2165/11533040-000000000-00000 PMid:20166768

24. Roer L, et al. WGS-based surveillance of third-generation cephalosporin-resistant Escherichia coli from bloodstream infections in Denmark. J Antimicrob Chemother. 2017; 72(7):1922-1929. https://doi.org/10.1093/jac/dkx092 PMid:28369408

25. Perez F, et al. The continuing challenge of ESBLs. Curr Opin Pharmacol. 2007; 7(5):459-69. https://doi.org/10.1016/j.coph.2007.08.003 PMid:17875405 PMCid:PMC2235939

26. Leistner R, et al. Bloodstream infection due to extended-spectrum beta-lactamase (ESBL)-positive K. pneumoniae and E. coli: an analysis of the disease burden in a large cohort. Infection. 2014; 42(6):991-7. https://doi.org/10.1007/s15010-014-0670-9 PMid:25100555

27. Meng X, et al. Risk factors and medical costs for healthcare-associated carbapenem-resistant Escherichia coli infection among hospitalized patients in a Chinese teaching hospital. BMC Infect Dis. 2017; 17(1):82. https://doi.org/10.1186/s12879-016-2176-9 PMid:28095785 PMCid:PMC5242049

28. Serefhanoglu K, et al. Bloodstream infections caused by ESBL-producing E. coli and K. pneumoniae: risk factors for multidrug-resistance. Braz J Infect Dis. 2009; 13(6):403-7. https://doi.org/10.1590/S1413-86702009000600003 PMid:20464329

29. Martelius T, et al. Nosocomial bloodstream infections caused by Escherichia coli and Klebsiella pneumoniae resistant to third-generation cephalosporins, Finland, 1999-2013: Trends, patient characteristics and mortality. Infect Dis. 2016; 48(3):229-34. https://doi.org/10.3109/23744235.2015.1109135 PMid:26577519

ID Design Press, Skopje, Republic of Macedonia
Open Access Macedonian Journal of Medical Sciences. 2019 Dec 30; 7(24):4406-4410.
https://doi.org/10.3889/oamjms.2019.871
eISSN: 1857-9655
Basic and Clinical Medical Researches in Vietnam

Antibiotic Resistance Profile and Methicillin-Resistant Encoding Genes of *Staphylococcus aureus* Strains Isolated from Bloodstream Infection Patients in Northern Vietnam

Le Van Nam[1], Do Quyet[2], Pham Ngoc Hung [3,4], Tran Viet Tien[1], Kieu Chi Thanh[5], Quan Anh Dung[6], Do Dieu Linh[7], Ha The Tan[3], Nguyen Duy Bac[4], Thien Chu Dinh[8], Dinh Cong Pho[6*]

[1]Department of Infectious Diseases, Military Hospital 103, Vietnam Military Medical University, Hanoi, Vietnam; [2]Director of Vietnam Military Medical University, Department of Tuberculosis and Lung Diseases, Military Hospital 103, Vietnam Military Medical University, Hanoi, Vietnam; [3]Department of Epidemiology, Vietnam Military Medical University, Hanoi, Vietnam; [4]Department of Training, Vietnam Military Medical University, Hanoi, Vietnam; [5]Department of Hospital Infection Control, Military Hospital 103, Vietnam Military Medical University, Hanoi, Vietnam; [6]Faculty of Medicine, Vietnam Military Medical University, Hanoi, Vietnam; [7]Faculty of Medicine, Hai Phong Medical University, 72A Nguyen Binh Khiem, Hai Phong, Vietnam; [8]Institute for Research and Development, Duy Tan University, 03 Quang Trung, Danang, Vietnam

Citation: Nam LV, Quyet D, Hung PN, Tien TV, Thanh KC, Dung QA, Linh DD, Tan HT, Bac ND, Dinh TC, Pho DC. Antibiotic Resistance Profile and Methicillin-Resistant Encoding Genes of *Staphylococcus aureus* Strains Isolated from Bloodstream Infection Patients in Northern Vietnam. Open Access Maced J Med Sci. 2019 Dec 30; 7(24):4406-4410.
https://doi.org/10.3889/oamjms.2019.871

Keywords: Antibiotic resistance; Staphylococcus aureus (S. aureus); MRSA (methicillin-resistant staphylococcus aureus); MSSA (methicillin-susceptible staphylococcus aureus); MRSA encoding genes; bloodstream infections (BSIs)

***Correspondence:** Dinh Cong Pho. Faculty of Medicine, Vietnam Military Medical University, Ha Dong District, Ha Noi City, Vietnam. Phone number: +84333697065. ORCID: https://orcid.org/0000-0002-0810-8521. E-mail: dcpho@vmmu.edu.com

Received: 11-Nov-2019; **Revised:** 26-Nov-2019; **Accepted:** 27-Nov-2019; **Online first:** 20-Dec-2019

Funding: This research did not receive any financial support

Competing Interests: The authors have declared that no competing interests exist

Abstract

BACKGROUND: Evaluating the antibiotic susceptibility and resistance genes is essential in the clinical management of bloodstream infections (BSIs). Nevertheless, there are still limited studies in Northern Vietnam**.**

AIM: This study aimed to determine the antibiotic resistance profile and methicillin-resistant encoding genes of *Staphylococcus aureus (S. aureus)* causing BSIs in Northern Vietnam.

METHODS: The cross-sectional study was done from December 2012 to June 2014 in two tertiary hospitals in Northern Vietnam. Tests performed at the lab of the hospital.

RESULTS: In 43 *S. aureus* strains isolating, 53.5 % were MRSA. Distribution of gene for overall, MRSA, and MSSA strains were following: *mecA* gene (58.1 %; 95.7%, and 15%), *femA* gene (48.8%, 47.8%, and 50%), *femB* gene (88.4%, 82.6%, and 95%). Antibiotic resistance was highest in penicillin (100%), followed by erythromycin (65.1%) and clindamycin (60.5%). Several antibiotics were susceptible (100%), including vancomycin, tigecycline, linezolid, quinupristin/dalfopristin. Quinolone group was highly sensitive, include ciprofloxacin (83.7%), levofloxacin (86%) and moxifloxacin (86%).

CONCLUSION: In *S. aureus* causing BSIs, antibiotic resistance was higher in penicillin, erythromycin, and clindamycin. All strains were utterly susceptible to vancomycin, tigecycline, linezolid, quinupristin/dalfopristin.

Introduction

Bloodstream infections (BSIs) became a significant concern with increasing in incidence [1]. Understanding the aetiology of BSI was essential for management. In Asian countries, *S. aureus* was one of the leading causes of bloodstream infections [2], and its incidence was increasing worldwide [3], [4]. It was responsible for many severe clinical conditions, especially in bloodstream infections [5] with rates of mortality was 50% [6]. With subtype of methicillin-resistant staphylococcus aureus (MRSA), the prevalence and mortality were higher than methicillin-susceptible staphylococcus aureus (MSSA) [7]. The burden of MRSA disease was quantifiable and substantial [8]. In European, Cassini et al. used population-level model estimating that MRSA *caused* 148 thousand infections and 32.6 thousand BSIs in 2015 [9]. In Asia, among patients with community-associated *S. aureus* infections, MRSA accounted for 25.5% [10]. Under increasing in prevalence, increasing resistance also reported, especially MRSA [11]. It caused many clinical conditions with poor outcomes [12]. Patients with MRSA in BSIs had a worse prognosis because of partially effect on correct empirical treatment [13]. It became a global concern [14] with the increasing burden of cost [15] and the

resistance to all classes of antibiotics [16]. Therefore, evaluation of the antibiotic susceptibility of bacteria is essential to decide what types of medicines and what appropriate doses that are improving treatment efficiency and minimising the antibiotic resistance rate.

In Vietnam, MRSA accounted for 67.4% of *S. aureus* healthcare-associated infections [10]. The study of causes in BSIs patients in Northern Vietnam showed 37% of methicillin-resistance among *S. aureus* [17], but there are still limited studies in Northern Vietnam. Thus, our research aims is to determine the antibiotic resistance profile and the prevalence of methicillin-resistant encoding genes in *S. aureus,* causing bloodstream infections in Northern Vietnam.

Materials and Methods

The cross-sectional study was done from 12/2012 to 6/2014 in the National Hospital of Tropical Diseases and 103 Military Hospital. Isolating blood samples from septicemia patients in two hospitals, 43 *S. aureus* strains were identified at the labs of those hospitals. The information of patients collected on the same forms.

Antimicrobial susceptibility assessed through MIC test by VITEK®2 Compact (BioMérieux, France and provided by DEKA *Limited Liability Company)* standardised by CLSI [18]. Antibiotics which have been used are*were (with number coding – abbreviation for Figure 3):* penicillin (1-PEN), gentamycin (2-GM), ciprofloxacin (3-CIP), levofloxacin (4-LVX), moxifloxacin (5- MXF), tetracycline (6-TE), erythromycin (7-ERY), clindamycin (8-CM), trimethoprim/sulfamethoxazole (9-SXT), vancomycin (10-VAN), rifampin (11-RIF), quinupristin/dalfopristin (12-QD), linezolid (13-LZD), oxacillin (14-OXA), tigecycline (15-TGE).

Using QIAamp DNA Mini Kit (USA) for DNA extraction (including isolation and quantification), we performed the experimental procedure according to manufacturer's instruction. PCR amplification performed in PCR master mix (Invitrogen – USA) that consisted of 200 µM of each dNTPs (dATP, dCTP, dGTP, dTTP), 100 pM primers, 1 U Taq DNA polymerase, 10 mM Tris-HCl, 1.5 mM $MgCl_2$ and 10 µl DNA template. Specific primers for *mecA*, *femA*, and *femB* genes showed in table 1. The experiments were performed using the protocol with 25 cycles that each of them consisted of 3 steps including denaturing (94^0C for 1 minute), priming (57^0C for 1 minute), synthesising of sequence (72^0C for 1 minute). PCR products were performed electrophoresis, imaged routinely and sequenced. The sequence of PCR products was compared with the original gene's sequence on GenBank to confirm *mecA, femA, and femB* genes.

Table 1: Specific primers for mecA gene

Target gene	Primer	Nucleotide sequence (5' – 3')	Size (bp)	Location
mecA	Mec-A1	5' – AAA ATC GAT GGT AAA GGT TGG C – 3'	533	1282-1303
	Mec-A2	5' – AGT TCT GCA GTA CCG GAT TTG C – 3'		1739-1814
femA	Fem-A1	5' – AGA CAA ATA GGA GTA ATG AT – 3'	509	595-614
	Fem-A2	5' – AAA TCT AAC ACT GAG TGA TA – 3'		1084-1103
femB	Fem-B1	5' – TTA CAG AGT TAA CTG TTA CC – 3'	651	1904-1923
	Fem-B2	5' – ATA CAA ATC CAG CAC GCT CT – 3'		2535-2554

Ethical considerations

The Ethics Committee of the National Hospital of Tropical Diseases and Military Hospital 103 approved the protocol of the study. The study was in line with the Declaration of Helsinki. Written informed consent has been signed by all participants after full explanation. After that, the blood samples were collected.

Statistical Analysis

The statistical analysis was conducted using the R language. Graphics also were performed by the R language. In this study, the analysis of such enormous volumes of information in the acquisition of data from 43 strains, each strain companion with genes (*mecA, femA, and femB*) and 15 antibiotics with 3 levels of resistance (susceptible, intermediate, resistance). For this reason, we used R language to analyse.

Results

Characteristics of the patient in this study showed in Table 2.

Table 2: Characteristics of patients

Characteristics		Number (Percentage)
Age (subgroup)		
	16-19	5 (11.63)
	20-29	5 (11.63)
	30-39	11 (25.58)
	40-49	7 (16.28)
	50-59	9 (20.93)
	≥ 60	6 (13.95)
Gender		
	Male	40 (93.02 %)
	Female	3 (6.98 %)
History of the medical conditions		
	Cirrhosis	4 (9.3)
	Self-report alcoholism	4 (9.3)
	Spinal cord injury	3 (6.98)
	Diabetes	2 (4.65)
	Hypertension	2 (4.65)
	Hepatitis	2 (4.65)
	Chronic arthritis	2 (4.65)
	Urinary tract stone	1 (2.33)
	Heart failure	1 (2.33)
	Deep vein thrombosis	1 (2.33)
	No	21 (48.83)
Time to hospitalization		
	< 5	17 (39.53)
	5-14	21 (48.84)
	>14	5 (11.63)

Among 43 *S. aureus* strains isolated analysed, 23 S. aureus strains were MRSA strains (53.5 %), and 20 S. aureus strains were MSSA strains (46.5%). Detail information of showed in Table 3.

Table 3: Methicillin-resistant S. aureus and methicillin-resistant encoding genes

Result	Number of strains (n = 43) Percentage (%)
MRSA	23 (53.49%)
MSSA	20 (46.51%)
mecA	25 (58.13%)
femA	21 (48.84%)
femB	38 (88.37%)
mecA + femA	11 (25.58%)
mecA + femB	23 (53.84%)
mecA + femA + femB	10 (23.25%)

And among that, 58.1 % strains were identified as producing *mecA*, and 22 of 23 MRSA strains (95.7%) proved to be having *mecA* gene when 15% strains in the MSSA group possessed this gene. The prevalence of *femB* gene of overall strains, MRSA, and MSSA was 88.4%, 82.6%, and 95%, respectively. The prevalence of *femA* gene of whole strains, MRSA, and MSSA was 48.8%, 47.8%, and 50%, respectively. More information showed in Table 4.

Table 4: Encoding genes of methicillin-resistant in S. Aureus

Gene	MRSA (n = 23)				MSSA (n = 20)			
	Positive (+)		Negative (-)		Positive (+)		Negative (-)	
	n	(%)	n	(%)	n	(%)	n	(%)
mecA	22	95.65	1	4.34	3	15	17	85
femA	11	47.83	12	52.17	10	50	10	50
femB	19	82.6	4	17.4	19	95	1	5
mecA + femA	10	43.47	13	56.53	1	5	19	95
mecA + femB	17	73.91	6	26.09	6	30	14	70
mecA + femA + femB	9	39.13	14	60.87	1	5	19	95

Figure 1 showed the highest prevalence of resistance to penicillin (PEN -100%), followed by erythromycin (ERY - 65.1%) and clindamycin (CM - 60.5%).

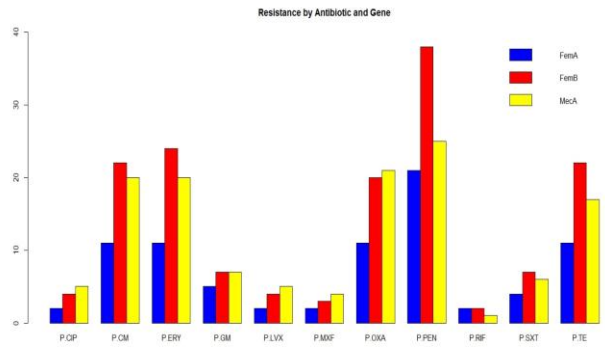

Figure 1: Antibiotic resistant profile

While Figure 2 showed highly active antibiotics in quinolone group, include ciprofloxacin (CIP - 83.7% of isolates), levofloxacin (LVX - 86.1% of isolates) and moxifloxacin (MXF - 86.1% of isolates). Several antibiotics were susceptible (100%), include vancomycin, tigecycline, linezolid, quinupristin/ dalfopristin.

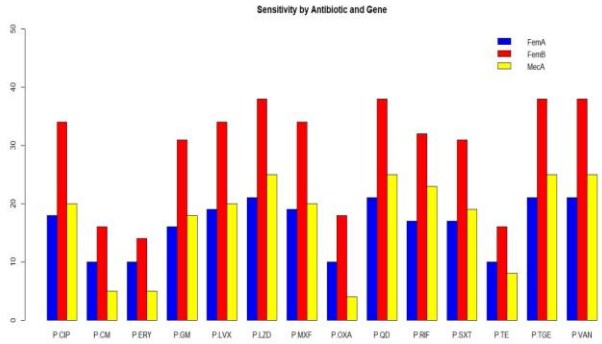

Figure 2: Antibiotic sensitivity profile

The level of resistance (MIC) in MRSA group to clindamycin, erythromycin, tetracycline, levofloxacin, ciprofloxacin, moxifloxacin was higher than MSSA group. In each antibiotic, detail information of genes showed. Figure 3 showed that the distribution of three *femA*, f*emB*, and *mecA* genes is equivalent to 15 antibiotics.

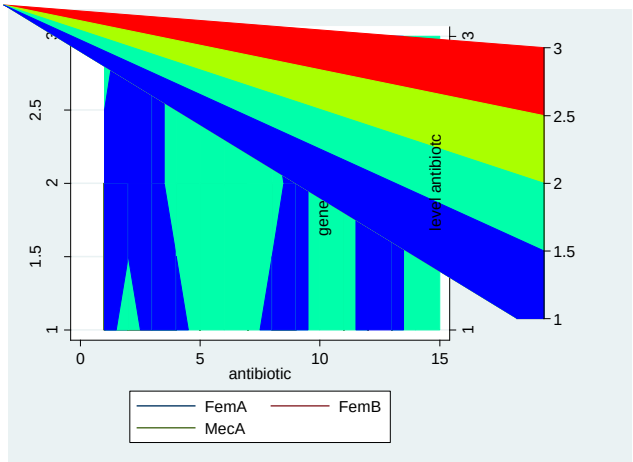

Figure 3: Distribution the antibiotic resistance level with genes. Antibiotic gene: 1.FemA; 2.FemB; 3.MecA. Antibiotic resistance level: From 1 to 3 are R, S, I, respectively; Antibiotic: From 1 to 15 is the ordinal number of 15 antibiotics

The rate of sensitivity also accounts for the majority of ciprofloxacin, levofloxacin, moxifloxacin, linezolid, quinupristin/ dalfopristin, rifampin, tigecycline, vancomycin distributed in all three genes but most in the *femB* gene. The intermediate response is concentrated in moxifloxacin and rifampin antibiotics. Antibiotic resistance focused on antibiotics clindamycin, erythromycin, oxacillin, penicillin, and tetracycline. Figure 3 supported figures 1 and 2 to visualise the association between the gene and antibiotic resistance.

Table 5 clarified the detail of antibiotic resistance with *S. aureus*. While MRSA strains were highly resistant to penicillin, erythromycin, clindamycin, and tetracycline with the rate following: 100%, 82.6%, 87%, 73.9%, respectively, MSSA strains showed a lower prevalence of resistance to these agents with the rate following: 20%, 9%, 6%, 3%, respectively. Both groups were susceptible to vancomycin, tigecycline, linezolid, quinupristin/ dalfopristine at the rate of 100%.

Table 5: The antibiotic resistance profile of S. Aureus

Antimicrobial agents	MRSA			MSSA		
	S (%)	I (%)	R (%)	S (%)	I (%)	R (%)
Penicillin			23 (100)			20 (100)
Erythromycin	4 (17.39)		19 (82.61)	11 (55)		9 (45)
Clindamycin	3 (17.04)		20 (86.96)	14 (70)		6 (30)
Tetracycline	6 (26.09)		17 (73.91)	17 (65)		3 (35)
Gentamycin	16 (69.57)		7 (30.43)	17 (85)		3 (15)
Trimethoprim/sulfamethoxazole	17 (73.91)		6 (26.09)	16 (80)		4 (20)
Ciprofloxacin	18 (78.26)	0 (0)	5 (21.74)	18 (90)	1 (5.0)	1 (5.0)
Levofloxacin	18 (78.26)		5 (21.74)	19 (95)		1 (5.0)
Moxifloxacin	18 (78.26)	1 (4.35)	4 (17.39)	19 (95)	0 (0)	1 (5.0)
Rifampin	22 (95.65)	0 (0)	1 (4.35)	14 (70)	5 (25)	1 (5.0)
Vancomycin	23 (100)			20 (100)		
Quinupristin/dalfopristin	21 (100)			22 (100)		
Linezolid	23 (100)			20 (100)		
Tigecycline	23 (100)			20 (100)		

Discussion

The methicillin-resistant in *S. aureus* strains are encoded by mobile genes with the *mecA* and *femB* gene was the most frequently. The incidence of MRSA varies from region to region. In our study, among 43 *S. aureus* strains have been analysed in BSI patients, 53.5% strains were identified as MRSA that was higher than study in Northern Vietnam (37%) [17]. Comparing with other countries, it was higher than the Philippines (38.1%), India (22.6%) [19] but lower than that of Korea (77.6%), Taiwan (65%), Hong Kong (56.8%), Sri Lanka (86.5%) [19].

Almost cases (22/23) with MRSA had *mecA* gene and the 100% resistance to penicillin was found that in line with the present study [20]. Our results about *mecA* gene have been shown that the *mecA* gene is responsible for resistance to methicillin [21] with the mechanisms have been proved [11] and 15% strains in MSSA group possessed this gene. Mohanasoundaram et al. showed similar findings with 100% MRSA possessed *mecA* gene, and only one MSSA strain had maintained this gene [22]. The 15% rate of MSSA positive for the *mecA* gene is quite high, and field literature reported a rate of 3% for MSSA positive for *mecA* [23]. The potential explanation regarding this high number is that the resistance gene transmitted in the hospital between bacteria. Thus, this finding in our study provides useful information to determine the prevalence of *mecA* gene in MSSA patients. In our study, *femB* gene was detected in almost *S. aureus* isolates, 82.6% in MRSA and 95% in the MSSA group, respectively. This result corroborated with Kobayashi et al. [24] but the differences between two studies that needed to highlight were the expression of *femA* gene showed very high (89.4%) [24] in Kobayashi's study and lower rate in our research (48.8%). Further analysis of the expression of these genes in staphylococci will be needed.

MRSA in BSIs has been shown substantial increase in the 21 century [25]. As a result, its burden was growing not only in Europe [15], [26] but also worldwide [27]. Finding the appropriate therapy became crucial and glycopeptides had been used as an effective empirical antibiotic therapy for MRSA[28]. But in the time of antibiotics and resistance becoming popular, *S. aureus* also starts resistance to vancomycin that leading high financial burden and increased mortality [29], [30], [31]. The knowledge of antibiotic resistance profile is critical in clinical practice. In our study, some routine antibiotic agents used commonly in our area showed high resistance. The results of our study also showed that vancomycin, tigecycline, linezolid, quinupristin/dalfopristin emerged as choices for empiric therapy instead. Fan Zhang et al. showed similar findings with a high rate of resistance to penicillin (100%), erythromycin (73.3%) and clindamycin (57.3%) and the clear choice for treatment were vancomycin in these cases [20]. In our study, methicillin-resistant encoding genes showed high correlation with antibiotic resistance. Penicillin, erythromycin, clindamycin, and tetracycline showed resistant to MRSA but susceptibility to MSSA. The remarkable results in our study were that vancomycin, tigecycline, linezolid, quinupristin/dalfopristin were entirely susceptible to both groups. It guides to use antibiotics in case of suspecting bloodstream infection caused by *S. aureus.*

Limitation of study: The isolates of *S. aureus* strains included seem to be quite old (2012-2014), but it still plays an important role in the reflection of the current epidemiological situation. The isolates included were small (43 isolates) because we focused on only bloodstream infection patients and these results of our study were useful for this kind of patient.

As a conclusion, in *S. aureus* causing bloodstream infections, antibiotic resistance was higher in penicillin, erythromycin, and clindamycin. All strains were entirely susceptible to vancomycin, tigecycline, linezolid, quinupristin/dalfopristin.

Ethical approval

This study is approved by the ethics committee of National Hospital of Tropical Diseases and Military Hospital 103.

Informed consent

The consent and commitment were signed by the patients in the study.

References

1. Laupland KB. Incidence of bloodstream infection: a review of population-based studies. Clinical microbiology and infection. 2013; 19(6): 492-500. https://doi.org/10.1111/1469-0691.12144 PMid:23398633

2. Kang CI, Song JH. Antimicrobial resistance in Asia: current epidemiology and clinical implications. Infect Chemother. 2013; 45(1): 22-31. https://doi.org/10.3947/ic.2013.45.1.22 PMid:24265947 PMCid:PMC3780932

3. De Kraker M, et al. The changing epidemiology of bacteraemias in Europe: trends from the European Antimicrobial Resistance Surveillance System. Clinical Microbiology and Infection. 2013; 19(9): 860-868. https://doi.org/10.1111/1469-0691.12028 PMid:23039210

4. Khatib R, et al. Persistent Staphylococcus aureus bacteremia: incidence and outcome trends over time. Scandinavian journal of infectious diseases. 2009; 41(1):4-9. https://doi.org/10.1080/00365540802441711 PMid:18821135

5. Wang JL, et al. Comparison of both clinical features and mortality risk associated with bacteremia due to community-acquired methicillin-resistant Staphylococcus aureus and methicillin-susceptible S. aureus. Clin Infect Dis. 2008; 46(6): 799-806. https://doi.org/10.1086/527389 PMid:18266610

6. Nickerson EK, et al. Staphylococcus aureus disease and drug resistance in resource-limited countries in south and east Asia. Lancet Infect Dis. 2009; 9(2):130-5. https://doi.org/10.1016/S1473-3099(09)70022-2

7. Cosgrove SE, et al. Comparison of mortality associated with methicillin-resistant and methicillin-susceptible Staphylococcus aureus bacteremia: a meta-analysis. Clin Infect Dis. 2003; 36(1):53-9. https://doi.org/10.1086/345476 PMid:12491202

8. Kuehnert MJ, et al. Methicillin-resistant-Staphylococcus aureus hospitalizations, United States. Emerging infectious diseases. 2005; 11(6):468. https://doi.org/10.3201/eid1106.040831 PMid:15963281 PMCid:PMC3367609

9. Cassini A, et al. Attributable deaths and disability-adjusted life-years caused by infections with antibiotic-resistant bacteria in the EU and the European Economic Area in 2015: a population-level modelling analysis. The Lancet Infectious Diseases. 2019; 19(1):56-66. https://doi.org/10.1016/S1473-3099(18)30605-4

10. Song J-H, et al. Spread of methicillin-resistant Staphylococcus aureus between the community and the hospitals in Asian countries: an ANSORP study. Journal of Antimicrobial Chemotherapy. 2011; 66(5):1061-1069. https://doi.org/10.1093/jac/dkr024 PMid:21393157

11. Grundmann H, et al. Emergence and resurgence of meticillin-resistant Staphylococcus aureus as a public-health threat. The Lancet. 2006; 368(9538): 874-885. https://doi.org/10.1016/S0140-6736(06)68853-3

12. Deresinski S. Methicillin-Resistant Staphylococcus aureus: An Evolutionary, Epidemiologic, and Therapeutic Odyssey. Clinical Infectious Diseases. 2005; 40(4):562-573. https://doi.org/10.1086/427701 PMid:15712079

13. Thaden JT, et al. Survival benefit of empirical therapy for Staphylococcus aureus bloodstream infections in infants. The Pediatric infectious disease journal. 2015; 34(11):1175. https://doi.org/10.1097/INF.0000000000000850 PMid:26222060 PMCid:PMC4604046

14. Drews TD, Temte JL, Fox BC. Community-associated methicillin-resistant Staphylococcus aureus: review of an emerging public health concern. WMJ-MADISON-. 2006; 105(1):52.

15. Lee BY, et al. The economic burden of community-associated methicillin-resistant Staphylococcus aureus (CA-MRSA). Clinical Microbiology and Infection. 2013; 19(6):528-536. https://doi.org/10.1111/j.1469-0691.2012.03914.x PMid:22712729 PMCid:PMC3463640

16. Vestergaard M, Frees D, Ingmer H. Antibiotic Resistance and the MRSA Problem. Microbiol Spectr. 2019; 7(2). https://doi.org/10.1128/microbiolspec.GPP3-0057-2018 PMid:30900543

17. Dat VQ, et al. Bacterial bloodstream infections in a tertiary infectious diseases hospital in Northern Vietnam: aetiology, drug resistance, and treatment outcome. BMC Infect Dis. 2017; 17(1):493. https://doi.org/10.1186/s12879-017-2582-7 PMid:28701159 PMCid:PMC5508750

18. Clinical and L.S. Institute, Performance Standards for Antimicrobial Susceptibility Testing of Anaerobic Bacteria: Informational Supplement. Clinical and Laboratory Standards Institute (CLSI), 2009.

19. Song JH, et al. Spread of methicillin-resistant Staphylococcus aureus between the community and the hospitals in Asian countries: an ANSORP study. J Antimicrob Chemother. 2011; 66(5):1061-9. https://doi.org/10.1093/jac/dkr024 PMid:21393157

20. Zhang F, et al. Bacterial susceptibility in bloodstream infections: Results from China Antimicrobial Resistance Surveillance Trial (CARST) Program, 2015-2016. Journal of global antimicrobial resistance. 2019. https://doi.org/10.1016/j.jgar.2018.12.016 PMid:30611932

21. Ubukata K, et al. Homology of mecA gene in methicillin-resistant Staphylococcus haemolyticus and Staphylococcus simulans to that of Staphylococcus aureus. Antimicrobial agents and chemotherapy. 1990; 34(1):170-172. https://doi.org/10.1128/AAC.34.1.170 PMid:1691614 PMCid:PMC171544

22. Mohanasoundaram K, Lalitha M. Comparison of phenotypic versus genotypic methods in the detection of methicillin resistance in Staphylococcus aureus. Indian Journal of Medical Research. 2008; 127(1):78.

23. Proulx MK, et al. Reversion From Methicillin Susceptibility to Methicillin Resistance in Staphylococcus aureus During Treatment of Bacteremia. J Infect Dis. 2016; 213(6):1041-8. https://doi.org/10.1093/infdis/jiv512 PMid:26503983 PMCid:PMC4760414

24. Kobayashi N, et al. Detection of mecA, femA, and femB genes in clinical strains of staphylococci using polymerase chain reaction. Epidemiology & Infection. 1994; 113(2):259-266. https://doi.org/10.1017/S0950268800051682 PMid:7925664 PMCid:PMC2271538

25. Johnson AP, Pearson A, Duckworth G. Surveillance and epidemiology of MRSA bacteraemia in the UK. Journal of Antimicrobial Chemotherapy. 2005; 56(3):455-462. https://doi.org/10.1093/jac/dki266 PMid:16046464

26. Köck R, et al. Methicillin-resistant Staphylococcus aureus (MRSA): burden of disease and control challenges in Europe, 2010. https://doi.org/10.2807/ese.15.41.19688-en PMid:20961515

27. Liebowitz LD. MRSA burden and interventions. International journal of antimicrobial agents. 2009; 34:S11-S13. https://doi.org/10.1016/S0924-8579(09)70551-5

28. Gemmell CG, et al. Guidelines for the prophylaxis and treatment of methicillin-resistant Staphylococcus aureus (MRSA) infections in the UK. Journal of antimicrobial chemotherapy. 2006; 57(4):589-608. https://doi.org/10.1093/jac/dkl017 PMid:16507559

29. Hawkey P. The growing burden of antimicrobial resistance. Journal of antimicrobial chemotherapy. 2008; 62(suppl_1): i1-i9. https://doi.org/10.1093/jac/dkn241 PMid:18684701

30. Johnson LB, et al. Staphylococcus aureus bacteremia: compliance with standard treatment, long-term outcome and predictors of relapse. Scandinavian journal of infectious diseases. 2003; 35(11-12): 782-789. https://doi.org/10.1080/00365540310016682 PMid:14723349

31. Chang F-Y, et al. Staphylococcus aureus bacteremia: recurrence and the impact of antibiotic treatment in a prospective multicenter study. Medicine. 2003; 82(5):333-339. https://doi.org/10.1097/01.md.0000091184.93122.09 PMid:14530782

ID Design Press, Skopje, Republic of Macedonia
Open Access Macedonian Journal of Medical Sciences. 2019 Dec 30; 7(24):4406-4410.
https://doi.org/10.3889/oamjms.2019.871
eISSN: 1857-9655
Basic and Clinical Medical Researches in Vietnam

Antibiotic Resistance Profile and Methicillin-Resistant Encoding Genes of *Staphylococcus aureus* Strains Isolated from Bloodstream Infection Patients in Northern Vietnam

Le Van Nam[1], Do Quyet[2], Pham Ngoc Hung [3,4], Tran Viet Tien[1], Kieu Chi Thanh[5], Quan Anh Dung[6], Do Dieu Linh[7], Ha The Tan[3], Nguyen Duy Bac[4], Thien Chu Dinh[8], Dinh Cong Pho[6*]

[1]Department of Infectious Diseases, Military Hospital 103, Vietnam Military Medical University, Hanoi, Vietnam; [2]Director of Vietnam Military Medical University, Department of Tuberculosis and Lung Diseases, Military Hospital 103, Vietnam Military Medical University, Hanoi, Vietnam; [3]Department of Epidemiology, Vietnam Military Medical University, Hanoi, Vietnam; [4]Department of Training, Vietnam Military Medical University, Hanoi, Vietnam; [5]Department of Hospital Infection Control, Military Hospital 103, Vietnam Military Medical University, Hanoi, Vietnam; [6]Faculty of Medicine, Vietnam Military Medical University, Hanoi, Vietnam; [7]Faculty of Medicine, Hai Phong Medical University, 72A Nguyen Binh Khiem, Hai Phong, Vietnam; [8]Institute for Research and Development, Duy Tan University, 03 Quang Trung, Danang, Vietnam

Citation: Nam LV, Quyet D, Hung PN, Tien TV, Thanh KC, Dung QA, Linh DD, Tan HT, Bac ND, Dinh TC, Pho DC. Antibiotic Resistance Profile and Methicillin-Resistant Encoding Genes of *Staphylococcus aureus* Strains Isolated from Bloodstream Infection Patients in Northern Vietnam. Open Access Maced J Med Sci. 2019 Dec 30; 7(24):4406-4410.
https://doi.org/10.3889/oamjms.2019.871

Keywords: Antibiotic resistance; Staphylococcus aureus (S. aureus); MRSA (methicillin-resistant staphylococcus aureus); MSSA (methicillin-susceptible staphylococcus aureus); MRSA encoding genes; bloodstream infections (BSIs)

***Correspondence:** Dinh Cong Pho. Faculty of Medicine, Vietnam Military Medical University, Ha Dong District, Ha Noi City, Vietnam. Phone number: +84333697065. ORCID: https://orcid.org/0000-0002-0810-8521. E-mail: dcpho@vmmu.edu.com

Received: 11-Nov-2019; **Revised:** 26-Nov-2019; **Accepted:** 27-Nov-2019; **Online first:** 20-Dec-2019

Funding: This research did not receive any financial support

Competing Interests: The authors have declared that no competing interests exist

Abstract

BACKGROUND: Evaluating the antibiotic susceptibility and resistance genes is essential in the clinical management of bloodstream infections (BSIs). Nevertheless, there are still limited studies in Northern Vietnam**.**

AIM: This study aimed to determine the antibiotic resistance profile and methicillin-resistant encoding genes of *Staphylococcus aureus (S. aureus)* causing BSIs in Northern Vietnam.

METHODS: The cross-sectional study was done from December 2012 to June 2014 in two tertiary hospitals in Northern Vietnam. Tests performed at the lab of the hospital.

RESULTS: In 43 *S. aureus* strains isolating, 53.5 % were MRSA. Distribution of gene for overall, MRSA, and MSSA strains were following: *mecA* gene (58.1 %; 95.7%, and 15%), *femA* gene (48.8%, 47.8%, and 50%), *femB* gene (88.4%, 82.6%, and 95%). Antibiotic resistance was highest in penicillin (100%), followed by erythromycin (65.1%) and clindamycin (60.5%). Several antibiotics were susceptible (100%), including vancomycin, tigecycline, linezolid, quinupristin/dalfopristin. Quinolone group was highly sensitive, include ciprofloxacin (83.7%), levofloxacin (86%) and moxifloxacin (86%).

CONCLUSION: In *S. aureus* causing BSIs, antibiotic resistance was higher in penicillin, erythromycin, and clindamycin. All strains were utterly susceptible to vancomycin, tigecycline, linezolid, quinupristin/dalfopristin.

Introduction

Bloodstream infections (BSIs) became a significant concern with increasing in incidence [1]. Understanding the aetiology of BSI was essential for management. In Asian countries, *S. aureus* was one of the leading causes of bloodstream infections [2], and its incidence was increasing worldwide [3], [4]. It was responsible for many severe clinical conditions, especially in bloodstream infections [5] with rates of mortality was 50% [6]. With subtype of methicillin-resistant staphylococcus aureus (MRSA), the prevalence and mortality were higher than methicillin-susceptible staphylococcus aureus (MSSA) [7]. The burden of MRSA disease was quantifiable and substantial [8]. In European, Cassini et al. used population-level model estimating that MRSA *caused* 148 thousand infections and 32.6 thousand BSIs in 2015 [9]. In Asia, among patients with community-associated *S. aureus* infections, MRSA accounted for 25.5% [10]. Under increasing in prevalence, increasing resistance also reported, especially MRSA [11]. It caused many clinical conditions with poor outcomes [12]. Patients with MRSA in BSIs had a worse prognosis because of partially effect on correct empirical treatment [13]. It became a global concern [14] with the increasing burden of cost [15] and the

resistance to all classes of antibiotics [16]. Therefore, evaluation of the antibiotic susceptibility of bacteria is essential to decide what types of medicines and what appropriate doses that are improving treatment efficiency and minimising the antibiotic resistance rate.

In Vietnam, MRSA accounted for 67.4% of *S. aureus* healthcare-associated infections [10]. The study of causes in BSIs patients in Northern Vietnam showed 37% of methicillin-resistance among *S. aureus* [17], but there are still limited studies in Northern Vietnam. Thus, our research aims is to determine the antibiotic resistance profile and the prevalence of methicillin-resistant encoding genes in *S. aureus,* causing bloodstream infections in Northern Vietnam.

Materials and Methods

The cross-sectional study was done from 12/2012 to 6/2014 in the National Hospital of Tropical Diseases and 103 Military Hospital. Isolating blood samples from septicemia patients in two hospitals, 43 *S. aureus* strains were identified at the labs of those hospitals. The information of patients collected on the same forms.

Antimicrobial susceptibility assessed through MIC test by VITEK®2 Compact (BioMérieux, France and provided by DEKA *Limited Liability Company)* standardised by CLSI [18]. Antibiotics which have been used are*were (with number coding – abbreviation for Figure 3):* penicillin (1-PEN), gentamycin (2-GM), ciprofloxacin (3-CIP), levofloxacin (4-LVX), moxifloxacin (5- MXF), tetracycline (6-TE), erythromycin (7-ERY), clindamycin (8-CM), trimethoprim/sulfamethoxazole (9-SXT), vancomycin (10-VAN), rifampin (11-RIF), quinupristin/dalfopristin (12-QD), linezolid (13-LZD), oxacillin (14-OXA), tigecycline (15-TGE).

Using QIAamp DNA Mini Kit (USA) for DNA extraction (including isolation and quantification), we performed the experimental procedure according to manufacturer's instruction. PCR amplification performed in PCR master mix (Invitrogen – USA) that consisted of 200 µM of each dNTPs (dATP, dCTP, dGTP, dTTP), 100 pM primers, 1 U Taq DNA polymerase, 10 mM Tris-HCl, 1.5 mM $MgCl_2$ and 10 µl DNA template. Specific primers for *mecA*, *femA*, and *femB* genes showed in table 1. The experiments were performed using the protocol with 25 cycles that each of them consisted of 3 steps including denaturing (94^0C for 1 minute), priming (57^0C for 1 minute), synthesising of sequence (72^0C for 1 minute). PCR products were performed electrophoresis, imaged routinely and sequenced. The sequence of PCR products was compared with the original gene's sequence on GenBank to confirm *mecA, femA, and femB* genes.

Table 1: Specific primers for mecA gene

Target gene	Primer	Nucleotide sequence (5' – 3')	Size (bp)	Location
mecA	Mec-A1	5' – AAA ATC GAT GGT AAA GGT TGG C – 3'	533	1282-1303
	Mec-A2	5' – AGT TCT GCA GTA CCG GAT TTG C – 3'		1739-1814
femA	Fem-A1	5' – AGA CAA ATA GGA GTA ATG AT – 3'	509	595-614
	Fem-A2	5' – AAA TCT AAC ACT GAG TGA TA – 3'		1084-1103
femB	Fem-B1	5' – TTA CAG AGT TAA CTG TTA CC – 3'	651	1904-1923
	Fem-B2	5' – ATA CAA ATC CAG CAC GCT CT – 3'		2535-2554

Ethical considerations

The Ethics Committee of the National Hospital of Tropical Diseases and Military Hospital 103 approved the protocol of the study. The study was in line with the Declaration of Helsinki. Written informed consent has been signed by all participants after full explanation. After that, the blood samples were collected.

Statistical Analysis

The statistical analysis was conducted using the R language. Graphics also were performed by the R language. In this study, the analysis of such enormous volumes of information in the acquisition of data from 43 strains, each strain companion with genes (*mecA, femA, and femB*) and 15 antibiotics with 3 levels of resistance (susceptible, intermediate, resistance). For this reason, we used R language to analyse.

Results

Characteristics of the patient in this study showed in Table 2.

Table 2: Characteristics of patients

Characteristics		Number (Percentage)
Age (subgroup)		
	16-19	5 (11.63)
	20-29	5 (11.63)
	30-39	11 (25.58)
	40-49	7 (16.28)
	50-59	9 (20.93)
	≥ 60	6 (13.95)
Gender		
	Male	40 (93.02 %)
	Female	3 (6.98 %)
History of the medical conditions		
	Cirrhosis	4 (9.3)
	Self-report alcoholism	4 (9.3)
	Spinal cord injury	3 (6.98)
	Diabetes	2 (4.65)
	Hypertension	2 (4.65)
	Hepatitis	2 (4.65)
	Chronic arthritis	2 (4.65)
	Urinary tract stone	1 (2.33)
	Heart failure	1 (2.33)
	Deep vein thrombosis	1 (2.33)
	No	21 (48.83)
Time to hospitalization		
	< 5	17 (39.53)
	5-14	21 (48.84)
	>14	5 (11.63)

Among 43 *S. aureus* strains isolated analysed, 23 S. aureus strains were MRSA strains (53.5 %), and 20 S. aureus strains were MSSA strains (46.5%). Detail information of showed in Table 3.

Table 3: Methicillin-resistant S. aureus and methicillin-resistant encoding genes

Result	Number of strains (n = 43) Percentage (%)
MRSA	23 (53.49%)
MSSA	20 (46.51%)
mecA	25 (58.13%)
femA	21 (48.84%)
femB	38 (88.37%)
mecA + femA	11 (25.58%)
mecA + femB	23 (53.84%)
mecA + femA + femB	10 (23.25%)

And among that, 58.1 % strains were identified as producing *mecA*, and 22 of 23 MRSA strains (95.7%) proved to be having *mecA* gene when 15% strains in the MSSA group possessed this gene. The prevalence of *femB* gene of overall strains, MRSA, and MSSA was 88.4%, 82.6%, and 95%, respectively. The prevalence of *femA* gene of whole strains, MRSA, and MSSA was 48.8%, 47.8%, and 50%, respectively. More information showed in Table 4.

Table 4: Encoding genes of methicillin-resistant in S. Aureus

Gene	MRSA (n = 23)				MSSA (n = 20)			
	Positive (+)		Negative (-)		Positive (+)		Negative (-)	
	n	(%)	n	(%)	n	(%)	n	(%)
mecA	22	95.65	1	4.34	3	15	17	85
femA	11	47.83	12	52.17	10	50	10	50
femB	19	82.6	4	17.4	19	95	1	5
mecA + femA	10	43.47	13	56.53	1	5	19	95
mecA + femB	17	73.91	6	26.09	6	30	14	70
mecA + femA + femB	9	39.13	14	60.87	1	5	19	95

Figure 1 showed the highest prevalence of resistance to penicillin (PEN -100%), followed by erythromycin (ERY - 65.1%) and clindamycin (CM - 60.5%).

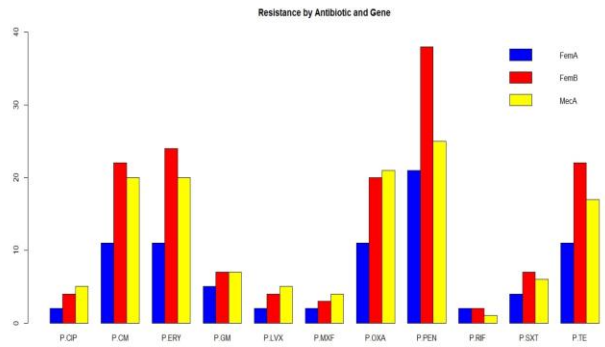

Figure 1: Antibiotic resistant profile

While Figure 2 showed highly active antibiotics in quinolone group, include ciprofloxacin (CIP - 83.7% of isolates), levofloxacin (LVX - 86.1% of isolates) and moxifloxacin (MXF - 86.1% of isolates). Several antibiotics were susceptible (100%), include vancomycin, tigecycline, linezolid, quinupristin/ dalfopristin.

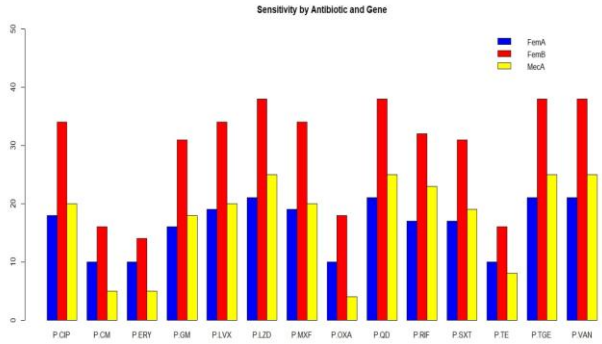

Figure 2: Antibiotic sensitivity profile

The level of resistance (MIC) in MRSA group to clindamycin, erythromycin, tetracycline, levofloxacin, ciprofloxacin, moxifloxacin was higher than MSSA group. In each antibiotic, detail information of genes showed. Figure 3 showed that the distribution of three *femA*, f*emB*, and *mecA* genes is equivalent to 15 antibiotics.

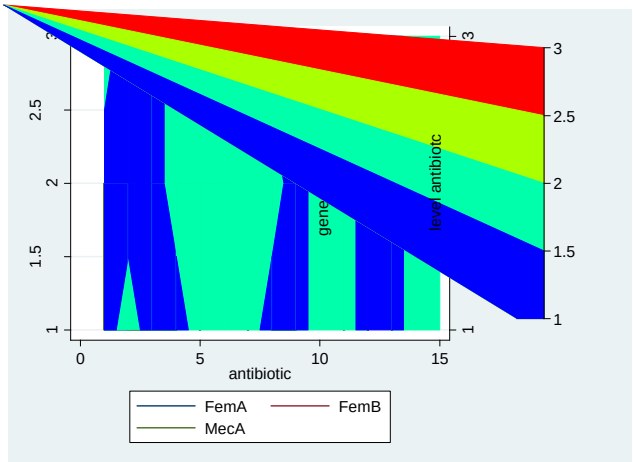

Figure 3: Distribution the antibiotic resistance level with genes. Antibiotic gene: 1.FemA; 2.FemB; 3.MecA. Antibiotic resistance level: From 1 to 3 are R, S, I, respectively; Antibiotic: From 1 to 15 is the ordinal number of 15 antibiotics

The rate of sensitivity also accounts for the majority of ciprofloxacin, levofloxacin, moxifloxacin, linezolid, quinupristin/ dalfopristin, rifampin, tigecycline, vancomycin distributed in all three genes but most in the *femB* gene. The intermediate response is concentrated in moxifloxacin and rifampin antibiotics. Antibiotic resistance focused on antibiotics clindamycin, erythromycin, oxacillin, penicillin, and tetracycline. Figure 3 supported figures 1 and 2 to visualise the association between the gene and antibiotic resistance.

Table 5 clarified the detail of antibiotic resistance with *S. aureus*. While MRSA strains were highly resistant to penicillin, erythromycin, clindamycin, and tetracycline with the rate following: 100%, 82.6%, 87%, 73.9%, respectively, MSSA strains showed a lower prevalence of resistance to these agents with the rate following: 20%, 9%, 6%, 3%, respectively. Both groups were susceptible to vancomycin, tigecycline, linezolid, quinupristin/ dalfopristine at the rate of 100%.

Table 5: The antibiotic resistance profile of S. Aureus

Antimicrobial agents	MRSA			MSSA		
	S (%)	I (%)	R (%)	S (%)	I (%)	R (%)
Penicillin			23 (100)			20 (100)
Erythromycin	4 (17.39)		19 (82.61)	11 (55)		9 (45)
Clindamycin	3 (17.04)		20 (86.96)	14 (70)		6 (30)
Tetracycline	6 (26.09)		17 (73.91)	17 (65)		3 (35)
Gentamycin	16 (69.57)		7 (30.43)	17 (85)		3 (15)
Trimethoprim/sulfamethoxazole	17 (73.91)		6 (26.09)	16 (80)		4 (20)
Ciprofloxacin	18 (78.26)	0 (0)	5 (21.74)	18 (90)	1 (5.0)	1 (5.0)
Levofloxacin	18 (78.26)		5 (21.74)	19 (95)		1 (5.0)
Moxifloxacin	18 (78.26)	1 (4.35)	4 (17.39)	19 (95)	0 (0)	1 (5.0)
Rifampin	22 (95.65)	0 (0)	1 (4.35)	14 (70)	5 (25)	1 (5.0)
Vancomycin	23 (100)			20 (100)		
Quinupristin/dalfopristin	21 (100)			22 (100)		
Linezolid	23 (100)			20 (100)		
Tigecycline	23 (100)			20 (100)		

Discussion

The methicillin-resistant in *S. aureus* strains are encoded by mobile genes with the *mecA* and *femB* gene was the most frequently. The incidence of MRSA varies from region to region. In our study, among 43 *S. aureus* strains have been analysed in BSI patients, 53.5% strains were identified as MRSA that was higher than study in Northern Vietnam (37%) [17]. Comparing with other countries, it was higher than the Philippines (38.1%), India (22.6%) [19] but lower than that of Korea (77.6%), Taiwan (65%), Hong Kong (56.8%), Sri Lanka (86.5%) [19].

Almost cases (22/23) with MRSA had *mecA* gene and the 100% resistance to penicillin was found that in line with the present study [20]. Our results about *mecA* gene have been shown that the *mecA* gene is responsible for resistance to methicillin [21] with the mechanisms have been proved [11] and 15% strains in MSSA group possessed this gene. Mohanasoundaram et al. showed similar findings with 100% MRSA possessed *mecA* gene, and only one MSSA strain had maintained this gene [22]. The 15% rate of MSSA positive for the *mecA* gene is quite high, and field literature reported a rate of 3% for MSSA positive for *mecA* [23]. The potential explanation regarding this high number is that the resistance gene transmitted in the hospital between bacteria. Thus, this finding in our study provides useful information to determine the prevalence of *mecA* gene in MSSA patients. In our study, *femB* gene was detected in almost *S. aureus* isolates, 82.6% in MRSA and 95% in the MSSA group, respectively. This result corroborated with Kobayashi et al. [24] but the differences between two studies that needed to highlight were the expression of *femA* gene showed very high (89.4%) [24] in Kobayashi's study and lower rate in our research (48.8%). Further analysis of the expression of these genes in staphylococci will be needed.

MRSA in BSIs has been shown substantial increase in the 21 century [25]. As a result, its burden was growing not only in Europe [15], [26] but also worldwide [27]. Finding the appropriate therapy became crucial and glycopeptides had been used as an effective empirical antibiotic therapy for MRSA[28]. But in the time of antibiotics and resistance becoming popular, *S. aureus* also starts resistance to vancomycin that leading high financial burden and increased mortality [29], [30], [31]. The knowledge of antibiotic resistance profile is critical in clinical practice. In our study, some routine antibiotic agents used commonly in our area showed high resistance. The results of our study also showed that vancomycin, tigecycline, linezolid, quinupristin/dalfopristin emerged as choices for empiric therapy instead. Fan Zhang et al. showed similar findings with a high rate of resistance to penicillin (100%), erythromycin (73.3%) and clindamycin (57.3%) and the clear choice for treatment were vancomycin in these cases [20]. In our study, methicillin-resistant encoding genes showed high correlation with antibiotic resistance. Penicillin, erythromycin, clindamycin, and tetracycline showed resistant to MRSA but susceptibility to MSSA. The remarkable results in our study were that vancomycin, tigecycline, linezolid, quinupristin/dalfopristin were entirely susceptible to both groups. It guides to use antibiotics in case of suspecting bloodstream infection caused by *S. aureus.*

Limitation of study: The isolates of *S. aureus* strains included seem to be quite old (2012-2014), but it still plays an important role in the reflection of the current epidemiological situation. The isolates included were small (43 isolates) because we focused on only bloodstream infection patients and these results of our study were useful for this kind of patient.

As a conclusion, in *S. aureus* causing bloodstream infections, antibiotic resistance was higher in penicillin, erythromycin, and clindamycin. All strains were entirely susceptible to vancomycin, tigecycline, linezolid, quinupristin/dalfopristin.

Ethical approval

This study is approved by the ethics committee of National Hospital of Tropical Diseases and Military Hospital 103.

Informed consent

The consent and commitment were signed by the patients in the study.

References

1. Laupland KB. Incidence of bloodstream infection: a review of population-based studies. Clinical microbiology and infection. 2013; 19(6): 492-500. https://doi.org/10.1111/1469-0691.12144 PMid:23398633

2. Kang CI, Song JH. Antimicrobial resistance in Asia: current epidemiology and clinical implications. Infect Chemother. 2013; 45(1): 22-31. https://doi.org/10.3947/ic.2013.45.1.22 PMid:24265947 PMCid:PMC3780932

3. De Kraker M, et al. The changing epidemiology of bacteraemias in Europe: trends from the European Antimicrobial Resistance Surveillance System. Clinical Microbiology and Infection. 2013; 19(9): 860-868. https://doi.org/10.1111/1469-0691.12028 PMid:23039210

4. Khatib R, et al. Persistent Staphylococcus aureus bacteremia: incidence and outcome trends over time. Scandinavian journal of infectious diseases. 2009; 41(1):4-9. https://doi.org/10.1080/00365540802441711 PMid:18821135

5. Wang JL, et al. Comparison of both clinical features and mortality risk associated with bacteremia due to community-acquired methicillin-resistant Staphylococcus aureus and methicillin-susceptible S. aureus. Clin Infect Dis. 2008; 46(6): 799-806. https://doi.org/10.1086/527389 PMid:18266610

6. Nickerson EK, et al. Staphylococcus aureus disease and drug resistance in resource-limited countries in south and east Asia. Lancet Infect Dis. 2009; 9(2):130-5. https://doi.org/10.1016/S1473-3099(09)70022-2

7. Cosgrove SE, et al. Comparison of mortality associated with methicillin-resistant and methicillin-susceptible Staphylococcus aureus bacteremia: a meta-analysis. Clin Infect Dis. 2003; 36(1):53-9. https://doi.org/10.1086/345476 PMid:12491202

8. Kuehnert MJ, et al. Methicillin-resistant-Staphylococcus aureus hospitalizations, United States. Emerging infectious diseases. 2005; 11(6):468. https://doi.org/10.3201/eid1106.040831 PMid:15963281 PMCid:PMC3367609

9. Cassini A, et al. Attributable deaths and disability-adjusted life-years caused by infections with antibiotic-resistant bacteria in the EU and the European Economic Area in 2015: a population-level modelling analysis. The Lancet Infectious Diseases. 2019; 19(1):56-66. https://doi.org/10.1016/S1473-3099(18)30605-4

10. Song J-H, et al. Spread of methicillin-resistant Staphylococcus aureus between the community and the hospitals in Asian countries: an ANSORP study. Journal of Antimicrobial Chemotherapy. 2011; 66(5):1061-1069. https://doi.org/10.1093/jac/dkr024 PMid:21393157

11. Grundmann H, et al. Emergence and resurgence of meticillin-resistant Staphylococcus aureus as a public-health threat. The Lancet. 2006; 368(9538): 874-885. https://doi.org/10.1016/S0140-6736(06)68853-3

12. Deresinski S. Methicillin-Resistant Staphylococcus aureus: An Evolutionary, Epidemiologic, and Therapeutic Odyssey. Clinical Infectious Diseases. 2005; 40(4):562-573. https://doi.org/10.1086/427701 PMid:15712079

13. Thaden JT, et al. Survival benefit of empirical therapy for Staphylococcus aureus bloodstream infections in infants. The Pediatric infectious disease journal. 2015; 34(11):1175. https://doi.org/10.1097/INF.0000000000000850 PMid:26222060 PMCid:PMC4604046

14. Drews TD, Temte JL, Fox BC. Community-associated methicillin-resistant Staphylococcus aureus: review of an emerging public health concern. WMJ-MADISON-. 2006; 105(1):52.

15. Lee BY, et al. The economic burden of community-associated methicillin-resistant Staphylococcus aureus (CA-MRSA). Clinical Microbiology and Infection. 2013; 19(6):528-536. https://doi.org/10.1111/j.1469-0691.2012.03914.x PMid:22712729 PMCid:PMC3463640

16. Vestergaard M, Frees D, Ingmer H. Antibiotic Resistance and the MRSA Problem. Microbiol Spectr. 2019; 7(2). https://doi.org/10.1128/microbiolspec.GPP3-0057-2018 PMid:30900543

17. Dat VQ, et al. Bacterial bloodstream infections in a tertiary infectious diseases hospital in Northern Vietnam: aetiology, drug resistance, and treatment outcome. BMC Infect Dis. 2017; 17(1):493. https://doi.org/10.1186/s12879-017-2582-7 PMid:28701159 PMCid:PMC5508750

18. Clinical and L.S. Institute, Performance Standards for Antimicrobial Susceptibility Testing of Anaerobic Bacteria: Informational Supplement. Clinical and Laboratory Standards Institute (CLSI), 2009.

19. Song JH, et al. Spread of methicillin-resistant Staphylococcus aureus between the community and the hospitals in Asian countries: an ANSORP study. J Antimicrob Chemother. 2011; 66(5):1061-9. https://doi.org/10.1093/jac/dkr024 PMid:21393157

20. Zhang F, et al. Bacterial susceptibility in bloodstream infections: Results from China Antimicrobial Resistance Surveillance Trial (CARST) Program, 2015-2016. Journal of global antimicrobial resistance. 2019. https://doi.org/10.1016/j.jgar.2018.12.016 PMid:30611932

21. Ubukata K, et al. Homology of mecA gene in methicillin-resistant Staphylococcus haemolyticus and Staphylococcus simulans to that of Staphylococcus aureus. Antimicrobial agents and chemotherapy. 1990; 34(1):170-172. https://doi.org/10.1128/AAC.34.1.170 PMid:1691614 PMCid:PMC171544

22. Mohanasoundaram K, Lalitha M. Comparison of phenotypic versus genotypic methods in the detection of methicillin resistance in Staphylococcus aureus. Indian Journal of Medical Research. 2008; 127(1):78.

23. Proulx MK, et al. Reversion From Methicillin Susceptibility to Methicillin Resistance in Staphylococcus aureus During Treatment of Bacteremia. J Infect Dis. 2016; 213(6):1041-8. https://doi.org/10.1093/infdis/jiv512 PMid:26503983 PMCid:PMC4760414

24. Kobayashi N, et al. Detection of mecA, femA, and femB genes in clinical strains of staphylococci using polymerase chain reaction. Epidemiology & Infection. 1994; 113(2):259-266. https://doi.org/10.1017/S0950268800051682 PMid:7925664 PMCid:PMC2271538

25. Johnson AP, Pearson A, Duckworth G. Surveillance and epidemiology of MRSA bacteraemia in the UK. Journal of Antimicrobial Chemotherapy. 2005; 56(3):455-462. https://doi.org/10.1093/jac/dki266 PMid:16046464

26. Köck R, et al. Methicillin-resistant Staphylococcus aureus (MRSA): burden of disease and control challenges in Europe, 2010. https://doi.org/10.2807/ese.15.41.19688-en PMid:20961515

27. Liebowitz LD. MRSA burden and interventions. International journal of antimicrobial agents. 2009; 34:S11-S13. https://doi.org/10.1016/S0924-8579(09)70551-5

28. Gemmell CG, et al. Guidelines for the prophylaxis and treatment of methicillin-resistant Staphylococcus aureus (MRSA) infections in the UK. Journal of antimicrobial chemotherapy. 2006; 57(4):589-608. https://doi.org/10.1093/jac/dkl017 PMid:16507559

29. Hawkey P. The growing burden of antimicrobial resistance. Journal of antimicrobial chemotherapy. 2008; 62(suppl_1): i1-i9. https://doi.org/10.1093/jac/dkn241 PMid:18684701

30. Johnson LB, et al. Staphylococcus aureus bacteremia: compliance with standard treatment, long-term outcome and predictors of relapse. Scandinavian journal of infectious diseases. 2003; 35(11-12): 782-789. https://doi.org/10.1080/00365540310016682 PMid:14723349

31. Chang F-Y, et al. Staphylococcus aureus bacteremia: recurrence and the impact of antibiotic treatment in a prospective multicenter study. Medicine. 2003; 82(5):333-339. https://doi.org/10.1097/01.md.0000091184.93122.09 PMid:14530782

ID Design Press, Skopje, Republic of Macedonia
Open Access Macedonian Journal of Medical Sciences. 2019 Dec 30; 7(24):4411-4415.
https://doi.org/10.3889/oamjms.2019.872
eISSN: 1857-9655
Basic and Clinical Medical Researches in Vietnam

The Role of Serial NT-ProBNP Level in Prognosis and Follow-Up Treatment of Acute Heart Failure after Coronary Artery Bypass Graft Surgery

Bui Duc Thanh[1], Nguyen Hong Son[2], Dinh Cong Pho[3], Nguyen Duy Bac[4], Vu Thi Nga[5], Quan Anh Dung[3], Do Duc Anh[6], Do Dieu Linh[7], Hoang Thi Bich Viet[8], Bui Dang The Anh[9], Ha The Tan[9], Pham Ngoc Hung[4,9*]

[1]Intensive Care Unit, 175 Military Hospital, Ho Chi Minh City, Vietnam; [2]175 Military Hospital, Ho Chi Minh City, Vietnam; [3]Faculty of Medicine, Vietnam Military Medical University, Hanoi, Vietnam; [4]Department of Training, Vietnam Military Medical University, Hanoi, Vietnam; [5]Institute for Research and Development, Duy Tan University, 03 Quang Trung, Danang, Vietnam; [6]Faculty of Medicine, University of Medical Sciences of Revolutionary Armed Force (UCIMED de Las FAR), Marianao, Havana, Cuba; [7]Faculty of Medicine, Hai Phong Medical University, 72A Nguyen Binh Khiem, Hai Phong, Vietnam; [8]Department of Occupational Lung Disease, National Lung Hospital, 463 Hoang Hoa Tham, Ba Dinh, Ha Noi, Vietnam; [9]Department of Epidemiology, Vietnam Military Medical University, Hanoi, Vietnam

Citation: Thanh BD, Son NH, Pho DC, Bac ND, Nga VT, Dung QA, Anh DD, Linh DD, Viet HTB, Anh BDT, Tan HT, Hung PN. The Role of Serial NT-ProBNP Level in Prognosis and Follow-Up Treatment of Acute Heart Failure after Coronary Artery Bypass Graft Surgery. Open Access Maced J Med Sci. 2019 Dec 30; 7(24):4411-4415. https://doi.org/10.3889/oamjms.2019.872

Keywords: N-terminal pro-B-type natriuretic peptide (NT-proBNP); serial measurements; acute heart failure (AHF); coronary artery bypass graft surgery (CABG); prognosis; follow-up treatment

***Correspondence:** Pham Ngoc Hung, Assoc. Prof, PhD, MD. Department of Epidemiology, Vietnam Military Medical University; Department of Training, Vietnam Military Medical University. Phone number: +84939613388. ORCID: https://orcid.org/0000-0002-5458-8001. Email: pnhungqy@vmmu.edu.vn

Received: 11-Nov-2019; **Revised:** 26-Nov-2019; **Accepted:** 27-Nov-2019; **Online first:** 20-Dec-2019

Funding: This research did not receive any financial support

Competing Interests: The authors have declared that no competing interests exist

Abstract

BACKGROUND: After coronary artery bypass graft (CABG) surgery, heart failure is still major problem. The valuable marker for it is needed.

AIM: Evaluating the role of serial NT-proBNP level in prognosis and follow-up treatment of acute heart failure after CABG surgery.

METHODS: The prospective, analytic study evaluated 107 patients undergoing CABG surgery at Ho Chi Minh Heart Institute from October 2012 to June 2014. Collecting data was done at pre- and post-operative days with measuring NT-proBNP levels on the day before operation, 2 hours after surgery, every next 24 h until the 5th day, and in case of acute heart failure occurred after surgery.

RESULTS: On the first postoperative day (POD1), the NT-proBNP level demonstrated significant value for AHF with the cut-off point = 817.8 pg/mL and AUC = 0.806. On the second and third postoperative day, the AUC value of NT- was 0.753 and 0.751. It was statistically significant in acute heart failure group almost at POD 1 and POD 2 when analyzed by the doses of dobutamine, noradrenaline, and adrenaline (both low doses and normal doses).

CONCLUSION: Serial measurement of NT-proBNP level provides useful prognostic and follow-up treatment information in acute heart failure after CABG surgery.

Introduction

Acute heart failure emerged as the primary cause of mortality after heart surgery in general and CABG surgery in particular [1]. It needs to early recognize before operation that helps clinicians consider patients who had heart failure into subgroups and allocate resources to maximize benefit from treatment and minimize risks such as adverse events. To predict early outcomes from cardiac surgery, both clinical tools (scoring systems) and biochemical tests were used. The two most common scoring systems were the EuroSCORE [2] and the Parsonnet score [3]. Although frequently used, it also had some limitations [4], [5]. To resolve, some biochemical tests were considered. Among that, NT-proBNP was emerged as one of the promise markers in heart disease, especially in heart failure [6]. It was used to predict postoperative outcomes in heart surgery in both early [7] and long-term effects [8]. The Canadian guideline recommended using it in persons with HF as a prognostic factor [9].

The guideline of ESC also remarked NT-proBNP as one of prognostic factors [10]. Moreover, in CABG surgery, it independently predicted postoperative outcome [11]. In combination with existing clinical tools such as EuroSCORE II, it showed more accuracy than using it alone [12].

Besides predictive ability before cardiac surgery [13], NT-proBNP levels contribute a valuable role in heart failure management [14] evenly in acute or unstable state [15]. Elevating NT-proBNP levels in these situations was associated with poor clinical outcomes [16], [17]. To optimize medical therapy, serial NT-proBNP measurement was used in stable CHF patients [18]. But in acute heart failure after CABG surgery, data of this biochemical marker were too limited.

Therefore, this study aimed to evaluate the serial NT-proBNP level that could provide prognostic and follow-up treatment information of acute heart failure after CABG surgery.

Materials and Methods

We conducted this prospective study on 107 patients who underwent CABG surgery at Ho Chi Minh Heart Institute from October 2012 to June 2014. Inclusion criteria included patients with established diagnoses of coronary artery stenosis based on angiography; aged 18 and older; consultation of internal medicine and surgery, and indication for CABG according to the recommendation American Internal Medicine Association (ACC/AHA/ACP /ASIM).

The exclusion criteria were: aged <18; damage of 1 or 2 branches of coronary artery; overall 50 - 60% of coronary artery stenosis with excepting main body; < 50% diameter of coronary artery stenosis; concomitant cardiac surgery such as valve surgery and septal surgery ; renal function insufficiency (eGFR <30 ml/min/1.73m^2).

Monitoring

Chronic heart failure (CHF) before surgery was diagnosed according to the Framingham criteria, while postoperative diagnosis of acute heart failure (AHF) was followed the guidelines of Viet Nam Heart Association 2015 with staging A, B, C and D according to ACC/AHA and grading according to NYHA. Indexes in heart failure were recorded in echocardiography. The main prognosis factor of heart failure after surgery were EuroSCORE and the level of serial NT-proBNP. NT-proBNP level was quantified at the Department of Biochemistry at Ho Chi Minh Heart Institute, using the electrochemiluminescence immunoassay (ECLIA). The optimal cutting points of NT-proBNP to determine acute heart failure for ages younger than 50, from 50 to 75 and older than 75 years are 450, 900 and 1800 pg/ml, respectively. The NT-proBNP-independent age cut point less than 300 pg/ml had a negative diagnostic value to rule out acute heart failure at 98%.Collecting time was noted as following: B0: the day before surgery; B1: 2 hours after surgery; B2, B3, B4, B5 were collected at 8 a.m on days 2, 3, 4, 5 after surgery; Bx: at the time of expression of cardiac dysfunction (continuous monitoring of cardiac index on the Flo-Trac system) or when the patient presents with acute heart failure.

We also recorded data about dosage and using time of dobutamine, noradrenaline, and adrenaline in collecting time after surgery to follow-up treatment. Collecting time was noted as following: N0: the day before surgery; N1: 2 hours after surgery; N2, N3, N4, N5 were collected at 8 a.m on days 2, 3, 4, 5 after surgery. In addition, follow-up at times when patients showed cardiac impairment or when acute heart failure occurred.

Statistical analysis

Statistical analysis was performed by Epidata 6 and STATA version 14.0 software.

Descriptive analysis presented as mean ± standard deviation (95% confidence interval). Testing t-Student/Mann-Withney U test/Wilcoxon/ANOVA and Chi-square/ Fisher's exact test, Kolmogorov test, Person correlation, single and multivariate linear regression methods used in the study. p-value < 0.05 was known as statistically significant.

Results

Out of 107 patients, 67.3% was male. Medical history was chest pain (98.1%), hypertension (77.6%), myocardial ischemia (77.6%), heart failure (28.0%), diabetes (24.3%), myocardial infarction (9.4%), dyslipidemia (7.5%), arrhythmias (4.7%), COPD (3.7%), and renal failure (1.9%). Demographics of CHF before surgery and AHF after surgery showed in Table 1.

Table 1: Demographics of chronic heart failure before surgery and acute heart failure after surgery

Pre-operative condition	Post-operative condition			
	Without AHF	AHF	Total	p-value
Without CHF	64 (78.1 %)	7 (28.0 %)	71 (66.4 %)	< 0.0001
CHF	18 (21.9 %)	18 (72.0 %)	36 (33.6 %)	< 0.0001
Total	82 (76.6 %)	25 (23.4 %)	107 (100%)	< 0.0001

Note: CHF: Chronic heart failure; AHF: Acute heart failure.

On the first postoperative day (POD1), the NT-proBNP level demonstrated significant value for AHF in patients undergoing CABG surgery with the cut-off point = 817.8 pg/mL and AUC = 0.806 (95% CI = 0.71 to 0.90; p<0.0001; sensitivity = 70%; and specificity = 80.5%). The values of NTproBNP for AHF on the second and third postoperative days (POD 2 and POD3) showed detail in Table 2.

Table 2*:* Cut-off values of NT-proBNP according to Euro-score

Post-operative day (POD)	Cut-off value	Sensitivity	Specificity	AUC (95% CI)	Youden – Index
POD 1	817.8	70.0 %	80.5 %	0.806 (0.71 – 0.90)	0.505
POD 2	2,516	66.7 %	77.9 %	0.753 (0.64 – 0.87)	0.446
POD 3	3,556	60.0 %	81.6 %	0.751 (0.64 – 0.86)	0.416

Note: AUC: Area under the curve; CI: Confidence Interval.

Table 3 performed detail analysis of NT-proBNP cut-off value according to EuroSCORE.

Table 3: Detail analysis of cut-off value of NT-proBNP according to EuroSCORE

		EuroSCORE						Cut-off NT-proBNP					
		L and I risk	High risk	Indexes Sen	Spe	Acc	P-value	≤ Cut-off	> Cut-off	Indexes Sen	Spe	Acc	P-value
Pre-operative Cut-off (508.8 pg/ml)	Without CHF (71)	58 (81.7)	13(18.3)	47.2	81.7	70.1	0.002	56 (78.9)	15 (21.1)	80.6	78.9	79.44	0.000
	CHF (36)	19 (52.8)	17 (47.2)					7 (19.4)	29 (80.6)				
POD 1 Cut-off (871.8 pg/ml)	No AHF (94)	73 (77.7)	21 (22.3)	77.7	69.2	76.64	0.002	70 (74.5)	24 (25.5)	74.5	92.3	76.64	0.000
	AHF (13)	4 (30.8)	9 (69.2)					1 (7.7)	12 (92.3)				
POD 2 Cut-off (2516 pg/ml)	No AHF (98)	74 (75.5)	24(24.5)	75.5	66.7	74.8	0.014	68(69.4)	30(30.6)	69.4	77.8	70.1	0.008
	AHF (9)	3 (33.3)	6 (66.7)					2(22.2)	7 (77.8)				
POD 3 Cut-off (3556 pg/ml)	Without AHF(104)	76(73.1)	28(26.9)	66.7	73.1	72.9	0.189	74(71.8)	29(28.2)	100	71.8	72.6	0.026
	AHF (3)	1 (33.3)	2 (66.7)					0 (0)	3 (100)				

Note: Sensitivity = Sen; Specificity = Spe ;Accurac = ACC , POD: Postoperative day; CHF: Chronic heart failure; AHF: Acute heart failure; Low and Intermediate risk = L and I risk.

To follow-up treatment, the general dosage and using time of inotrope was shown in Table 4.

Table 4: Dosage and using time of inotrope (µg/kg/min)

Factors		Post-operative condition Without AHF (n=82)	AHF (n=25)	p-values
Noradrenalin	Dosage	0.85 ± 1.59	0.14 ± 0.12	0.75[f]
	Using time	43.1 ± 28.9	112.9 ± 37.5	0.000[c]
Dobutamine	Dosage	3.32 ± 1.82	6.25 ± 2.47	0.000[f]
	Using time	29.1 ± 28.2	101.1 ± 47.3	0.000[f]
Adrenalin	Dosage	0.026 ± 0.048	0.15 ± 0.15	0.000[f]
	Using time	16.6 ± 30.7	82.9 ± 55.6	0.000[f]

Note: AHF: Acute heart failure.

More detail showed in Table 5 (dobutamine), table 6 (noradrenaline), and table 7 (adrenaline). The level of NT-proBNP level in AHF group was statistically significant compared to the without AHF group at POD 1 and POD 2 when analyzed by the normal doses of dobutamine. In low doses, it just showed statistically significant at POD 2 (Table 5). In AHF group it was statistically significant compared to the without AHF group at POD 1 and POD 2 when analyzed by the low doses of noradrenaline. In low doses, it did not show statistically significant at POD all three days after surgery (Table 6).

Table 5: Level of serum NT-proBNP and dobutamine doses

Time	Dobutamin doses	Post-operative condition Without AHF	AHF	p-values
POD 1	Low doses (< 5 µg)	496.1 ± 609.9	2885	0.1[f]
	Normal doses (5-15 µg)	1.077.5 ± 2.154.5	2.499.8 ± 1.646.7	0.000[f]
	p-values	0.041[f]	0.59[f]	
POD 2	Low doses (< 5 µg)	1.956.8 ± 1.728.9	6.088 ± 4.774.8	0.023[f]
	Normal doses (5-15 µg)	3.465.2 ± 3.224.7	9.387.5 ± 8.623.8	0.036[f]
	p-values	0.049[f]	0.796[f]	
POD 3	Low doses (< 5 µg)	3.653.3 ± 4.984.2		
	Normal doses (5-15 µg)	5.797.8 ± 3.937	8.123.7 ± 4.636.0	0.393[f]
	p-values	0.001[f]		

Note: POD: Post-operative day; AHF: Acute heart failure.; f. Mann-Withney U test.

When analyzed by the normal doses of adrenaline, in AHF group it was statistically significant compared to the without AHF group at POD 1 and POD 2.

Table 6: Level of serum NT-proBNP and noradrenalin doses

Time	Noradrenalin dosage	Post-operative condition Without AHF	AHF	p-values
POD 1	Low dosage (<0.01 µg)	862.7 ± 1.855.5	2.447.2 ± 628.5	0.0001[f]
	Normal dosage (≥0.01 µg)	749.8 ± 871.9	2.578.7 ± 2.172.9	0.062[f]
	p-values	0.7[f]	0.81[f]	
POD 2	Low dosage (<0.01 µg)	2.335.5 ± 2.436.2	9.252.8 ± 9.681.3	0.014[f]
	Normal dosage (≥0.01 µg)	3.509 ± 2751.1	7.081.3 ± 4.235.8	0.073[f]
	p-values	0.03[f]	0.807[f]	
POD 3	Low dosage (<0.01 µg)	3.952.7 ± 5.067.4	13.415	0.13[f]
	Normal dosage (≥0.01 µg)	5.804.9 ± 3.476.9	5.478 ± 994.2	0.89[f]
	p-values	0.003[f]	0.221[f]	

Note: POD: Post-operative day; AHF: Acute heart failure.; f. Mann-Withney U test.

It is statistically significant in POD 2 and POD 3 when analyzed by the low doses of adrenaline (Table 7).

Table 7: Level of serum NT-proBNP and adrenalin doses

Time	Adrenalin	Post-operative condition Without AHF	AHF	p-values
POD 1	Low dosage (<0.05 µg)	585.3 ± 726.6	2.595	0.12[f]
	Normal doage (≥0.05)	1.444.4 ± 2.911	2.523.9 ± 1.650.3	0.004[f]
	p-values	0.051[f]	1[f]	
POD 2	Low dosage (<0.05 µg)	1.855.6 ± 1.725.2	2.733.8 ± 8.32.3	0.07[f]
	Normal doage (≥0.05)	4.047.4 ± 3.237.4	12.730.8 ± 7.332.3	0.004[f]
	p-values	0.000[f]	0.014[f]	
POD 3	Low dosage (<0.05 µg)	3.140.1 ± 3.890.3	9.095 ± 6.109.4	0.045[f]
	Normal doage (≥0.05)	8.015.2 ± 5.590.9	6.181	0.694
	p-values	0.000[f]	1[f]	

Note: POD: Post-operative day; AHF: Acute heart failure.; f. Mann-Withney U test.

Discussion

NT-proBNP reflected the grade of heart failure [19] and proved to be useful indicator for evaluating heart failure [16] In cardiac surgery, it pointed out as independent indicator to predict postoperative outcomes [20]. Compared with other indicators, it seems to be equal to euroSCORE but superior than ejection fraction [21]. It was used in various types of cardiac surgery such as percutaneous coronary

intervention [22], surgery for aortic stenosis.[23], and CABG [11]. As the role of prognosis in CABG patients, NT-proBNP in combined with EuroSCORE II provided better prognosis accuracy with AUC = 0.93 and the cut-off point of NT-proBNP level was 1028 pg/ml [12]. When using it alone as an independent indicator to predict postoperative mortality, NT-proBNP also showed as valuable factor with HR = 2.02 and the cut-off point was 2,000 pg/ml [24]. To maximize the accuracy of NT-proBNP level, the cofounders that affected it must be eliminated. In general, factor affecting systolic function such as valve disease that can be elevated NT-proBNP level through elevating filling pressure of left ventricle [6]. Patients with heart valve abnormality (aortic or mitral stenosis) often had higher pre-operative levels than coronary diseases [25]. In our study, there was no patient with concomitant valve disease that reduced the risk of bias. The other important element affecting NT-ProBNP level was renal function. The relation between them was associated inversely [26] with increasing NT-proBNP level as decreasing eGFR [27]. Thus, in our study we excluded patients with renal function insufficiency to reduce the bias of NT-proBNP level.

NT-proBNP had shown evidence as a predictor of prognosis but what collecting time was better to predict also remained unknown [28]. One of the most advantages in our study was serial measurements of the NT-ProBNP that help to optimize the cut off value for specific circumstances. Using single NT-proBNP level measured before surgery to predict both severe circulatory failure and mortality in hospital after surgery [11]. Although preoperative measurement was independently predictive of postoperative outcome [29], [30], clinical assessment combined with biomarker tests also showed more useful value [7], [31]. However, natriuretic peptides were not included in post-operation follow-up. To further understanding, evaluating NT-proBNP in this period was needed. It was more valuable in prediction of mortality when using serial measurements within 12 hours [32]. It showed as strong predictors for both short-term and long-term prognosis [33].

When acute heart failure develops, NT-proBNP also increases and vice versa. That is why we used serum NT-proBNP level as an indicator of follow-up treatment in this study. It had been proved superior to standard care in guiding heart failure treatment with cost-effective, improving quality of life, and reversing ventricular remodeling [34]. Single NT-proBNP measurements can provide a diagnostic index, but it is unreasonable for treatment because of disease changing rapidly and need to use medical therapy to stabilize individual patients directly. Serial NT-proBNP measurements may provide intraindividual variation of NT-proBNP that reflects the real condition of patients. In our study, we used day by day measurements to follow continuously.The exact interpretation will lead to set up suitable treatment strategies. It can predict predicts adverse events during follow-up [35] and from that individually optimizing medical therapy for each patient [18]. In our study, level of NT-proBNP in AHF group was statistically significant compared to the without AHF group almost at POD 1 and POD 2 when analyzed by the doses of dobutamine, noradrenaline, and adrenaline (both low doses and normal doses). The dose of inotrope drugs was in line with NT-proBNP level. These results provide a valuable indicator in intensive management after CABG.

In conclusion, serial measurement of NT-proBNP level provides useful prognostic and follow-up treatment information in acute heart failure after CABG surgery.

Ethical approval

This study is approved by the ethics committee of 108 Military Central Hospital.

Informed consent

The consent and commitment were signed by the patients in the study

References

1. O'Connor GT, et al. Results of a regional study of modes of death associated with coronary artery bypass grafting. Northern New England Cardiovascular Disease Study Group. Ann Thorac Surg. 1998; 66(4):1323-8.

2. Roques F, et al. Risk factors and outcome in European cardiac surgery: analysis of the EuroSCORE multinational database of 19030 patients. Eur J Cardiothorac Surg. 1999; 15(6):816-22; discussion 822-3. https://doi.org/10.1016/S1010-7940(99)00106-2

3. Parsonnet V, Dean D, Bernstein AD. A method of uniform stratification of risk for evaluating the results of surgery in acquired adult heart disease. Circulation. 1989; 79(6 Pt 2):I3-12.

4. Wynne-Jones K, et al. Limitations of the Parsonnet score for measuring risk stratified mortality in the north west of England. The North West Regional Cardiac Surgery Audit Steering Group. Heart. 2000; 84(1):71-8. https://doi.org/10.1136/heart.84.1.71 PMid:10862595 PMCid:PMC1729412

5. Bhatti F, et al. The logistic EuroSCORE in cardiac surgery: how well does it predict operative risk? Heart. 2006; 92(12):1817-20. https://doi.org/10.1136/hrt.2005.083204 PMid:16547206 PMCid:PMC1861312

6. Weber M, Hamm C. Role of B-type natriuretic peptide (BNP) and NT-proBNP in clinical routine. Heart. 2006; 92(6):843-849. https://doi.org/10.1136/hrt.2005.071233 PMid:16698841 PMCid:PMC1860679

7. Cuthbertson BH, et al. N-terminal pro-B-type natriuretic peptide levels and early outcome after cardiac surgery: a prospective cohort study. Br J Anaesth. 2009; 103(5):647-53. https://doi.org/10.1093/bja/aep234 PMid:19713279

8. Cuthbertson BH, et al. N-terminal pro-B-type natriuretic peptide concentrations and long-term outcome after cardiac surgery: a prospective cohort study. Br J Anaesth. 2013; 110(2):214-21. https://doi.org/10.1093/bja/aes379 PMid:23183321

9. McKelvie RS, et al. The 2012 Canadian Cardiovascular Society heart failure management guidelines update: focus on acute and chronic heart failure. Canadian Journal of Cardiology. 2013; 29(2):168-181. https://doi.org/10.1016/j.cjca.2012.10.007 PMid:23201056

10. Members ATF, et al. ESC Guidelines for the diagnosis and treatment of acute and chronic heart failure 2012: The Task Force for the Diagnosis and Treatment of Acute and Chronic Heart Failure 2012 of the European Society of Cardiology. Developed in collaboration with the Heart Failure Association (HFA) of the ESC. European journal of heart failure. 2012; 14(8):803-869.

11. Holm J, et al. Preoperative NT-proBNP independently predicts outcome in patients with acute coronary syndrome undergoing CABG. Scand Cardiovasc J Suppl. 2013; 47(1):28-35. https://doi.org/10.3109/14017431.2012.731518 PMid:22989031

12. Holm J, et al. EuroSCORE II and N-terminal pro-B-type natriuretic peptide for risk evaluation: an observational longitudinal study in patients undergoing coronary artery bypass graft surgery. Br J Anaesth. 2014; 113(1):75-82. https://doi.org/10.1093/bja/aeu088 PMid:24727704

13. Polineni S, et al. Predictive Ability of Novel Cardiac Biomarkers ST2, Galectin-3, and NT-ProBNP Before Cardiac Surgery. J Am Heart Assoc. 2018; 7(14). https://doi.org/10.1161/JAHA.117.008371 PMid:29982227 PMCid:PMC6064859

14. Newton PJ, Betihavas V, Macdonald P. The role of b-type natriuretic peptide in heart failure management. Aust Crit Care. 2009; 22(3):117-23. https://doi.org/10.1016/j.aucc.2009.06.001 PMid:19589695

15. Bhardwaj A, Januzzi Jr. JL. Natriuretic peptide-guided management of acutely destabilized heart failure: rationale and treatment algorithm. Crit Pathw Cardiol. 2009; 8(4):146-50. https://doi.org/10.1097/HPC.0b013e3181c4a0c6 PMid:19952548

16. Di Angelantonio E, et al. B-type natriuretic peptides and cardiovascular risk: systematic review and meta-analysis of 40 prospective studies. Circulation. 2009; 120(22):2177-87. https://doi.org/10.1161/CIRCULATIONAHA.109.884866 PMid:19917883

17. Bettencourt P, et al. N-terminal-pro-brain natriuretic peptide predicts outcome after hospital discharge in heart failure patients. Circulation. 2004; 110(15):2168-74. https://doi.org/10.1161/01.CIR.0000144310.04433.BE PMid:15451800

18. Franke J, et al. Is there an additional benefit of serial NT-proBNP measurements in patients with stable chronic heart failure receiving individually optimized therapy? Clin Res Cardiol. 2011; 100(12):1059-67. https://doi.org/10.1007/s00392-011-0340-1 PMid:21779816

19. Clerico A, Emdin M. Diagnostic accuracy and prognostic relevance of the measurement of cardiac natriuretic peptides: a review. Clin Chem. 2004; 50(1):33-50. https://doi.org/10.1373/clinchem.2003.024760 PMid:14633912

20. Nashef SA, et al. EuroSCORE II. Eur J Cardiothorac Surg. 2012; 41(4):734-44; discussion 744-5.

21. Eliasdottir SB, et al. Brain natriuretic peptide is a good predictor for outcome in cardiac surgery. Acta Anaesthesiol Scand. 2008; 52(2):182-7. https://doi.org/10.1111/j.1399-6576.2007.01451.x PMid:17949462

22. Jaberg L, et al. Prognostic value of N-terminal pro-B-type natriuretic peptide in patients with acute coronary syndromes undergoing left main percutaneous coronary intervention. Circ J. 2011; 75(11):2648-53. https://doi.org/10.1253/circj.CJ-11-0095 PMid:21891968

23. Jiang H, et al. NT-proBNP and postoperative heart failure in surgery for aortic stenosis. Open Heart. 2019; 6(1):e001063. https://doi.org/10.1136/openhrt-2019-001063 PMid:31218010 PMCid:PMC6546186

24. Hinderliter AL, et al. Independent prognostic value of echocardiography and N-terminal pro-B-type natriuretic peptide in patients with heart failure. Am Heart J. 2008; 156(6):1191-5. https://doi.org/10.1016/j.ahj.2008.07.022 PMid:19033018 PMCid:PMC3665504

25. Jiang H, et al. Impact of underlying heart disease per se on the utility of preoperative NT-proBNP in adult cardiac surgery. PloS one. 2018; 13(2):e0192503. https://doi.org/10.1371/journal.pone.0192503 PMid:29420603 PMCid:PMC5805306

26. McCullough PA, et al. B-type natriuretic peptide and renal function in the diagnosis of heart failure: an analysis from the Breathing Not Properly Multinational Study. American Journal of Kidney Diseases. 2003; 41(3):571-579. https://doi.org/10.1053/ajkd.2003.50118 PMid:12612980

27. Chenevier-Gobeaux C, et al. Influence of renal function on N-terminal pro-brain natriuretic peptide (NT-proBNP) in patients admitted for dyspnoea in the Emergency Department: comparison with brain natriuretic peptide (BNP). Clin Chim Acta. 2005; 361(1-2):167-75. https://doi.org/10.1016/j.cccn.2005.05.021 PMid:15993397

28. Balion C, et al. Testing for BNP and NT-proBNP in the diagnosis and prognosis of heart failure. Evid Rep Technol Assess (Full Rep). 2006; 142:1-147.

29. Fellahi JL, et al. Does preoperative B-type natriuretic peptide better predict adverse outcome and prolonged length of stay than the standard European System for Cardiac Operative Risk Evaluation after cardiac surgery? J Cardiothorac Vasc Anesth. 2011; 25(2):256-62. https://doi.org/10.1053/j.jvca.2010.05.009 PMid:20674395

30. Pedrazzini GB, et al. Comparison of brain natriuretic peptide plasma levels versus logistic EuroSCORE in predicting in-hospital and late postoperative mortality in patients undergoing aortic valve replacement for symptomatic aortic stenosis. Am J Cardiol. 2008; 102(6):749-54. https://doi.org/10.1016/j.amjcard.2008.04.055 PMid:18774001

31. De Maria R, et al. Predictive value of EuroSCORE on long term outcome in cardiac surgery patients: a single institution study. Heart. 2005; 91(6):779-784. https://doi.org/10.1136/hrt.2004.037135 PMid:15894777 PMCid:PMC1768917

32. Luers C, et al. Serial NT-proBNP measurements for risk stratification of patients with decompensated heart failure. Herz. 2010; 35(7):488-95. https://doi.org/10.1007/s00059-010-3377-4 PMid:20927502

33. Sargento L, et al. Serial measurements of the Nt-ProBNP during the dry state in patients with systolic heart failure are predictors of the long-term prognosis. Biomarkers. 2014; 19(4):302-13. https://doi.org/10.3109/1354750X.2014.910549 PMid:24735006

34. Januzzi JL, Troughton R. Are serial BNP measurements useful in heart failure management? Serial natriuretic peptide measurements are useful in heart failure management. Circulation. 2013; 127(4):500-7; discussion 508. https://doi.org/10.1161/CIRCULATIONAHA.112.120485 PMid:23357662

35. Bayes-Genis A, et al. Serial NT-proBNP monitoring and outcomes in outpatients with decompensation of heart failure. Int J Cardiol. 2007; 120(3):338-43. https://doi.org/10.1016/j.ijcard.2006.10.009 PMid:17174423

ID Design Press, Skopje, Republic of Macedonia
Open Access Macedonian Journal of Medical Sciences. 2019 Dec 30; 7(24):4416-4419.
https://doi.org/10.3889/oamjms.2019.873
eISSN: 1857-9655
Basic and Clinical Medical Researches in Vietnam

Risk Factors for Stroke Associated Pneumonia

Do Quyet[1], Nguyen Minh Hien[2], Mai Xuan Khan[1], Pham Dinh Dai[2], Do Duc Thuan[2], Dang Minh Duc[2], Nguyen Dang Hai[2], Bui Van Nam[2], Pham Quoc Huy[3], Mai Duy Ton[4], Dang Tien Truong[5], Vu Thi Nga[6], Dang Phuc Duc[2*]

[1]Respiratory Center, Military Hospital 103, Hanoi, Vietnam; [2]Stroke Department, Military Hospital 103, Hanoi, Vietnam; [3]Emergency Department, Military Hospital 103, Hanoi, Vietnam; [4]Emergency Department, Bach Mai Hospital, Hanoi, Vietnam; [5]Vietnam Military Medical University, Hanoi, Vietnam; [6]Institute for Research and Development, Duy Tan University, Danang, Vietnam

Citation: Quyet D, Hien NM, Khan MX, Dai PD, Thuan DD, Duc DM, Hai ND, Nam BV, Huy PQ, Ton MD, Truong DT, Nga VT, Duc DP. Risk Factors for Stroke Associated Pneumonia. Open Access Maced J Med Sci. 2019 Dec 30; 7(24):4416-4419. https://doi.org/10.3889/oamjms.2019.873

Keywords: stroke; stroke-associated pneumonia (SAP); National Institutes of Health Stroke Scale (NIHSS); Gugging Swallowing Screen (GUSS)

***Correspondence:** Dang Phuc Duc. Department of Stroke, Military Hospital 103, No 261 Phung Hung str, Ha Dong distr, Hanoi, Vietnam. Phone: +84 976819546. E-mail: dangphucduc103@gmail.com or dangphucduc@vmmu.edu.vn

Received: 01-Nov-2019; **Revised:** 20-Nov-2019; **Accepted:** 25-Nov-2019; **Online first:** 20-Dec-2019

Funding: This research did not receive any financial support

Competing Interests: The authors have declared that no competing interests exist

Abstract

BACKGROUND: Stroke patients are at high risk for stroke-associated pneumonia (SAP). If patients suffer from pneumonia their prognosis will worsen.

AIM: To identify factors that increases the risk of SAP in stroke patients.

METHODS: A group of 508 patients hospitalized within 5 days after the onset of stroke were enrolled prospectively.

RESULTS: The incidence of SAP was 13.4%. Some major risk factors for SAP are: mechanical ventilation (MV) had odds ratio (OR) 16.4 (p <0.01); the National Institutes of Health Stroke Scale (NIHSS) > 15 OR 9.1 (p <0.01); the Gugging Swallowing Screen (GUSS) 0-14 OR 11.7 (p <0.01).

CONCLUSION*:* SAP is a frequent complication. We identified some risk factors of SAP, especially stroke severity (NIHSS > 15), swallowing disorder (GUSS < 15) and mechanical ventilation.

Introduction

Stroke is dangerous because it causes cause high rates of death and disability. Stroke-related DALYs (disability-adjusted life-years) ranked second in the list of 10 leading causes of DALYs [1]. The proportion of DALYs and deaths caused by stroke had been increased when compared with all diseases, from 3.5% (in 1990) to 4.6% (in 2013) [1]. Previous studies demonstrated that complications have a bad effect on the disability rate and mortality rate. Of all post-stroke complications, SAP is considered a major one with a strong impact on the outcome [2]. SAP is associated with increased mortality, prolonged the time of stay in hospital, and poor outcome on discharge [2]. Early identification of the probability of SAP is required to improve outcomes of SAP patients. Although various studies on risk factors for SAP were conducted, their results were inconsistent. In particular, according to our search results at the National Library of Vietnam, there is currently no research on this topic in Vietnam. So we conducted this study to identify the risk factors for stroke-related pneumonia in stroke patients.

Subjects and Methods

Patient selection

All adult patients aged from 18 years and

more admitted to the Stroke Department from March 2014 to April 2016, were diagnosed with stroke based on the WHO definition [3].

SAP diagnosis was based on Pneumonia In Stroke Consensus (PISCES) [4]: pneumonia (according to CDC standards) occurred within 7 days after onset of stroke.

Methods

We enrolled prospectively 508 stroke patients during the first 24 hours after admission and followed continuously until discharge. The collected data included medical history, routine blood test, chest X-rays, electrocardiogram and cranial computed tomography. The severity of stroke was evaluated by NIHSS [5]. NIHSS is a simple, reliable and validated scale whereby higher scores indicate a more severe stroke. NIHSS is a scale with values from 0 (normal neurological functions) to 42 (absolutely neurological deficiency). Patients' swallowing ability was evaluated by the GUSS [6]. Total GUSS score ranges from 20 (normal swallowing function) to 0 (absolutely no ability to swallow).

During the prospective follow-up, SAP occurrence was recorded. Descriptive measures were applied for quantitative variables. We used Student t-test for normality distribution and Mann-Whitney test for abnormality distribution. Two categorical variables were compared by the Chi-Square test. Odds ratios (OR) were used in discovery the relation between pneumonia and the risk factors. All the tests in this study were 2-tailed and we determined the statistical significance level of 0.01. Data were analyzed by IBM SPSS version 22.

Results

We collected data from 508 patients admitted to the Stroke Department, Military Hospital 103. The results in Table 1 show the characteristics of the patient. The mean age was 65.6 ± 12.4 years. Ischemic stroke accounted for 60% and the incidence rate of SAP was 13.4%.

Comparing results between SAP and non-SAP groups showed that: SAP group had higher NIHSS (15.1 ± 8.6 and 7.7 ± 5.9, respectively, $p < 0.01$) lower GCS (12.6 ± 2.8 and 14.2 ± 1.7, respectively, $p < 0.01$), and lower GUSS (9.2 ± 6.6 vs 17.0 ± 4.8, respectively, $p < 0.01$), all differences were significant ($p < 0.01$). The SAP group had a higher mechanical ventilation rate than the non-SAP group (39.7% and 3.9%, respectively, $p < 0.01$).

Table 1: Characteristics of patients

Characteristics	SAP n (%)	non-SAP n (%)	Total n (%)	p
Stroke types				
Ischemic	31 (45.6)	274 (62.3)	305 (60.0)	0.070
Hemorrhagic	37 (54.4)	166 (37.7)	203 (40.0)	
Sex				
Female	26 (38.2)	160 (36.4)	186 (36.6)	0.432
Male	42 (61.8)	280 (63.6)	322 (63.4)	
Age (years)				
≤ 70	35 (51.5)	**279 (63.4)**	314 (61.8)	**0.620**
> 70	33 (48.5)	161 (36.6)	194 (38.2)	
Mean ± SD	69.2 ± 12.2	65.6 ± 12.4	66.0 ± 12.5	0.024
GCS (median)	13	15	15	< 0.01
NIHSS (median)	15	6	7	< 0.01
GUSS (median)	11	19	18	< 0.01
Diabetes				
Yes	18 (26.5)	42 (9.5)	60 (11.8)	< 0.01
Smoke				
Yes	5 (7.4)	34 (7.7)	39 (7.7)	0.910
Mechanical ventilation				
Yes	27 (39.7)	17 (3.9)	44 (8.7)	< 0.01
Total	68 (13.4)	440(86.6)	508 (100)	

The univariate logistic regression analysis showed that hemorrhagic type, prior medical history of diabetes mellitus, mechanical ventilation, Glasgow 3-8, NIHSS 16-42, GUSS 0-14 and hyperglycemia at admission were associated with SAP (shown in Table 2). Among them, 3 outstanding SAP risk factors are mechanical ventilation (OR 16.4, 95%CI 8.2-32.5, $p < 0.01$), GUSS < 15 (OR 11.7, 95%CI 6.6 - 20.8, $p < 0.01$) and NIHSS > 15 (OR 9.1, 95%CI 5.2 - 16.0, $p < 0.01$).

Table 2: Some risk factors of SAP (n = 508)

Risk factors	OR, CI 95%	p
Stroke type: Hemorrhagic	2.0 (1.2 - 3.3)	< 0.01
Diabetes	3.4 (1.8-6.4)	< 0.01
Mechanical ventilation	16.4 (8.2-32.5)	< 0.01
GCS ≤ 8	7.2 (3.2 - 16.0)	< 0.01
NIHSS > 15	9.1 (5.2 - 16.0)	< 0.01
GUSS < 15	11.7 (6.6 - 20.8)	< 0.01
Hyperglycemia at admission	3.0 (1.7 - 5.2)	< 0.01

Discussion

SAP is a common complication after stroke [7]. In our study, 13.4% (68/508) developed SAP.

A lot of studies were conducted to find out factors that increase the probability of SAP. Some of them developed prognosis scales of the pneumonia risk in stroke patients (Table 3).

Because of too many scoring systems for the prognosis of the pneumonia risk are existent, Kishore et al. conducted a study investigating the accuracy of the existing scales of risk factors for pneumonia in 2016 [16]. The authors found that prognostic factors included in the scoring systems are: age; sex; NIHSS; GCS; speech disorder; swallowing disorder; falls at onset of stroke; blood pressure increase > 200mmHg; disability before stroke; atrial fibrillation; heart failure; COPD; smoking; drinking a lot of alcohol; prior medical history of pneumonia; diabetes mellitus; mechanical ventilation; CT or MR brain images

(location of lesions, intra-ventricular hemorrhage, hematoma volume).

Table 3: Risk factors for SAP in some scales

Risk factor	Schepp et al (2012) [8]	Friedant et al (2015) [9]	Smith et al (2015) [10]	Chumbler et al (2010) [11]	Hoffmann et al (2012) [12]	Kumar et al (2017) [13]	Harms et al (2013) [14]	Ji et al (2013) [15]
Old age	×	×	×	×	×	×	×	×
Male			×					
mRS prior to hospital			×					×
Prior history of pneumonia				×	×			
AF	×							×
COPD	×							×
Diabetes		×						
Heart failure						×		×
Smoking								×
Drinking too much								×
Hemorrhagic stroke	×							
GCS decreased							×	×
Falls at onset				×				
NIHSS increased	×	×	×	×	×			×
Swallowing disorders				×	×	×		×
Systolic blood pressure> 200mmHg							×	
Hyperglycemia								×

Hemorrhagic stroke was related to the risk of SAP with OR = 2.0. Our research results are consistent with those of Divani et al that: hemorrhagic type was related to a higher risk of SAP [17]. Schepp et al. conducted their research on 1,008 stroke patients and found that: hemorrhagic stroke patients have a higher risk of SAP than cerebral infarction patients with OR = 1.67 [8] .

Diabetes is a common risk factor of stroke. Hyperglycemia was an independent prognostic factor for bacteria infection and SAP [18]. In our study, patients with a history of diabetes in the SAP group was 26.5%, higher than that of the non-SAP group (9.5%), the difference was significant ($p < 0.01$). Patients who had a history of diabetes had an increased risk of SAP with OR 3.4. The study by Zhang in 2016, conducted on 1,149 ischemic stroke patients showed that the proportion of diabetes in the SAP group is 24.4% higher than in the non-SAP group (18.4%). According to Sari et al. (2017) diabetes was related to the risk of SAP (OR = 2.09; 95% CI: 0.83-5.29; $p = 0.12$) [19].

Patients with consciousness disorders which lead to an increased risk of swallowing disorder, aspiration, reduction in the ability to cough, spit. GCS at admission below 8 was an independent prognostic factor of infection and SAP [18]. These factors increase the risk of SAP. As our results, stroke patients with severe consciousness disorders (Glasgow 3-8) had a high risk of SAP with OR 7.2, $p < 0.01$.

The proportion of severe stroke (the NIHSS over 15) in the SAP group was higher than that in the non-SAP group (47.1% and 9.1%, respectively, $p < 0.01$). NIHSS > 15 increased the risk of SAP with OR 16.4 (95%CI 8.2 - 32.5, $p < 0.01$). Our results are consistent with other authors, such as Smith et al., the patients who had NIHSS > 15 caused the risk of pneumonia with OR=9.58 [10]. Results from other studies had also shown that high scores of NIHSS increased the risk of SAP [11], [12], [13], [15], [19], [20].

A stroke happens in the cerebral hemisphere, cerebellum, or brain stem can damage swallowing physiology. Cerebral stroke lesions can destroy the voluntary function of mastication and interrupt the bolus transport process of the oral phase. The lesions in the precentral gyrus may cause not only contralateral disorder in facial, tongue and lip motor function but also contralateral compromise in peristalsis of pharynx. Brain stem stroke may cause sensation loss of the mouth, cheek, and tongue, delay the trigger of the pharynx and glottis. [21]. Due to swallowing disorders, foreign objects, food, pathogens easily enter the lower respiratory of pneumonia patients. The study conducted by Bray et al., (2016) with nearly 60,000 stroke patients showed that if the patient were examined for early swallowing disorders in order to have appropriate preventive measures, the rate of pneumonia after stroke would reduce from 13.8 % to 8% [22].

The patients who had GUSS 0-14 would have a higher risk of pneumonia than patients with GUSS 15-20: OR = 11.7, $p < 0.01$. There are various scales to measure swallowing disorders, of which GUSS is the most popular one. According to Trapl et al., when comparing the diagnostic value of swallowing disorder by GUSS with the esophageal endoscopy, Kappa coefficient was 0.835 [23]. The author divided swallowing disorder into 4 levels: severe (GUSS 0-9 scores); medium (GUSS 10-14); mild (GUSS 15-19) and no swallowing disorder (GUSS 20). Of which, risk of aspiration will be high for the patients with GUSS ≤ 14 scores [23]. GUSS had 100% sensitivity, 69% specificity in assessing the risk of aspiration [24]. The study conducted by Zhang et al. in 2016 [25] on 1,149 patients with ischemic stroke showed that swallowing disorder was a risk of pneumonia with OR = 16.68 (95% CI: 10.28-27.07; $p <0.05$). Sari et al. (2017) [19] studied on SAP in Indonesia and Japan. The results showed that swallowing disorder is a risk of pneumonia, OR = 12.62 ($p = 0.001$). Therefore the authors concluded that swallowing impairment is an independent risk for pneumonia [26].

Mechanical ventilation caused a high risk of pneumonia with OR 16.4 ($p <0.01$). Hinduja et al. (2015) [18] conducted research on 202 primary intracerebral hemorrhage patients: mechanical ventilation was an independent prognostic factor infection and SAP. Alsumarain et al. [27] studied on 290 stroke patients with cerebral hemorrhage and

found that mechanical ventilation increased the risk of pneumonia with OR = 9.42

In conclusion, our study identified the risk factors related to SAP in stroke patients. We have shown that SAP is a frequent complication. We identified some risk factors of SAP, especially stroke severity (NIHSS > 15), swallowing disorder (GUSS < 15) and mechanical ventilation.

Ethical statements

This study was started after being approved by the ethics committee of the Vietnam Military Medical University.

References

1. Feigin VL, Norrving B, Mensah GA. Global burden of stroke. Circulation research. 2017; 120(3):439-448. https://doi.org/10.1161/CIRCRESAHA.116.308413 PMid:28154096

2. Teh W-H, et al. Impact of stroke-associated pneumonia on mortality, length of hospitalization, and functional outcome. Acta Neurologica Scandinavica. 2018; 138(4):293-300. https://doi.org/10.1111/ane.12956 PMid:29749062

3. Aho K, et al. Cerebrovascular disease in the community: results of a WHO collaborative study. Bulletin of the World Health Organization. 1980; 58(1):113.

4. Smith CJ, et al. Diagnosis of Stroke-Associated Pneumonia: Recommendations From the Pneumonia in Stroke Consensus Group. Stroke. 2015; 46(8):2335-2340. https://doi.org/10.1161/STROKEAHA.115.009617 PMid:26111886

5. World Health Organization. WHO STEPS stroke manual: the WHO STEPwise approach to stroke surveillance, 2005.

6. Trapl M, et al. Dysphagia bedside screening for acute-stroke patients: the Gugging Swallowing Screen. Stroke. 2007; 38(11):2948-2952. https://doi.org/10.1161/STROKEAHA.107.483933 PMid:17885261

7. Cugy E, Sibon I. Stroke-Associated Pneumonia Risk Score: Validity in a French Stroke Unit. Journal of Stroke and Cerebrovascular Diseases. 2017; 26(1):225-229. https://doi.org/10.1016/j.jstrokecerebrovasdis.2016.09.015 PMid:27839768

8. Schepp SK, Tirschwell DL, Longstreth WT. Abstract 2695: A Clinical Prediction Rule for Pneumonia after Acute Stroke. Stroke. 2012; 43(1):A2695. https://doi.org/10.1161/STROKEAHA.111.638254 PMid:22156697 PMCid:PMC3288702

9. Friedant AJ, et al. A simple prediction score for developing a hospital-acquired infection after acute ischemic stroke. Journal of Stroke and Cerebrovascular Diseases. 2015; 24(3):680-686. https://doi.org/10.1016/j.jstrokecerebrovasdis.2014.11.014 PMid:25601173 PMCid:PMC4359649

10. Smith CJ, et al. Can a Novel Clinical Risk Score Improve Pneumonia Prediction in Acute Stroke Care? A UK Multicenter Cohort Study. Journal of the American Heart Association. 2015; 4(1):1-10. https://doi.org/10.1161/JAHA.114.001307 PMid:25587017 PMCid:PMC4330058

11. Chumbler NR, et al. Derivation and validation of a clinical system for predicting pneumonia in acute stroke. Neuroepidemiology. 2010; 34(4):193-199. https://doi.org/10.1159/000289350 PMid:20197702 PMCid:PMC2883837

12. Hoffmann S, et al. Development of a clinical score (A2DS2) to predict pneumonia in acute ischemic stroke. Stroke. 2012; 43(10):2617-2623. https://doi.org/10.1161/STROKEAHA.112.653055 PMid:22798325

13. Kumar S, et al. ACDD4 score: A simple tool for assessing risk of pneumonia after stroke. Journal of the neurological sciences. 2017; 372:399-402. https://doi.org/10.1016/j.jns.2016.10.050 PMid:27823836

14. Harms H, et al. Predicting post-stroke pneumonia: the PANTHERIS score. Acta neurologica Scandinavica. 2013; 128(3):178-184. https://doi.org/10.1111/ane.12095 PMid:23461541

15. Ji R, et al. Novel risk score to predict pneumonia after acute ischemic stroke. Stroke. 2013; 44(5):1303-1309. https://doi.org/10.1161/STROKEAHA.111.000598 PMid:23482598

16. Kishore AK, et al. Clinical risk scores for predicting stroke-associated pneumonia: A systematic review. European Stroke Journal. 2016; 1(2):76-84. https://doi.org/10.1177/2396987316651759 PMid:31008268 PMCid:PMC6301233

17. Divani AA, et al. Predictors of nosocomial pneumonia in intracerebral hemorrhage patients: a multi-center observational study. Neurocritical care. 2015; 22(2):234-242. https://doi.org/10.1007/s12028-014-0065-x PMid:25231530

18. Hinduja A, et al. Nosocomial infections in patients with spontaneous intracerebral hemorrhage. American Journal of Critical Care. 2015; 24(3):227-231. https://doi.org/10.4037/ajcc2015422 PMid:25934719

19. Sari IM, et al. Comparison of Characteristics of Stroke-Associated Pneumonia in Stroke Care Units in Indonesia and Japan. Journal of Stroke and Cerebrovascular Diseases. 2017; 26(2):280-285. https://doi.org/10.1016/j.jstrokecerebrovasdis.2016.09.018 PMid:27746080

20. Walter U, et al. Predictors of pneumonia in acute stroke patients admitted to a neurological intensive care unit. J Neurol. 2007; 254(10):1323-9. https://doi.org/10.1007/s00415-007-0520-0 PMid:17361338

21. Martino R, et al. Dysphagia after stroke incidence, diagnosis, and pulmonary complications. stroke. 2005; 36(12):2756-2763. https://doi.org/10.1161/01.STR.0000190056.76543.eb PMid:16269630

22. Bray BD, et al. The association between delays in screening for and assessing dysphagia after acute stroke, and the risk of stroke-associated pneumonia. J Neurol Neurosurg Psychiatry. 2016; 88:25-30. https://doi.org/10.1136/jnnp-2016-313356 PMid:27298147

23. Trapl M, et al. Dysphagia bedside screening for acute-stroke patients. Stroke. 2007; 38(11):2948-2952. https://doi.org/10.1161/STROKEAHA.107.483933 PMid:17885261

24. St John J, Berger L. Using the gugging swallowing screen (GUSS) for dysphagia screening in acute stroke patients. The Journal of Continuing Education in Nursing. 2015; 46(3):103-104. https://doi.org/10.3928/00220124-20150220-12 PMid:25723329

25. Zhang X, et al. The A2DS2 score as a predictor of pneumonia and in-hospital death after acute ischemic stroke in Chinese populations. PloS one. 2016; 11(3):1-9. https://doi.org/10.1371/journal.pone.0150298 PMid:26950337 PMCid:PMC4780726

26. De Castillo LLC, D.E.P. Sumalapao, and J.L.R. Pascual, Risk factors for pneumonia in acute stroke patients admitted to the Emergency Department of a Tertiary Government Hospital. National Journal of Physiology, Pharmacy and Pharmacology. 2017; 7(8):855-859. https://doi.org/10.5455/njppp.2017.7.0411008052017

27. Alsumrain M, et al. Predictors and outcomes of pneumonia in patients with spontaneous intracerebral hemorrhage. Journal of intensive care medicine. 2013; 28(2):118-123. https://doi.org/10.1177/0885066612437512 PMid:22337709

ID Design Press, Skopje, Republic of Macedonia
Open Access Macedonian Journal of Medical Sciences. 2019 Dec 30; 7(24):4420-4426.
https://doi.org/10.3889/oamjms.2019.874
eISSN: 1857-9655
Basic and Clinical Medical Researches in Vietnam

Neuromuscular Blockade Agents Reversal with Sugammadex Compared to Neostigmine in the Living Kidney Donors

Thuy Luu Quang[1], Huyen Nguyen Thi Thu[1], Kinh Nguyen Quoc[1], Ha Nguyen Thu[2], Dong Pham Van[3], Nguyen Le Bao Tien[4], Vo Van Thanh[4,5], Vu Thi Nga[6], Chu Dinh Toi[7*]

[1]Center for Anesthesia and Surgical Intensive Care, Viet Duc Hospital, Hanoi, Vietnam; [2]Anesthesia & Intensive Care Departement, Hanoi Medical University, Hanoi, Vietnam; [3]Anesthesia and Pain Medicine, Cho Ray Hospital, Ho Chi Minh City, Viet Nam; [4]Institute of Orthopaedics and Trauma Surgery, Viet Duc Hospital, Hanoi, Vietnam; [5]Department of Surgery, Hanoi Medical University, Hanoi, Vietnam; [6]Institute for Research and Development, Duy Tan University, Danang, Vietnam; [7]Department of Human and Animaly Physiology, Faculty of Biology, Hanoi National University of Education, Hanoi, Vietnam

Citation: Quang TL, Thu HNT, Quoc KN, Thu HN, Van DP, Tien NLB, Thanh VV, Nga VT, Toi CD. Neuromuscular Blockade Agents-- Reversal with Sugammadex Compared to Neostigmine in the Living Kidney Donors. Open Access Maced J Med Sci. 2019 Dec 30; 7(24):4420-4426. https://doi.org/10.3889/oamjms.2019.874

Keywords: muscle relaxants; living kidney donors; sugammadex

***Correspondence:** Chu Dinh Toi. Department of Human and Animaly Physiology, Faculty of Biology, Hanoi National University of Education, Hanoi, Vietnam. E-mail: chudinhtoi.hnue@gmail.com

Received: 10-Nov-2019; **Revised:** 16-Nov-2019; **Accepted:** 17-Nov-2019; **Online first:** 20-Dec-2019

Funding: This research did not receive any financial support

Competing Interests: The authors have declared that no competing interests exist

Abstract

BACKROUND: The reversation of NMBA (neuromuscular blocking agents) prevents numerous postoperative complications, increases quality of recovery and decreases the time, expenditure spending in hospital. The choice of medicine used to reverse NMBA depends considered as a key fators to gain the best outcome and to avoid the side effects.

AIM: To evaluate the postoperative effect on muscle relaxation reversal and side effects of sugammadex 2 mg/kg versus the combination of neostigmine and atropine sulfate in the living kidney donors.

METHODS: A randomised controlled trial on 70 patients undergoing living kidney donation surgery were allocated to 2 groups. Patients in group I (SUGA) were reversed with sugammadex 2 mg/kg and in group II (NEO/ATR) with the combination of neostigmine and atropine sulfat.

RESULTS: With 35 patients in each group, the study results showed that after 3 mintutes of reversal patients reaching TOF value ≥ 0.9 in group SUGA is 91.4%, after 5 minutes 100% of patients in group SUGA reached TOF value ≥ 0.9 . In group NEO/ATR after 3 minutes 28.6% patients reached TOF ≥ 0.9 and 40% patients reached TOF≥ 0.9 after 5 minutes. The difference in percentage of patients reaching TOF ≥ 0.9 after 3 minutes, 5 minutes of reversal between two groups is significant ($p<0.05$). After 10 minutes, 100% patients in both group got TOF ≥ 0.9. Time to exutubation of group SUGA was 249.43 ± 81.75 seconds and it was 456.29 ± 146.45 seconds in group NEO/ATR. Nausea, bradycardia, and increased phlegm production in group NEO/ATR was 22.9%; 28.5%; 25.7% respectively; while those side effects were not met in group SUGA, the difference was significant ($p<0.05$).

CONCLUSION: The muscle relaxation reversal effect of sugammadex was faster than that of neostigmine, the duration TOF ≥ 0.9 and the time to extubation was significantly faster. Sugammadex did not cause hemodynamic changes before and after muscle relaxation reversal, neostigmine resulted in the bradycardia, increased phlegm secreting and other side effects. The renal function after 24 hours postoperatively of two groups was similar.

Introduction

Nowadays, living donor nephrectomy in Viet Nam is usually performed under laparascopic methods, due to numerous advantages for the donors such as reduced blood loss, decreased tissue trauma, lower analgesia requirement, faster resumption of food and drinks intake, shorter hospitalisation and better postoperative cosmetic appearance. However, increasing abdominal pressure due to pneunoperitonium can affect the kidney function by impairing renal perfusion flow and does not facilitate surgeon's procedure [1]. Therefore, profound neuromuscular blockade plays essential role in limitting the increase in abdominal pressure and facilitating surgical field for kidney removal. Postoperative residual curarization is a common complication after surgery that impacts the patient's safety. Postoperative residual curarization reduces ventilation response to hypoxia; induces laryngeal muscle and esophageal sphincter dysfunction which causes reflux, choking lungs; thus increasing risk of postoperative respiratory complications. Therefore, finding a safe way to reverse muscles relaxation is fundamental to achieving successful outcomes of

surgery. Neostigmine is a common neuromuscular blockade reversal agent; with anticholinesterase mechanism which allows acetylcholine to build up at the neuromuscular junction and subsequently results in competitively inhibiting non-depolarizing blocking drugs at the nicotinic receptor of motor nerve terminals. On the other hand, this drug simultaneously acts on muscarinic receptor that leads to several side effects, so neostigmine is frequently used with anticholinergic drugs such as atropine. The dose of neostigmine should be adjusted according to TOF count, and postoperative residual curarization may still exist after neostigmin administration [2], [3]. If neostigmine is used when TOF < 0.9, it may also increase the residual neuromuscular blockade [4], [5], [6]. Sugammadex, a cyclodextrin, is thought to be an antagonist - a selective relaxant-binding agent (SRBA), which reverses the aminosteroid group like rocuronium through an encapsulating mechanism to form a rigid sugammadex-rocuronium complex and then excreted in urine. Sugammadex has some advantages such as allowing reversal of profound blockade, rapid onset as well as no muscarinic side effects and no atropine combination requirement [7], [8], [9]. Dose of sugammadex and neostigmin chosen for reversal are based on TOF value [10]. In the world, there are several studies demonstrating the safety and efficacy of sugammadex and comparing the neuromuscular blockade reversal effect of sugammadex versus that of neostigmine.

An analyzed randomized controlled trial on the reversal function of sugammadex and neostigmine conducted by M.Carron et al in 2016 shows that in comparison to neostigmine, sugammadex reverses the neuromuscular block faster ($p < 0.0001$), has a stronger relation to TOF during extubation period, and decreases risk of recurarization after endotracheal tube withdrawing (OR = 0.05, CI 95%: 0.01 – 0.43; $p = 0.0068$). Sugammasex also has a significant relation to reduction of all complications ($p < 0.00016$) [1].

In Vietnam, there have been rare studies comparing the reversal effectiveness and side effects between sugammadex and the combination of neostigmine and atropine, especially on patients experiencing living donor nephrectomy. For that reason, we conducted this study to evaluate the differences in efficacy, undesirable effects between sugammadex 2 mg/kg and the combination of neostigmine and atropine at different doses and atropine sulfate in the living kidney donors.

Materials and Methods

Criteria for selection

- Age 18-60 years old, ASA I - III.
- Laparocopic donor nephrectomy.
- General anesthesia.
- Normal results of complete blood count, physiochemical tests, echocardiogram.
- Surgery duration > 60 minutes.

Criteria for exclusion

- Patient's disagreement to participate in study.
- Patients did not meet selection requirement.
- Patients who have renal or hepatic dysfunction.
- Patients having history of malignant hyperthermia or neuromuscual diseases.
- Patients with difficult airway.
- Prolonged diabetes patients with complication, neurological complication.
- Patients with BMI < 17 kg/m^2 or > 30 kg/m^2.
- Patients taking medications interacting with neuromuscular relaxants such as anticonvulsants, magnesium, and some antibiotics.
- Patients having allergy to opioid, NMBA, anesthetics.

Patients rejected from study

- Patients had allergy to medications, or anaphylaxis shock to anesthetics.
- Patients with surgical complications.
- Patients had postoperative severe condition which required treatment in ICU and mechanical ventilation > 24h.

Study methods

This study was a single blinded randomized controlled trial. Patients were allocated to 2 groups:

- Group I (SUGA) : Sugammadex 2 mg/kg were used to reverse NMBA.
- Group II (NEO/ATR): Different doses of neostigmine combined with atropine sulfate were used

The study was perfomed at Center of Anestheisa and Surgical intensive care, Viet Duc hospital from March to September of 2018. Convenience sampling with 35 patients in each group, and patients were ramdomly assigned into group SUGA or NEO/ ATR by ballot when they were in operation center.

Research process

Preparing patients included: Anesthesia examination, explaining to patients about anesthesia

method and research. After ASA standard monitoring was applied, induction was carried out with fentanyl 1.5 mcg/kg, propofol 2 mg/kg, rocoronium 0.6 mg/kg, then an endotracheal tube was intubated when the TOF was 0. Anesthesia was maintained by sevoflurane at the MAC of 1-1.5 and intraoperative TOF was observed, additional dose of rocuronium (0.15 mg/kg) was utilised when TOF count reached 2 out of 4. TOF value after surgery was recorded right after operation. The patients were reversed neuromuscular blockade when TOF count > 0: Group SUGA (n = 35) was reversed with sugammadex 2 mg/kg, group NEO/ATR (n = 35) was reversed with neostigmine at different doses based on TOF Scan which were 60; 50; 40; 30 mcg/kg to TOF value of 1;2;3;4 respectively [10] and neostigmine was combined with atropine at ratio of 3:1. The TOF values were recorded at the time of blockade reversal, after reversal every minute until 20 minutes and then at 30 minutes and 60 minutes. Endotracheal tube extubation was performed when patients met criteria of full awareness; heart rate < 100 bpm; systolic blood pressure > 90mmHg; respiratory rate 10-12 rates/min; SpO2 > 95%; body temperature >35.5^{0}C; TOF ratio ≥ 0.9 [11].

Analyzing data

The research data was analyzed and processed by SPSS 20.0 software. Quantitative variables were described in average and standard deviations. Qualitative variables were described in percentage (%). Chi square, T-test with 95% confidence, the difference was statistically significant when p <0.05.

Results

Common features of study groups

Of 70 patients assessed for eligibility, 35 patients were randomly allocated to two groups. There are no significant differences in baseline characteristics between 2 groups such as gender, age, BMI, hemoglobin concentration or serum electrolyte (Table 1).

Table 1: Patients demographic

Features	Group SUGA (n = 35)	Group NEO/ATR (n = 35)	P
Gender (male/female)	28/7	25/10	
Age (yrs): X ± SD	33 ± 7.37	31.83 ± 7.70	
BMI (kg/m²): X ± SD	21.86 ± 3.39	20.77 ± 2.32	
Hemoglobin: X ± SD	147.09 ± 9.81	147.17 ± 9.82	
Serum sodium (mmol/l): X ± SD	136.8 ± 1.98	136.66 ± 2.04	> 0.05
Serum potassium (mmol/l): X ± SD	3.88 ± 0.33	3.82 ± 0.30	
Serum calcium (mmol/l): X ± SD	2.30 ± 0.12	2.27 ± 0.11	
Serum creatinine (mmol/l): X ± SD	80.69 ± 14.20	81.66 ± 13.28	
Serum albumin (mmol/l): X ± SD	45.49 ± 2.67	44.58 ±2.58	
Blood loss (ml): X ± SD	114.29 ± 53.64	118.57 ± 40.38	

In our study, the rate of right kidney collection in group I was 60% and group II was 71.4%, there was no significant difference in the two groups (p> 0.05). The average anesthesia time of group I was 178.43 ± 36.54 minutes and group II was 171.43 ± 25.71 minutes, this time of the two groups did not differ significantly (p > 0.05). The average amount of blood loss between the two groups was not statistically significant with p > 0.05.

Anesthesia time and medication used in surgery

The total amount of propofol, fentanyl and sevoflurane used to induce and maintain anesthesia in the two groups were matching. The average rocuronium used in group I, II are the same which are 76.15 ± 17.78 mg and 71.20 ± 11.53 respectively. There was no difference in the total amount of rocuronium used as well as the quantity of rocuronium in the last 45 minutes of the operation and the repeated dose of rocuronium of the two groups (p> 0.05) (Table 2).

Table 2: Characteristics of drugs used in surgery

Group / Index	Group I (n = 35)	Group II (n = 35)	P
Fentanyl (mg)	0.21 ± 0.05	0.9 ± 0.04	
Propofol (mg)	125.71 ± 24.53	117.74 ± 18.43	
Sevoflurane (ml)	29.69 ± 6.69	28.14 ± 6.95	> 0.05
Rocuronium (mg)	76.15 ± 17.78	71.20 ± 11.53	
Rocuronium used in the last 45 min (mg)	9.0 ± 2.56	8.17 ± 2.68	
Times of repeating rocuronium	3.14 ± 0.73	3.17 ± 0.66	

Postoperative indexes

Patients were monitored at the end of surgery the temperature; MAC (Minimum aveolar concentration) and Et Sevoflurane (expiratory sevoflurane concentration). The temperature at the end of surgery in group SUGA was 36.42 ± 0.37^{0}C which is 36.41 ± 0.37^{0}C in group NEO/ATR. MAC got to 0.44 ± 0.07 and 0.43 ± 0.06 in group SUGA and NEO/ATR. The expiratoty Sevoflurane concentration of group SUGA is 0.5 ± 0.06 comparing to 0.47 ± 0.07 in group NEO/ATR. All showed no differences with p value > 0.05

Rate of TOF ≥ 0.7 and ≥ 0.9 after reversal of NMBAs over time

After 2 minutes of reversal: 94.3% of patients in group SUGA achieved TOF ≥ 0.7, while only 31.4% of patients achieved TOF ≥ 0.7 in group NEO/ATR, the variance was statistically substantial with p <0.05. After 4 minutes of reversal: 100% patients of group SUGA achieved TOF ≥ 0.7, which statistically significantly distinguished from 65.7% in group NEO/ATR with p < 0.05. After 7 minutes of reversal: 100% of patients in both study groups achieved TOF ≥ 0.9 (Figure 1).

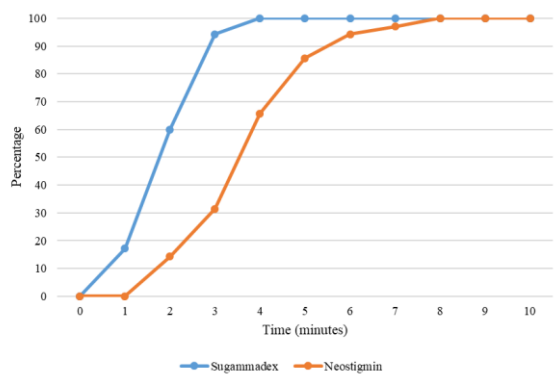

Figure 1: The ratio reaches TOF 0.7 after reversal of NMBAs over time

After 3 minutes of reversal: group SUGA had 91.4% patients achieving TOF ≥ 0.9, contrasting with only 28.6% patients in group NEO/ATR and the difference was also statistically significant with p <0.05 . After 5 minutes of reversal: 100% patients in group I gained TOF ≥ 0.9, whereas in group II only 40% of patients obtained TOF ≥ 0.9 and the mismatch was also substantial with p <0.05. After 10 minutes of reversal: 100% patients in the two study groups acquired TOF ≥ 0.9 (Figure 2).

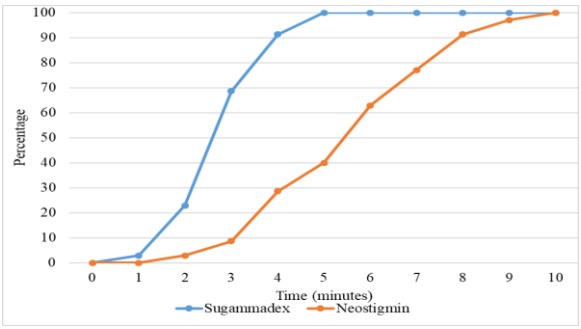

Figure 2: The ratio reaches TOF ≥ 0.9 after reversal of NMBAs over time

Time to TOF ≥ 0.7; ≥ 0.9 and time to extubation

Time from starting reversing neuromuscular block to reach TOF ≥ 0.7 and TOF ≥ 0.9 in group I is faster signigicantly than the one in group II with p <0.05 (Table 3).

Table 3: Time to TOF ≥ 0.7; ≥ 0.9 and time to extubation

Group Time (second)	Group I (n = 35)	Group II (n = 35)	p
Time to TOF ≥ 0.7			
$\bar{X}$ ± SD	107.57 ± 54.87	215.57 ± 81.76	<0.05
Min – Max	30-300	75-435	
Time to TOF ≥ 0.9			
$\bar{X}$ ± SD	155.29 ± 62.51	313.29 ± 105.77	<0.05
Min – Max	45-360	120-570	
Time to extubation after NMBAs reveral	249.43 ± 81.75	456.29 ± 146.45	<0.05

Side effects of NMBAs reversal

Sugammadex did not cause changes in the heart rate and blood pressure as well as other side effects, while heart rate was recorded to decrease in the neostigmine and atropine group. There were 2.9% patients experiencing xerostomia, 2.9% patients undergoing headaches in sugammadex group. In group used combination of neostigmine and atropine: 28.5% patients had bradycardia; 25.7% increased phlegm production; 11.4% suffered xerostomia; 11.4% had headaches; 22.9% represented nausea. Among them, bradycardia, increased secretion of mucus, and nausea were statistically significantly different from group S with p <0.05. All patients in both groups had neither arrhythmias nor bronchospasm. 28.5% patients with bradycardia were sinus one (Table 4).

Table 4: Side effects

Group Side effect	Group I n (%)	Group II n (%)	P
Nausea	1(2.9)	8(22.9)	<0.05
Bradycardia	0	10(28.5)	<0.05
Increased phlegm production	0	9(25.7)	<0.05
Xerostomia	1(2.9)	4(11.4)	>0.05
Headache	1(2.9)	4(11.4)	>0.05

Discussion

The patients in the two study groups did not differ in terms of common characteristics: patient age, height, weight, BMI classification. As far as surgical type, perioperative used drugs, postoperative parameters, arterial blood gas of the two groups were concerned, there were not significant difference.

In the regard of the effect of neuromuscular blockade reversal agent, the results of the study showed that the group of patients receiving dose of 2 mg/kg sugamadex had a significantly faster recovery time of TOF compared with the patients receiving the combination of neostigmine and atropine at the ratio 3:1. The dose of sugammadex or neostigmine was adjusted according to TOF count value mearsured right after operation. In the study, time to start reversing neuromuscular blockade was when there was at least one twitch of TOF [12]. Acorrding to Hristovska's study, time to get TOF 0.9 when reversed by sugammadex is significantly faster than that by neostigmine at every different dose in patients who were maintained by either intravenous anesthetics or volatile agents during anesthesia [13]. After 3 minutes of sugammadex injection, 91.4% patients achieved TOF ≥ 0.9, whereas only 28.6% of patients obtained TOF ≥ 0.9 after 4 minutes of neostigmine injection, this difference was statistically significant with p <0.05. After 5 minutes of reversal, 100% patients of group I achieved TOF ≥ 0.9, while the figure for group 2 was 40%.

Neostigmine is a neuromuscular blockade

reversal agent that has been used for a long time and is clinically popular. The drug causes inactivation of acetyl cholinesterase through the irreversible carbamylation process. Neostigmine cannot resolve the muscle relaxant when the neuromuscular blockade is deep. Neostigmine's neuromuscular blockade reversal effect usually initiates in about 1-2 minutes and reaches maximum within 6-10 minutes, so it takes about 10 minutes for neostigmine to fully perform [14],[15]. In our study, the group treated with neostigmine combined with atropine had an average recovery time of TOF ≥ 0.7 was 215.57 ± 81.76 seconds, the slowest recovery time of TOF ≥ 0.7 was 435 seconds; the average recovery time of TOF ≥ 0.9 was 313.29 ± 105.77 seconds, the latest was after 570 seconds. In this group, the number of patients who received neostigmine when there was 1-2-3-4 stimulating response (TOF 1/4) was 4-13-7-11 respectively. In our study, the time to achieve TOF ≥ 0.9 was shorter than that of Manfred, Blobner [16], and Tiffany Woo [17], Cheong Ho [18]; in the study of Blobner and plus, the average recovery time of TOF ≥ 0.7 is 7.2 minutes, recovery of TOF ≥ 0.9 is 18.6 minutes. This difference may be due to the fact that Blobner and Woo administered reversal agent at the time of TOF =2/4, while we injected reversal agent at times of different TOF values. In our study, patients who recieved neuromuscular blockade reversal at the time of TOF=2/4 had average recovery time of TOF ≥ 0.7 and TOF ≥ 0.9 was 238.85 ± 80.89 seconds and 339.23 ± 115.80 seconds respectively. This result is longer than that of Wu Xinmin [19], this difference can be attributed to the fact that we used sevofluran for anaesthesia maintenance. Sevofluran has been shown to slow neostigmine's muscle relaxant recovery [20].

Sugammadex was approved for use in Europe in 2008 by the European, Pharmaceutical Authorities. In 2015, sugammadex was accepted by the American Pharmaceutical Society, and now it has been used in 70 countries [21]. With the mechanism of direct action through rapid chemical interaction, sugammadex forms a stable complex with non-depolarizing muscle relaxants. Sugammadex 16 mg/kg can be used in case of rescue when intubation is not possible after 1.2 mg/kg rocuronium injected, TOF achieved the value of ≥ 0.9 after 2 - 3 minutes [22]. In our study, we used dose of 2mg/kg sugammadex for all TOF count values. The results showed that after sugammadex injection, average time of TOF achieved ≥ 0.7 was 107.57 ± 54.87 seconds; and TOF ≥ 0.9 was 155.29 ± 62.51 seconds. The fastest time to recover TOF ≥ 0.7 was 0.30; and the fastest time to reach TOF ≥ 0.9 was 45 seconds. In this group, the number of patients receiving neuromuscular blockade reversal agent at the moment of TOF count = 1-2-3-4 stimulus response was 15-14-5-1 respectively. In patients who were reversed at TOF score of 2 stimuli, the average recovery time of TOF ≥ 0.7 and TOF ≥ 0.9 was 84.64 ± 24.67 seconds and 136.43 ± 32.10 seconds, correspondingly. Our results was similar to other studies, which showed that sugammadex can quickly dissolves rocuronium molecule: the average time of TOF ≥ 0.9 was 155.29 seconds; after 3 minutes, 91.4% patients recovered TOF ≥ 0.9; after 5 minutes, 100% patients recover TOF ≥ 0.9.

In the regard of undesirable effects: The rate of patients with bradycardia, nausea, and increased secretion of group 2 was significantly higher than group I, this result is shown in Table 3.7. Group 2 had 10 patients with heart rate <50 beats/minute accounting for 28.5%, 9 patients had increased sputum secretion mounting to 25.7%, 4 patients with dry mouth and 4 patients with headache occupying 11.4% and 8 patients (22.9%) had nausea. On the contrary, Group I had only 1 patient with headache, 1 patient with nausea, 1 patient with xerostomia, each accounting for 2.9%. In our study, we did not see any patients with allergies, dizziness, hypotension ... after reversal. Nausea and vomiting are common concern after surgery. There are many factors that are thought to be related to postoperative vomiting and nausea such as laparoscopic surgery with pneumoperitoneum, usage of atropine for neuromuscular blockade reversal compared to patients without postoperative reversal (68% vs. 32%) [23]. In our study, we had 8 patients (22.9%) with nausea in group II, including 2 patients had severe nausea, this patient was given metoclopramide 10 mg intravenously, and responded well to treatment. In the group of using sugammadex for neuromuscular blockade reversal there was 1 patients (2.9%) who suffered from nausea and vomiting after surgery. Some other studies recorded the rate of postoperative nausea and vomiting in patients with neuromuscular blockade reversal by sugammadex: Blobner 4%, Tiffany Woo 7%, Yazar 5%; [16], [17], [22]. We did not document any patients with bronchospasm after extubation. But 25.7% patients in group II increased sputum production, whilst in group I there was no patient with this symtom. Emine Yazar noted that 2 patients (3.4%) had bronchospasm after neuromuscular blockade reversal with sugammadex, but the author did not describe these two cases [22]. 1 patient (2.9%) in group I and 4 patients (11.4%) in group II had headache after surgery, there was no difference between the two groups, p > 0.05. In Tiffany Woo's study, the headache rate of neuromuscular blockade reversal with sugammadex and neostigmine was 12% and 15% respectively [11]. The rate of dry mouth in group II was 11.4%; group I is 2.9%. Xerostomia in patients receiving neuromuscular blockade reversal with neostigmine are associated with the use of combined atropine. In addition, the evaluation of this symptom is also difficult, because the patient must fast to prepare for surgery, so the patient had a feeling of dry mouth before. In the Blobner study, the rate of dry mouth was 6% in both groups used neostigmine and sugammadex [16].

The objects of our study were patients who experienced laparoscopic nephrectomy, so it is necessary to monitor and evaluate plasma creatinine level before and after 24 hour of surgery which were shown to be not significantly different between the two groups.

In conclusion, Sugammadex has better neuromuscular block reversal effects than neostigmine. Recovery time reaching TOF ≥ 0.9 of group using sugammadex 2mg/kg is significantly faster than the one of group using neostigmine combined with atropine at the rate of 3:1 following TOF count. Sugammadex also reduces side effects induced by neuromuscular blockade reversal agents in living donor nephrectomy surgery.

Ethical approval

All procedures performed in studies involving human participants were in accordance with the ethical standards of institutional and/or national research committee and with the 1964 Helsinki declaration and its later amendments or comparable ethical standards. The study has been approved by Science and Medical Ethics Review Board of Viet Duc hospital and Committee of Science and Ethics of Hanoi Medical University.

Informed consent

The patient's family was fully explained about the research process and agreed to participate. Risk patients had been excluded to minimize the unwanted effects of monitoring methods. Information about medical records and images were kept confidentially. Informed consents were obtained from the patients included in the study.

Acknowledgement

We would like to send our sincere thanks to all patients and their families for their believes, consensus to participate in and help us complete this study. We are also grateful to all staffs from Center of anesthesia and surgical intensive care, Center of organ transplantation, Department of renal diseases and hemodialysis of Viet Duc Hospital for facilitating and supporting this study.

References

1. Carron M, Zarantonello F, Tellaroli P, Ori C. Efficacy and safety of sugammadex compared to neostigmine for reversal of neuromuscular blockade: a meta-analysis of randomized controlled trials. Journal of clinical anesthesia. 2016; 35:1-2. https://doi.org/10.1016/j.jclinane.2016.06.018 PMid:27871504

2. Kim KS, Cheong MA, Lee HJ, Lee JM. Tactile assessment for the reversibility of rocuronium-induced neuromuscular blockade during propofol or sevoflurane anesthesia. Anesthesia & Analgesia. 2004; 99(4):1080-5. https://doi.org/10.1213/01.ANE.0000130616.57678.80 PMid:15385354

3. Donati F. Neuromuscular MonitoringMore than Meets the Eye. Anesthesiology: The Journal of the American Society of Anesthesiologists. 2012; 117(5):934-6. https://doi.org/10.1097/ALN.0b013e31826f9143 PMid:23011318

4. Kopman AF, Kopman DJ, Ng J, Zank LM. Antagonism of profound cisatracurium and rocuronium block: the role of objective assessment of neuromuscular function. Journal of clinical anesthesia. 2005; 17(1):30-5. https://doi.org/10.1016/j.jclinane.2004.03.009 PMid:15721727

5. Bevan JC, Collins L, Fowler C, Kahwaji R, Rosen HD, Smith MF, Scheepers LD, Stephenson CA, Bevan DR. Early and late reversal of rocuronium and vecuronium with neostigmine in adults and children. Anesthesia & Analgesia. 1999; 89(2):333-9. https://doi.org/10.1213/00000539-199908000-00016

6. Tramer MR, Fuchs-Buder T. Omitting antagonism of neuromuscular block: effect on postoperative nausea and vomiting and risk of residual paralysis. A systematic review. British journal of anaesthesia. 1999; 82(3):379-86. https://doi.org/10.1093/bja/82.3.379 PMid:10434820

7. Bom A, Bradley M, Cameron K, Clark JK, van Egmond J, Feilden H, MacLean EJ, Muir AW, Palin R, Rees DC, Zhang MQ. A novel concept of reversing neuromuscular block: chemical encapsulation of rocuronium bromide by a cyclodextrin-based synthetic host. Angewandte Chemie International Edition. 2002; 41(2):265-70. https://doi.org/10.1002/1521-3773(20020118)41:2<265::AID-ANIE265>3.0.CO;2-Q

8. Sorgenfrei IF, Norrild K, Larsen PB, Stensballe J, Østergaard D, Prins ME, Viby-Mogensen J. Reversal of Rocuronium-induced Neuromuscular Block by the Selective Relaxant Binding Agent SugammadexA Dose-finding and Safety Study. Anesthesiology: The Journal of the American Society of Anesthesiologists. 2006; 104(4):667-74. https://doi.org/10.1097/00000542-200604000-00009 PMid:16571960

9. Sparr HJ, Vermeyen KM, Beaufort AM, Rietbergen H, Proost JH, Saldien V, Velik-Salchner C, Wierda JM. Early reversal of profound rocuronium-induced neuromuscular blockade by sugammadex in a randomized multicenter study: efficacy, safety, and pharmacokinetics. Anesthesiology. 2007; 106(5):935-43. https://doi.org/10.1097/01.anes.0000265152.78943.74 PMid:17457124

10. Cedborg AI, Sundman E, Bodén K, Hedström HW, Kuylenstierna R, Ekberg O, Eriksson LI. Pharyngeal function and breathing pattern during partial neuromuscular block in the elderlyeffects on airway protection. Anesthesiology: The Journal of the American Society of Anesthesiologists. 2014; 120(2):312-25. https://doi.org/10.1097/ALN.0000000000000043 PMid:24162461

11. Adembesa I, Mung'ayi V, Premji Z, Kamya D. A randomized control trial comparing train of four ratio> 0.9 to clinical assessment of return of neuromuscular function before endotracheal extubation on critical respiratory events in adult patients undergoing elective surgery at a tertiary hospital in. African health sciences. 2018; 18(3):807-16. https://doi.org/10.4314/ahs.v18i3.40 PMid:30603015 PMCid:PMC6306997

12. Brueckmann B, Sasaki N, Grobara P, Li MK, Woo T, De Bie J, Maktabi M, Lee J, Kwo J, Pino R, Sabouri AS. Effects of sugammadex on incidence of postoperative residual

neuromuscular blockade: a randomized, controlled study. BJA: British Journal of Anaesthesia. 2015; 115(5):743-51. https://doi.org/10.1093/bja/aev104 PMid:25935840

13. Hristovska AM, Duch P, Allingstrup M, Afshari A. Efficacy and safety of sugammadex versus neostigmine in reversing neuromuscular blockade in adults. Cochrane Database of Systematic Reviews. 2017; (8): CD012763-CD012763. https://doi.org/10.1002/14651858.CD012763 PMid:28806470 PMCid:PMC6483345

14. Beemer GH, Bjorksten AR, Dawson PJ, Dawson RJ, Heenan PJ, Robertson BA. Determinants of the reversal time of competitive neuromuscular block by anticholinesterases. British Journal of Anaesthesia. 1991; 66(4):469-75. https://doi.org/10.1093/bja/66.4.469 PMid:2025474

15. Kirkegaard H, Heier T, Caldwell JE. Efficacy of tactile-guided reversal from cisatracurium-induced neuromuscular block. Anesthesiology. 2002; 96(1):45-50. https://doi.org/10.1097/00000542-200201000-00013 PMid:11753000

16. Blobner M, Eriksson LI, Scholz J, Motsch J, Della Rocca G, Prins ME. Reversal of rocuronium-induced neuromuscular blockade with sugammadex compared with neostigmine during sevoflurane anaesthesia: results of a randomised, controlled trial. European Journal of Anaesthesiology (EJA). 2010; 27(10):874-81. https://doi.org/10.1097/EJA.0b013e32833d56b7 PMid:20683334

17. Woo T, Kim KS, Shim YH, Kim MK, Yoon SM, Lim YJ, Yang HS, Phiri P, Chon JY. Sugammadex versus neostigmine reversal of moderate rocuronium-induced neuromuscular blockade in Korean patients. Korean journal of anesthesiology. 2013; 65(6):501. https://doi.org/10.4097/kjae.2013.65.6.501 PMid:24427455 PMCid:PMC3888842

18. Cheong SH, Ki S, Lee J, Lee JH, Kim MH, Hur D, Cho K, Lim SH, Lee KM, Kim YJ, Lee W. The combination of sugammadex and neostigmine can reduce the dosage of sugammadex during recovery from the moderate neuromuscular blockade. Korean journal of anesthesiology. 2015; 68(6):547. https://doi.org/10.4097/kjae.2015.68.6.547 PMid:26634077 PMCid:PMC4667139

19. Wu X, Oerding H, Liu J, Vanacker B, Yao S, Dahl V, Xiong L, Claudius C, Yue Y, Huang Y, Abels E. Rocuronium blockade reversal with sugammadex vs. neostigmine: randomized study in Chinese and Caucasian subjects. BMC anesthesiology. 2014; 14(1):53. https://doi.org/10.1186/1471-2253-14-53 PMid:25187755 PMCid:PMC4153006

20. Reid JE, Breslin DS, Mirakhur RK, Hayes AH. Neostigmine antagonism of rocuronium block during anesthesia with sevoflurance, isoflurane or propofol. Canadian journal of anaesthesia. 2001; 48(4):351. https://doi.org/10.1007/BF03014962 PMid:11339776

21. Nag K, Singh DR, Shetti AN, Kumar H, Sivashanmugam T, Parthasarathy S. Sugammadex: a revolutionary drug in neuromuscular pharmacology. Anesthesia, essays and researches. 2013; 7(3):302. https://doi.org/10.4103/0259-1162.123211 PMid:25885973 PMCid:PMC4173552

22. Yazar E, Yılmaz C, Bilgin H, Karasu D, Bayraktar S, Apaydın Y, Sayan HE. A comparision of the effect of sugammadex on the recovery period and postoperative residual block in young elderly and middle-aged elderly patients. Balkan medical journal. 2016; 33(2):181. https://doi.org/10.5152/balkanmedj.2016.16383 PMid:27403387 PMCid:PMC4924962

23. King MJ, Milazkiewicz R, Carli F, Deacock AR. Influence of neostigmine on postoperative vomiting. BJA: British Journal of Anaesthesia. 1988; 61(4):403-6. https://doi.org/10.1093/bja/61.4.403 PMid:3190971

ID Design Press, Skopje, Republic of Macedonia
Open Access Macedonian Journal of Medical Sciences. 2019 Dec 30; 7(24):4427-4431.
https://doi.org/10.3889/oamjms.2019.875
eISSN: 1857-9655
Basic and Clinical Medical Researches in Vietnam

Preimplantation Genetic Testing of Aneuploidy by Next Generation Sequencing: Association of Maternal Age and Chromosomal Abnormalities of Blastocyst

Tien-Truong Dang[1], Thi-Mui Phung[1], Hoang Le[1, 2], Thi-Bich-Van Nguyen[3], Thi-Sim Nguyen[4], Thi-Lien-Huong Nguyen[3], Vu Thi Nga[5], Dinh-Toi Chu[6, 7], Van-Luong Hoang[1], Duy-Bac Nguyen[1*]

[1]Vietnam Military Medical University, Hanoi, Vietnam; [2]Tam Anh Hospital, Hanoi, Vietnam; [3]National Hospital of Obstetrics and Gynecology, Hanoi, Vietnam; [4]Hanoi Obstetrics and Gynecology Hospital, Hanoi, Vietnam; [5]Institute for Research and Development, Duy Tan University, Danang 550000, Vietnam; [6]Faculty of Biology, Hanoi National University of Education, Hanoi, Vietnam; [7]School of Odonto Stomatology, Hanoi Medical University, Hanoi, Vietnam

Citation: Dang T-T, Phung T-M, Hoang Le, Nguyen T-B-V, Nguyen T-S, Nguyen T-L-H, Nga VT, Chu D-T, Hoang V-L, Nguyen D-B. Preimplantation Genetic Testing of Aneuploidy by Next Generation Sequencing: Association of Maternal Age and Chromosomal Abnormalities of Blastocyst. Open Access Maced J Med Sci. 2019 Dec 30; 7(24):4427-4431. https://doi.org/10.3889/oamjms.2019.875

Keywords: Blastocyst embryos; Preimplantation genetic testing aneuploidy; Next-generation sequencing; Aneuploidy; In vitro fertilization

***Correspondence:** Duy-Bac Nguyen. Vietnam Military Medical University, Hanoi, Vietnam. E-mail: nguyenduybac@vmmu.edu.vn

Received: 13-Nov-2019; **Revised:** 22-Nov-2019; **Accepted:** 25-Nov-2019; **Online first:** 20-Dec-2019

Funding: This study was funded by KC10/16-20 Program, Vietnam

Competing Interests: The authors have declared that no competing interests exist

Abstract

BACKGROUND: Aneuploidy is a major cause of miscarriages and implantation failure. Preimplantation genetic testing for aneuploidy (PGT-A) by Next Generation Sequencing (NGS) is able to detect of the numeral and structural chromosomal abnormalities of embryos *in vitro* fertilization (IVF).

AIM: This study was aimed to assess the relationship between maternal age and chromosomal abnormalities NGS technology.

METHODS: A group of 603 human trophectoderm (TE) biopsied samples were tested by Veriseq kit of Illumina. The relation of marternal age and chromosomal abnormality of blastocyst embryo was evaluated.

RESULTS: Among the 603 TE samples, 247 samples (42.73%) presented as chromosomal abnormalities. The abnormalities occurred to almost chromosomes, and the most popular aneuploidy observed is 22. Aneuploidy rate from 0.87% in chromosome 11 to 6.06% in chromosome 22. The rate of abnormal chromosome increased dramatically in group of mother's ages over 37 (54.17%) comparing to group of mother's ages less than 37 (38.05%) ($p < 0.000$). The Abnormal chromosome and maternal age has a positive correlation with $r = 0.4783$ ($p<0.0001$).

CONCLUSION: These results showed high rate abnormal chromosome and correlated with advanced maternal age of blastocyst embryos.

Introduction

Maximizing the success rate of *in vitro* fertilization (IVF) treatments is challenge, and a reliable mean of determining the embryos with the most significant capacity for pregnancy is required [1]. There are several molecular methods to assess embryos, which are available to be applied. The major cause of IVF failure was showed to be abnormal chromosome. Recent years, aneuploidy rates were higher in oocytes and embryos from women of advanced maternal age [2], [3], [4]. The number of women intentionally, delaying pregnancy after year-old age of 35, has increased significantly last decades because the clash between the optimal biological period for women to have children and to obtain additional education, and building a career. In fact, for women over 40 years old, it is common for more than fifty percent of the oocytes retrieved to be aneuploidy [1], [5]. In miscarriage couples, an abnormal embryonic karyotype has been found to represent the most frequent cause [3].

PGT-A has been applied for the last over ten years to assess the chromosome abnormality of embryos to satiate the reproductive outcome of specific patient groups. Aneuploidies are common in early human embryos such as day 3 to day 5. Most methodologies of embryo assessment involve morphologic analysis at different developmental stages of the embryo. Blastomere number, multi-nucleation, fragmentation of embryo, and blastocyst formation are the key factors associated with viability

of embryo. The relationship between morphology and embryo aneuploidy was first evaluated with Fluorescence *in situ* hybridization (FISH) studies for 7–8 chromosomes [6]. Pellicer's experience showed that a remarkable rate of embryos with chromosomal abnormality was able to develop to the blastocyst with suitable morphology parameters; in fact, 42.8% of chromosomally abnormal embryos reached blastocyst stage [7]. However, the failure of finding a better morphologic indicator of aneuploidy in previous researches had been a consequence of technical insufficiency. Virtually all study has evaluated only a few specific chromosomes in each embryo, and it is therefore unavoidable that some of the embryos categorized as aneuploidy were, in fact, abnormal, with aneuploidies affecting chromosomes that were not tested [1].

More recently, in a study, array comparative genomic hybridization (A- CGH) could be used to detect 24 embryonic chromosomes. A-CGH was the first technology to be widely available for comprehensive aneuploidy screening and is now used extensively around the world [8]. The rapid development of next generation sequencing (NGS) technologies has generated an increasing interest to apply in PGT-A purposes and the technique offer improvements for the detection of chromosomal aneuploidy in IVF embryos compared with current technologies by reduced costs and enhanced precision as well as parallel and customizable analysis of multiple embryos in a single sequencing run [8], [9]. In this study, we applied NGS technology to screening 24-chromosome aneuploidy on embryos at blastocyst stages. This approach with trophectoderm samples from blastocyst biopsies, both whole chromosome aneuploidy and segmental chromosome imbalances would be detected. We also determined the chromosomal abnormalities of blastocyst-stage embryos *in vitro* fertilization using PGS-NGS technique and evaluating the correlation between the chromosomal status of blastocyst-stage embryos and the maternal age.

Materials and Methods

Material

The study population consisted of 603 embryos from consecutive patients planning to undergo PGS with trophectoderm (TE) biopsy. All IVF cycles were performed at the Andrology and Fertility Hospital of Hanoi, and Hanoi Hospital of Obstetrics and Gynecology in the period between June 2017 and February 2018. Genetic testing was performed at the DNA laboratory - Vietnam Military Medical Academy.

Whole genome amplification (WGA)

For whole genome amplification, TE samples, negative and positive controls were lysed, and genomic DNA was amplified by SurePlex kit (Illumina, Inc., San Diego, CA, USA), as the manufacturer's recommendation. Then, 5 µl of each product plus 5 µl gel loading dye were tested by agarose electrophoresis to determine the success of the amplification.

Libraries preparation

Libraries were prepared at DNA Lab using the VeriSeq PGS workflow (Illumina, Inc.), was briefly following: One nanogram of quantified dsDNA template at 0.2 ng/ml was added to 5 µl of Amplicon Tagmentation Mixture (ATM) and 10 µl of Tagmentation DNA Buffer (TD). The segmentation step was carried out at 55^{o}C for 5 min and hold at 10^{o}C. The resulting segmented mixture was neutralized by adding 5µl of proprietary neutralization buffer (NT). Post-homogenization, the Tagmentation plate was held at room temperature for 5 min. The fragmented DNA was amplified via a limited-cycle PCR programme (one cycle of 72^{o}C for 3 min, followed by 12 cycles of 95^{o}C for 10 s, 55^{o}C for 30 s and 72^{o}C for 30 s, one cycle at 72^{o}C for 30 s, followed by a hold at 4^{o}C) after the adding of 5µl of index 1 (i7), 5µl of index 2 (i5), and 15µl of Nextera PCR Master Mix (NPM) to each well. PCR product clean-up used AMPureXP beads (Beckman Coulter, Brea, CA, USA) to purify the library DNA with no salt carryover, providing a size selection step that removes short library fragments including index 1 (i7) and index 2 (i5) from the population. 45 µl of the PCR product was transferred to 96-well storage plates containing 45 µl of AMPure XP beads. Sealed plates were mixed using a microplate shaker at 1000 rpm for 2 min, then incubated at ambient temperature without shaking for 5 min. Thereafter, the plate was placed on a magnetic stand for 2 min or until the supernatant cleared. While the plates were kept on the magnetic stand, the magnetic beads were washed twice with 200 µl of freshly prepared 80% ethanol. Purified libraries were eluted with 50 µl of the Nextera XT Resuspension Buffer. It could be found more detail elsewhere [8], [9].

Sequencing

Single-end, dual index 36 base pair reads sequencing was performed at DNA Laboratory following the Illumina chemistry workflow on a MiSeq (Illumina, Inc.), using the MiSeq Reagent Kit v3 PGS kit (Illumina, Inc.) which contains the ready to load onboard clustering and SBS chemistry reagents.

Processing and analysing data

The following bioinformatics analysis was accomplished with a pre-release version of BlueFuse Multi for NGS (Illumina, Inc.). "Embryos were diagnosed as "euploidy" if the generated plot showed no gain or loss [8]. Secondary analysis included statistics; description, processing, and data analysis were performed by STATA software version 14. We compared the average values by t-testst and the

ratios by Chi quare test, CI 95%. We use simple linear regression and Pearson's correlation to find the relationship.

Results

Of the blastocyst-stage embryos, 95.9% were succeeding in whole genome amplification (578 out of 603). We investigated 410 embryos belong group mother's age <37 years old Group 1 (32.6 ± 3.43) and 168 embryos belong group mother's age >37 years old – Group 2 (39.63 ± 2.96) (Table 1).

Table 1: PGS-NGS results in 578 embryos at blastocyst stage, (Pearson chi2(1) = 12.6506 pr = 0.000)

	Group 1 (<37 years old)	Group 2 (≥37 years old)	Total	P (Group 1 vs Group 2)
Average age (Mean±SD	32.06 ± 3.43	39.63 ± 2.96	34.26 ± 4.76	0.0000
Normal embryos (n, %)	254 61.95%	77 45.83%	331 57.27%	0.0000
Abnormal embryo (n, %)	156 38.05%	91 54.17%	247 42.73%	0.0000
Total embryo (n, %)	410 100%	168 100%	578 100%	

Note: P values were determined by t test and Chi square test.

A wide variety of aneuploidies was detected. Indeed, the results showed that any chromosome can be affected by aneuploidy at the blastocyst stage. A total of 322 chromosomal abnormalities were detected in the aneuploidy embryos represented monosomy, trisomy (Figure 1). Top 3 chromosomal 22, 16 and 21 were much more represented by abnormal than others (35, 32 and 24, respectively) (Table 2).

Table 2: Characteristics of aneuploidy

Chrom-osome	Total chromosome tested	Aneuplody		Euploidy	
		n	%	n	%
1	578	9	1.56%	569	98.44%
2	578	11	1.90%	567	98.10%
3	578	12	2.08%	566	97.92%
4	578	15	2.60%	563	97.40%
5	578	13	2.25%	565	97.75%
6	578	9	1.56%	569	98.44%
7	578	7	1.21%	571	98.79%
8	578	17	2.94%	561	97.06%
9	578	6	1.04%	572	98.96%
10	578	17	2.94%	561	97.06%
11	578	5	0.87%	573	99.13%
12	578	12	2.08%	566	97.92%
13	578	15	2.60%	563	97.40%
14	578	10	1.73%	568	98.27%
15	578	19	3.29%	559	96.71%
16	578	32	5.54%	546	94.46%
17	578	10	1.73%	568	98.27%
18	578	11	1.90%	567	98.10%
19	578	7	1.21%	571	98.79%
20	578	8	1.38%	570	98.62%
21	578	24	4.15%	554	95.85%
22	578	35	6.06%	543	93.94%
XY	578	18	3.11%	560	96.89%
Total	13294	322	2.42%	12972	97.58%

As expected, a strong association between advancing maternal age and aneuploidy was observed, but interestingly individual chromosomes were not equally affected by this phenomenon. There were 54.1% embryos had chromosomal abnormality in group 1 whereas only 38.05% in Group 1 (Table 1).

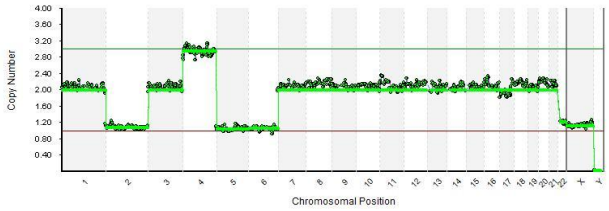

Figure 1: Examples of chromosomal abnormalities detection by next-generation sequencing. Embryo number HU3 of patient N. T. H.: 42, XY, -2, -5, -6, -22, +4

Results from the embryos of group 1 were compared with those from patients in group 2. Chromosome 14 showed the greatest increase in the risk of aneuploidy (3.7-fold increase). Chromosomes 7 and 18 displayed a 3.3 and a 2.9-fold increase, respectively. For chromosomes 2, 3, 12, 13, 15, 17, 19, 20, 21 and 22 the increase was around from 1.5 to 2-fold. Other chromosomes were found little or no change in aneuploidy rate with advancing age (Figure 2).

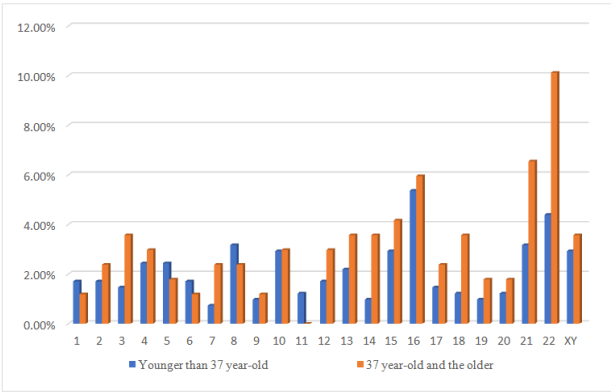

Figure 2: Incidence of chromosomal abnormalities between two groups

We evaluated the relationship between blastocyst-stage chromosomal abnormalities and maternal age using linear regression and Pearson's correlation (Figure 3). The correlation coefficients r = 0.4783 (CI 95%) are illustrated as formula:

Abnormalities probity of chromosomes = -0.7 + 0.01 x (maternal age)

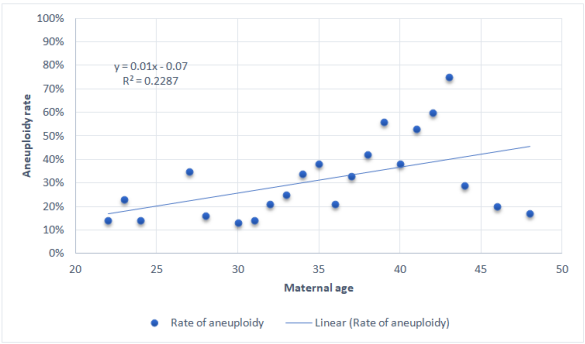

Figure 3: The linear regression line shows the correlation between maternal age and the rate of aneuploidy. R^2: coefficient index

Discussion

The evaluation of genetic normality embryo is the most important criterion for the selection of embryos to be transferred. Thus, the present study attempted to re-evaluate previous studies that had described the relationship between chromosome abnormalities and maternal age using newest PGS method based on NGS technology [10], [11], [12], [13], [14], [15]. The analysis of more than 603 embryos for 23 chromosome pairs makes this study the most extensive and comprehensive to date on chromosome abnormalities in human cleavage stage embryos.

In this study showed that the abnormal chromosomal IVF in Vietnam population was 42.7% (Confident interval 95%). This number indicated with Rubio's study in 2003 analyzing similar maternal age that there were 45.1% embryo had abnormal chromosomal [16]. In 2003, Alfarawati showed that there was more than half of embryos tested had abnormal (56.7%) [17]. However, their study focused on recurrent miscarriage and high maternal age (average 37.5 years) whereas this study focused on patient had average age lower (34.4 years). In 1991, Zenzes and Casper represented the rate of abnormalities in embryo was fluctuate from 23% to 40% [18]. It is possible to project used NGS method with high accuracy compare with karyotyping used by Zenzes.

Aneuploidy is the most error observed on the embryo at the blastocyst stage [19]. Notably, the proportion of each chromosome is the difference in order that testing individual chromosomal or some chromosomes was concluded healthy embryo due to an increasing false negative. Therefore, the high aneuploidy rates observed suggest that chromosome screening at the blastocyst stage may be beneficial, particularly for women >34 years [20].

On the other hand, the results agreed with previous trends, such as that aneuploidy increases in cleavage stage embryos with maternal age. It is clear that maternal age is only one of the causes of chromosome abnormalities. The present study confirms that only 61.95% of embryos from young patients are healthy for the chromosomes studied (< 37 years), and this frequency decreases to 45.83% with advancing maternal age (>37 years) (CI: 95%, $p < 0.05$). In 2003, Rubio's study illustrated that the abnormalities rate of chromosomes were 33.3% at patients age <37 years and increased to 57.7% at patients age >37 years [16]. Of research made, Aneuploidy reached over 50% with maternal age >40 years [20]. In addition, in the year 2017, Upadhyaya concluded that the number of normal embryos in group < 37 years was 65.5% and fallen at 40.6% when maternal age increasing [21]. This proportion for this study was very similar to the proportion of our study. Even Upadhyaya et al. used another technology (array CGH) to detected comprehensive chromosomes.

The results make us believe that chromosomal abnormalities of the embryo in IVF blastocyst stage have a relationship with maternal age, although the correlation coefficient is not really high ($r = 0.4783$, CI:95%). In fact, this coefficient is positive, that means the higher the mother's age will have more chromosomal abnormalities of embryos. Figure 3 shows that each 22.87% variation in the incidence of chromosome abnormalities is explained by the variation of maternal age factor (coefficient of determination R-square = 0.2287). When maternal age increases by one unit, the incidence of chromosome numbers increases by 0.01 units, and this change is significant, with 95% confidence [22].

Overall, the probability of embryo aneuploidy increases when maternal age higher. This effect becomes more impressive for some chromosomes. The chromosome most affected by age is chromosome 14; the data show that the rate of multiple deviations increased by 3.7 times in the elderly group (≥ 37 years). Then came chromosome 7, the rate of multiple deviations increased by 3.3 times and chromosome 18 increased by 2.9 times when the mother's age increased compared with the average increase of about 1.5 to 2 times for all chromosomes 2, 3, 12, 13, 15, 17, 18, 19, 20, 21, 22. In addition to the study of Alfarawati and colleagues in 2011, chromosomes 7 and 14 were the most prevalent group with the highest increase in maternal age (5-6 times higher), and for infection chromosomes 2, 15, 17, 20, 22 doubled [17]. This conclusion is quite similar to our results, thus confirming the reliability of this study.

In conclusion, the rate of chromosomal abnormalities of embryos at blastocyst stage in vitro fertilization in the Vietnamese population is 42.7%. The most common groups of chromosomes were observed including chromosome number 15, 16, 21, 22 and sex chromosomes.

The proportion of embryos with abnormal chromosome and maternal age has a positive correlation with the average level of contact ($r = 0.4783$), meaning that the higher the age of the mother will make greater the risk of creating embryos have chromosomal abnormalities.

Ethical approval

All procedures performed in studies involving human participants were in accordance with the ethical standards of the institutional and/or national research committee and with the 1964 Helsinki declaration and its later amendments or comparable

ethical standards. This study was approved by the ethics committee Vietnam Military Medical University.

Informed consent

The informed consents were signed by patients.

References

1. Alfarawati S, Fragouli E, Colls P, Stevens J, Gutiérrez-Mateo C, Schoolcraft WB, Katz-Jaffe MG, Wells D. The relationship between blastocyst morphology, chromosomal abnormality, and embryo gender. Fertility and sterility. 2011; 95(2):520-4. https://doi.org/10.1016/j.fertnstert.2010.04.003 PMid:20537630

2. Gutiérrez-Mateo C, Benet J, Wells D, Colls P, Bermudez MG, Sanchez-Garcia JF, Egozcue J, Navarro J, Munné S. Aneuploidy study of human oocytes first polar body comparative genomic hybridization and metaphase II fluorescence in situ hybridization analysis. Human Reproduction. 2004; 19(12):2859-68. https://doi.org/10.1093/humrep/deh515 PMid:15520023

3. Kuliev A, Cieslak J, Ilkevitch Y, Verlinsky Y. Chromosomal abnormalities in a series of 6733 human oocytes in preimplantation diagnosis for age-related aneuploidies. Reproductive biomedicine online. 2003; 6(1):54-9. https://doi.org/10.1016/S1472-6483(10)62055-X

4. Selva J, Martin-Pont B, Hugues JN, Rince P, Fillion C, Herve F, Tamboise A, Tamboise E. Cytogenetic study of human oocytes uncleaved after in-vitro fertilization. Human Reproduction. 1991; 6(5):709-13. https://doi.org/10.1093/oxfordjournals.humrep.a137413 PMid:1939554

5. Hassold TJ, Jacobs PA. Trisomy in man. Annual review of genetics. 1984; 18(1):69-97. https://doi.org/10.1146/annurev.ge.18.120184.000441 PMid:6241455

6. Rubio C, Rodrigo L, Mir P, Mateu E, Peinado V, Milán M, Al-Asmar N, Campos-Galindo I, Garcia S, Simón C. Use of array comparative genomic hybridization (array-CGH) for embryo assessment: clinical results. Fertility and sterility. 2013; 99(4):1044-8. https://doi.org/10.1016/j.fertnstert.2013.01.094 PMid:23394777

7. Rubio C, Rodrigo L, Mercader A, Mateu E, Buendía P, Pehlivan T, Viloria T, De los Santos MJ, Simón C, Remohí J, Pellicer A. Impact of chromosomal abnormalities on preimplantation embryo development. Prenatal Diagnosis: Published in Affiliation With the International Society for Prenatal Diagnosis. 2007; 27(8):748-56. https://doi.org/10.1002/pd.1773 PMid:17546708

8. Fiorentino F, Biricik A, Bono S, Spizzichino L, Cotroneo E, Cottone G, Kokocinski F, Michel CE. Development and validation of a next-generation sequencing-based protocol for 24-chromosome aneuploidy screening of embryos. Fertility and sterility. 2014; 101(5):1375-82. https://doi.org/10.1016/j.fertnstert.2014.01.051 PMid:24613537

9. Fiorentino F, Bono S, Biricik A, Nuccitelli A, Cotroneo E, Cottone G, Kokocinski F, Michel CE, Minasi MG, Greco E. Application of next-generation sequencing technology for comprehensive aneuploidy screening of blastocysts in clinical preimplantation genetic screening cycles. Human Reproduction. 2014; 29(12):2802-13. https://doi.org/10.1093/humrep/deu277 PMid:25336713

10. Munné S, Alikani M, Tomkin G, Grifo J, Cohen J. Embryo morphology, developmental rates, and maternal age are correlated with chromosome abnormalities. Fertility and sterility. 1995; 64(2):382-91. https://doi.org/10.1016/S0015-0282(16)57739-5

11. Munní S, Ary J, Zouves C, Escudero T, Barnes F, Cinioglu C, Ary B, Cohen J. Wide range of chromosome abnormalities in the embryos of young egg donors. Reproductive biomedicine online. 2006; 12(3):340-6. https://doi.org/10.1016/S1472-6483(10)61007-3

12. Márquez C, Sandalinas M, Bahçe M, Munné S. Chromosome abnormalities in 1255 cleavage-stage human embryos. Reproductive biomedicine online. 2000; 1(1):17-26. https://doi.org/10.1016/S1472-6483(10)61988-8

13. Magli MC, Gianaroli L, Ferraretti AP. Chromosomal abnormalities in embryos. Molecular and Cellular Endocrinology. 2001; 183:S29-34. https://doi.org/10.1016/S0303-7207(01)00574-3

14. Gianaroli L, Magli MC, Ferraretti AP, Lappi M, Borghi E, Ermini B. Oocyte euploidy, pronuclear zygote morphology and embryo chromosomal complement. Human reproduction. 2007; 22(1):241-9. https://doi.org/10.1093/humrep/del334 PMid:16936301

15. Bielanska M, Tan SL, Ao A. High rate of mixoploidy among human blastocysts cultured in vitro. Fertility and sterility. 2002; 78(6):1248-53. https://doi.org/10.1016/S0015-0282(02)04393-5

16. Rubio C, Simon C, Vidal F, Rodrigo L, Pehlivan T, Remohi J, Pellicer A. Chromosomal abnormalities and embryo development in recurrent miscarriage couples. Human Reproduction. 2003; 18(1):182-8. https://doi.org/10.1093/humrep/deg015 PMid:12525464

17. Alfarawati S, Fragouli E, Colls P, Stevens J, Gutiérrez-Mateo C, Schoolcraft WB, Katz-Jaffe MG, Wells D. The relationship between blastocyst morphology, chromosomal abnormality, and embryo gender. Fertility and sterility. 2011; 95(2):520-4. https://doi.org/10.1016/j.fertnstert.2010.04.003 PMid:20537630

18. Zenzes MT, Casper RF. Cytogenetics of human oocytes, zygotes, and embryos after in vitro fertilization. Human genetics. 1992; 88(4):367-75. https://doi.org/10.1007/BF00215667 PMid:1740312

19. Mantikou E, Wong KM, Repping S, Mastenbroek S. Molecular origin of mitotic aneuploidies in preimplantation embryos. Biochimica et Biophysica Acta (BBA)-Molecular Basis of Disease. 2012; 1822(12):1921-30. https://doi.org/10.1016/j.bbadis.2012.06.013 PMid:22771499

20. Fragouli E, Wells D, Thornhill A, Serhal P, Faed MJ, Harper JC, Delhanty JD. Comparative genomic hybridization analysis of human oocytes and polar bodies. Human Reproduction. 2006; 21(9):2319-28. https://doi.org/10.1093/humrep/del157 PMid:16704993

21. Majumdar G, Majumdar A, Verma IC, Upadhyaya KC. Relationship between morphology, euploidy and implantation potential of cleavage and blastocyst stage embryos. Journal of human reproductive sciences. 2017; 10(1):49. https://doi.org/10.4103/jhrs.JHRS_98_17 PMid:28904506 PMCid:PMC5586090

22. Pellestor F, Andréo B, Anahory T, Hamamah S. The occurrence of aneuploidy in human: lessons from the cytogenetic studies of human oocytes. European journal of medical genetics. 2006; 49(2):103-16. https://doi.org/10.1016/j.ejmg.2005.08.001 PMid:16530707

ID Design Press, Skopje, Republic of Macedonia
Open Access Macedonian Journal of Medical Sciences. 2019 Dec 30; 7(24):4432-4434.
https://doi.org/10.3889/oamjms.2019.876
eISSN: 1857-9655
Basic and Clinical Medical Researches in Vietnam

Torsion of Ileum Due To Giant Meckel's Diverticulum – A Case Report

Nguyen Duy Hung[1,2*], Trinh Anh Tuan[2], Than Van Sy[2], Vu Duc Thinh[3], Vo Truong Nhu Ngoc[4], Vu Thi Nga[5], Van Thai Than[6]

[1]Department of Radiology, Hanoi Medical University, Hanoi, Vietnam; [2]Department of Radiology, Viet Duc Hospital, Hanoi, Vietnam; [3]Digestive Surgery Department, Viet Duc Hospital, Hanoi, Vietnam; [4]School of Odonto Stomatology, Hanoi Medical University, Hanoi, Vietnam; [5]Institute for Research and Development, Duy Tan University, Danang, Vietnam; [6]NTT Institute of High Technology, Nguyen Tat Thanh University, Ho Chi Minh City, Vietnam

Citation: Hung ND, Tuan TA, Sy TV, Thinh VD, Ngoc VTN, Nga VT, Than VT. Torsion of Ileum Due To Giant Meckel's Diverticulum – A Case Report. Open Access Maced J Med Sci. 2019 Dec 30; 7(24):4432-4434. https://doi.org/10.3889/oamjms.2019.876

Keywords: Meckel's diverticulum; gastrointestinal tract; abdominal pain; abdominal distension

***Correspondence:** Nguyen Duy Hung. Department of Radiology, Hanoi Medical University, Hanoi, Vietnam; Department of Radiology, Viet Duc Hospital, Hanoi, Vietnam. E-mail: nguyenduyhung_84@yahoo.com

Received: 11-Nov-2019; **Revised:** 26-Nov-2019; **Accepted:** 27-Nov-2019; **Online first:** 20-Dec-2019

Funding: This research did not receive any financial support

Competing Interests: The authors have declared that no competing interests exist

Abstract

BACKGROUND: Meckel's diverticulum (MD) is detected in approximately 2% of all individuals and only 2-4% MD patients may develop symptoms. Small intestinal obstruction is a frequent complication in adults.

CASE REPORT: A 48-year-old male was admitted to emergency department for high intestinal obstruction symptoms. The imaging examinations were failed to detect the underlying causes. A median laparotomy revealed small bowel obstruction (SBO) due to a segment of ileum twisted around a giant MD axis.

CONCLUSION: Thus, a giant MD generating torsion of ileum is an unusual complication. Preoperative diagnosis is challenging. Emergency surgery is preferred to make an accurate diagnosis and for treatment.

Introduction

Meckel's diverticulum (MD) is a frequent congenital defect of the gastrointestinal tract, presenting in approximately 2% of whole population. Only 2-4% of this anomaly may become symptomatic [1]. Its location and size are known by "the rule of twos", in which the diverticulum is frequently located 2 feet (60 cm) from the ileocecal valve and does not exceed 2 inches (5 cm) in length [2]. Gastrointestinal bleeding, inflammation, intussusception or SBO are the principle complications of MD [1].

According to previous studies, the complication rate likely increases in the giant MD (diameter ≥ 5 cm) cases [3]. In these cases, small bowel obstruction (SBO) because of torsion around the giant diverticulum axis is rare but is the most serious complication [3]. Preoperative imaging diagnosis is always challenging because the diverticulum may resemble a normal bowel loop on ultrasound and computed tomography (CT) scan [3]. Hence, we report an unusual SBO case causing axial volvulus of a giant MD successfully treated by operation.

Case report

A 48-year-old male patient was hospitalized with increasing abdominal pain, abdominal distension, failure of passage gas and bowel movement for over 24 hours. No abnormal medical and surgical history was detected. The patient reported no nausea and no vomiting experience, along with a normal blood pressure (110/80 mmHg) and heart rate (90 bpm). Abdominal tenderness on palpation with muscular defense and no palpable hernias was detected on physical examination.

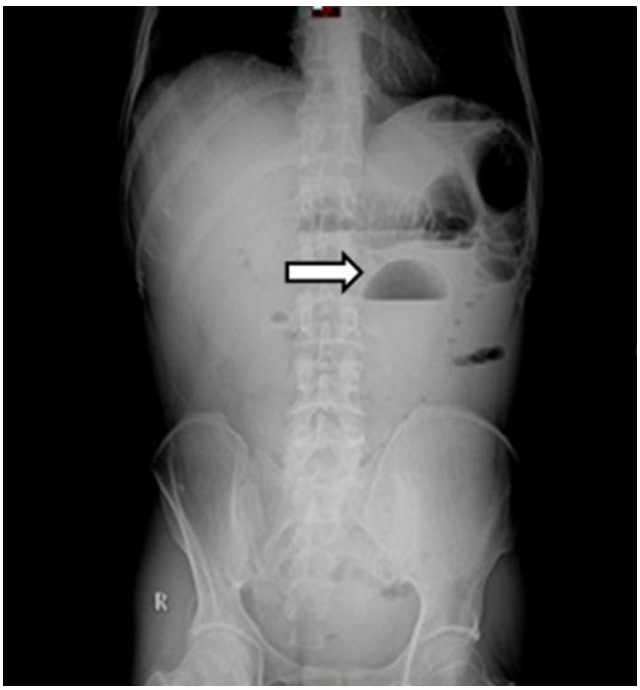

Figure 1: Abdominal X-ray findings. Air fluid levels in small bowel (arrow)

Air fluid levels were showed in small bowel at the left upper quadrant and ruled out pneumoperitoneum on abdominal X-ray (Fig. 1). Ultrasound revealed SBO with dilated bowel loop, decreased bowel peristalsis and homogenous free fluid mainly located in pouch of Douglas. On CT, SBO signs were also detected. The most distended loop (52 mm in diameter) proximal to transition point (Fig. 2A) and the thickened small bowel loops (Fig. 2B) were found at the left upper quadrant. Moreover, the whirlpool sign indicated mesenteric volvulus was showed at this area (Fig. 2C). No free gas, and no hernia was found. Blood count revealed that white blood cell count was 18.2 g/l, and percentage of neutrophil was 87.7%.

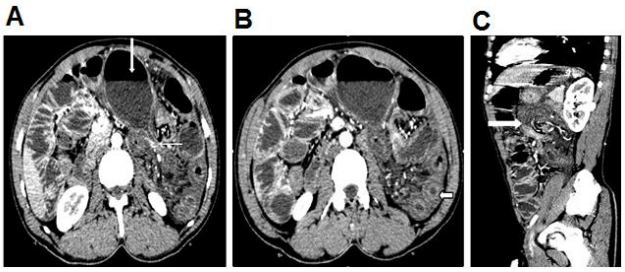

Figure 2: CT findings. A. Axial CT scan reveals the most distended loop (white arrow) proximal to transition point (small arrow). B. Axial CT reveals the thickened small bowel loops (arrow). C. Sagittal CT scan shows the whirlpool sign indicated mesenteric volvulus (arrow)

A median laparotomy was performed due to SBO with mesenteric volvulus. Operatory findings pointed out a 10-cm in length MD from 40 cm of ileocecal junction and 50 cm long of ileum twisted around MD axis. Segmental ileum containing the diverticulum was resected followed by ileo-ileostomy. Pathologic findings demonstrated inflammation, necrosis and hemorrhage of a MD and necrosis of the small bowel segment. The patient was discharged after 10 days.

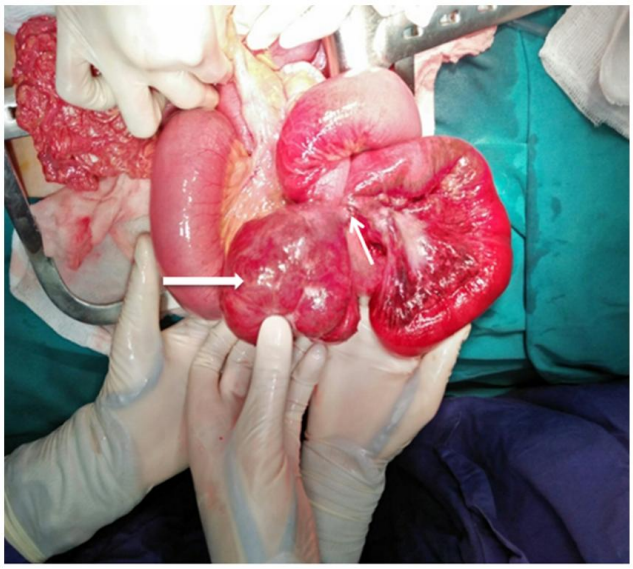

Figure 3: Intra-operative findings. Intra-operative photograph shows a giant MD (white arrow) and the location where the ileal loops twisted around MD axis (small arrow)

Discussion

MD results from the incomplete obliteration in the omphalomesenteric (vitelline) duct. As it is consisted of all layers of the small bowel, MD is considered a true diverticulum [3]. While gastrointestinal bleeding is one of the popular complications in children, intestinal obstruction is more frequently found to be a clinical symptom among adults (3). Based on hypothesis of Halstead *et al*, MD can be divided in two types - unattached and attached diverticulum. The former type is rarer and can cause obstruction due to its mobility. The latter has a fibrous band at its apex attaches to the umbilicus or to other viscera. Inflammation, adhesion or inversion of the mucous membrane of the diverticulum and adjacent bowel may lead a volvulus by twisting of the gut in upon itself at the point where the diverticulum attached. Furthermore, the appearance and the size of MD may increase the complication rate, hence, may change the treatment strategy. Many authors discouraged the resection of a broad-base or of a short length MD without palpable mass in the lumen in case of casually found [4, 5]. In contrast, a long and narrow base diverticulum is prone to diverticulitis and torsion, while intussusception is a frequent complication detected with a short and stumpy base diverticulum [2]. Regarding the size of MD, those which the diameter is ≥ 5 cm may result in SBO [2].

Preoperative diagnosis is difficult in the symptomatic patients without per-rectal bleeding and can be misdiagnosed as acute appendicitis. The clinical symptoms of SBO by reason of volvulus of MD are untypical to the other causes such as hernias, intra-abdominal adhesions or intussusception. Imaging exams can easily diagnose the SBO. Mallo et al. showed that CT scan sensitivity and specificity were 92 and 94% respectively for detecting SBO [6]. However, the potential diagnostic tools such as ultrasound and CT scan have limited value in detecting MD even in symptomatic cases [7]. Ultrasound has a narrow field of view and a limitation due to bowel gas. Besides, it is challenging to make a distinction between small bowel loops and MD on CT by reason of similarity of two structures. Scintigraphy with technetium-99m is a valuable non-invasive diagnostic exam in case of gastrointestinal bleeding [7].

Emergency surgery via laparotomy or laparoscopic is the first-line option to treat SBO due to MD. The principle purpose of this procedure is to remove the diverticulum and to correct the associated pathologies [8]. In cases where the adjacent ileum has inflammatory or ischemia changes, the resection of involved bowel with ileo-ileostomy is favored [9]. According to Cullen *et al.* study, the mortality and morbidity rates of Meckel's diverticulectomy were 2% and 12%, respectively, moreover, the cumulative risk of long-term post-operative complications was 7%. The author also recommended that the casually found MD should be resected regardless of the patient's age [10]. Our unusual case shows a SBO because of the torsion of adjacent ileum around a giant MD axis. The clinical symptoms and the imaging examinations were typical of SBO, however, they failed to demonstrate the etiology which was MD. A median laparotomy was performed to detect the underlying cause and successfully managed the SBO condition.

In conclusion, a segment of ileum twisted around a giant MD axis causing SBO is exceptional. The preoperative diagnosis of etiology in this condition is limited. Hence, MD should be considered in cases with an unrecognized cause of SBO and without surgical history.

Ethical approval

The patient and patient's family were informed about the imaging exams, surgical protocol, surgical complications and the research. All study protocols were approved by a local ethics committee of the Department of radiology, Vietduc hospital.

Informed consent

Informed consents were obtained from department of radiology and digestive surgery department, Vietduc hospital, the patient and patient's family.

References

1. Lee NK, et al. Complications of congenital and developmental abnormalities of the gastrointestinal tract in adolescents and adults: evaluation with multimodality imaging. Radiographics. 2010; 30(6):1489-507. https://doi.org/10.1148/rg.306105504 PMid:21071371

2. Capelão G, et al. Intestinal Obstruction by Giant Meckel's Diverticulum. GE Portuguese journal of gastroenterology. 2017; 24(4):183-187. https://doi.org/10.1159/000452690 PMid:29255748 PMCid:PMC5729947

3. Akbulut S, Yagmur Y. Giant Meckel's diverticulum: An exceptional cause of intestinal obstruction. World journal of gastrointestinal surgery. 2014; 6(3):47-50. https://doi.org/10.4240/wjgs.v6.i3.47 PMid:24672650 PMCid:PMC3964415

4. Robijn J, Sebrechts E, Miserez M. Management of incidentally found Meckel's diverticulum a new approach: resection based on a Risk Score. Acta Chir Belg. 2006; 106(4):467-70. https://doi.org/10.1080/00015458.2006.11679933 PMid:17017710

5. Varcoe RL, et al. Diverticulectomy is inadequate treatment for short Meckel's diverticulum with heterotopic mucosa. ANZ J Surg. 2004; 74(10):869-72. https://doi.org/10.1111/j.1445-1433.2004.03191.x PMid:15456435

6. Mallo RD, et al. Computed tomography diagnosis of ischemia and complete obstruction in small bowel obstruction: a systematic review. J Gastrointest Surg. 2005; 9(5):690-4. https://doi.org/10.1016/j.gassur.2004.10.006 PMid:15862265

7. Shelat VG, et al. Meckel's diverticulitis causing small bowel obstruction by a novel mechanism. Clin Pract. 2011; 1(3):e51. https://doi.org/10.4081/cp.2011.e51 PMid:24765312 PMCid:PMC3981389

8. Sharma RK, Jain VK. Emergency surgery for Meckel's diverticulum. World J Emerg Surg. 2008; 3:27. https://doi.org/10.1186/1749-7922-3-27 PMid:18700974 PMCid:PMC2533303

9. Mukai M, et al. Does the external appearance of a Meckel's diverticulum assist in choice of the laparoscopic procedure? Pediatr Surg Int. 2002; 18(4):231-3. https://doi.org/10.1007/s003830100663 PMid:12021967

10. Cullen JJ, et al. Surgical management of Meckel's diverticulum. An epidemiologic, population-based study. Ann Surg. 1994; 220(4):564-8; discussion 568-9. https://doi.org/10.1097/00000658-199410000-00014 PMid:7944666 PMCid:PMC1234434